Kraft recovery boilers - Principles and practice

Vakkilainen
Esa K.

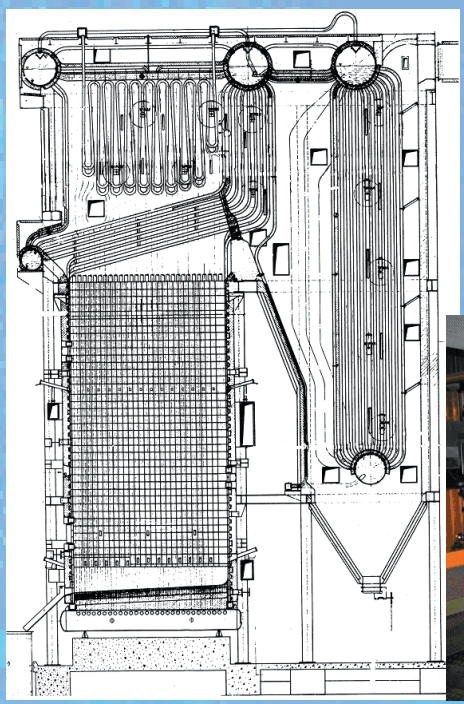

KRAFT RECOVERY BOILERS

Principles and practice

Esa K. Vakkilainen

Title/Nimi: Kraft recovery boilers - Principles and ptractice
Author/Tekijä: Vakkilainen, Esa K.

Publisher/Julkaisija: Suomen Soodakattilayhdistys r.y.
Printer/Painopaikka: Valopaino Oy, Helsinki, Finland
Year/Painovuosi: 2005
Pages/Sivuja: 246

ISBN 952-91-8603-7

Preface

This book was created as postgraduate lecture notes for Lappeenranta University of Technology's special course of steam power plants. But as with anything ever written the ideas shown have nurtured for a long time. Parts of these chapters have appeared elsewhere as individual papers or work documents. One of the most helpful episodes have been presentations and discussions during Pohto Operator training seminars. Input from those sessions can be seen in chapter firing. You who run recovery boilers, I salute you.

The purpose of this text is to give the reader an overview of recovery boiler operation. Most parts of the recovery boiler operation are common to boilers burning other fuels. The furnace operation differs significantly from operation of other boiler furnaces. Oxygen rich atmosphere is needed to burn fuel efficiently. But the main function of recovery boiler is to reduce spent cooking chemicals. Reduction reactions happen best in oxygen deficient atmosphere. This dual, conflicting nature of recovery furnace makes understanding it so challenging.

To understand the processes happening in the recovery furnace one must try to understand the detailed processes that might occur and their limitations. Therefore chapters on materials, corrosion and fouling have been added.

Many thanks to Marja and Ari Heinola, who not only read through the manuscript, but provided many valuable comments. The book greatly benefited from drawings, illustrations and other material given by Esa Vihavainen and Kari Haaga. As always all the errors, omissions and incomprehensible ideas are solely my own fault.

Helsinki, 25.3.2005

About the author

Esa Vakkilainen is a graduate of Lappeenranta University. He made his M.Sc., Licentiate and Ph. D. there. He concluded his graduate studies by enrolling to Institute of Paper Science and Technology in Atlanta, USA. Esa Vakkilainen started his professional career in Lappeenranta University as an assistant professor (yliassistentti) of Power plants teaching and researching furnace heat transfer, optimization of combined cycle processes, district heating (a Finnish specialty) and combustion of biofuels.

After four years of academics Esa Vakkilainen joined A. Ahlström Corporation and started working at their Varkaus Boiler works. He was responsible for developing a new generation of dimensioning programs for steam generator thermal design. It was time of extensive development as circulating fluidized beds were making their way to the mainstream of steam power plants. After several changes of ownership these boilers are now part of the Foster Wheeler Corporation.

In 1989 Esa Vakkilainen found himself involved with kraft recovery boilers, his destiny for the next 15 years. The years with A. Ahlström Corporation, then Ahlstrom Machinery were spent with various technical aspects of kraft recovery boilers. Main interests have been fouling of heat transfer surfaces, liquor spraying, air distribution and black liquor combustion. He has extensive list of publications in these areas.

In 2001 Esa Vakkilainen was employed by Jaakko Pöyry Oy, international consultants to pulp and paper. He has been involved with majority of recent worldwide recovery boiler purchases.

Esa Vakkilainen is currently an associate professor (dosentti) in Lappenranta University and Helsinki University of Technology. He has directed over 20 M. Sc. and 3 Ph. D. theses. Esa Vakkilainen has lectured of recovery boilers in technical conferences at all major continents. He was the technical chairman for the 2004 International Chemical Recovery Conference.

Contents

Nomenclature

A	surface area, m^2
A_d	droplet surface area, m^2
a_d	dust emission coefficient, -
B_d	dust loading, kg/m^3
b	correction coefficient, -
C	heat capacity, W/K
c_p	specific heat capacity, kJ/kgK
D_p	particle diameter, m
d	diameter, m
d_o	outside tube diameter, m
d_s	inside tube diameter, m
f	correction factor for heat transfer, -
f_n	form correction
f_o	overall correction (fouling correction, etc.)
G	conductance, W/K
h	convective heat transfer coefficient, W/m^2K
k	heat transfer coefficient, W/m^2K
k_c	convective heat transfer coefficient
k_i	inside heat transfer coefficient referred to the outside surface
k_o	outside heat transfer coefficient
k_r	radiative heat transfer coefficient
k_{ex}	external heat transfer arranged to represent a heat transfer coefficient
L	length, m
l	heat of vaporization, kJ/kg stopping distance, m
n	number of, -
m_w	mass of water in droplet, kg
m_o	mass of pyrolysable material in droplet, kg
Pr	Prandtl number based on gas phase, -
p	pressure, bar abs
p_x	partial pressure of substance x, bar
Q	heat flow, J
q_m	mass flow, kg/s
Re_d	Reynolds number based on droplet diameter and relative speed, -
R	ratio of steam side heat capacity to gas side heat capacity, -
r	radius, m
s	radiation beam length, m, tube wall thickness, m
S_l	longitudinal pitch, m
S_t	transverse pitch, m
s_l	dimensionless longitudinal pitch, -
s_t	dimensionless transverse pitch, -
T	temperature, K or ^oC
T_g	gas temperature, K
T_d	droplet temperature, K
U	free stream velocity, m/s
w	flow velocity, m/s
X	fraction, -
x	dry solids, -
z	number of transfer units, -

Δ	difference, -
ΔT	temperature difference, K or ^oC
$\Delta\varepsilon_g$	overlapping correction for emissivity, -
$\Delta\alpha_g$	overlapping correction for absorptivity, -
Φ	heat flow, W
α_d	absorption coefficient of dust, -
α_{dg}	absorptivity of the dusty gas, -
ε	ratio of gas temperature drop to total temperature difference, -, emissivity, -
ε_{dg}	emissivity of the dusty gas, -
ε_α	background emissivity, -
ε_w	emissivity of the wall, -
ζ	loss coefficient, -
η	viscosity, Pas, efficiency, -
θ	total temperature difference, ^oC
λ	heat conductivity, W/m^oC
ξ	friction factor, -
ρ	density, kg/m^3
σ	Stefan Bolzman coefficient, W/m^2K^4
τ	particle relaxation time, s

1 Principles of kraft recovery

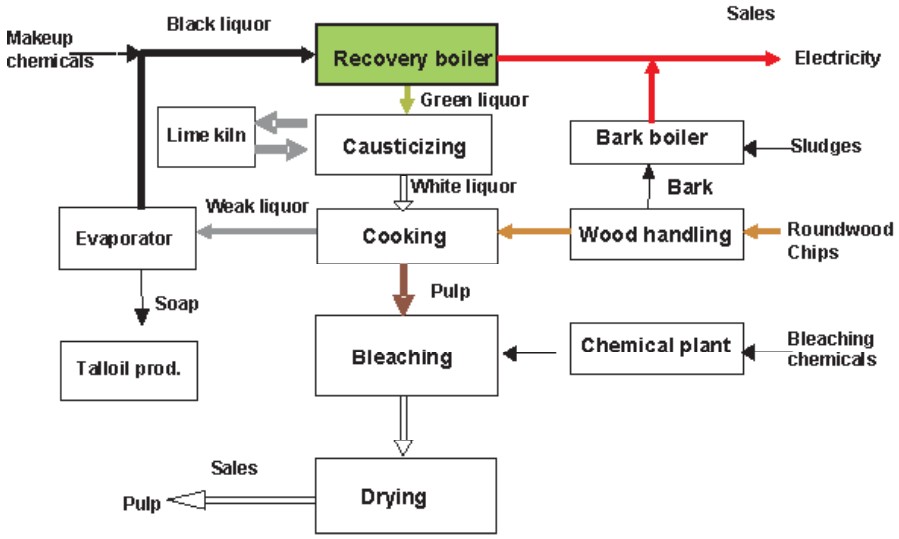

Figure 1-1, Kraft mill unit operations.

Spent cooking chemicals and dissolved organics are separated from pulp during washing. This black, alkaline liquor was at first dumped. Various chemical recovery systems were then developed (Niemelä, 2004), but it was in the 1930's and 40's when modern type of regeneration of spent liquor was widely adopted. New type of equipment increased line size and led to more favorable economic situation.

Recovery of black liquor has other advantages. Concentrated black liquor can, when burnt, produce energy for generation of steam and electricity. In the most modern pulp mills, this energy is more than sufficient to cover all internal use, The principal kraft recovery unit operations are, Figure 1-1, evaporation of black liquor, combustion of black liquor in recovery boiler furnace including of formation of sodium sulfide and sodium carbonate, causticizing of sodium carbonate to sodium hydroxide and regeneration of lime mud in lime kiln.

There are other minor operations to ensure continuous operation of recovery cycle. Soap in the black liquor can be removed and tall oil produced. Control of sodium - sulfate balance is done by addition of makeup chemicals such as sodium sulfate to mix tank or removal of recovery boiler ash. Dumping of recovery boiler ash removes mostly sodium and sulfur, but serves as an important purge for chloride and potassium. Buildup of non process elements is prevented by disposal of dregs and grits at causticizing. Malodorous non condensable gases are processed by combustion at recovery boiler or lime kiln. In some modern and closed mills chloride and potassium removal processes are employed. With additional closure new internal chemical manufacturing methods are sometimes applied.

1.1 FUNCTION OF RECOVERY BOILER

Concentrated black liquor contains organic dissolved wood residue in addition of cooking chemicals. Combustion of the organic portion of chemicals produces heat. In the recovery boiler heat is used to produce high pressure steam,

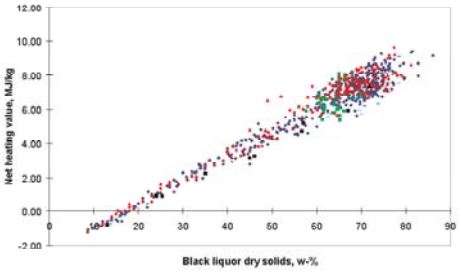

Figure 1-2, Net heating value of typical kraft liquor at various dry solid content.

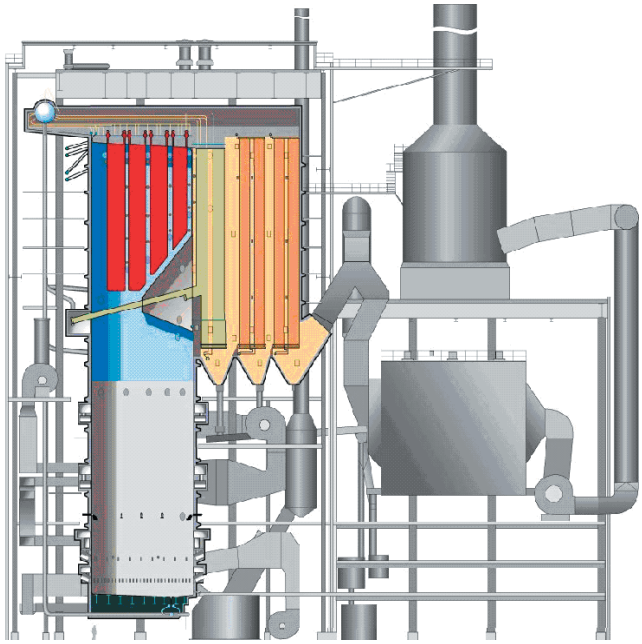

Figure 1-3, One of the latest recovery boilers, Gruvö from Kvaerner.

which is used to generate electricity in a turbine. The turbine exhaust, low pressure steam is used for process heating. Medium pressure extraction steam from between turbine stages is used in cooking, sootblowing and high solids evaporation.

Combustion in the recovery boiler furnace needs to be controlled carefully. High level of sulfur in the black liquor requires optimum process conditions to avoid production of sulfur dioxide and reduced sulfur gases emissions. In addition to environmentally clean combustion, reduction of inorganic sulfur must be achieved in the char bed.

The recovery boiler process has several unit processes
1. Combustion of organic material in black liquor to generate steam
2. Reduction of inorganic sulfur compounds to sodium sulfide
3. Production of molten inorganic flow of mainly sodium carbonate and sodium sulfide and dissolution of said flow to weak white liquor to produce green liquor
4. Recovery of inorganic dust from flue gas to save chemicals
5. Production of sodium fume to capture combustion residue of released sulfur compounds

1.2 EARLY RECOVERY TECHNOLOGY

Early recovery technology concentrated on chemical recovery (Deeley and Kirkby, 1967). Chemicals cost money and it was easy to discover that recycling these chemicals would improve the profitability of pulp manufacture.

Recovery of pulping chemicals could be based to French chemist Nicholas LeBlanc's process for producing soda at reducing furnace. A flame oven was hand filled with black liquor, Figure 1-4. Then the black liquor was dried with flue gases from burning wood. The dried black liquor was then scraped to floor, collected and sent to separate

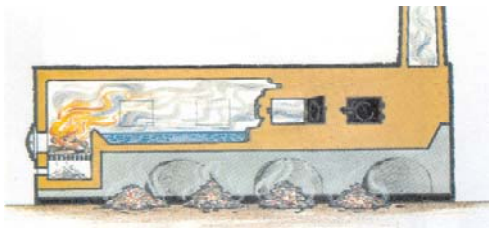

Figure 1-4, Early flame oven from late 1800 (Edling, 1981).

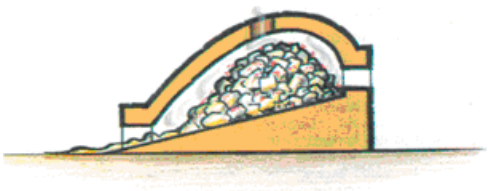

Figure 1-5, Early smelt pot from late 1800 (Edling, 1981).

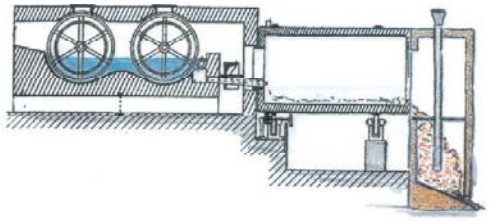

Figure 1-6, Rotating oven from 1890, liquor in at 20 % ds (Edling, 1981).

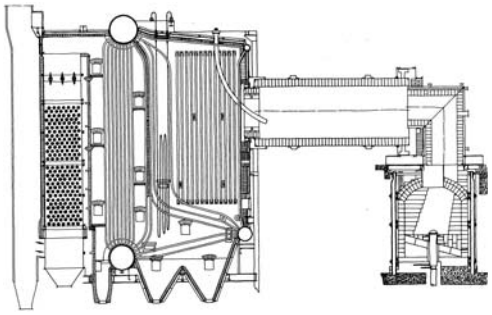

Figure 1-7, Early Tampella rotary furnace from about 1925 (Tampella).

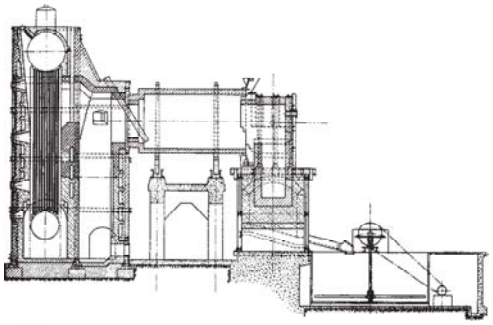

Figure 1-8, Early S-S rotary furnace from about 1945 (Vannerus et al., 1948).

smelt pot, Figure 1-5, for reduction and burning the remaining organics (Rydholm, 1965). Recovery of chemicals with this type of system was inefficient. Chemicals recovery hardly exceeded 60 % (Whitney, 1968).

Hand operated recovery grew more complicated with additional heat recovery surfaces. Pre-evaporation and scrubbing in a rotary device was invented by Adolph W. Waern (Combustion Engineering, 1949). The direct contact evaporator improved the heat economy of the recovery system. The hand feeding operation was soon replaced by rotative oven, Figure 1-6.

Use of rotary oven improved the heat economy. Then it was a small step to introduce heat recovery equipment as was done with other types of boilers at that time. In 1912 the S-S system (Sundblad-Sandberg) was taken online at Skutskär. In it liquor was sprayed into rotary furnace at 50 % ds. The evaporation took place in a four stage evaporator. The heat was recovered with vertical tube boiler.

Tampella was among the first manufacturers to build S-S type furnaces, Figure 1-7. Preventing unnecessary air flow through sealing arrangement between rotary drum and fixed parts was one of the major operating problems. The combustion was often conducted at very high air ratio leading to inefficient energy use. One could generate 3000 … 4000 kg of 3.0 MPa steam for each ton of pulp (Roschier, 1952).

The main recovery equipment itself remained unchanged, but details were improved on. Smelt dissolving tank was introduced, final smelting was improved on and capacities grew, Figure 1-8. The use of refractory and rotative oven tended to limit the recovery capacity to 70 … 75 tds/d (Sebbas *et al.*, 1983). Rotary part lengths were 7 … 10 m and diameter about 1.5 m (Swatrz and MacDonald, 1962).

The boilers parts were improved on. In 1930s even LaMont type forced circulation units were built, Figure 1-9. The use of rotary furnaces pinnacled in Murray-Waern type units which were successfully built around the world. In these the rotary precombustion was combined with totally water-cooled furnace with lower part refractory lined. The Murray-Waern recovery units were popular until the fifties.
An epitome of inventivness of that age was the Godell recovery unit at Stevens Point Wise in 1940's. There the liquor was completely dried in a chamber after the boiler (Edling 1983). But that

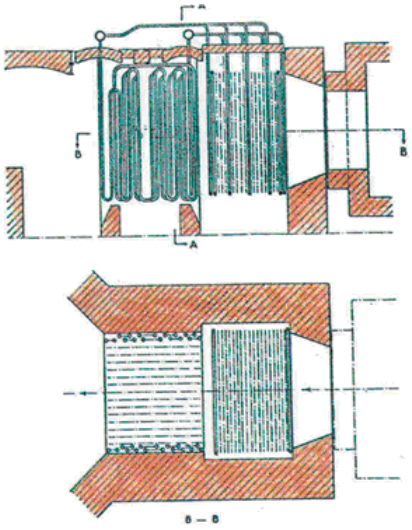

Figure 1-9, LaMont type construction used in Kotka, Moss and Frantsach ~1930 (Edling, 1981).

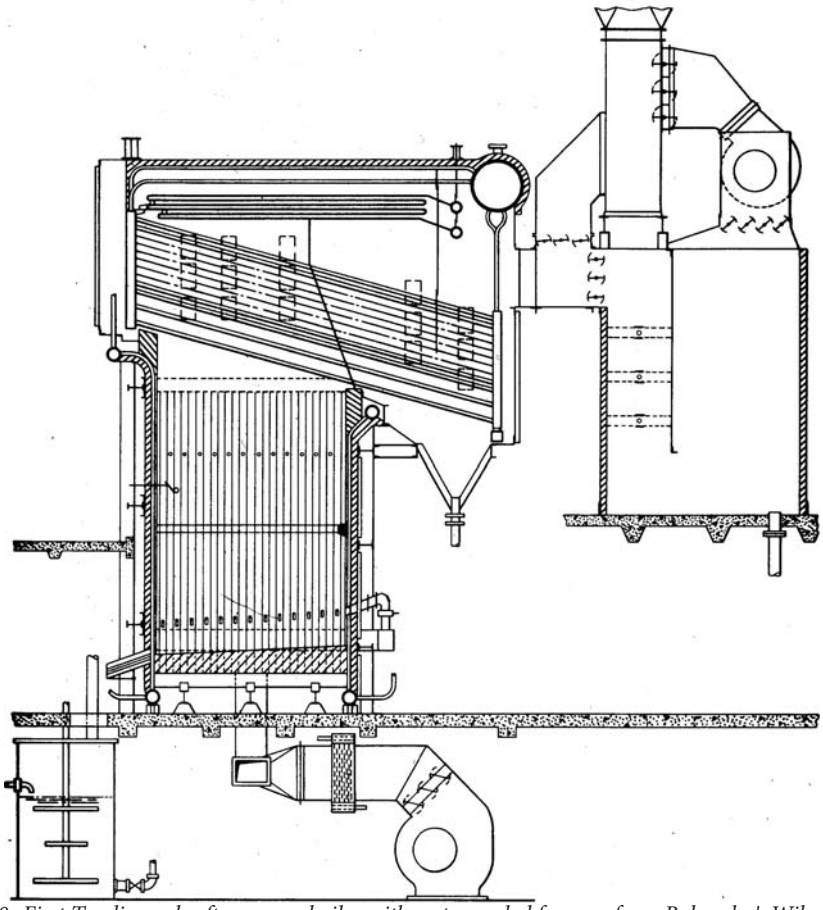

Figure 1-10, First Tomlinson kraft recovery boiler with water cooled furnace from Babcock & Wilcox in 1934 (Steam, 1992). Note spray tower using weak black liquor before the ID fan.

unit and most of those other alternative systems were hard to operate and did not achieve high availability.

1.3 FIRST RECOVERY BOILERS

The modern recovery boiler has a few strong ideas that have remained unchanged until today. It was the first recovery equipment type where all processes occurred in a single vessel. The drying, combustion and subsequent reactions of black liquor all occur inside a cooled furnace. This is the main idea in Tomlinson's work.

Secondly the combustion is aided by spraying the black liquor into small droplets. Controlling process by directing spray proved easy. Spraying was used in early rotary furnaces and with some success adapted to stationary furnace by H. K. Moore. Thirdly one can control the char bed by having primary air level at char bed surface and more levels above. Multiple level air system was introduced by C. L. Wagner.

Recovery boiler also improved the smelt removal. It is removed directly from the furnace through smelt spouts into a dissolving tank. Some of the first recovery units employed the use of Cottrell's electrostatic precipitator for dust recovery.

Babcock & Wilcox was founded in 1867 and gained early fame with its water tube boilers. It built and put into service the first black liquor recovery boiler in the world in 1929 (Steam, 1992). This was soon followed by a unit with completely water cooled furnace at Windsor Mills in 1934. After reverberatory and rotating furnaces the recovery boiler was on its way (Jones, 2004).

The second early pioneer, Combustion Engineering based its recovery boiler design on the pioneering work of William M. Cary, who in 1926 designed three furnaces to operate with direct liquor spraying and on work by Adolph W. Waern and his recovery units.

The first CE recovery unit, Figure 1-11, looks a lot like a modern recovery boiler. Note direct contact evaporator on the left, cooled floor tubes and

three drum construction.

Recovery boiler were soon licensed and produced in Scandinavia and Japan. These boilers were built by local manufacturers from drawings and with instructions from licensors. One of the early Scandinavian Tomlinson units employed a 8.0 m high furnace that had 2,8*4,1 m furnace bottom which expanded to 4,0*4,1 m at superheater entrance (Pettersson, 1983). This unit stopped production for every weekend. In the beginning economizers had to be water washed twice every day, but after installation of shot sootblowing in the late 1940s the economizers could be cleaned at the regular weekend stop.

The construction utilized was very successful. One of the early Scandinavian boilers 160 t/day at Korsnäs, Figure 1-12, operated still almost 50 years later (Sanquist, 1987). Edling states in 1937 that more than 20 units had already been built of which 10 in Scandinavia.

1.4 DEVELOPMENT OF RECOVERY BOILER TECHNOLOGY

Spread of kraft recovery boilers was fast as functioning chemical recovery gave kraft pulping an economic edge over sulfite pulping (Boniface, 1985). They had about 20 % better energy efficiency as more than 5000 kg of 3.0 MPa steam for each ton of pulp could be generated (Roschier, 1952, Alava, 1955). The first recovery boilers had horizontal evaporator surface followed with superheaters and more evaporation, Figure 1-13. These boilers resembled the state-of-the-art boilers of some 30 years earlier. This trend has continued until today. It is easy to understand that when any stop will cost a lot of money the adopted technology tends to be conservative. Conservatism meant that e.g. the new Oulu Oy, 100 000 t/a sulphate mill installed four Tomlinson boilers when it started operating in 1937 (Oulu, 1937).

The first recovery boilers had severe problems with fouling (Deeley and Kirkby, 1967, Roschier, 1952). Tube spacing wide enough for normal operation of a coal fired boiler had to be wider for recovery boilers. This gave satisfactory performance of about a week before a water wash. Mechanical steam operated sootblowers were also quickly adopted, Figure 1-13. To control chemical losses and lower the cost of purchased chemicals electrostatic precipitators were added. Lowering dust losses in flue gases has more than 60 years of practice.

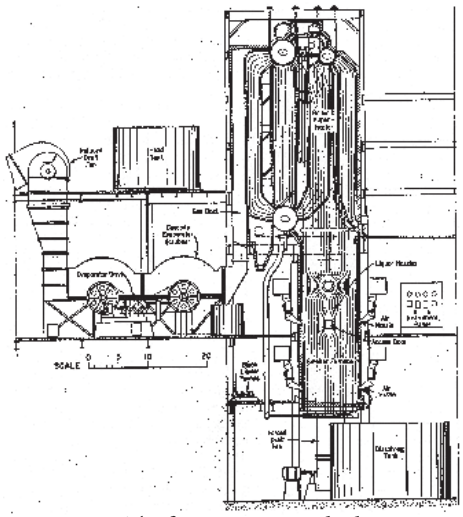

Figure 1-11, The first CE recovery boiler 1938 (Combustion Engineering, 1949).

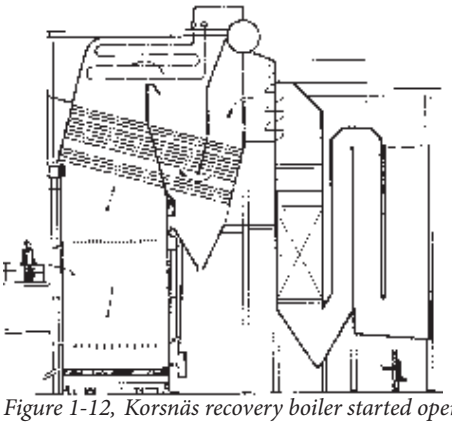

Figure 1-12, Korsnäs recovery boiler started operation in 1943 (Götaverken).

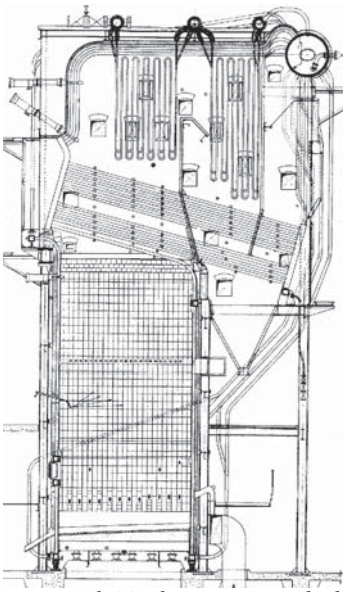

Figure 1-13, Early Tomlinson recovery boiler (Vannérus et al., 1948).

One should also note square headers in the 1940 recovery boiler (Vannérus *et al*., 1948), Figure 1-13.

The air levels in recovery boilers soon standardized to two. The primary air level was placed at the char bed level and the secondary above the liquor guns.

In the first tens of years the furnace lining was often of refractory brick or refractory on cast blocks. The flow of smelt on the walls causes extensive replacement and soon designs that eliminated the use of refractory were developed. The standard then became the tangent furnace wall. Membrane wall use became widespread in the 60's.

B&W-design

B&W favored use typically a single black liquor gun at front wall. In larger units additional gun was placed on back wall (Tomlinson and Richter, 1969). They preferred a significant part of the liquor to be sprayed to walls for drying. Boiler bottom was in angle causing smelt to flow quickly out. Hardly any space was reserved for smelt layer in the furnace. Thus this kind of furnace is named sloping bottom type.

Final black liquor evaporation was often carried in a direct contact evaporator of venturi scrubber or cyclone evaporator type. The highest practical black liquor solids was 60 … 65 % depending on black liquor properties. Use of wall spraying was promoted by B&W and its licensees Götaverken and Babcock Hitachi. B&W adopted three level air in the late 1960s.

CE-design

Early on the CE design stressed use of multiple guns in all walls (Tomlinson and Richter, 1969). Boiler bottom was flat with space for smelt layer on top of the whole floor. Thus this kind of furnace is named decanting floor type. Final black liquor evaporation was carried in a direct contact evaporator of cascade evaporator type.

The basic aims of recovery boiler design could soon be summarized as; highest possible recovery of chemicals, high efficiency, high utilization of the calorific values in black liquor and highest safety of operation (Hochmuth, 1953).

CE sticked for a long time with a two level air system that had corned fired secondary. They used similar system in PCF-boilers.

Single drum design

There are some early examples of single drum recovery boilers. Both B&W and Ahlstrom delivered a single drum boiler in the late 1950's. The first modern single drum recovery boiler was delivered in 1984 by Götaverken to Leaf River at Hattiesburg, Mississippi. The boiler size was 1966 tds/d. By 1990 all manufacturers started providing single drum boilers. Excluding very small boilers, all modern boilers are now of single drum design.

There are several advantages in a single drum boiler. Single drum construction eliminates the possibility of water leakage to furnace as it is placed outside the furnace. There are significantly less holes in a drum wall. Therefore it can be built thinner. Thinner wall of drum allows faster start up and stop-down. The gas flow to the boiler bank is smoother and heating surface arrangement is simple. The erection period is shorter because of large block construction. There is no rolled tube work. Enhanced and steady water circulation by separated and unheated downcomers.

The largest advantage is that single drum boilers can be made larger. Tube stiffness limits cross flow two drum arrangement to about 2300 tds/d size (Steam, 1992). Vertical flow two drum constructions have suffered from plugging because of vibration stiffeners.

Furnace protection

First recovery units had brick lined lower furnace with straight tubes forming cooling section behind bricks. This design persisted until the 1960s. Some of these units are still operating today. Another design provided corrosion protection of furnace tubes with studs and refractory. Some manufacturers use studs even today, but need of stud replacement has led to decline of stud use. From late fifties onwards the membrane wall design took over, first with carbon steel walls. Tangent tube design was replaced with membrane design. The drawbacks of tangent design were the difficulties in inspecting welds and doing maintenance work

First furnace walls were of carbon steel. With increasing design pressure there were several corrosion problems in lower furnace. The advantage of chrome containing alloys as wall corrosion inhibitor was discovered as an answer to high pressure boiler sulfidation corrosion (Moberg, 1974). In 1972 Tampella delivered first totally compound tube recovery boiler furnace to ASSI Lövholmen mill in Piteå, Sweden. By 1982 there were 30 recovery boilers with 304 compound tube

bottoms in Scandinavia (Westerberg, 1983). Use of composite tubing in United States started only in 1981.

Sanicro 38 is a widespread material that offers improved corrosion protection for lower furnace. The first lower furnace made from Sanicro 38 was delivered by Kvaerner. They used Sanicro 38 in the lower furnace up to primary ports in 1994 for their Rauma recovery boiler.

Economizer

Earlier the recovery boilers had horizontal tube economizers. They plugged fast and had to be water washed at intervals of 1- 4 weeks (Rissanen, 1965). It was not until the early 1960 that installing vertical economizers started. In economizers of vertical flow design the gas flows downwards and water counter currently upwards (Hyöty, 1994). In a period of few years the current long flow economizer design emerged, Figure 1-14 (Moberg, 1967). Vertical economizer design spread fast in Scandinavia where by mid 1970's more than half of the recovery boilers had long flow economizers without direct contact evaporator (Environmental, 1976).

In competition to purely vertical, the three pass design featured gas flow which was forced crosswise the economizer tubes to improve heat transfer.

There have been several rounds of economizer header designs. In a typical old design each economizer tube is connected to a common large header. As maximum number of tube rows that fit to this type header is about 8 … 10. The larger economizers must have front and back headers. This design has the disadvantage of having a header in the gas flow. The header can corrode and the welded joints tend to receive thermal stress. Modern economizers have flat horizontal headers.

1.5 HIGH DRY SOLIDS

Dry solids at as fired black liquor was between 60 and 65 % in Sweden at the beginning of the 1960's (Jönsson, 1961). In the beginning of 1950's the typical as fired black liquor concentration was 50 % (Vegeby, 1961). The final concentration was often done with cascade or cyclone evaporator. In practice the as fired dry solids could remain dangerously low before refractometers started to be applied in late 1960s and early 1970s (Hellström, 1970). The only reasons seen for higher dry solids were the energy economy and increase of bottom

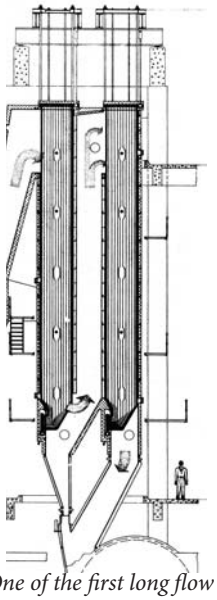

Figure 1-14, One of the first long flow economizers, Sunila (Moberg, 1967).

loading (Vegeby, 1961). One advantage noted was that partial load capability improved with higher dry solids. Increasing black liquor dry solids from 60 % to 68 % enabled running recovery boiler without auxiliary fuel firing at 65 % of rated MCR (Rissanen, 1965). At 60 % dry solids hardly any partial load could be run.

In 1980's the first high dry solids units started coming on line. Extensive tests of effect of increasing dry solids from 72 % to 84 % were run at Metsä-Botnia Kemi and Rosenlew, Pori, Finland recovery boilers (Hyöty and Ojala, 1987). They noticed that above 75 % dry solids the SO_2 and H_2S emissions were practically zero. Also reduction increased more than one percentage point. Other benefits listed were steam generation increase and boiler controllability increase. High dry solids require that ESP ash is mixed to the black liquor with 62 … 65 % liquor. Higher retention time also improves the stability of resulting black liquor.

1.6 IMPROVING AIR SYSTEMS

Air system development continues and has been continuing as long as recovery boilers existed (Vakkilainen, 1996). As soon as the target set for the air system has been met other new targets are given. Currently the new air systems have achieved low NOx, but are still working on with lowering fouling.

The first generation air system in the 1940's and 1950's consisted of a two level arrangement; pri-

Table 1-1, *Development of air systems (Vakkilainen, 1996).*

Air system	Main target	But also should
1st generation		Stable burning of black liquor
2nd generation	high reduction	Burn liquor
3rd generation	decrease sulfur emissions	Burn black liquor, high reduction
4th generation	low NOx	Burn black liquor, high reduction and low sulfur emission
5th generation	decrease superheater and boiler bank fouling	Burn black liquor, high reduction, low emissions

mary air for maintaining reduction zone and secondary air below the liquor guns for final oxidation (Llinares and Chapman, 1989). The recovery boiler size was 100 … 300 tds/d and black liquor concentration 45 … 55 %. Frequently to sustain combustion auxiliary fuel needed to be fired. Primary air was 60 … 70 % of total air with secondary the rest. In all levels openings were small and design velocities were 40 … 45 m/s. Both air levels were operated at 150 °C. Liquor gun or guns were oscillating. Main problems were high carryover, plugging and low reduction. But the main target, burning of black liquor could be done.

The second generation air system targeted high reduction. In 1954 CE moved their secondary air from about 1 m below the liquor guns to about 2 m above them (Llinares and Chapman, 1989). The air ratios and temperatures remained the same, but to increase mixing 50 m/s secondary air velocities were used.

CE changed their frontwall/backwall secondary to tangential firing at that time. In tangential air system the air nozzles are in the furnace corners. The preferred method is to create a swirl of almost the total furnace width. In large units the swirl caused left and right imbalance. This kind of air system with increased dry solids managed to increase lower furnace temperatures and achieve reasonable reduction. B&W had already adopted the three level air by then, Figure 1-15.

At first the air port openings were made by bending one tube away from the opening sideways and making room for this by bending another tube back, Figure 1-16. Airport width was about tube spacing and large plate areas were needed to make airport gas tight. In 1978 CE began experimenting with two level primary air. Upper primary was designed to about 20 % of total air with velocity up to 60 m/s. Total air split remained the same. The aim was to increase hearth temperatures.

Third generation air system was the three level air. In Europe the use of three level air with primary and secondary below the liquor guns started about 1980. At the same time stationary firing gained

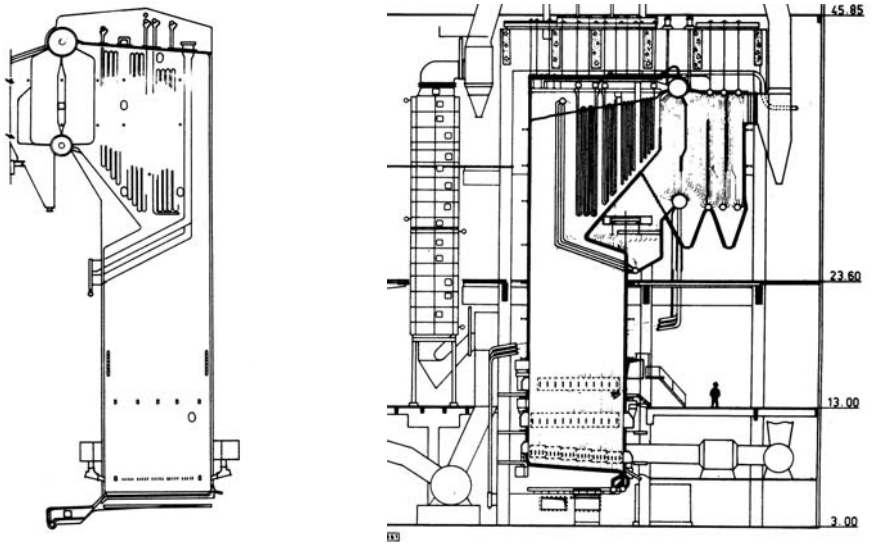

Figure 1-15, Typical two level air CE, left and three level air BW, right from early 1960 (Roos, 1963).

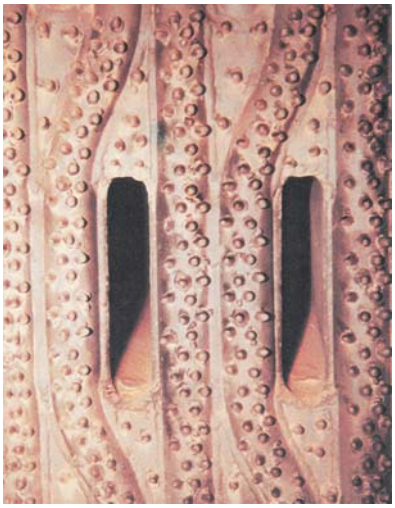

Figure 1-16, Typical air port from 1960's (Soodakattiloiden, 1968).

ground. Use of about 50 % secondary seemed to give hot and stable lower furnace (Westerberg, 1983). Higher black liquor solids 65 … 70 % started to be in use. Hotter lower furnace and improved reduction were reported. With three level air and higher dry solids the sulfur emissions could be kept in place.

Fourth generation air systems are the multilevel air and the vertical air. As black liquor dry solids to the recovery boiler have increased, achieving low sulfur emissions is not anymore the target of the air system. Instead low NOx and low carryover are the new targets.

Multilevel air

The three level air system was a significant improvement, but better results were required. Use of CFD models offered a new insight of air system workings. The first to develop a new air system was Kvaerner (Tampella) with their 1990 multilevel secondary air in Kemi, Finland, which was later adapted to a string of large recovery boilers (Mannola and Burel, 1995).

Kvaerner also patented the four level air system, where additional air level is added above the tertiary air level. This enables significant NOx reduction.

Vertical air

In vertical air primary is arranged conventionally. Rest of the air ports are placed on interlacing 2/3 or 3/4 arrangement, Figure 1-17. Vertical air was invented by Erik Uppstu (1995). His idea is to turn

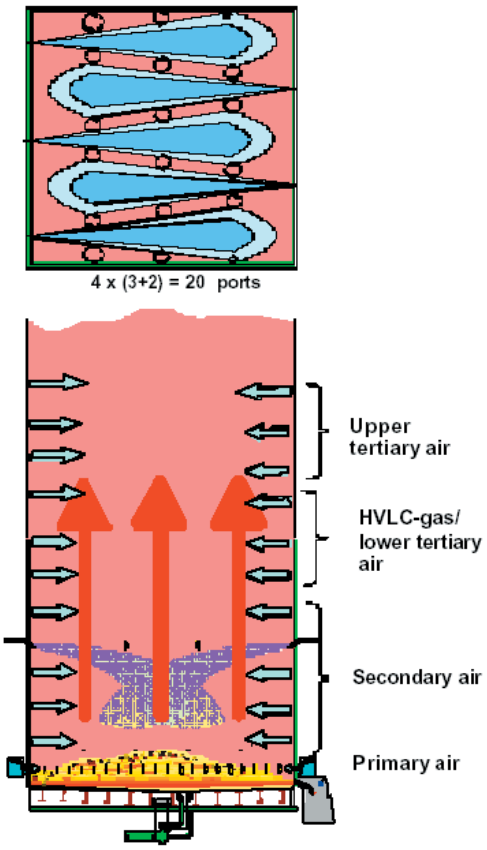

Figure 1-17, Principle of vertical air (Kaila and Saviharju, 2003.

traditional vertical mixing to horizontal mixing. Closely spaced jets will form a flat plane. In traditional boilers this plane has been formed by secondary air. By placing the planes to 2/3 or 3/4 arrangement improved mixing results. Vertical air has a potential to reduce NOx as staging air helps in decreasing emissions (Forssén *et al.*, 2000b).

1.7 HIGH TEMPERATURE AND PRESSURE RECOVERY BOILER

Development of recovery boiler main steam pressure and temperature was rapid at the beginning, Figure 1-18. By 1955, not even 20 years from birth of recovery boiler highest steam pressures were 10.0 MPa and 480 °C (Vakkilainen *et al.*, 2004). The typical pressures and temperatures then backed downward somewhat due to safety (McCarthy, 1968). By 1980 there were about 700 recovery boilers in the world (Westerbeg, 1983). In Japan, because of high electricity prices, more than ten high temperature and pressure recovery boilers are in use (Tsuchiya *et al.*, 2002). The biggest one is the 2700 tds/d, 10.3 MPa and 505 °C

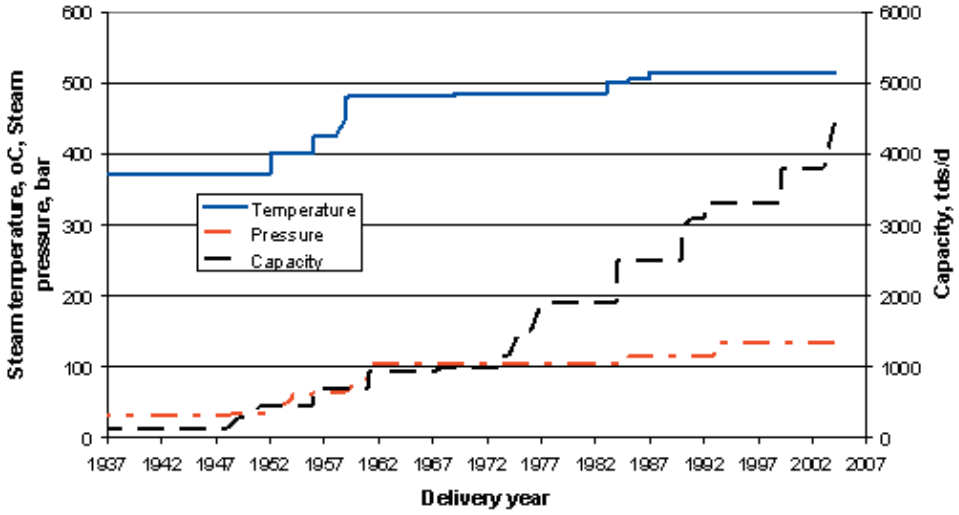

Figure 1-18, Development of recovery boiler pressure, temperature and capacity.

recovery boiler at Iwakuni mill (Ohtomo, 2000).

New large recovery boilers seem to favor high main steam temperatures and pressures (Vakkilainen, 2004). These increase the amount of back pressure electricity.

1.8 GASIFICATION

Gasification provides a way to convert solid fuel into gaseous. Energy conversion always involves exergy and energy losses. Gaseous fuel enables use of combined cycle power generation, where both gas turbine and steam process produce electricity. This increases energy efficiency (Demirbaş, 2001, Consonni *et al.*, 2003). Higher yield of biofuel based electricity fits with national and international targets and reduces production of fossil CO_2 (Raymond, 2003). More efficient process must be pursued also to offset higher unit cost of gasification (per ton of mass production). One way to increase electricity production is to perform gasification under pressure. Another is to use oxygen gasification instead of air gasification (Donovan and Brown, 2003). An overview of potential process improvements has been presented by McKeough (2003).

Production of extra electricity and high unit cost of recovery boiler are the main driving forces for the development of gasification. From energy efficiency standpoint the recovery boiler has several weaknesses; the main steam temperature and pressure are low, the energy in smelt is not recov-

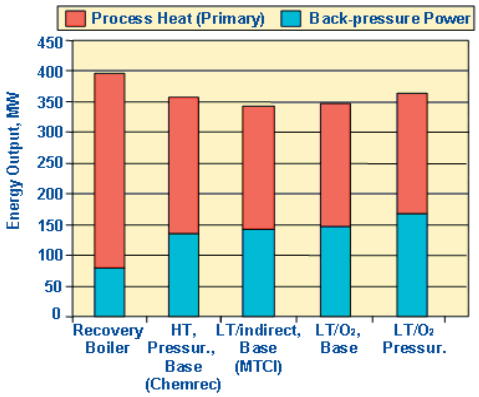

Figure 1 19, Estimated net power and heat outputs from recovery boiler and gasification of black liquor, Pulp production 600 000 ADt/a (McKeough, 2004).

Table 1-2, *Effectiveness of converting black liquor HHV into fuel value in net product gas (Grace and Timmer, 1995).*

Original HHV, MJ/kgbl	14.7	13.3
	HHV in net gas, % of original	HHV in net gas, % of original
Commercial		
Chemrec	55.9	50.7
StoneChem TCI)	49.0	42.6
Piloted processes		
ABB	70.4	66.6
Tampella	60.7	55.9
Conventional RB	61.1	58.6

ered and combustion temperature is only moderate. Dealing with reductive/oxidative process, rare feature of smelt water explosion and corrosive process media cause high unit costs and require extra safety features. The modern recovery boiler has a very good record for environmental cleanness. In spite of this improvements are in need.

The two main process alternatives for black liquor gasification are high temperature gasification and low temperature gasification (Backman *et al*., 1993, Warnqvist *et al*., 2000, Whitty and Verrill, 2004). In low temperature gasification, the black liquor is kept below the melting point of ash. This temperature usually corresponds to significantly less than 700 °C. Heat to low temperature gasification can be supplied either directly or indirectly. A typical process problem in low temperature gasification pilot plants has been plugging due to sintering. At low temperature the pyrolysis phase is still relatively fast, but char gasification requires considerable time.

In high temperature gasification the reaction temperature is at about 1000 °C or higher. High temperature gasification is fast but means of dealing with molten smelt and protection from corrosive athmosphere need to be developed. Both gasification processes require flue gas cleaning to reduce sulfur and sodium emissions. There is less sulfur release but more alkali release in the high temperature gasification process (Berglin and Berntsson, 1998).

In gasification higher steam temperature and pressure could be used if the product gas is cleaned. A part of the energy in smelt can be recovered if dissolving is done under pressure. Still higher combustion temperatures can be achieved with oxygen gasification.

Gasification research has been done by all leading recovery boiler manufacturers. There have been several key issues in the development. Energy conversion causes always extra losses. Processes have tended to go for multiple heat exchangers and recuperators to increase efficiency. It is very costly and technically difficult to clean gases to required cleanliness for gas turbine. Quench needs to be applied. So far all commercial processes lack behind the energy efficiency of conventional recovery boiler, Table 1-2 and Figure 1-19.

Main technical obstacles in the low temperature gasification (e.g. Thermochem) have been achieving high enough carbon conversion and keeping the gasifier from plugging. The main factors which lower the overall efficiency of current processes include; use of air in place of O_2 as gasification medium, operation of gasifier at atmospheric pressure, application of quench cooling and high steam content in gas from gasifier (McKeough, 2004).

The practical gasification process is still a long way of becoming a commercially attractive solution (Hood and Henningsen, 2002). Industry visions of early nineties that black liquor gasification could within next ten years become a viable alternative have not materialized. Even though there are significant gains to be made, there still remain a lot of unresolved issues; finding materials that survive in a gasifier, mitigating increased causticizing load and how to make startup and shutdown (Tucker, 2002).

1.9 ALTERNATIVE RECOVERY

There are other processes developed to replace conventional evaporator, recovery boiler, causticizing, lime kiln process. One driving force is the relative inefficiency of the recovery boiler. Even though the recovery boiler compares well with modern power production it is still the greatest entropy producing unit process in the kraft mill (Richards, 2001).

$$Na_2CO_3 + Fe_2O_3 \rightarrow Na_2Fe_2O_4 + CO_2 \qquad 1\text{-}1$$
$$Na_2Fe_2O_4 + H_2O \rightarrow 2NaOH + Fe_2O \qquad 1\text{-}2$$

Most of the proposed new processes involve a number of new stages. This means that much experimenting and heavy investment is needed. Maybe this is why there are only a few alternative processes that have evolved to the mill scale.

Direct alkali recovery

Australian Paper has employed a process where liquor from soda pulping is processed in fluidized bed with ferric oxide (Scott-Young and Cukier, 1995). The product, sodium ferrite is dissolved in water. Sodium hydroxide and iron oxide are formed. The mill achieved several years of operation before it shut down due to uneconomical size of the mill.

A mill in Denmark used straw to make pulp for various applications using direct alkali recovery with ferric oxide. In spite of the partially successful recovery operation the mill closed down because of economical reasons.

The development of direct alkali recovery system (DARS) process is slow because the use of fluidized bed and subsequent pelletizing and leaching operations are new for typical pulp mill personnel.

DARS has about 10 % lower thermal efficiency than recovery boiler (Maddern, 1988). This is due to extra heat in sodium iron leaving furnace and higher amount of water in incoming liquor per unit of virgin black liquor. This may be large enough penalty to offset the savings when lime kiln is not needed.

Other much studied component has been titanium dioxide (Kiiskilä, 1979 and Richards, 2001).

Autocausticization

In autocausticization an additional component is added to the liquor. This component needs to react with sodium hydroxide at furnace and dissolve back at green liquor. One such chemical is sodium borate discovered by Janson (1978) and recently studied by Tran *et al*., (2001).

$$Na_2CO_3 + NaBO_2 \rightarrow Na_3BO_3 + CO_2 \qquad 1\text{-}3$$

$$Na_3BO_3 + H_2O \rightarrow 2NaOH + NaBO_2 \qquad 1\text{-}4$$

2 Recovery boiler design

Figure 2-1, Typical recovery boiler in operation, Gruvön (Wallén et al., 2002).

In a pulp mill recovery boiler fulfills three main functions. The first is to burn the organic material in the black liquor to generate high pressure steam. The second is to recycle and regenerate spent chemicals in black liquor. The third is to minimize discharges from several waste streams in an environmentally friendly way. In a recovery boiler, concentrated black liquor is burned in the furnace and at the same time reduced inorganic chemicals emerge molten. A modern recovery boiler, Figure 2-1, has evolved a long way from the first recovery boilers, Figure 2-2.

One noticeable trend has emerged in recent years. The average size of recovery boiler has grown significantly in each year, Figure 2-3. The nominal capacity of new recovery boilers at the beginning of the 1980s was 1700 metric tons of dry solids per day. This was regarded as the maximum at that time (Pantsar, 1988).

By year 2000 more than ten recovery boilers, capable of handling 2500 … 3500 metric tons of dry solids per day were built. At 2004 recovery boilers with nominal capacity of 4450 and 5000+ tds/d were started. The maximum design capacity has increased because there is less water in black liquor, liquor spraying is now more uniform, new computer controls mean better stability and controllability and most importantly, new pulping lines of corresponding capacity can be built.

2.1 KEY RECOVERY BOILER DESIGN ALTERNATIVES

There are alternative solutions to design of recov-

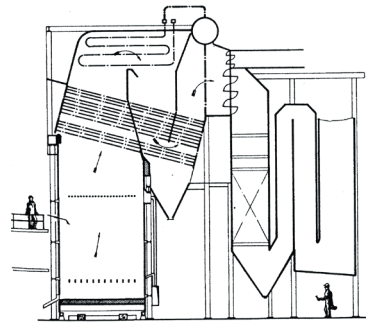

Figure 2-2, One of the first Scandinavian recovery boilers Korsnäs from 1943, 160 tds/d, 4 MPa, 400 °C (Sandquist, 1987).

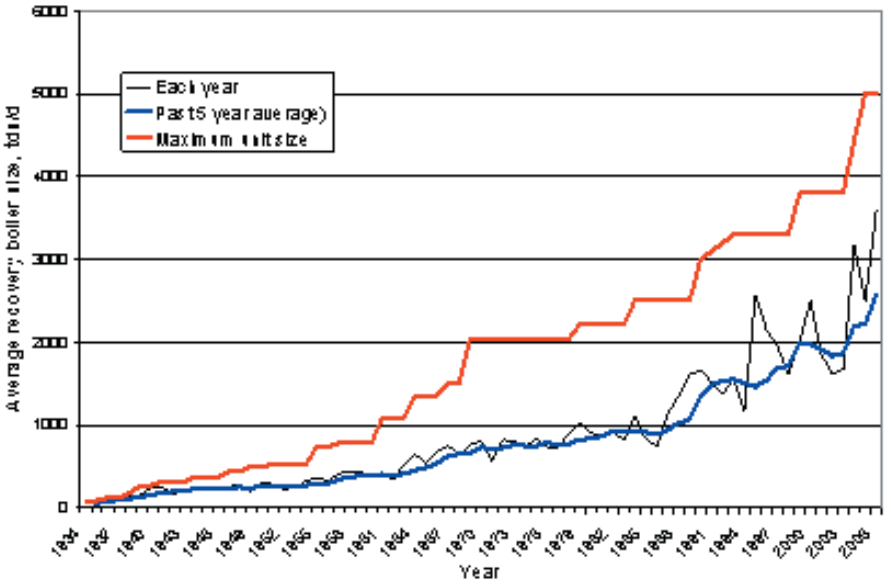

Figure 2-3, Size of recovery boiler versus startup year.

ery boilers. Major recovery boiler design options are; screen or screenless superheater area layout, single drum or two-drum, lower furnace tubing material, furnace bottom tubing material, vertical or horizontal boiler bank, economizer arrangement and number and type of air levels.

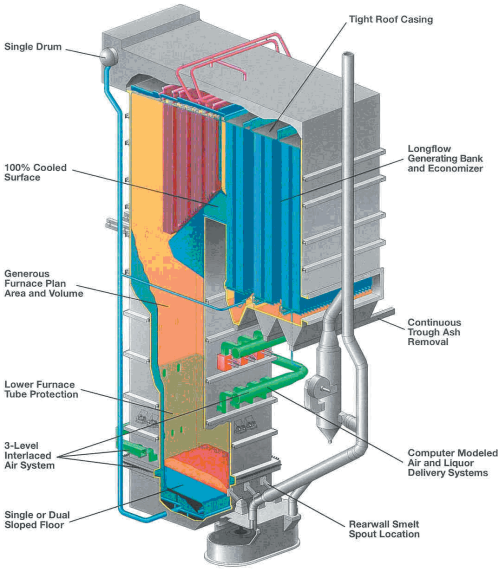

Figure 2-4, Design features of Babcock & Wilcox recovery boiler (Babcock & Wilcox, 2001).

In addition to major design features the manufacturers like to advertise their equipment with minor design features. In Figure 2-4, Babcock & Wilcox, presents their design features.

Key design specifications

When sizing a recovery boiler some key design specifications are usually given to the boiler vendor to do the design. Typically given are dry solids capacity, black liquor gross heat value, black liquor elementary analysis, black liquor dry solids % from evaporation, desired main steam conditions, feed water inlet temperature and economizer flue gas outlet temperature. Sometimes also desired superheated steam temperature control point (% of MCR) is given.

Black liquor dry solids flow is the key design criteria. It establishes the required size of the boiler. With black liquor heating value this defines the recovery boiler capacity (Rickard, 1993). Using elementary analysis and dry solids one can calculate the heat released in the furnace. With water and steam values the MCR (Maximum continuous rating) steam flow is established. It should be noted that when black liquor is sprayed to the furnace it contains ash collected from the electrostatic precipitator and ash hoppers. Because ash free black liquor is the input flow to the recovery plant, it is usually chosen as the design base.

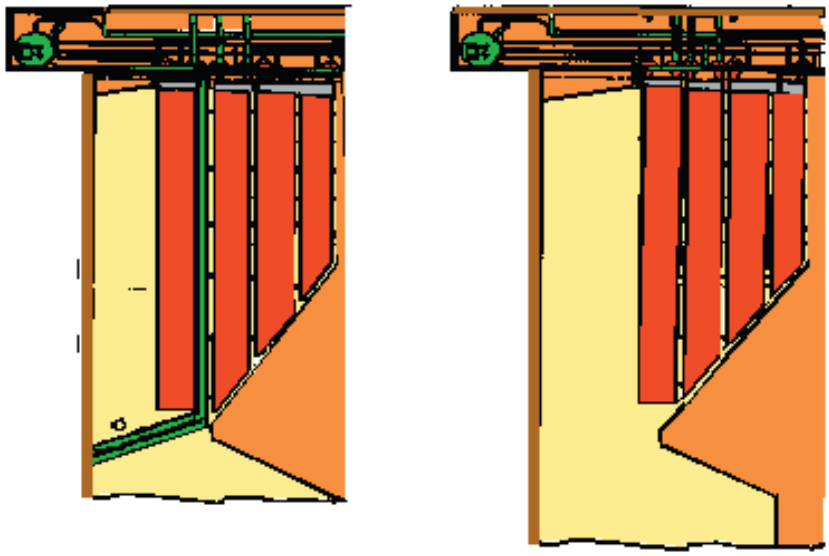

Figure 2-5, Screen at left, screenless boiler at right.

Single drum

All modern recovery boilers are of single drum type. The single drum has replaced the two drum (or bi-drum) construction in all but the smallest, low pressure boilers. The same trend but 20 years earlier happened with coal fired boilers.

Screen or screenless boiler

One of the key design issues is whether to have a screen in the recovery boiler. A screen is a low temperature heat surface that is put in front of the superheater area. Almost always the screen is an evaporative surface. There are a few screens with saturated steam entering them, but the experience has not been too favorable.

Benefits of the screen are

- Screen stops part of the carryover from furnace
- Screen blocks radiation from the furnace and reduces superheater surface temperatures. A screen protects superheater from corrosion
- Screen itself is cold surface with very minor corrosion
- Screen captures unburnt liquor partcles. Less unburnt reaches superheater surfaces, especially lower bends. This decreases superheater corrosion rates.
- Screen evens out the flow somewhat. This blocking effect is small if the screen is not covered with deposits.
- Screenless superheater section is higher and so has higher building volume and cost.

Negative issues with the screen are

- There has been number of cases where fallen deposits have caused the screen to rupture. This has caused boiler explosions and long shutdown times for repairs.
- Superheater surfaces are more affected with radiation behind the screen than behind the nose
- Screen captures heat. This reduces superheating.

Fear of boiler accidents caused by fallen deposits caused the boiler purchasers in US to avoid buying new boilers with screen. In Scandinavia boilers with screen have been bought all the time. Even in US some new boilers with screen have been bought.

2.2 EVOLUTION OF RECOVERY BOILER DESIGN

There have been significant changes in kraft pulping in recent years (Lindberg and Ryham, 1994, Vakkilainen, 1994b, Ryham, 1992). Increased use of new modified cooking methods and oxygen delignification have increased the degree of organic residue recovery. Black liquor properties have reflected these changes, Table 2-1.

Changes in investment costs, increases in scale,

***Table 2-1**, Development of black liquor properties (Vakkilainen, 2000).*

Property	Two drum	Modern	Current
	1982	1992	2002
Liquor dry solids,			
kg dry solids/ton pulp	1700	1680	1780
Sulphidity, $Na_2S/(Na_2S+NaOH)$	42	45	41
Black liquor HHV, MJ/kg dry solids	15.0	13.9	13.0
Liquor dry solids, %	64	72	80
Elemental analysis, % weight			
C	36.4	34	31.6
H	3.75	3.5	3.4
N	0.1	0.1	0.1
Na	18	18.4	19.8
S	5.4	5.9	6
Cl	0.2	0.4	0.8
K	0.75	1.0	1.8
$Cl/(Na_2+K_2)$, mol-%	0.35	0.68	1.24
K/(Na+K), mol-%	2.39	3.10	5.07
Net heat to furnace, kW/kg dry solids	13600	12250	11200
Combustion air* required, m^3n/kg dry solids	4.1	3.7	3.4
Flue gas* produced, m^3n/kg dry solids	4.9	4.3	3.9

* At air ratio 1.2

demands placed on energy efficiency and environmental requirements are the main factors directing development of the recovery boiler (Vakkilainen, 1994). Steam generation increases with increasing black liquor dry solids content. For a rise in dry solids content from 65% to 80% the main steam flow increases by about 7%. The increase is more than 2% per each 5% increase in dry solids. Steam generation efficiency improves slightly more than steam generation itself. This is mainly because the drier black liquor requires less preheating.

There are recovery boilers that burn liquor with solids concentration higher than 80%. Unreliable liquor handling, the need for pressurized storage and high pressure steam demand in the concentrator have frequently prevented sustained operation at very high solids. The main reason for the handling problems is the high viscosity of black liquor associated with high solids contents. Black liquor heat treatment (LHT) can be used to reduce viscosity at high solids (Kiiskilä *et al.*, 1993).

For pulp mills the significance of electricity generation from the recovery boiler has been secondary. The most important factor in the recovery boiler has been high availability. The electricity generation in recovery boiler process and steam cycle can be increased by elevated main steam pressure and temperature or by higher black liquor dry solids (Raukola *et al.*, 2002).

Increasing main steam outlet temperature increases the available enthalpy drop in the turbine. The normal recovery boiler main steam temperature 480°C is lower than the typical main steam temperature of 540°C for the coal and oil fired utility boilers. The main reason for choosing a lower steam temperature is to control superheater corrosion. Requirement for high availability and use of less expensive materials are often cited as other important reasons.

Two drum recovery boiler

Most of the recovery boilers operating today are of two drum design. Their main steam pressure is typically about 8.5 MPa and temperature 480 °C. The maximum design solids handling capacity of the two drum recovery boiler is about 1700 tds/d.

Three level air and stationary firing are employed. Two drum boiler represents one successful stage in a long evolutionary path and signified a design with which the sulfur emissions could be successfully minimized. Main steam temperature was increased to 480 °C using this design.

Two drum recovery boilers are constructed with water screen to protect superheaters from direct furnace radiation, lower flue gas temperatures and to decrease combustible material carry-over to superheaters. The two drum boiler was the first type to use vertical flow economizers, which replaced horizontal economizers because of their improved resistance to fouling.

Currently the two drum boilers start to get modified with single drum vertical boiler bank design (Lovo *et al*., 2004).

Modern recovery boiler

The modern recovery boiler is of a single drum design, with vertical steam generating bank and wide spaced superheaters. The most marked change around 1985 was the adoption of single drum construction. The construction of the vertical steam generating bank is similar to the vertical economizer. Vertical boiler bank is easy to keep clean. The spacing between superheater panels increased and leveled off at over 300 but under 400 mm. Wide spacing in superheaters helps to minimize fouling. This arrangement, in combination with sweetwater attemperators, ensures maximum protection against corrosion. There have been numerous improvements in recovery boiler materials to limit corrosion (Ahlers, 1983, Hänninen, 1994, Klarin, 1992, Nikkanen *et al*., 1989).

The effect of increasing dry solids concentration has had a significant effect on the main operating variables. The steam flow increases with increasing black liquor dry solids content. Increasing closure of the pulp mill means that less heat per unit of black liquor dry solids will be available in the furnace. The flue gas heat loss will decrease as the flue gas flow diminishes. Increasing black liquor dry solids is especially helpful since the recovery boiler capacity is often limited by the flue gas flow.

A modern recovery boiler, Figure 2-7, consists of heat transfer surfaces made of steel tube; furnace-1, superheaters-2, boiler generating bank-3 and economizers-4. The steam drum-5 design is of single-drum type. The air and black liquor are introduced through primary and secondary air ports-6, liquor guns-7 and tertiary air ports-8. The combustion residue, smelt exits through smelt spouts-9 to the dissolving tank-10.

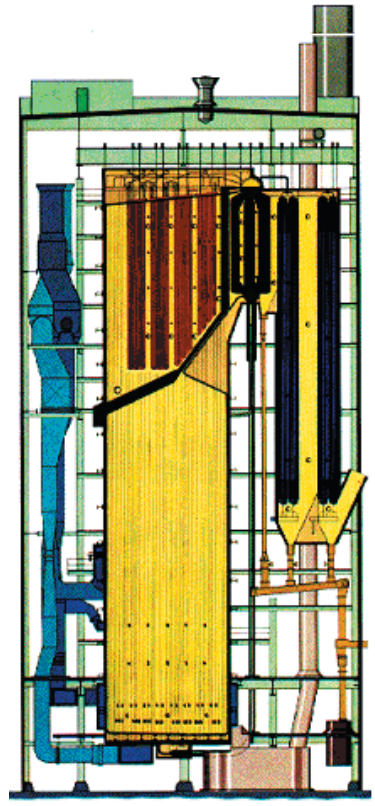

Figure 2-6, Two drum recovery boiler.

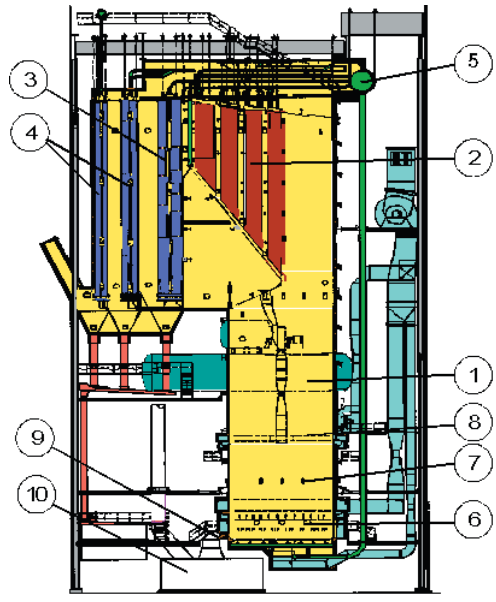

Figure 2-7, Modern recovery boiler.

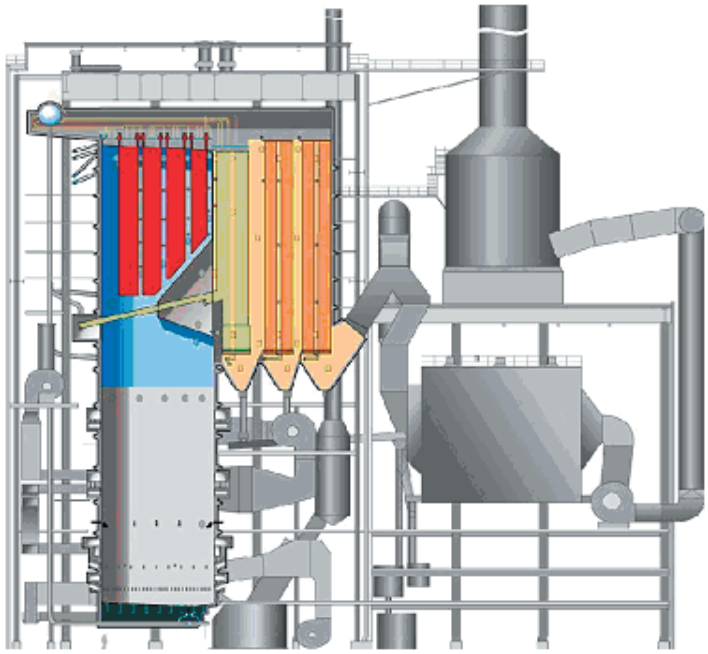

Figure 2-8, One of the most modern boilers, Gruvön (Wallén et al., 2002).

The nominal furnace loading has increased during the last ten years and will continue to increase (McCann, 1991). Changes in air design have increased furnace temperatures (Adams, 1994, Lankinen *et al*., 1991, MacCallum, 1992, MacCallum and Blackwell, 1985). This has enabled an significant increase in hearth solids loading (HSL) with only a modest design increase in hearth heat release rate (HHRR). The average flue gas flow decreases as less water vapor is present. So the vertical flue gas velocities can be reduced even with increasing temperatures in lower furnace.

The most marked change has been the adoption of single drum construction. This change has been partly affected by the more reliable water quality control. The advantages of a single drum boiler compared to a bi drum are the improved safety and availability. Single drum boilers can be built to higher pressures and bigger capacities. Savings can be achieved with decreased erection time. There is less tube joints in the single drum construction so drums with improved startup curves can be built.

The construction of the vertical steam generating bank is similar to the vertical economizer, which based on experience is very easy to keep clean (Tran, 1988). Vertical flue gas flow path improves the cleanability with high dust loading (Vakkilainen and Niemitalo, 1994). To minimize the risk for plugging and maximize the efficiency of cleaning both the generating bank and the economizers are arranged on generous side spacing. Two drum boiler bank pluggage is often caused by the too tight spacing between the tubes.

The spacing between superheater panels has increased. All superheaters are now wide spaced to minimize fouling. This arrangement, in combination with sweetwater attemperators, ensures maximum protection against corrosion. With wide spacing plugging of the superheaters becomes less likely, the deposit cleaning is easier and the sootblowing steam consumption is lower. Increased number of superheaters facilitates the control of superheater outlet steam temperature especially during start ups.

The lower loops of hottest superheaters can be made of austenitic material, with better corrosion resistance. The steam velocity in the hottest superheater tubes is high, decreasing the tube surface temperature. Low tube surface temperatures are essential to prevent superheater corrosion. A high steam side pressure loss over the hot superheaters ensures uniform steam flow in tube elements.

Current recovery boiler

Recovery boiler evolution is continuing strongly. Maximizing electricity generation is driving increases in main steam pressures and temperatures.

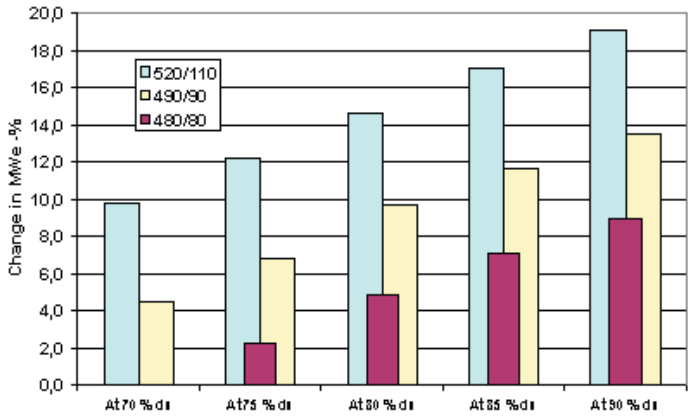

Figure 2-9, Effect of black liquor dry solids and main steam parameters to electricity generation from recovery boiler.

If the main steam pressure is increased to 10.4 MPa and temperature 520 °C, then the electricity generation from recovery boiler plant increases about 7 %. For design dry solids load of 4000 tds/d this means an additional 7 MW of electricity.

The current recovery boiler, Figure 2-8, can be much larger than the previous ones. Boilers with over 200 square meter bottom area have been bought. Largest recovery boilers are challenging circulating fluidized boilers for the tittle of largest bio-fuel fired boiler.

The superheater arrangement is designed for optimum heat transfer with extra protection to furnace radiation. Mill closure and decreased emissions mean higher chloride and potassium contents in black liquor. Almost all superheaters are placed behind the bullnose to minimize the direct radiative heat transfer from the furnace. Increasing superheating demand with increasing pressure decreases the need for boiler bank and water screen arrangement.

The higher main steam outlet temperature requires more heat to be added in the superheating section. Therefore the furnace outlet gas temperature has increased. The alternative is to significantly increase superheating surface and decrease boiler bank inlet flue gas. If boiler bank inlet gas temperature is reduced the average temperature difference between flue gas and steam is also decreased. This reduces heat transfer and substantially more superheating surface is needed. This approach has been abandoned because of increased cost. With increasing dry solids content the furnace exit temperature can safely increase without fear of corrosion caused by carryover.

Increasing recovery boiler main steam temperature affects the corrosion of the superheaters. Designing for higher recovery boiler main steam pressure increases the design pressure for all boiler parts. The recovery boiler lower furnace wall temperatures increase with higher operating pressure. New better but more expensive lower furnace materials are used. The air flow per unit of black liquor burned in the recovery boiler furnace decreases. Therefore the number of air ports will decrease.

State of the art and current trends

Recovery boiler design changes slowly. There are however some features that boilers bought today have in common. State of the art recovery boiler has the following features;

- One drum boiler with 3-part superheater and water screen (optional)
- Steam design data 9.2 MPa / 490 °C
- Design black liquor dry solids 80 % with pressurized heavy liquor storage tank
- Liquor temperature control with flash tank, indirect liquor heaters for backup
- DNCG burning in the boiler
- Low emissions of TRS, SO_2 and particulates
- Flue gas cleaning with ESP (no scrubbers)

The design changes occurring can be listed. Current trends for recovery boilers are

- Higher design pressure and temperature due to increasing demands of power generation
- Use of utility boiler methods to increase steam generation
- Superheater materials of high-grade alloys

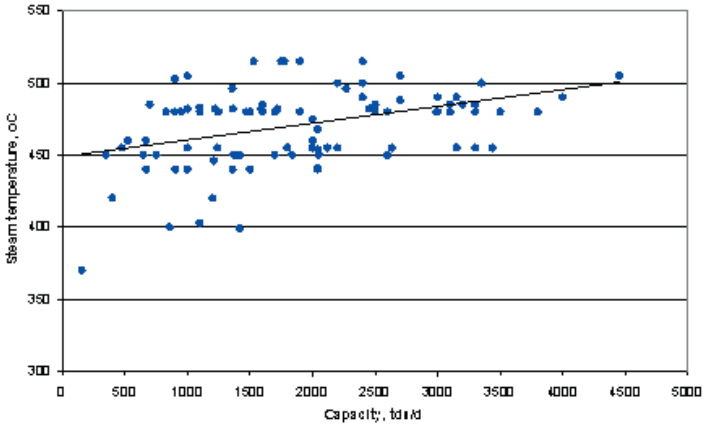

Figure 2-10, Main steam temperature as a function of recovery boiler capacity.

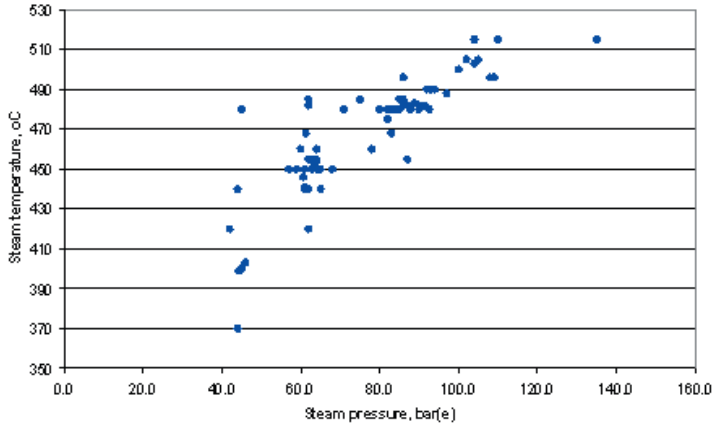

Figure 2-11, Main steam temperature as a function of recovery boiler main steam pressure.

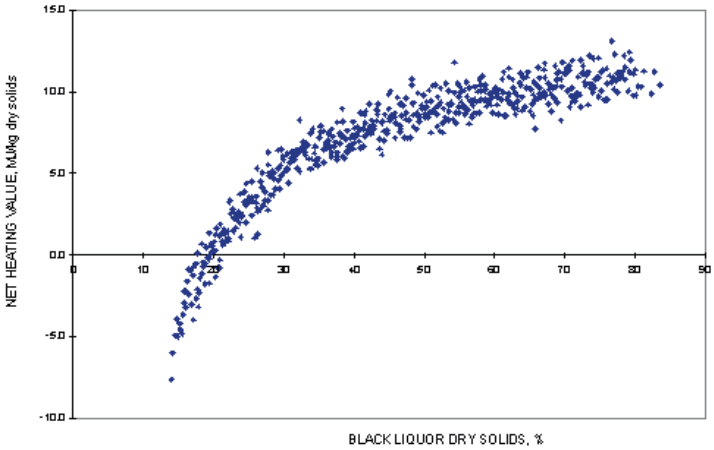

Figure 2-12, Net heating values of typical kraft liquors at various concentrations.

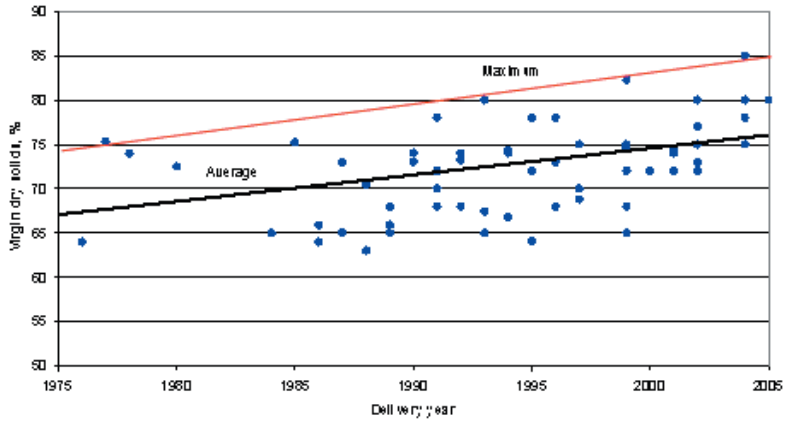

Figure 2-13, Virgin black liquor dry solids as a function of purchase year of the recovery boiler.

- Further increase in black liquor solids towards 90 % by concentrators using elevated steam pressure
- Burning of biological effluent treatment sludge and bark press filtrate effluent
- CNCG burner (LVHC gases)

Dissolving tank vent gases returned to the boiler
Advanced air systems for NOx control

2.3 CHOOSING RECOVERY BOILER MAIN PARAMETERS

As stated the recovery boiler main parameters are often given by the customer to the boiler vendor. So when the recovery boiler purchase is considered these main parameters must be chosen after careful study.

Higher black liquor dry solids generates more steam. This has been seen as a significant path to increased steam generation (Ryham, 1992). The main steam parameters (pressure and temperature) can be increased from traditional values. Increase of main steam values results in significantly more power generation, Figure 2-9. The change in steam data is as important as about 5 % change in black liquor dry solids.

The trend in recent years has been definitely in favor of increased temperatures and pressures. Newest Scandinavian lines, have chosen main steam values in excess of 8.0 MPa and 480 °C (Vakkilainen and Holm, 2000, Wallén *et al.*, 2000). The overall mill heat balance should be used to optimize the feed water and flue gas temperatures (Suutela and Fogelholm, 2000).

Main steam temperature

Main steam temperature of recovery boilers is shown in Figure 2-10 as a function of MCR capacity of that boiler.

The average steam temperature increases with size. Small boilers tend to have low pressure to reduce specific cost. There are many boilers with main steam parameters higher than 500 °C. Most of them are in Japan.

Main steam pressure

Main steam temperature of recovery boilers is shown in Figure 2-11 with corresponding main steam pressure. Increase in main steam temperature is usually accompanied with increase in main steam pressure, to keep exhaust steam wetness in control.

Main steam pressure of above 80 bar but below 90 has been the most typical chosen value in the recent years. Main steam pressure has been limited to about 60 … 65 bars in Sweden to control lower furnace corrosion (Bruno, 1995). In Japan several boilers have been recently built with more than 100 bar main steam pressure (Akiyama *et al.*, 1988).

Black liquor dry solids

As fired black liquor is a mixture of organics inorganics and water. Typically the amount of water is expressed as mass ratio of dried black liquor to unit of black liquor before drying. This ratio is called the black liquor dry solids.

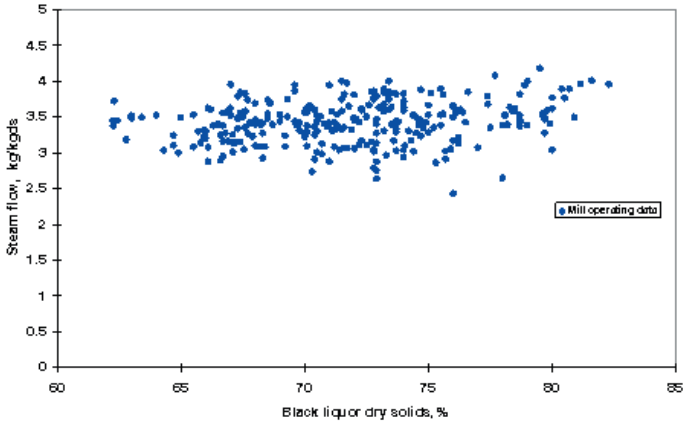

Figure 2-14, Specific steam generation kgsteam/kgBLdry solids as function of black liquor dry solids.

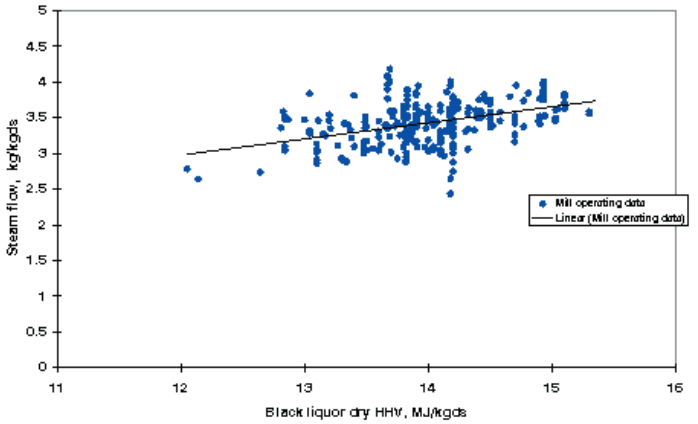

Figure 2-15, Specific steam generation kgsteam/kgBLdry solids as function of black liquor higher heating value.

If the black liquor dry solids is below 20 % or water content in black liquor is above 80 % the net heating value of black liquor is negative, Figure 2-12. This means that all heat from combustion of organics in black liquor is spent evaporating the water it contains. The higher the dry solids, the less water the black liquor contains and the hotter the adiabatic combustion temperature.

Black liquor dry solids has always been limited by the ability of available evaporation technology to handle highly viscous liquor (Holmlund and Parviainen, 2000). Virgin black liquor dry solids of recovery boilers is shown in Figure 2-13 as a function of purchase year of that boiler.

When looking at the virgin black liquor dry solids we note that on average dry solids has increased. This is especially true for latest very large recovery boilers. Design dry solids for green field mills have been either 80 or 85 % dry solids. 80 % (or before that 75 %) dry solids has been in use in Asia and South America. 85 % (or before that 80 %) has been in use in Scandinavia and Europe.

Steam generation

Steam generation will depend on recovery boiler design parameters. A rough estimate can be seen from Figure 2-14 and Figure 2-15. About 3.5 kgsteam/kgBL dry solids is often used as a base value. Specific steam production can be used to presize other components in recovery boiler plant.

Both black liquor dry solids and higher heating value affect the steam generation. Also black liquor sulfidity and main steam values affect the steam generation efficiency. For accurate steam generation one should always calculate the mass and energy balances.

2.4 PROJECTING A RECOVERY BOILER

The designer/owner/operator needs to consider several factors when projecting a new recovery boiler. The main tasks are

- Determine the steam/power requirement
- Determine the fuels available
- Determine possible locations and place ments
- Compare different types of equipment from different vendors
- Anticipate future needs
- Permitting

Selection process is influenced by applicable emission requirement, project time schedule and reliability.

Often also several iterations need to be done. Improving thermal efficiency and so electricity generation requires extra investments. Investments can be partially or totally offset by savings in operating cost. Annual costs of owning and operating a recovery boiler plant are a sum of annual charges for capital, fuel, maintenance, manpower, ash and waste disposal (Advances in …, 1986). Best configuration thus depends on actual site conditions.

Boiler purchasing

The main purchase is the pressure vessel with the steel structure. Boiler purchasing requires also choosing and buying the boiler auxiliary equipment such as choosing equipment for black liquor handling, pumps, fans and environmental equipment. Typically a building contractor does the building and foundations. Similarly a company specializing in erection does the pressure part erection often as a subcontractor to recovery boiler vendor. A score of smaller subcontractors works on the site installing e.g. electrification, automation and insulation. Depending on the project type chosen these subcontractors work for the boiler vendor or the purchaser.

Because of large sums involved there has to be a tight financial control for the whole project. Loans must be scheduled, payments should be given only against work done and purchases made. Cost of project capital can be significant.

In addition permitting process should be early started and closely monitored. A boiler with environmental performance acceptable in the future should be purchased. Timing of permitting process is crucial.

Equipment selection criteria

Boiler equipment should be selected based on satisfactory expected life span and acceptable maintenance costs. This decision is often based on satisfactory previous references.

All equipment should have adequate permanent strength. The equipment must be placed so that it is accessible for inspection and repair. Especially easiness of future large maintenance tasks, such as changing pump and fan motors, seals etc. needs to be considered.

When making the purchasing decision availability of spare parts and service should be looked at.

CE norms regulate the working environment in Europe and OSHA in North America. For other countries often similar equipment is proposed and bought. In summary safe, reliable operation is the main target with pleasing working conditions.

Permitting

The operation of a recovery boiler requires permits.

Zoning requirements place boiler to area that is reserved for industry and especially energy generation. Recovery boiler sites should be chosen so as not to cause harm to zones where people live.

Boiler equipment needs to be authorized for use. Boiler must be made according to the required pressure vessel code. The electrical system and instrumentation need to fill applicable laws. Often special requirements for chemical handling must be met.

Operating permits are needed. Environmental permits are used to regulate loads of effluents to environment. These include gaseous effluents, effluents to the water (also heat) and dumping of solid waste (mostly ash). Boiler operators are often codified.

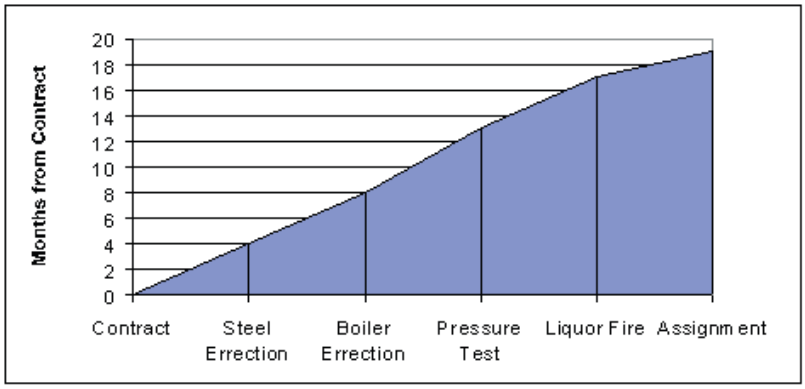

Figure 2 -16, Delivery time of a complete recovery boiler (EPS).

Delivery time

One of the most critical factors in a successful project is the delivery time of a new recovery boiler. In some projects 18 months have been achieved, Figure 2-16 (Vakkilainen and Holm, 2000). Delivery time is somewhat affected by the amount of work the boiler manufacturer has. The biggest factor is however whether one can start construction work right after contract and how easy the installation site is. From the pressure part delivery point of view the steam drum is the most critical part.

3 Material and energy balance

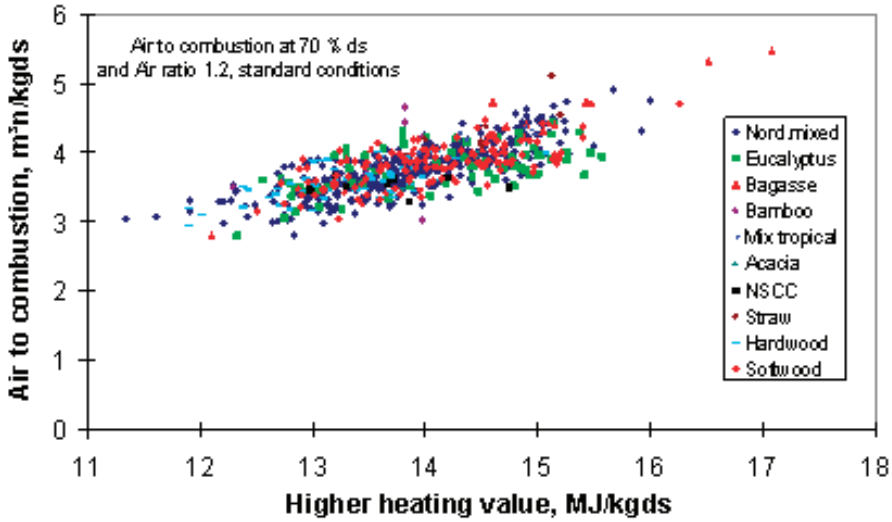

Figure 3-1, Black liquor air demand as function of the higher heating value.

Calculation of material and energy balances is fundamental. Dimensioning of recovery boiler heat transfer surfaces can not be done if mass and energy flows are unknown. Proper calculation is important for mill energy and mass balances. These are needed to evaluate economics and running costs. Recovery boiler mass and energy balances have been presented by Gullichsen (1968b), Clement *et al.* (1963), Adams and Frederick (1988) and Vakkilainen (2000b). The only standard that covers recovery boiler mass and energy balance calculation is the so called Tappi standard (Performance, 1996).

3.1 MATERIAL BALANCE

Control of combustion requires air flow that matches fuel flow. The amount of air required to burn a mass unit of black liquor depends mainly on water content and the heating value of the fuel. Black liquor higher heating value increase, Figure 3-1, means more air for combustion is needed. Figures like Figure 3-1 can be used to estimate the required air flow for dimensioning the fans. More importantly they should be used to estimate the possible range of air flows. A recovery boiler should be able to handle not only the design black liquor, but a range of typical black liquors. Often design and performance estimation is done using only the actual black liquor elemental composition.

Typical biofuels consist of carbon, hydrogen, nitrogen, sulfur and oxygen. Black liquor contains also a high amount of ash; sodium, potassium and chloride compounds. It is often impossible to define the individual chemical compounds that form the fuel. The stoichiometric air demand, I, can be calculated assuming that the fuel can be divided into three fractions

1. Organic portion, which combusts fully
2. Reactive inorganic portion, which reacts to predefined end products
3. Inactive portion, which passes through combustion system unchanged

In calculating recovery boiler inorganic reactions it can be assumed that e.g. ratio of sodium sulfide to potassium sulfide equals the ratio of sodium to potassium in smelt. Similarly all chloride reacts to form sodium and potassium chloride. To facilitate mass balances it can be assumed that all sulfur that is not escaping with flue gas is reacted either to sulfide or sulfate. It can also be assumed (mainly for the lack of thermodynamical data) that only sodiumborate compounds exists.

The basis for material calculations is typically one mass unit of black liquor. If mass balance values for one mass unit are known it is easy to multiply these values for the desired load.

The boiler house forms a convenient system

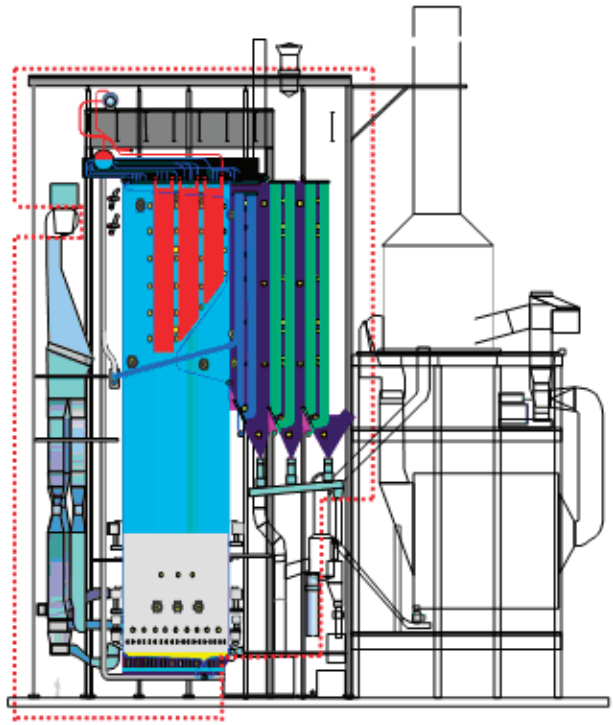

Figure 3-2, Modern recovery boiler with balance boundaries shown.

Table 3-1, *Example black liquor analysis for flows in Figure 3-2.*

Element	Value
C	32.5
H	3.3
N	0.09
S	6.1
Na	20.0
K	3.0
Cl	0.25
B	0.5
Inert (NPE)	0.1
Oxygen (by difference)	34.16

Table 3-2, *Example dust for flows in Figure 3-2.*

Element	Flow, g/kgds
Na	0.1158
K	0.0260
Cl	0.0035
$-CO_3$	0.0662
$-SO_4$	0.1682
-S	0.0004
-B	0.0000

boundary. It has been pointed out that losses and heat input caused by fans, blowers and pumps should not affect the boiler efficiency. On the other hand, forced circulation pumps, flue gas re-circulation fans and other internal process devices should be taken into account, because they play a role when boiler efficiency between different types of boilers is compared. Therefore the system boundary for boiler efficiency loosely includes some but not all equipment in the boiler house. The balance boundaries for a recovery boiler are shown in Figure 3-2. This system boundary for boiler efficiency measurement is then determined in equivalent way to definition in European standard EN 12952-15. All flow values are recorded when they cross the system boundary.

Example

Calculate required air flow for boiler shown in Figure 3-2. As fired liquor dry solids analysis as mass percent is shown in Table 3-1. Note that the corresponding virgin dry solids analysis would not include the ash that is recycled back to the boiler.

In addition assume that the reduction degree is 96 % expressed as the mole ratio of sulfide to sum of sulfate and sulfide in smelt. Black liquor dry solids is 85 %. Air ratio is 1.1625 (~3% O_2 in flue

Table 3-3, *Example ash for flows in Figure 3-2.*

Element	Flow, g/kgds
Na	30.47
K	6.84
Cl	0.93
$-CO_3$	17.41
$-SO_4$	44.25
-S	0.10
-B	0.00

gas), SO_2 emissions are 0.052 mg/kgds and HCl emissions are 0.010 mg/kgds. Sootblowing steam consumption is 150 g/kgds. The ESP ash to recycle and the dust to stack have the same analysis. Dust loss is 380 mg/kgds and the ash recycle is 100 g/kgds.

Input flow per 1 kg of as fired black liquor dry solids is from liquor analysis

	mass, g/kgds	mol/kgds	end product
Carbon	325	325/12,011 =27,059	CO_2, Na_2CO_3
Hydro-gen	33	33/2,016 =16,369	H_2O, HCl
Nitrogen	0,9	0,9/28,0134 =0,032	N_2
Oxygen	341,6	341,6/31,999 = 10,675	CO_2, SO_2, Na_2CO_3, Na_2SO_4, K_2SO_4, K_2CO_3, H_2O, $NaBO_2$, Na_3BO_3
Chloride	2,5	2,5/35,453 =0,071	NaCl, KCl, HCl
Potas-sium	30	30/78,204 =0,384	K_2S, K_2SO_4, K_2CO_3, KCl,
Sulfur	61	61/32,060 =1,903	SO_2, K_2S, Na_2S, Na_2SO_4
Sodium	200	200/45,980 =4,350	NaCl, Na_2S, Na_2SO_4, Na_2CO_3, $NaBO_2$, Na_3BO_3
Boron	5	5/10,811 =0,462	$NaBO_2$, Na_3BO_3
Water	1000* (1/0,85 - 1) =175,5	175,5/18,015 =9,796	H_2O

Sulfur balance can be calculated by first adding up all sulfur inputs and losses to get sulfur flow with smelt. Then this sulfur flow can be divided to sulfide and sulfate.

	molS/kgds	mass, gS/kgds	end product
	1,903	61,0	available sulfur
	0,333	10,7	in NCG
	-0,000	-0,0	SO_2
	-0,002	-0,1	dust as $-SO_4$
	-0,000	-0,0	dust as -S
	-0,461	-14,8	ash as $-SO_4$
	-0,003	-0,1	ash as -S
Sum	1,770	56,7	S in smelt
	0,04*1,770=0,071	2,3	$-SO_4$ in smelt
	0,96*1,770=1,699	54,5	-S in smelt

Chloride balance can be calculated by subtracting from chloride in black liquor losses as dust, ash and HCl. This is chloride in smelt.

	molCl/kgds	mass, gCl/kgds	end product
	0,071	2,5	available chloride
	0,000	-0,0	NaCl and KCl in dust
	-0,026	-0,9	NaCl and KCl in ash
	-0,000	-0,0	HCl in flue gases
Sum	0,044	1,6	Cl in smelt

Borate balance can similarly be calculated with known flow in black liquor and losses to arrive at borate in smelt. This can further be divided to sodiumtriborate and sodium metaborate.

	molB/kgds	mass, gB/kgds	end product
	0,462	5,0	available boron
	-0,000	-0,0	loss in dust
	-0,000	-0,0	loss in ash
Sum	0,462	5,0	boron in smelt
	0,80*0,462=0,370	4,0	Na_3BO_3 in smelt
	0,20*0,462=0,092	1,0	$NaBO_2$ smelt

Sodium and potassium balances need to be calculated together. In addition it is assumed that borate forms components only with sodium and other smelt compounds are formed in proportion of total sodium and potassium in smelt. The actual distribution between e.g. Na_2S and K_2S is not known, but it does not affect the mass balance.

Sodium balance to smelt can be calculated by subtracting from incoming sodium the sodium in dust and ash.

	$molNa_2$/kgds	mass, gNa/kgds	end product
	4,350	200,0	available sodium
	-0,003	-0,1	Na_2SO_4, Na_2CO_3 and NaCl in dust
	-0,663	-30,5	Na_2SO_4, Na_2CO_3 and NaCl in ash
Sum	3,684	169,4	sodium in smelt

Potassium balance to smelt can be calculated by subtracting from incoming potassium the potassium in dust and ash.

	$molK_2$/kgds	mass, gK/kgds	end product
	0,384	30,0	available potassium
	-0,000	-0,0	K_2SO_4, K_2CO_3 and KCl in dust
	-0,087	-6,8	K_2SO_4, K_2CO_3 and KCl in ash
Sum	0,296	23,1	potassium in smelt

Mole percent of potassium to sum of sodium and potassium in smelt is

100*0,296/(3,684+0,296) = 7,4 %

Mole percent of sodium to sum of sodium and potassium in smelt is

100*3,684/(3,684+0,296) = 92,6 %

Sodium balance for smelt compounds can be calculated by first subtracting from sodium in smelt the amounts of sodiumsulfide and sodium sulfate. Then amounts of sodiumborates are subtracted. Finally the amount of sodiumchloride is subtracted to arrive at the amount of sodiumcarbonate.

	$molNa_2$/kgds	mass, gNa/kgds	end product
Sum	3,684	169,4	sodium in smelt
	0,926*0,071=0,066	3,0	Na_2SO_4 in smelt
	0,926*1,699=1,573	72,3	Na2S in smelt
	0,555	25,5	Na_3BO_3 in smelt
	0,046	2,1	$NaBO_2$ in smelt
	0,926*0,022=0,020	0,9	NaCl in smelt
	3,684-Σ=1,425	65,5	Na_2CO_3 in smelt

Potassium balance for smelt compounds can similarly be calculated by first subtracting from potassium in smelt the amounts of potassiumsulfide and potassium sulfate. Then the amount of potassiumchloride is subtracted to arrive at the amount of potassiumcarbonate.

	$molK_2$/kgds	mass, gK_2/kgds	end product
Sum	0,296	23,1	potassium in smelt
	0,074*0,071=0,005	0,4	K_2SO_4 in smelt
	0,074*1,699=0,126	9,9	K_2S in smelt
	0,074*0,022=0,002	0,1	KCl in smelt
	0,296- Σ =0,162	12,7	K_2CO_3 in smelt

Other inorganic 1 g/kgds is assumed to pass through to smelt unreacted.

Carbon balance can be calculated after the smelt compounds are known by subtracting from carbon in black liquor the amount of carbon in carbonates. This results in the amount of carbon that is burned to carbon dioxide.

	molC/kgds	mass, gC/kgds	end product
	27,059	325,0	available carbon
	-0,001	-0,0	Na_2CO_3 and K_2CO_3 in dust
	-0,290	-3,5	Na_2CO_3 and K_2CO_3 in ash
	-1,425-0,162= -1,587	-19,1	Na_2CO_3 and K_2CO_3 in smelt
Sum	25,181	302,4	CO_2

Oxygen balance requires subtracting from oxygen in black liquor oxygen in all outgoing compounds.

	$molO_2$/kgds	mass, gO_2/kgds	end product
	10,675	341,6	available oxygen
	-25,180	-805,7	CO_2
	-0,005	-0,2	CO_3 and SO_4 in dust
	-1,357	-43,4	CO_3 and SO_4 in ash
	-0,000	-0,0	SO_2
	-0,142	-4,5	Na_2SO_4 and K_2SO_4 in smelt
	-2,381	-76,2	Na_2CO_3 and K_2CO_3 in smelt
	-0,555	-17,8	Na_3BO_3 in smelt
	-0,092	-3,0	$NaBO_2$ in smelt
	-8,185	-261,9	H_2O
Sum	-27,223	-871,1	

The humid air demand is then
1.1625*0,8711/0.22925= 4.4173 kg/kgds

If we apply the carbon content versus higher heating value equation (see appendix) we get for HHV 13.3 MJ/kgds. From Figure 3-1 the air demand is from 3.2 to 4 m^3n/kgds or from 3.8 to 4.8 kg/kgds.

The smelt flow can be calculated if we add up all mass flows to smelt.

Smelt balance

	mol/ kgds	mass, g/kgds	end product
	0.126	0.126*110.26=13.9	K_2S in smelt
	1.573	1.573*78.04=122.8	Na_2S in smelt
	0.066	0.066*142.04=9.3	Na_2SO_4 in smelt
	0.005	0.005*174.25=0.9	K_2SO_4 in smelt
	0.041	0.041*58.443=2.4	NaCl in smelt
	0.003	0.003*74.55=0.2	KCl in smelt
	1.424	1.424*105.99=150.9	Na_2CO_3 in smelt
	0.163	0.163*138.2=22.5	K_2CO_3 in smelt
	0,370	0,370*127,76=47.3	Na_3BO_3 in smelt
	0,092	0,092*68,5=6,1	$NaBO_2$ in smelt
	-	1	Other inorganics
Sum		377.3	

The smelt flow is then 0.377 kg/kgds.

Black liquor flue gas production depends on the black liquor heating value, Figure 3-3. For the simple analysis estimation based on predetermined mass ratio of flue gas to air can be done. An accurate flue gas flow can be calculated from simple mass balance if air flow, black liquor flow and smelt flow are known.

Example

Calculate flue gas flow for the previous example.

Mass balance

	mass, g/kgds	product
	1000	dry black liquor
	175.5	water with black liquor
	4417.3	air
	150	sootblowing steam
	0.4	loss in dust
	100.0	ash recycle
	-377.3	smelt
Sum	5265	flue gas

The flue gas flow is then 5.265 kg/kgds. For environmental reporting it is often useful to know the dry flue gas flow. The dry flue gas flow can be calculated by subtracting water with black liquor, sootblowing steam, water with air and water from hydrogen in black liquor from flue gas flow.

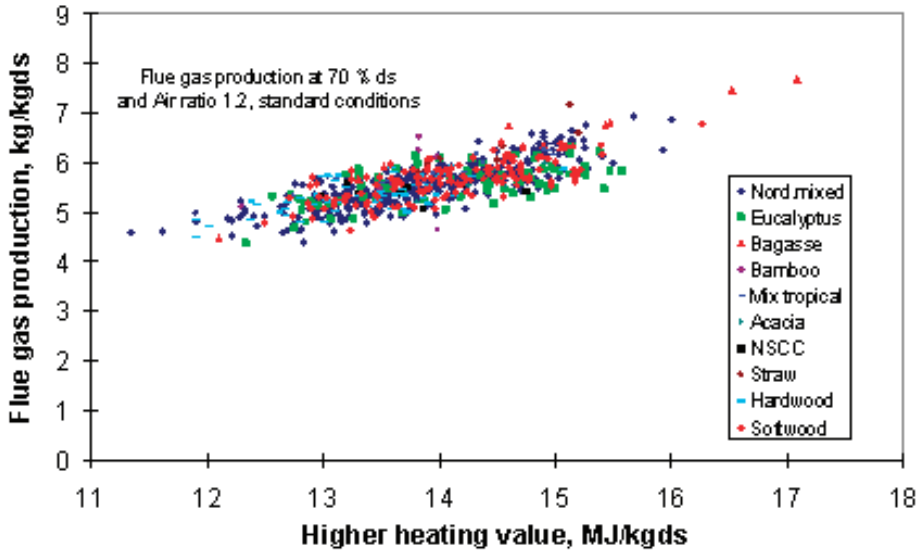

Figure 3-3, Black liquor flue gas production as function of the higher heating value.

Mass balance

	mass, g/kgds	product
	5.265	wet flue gas flow
	-175.5	water with black liquor
	-150	sootblowing steam
	-0.0135*4.417	water with air
	-16.369*18.02	water from hydrogen in black liquor
Sum	4.645	dry flue gas

When calculating real recovery boiler air and flue gas flows leakage should be taken into account. Air flow through air fans is less than calculated as some of the air is infiltration air through various openings. Flue gas flow at stack can be significantly higher that through economizers because of the same reason.

3.2 ENERGY BALANCE

To calculate energy balance for a recovery boiler one must make a boundary around the recovery boiler and then calculate all energy flows in and out of the boiler. It is easy once all mass flows have been determined.

The basis for energy balance calculation is so called heat loss method. First the sum of all input energy flows is calculated. Then from this the energy losses are subtracted. The result is the net heat available for steam generation.

As one can see from the Figure 3-4, most of the heat input comes from the heat that can be released in the combustion of black liquor. Other large sources are sensible heat in black liquor and air preheating.

Similarly looking at the Figure 3-5, most of the released heat is converted to steam. Reduction reactions take a lot of heat as does outgoing molten smelt. It should be noted that instead of traditional higher heating value, the lower heating value of black liquor is used.

Example

Calculate main steam flow and feedwater flow for the previous example. The main steam values are 9.1 MPa(a) and 490 °C. Feedwater process values are 11.0 MPa(a) and 115 °C. Flue gas flow exits at 155 °C. Air enters at 30 °C and is preheated as average value to 108.8 °C. The blowdown is 0.10 kg/kgds at drum pressure 103.6 MPa(a). Black liquor enters at 140 °C. Sootblowing is from outside with enthalpy of 3054.8 kJ/kg. Radiation and convection losses are 0.283 % of total heat input. Unaccounted losses and margin are 0.3 % and 0.5 % of total heat input respectively.

Lower heating value of as fired black liquor is the higher heating value corrected with the hydrogen and water in fuel losses.

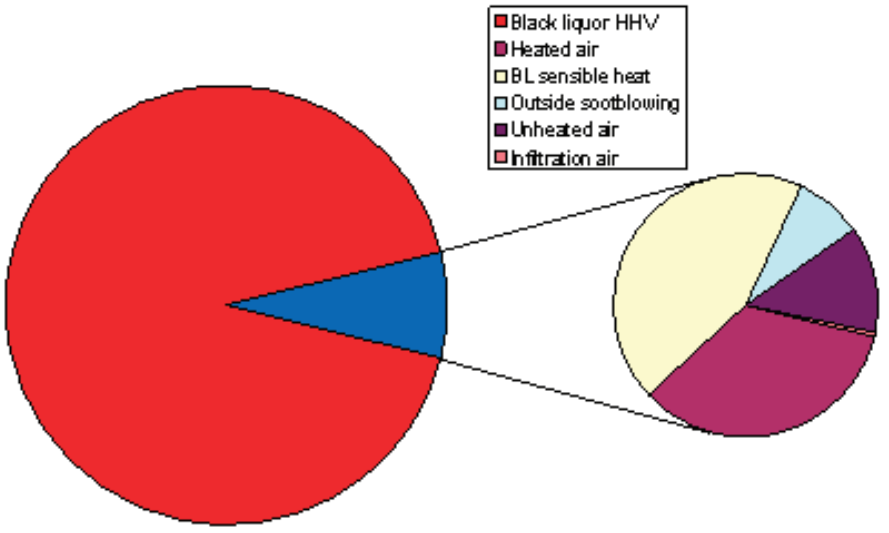

Figure 3 4, Example heat inputs to recovery boiler.

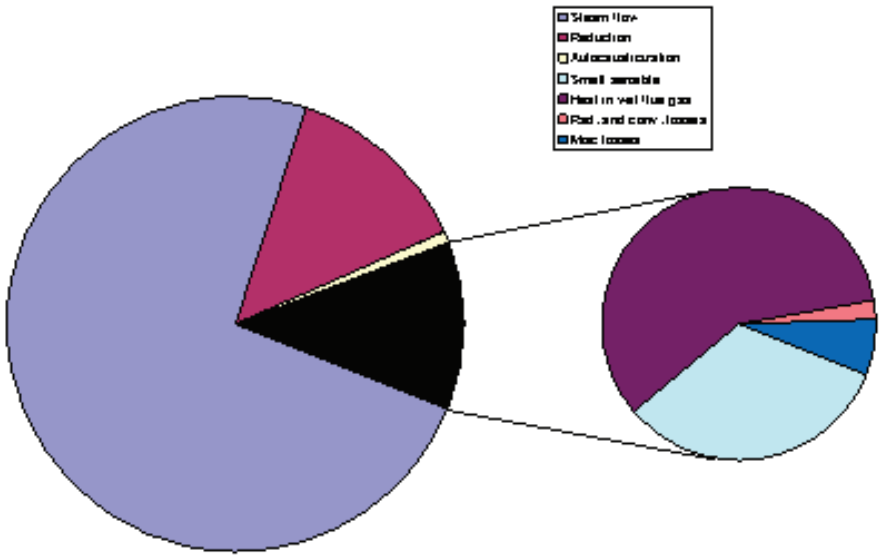

Figure 3-5, Example heat outputs form recovery boiler.

Input	mass flow kg/kgds	Enthalpy kJ/kg	kJ/kgds
Higher heating value of BL	1	13000	13000.0
Hydrogen in black liquor	0.038	-21806.3	-719.6
Lower heating value of dry BL liquor	1		12280.4
Water in black liquor	0.1755	-2440	-430.3
Lower heating value of wet BL	1.1755		11849.8

The total heat input to the boiler is the sum of heat in fuel value, heat in fuel sensible, heat in air preheating and heat in sootblowing.

Input	mass flow kg/kgds	Enthalpy kJ/kg	kJ/kgds
Heating value of black liquor	1.1755	11849.8	11849.8
Black liquor sensible	1.1755	140*2.64	434.8
Air	4.196	(30-0)*1.0336	130.1
Air preheat	4.196	(140-30) *1.0336	341.8
Infiltration	0.221	(30-0)*1.0336	6.8
Sootblowing	0.150	3054.8-2500.9	83.1
Total heat input			12846.5

To find out the heat available to steam generation one needs first to calculate the losses. Necessary energy uses are the heats needed for reduction and autocausticization reactions. They can be found for individual compounds from thermodynamical tables. The two main losses are the loss in heat of smelt and the loss in wet flue gas.

Losses			
Wet flue gas	5.265	155*1.107	903.8
Reduction to Na_2S	0.123	13099	1607.3
Reduction to K_2S	0.0139	9629	134.0
Reduction to SO_2	0.00052	5531	0.3
Autocausticization of Na_3BO_3	0.0473	1535	72.6
Loss in smelt sensible	0.377	0.377*1350	509.0
Radiation & con-vection	-	0.283*12846.5	36.4
Unaccounted losses	-	0.3*12846.5	38.5
Margin		0.5*12846.5	64.2
Total losses			3366.1

Net heat available is then 12846.5-3366.1= 9480.4

Enthalpy of steam (9.1 MPa,490 °C) is 3360.7 kJ/kg.
Enthalpy of water (11.0 MPa,115 °C) is 490.3 kJ/kg.
Enthalpy of sat. water (103.6 MPa) is 1423.3 kJ/kg.
Enthalpy of sootbl. steam (155 °C) is 2792.0 kJ/kg.

Steam mass flow x can then be calculate from the simple balance

x*3360.7+0.100*1423.3-(x+0.100)*490.3+0.000*2792.0 = 9480.4

Steam mass flow, x is then 3.270 kg/kgds.

Feedwater mass flow is

3.270+0.100+0.000 = 3.370 kg/kgds.

3.3 RADIATION AND CONVECTION HEAT LOSSES

Radiation and convection heat losses from recovery boiler are hard to measure because there are many flows in and out to the space surrounding boiler proper inside the recovery boiler building. Radiation and convection heat loss can be estimated through equation 3-1. The coefficient 0.0257 is between coal (0.022) and lignite (0.0315) boiler values. This equation with Tappi loss function (Performance, 1996) is presented graphically in Figure 3-6.

$$\Phi_{RC} = 0.0257 * \Phi_s^{0.7} \qquad 3\text{-}1$$

where

Φ_{RC} is the rad. and convection heat loss, MW
Φ_s is the useful heat output, MW

Losses calculated from equation 3-1, losses from Tappi (Performance, 1996) and measured losses are compared in Table 3-4. Tappi loss function is not valid for boilers above 3500 tds/d.

Table 3-4, *Calculated heat losses (equation 3-1 and Tappi) compared to measured heat losses from Finnish recovery boilers (Ahtiala, 1997).*

Boiler	Capacity tds/d	Calc. heat loss kJ/kgds	kW	Tappi loss kJ/kgds	Measured kW
Sunila SK11	1000	63.3	734	72.9	870
Kaukopää, SK6	3000	45.6	1582	44.6	1590
Rauma, SK3	3200	44.7	1655	43.3	1600
Kaukas, SK3	3350	44.1	1709	42.6	2000

Most of the heat losses are from pipes (50 %). Furnace accounts for roughly a part (22%). Another large portion of heat losses is from electrical equipment (18%). Ducts and tanks account for only a minor portion (10%) (Ahtiala, 1997).

3.4 STEAM GENERATION EFFICIENCY

Steam generation efficiency depends on how it is determined. Most general efficiencies are ones based on total heat input and fuel heat input. Using the values in previous example we get

$$\eta_{LHV} = \frac{\text{Heat to steam}}{\text{Total heat input}} = \frac{9480.4}{12846.5} = 73.8\% \qquad 3\text{-}2$$

If we had based the efficiency to the higher heating value in fuel heat input as is customary in North America.

$$\eta_{HHV} = \frac{\text{Heat to steam}}{\text{Fuel heat input (HHV)}} = \frac{9480.4}{12846.5 + 13000 - 11849.8} = 67.7\% \qquad 3\text{-}3$$

A recovery boiler needs to spend part of the heat in fuel to reduce chemicals. It is thus more customary especially in Europe to look at boiler efficiencies based on lower heating value and subtract the heat used to process purposes. This is called the net heating method. Net heating value or effective heating value of a boiler can be calculated by subtracting from total heat input, the reduction heats and the autocausticizing heat (Adams and Frederick, 1988).

$$\eta_{NHV} = \frac{\text{Heat to steam}}{\text{Effective heat input}} = \frac{9480.4}{12846.5 - 1607.3 - 134.0 - 72.6} = 87.9\% \qquad 3\text{-}4$$

Efficiencies based on lower heating value are ones that a well built boiler in practice can achieve. So actually recovery boiler is doing a very good job. Out of available heat it can transfer about 90 % to steam. A recovery boiler is well in range of efficiencies of the modern biofuel boilers.

3.5 HIGH DRY SOLIDS BLACK LIQUOR

One of the major trends of current years has been the increase of dry solids from evaporators. The data presented is for study of a 3000 tds/d recovery boiler. Even though this size of recovery boiler is chosen as example, the results should be applicable to most of the current recovery boilers (Lankinen *et al.*, 1991, Vakkilainen and Niemitalo,

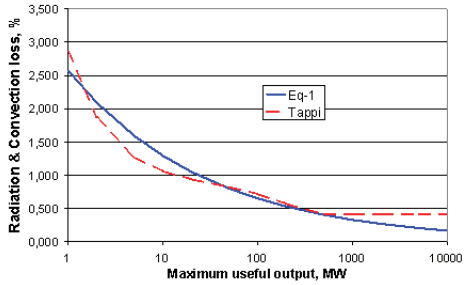

Figure 3-6, Radiation and convection losses equation 3-1, Tappi.

Table 3-5, *3000 tds/d recovery boiler main parameters.*

Max. continuous firing rate	ton ds/day	3000
Steam pressure	bar(g)	90.0
Steam temperature	°C	490
Feedwater pressure	bar(g)	109
Feedwater temperature	°C	115
Primary air percentage	%	35.0
Primary air temperature	°C	120
Secondary air percentage	%	50.0
Secondary air temperature	°C	120
Tertiary air percentage	%	15.0
Tertiary air temperature	°C	50
Flue gas temperature after eco	°C	150
Black liquor analysis		
C	% weight	34.6
Na	% weight	19.9
S	% weight	4.8
O_2	% weight	35.9
H_2	% weight	3.5
K	% weight	1.0
Cl	% weight	0,1
Others	% weight	0.2
Higher heating value	MJ/kg ds	14.0
Dry solids content as fired	% weight	65-90
Liquor temperature as fired	°C	140.0
Chemical loss to stack	g/kgds	0.2
Reduction	%	97
Sootblowing steam flow	kg/s	5.0
Balance reference temperature	°C	0

1994, Vakkilainen *et al.*, 1998b).

The design parameters for the studied recovery boiler are shown in Table 3-5. Material balance data from low dry solids value of 60 % to high value of 90 % is presented in Table 3-6. In these calculations the black liquor elemental composition is assumed to remain constant. The typical change in existing recovery boilers has been increase of liquor solids content from 65 to about 80 % dry solids. For same cases the corresponding energy balance values and steam flows are presented in Table 3-7.

In the material balance the combustion air flow and black liquor dry solids flow remain constant. The flue gas flow decreases as less water enters the furnace with increasing black liquor dry solids content. The flow of smelt remains constant as reduction degree has been assumed to remain at 95 %.

Even though the steam flow increases with increasing black liquor dry solids content, the sootblowing can remain constant. The blowdown has been increased with increasing steam flow as it depends mainly on the quality of incoming feedwater. The total heat input falls slightly with increasing dry solids, as the heat in the black liquor preheat will decrease. Because of this decrease, less heat will be available in the furnace, the reduction and smelt losses being constant, Figure 3-7.

Flue gas heat loss will decrease as the flue gas mass flow decreases. The heat loss due to water vapor in flue gas will decrease as there is less water to be evaporated. The heat available to steam production will increase as the heat losses decrease more

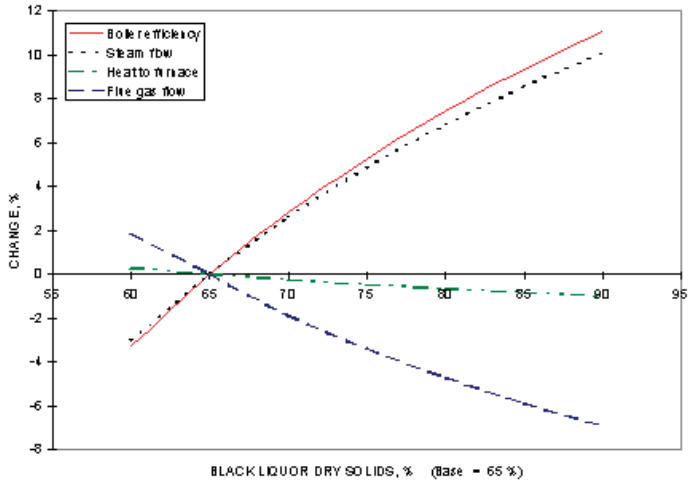

Figure 3-7, Effect of black liquor dry solids at amount of flue gas, boiler efficiency, steam flow and heat input to furnace.

Table 3-6, *Material balance for the example boiler.*

Liquor dry solids, %	65	70	75	80	85	90
Liquor flow, kg/s	53.4	49.6	46.3	43.4	40.8	38.5
Air flow, kg/s	161.9	161.9	161.9	161.9	161.9	161.9
Sootblowing, kg/s	5.0	5.0	5.0	5.0	5.0	5.0
Ash and dust, kg/s	-3.5	-3.5	-3.5	-3.5	-3.5	-3.5
Smelt flow, kg/s	-12.8	-12.8	-12.8	-12.8	-12.8	-12.8
Flue gas flow, kg/s	-204.0	-200.2	-196.9	-194.0	-191.4	-189.2

Table 3-7, *Energy balance for the example boiler.*

Liquor dry solids, %	65	70	75	80	85	90
Black liquor LHV, kJ/kgds	11923	12191	12423	12627	12806	12966
Sensible heat in BL, kJ/kgds	569	528	493	462	435	411
Air preheating, kJ/kgds	509	509	509	509	509	509
Sootblowing, kJ/kgds	80	80	80	80	80	80
Total heat available, kJ/kgds	13080	13307	13505	13677	13829	13965
Heat in smelt, kJ/kgds	-545	-545	-545	-545	-545	-545
Reduction, kJ/kgds	-1024	-1024	-1024	-1024	-1024	-1024
Heat in wet FG, kJ/kgds	-976	-958	-942	-928	-916	-905
Unacc.etc. losses, kJ/kgds	-142	-144	-146	-148	-150	-151
Total losses, kJ/kgds	-2687	-2671	-2657	-2645	-2635	-2625
Heat for steam, kJ/kgds	10393	10636	10847	11032	11194	11339
Steam flow, kg/kgds	3.588	3.673	3.7465	3.811	3.868	3.918
Steam flow, kg/s	124.6	127.5	130.1	132.3	134.3	136.0
Efficiency, %	87.3	87.6	87.9	88.1	88.3	88.5

than the total heat input.

Steam generation increases with increasing dry solids. For a rise in dry solids content from 65 % to 80 % the main steam flow increases by 7 %. The increase is typically more than 2 % per each 5 % raise in dry solids. The superheater pressure loss also increases as main steam generation is raised. To keep steam pressure losses in superheaters in reasonable level larger tubes or more parallel tubes should be used.

Steam generation efficiency improves more than steam generation itself. This is because preheating the higher dry solids black liquor requires less heat. For a rise in dry solids content from 65 % to 80 %, the steam generating efficiency improves from about 65 % to close to 70 %. The decrease in flue gas flow causes the greatest increase in steam generating efficiency. For the same rise of dry solids the amount of flue gas generated falls by 7 %. The flue gas passages can be made smaller as the flue gas flow decreases. At the same time, a smaller flue gas fan will be required.

Liquor heat treatment and storage in high temperature cause some of the combustible material to be released as non-condensable gases. The main effect is a decrease in black liquor sulphur content. Release of NCG affects recovery boiler performance in the same way as the increase in black liquor dry solids. The efficiency of steam generation goes up and the amount of flue gas decreases. The lower sulphur load to the furnace results in a sharp decrease in the heat required for reduction of sulfur compounds. If CNCGs are burned in the recovery boiler there is no net effect.

4 Combustion of black liquor

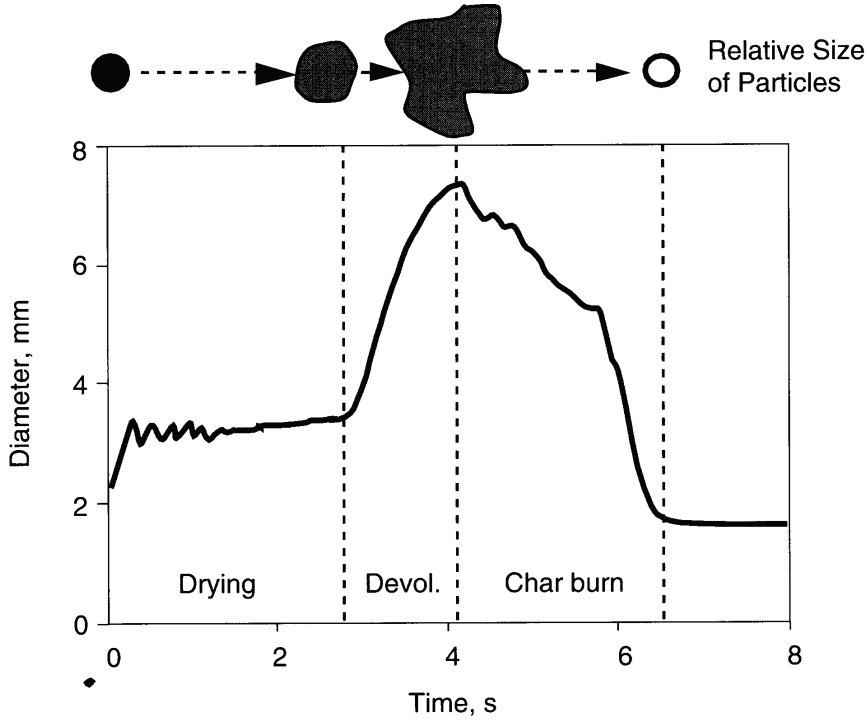

Figure 4-1, Characteristic swelling behavior of black liquor during combustion.

The black liquor is composed of a large number of organic and inorganic compounds. The amount and the composition of the black liquor depend on the wood species, the cooking method and the pulping process. Properties and processes for e.g. sulfite liquor combustion can be different (Hupa *et al.*, 1994). This text considers only kraft liquor combustion. The organic matter of black liquor is combusted in the recovery boiler furnace, while part of the inorganic matter is recovered as smelt. Black liquor has one of the lowest heating values of industrial fuels. This is because of the large inorganic portion of the black liquor. High water content, low heating value and huge ash content make combustion of black liquor difficult.

Black liquor combustion occurs either as a droplet sprayed to the furnace from a liquor gun or in the char bed at the bottom of the recovery boiler furnace (Hupa and Solin, 1985). Black liquor is sprayed into the furnace through a number of liquor guns. In many combustion applications the aim is to produce very small droplets to maximize combustion rates and temperature. Black liquor is not finely atomized as it enters the furnace. Rather black liquor is sprayed as coarse droplets. The average droplet diameter is about 2 ... 3 mm, so that unburned material can reach char bed. The black

***Table 4-1**, Main stages in black liquor combustion in furnace for a 2 mm droplet*

Stage	Characterized by	Time scale in furnace
Drying	Water evaporation, constant diameter after initial swelling	0.1 … 0.2 s
Devolatilization	Appearance of flame, ignition, swelling of the droplet, release of volatiles	0.2 … 0.3 s
Char burning	Disappearance of flame, reduction reactions, decreasing diameter	0.5 … 1 s
Smelt	Constant or increasing diameter, reoxidation	Long

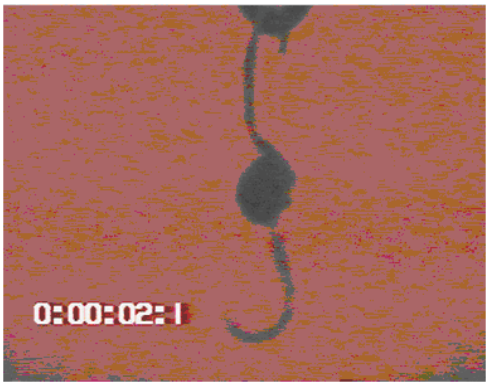

Figure 4-2, Example of drying black liquor droplet, laboratory conditions (Åbo Akademi).

liquor droplet combustion is typically divided into four stages, Table 4-1. This division is similar than for other biofuels. As most of the combustible material in black liquor originates from wood (Söderhjelm, 1994), this can be expected.

During combustion, Figure 4-1, black liquor swells (Hupa *et al.*, 1994). No other industrial fuel swells as much as black liquor during combustion. The swelling behavior is caused by high volatiles yields and suitable surface properties (Milanova, 1988, Miller *et al.*, 1986, Noopila et al., 1991). Order of different combustion steps is shown as vertical lines in Figure 4-1. In reality the combustion stages overlap somewhat (Verrill and Wessel, 1995, Järvinen *et al.*, 2000) at least for the larger droplets. A reason for this is the different combustion speeds at different parts of droplets. While black liquor can already be dry and undergoing volatiles release at surface, drying is not complete at droplet centre.

4.1 DRYING

Drying is characterized by evaporation of water from the black liquor droplet. It is often experimentally defined by absence of combustion (visible flame), Figure 4-2. Evaporation of water requires heat. Drying of black liquor droplet proceeds as fast as the heat is transferred to the droplet. Even in the furnace temperatures drying is limited by the heat flux to the droplet.

The black liquor diameter increases to 1.3 - 1.6 times the original diameter during the first couple of milliseconds after insertion into the furnace. As water is evaporated, the density decreases, but the diameter stays constant. Swelling restarts with the onset of the volatiles release. The black liquor droplet is not completely dry at the onset of volatiles release. Typically about five percent of moisture remains (Frederick and Hupa, 1993). The drying rate for pine, birch and sodium sulfite liquors is constant for black liquor droplets with various dry solids contents at 700 °C and 800 °C.

Initially the black liquor is thought to consist of water and pyrolysable material that remains after drying. Black liquor mass can then be divided into

$$m_o = m_p + m_w \qquad 4\text{-}1$$

where

m_o is the initial droplet mass, kg
m_w is the mass of water in droplet, kg
m_p is the mass of pyrolysable material in droplet, kg

The dry solids at start of combustion is

$$x_d = m_p/(mp+m_w) \qquad 4\text{-}2$$

where

x_d is the droplet dry solids, -

The black liquor droplet temperature correspond to boiling point rise (BPR_{max} = 650 K)

$$T_d = 100+BPR_{max}*x_d^{2.74} \qquad 4\text{-}3$$

The heat to droplet is (c_p = 2.5 kJ/kg, l = 2450 kJ/kg)

$$\frac{\partial}{\partial t}Q_d = m_p c_p \frac{\partial}{\partial t}T_d + l\frac{\partial}{\partial t}m_w \qquad 4\text{-}4$$

where

$\frac{\partial}{\partial t}m_w$ is the loss as water vapor

Heat to droplet is

$$Q_d = Q_c + Q_r \qquad 4\text{-}5$$

The liquor droplet diameter is constant D_d.

$$D_d = 1.54*D_o \qquad 4\text{-}6$$

The droplet area is

$$A_d = \pi D_d^2 \qquad 4\text{-}7$$

The convective heat flux is ($h_c \sim 10$ W/m^{2}K)

$$\frac{\partial Q_c}{\partial t} = h_c A_d (T_g - T_d) \qquad 4\text{-}8$$

For modelling of convective heat transfer a model of Ranz and Marshal (1986) can be used.

$$Nu = \frac{h D_d}{\lambda} = 2.0 + 0.6\, Re_d^{\frac{1}{2}} Pr^{\frac{1}{3}} \qquad 4\text{-}9$$

where

D_d particle diameter, m
h convective heat transfer coefficient, W/m²K
R_{ed} Reynolds number based on droplet diameter and relative speed, -
Pr Prandtl number based on gas phase, -

The radiative heat flux (ε = 0.8)

$$\frac{\partial Q_r}{\partial t} = \varepsilon A_d \sigma (T_g^4 - T_d^4) \qquad 4\text{-}10$$

The basic radiation heat transfer equation for droplet in gray gas is

$$\Phi_r = \varepsilon \sigma A_d (T_g^4 - T_d^4) \qquad 4\text{-}11$$

where

A_d droplet surface area, m²
T_g gas temperature, K
T_d droplet temperature, K

This type of equation is applicable to the real processes in the recovery boiler furnace.

In most of the experimental studies the main radiative component is the hot furnace wall so different type of radiative heat transfer equation needs to be used. In the Åbo Akademi experiments where the view port was small the resulting equation was (Frederick *et al.*, 1989)

$$\Phi_r = \varepsilon \sigma (T_w^4 - T_d^4) \qquad 4\text{-}12$$

In the IPC experiments where the view port was large the resulting equation was (Frederick *et al.*, 1989)

$$\Phi_r = {}^1/_2 \varepsilon \sigma A_d (T_w^4 - T_d^4) + {}^1/_3 \varepsilon \sigma A_d (T_g^4 - T_d^4) \qquad 4\text{-}13$$

4.2 DEVOLATILIZATION

As black liquor dries and temperature increases reactions with lowest activation energies start taking place. For organic fuels, release of low molecular weight component gases such as methane, carbon dioxide, hydrogen and hydrogen sulfide starts. Hydrogen, carbon monoxide, carbon dioxide, light hydrocarbons, tar and light sulfur-containing gases have been reported to be main product gases during devolatilization (Jing and Iisa, 2001). Devolatilization is characterized by the increase of black liquor droplet volume, release

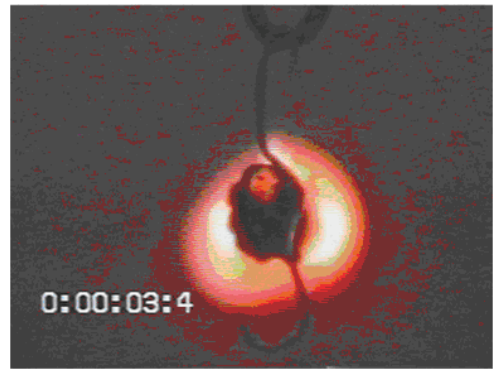

Figure 4-3, Example of black liquor droplet at the start of devolatilization, laboratory conditions (Åbo Akademi).

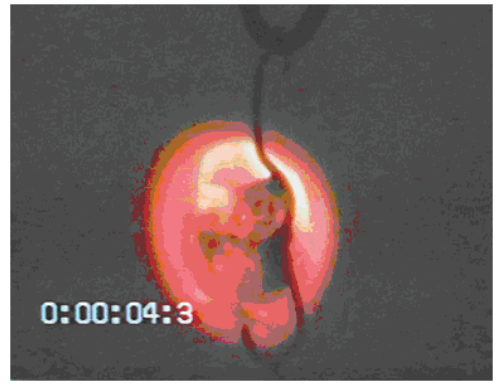

Figure 4-4, Example of black liquor droplet at the end of devolatilization, laboratory conditions (Åbo Akademi).

of volatile gases from the black liquor droplet and appearance of visible flame, Figure 4-3. The last one is the most typical criteria for determining the length of devolatilization time in experimental droplet combustion studies.

During devolatilization usually the gas release is large enough so no oxygen can contact the droplet surface. Therefore the conditions at droplet resemble those of pyrolysis or heating in inert athmosphere. The term Pyrolysis is often used incorrectly to mean devolatilization. So the release of volatile fraction occurs whether or not there is oxygen present.

Devolatilization of black liquor tends to be a fast proces and depends essentially on the heat transfer to the liquor. Devolatilization tends to occur in an outer shell of expanding thickness for the larger droplets, while a core of colder, unpyrolyzed material remains within (Järvinen *et al.*, 2000, Sricharoenchaikul *et al.*, 2001).

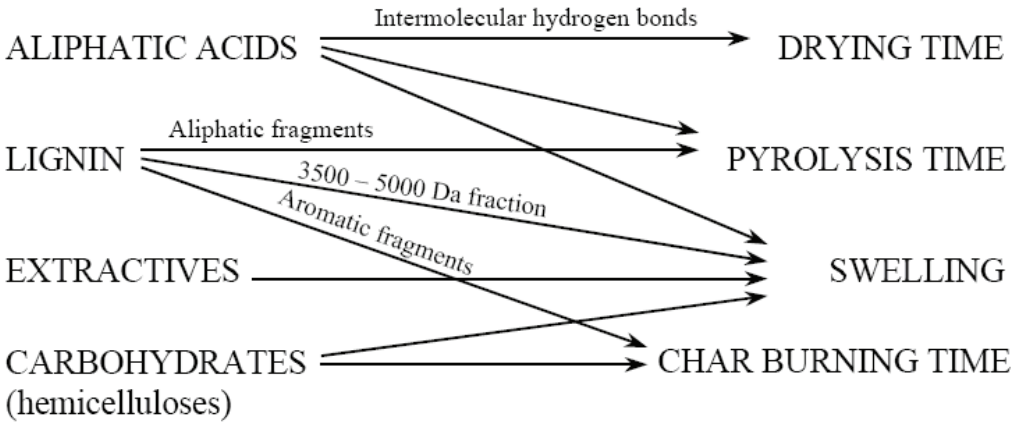

Figure 4-5, Relationships between the main organic constituents and the different combustion stages of a kraft black liquor droplet (Alén, 2000).

Swelling

During the devolatilization, the black liquor droplets swell considerably. The swelling is continuous from the onset of ignition until the devolatilization is complete, Figure 4-4. The swollen devolatilized particles exhibit extensive macroporosity and often a hollow central core is found.

Two conditions have to be met for swelling; there must be gas generation and the droplet must have plastic surface properties. The maximum swelling changes from one type of liquor to another. The maximum swollen volume for kraft black liquors varies from less than 10 to 50 cm^3/g.

During the devolatilization, the black liquor droplets swell considerably. The swelling is continuous from the onset of ignition until the devolatilization is complete. Noopila *et al.* (1991) have studied the effect of wood species and cooking time. They concluded that the swelling both for softwood and hardwood is proportional to the ratio of lignin to aliphatic acids. Typically a longer cooking time increases swelling (Alén, 2004). Liquor from soda cooks and NSSC cooks seem generally to swell less than kraft liquors. Adding of sodiumsulfate or sodiumcarbonate to virgin black liquor decreases swelling.

The rate of combustion reactions is increased with higher swelling, Figure 4-6 (Vakkilainen *et al.*, 1998). This can be explained by the larger available surface area for highly swelling black liquors. Backman *et al.* (1996) found that the swelling and organic combustion time correlate for typical mill liquors. Swelling is dependent on liquor specific properties (Alén, 1997). Swelling decreases with increasing furnace temperature (Hupa *et al.*, 1994).

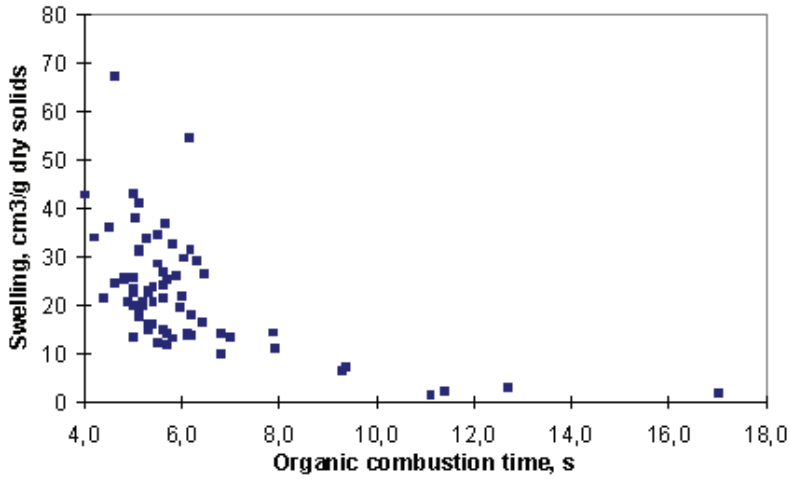

Figure 4-6, Swelling versus organic combustion time for single droplet studies at 800 °C (=sum of devolatilization and char burning times).

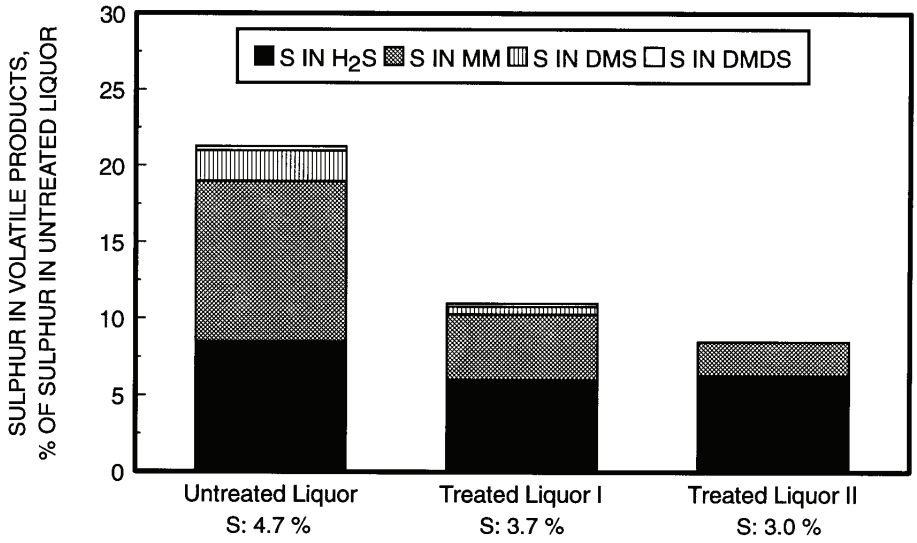

Figure 4-7, Sulfur species during pyrolysis of black liquor (McKeough et al., 1995).

Sulfur release

During devolatilization a large number of reactions take place. The main form of sulfur release is dimethyl sulphide and methyl mercaptane, Figure 4-7. Hydrogen sulfide, H_2S is formed rapidly with decomposition reactions after gases are released from the droplet.Formation of dimethyl disulfide is small.

Sodium release

There is some experimental evidence that during devolatilization fragmentation though ejection of small particles occurs (Frederick *et al*., 1995). This process is partly responsible for sodium loss from combusting black liquor droplets. In addition sodium associated with activated carboxylate and phenolate sites can volatilize (Frederick *et al*., 2004).

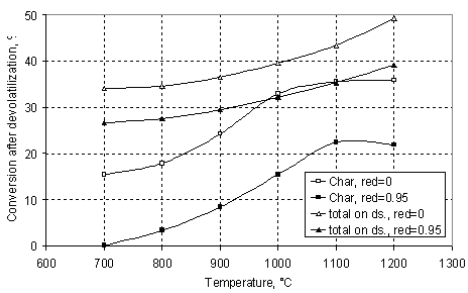

Figure 4-8, Effect of temperature on char conversion (Järvinen et al., 2000).

Carbon conversion

Devolatilization occurs very rapidly when black liquor solids are heated to temperatures substantially above 200 °C (Sricharoenchaikul *et al*., 2001). During devolatilization a significant portion of carbon in char is consumed, Figure 4-8. Increasing temperature results in higher pyrolysis yield. Volatiles release seems to decrease when swelling increases (Whitty *et al*., 1997). This is explained by increased heating rate with increased swelling.

As can be seen total of almost half of the char is reacted in normal recovery boiler lower furnace temperatures. This includes the about 6 to 7 percent that is involved in reduction reactions.

Kulas and Clay (1988) derived, using statistical methods, an equation for mass loss as a function of initial droplet diameter and oxygen partial pressure.

$$\frac{\partial}{\partial t}\frac{m}{m_{0d}} = \frac{0.001634}{d_{0d}} + 0.0034\frac{p_{O_2}}{d_{0d}} - 0.54\,p_{O_2} - 0.316 \qquad 4\text{-}14$$

Frederick *et al.* (1989) models the black liquor pyrolysis

$$Q_p = m_o[c_p(T_d - T_o) + l(1 - x_o/x_d)] + Q_{\Delta p} \qquad 4\text{-}15$$

$$Q_p = Q_c + Q_r \qquad 4\text{-}16$$

Horton (1991) models the black liquor pyrolysis as follows

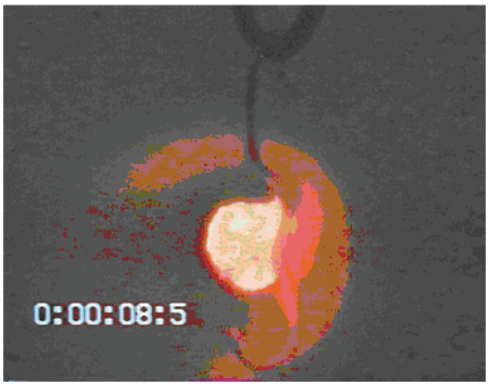

Figure 4-9, Example of black liquor droplet during char combustion, laboratory conditions (Åbo Akademi).

Table 4-2, *Composition of kraft char (Grace, 1990).*

Component		moles/ mole Na_2	weight, %
Sodium sulfide	Na_2S	1/6	9.0
Sodium sulfate	Na_2SO_4	1/6	16.4
Sodium carbonate	Na_2CO_3	2/3	49.0
Carbon	C	3	24.9
Hydrogen	H	1	0.7

$$D(t) = D_d + (D_p - D_d)(Q_p(t)/Q_p)^{Nv} \quad 4\text{-}17$$

$$Q_p = m_o x_o / x_p [c_p(T_p - T_d) + H_v(1 - x_d)] \quad 4\text{-}18$$

$$Q_p = Q_c + Q_r \quad 4\text{-}19$$

Frederick (1991) models the carbon remaining in the droplet after the devolatilization as

$$x_c = A - BT^* \quad 4\text{-}20$$

where
A = 0.513 for kraft liquors
B = 0.384 for kraft liquors
and
T* = T[K]/1000

Most of the char conversion cn be attributed to formation of volatiles. Sricharoenchaikul *et al.* (2002) found in their LFR-experiments that tar formation accounted to less than 5 % of cabon on all conditions studied.

4.3 CHAR COMBUSTION

Char combustion of black liquor starts as the volatiles release is finished. Often the combustible material remaining after volatiles release is termed fixed carbon. Fixed carbon does not include inorganic ash. In laboratory tests char combustion starts when the visible flame is extinguished, Figure 4-9. In practice char combustion and devolatilization overlap considerably. Often a term organic combustion time, that is the sum of devolatilization and char combustion times, is used to characterize combustion.

Almost all the inorganic matter except sulfur remains with majority of carbon in char. Black liquor char contains carbon, sodium carbonate, sodium sulfate and sodium sulfide. A representative composition of char is shown in Table 4-2.

We can see that about two thirds of carbon and less than a fourth of hydrogen is present but no organic oxygen is left. The reduction rate expressed as ratio of sodium sulfide to sodium sulfate is about 50 %. Char continues to burn with the particle temperature increasing from outside to inside. The inorganic residue eventually forms molten smelt.

During the char combustion reduction reactions take place (Grace, 1985). The carbon has a major role in the reduction reaction. Sodium sulfate Na_2SO_4 reacts with carbon to form sodium sulfide Na_2S. So while the carbon in the char bed burns it causes the reduction of sodium (Grace, 2004).

$$Na_2S + 2O_2 \rightarrow Na_2SO_4 \quad 4\text{-}21$$

$$Na_2SO_4 + 2C \rightarrow Na_2S + 2CO_2 \quad 4\text{-}22$$

$$Na_2SO_4 + 4C \rightarrow Na_2S + 2CO \quad 4\text{-}23$$

The rate of reduction reaction depends on the char carbon content. This rate was found to be

$$\frac{\partial [SO_4]}{\partial t} = -K_{Red} \frac{[SO_4]}{B + [SO_4]} [C] e^{-\frac{E_a}{RT}} \quad 4\text{-}24$$

The constants measured for kraft char were
K_{Red} = 1310±410, 1/s
B = 0.022±0.008, kmol/m³
E_a = 122, kJ/kmol

The reduction rate is dependent on temperature. In modern kraft recovery boilers high reduction efficiencies are typical. From thermodynamical equilibrium we note that there should be very little of sodium oxides and thiosulphite. The rate of reduction process is very slow when reduction degree is over 95%. Higher reduction degrees require significant residence time for the smelt.

If there is enough oxygen to reach the char surface, the carbon in the char reacts with the oxy-

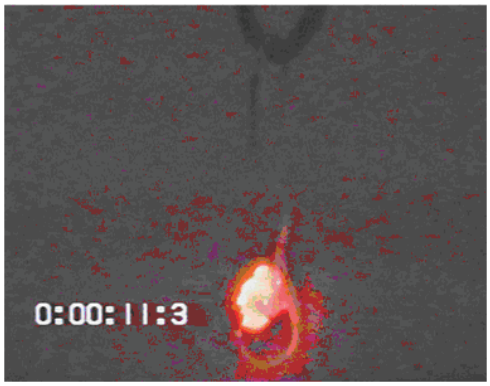

Figure 4-10, Example of black liquor droplet during smelt reactions, laboratory conditions (Åbo Akademi).

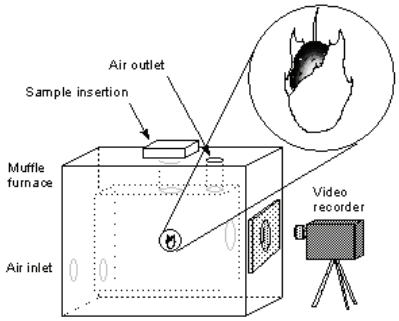

Figure 4-11, Single droplet furnace for combustion experiments.

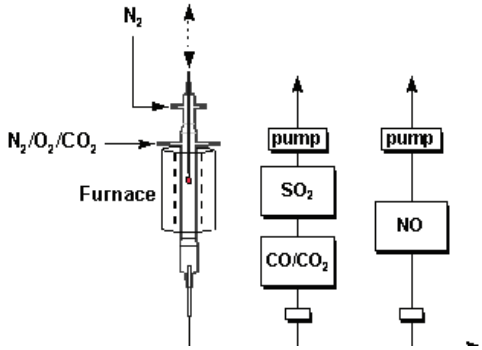

Figure 4-12, Single droplet tube reactor.

gen. If there is a deficiency of oxygen the char is gasified with carbon dioxide CO_2 and water vapor H_2O. Both carbon dioxide and water vapor react with char to form carbon monoxide CO.

$$C_{char} + CO_2 \rightarrow 2CO \qquad 4\text{-}25$$

$$C_{char} + H_2O \rightarrow CO + H_2 \qquad 4\text{-}26$$

The CO is further oxidized to CO_2 higher in the furnace when it reacts with oxygen.

4.4 SMELT REACTIONS

As the char combustion is finished the inorganic residue remains. The black liquor droplet has first enlarged and then shrunk to a liquid droplet, Figure 4-10. If oxygen contacts smelt, the sulfide in smelt is reoxidized to sodium sulfate Na_2SO_4. In recovery boiler it is important to have enough reacting material on top of smelt to avoid smelt reoxidation.

4.5 EXPERIMENTAL PROCEDURES TO LOOK AT BLACK LIQUOR COMBUSTION

Laboratory-scale devices are used for studying the combustion properties of the liquors: Single-droplet muffle furnace is maybe the most typical of these, Figure 4-11.

The duration of the pyrolysis and char burning times and swelling during combustion is recorded with a video camera. Experiments are performed in the single-droplet muffle furnace typically in air at 700 and 800 °C. The sample size is usually of order of 10 mg wet black liquor. The technique has been used by Hupa *et al.* (1994) and Whitty *et al.* (1997).

Another typical device is the single droplet tube reactor, Figure 4-12. The main benefit of the tube furnace to single droplet furnace is that gas analysis of combustion products can be made. In the Åbo Akademi one can follow the burning process of individual droplets with on-line gas analysis for CO_2, CO, SO_2 and NO. The experiments are typically performed on 40 mg samples at 900°C in different O_2 compositions.

The single droplet tube reactors have been described in more detail by Whitty (Whitty *et al.*, 1995) and Forssén (Forssén *et al.*, 1997).

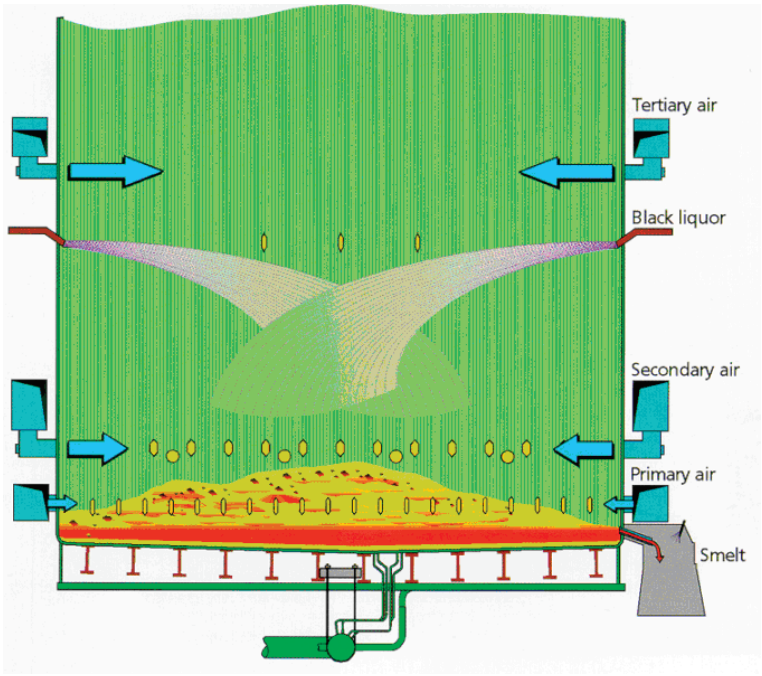

Figure 4-13, Recovery boiler lower furnace.

4.6 COMBUSTION OF BLACK LIQUOR DROPLET IN THE FURNACE

A typical lower part of recovery furnace is shown in Figure 4-13. It consists of three air levels; primary, secondary and tertiary levels. The furnace bottom is covered with a char bed. The black liquor is sprayed from black liquor guns. Combustion of black liquor in the furnace can be simulated. Results of one such simulation can be seen in Figure 4-14. In it black liquor droplets of 1.5 mm diameter, but of different dry solids contents are sprayed into the furnace. Each droplet is drawn about 0.1 s time intervals.

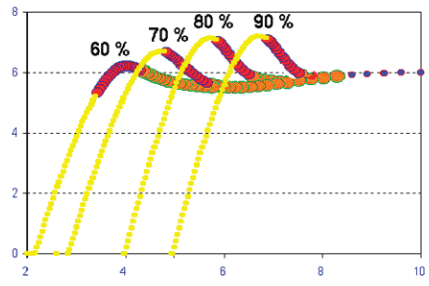

Figure 4-14, Effect of increased dry solids to combustion of 1.5 mm black liquor droplets fired to furnace.

Black liquor drying occurs close to the liquor gun at the right wall. Droplet velocity is initially high, about 10 m/s. When volatiles release starts the black liquor droplets swell. Increased drag then slows them down. At the same time droplets curve upward because of the drag from flue gases. During char burning the horizontal velocity is low. As char burning is completed the droplet density increases. Then it starts falling down until it hits the char bed.

Drops with higher initial dry solids start swelling faster and tend to burn higher in the furnace (Frederick and Hupa, 1992). All droplets in figure 4-14 burn at about liquor gun level. In practice this is too high and larger size droplets would be used.

4.7 COMBUSTION PROPERTIES OF HIGH DRY SOLIDS BLACK LIQUOR

The combustion properties of high dry solids black liquors have been studied by Åbo Akademi and VTT (Frederick and Hupa, 1993, McKeough *et al.*, 1995). The main interest has been the release of sodium, sulphur and chloride and the combustion properties of the drop.

The black liquor droplet is a poor heat conductor. The burning process is controlled by the slow rise of the temperature inside the droplet (Järvinen

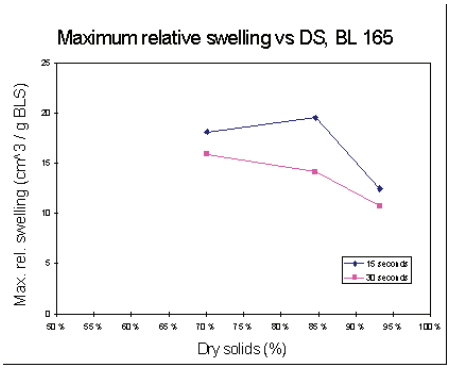

Figure 4-15, Swelling as a function of black liquor dry solids.

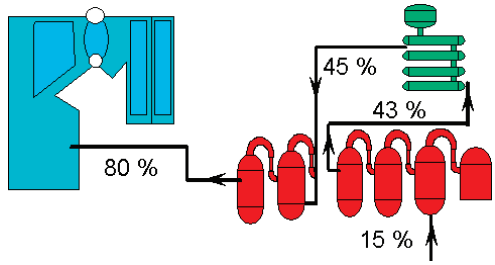

Figure 4-16, LHT plant.

et al., 2000). The increase of the dry solids affects only slightly the black liquor combustion when the dry solids of black liquor is raised. In Figure 4-15, the small decrease of swelling as dry solids is increased is shown.

The results of studies show that the increase in dry solids shortens the drying time, but it does not have an effect to the time for volatiles release nor to the char burning time. The increase of dry solids does not significantly affect the swelling of the black liquor, Table 4-3

***Table 4-3**, Effect of dry solids on combustion properties*

Dry solids %	Pyrolysis time, s	Pyrolysis m-loss, %	Swelling, cm^3/g	Char, g/cm^3
70.1	15	36	18.1	0.0486
70.1	30	51	15.9	0.0418
84.6	15	32	19.5	0.0502
84.6	30	48	14.1	0.0514
93.2	15	42	12.5	0.0712
93.2	30	48	10.7	0.0689

The tests with a very high dry solids have been performed only with the Northern softwood and hardwood liquors, so further research is needed with black liquors generated from grass and tropical woods.

Effects of liquor heat treatment on black liquor combustion

The heat treatment of black liquor can be defined as a thermal treatment method where residual alkali reacts with dissolved polysaccharides and lignin. These reactions are very slow in typical evaporator temperatures so the black liquor is heated up to 180 ... 190 °C. The effect is destruction of high molecular weight compounds and reduction of black liquor viscosity. The process has been employed to fire and store black liquor up to 90 % dry solids in atmospheric pressure in order to maximize the benefits of high dry solids in black liquor combustion (Ryham, 1990, Ryham and Nikkanen, 1992).

The main benefit of the liquor heat treatment (LHT) is viscosity reduction which allows the evaporation up to 90 % dry solids and keeps the black liquor in a pumpable form even at atmospheric pressure. This also allows storage of the strong liquor in atmospheric tanks. Viscosity reduction is especially beneficial, if the raw material and cooking method at the mill is such that the handling of strong liquor is a problem. One possible way to combine the LHT-process into an existing evaporation plant is shown in Figure 4-16.

The viscosity of the black liquor is determined by its composition. The polysaccharides like xylan are dissolved during the cook as long chain molecules which increase the original viscosity level of black liquor. The relationship is clearly shown when we compare the behavior of black liquors originating from different mills, Figure 4-17. In practice the effect of the lower viscosity and the reduced polysaccharide content shows up as decreased energy consumption in pumping and less severe

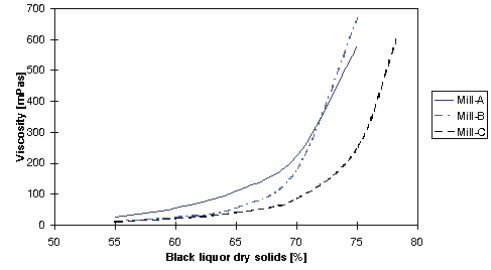

Figure 4-17, Viscosity of black liquors from three mills using liquor heat treatment; Mills A and B before heat treatment, Mill C after heat treatment.

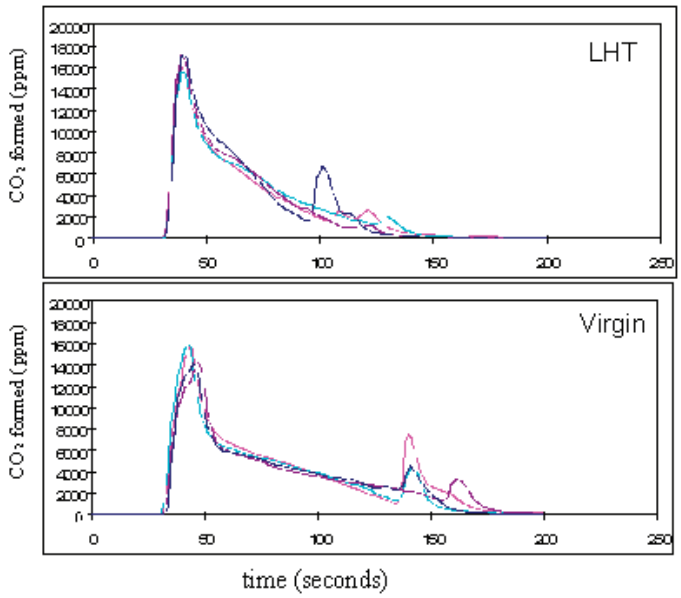

Figure 4-18, CO_2 profiles for liquors 3 and 4 at about 80 % dry solids for combustion at 3% O_2.

scaling in strong liquor pipes.

Simultaneously with the reaction of the polysaccharides and alkali there happens also another reaction. The sulfide in the liquor reacts with the lignin generating dimethylsulfide and methyl mercaptans. This gas is released from the liquor when the pressure is decreased after the treatment. However, the amount of DMS/MM formed can be controlled by adjusting the treatment conditions. The gas can be introduced into the malodorous gas treatment system and combusted in a lime kiln or in an existing NCG combustor.

The most of the benefits of using LHT are related to the boiler. Increasing the dry solids increases the boiler capacity and also efficiency. The benefits which are related to high dry solids combustion can be summarised as follows; reduced sulfur dioxide emission and higher temperature at the bottom part of the boiler. A well-known benefit of raising the dry solid level of black liquor is the reduced sulfur dioxide emission. The higher dry solids rises the temperature at the bottom part of the boiler. This gives higher sodium release from black liquor droplets. The Na can form Na_2SO_4 with the SO_2 present in the upper furnace. The achievable level of SO_2-emission is typically a function of two factors, the boiler load and the black liquor sulfidity.

LHT treatment splits long lignin chains. It has been observed (Backman *et al.*, 1996, Alèn, 1997) that increasing the amount of shorter (M_w 1500 … 3000) lignin chains increases swelling. Heat treatment of black liquor has also been found to increase the black liquor swelling during combustion (Backman *et al.*, 1996). The LHT can also affect beneficially to the NOx emissions (Forssén *et al.*, 1997). The amount of released NO convertible nitrogen and nitrogen remaining in the liquor is reduced with LHT.

Burning rate

For individual liquors an increased burning rate with LHT can be observed. The increased rate is more evident if we study the CO_2 content profile in the flue gas from combustion of individual droplets with on-line gas analysis. Figure 4-18 shows CO_2 profiles for a mill liquor with and without heat treatment. In the figure the disappearance of the CO_2 curve shows the end of char burning. The char combustion for the heat treated liquor was approximately 30% faster than for the untreated sample.

Swelling

Figure 4-19 shows the swelling during droplet combustion for all about 19 liquor samples (Vakkilainen *et al.*, 1998). First line in each series is swelling of a liquor sample without liquor heat treatment and subsequent 1 – 3 lines are for progressively more heat treatment. The swelling increased significantly for liquor 1->2 and clearly for liquors 3->6, 10->13, 14->16 and 17->19. Only for liquor 7->9 the swelling has decreased.

Liquor heat treatment increases swelling and decreases pyrolysis time and mass loss during

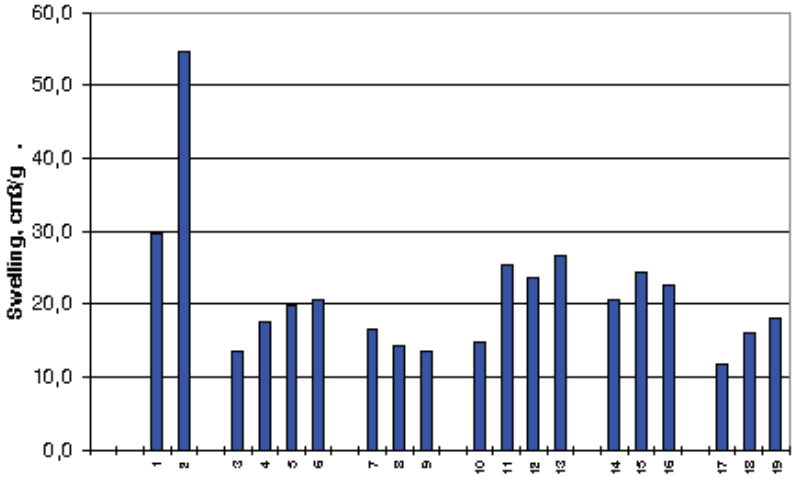

Figure 4-19, Swelling of black liquor.

pyrolysis. The increased burning rate is probably mostly a result of the increased swelling: Increased swelling increases the effective external surface area during the combustion process. This, again, gives higher heat transfer from the hot environment to the droplet and a higher heating rate during pyrolysis. Also, larger external surface increases the amount of oxygen diffused for char burning.

During liquor heat treatment volatile organic gases are released. It would seem natural to assume that the observed decrease in mass loss indicates that same compounds are released during pyrolysis. The mass loss during heat treatment is from 1 to 5 percent of incoming dry solids, Söderhjelm *et al.* (1998). The finding seems to suggest that in addition to mass loss, also other changes in the black liquor that affect combustion take place.

Milanova, 1998 states that two conditions have to be met for the char particle to swell. There must be gas generation inside the droplet and the droplet must have plastic surface properties. The liquor heat treatment affects the polysaccharide content and so also the surface properties of black liquor droplet.

The plot of polysaccharide versus swelling, Figure 4-20, shows decreased swelling with increased polysaccharide content. It is suspected that the change in liquor swelling can be attributed to changes in polysaccharide and low molecular weight lignin content.

Sulfur release

Sulfur release during pyrolysis at 900 °C for a mill

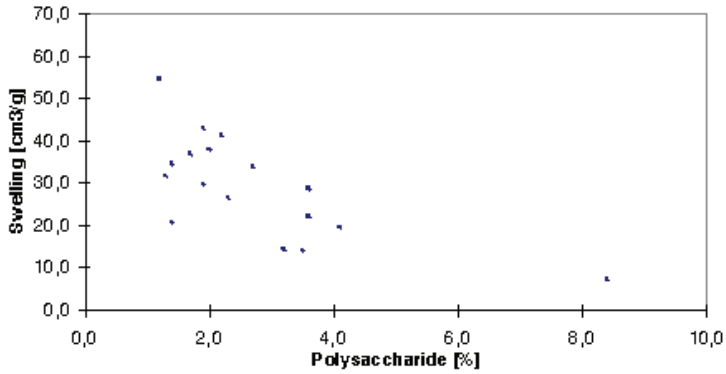

Figure 4-20, Swelling versus polysaccharides content.

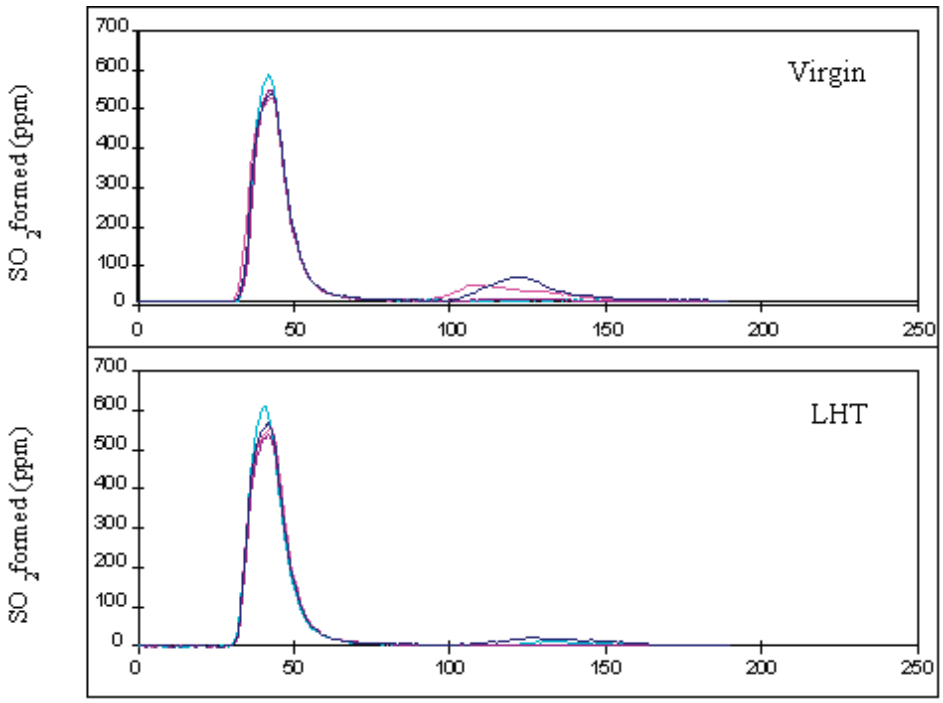

Figure 4-21, Sulfur release during combustion at 3 % O_2 and 900 °C for a mill liquors with and without LHT.

liquor is shown in Figure 4-21. The liquor heat treatment seems to decrease the sulfur release. Sricharoenchaikul *et al.* (1995) measured that the main pyrolysis products of black liquor droplets were dimethyl sulphide, methyl mercaptane and hydrogensulfide. The same products are the main species released during heat treatment. McKeough (1995) measured that of the main sulfur containing pyrolysis products of black liquor droplets the concentrations of dimethyl sulphide and methyl mercaptane decreased for heat treated liquors. This would seem to indicate that at least part of the sulfur released during pyrolysis comes from the lignin demethylation reactions. Manninen and Vakkilainen (1996) have modelled the black liquor droplets and found that changes in swelling do not wholly explain the changes in sulfur release.

Nitrogen release

Figure 4-22 shows from the on-line measurements amount of NO formed during the pyrolysis

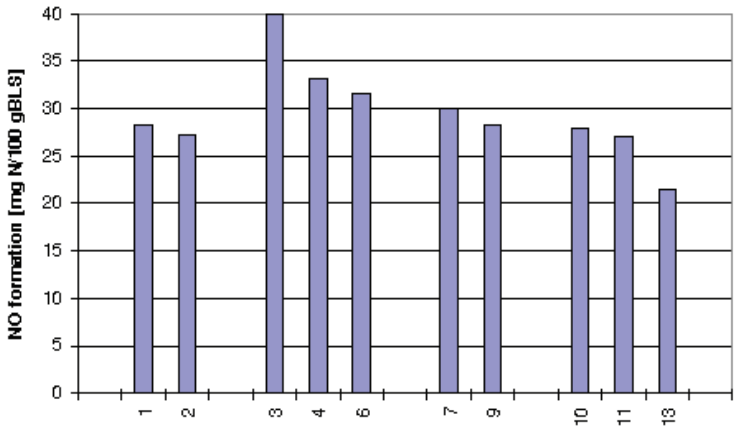

Figure 4-22, Nitrogen compound release as NO in flue gases during combustion at 3 % O_2 and 900 °C.

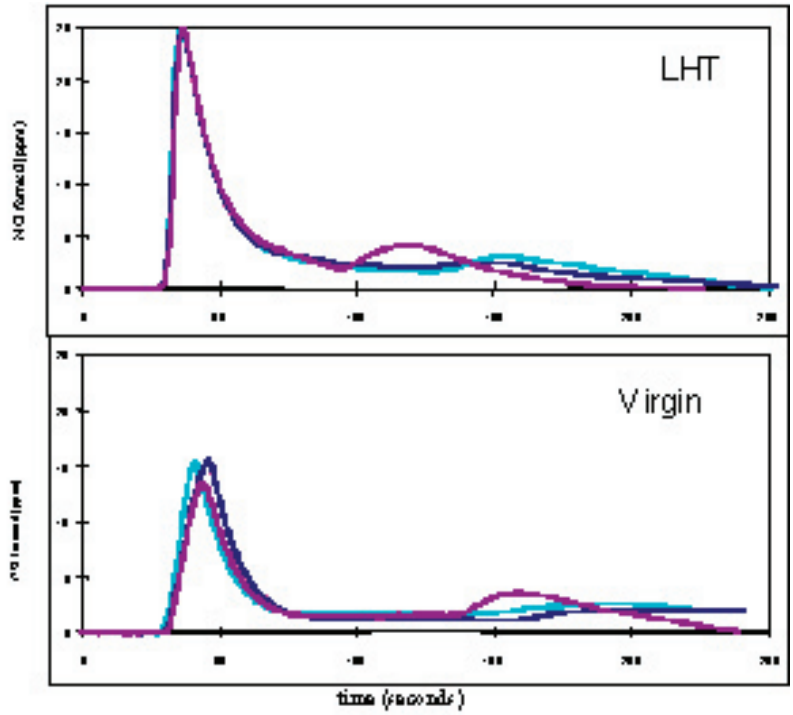

Figure 4-23, Nitrogen release during combustion at 3 % O_2 and 900 °C for a mill liquors with and without LHT.

stage. For the treated liquors the decrease in the NO formation is approximately 10 %. Decrease of nitrogen release during pyrolysis of heat treated liquors was also noted by Aho *et al.* (1993).

Base liquor nitrogen release (liquors 1, 3, 7 and 10) differs from each other. Heat treatment to these liquors decreases nitrogen release (liquors 2, 4, 9 and 11).

5 Chemical processes in furnace

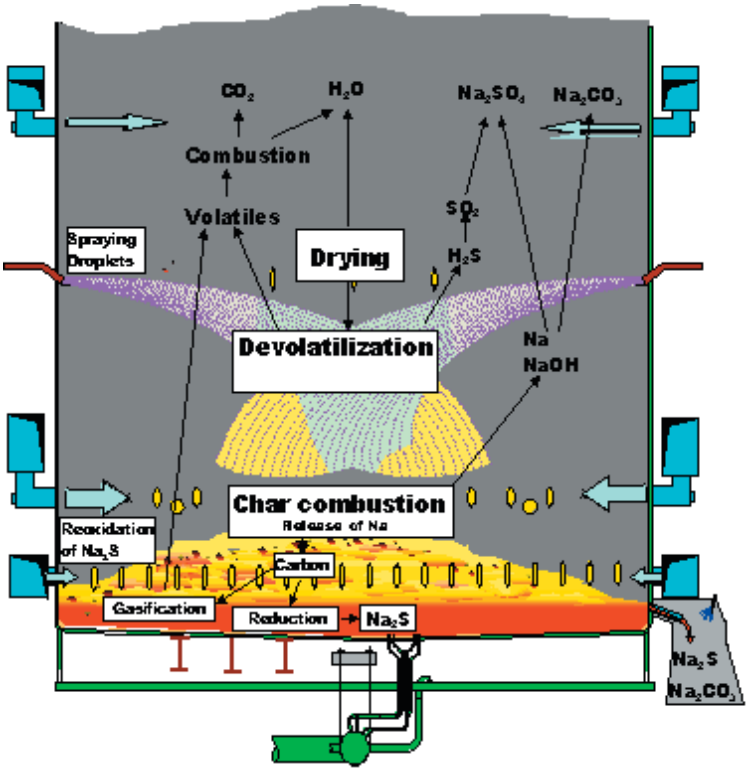

Figure 5-1, Some of the reactions in the lower furnace.

Recovery boiler processes efficiently inorganic and organic chemicals in the black liquor. Efficient inorganic chemicals processing can be seen as high reduction rate. The furnace also disposes of all organics in black liquor. This means stable and complete combustion. Reduction (removal of oxygen) and combustion (reaction with oxygen) are opposite reactions. It is difficult to achieve both at same unit operation, furnace.

Other furnace requirements are even more complex. A recovery boiler should have a high thermal efficiency. It should produce low fouling ash. Processes in the recovery boiler should be environmentally friendly and produce a low level of harmful emissions. In spite of successes, optimizing recovery boiler chemical processes is difficult. Processes are complex and there are several streams to and from the recovery boiler.

There are many simultaneous reactions going on in the lower furnace, Figure 5-1. First there are the black liquor burning processes described in Chapter 4. Drying occurs when water is evaporated, Devolatilization occurs when droplet size increases and gases generated inside the droplet are released. Finally char burning takes place when carbon is burned off. In the lowest part of the furnace there are char bed reactions. In addition to char burning, these consist mostly of inorganic salt, especially melt reactions. In the upper furnace there is volatiles combustion. Sodium sulfate and carbonate fume formation with other aerosol reactions take place. The best way to study the multitude of chemical reactions taking place in the recovery boiler is to look at first what we know of the conditions in the furnace and then individual reactions main component by main component.

5.1 FURNACE GAS PHASE

Above the char bed there is a mixture of air from primary and secondary air jets and combustion gases. Relatively few measurements of gaseous components in the recovery boiler furnace have been done. Most notably Roos (1968), Borg, Teder and Warnquist (1974) measured low solids boiler furnace gases. In addition equilibrium calculations of furnace have been done (Perjyd and Hupa, 1984).

***Table 5-1**, Concentration[ppm] in gas phase in the lower furnace, (Roos, 1968, Borg et al., 1974, Perjyd and Hupa, 1984).*

	Roos measured	Borg measured	Perjyd calculated
H_2		30 000	>10 000
H_2O		40 000	~100 000
CO	10..50 000	60 000	~100 000
CO_2	50..120 000	130 000	~100 000
O_2	1-40 000	50 000	~0
N_2		680 000	>10 0000
CH_4		10 000	
H_2S	1..10 000	300	~1 000
SO_2	10..100	1	10..1 000
Na			<10 000
NaOH			<10 000
NaCl			<1 000

***Table 5-2**, Measurements at the ninth floor (~10 m above nose).*

Component		Emission
SO_2	ppm	1
TRS	ppm	1
NOx	ppm	100
CO	ppm	85

***Table 5-3**, Measurements in the stack.*

Component		Emission
Water content	%	22.9
Temperature	°C	159.2
O_2 (wet)	%	3.2
CO_2 (wet)	%	15.7
CO	ppm	7.1
SO_2	ppm	1.1
TRS	ppm	1.2
NOx	ppm	105.6

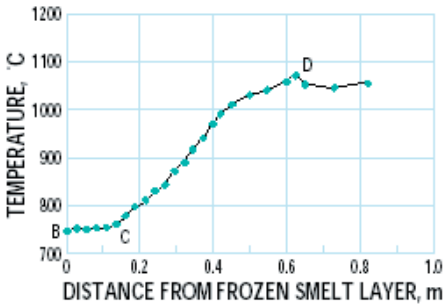

Figure 5-2, Char bed temperature profile (Tavares et al., 1998).

Experimental results and equilibrium calculations are compared in Table 5-1. It shows that there are large amounts of H_2 in the lower furnace. Multiple air levels can be seen as reducing atmosphere, which manifests itself with large concentrations of unburned CO in the lower furnace. Presence of O_2 as well as CH_4 shows that kinetic and/or mixing rates prevent reactions from reaching equilibrium. Use of equilibrium assumption in treating lower recovery furnace should be avoided.

Equilibrium calculations show that there are significant amounts of sodium compounds as fume in the lower furnace. Because furnace temperatures are rather low H_2S is the predominant result of free sulfur reactions. Formation of SO_2 would be significant with temperatures over 1100 °C.

The temperature of the gas immediately above the char bed is lower than the temperature of the gas 1 ... 2 m from bed surface. The IPC calculations (Jones, 1989) predicted a temperature gradient of 100 °C/m. Hellström (1977) and Jutila *et al.* (1978) measured similar gradients. When char bed temperatures are high, unprotected temperature probe will see almost constant temperature (Tavares *et al.*, 1998). In Figure 5-2 temperature of the char bed reaches close to 1100 °C. Distance 0 equals solid char bed. Measurements higher than distance D were made in lower furnace gas phase. The measured temperature profile is similar to the profile reported by Lundborg (1977) for an older boiler. The temperature at distance 0 was 783 °C and the gas temperature away char bed 1013 °C.

In all of the cases there was initially a temperature raise due to hot combustible gases from the char bed and the CO combustion. This was followed by a temperature drop of 100 ... 200 °C. The probable cause is the cooling effect of secondary air. Then the temperature increased again to reach a peak a few meters higher, where the main volatiles release/combustion takes place.

The published measured temperature maximums in the recovery boiler furnace are around 1100 ... 1200 °C (Jutila *et al.*, 1978, Shiang and Edwards, 1985). It should be noted that the boiler in question operated in extremely high load. It was also operated at combustion air deficiency of 10 %.

Vakkilainen and Holm (2000) present in furnace measurements in a modern high dry solids boiler. Tests were conducted with continuous emission measurement equipment. O_2-, CO-, SO_2-, TRS-, NO-, NO_2-content and temperature were recorded. Furnace gas measurements were done with air-cooled probes about 1.5 m from the walls. Furnace measurements were conducted at five

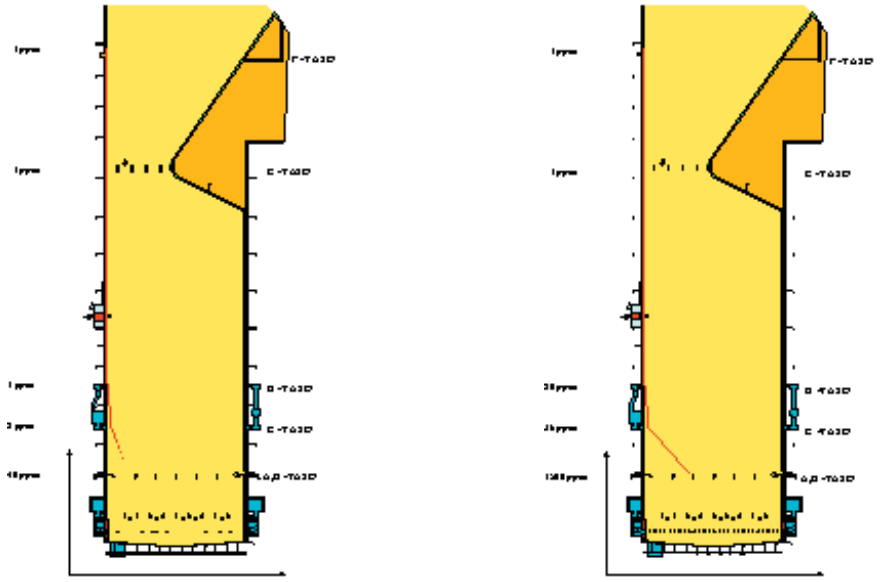

Figure 5-3, SO_2 (left) and TRS (right) from in furnace measurements.

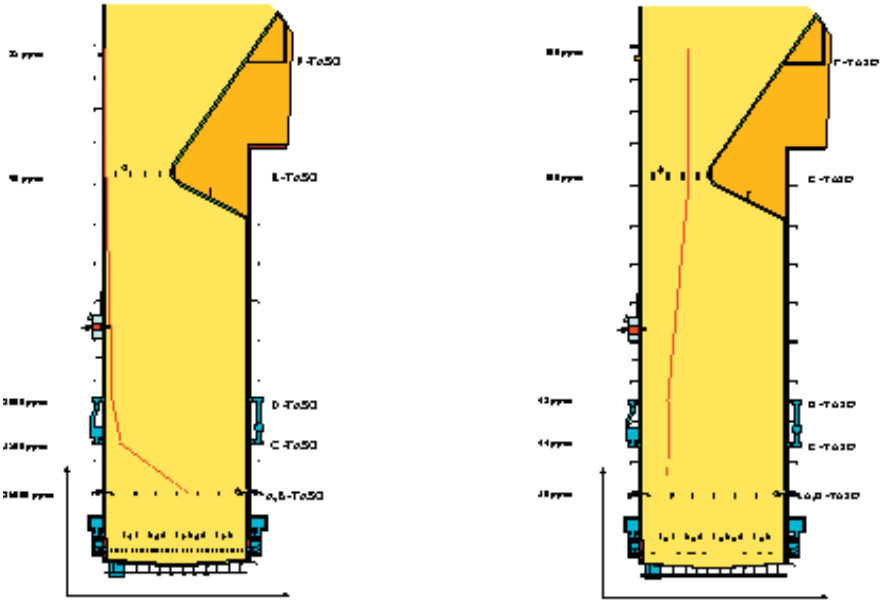

Figure 5-4, CO (left) and NOx (right) from in furnace measurements.

locations along different heights. Distance inside the furnace was about 2 m.

First emissions at approximately the nose level were measured. At the same time emissions were measured in the stack, Tables 5-2 and 5-3. It can be seen that the emissions remain constant from the nose to the stack. This being a modern high solids boiler can be seen as very low SO_2 and TRS contents. Earlier measurements (Boonsongsup *et al*., 1994) indicate higher emissions at the nose level and decreasing emissions from the nose level towards the boiler bank inlet. This might be explained by the differences in boiler size and higher solids fired. This boiler is much higher than the boilers in the earlier test. It has larger furnace and longer residence time.

The formation of emissions was studied by measuring emission profiles in the furnace. Similar but more limited studies have been reported from another boiler by (Vakkilainen *et al*., 1998). By looking at various measured emission profiles, Figure 5-3 and Figure 5-4, conclusions can be drawn for the emission performance of large boilers.

Sulfur emissions decrease to very low levels quickly, Figure 5-3. The sulfur release from sprayed black liquor droplets occurs mainly at or below the liquor gun level (Vakkilainen and Holm, 2000). Depending on the firing method it can extend down to the char bed level. The measured values of both SO_2 and TRS after the lower tertiary level were insignificant. The air system and consequently good mixing can explain the disappearance of TRS as it is oxidized to SO_2. It is possible that higher levels of sulfur compounds could have been measured close to the centerline of the recovery boiler. These measurements, however, clearly indicate that at or near the furnace walls the SO_2 will react with available fume. A full explanation of these results needs to wait until the reaction rates of several known sulfurdioxide-consuming reactions have been measured at high temperatures and a more comprehensive model of alkali release is available.

Good mixing by the air system is further seen in the decreasing trend for CO, figure 5-4. Most of the CO has reacted before the highest air level. The curves for CO and TRS look alike, probably because mixing heavily influences both.

Measured NOx profile is virtually identical to the earlier measurements (Vakkilainen *et al*., 1998) in another boiler, Figure 5-4. Fuel nitrogen species are released very fast, virtually with the volatiles release. It seems probable that much of the nitrogen species react after the last air level.

5.2 CHAR BEDS

The char bed is the heart of the recovery boiler. It is a pile of material that includes carbon, partially black liquor solids and smelt (Grace, 2001). The temperature in char bed changes from that of the water walls to that of flue gases. The materials in char bed can be molten, soft or solid. Without the char bed the main target of the recovery boiler, high reduction would be hard to achieve.

Char bed serves as repository of material. However the amount of incoming material must equal to the outflow of smelt and gases if the char bed is to remain stable. The bed grows locally if the rate of material reaching the bed exceeds that of material leaving the bed and decays if the rate of material reaching the bed is less than the rate of material leaving (Grace 2004).

The char bed receives new fresh include; liquor droplets from spraying, fallen residue from furnace walls and superheater area. In addition to falling char chunks, the material coming from the furnace walls includes molten smelt (Frederick, Singbeil and Kish, 2003).

Char bed takes care of a significant part of black liquor combustion. Dried and partially pyrolysed liquor droplets fall on it. Some of the carbonaceous material is gasified to be combusted in the upper furnace. The reduction of sodium sulfate in the char bed to sulfide is the main chemical process step in the recovery cycle. Sodium, potassium and chloride release takes place in the char bed.

Björkman and Warnquist (1985) state that only the region near the primary air ports is a site of efficient gasification. The rest of the bed being only a storage of pyrolyzed liquor. If this were true there would be large velocity and temperature gradients at the char bed surface. Viewing the char bed with the char bed imagining cameras reveals that also the secondary jets reach the char bed surface. Therefore the whole char bed surface serves as reaction zone.

Björkman & Warnquist further state that the gasification reaction creates inverted turbulent diffusion flames. It is clear that there exists mixing limitation above the char bed surface. Otherwise we could not measure high oxygen and high CO concentrations at the same time.

There have been different views of the importance of the char bed reactions. Björkman and Warnquist (1985) consider the weight fraction of particles that spend their 'life story' in flight to be insignificant. In the modern recovery boiler a

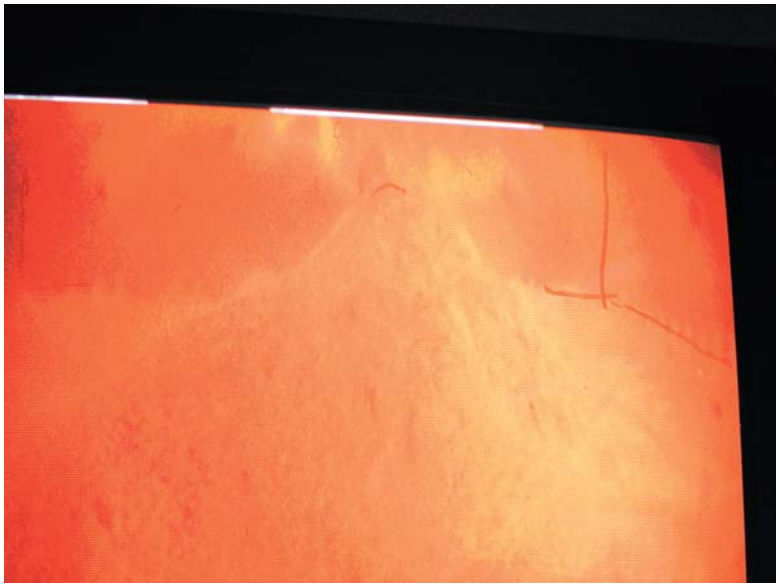

Figure 5-5, Char bed and boiler right and back wall through char bed camera (Saviharju and Pynnönen, 2003).

significant portion of the carbon release, maybe 60 … 70 % is happening in flight. Recent measurements (Tamminen *et al.*, 2002) have shown that maybe only 10 % of fume generation occurs in char bed.

There has been some char bed models produced to study the operation of char bed, (Richardson and Merriam, 1978, Shiang and Edwards, 1986, Sumnicht, 1989 and Sutinen *et al.*, 2002). They have provided insight on the basic events in the char bed. As there are only a few reported measurements of relevant char bed data those studies have formed the basis of our char bed understanding.

All these attempts have tried to model stationary char beds. In practice we see the char bed height and temperature changing. By creating a time dependent model of char bed it would be possible to model the real behavior of char bed. To create a time dependent char bed model, reaction rates for main reactions have to be determined. There are some measurements of char bed heat transfer behavior, from them time dependent behavior can be extrapolated. The flows in the char bed are a new challenge that has not been previously modeled.

Char bed physical characteristics

Char bed contains mainly carbonaceous char, sodium carbonate, sodium sulfate, sodium sulfide and sodium chloride with a smaller percentage of

***Table 5-4**, Thermal properties of char bed materials (Adams and Frederick, 1988).*

Material	Density kg/m^3	c_p J/kg^{o}C	λ W/m^{o}C	a 10^9 m^2/s
Inactive char	400-1330	1254	0.078	50-75
Active char	290-460	1254	0.28-0.38	500-1000
Smelt, liquid	923	1338	0.450	181
Smelt, solid	2163	1421	0.882	284

***Table 5-5**, Measured char bed composition (Heinävaara, 1991).*

Element		S1	S2	S3
Carbon, C*	%	0.5	2.4	0.3
Sulfur (tot), S	%	10.5	11.1	11.6
Sodium, Na	%	40.8	40.1	42.2
Potassium, K	%	3.9	4.0	4.2
Chloride, Cl	%	0.3	0.4	0.3
Magnesium, Mg	%	2.7	2.6	0.7
Calcium, Ca	10^{-6}	45.3	47.3	68.5
Iron, Fe	10^{-6}	69.8	161	161
Phosphor, P	10^{-6}	18.7	9.6	32.5
Na_2CO_3	%	66.2	74.1	63.6
Na_2SO_4	%	6.8	3.7	8.3
Na2S	%	21.6	24.9	23.3
$Na_2S_2CO_3$	%	0.9	1.0	0.8

* Measured as heating loss of the unsolvable portion of sample

potassium salts and unreacting material present. Typically the char bed shape is that of mostly flat pile with a 1 ... 2 m height and sloping sides. The top surface contains mounds and even smelt pools. The shape isn't constant, but changing with time so there are several other types of beds that have also been reported, Figure 5-5. In high beds there is a possibility of molten smelt pockets inside the bed. These pockets are not visible to the outside. The question remains whether there is a situation in char bed operation, which can be characterized as stationary.

The actual black liquor char content of the char bed is only 5 – 20 %. Most of it is inorganic salts (Warnqvist, 1994). Heinävaara (1991) has made measurements of char beds, Table 5-5.

The chloride in the char bed is only half the chloride in the incoming black liquor. This is because chloride volatilizes easily and thus participates in the dust recycle. The magnesium seems to enrich. The magnesium content in the char bed is about hundred times that of magnesium content of both the incoming liquor and the smelt. Reduction in the char bed is lower than at the outflowing smelt (Warnqvist, 1994).

During the ADL study (Merriam, 1978) a nitrogen cooled probe was used to get samples of incoming material. As can be expected the results from B&W and CE furnaces differed.

Most of the material reaching the char bed is either pyrolysed or gone through complete char burning. Sometimes portions of liquor reach the bed in a state of incomplete drying (Björkman & Warnquist, 1985).

Char bed temperature and density

The structure of char bed is mostly a mixture of frozen and liquid sodium salts in a carbon matrix. The char bed contains sections ranging from very porous to solid, glassy portions. Richardson and Merriam (1977) measured properties of several char beds during the ADL study. In their opinion only the top layer of the bed is hot and reacting. Measurements were made of temperatures, densities, thermal conductivities and thermal diffusivities. Some thermal properties of different char bed materials are shown in the Table 5-7. Richardson and Merriam (1977) observed that the bed surface temperature wasn't constant but there were cooler and hotter spots. They also measured temperatures and densities inside the bed, Table 5-7. In some measurements the maximum temperature in the bed was found to be up to 0.3 m deep in the char bed.

***Table 5-6**, Average composition of incoming material in char beds, weight percent. (Richardson and Merriam, 1977).*

Substance	Sample 1	Sample 2
C	10.7	7.1
Na_2S	8.6	3.7
Na_2SO_4	8.1	5.5
$Na_2S_2O_3$	6.2	2.6
Na_2CO_3	66.8	77.9
NaCl	-	-
NaOH	-	-
K_2S	-	-
K_2SO_4	-	-

***Table 5-7**, Measured temperatures and densities of char beds (Richardson and Merriam, 1977).*

Mill	Temperatures °C	Densities kg/m³
Westvaco CE, 1000 t/d	1060-1070, surface 1120-1150, surface	460, surface 2100, solid smelt
Brunswick	750-910, smelt BW	
Georgia	< 760, core, BW 795-810, smelt CE	
Ticonderoga BW, 500 t/d	650-705, core 770, 0.150 m deep 870-1100, surface	1300, char
Androscoggin CE, 600 t/d	960-1140, peak 770-830, core	

Table 5-8, *Measured thermal conductivities and diffusivities of char beds (Richardson and Merriam, 1977).*

Mill	Type, size	Conductivity, W/m²°C	Diffusivity W/m³°C
Ticonderoga	B&W, 500 t/d	0.078	160
Androscoggin	CE, 600 t/d	0.28, char 0.45, smelt	290

The surface temperatures measured in the ADL study are somewhat higher than the ones reported by Borg *et al.* (1973) Figure 5-6. STFI values were measured with a pyrometer.

New devices such as char bed imagining cameras (Harrison and Ariessohn, 1985) have revealed the cycling nature of char bed surface temperature. In

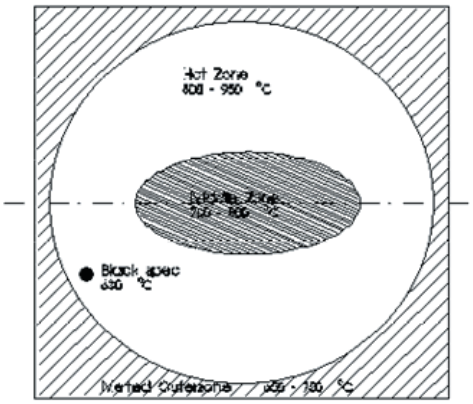

Figure 5-6, Char bed surface temperatures (reproduced from Borg et al., 1973).

addition growing and falling of bed surface up to 1 m/min was observed. Cyclic surface temperature variations of 80 °C/10 min were also observed.

The surface temperature of the char bed has a strong influence on emissions from recovery boilers. The higher the char bed surface temperature the higher the dust emissions and the lower the SO_2 and H_2S emissions (Chamberlain and Cairns, 1972). Borg *et al.* (1973) have stated that the H_2S emissions from the char bed decrease from 750 ppm to 250 ppm when the bed surface temperature increases from 825 to 860 °C. This is consistent with data from Lien *et al*, (2004) which state that fume and particle production from char bed start at about 850 °C.

Furnace loading and black liquor dry solids content have increased since 70's. This means that the surface temperatures are higher in the modern recovery boilers. The differences in density measurements were reportedly caused by uneven structures of char beds. The surface of the char bed is very porous. The deeper we go into the bed the denser it gets.

Thermal conductivity and diffusivity

In some mills char bed thermal conductivity and thermal diffusivity measurements were made, Table 5-8.

With high char beds cooldown times of 50 to 100 hours have been reported. This situation is aggravated if molten smelt pockets remain in the bed.

With high char beds cooldown times of 50 to 100 hours have been reported. This situation is aggravated if molten smelt pockets remain in the bed.

Bed cooldown and heat up

When recovery boiler is shut down the smelt bed remains. Typically oil firing is used to burn some of the bed out. To save the recovery boiler furnace bottom tubes all of it can't be removed.

Char bed cooling has been studied by Richardson and Merriam (1977, 1978). They conclude that, conditions leading to rapid cooldown of the bed are minimum height, high porosity in the top layers of the bed, and high content of solidified smelt in the remainder of the bed.

Char bed cooling rate is very slow as porous bed is a very good insulator. There can be molten smelt pockets remaining after 1 … 5 days from stop of firing. Bed inside temperature decay depends on the bed height, smelt content in the bed, and porosity and thickness of the top layers of the bed.

Heat transfer in char beds isn't solely conduction. Richardson and Merriam (1978) indicated that radiative heat transfer in the porous structure plays a role. Heat transferred with the flowing molten smelt is maybe the most significant heat transfer mode.

Char bed is a large heat sink. The typical hearth area loading of a modern recovery boiler is 0.2 kgds/s /m^2. With a HHV of 14.5 MJ/kgds this means heat input per char bed unit area of about 3 MW/m^2. Kelly *et al.* (1981) measured the smelt inventory of a CE boiler to be 250 kg/m^2. With an average smelt enthalpy of 1350 kJ/kg the heat in smelt per char bed unit area is about 340 MJ/m^2.

The average bed height is typically less than 2 m. The average char bed temperature is less than 800 °C. With average heat capacity of 2000 J/kg°C and density of 1300 kg/m^3 the heat in the char bed is less than 4200 MJ/m^2.

This means that the char bed contains about 1500 s worth of heat. The long cooling times observed are result of slow heat removal, not large heat content.

Safety

One of the main hazards in operation of recovery boilers is the smelt-water explosion. This can happen if even a small amount of water is mixed with the solids in high temperature. Smelt-water explosion is purely a physical phenomenon.

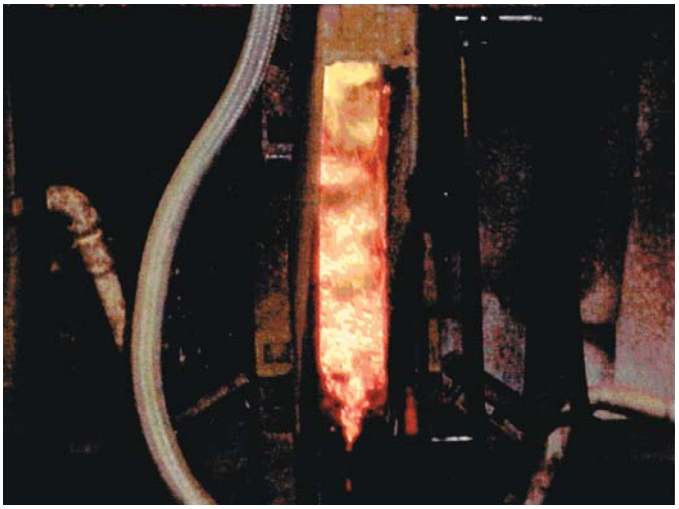

Figure 5-7, Smelt flow from char bed (Saviharju and Pynnönen, 2003).

The smelt water explosion phenomena have been studied by Grace (1988). The liquid - liquid type explosion mechanism has been established as one of the main causes of recovery boiler explosions.

In the smelt water explosion even a few liters of water, when mixed with molten smelt can violently turn to steam in few tenths of a second. Char bed and water can coexist as steam blanketing reduces heat transfer. Some trigger event destroys the balance and water is evaporated quickly through direct contact with smelt. This sudden evaporation causes increase of volume and a pressure wave of some 10 … 100 000 Pa. The force is usually sufficient to cause all furnace walls to bend out of shape. Safety of equipment and personnel requires an immediate shutdown of the recovery boiler if there is a possibility that water has entered the furnace. All recovery boilers have to be equipped with special automatic shutdown sequence.

The other type of explosions is the combustible gases explosion. For this to happen the fuel and the air have to be mixed before the ignition. Typical conditions are either a blackout (loss of flame) without purge of furnace or continuous operation in a substoichiometric state. To detect blackout flame monitoring devices are installed, with subsequent interlocked purge and startup. Combustible gas explosions are connected with oil/gas firing in the boiler. As also continuous O_2 monitoring is practiced in virtually every boiler the noncombustible gas explosions have become very rare.

5.3 SMELT

Smelt is the product of inorganic reactions in recovery furnace. At the same time the carbon is consumed the residual inorganic portion melts. Inorganics flow out of the furnace through smelt spouts, Figure 5-7. The amount of smelt inside recovery boiler furnace has been measured by Kelly *et al.* (1981). They found the smelt content per furnace unit area to be about 250 kg/m^2 for a decanting CE unit and about 140 kg/m^2 for a B&W unit. The residence times found were 44 and 25 minutes respectively.

Smelt temperature is about 100 °C higher than initial deformation temperature (Sandquist, 1987). In older low solids boilers the smelt temperatures are 750 … 810 °C (Lundborg, 1977). In modern high solids boilers the typical smelt temperatures are 800 … 850 °C.

The smelt flow corresponds typically from 0.400 to 0.480 kg per kilogram of incoming black liquor dry solids flow, Figure 5-8. The points highest from average are caused by very high potassium contents.

Reduction and sulfidity

The main process property of the smelt is the reduction. Reduction is usually expressed as the molar ratio of Na_2S to Na_2SO_4,

$$\textit{Reduction} = Na_2S/(Na_2S+Na_2SO_4) \qquad 5\text{-}1$$

The higher the reduction the lower the amount of sodium that reaches the cook unusable. Reduc-

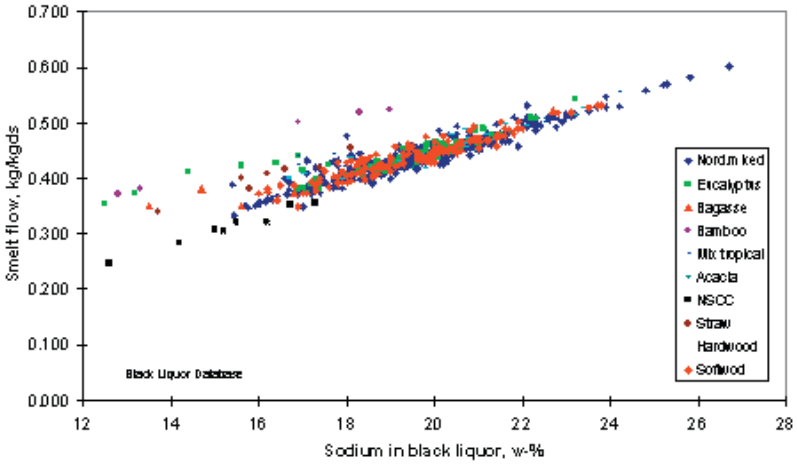

Figure 5-8, Smelt flow as function of sodium in black liquor.

tion rates of 95 ... 98 % are not uncommon in well operated recovery boilers. Usually the reduction efficiency increases as the char bed temperature increases. From thermodynamical equilibrium calculations we note that there should be very little of sodium oxides and thiosulfate.

Sulfidity is the molar ratio of sodium sulfide to the total alkali content.

$$Sulfidity = S_{tot}/(Na_2+K_2) \qquad 5\text{-}2$$

This equation is widely in use because of ease of measuring Sulfidity depends on the liquor circulation of the mill. Too high a sulfidity causes operating problems for the recovery boiler. Especially increased sulfidity increases SO_2 and TRS emissions (Chamberlain and Cairns, 1972).

Often the typical mill analysis of reduction rate is done for green liquor. Alkali in the green liquor will typically result in lower values that what is measured in smelt, Figure 5-9. Typically in modern mills the reduction in green liquor is 2 … 3 percent points lower that in smelt.

Smelt composition

Smelt compositions for modern recovery boilers don't vary much, Table 5-9. The amount of sodium chloride and potassium compounds is a function of their concentration in the black liquor. When we think of smelt composition it must be borne in mind that smelt having greater than 2 % carbon content is not flowing but rigid (Grace, 1997).

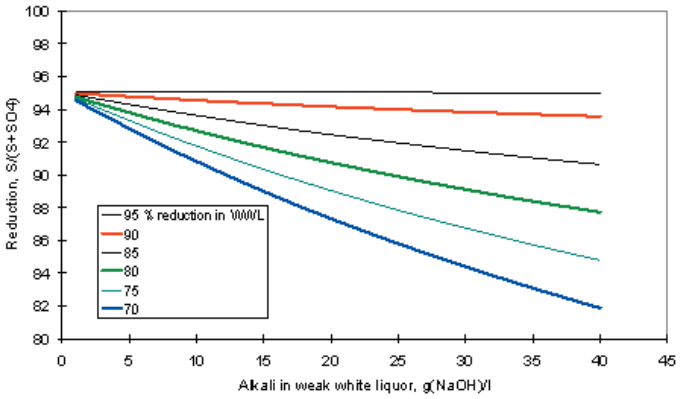

Figure 5-9, Effect of weak white liquor composition on reduction in green liquor, reduction is smelt 95 %, sulfidity 35 %.

***Table 5-9**, Smelt composition.*

		Softwood	Hardwood
Na_2S	%	25 – 28	19 - 21
Na_2CO_3	%	66 – 68	72 - 75
Na_2SO_4	%	0.4- 1.0	0.6- 1.4
$Na_2S_2O_3$	%	0.3- 0.4	0.2- 0.4
Others	%	5 - 6	3 - 5

***Table 5-10**, Properties of smelt (Wozniak, 1985).*

Property	Sub-stance	Tempera-ture, K	Measured value
Surface ten-sion, N/m	Na_2CO_3	1218 - 1244	0.208
	Na_2SO_4	1232	0.189
	Na_2SO_4	1261	0.188
	Na_2SO_4	1285	0.187
Density, kg/m^3	Na_2CO_3	1218 – 1244	1927 – 1917
	Na_2SO_4	1232 – 1261	2032 – 2018

***Table 5-11**, Physical properties of selected components (Himmelblau, 1989).*

Component	Melt. K	Boil. K	Density kg/m^3	Formula wt
Calcium carb., Ca_2CO_3	dec.	1098	2930	100.09
Calcium oxide, CaO	2873	3123	2620	56.08
Chromium, Cr	1888	2473	7100	52.01
Copper, Cu	1356	2855	8920	63.54
Ferric oxide, Fe_2O_3	1883	dec.	5120	159.77
Magnesium, Mg	923	1393	1740	24.32
Magnesium oxide, MgO	3173	3873	3650	40.32
Potassium, K	1032	dec.	860	39.10
Potassium carb., K_2CO_3	1264	dec.	2290	138.27
Potassium cyanide, KCN	907	-	1520	65.11
Potassium chloride, KCl	1063	1773	1988	74.56
Potassium hydr., KOH	653	1593	2044	65.10
Potassium sulfate, K_2SO_4	860	-	2662	174.25
Potassium sulfide, K_2S	333	-	-	200.33
Silicon dioxide, Si_2O	1883	2503	2250	60.09
Sodium, Na	371	1153	970	22.98
Sodium carb., Na_2CO_3	1126	dec.	2533	105.99
Sodium cyanide, NaCN	835	1770	-	49.01
Sodium chloride, NaCl	1081	1783	2163	58.45
Sodium hydroxide, NaOH	592	1662	2130	40.00
Sodium sulfate, Na_2SO_4	1163	-	2698	142.05
Sodium sulfide, Na_2S	1223	-	1856	78.05
Sulfur, S	386	718	2070	32.07

dec. = decomposes before this step

In poorly operating recovery boilers the dregs in green liquor reach 2 000 … 4 000 mg/l, while improved operation results in 100 … 1 000 mg/l (Clement *et al*., 1995). Saviharju and Pynnönen (2003) measured carbon contents in smelts from boilers equipped with vertical air. Carbon content ranged from 0.07 to 5.2 gC/kgNa or 5 … 500 mg/l while total dregs varied 400 … 4 000 mg/l. Carbon content was in one sample more than 50 %. This is significantly higher that the typical values reported by Lidén (1995). He found that carbon content in dregs rarely exceeded 5 w-%.

Some important smelt properties were measured in the IPC by Wozniak (1985), Table 5-10. Typically the smelt solidifies totally at about 550 °C. This temperature is however influenced by the minor constituents of the smelt. Ahlers has measured a quick drop of melting point from 750 °C to 580 °C, when the smelt NaCl composition increased from 0 to 10 % (Ahlers, 1971).

5.4 SODIUM

Sodium is released during the black liquor burning and char bed reactions through vaporization and reduction of sodium carbonate (Li and van Heiningen, 1990). Sodium release from combusting black liquor increases as a function of temperature, Figure 5-10. At beginning of combustion large portion of sodium is connected to the organic portion of the black liquor. At the end of volatiles release almost all of it is inorganically bound.

Sodium release in kraft recovery boilers increases with increasing lower furnace temperature, Figure 5-11. It has been assumed that in industrial boilers all of the ESP dust is from reactions with vaporized sodium. In addition the amount of sodium released as a function of carbonate in ESP dust seems to increase. Increase in carbonate indicates increase in lower furnace temperature (Vakkilainen, 2000). Sodium content in black liquors is around 20 w-%. This means that sodium release in recovery furnace is about 10 % of the sodium in black liquor.

Much studied reactions involving sodium are hydroxide formation, reduction reactions, and sulfate formation with hydroxides, sulfate formation with chlorides, sulfate formation with carbonate and carbonate formation.

Some of the sodium reactions occurring in recovery furnace are shown in Figure 5-12 and listed below.

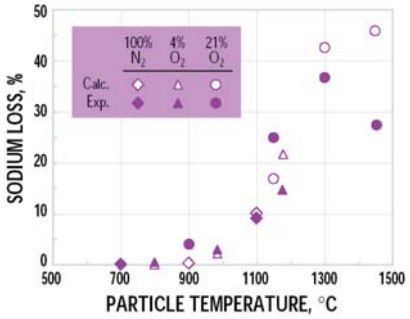

Figure 5-10, Sodium loss from combusting black liquor as a function of actual particle temperature in a LEFR for 100 µm particles (Wåg et al., 1997).

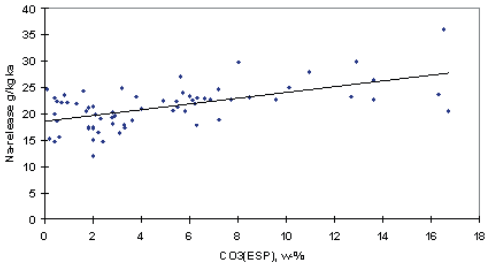

Figure 5-11, Sodium release to ESP ash as function of carbonate in ash in industrial boilers

$$Na_{(c)} \rightarrow Na_{(g)} \quad 5\text{-}3$$

$$Na_2CO_3 + 2C \rightarrow 2Na_{(g)} + 3CO \quad 5\text{-}4$$

$$Na_2S + CO_2 + H_2O \rightarrow Na_2CO_3 + H_2S \quad 5\text{-}5$$

$$Na_{(g)} + H_2O \rightarrow NaOH + H \quad 5\text{-}6$$

$$Na_2SO_4 + 4C \rightarrow Na_2S + 4CO \quad 5\text{-}7$$

$$NaOH + SO_3 \rightarrow Na_2SO_4 + H_2O \quad 5\text{-}8$$

$$NaOH + NaHSO_4 \rightarrow Na_2SO_4 + H_2O \quad 5\text{-}9$$

$$Na_2CO_3 + 2SO_2 + 0.5O_2 \rightarrow Na_2SO_4 + CO_2 \quad 5\text{-}10$$

Carbonate reduction

Carbonate reduction (reaction 5-4) seems to be the one of the main carbon consuming reactions after volatiles release above 900 °C (Järvinen, 2002). If carbonate reduction is the main sodium release reaction, then sodium and sulfur release are independent.

Reactions with oxygen

In the char bed, high concentrations of oxygen immediately above the bed has been measured. Borg *et al.* (1974) measured oxygen concentrations of 3 ... 5 %. The two implications of this are that either there was not enough mixing or the reactions are kinetically limited.

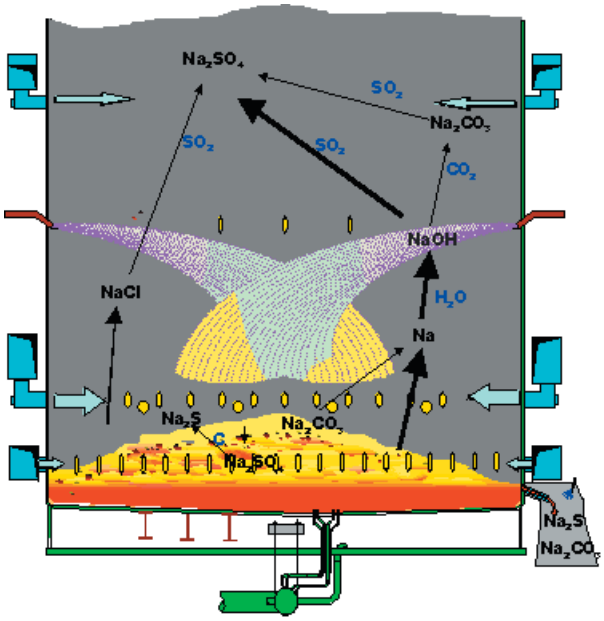

Figure 5-12, Reactions of sodium and potassium in the lower furnace (Reactions of potassium are similar to reactions of sodium).

Inside char particles there are gas producing reactions. Oxygen is consumed by reactions with carbon dioxide and hydrogen. Oxygen stays mainly outside the char (Wåg *et al.*, 1995, 2002). It seems that direct reactions of char with oxygen are rather limited.

Reactions with carbon dioxide and monoxide

$$Na_2S + CO_2 + H_2O \rightarrow Na_2CO_3 + H_2S \qquad 5\text{-}11$$

Sodium sulfide can react with carbon dioxide and produce hydrogen sulfide.

Reduction

The carbon has a dual role in the char bed (Grace, Cameron and Clay, 1985). During the sulfate-sulfide cycle the carbon reacts with Na_2SO_4 to form Na_2S. If smelt contacts air it can oxidize. The reduction process is slow requiring significant residence time to be completed to a high degree.

The sodium sulfate - sulfide cycle was discovered by Grace, Cameron and Clay. In it the three competing reactions take place; Oxidation of sulfide

$$Na_2S + 2O_2 \rightarrow Na_2SO_4 \qquad 5\text{-}12$$

and reduction of sulfate by char

$$Na_2SO_4 + 2C \rightarrow Na_2S + 2CO_2 \qquad 5\text{-}13$$

$$Na_2SO_4 + 4C \rightarrow Na_2S + 4CO \qquad 5\text{-}14$$

It can be observed that to achieve high reduction efficiencies the rate of sodium sulfide oxidation has to be much lower than the rate of sodium sulfate reduction. It is generally accepted that in kraft recovery boilers the sulfide oxidation is mass transfer controlled (Wåg *et al.*, 1997). High reduction can be achieved by having reactive, fresh char on top of char bed.

Cameron and Grace (1982) measured the rate of reduction reaction with the presence of carbon. The rate equation was found to be

$$\frac{\partial [SO_4]}{\partial t} = - K_{Red} \frac{[SO_4]}{B + [SO_4]} C e^{-\frac{E_a}{RT}} \qquad 5\text{-}15$$

The constants measured for kraft char were

K_{Red} = 1.31+0.41*103, 1/s
B = 0.022+0.008, kmol/m^3
E_a = 122, kJ/kmol

The rate is fairly independent of sulfate content up to about 94 % reduction, but then reduces sharply. This in addition of smelt surface oxidation explains why reduction rates of more than 95 % are hard to achieve. The air requirement to complete this cycle is about 20 ... 40 % of total air.

Sjöberg and Cameron (1984) studied the sodium sulfate reduction with CO.

$$Na_2SO_4 + 4CO \rightarrow Na_2S + 4CO_2 \qquad 5\text{-}16$$

They found the rate equation to be

$$\frac{\partial [SO_4]}{\partial t} = - K_{CO} p_{CO} e^{-\frac{E_{CO}}{RT}} \qquad 5\text{-}17$$

The constants measured were

K_{CO} = 31.7 kmol/m^{3}atms
E_{CO} = 115 kJ/kmol

Birk *et al.* (1971) have measured the sodium sulfate reduction by hydrogen.

$$Na_2SO_4 + 4H_2 \rightarrow Na_2S + H_2O \qquad 5\text{-}18$$

They found the hydrogen reduction rate to be about six times faster than with CO at 840 °C. Because of water shift reaction there is hydrogen inside char bed.

In addition to carbon monoxide and hydrogen, water vapor can reduce sodium sulfide. Rates of these reactions are more than two orders of magnitude slower than with carbon at recovery boiler conditions (Grace, 1997). Their role in kraft recovery boilers is insignificant (Sjöber and Cameron, 1984).

Reactions with water vapor

Water vapor can react with sulfide and create sodium bisulfide. This reaction is responsible for decrease in causticization rate. So it is very probable that until the black liquor droplet has dried there is some sodium hydroxide present.

$$Na_2S + H_2O \rightarrow Na_2S + 4H_2O \qquad 5\text{-}19$$

Sodium carbonate can react with water vapor and produce sodium hydroxide (Blackwell and King, 1985), but probably the rate controlling step is sodium carbonate decomposition.

$$Na_2CO_3 + H_2O \rightarrow 2NaOH + CO_2 \qquad 5\text{-}20$$

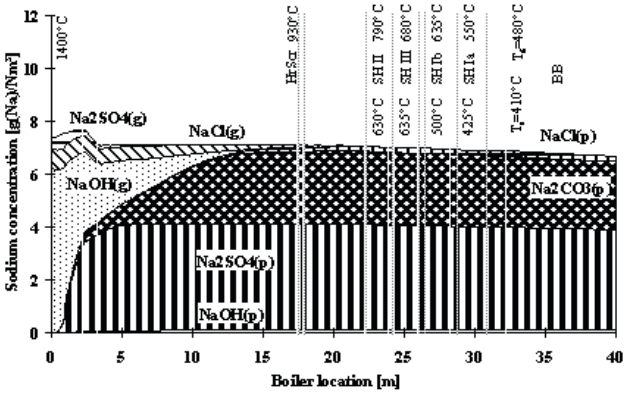

Figure 5-13, Equilibrium composition curves (Eskola et al., 1998).

Formation of sodium vapor

Based on Figure 5-13 the most probable gaseous components are sodium chloride and sodium hydroxide. Existence of metallic sodium is not thermodynamically favorable. There have been discussions as what is the form of sodium release. Gaseous sodium, sodium atoms and sodium oxide have been suggested as products. There is a large amount of water vapor in recovery boiler furnace. After release most of the sodium reacts fast to sodium hydroxide (NaOH) (Jokiniemi *et al*., 1993, Jokiniemi *et al.*, 1995). Furnace tests have detected as much as 26 w-% alkali hydroxides in lower furnace fume deposits (Tavares *et al*., 1995).

Iisa and Jing (2000) studied sodium vaporization in a laminar entrained flow reactor. In their experiments with nineteen black liquors the sodium release seemed to be fairly independent of the liquor Na content. They also added sodium salts to one black liquor. They found that the sodium release could best be correlated to amount of fixed C at the resulting liquor. This seems to indicate that none of the additions substantially changed sodium release reactions and that sodium release seems to be dependent on organic portion of the liquor.

Cameron (1988) showed that sodium can be released by oxidation of sodium sulfide.

$$Na_2S + O_2 \rightarrow 2Na + SO_2 \qquad 5\text{-}21$$

Sodiumsulfate and -carbonate decomposition

Sodium sulfate can decompose

$$Na_2SO_4 \rightarrow 2Na + SO_2 + O_2 \qquad 5\text{-}22$$

This reaction would produce sulfur dioxide and oxygen in addition to volatile sodium. The reaction is more favorable at high temperatures and low oxygen concentrations.

Sodium carbonate can decompose

$$Na_2CO_3 \rightarrow Na_2O + CO_2 \qquad 5\text{-}23$$

There is an abundance of water vapor present so probably sodium hydroxide is formed

$$Na_2O + H_2O \rightarrow 2NaOH \qquad 5\text{-}24$$

5.5 POTASSIUM

Potassium in the black liquor originates from the wood supply. Typically its content is 3 ... 5 % of the sodium content (Tran 1989).

Potassium is chemically related to sodium. Practically all sodium compounds will also exist as potassium compounds. They behave similarly in kraft recovery furnace. Potassium release seems to correlate well with sodium release in industrial boilers, Figure 5-14.

Potassium release is on average about 1,5 times higher than sodium release and a bit more than 15 w-% of potassium in black liquor. It has been suggested that significant amounts of potassium can be released through potassium chloride vaporization (Verrill and Wessel, 1998). Data from industrial boilers indicates that potassium enrichment and chlorine do not correlate, Figure 5-15. The potassium in the black liquor will enrich close

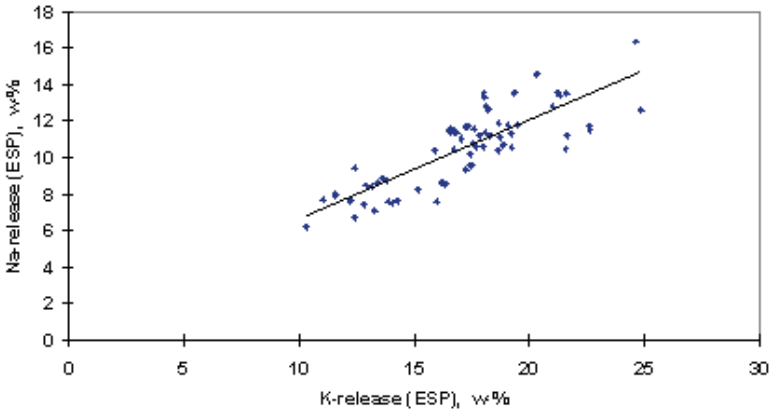

Figure 5-14, Sodium release versus potassium release in industrial boilers.

to the tube surface, Table 5-12 (Klarin 1992).

***Table 5-12**, Elementary analysis of char bed close to the tube surface (Klarin, 1992).*

Distance from tube surface, mm	2-5	5-10	10-30	>30
Color	Black	Grey	Yellow	Red
Solubility to water	Very good	Good	Fair	Slow
Aluminum, Al	0	0.27	0.33	0.08
Chloride, Cl	1.6	1.85	0.35	0.32
Iron, Fe	0	0	0.4	0.14
Potassium, K	12.0	5.77	5.09	7.15
Silica, Si	0.30	0.22	0.33	0.77
Sodium, Na	38.1	67.6	67.8	64.7
Sulfur, S	48.0	24.3	25.8	26.8
S/Na_2	2.52	0.72	0.76	0.83
K/Na_2	0.32	0.09	0.08	0.12

5.6 SULFUR

Sulfur emissions play a crucial role in the char bed reactions. The one main concern in any recovery boiler is; will we get low enough sulfur emissions. The sulfur in black liquor is for the most part in inorganic sulfur compounds. The main inorganic compounds are sulfide and sulfate. In addition minor amounts of thiosulfate, sulfite and polysulfates are present (Grace, 2001). 30 to 40 % of sulfur is bound to organosulfur compounds. Thiosulfate and organic sulfur are rapidly released from gaseous sulfur compounds (Jing and Iisa, 2001).

The sulfur as such is not stable compound at recovery boiler furnace conditions. Björkman

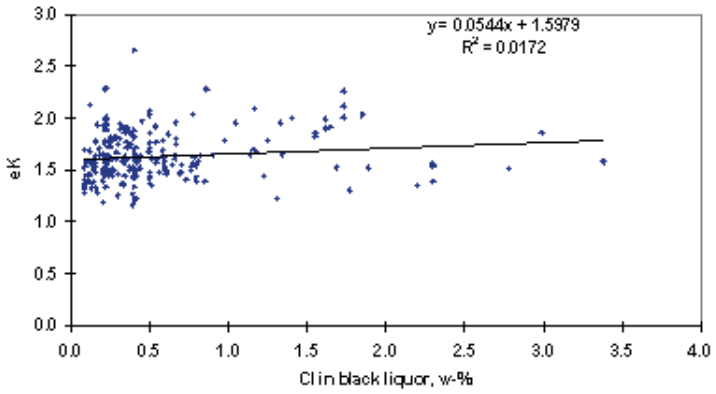

Figure 5-15, Potassium release versus chloride in black liquor in industrial boilers.

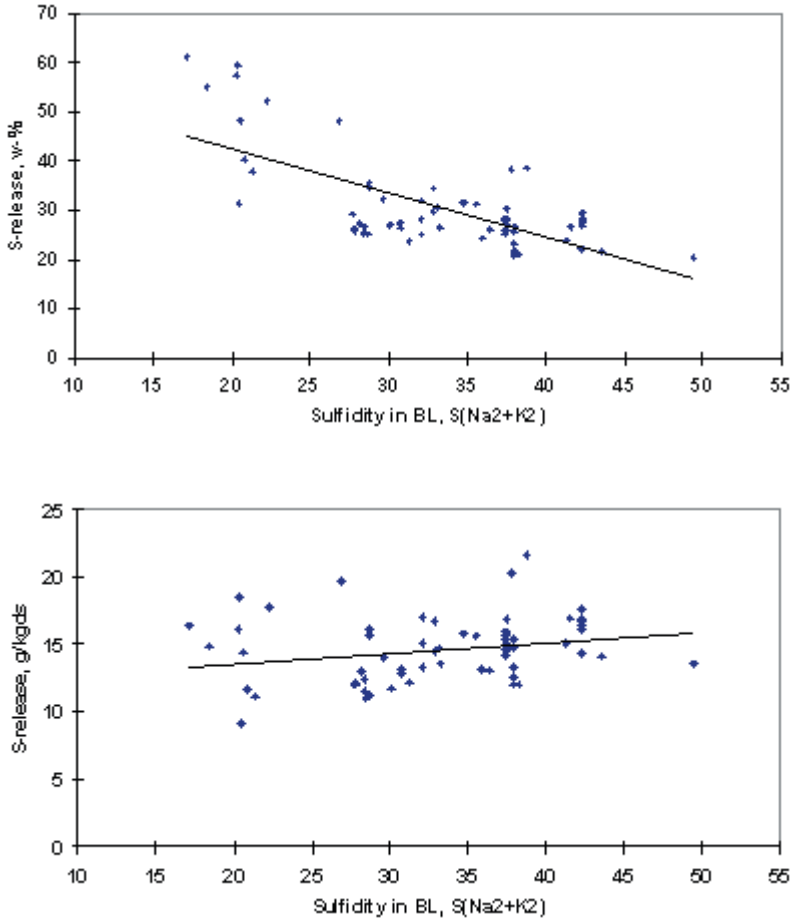

Figure 5-16, Sum of sulfur in SO_2 and sulfur in ESP dust in industrial boilers, upper figure % of sulfur released, lower figure total release as function of black liquor sulfidity. rofile, dry gases.

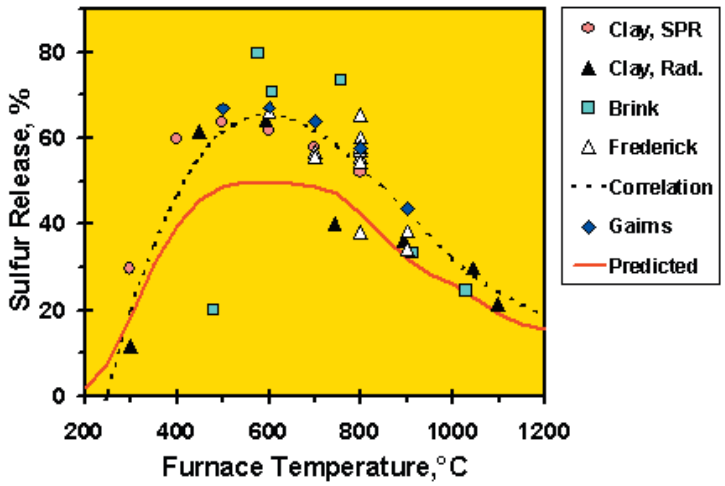

Figure 5-17, Sulfur release as function of temperature (Wessel and Kaufman, 2000).

and Warnquist (1985) claim that about 30 % of incoming sulfur leaves the recovery boiler furnace in the flue gas and fume. Ångpanneföreningen's measurements from ten boilers in Sweden indicated about 15 gS/kgds sulfur release when sulfidities were between 30 and 45 mol-% and about 20 gS/kgds sulfur release when sulfidity was around 50 mol-% (Moberg, 1973). Recent industrial data from modern boilers, Figure 5 – 16, show that sulfur release is between 10 and 20 gS/kgds. Dry solids does not have a strong correlation with sulfur release. It seems that sulfur release as sum of S in ESP dust and SO_2 is very insensitive to differences in virgin sulfidities of black liquor.

In upper part of Figure 5-16 released fraction of sulfur decreases with increased sulfidity. In lower part of Figure 5–16 total release is hardly affected by black liquor sulfidity. Sulfur release is about 15 g/kgds or 20 … 40 w-% of sulfur.

It should be pointed out that the form by which sulfur leaves the recovery boiler is very sensitive to dry solids. At high dry solids hardly any gaseous SO_2 is leaving the boiler.

In laboratory conditions the measured sulfur release as function of temperature resembles a bell shape (Forssén *et al*., 1992). Single droplet data, Figure 5-17, tends to overpredict the sulfur release. Therefore somewhat lower values have been used to arrive to realistic levels (Wessel and Kaufman, 2000). Generally it is believed that sulfur release is inversely proportional to the furnace temperature and that it is a function of black liquor droplet heating rate. Faster heating produces lower sulfur release.

Figure 5-18 shows theoretical predictions compared to experimental values in one furnace (McKeough and Janka, 2001). Actual parameter that varied was boiler load, but measured data was plotted versus lower furnace temperature. Increase in temperature of 100 °C would decrease sulfur release by 25 %. Magnusson (1977) states that recovery boiler load affects the sulfur release. Data from industrial boilers suggests that load does not affect the sulfur release above 2 MW/m^2 load.

Contrary to Figure 5-18 general trend from boilers seems to be that increase in dry solids does not affect the sulfur release, Figure 5-19. Similarly the boiler specific load does not seem to affect the sulfur release. Manninen and Vakkilainen (1996) found through their theoretical sulfur release model that droplet size affected somewhat the sulfur release. It is probable that differences on the results from various sources reflect also the way the boilers are fired.

Reactions leading to formation of H_2S

Sulfur release from the black liquor has been studied extensively. It is released as organic volatiles, through reduction of thiosulfate and from reaction of sulfide with gaseous species. The formation of hydrogen sulfide H_2S is considered the main pathway to the formation of sulfur emissions.

Li and Heiningen (1991) found that during pyrolysis about 22 % of all sulfur in the incoming black liquor was released. In addition after the sample reached about 470 °C the sulfur emissions in the nitrogen atmosphere stopped. The sample

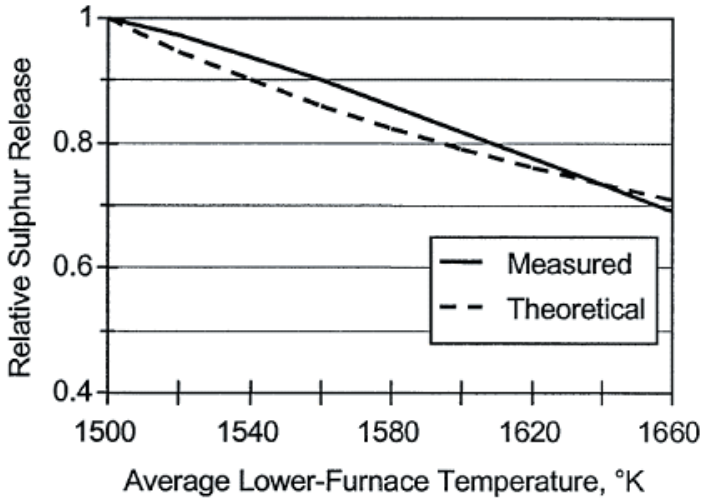

Figure 5-18, Sulfur release as function of furnace temperature (McKeough and Janka, 2001).

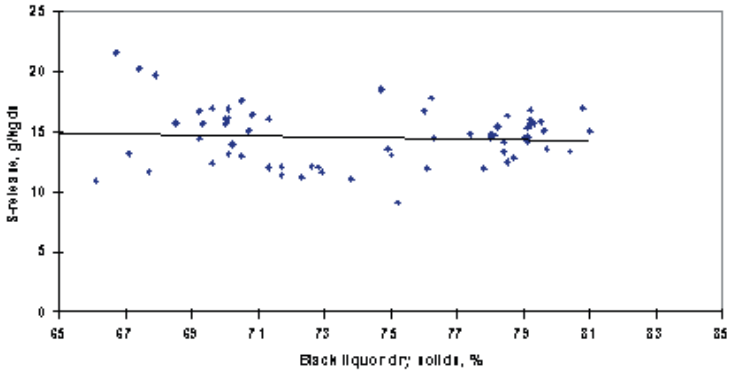

Figure 5-19, Sulfur release as function of black liquor dry solids.

must have also been dried by then so neither H_2O nor CO_2 gasification could take place. Typically sulfur release after volatiles release stops.

McKeough *et al.* (1995) attribute inorganic sulfur reactions to reaction of sulfide and reduction of thiosulfate. Thiosulfate in black liquor seems to decompose very fast < 0.3 seconds (Sricharoenchaikul *et al.*, 1995). In laboratory experiment about 40 – 50 % of sulfur in thiosulfate and 20 – 70 % of sulfur in sulfide was released (Kulas *et al.*, 1989).

$$Na_2S + CO_2 + H_2O \rightarrow Na_2CO_3 + H_2S \qquad 5\text{-}25$$

$$Na_2S_2O_3 + CO_2 \rightarrow Na_2CO_3 + SO_2 + S \qquad 5\text{-}26$$

$$Na_2S_2O_3 + 3CO \rightarrow Na_2S + S + CO_2 \qquad 5\text{-}27$$

In pyrolysis tests about 30 % of released sulfur was hydrogen sulfide. Most of the sulfur release came when methoxyl groups of dissolved lignin in black liquor react with hydrogen sulfide ions. Primary reaction is formation of methyl mercaptan (MM) and secondary reaction is formation of dimethyl sulfide (DMS) (McKeough *et al.*, 1995).

$$Liginin\text{-}OCH_3 + NaHS \rightarrow Lignin\text{-}ONa + CH_3SH \qquad 5\text{-}28$$

$$CH_3SH + NaOH \rightarrow CH_3SNa + H_2O \qquad 5\text{-}29$$

$$Liginin\text{-}OCH_3 + CH_3SH \rightarrow Lignin\text{-}ONa + (CH_3)_2S \qquad 5\text{-}30$$

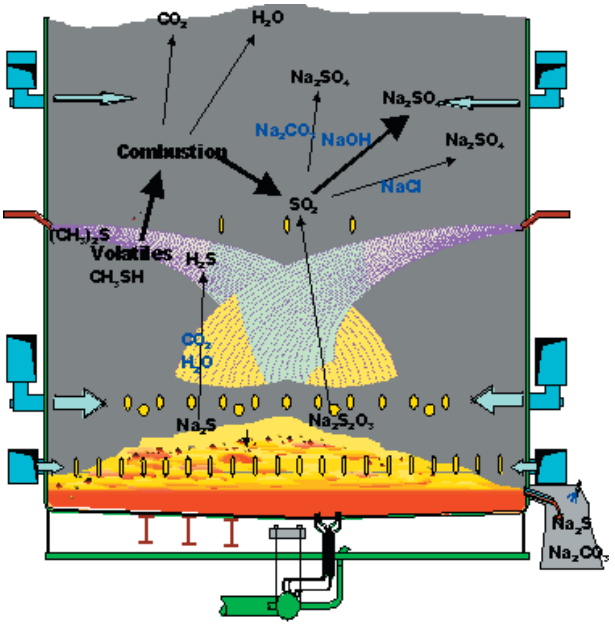

Figure 5-20, Reactions of sulfur in the lower furnace.

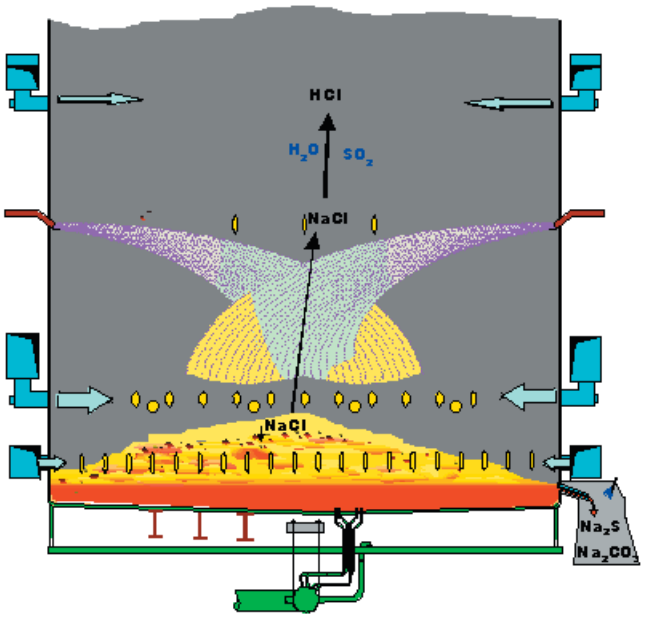

Figure 5-21, Chloride reactions in the lower furnace.

In high temperature conditions at lower furnace methyl mercaptan and dimethyl sulfide will quickly decompose to carbohydrates and hydrogen sulfide.

Gaseous reactions of sulfur

Oxidation of hydrogen sulfide is in furnace conditions fast and requires mostly proper mixing.

$$2H_2S + 3O_2 \rightarrow 2SO_2 + 2H_2O \quad 5\text{-}31$$

Other gas stream reactions involve fume reactions with sodium. Sulfate formation with hydroxides, sulfate formation with chlorides and sulfate formation with carbonate.

Some of the sulfur reactions occurring in recovery furnace are shown in Figure 5-20 and listed below.

$$Na_2S + \text{-}OCH_3 \rightarrow CH_3SH,(CH_3)_2S \quad 5\text{-}32$$

$$Na_2S_2O_3 \rightarrow Na_2S + SO_2 \quad 5\text{-}33$$

$$Na_2S + CO_2 + H_2O \rightarrow Na_2CO_3 + H_2S \quad 5\text{-}34$$

$$2H_2S + 3O_2 \rightarrow 2SO_2 + 2H_2O \quad 5\text{-}35$$

$$NaOH + SO_2 \rightarrow NaHSO_3 \quad 5\text{-}36$$

$$Na_2CO_3 + 2SO_2 + 0.5O_2 \rightarrow Na_2SO_4 + CO_2 \quad 5\text{-}37$$

Sulfation of sodium carbonate

Sulfation of sodium carbonate has been suggested as the capture mechanism for sulfur dioxide (Blackwell and King, 1985). Reaction rate of gaseous sulfur dioxide or trioxide with solid sodium carbonate is too small to affect significantly to sulfur capture (Frederick *et al.*, 1995).

$$Na_2CO_3 + 2SO_2 + 0.5O_2 \rightarrow Na_2SO_4 + CO_2 \quad 5\text{-}38$$

5.7 CHLORIDE

Chloride can be assumed to be entirely of NaCl. Chloride compounds found in the flue gas are mostly released due to direct vaporization.

The chloride is released from black liquor char by vapor pressure. It is unclear whether it is released as pure Cl(g), chloride gas Cl_2(g) or sodium chloride NaCl(g). It however reacts very fast to form hydrogen chloride HCl(g).

Some of the sodium chloride reactions occurring in recovery furnace are shown in Figure 5-21 and listed below.

$$NaCl_{(s,l)} \rightarrow NaCl_{(g)} \quad 5\text{-}39$$

$$NaCl + NaHSO_4 \rightarrow HCl + Na_2SO_4 \quad 5\text{-}40$$

$$NaCl + H_2O \rightarrow HCl + NaOH \quad 5\text{-}41$$

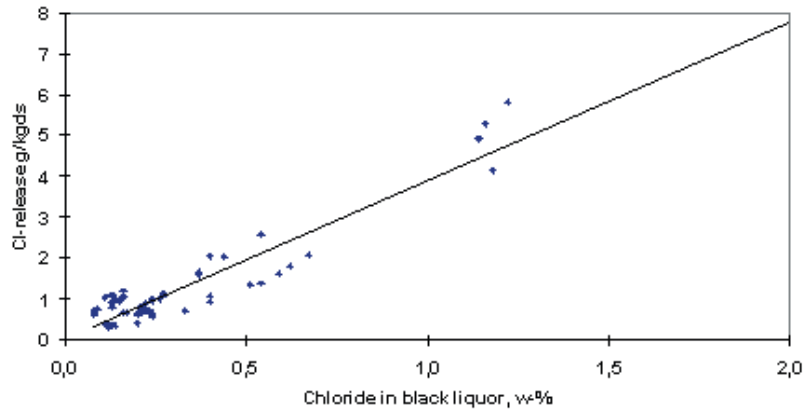

Figure 5-22, Chloride release from operating recovery boilers.

Chloride release

Iisa and Jing (2000) studied chloride vaporization in a laminar entrained flow reactor. In their experiments with nineteen black liquors the chloride release seemed to be linearly dependent of the liquor Cl content. They also added sodium chloride to two black liquors. The chloride release increased almost linearly to chloride content in the resulting liquor. Same linear regression in laminar entrained furnaces was observed for black liquor and black liquor with KCl addition (Khalaj *et al.*, 2004). Linear behavior is observed also for industrial boilers, Figure 5-22.

Increasing temperature increases chloride release in laminar entrained furnaces (Khalaj *et al.*, 2004). However the recovery boiler furnace temperature has weaker effect on chloride release than on sodium release (Janka *et al.*, 2004).

In earlier laminar entrained flow reactor experiments more than 60 % of chloride in black liquor was released (Wåg *et al.*, 1997). Because of large flue gas flow and small liquor flow the chloride release in LEFR experiments is not limited by sodium chloride vapor pressure, so results can be misleading.

Sulfation of sodium chloride

Sulfation of sodium chloride has been suggested as a capture mechanism for sulfur dioxide (Blackwell and King, 1985). Reaction rate of gaseous sulfur dioxide with solid sodium chloride at 400 … 600 °C is too small to affect significantly to sulfur capture to deposits (Frederick *et al.*, 1995). Equilibrium studies suggest that it is not possible to completely convert gaseous sodium chloride to sulfate before the superheater section (Iisa, 2004).

$$2NaCl + SO_2 + 0.5O_2 + H_2O \rightarrow Na_2SO_4 + 2HCl \quad 5\text{-}42$$

Hydrochloric acid found in recovery boiler flue gas corresponds roughly to 1/3 of sulfurdioxide present (Someshwar and Jain, 1995). This strongly supports the existence of this type of mechanism at recovery boiler.

Sodium chloride – hydrochloric acid

Sodium chloride can react with water vapor to hydrochloric acid. Equilibrium calculations suggest that equilibrium amount would be very small.

$$NaCl + H_2O \rightarrow NaOH + HCl \quad 5\text{-}43$$

5.8 REACTIONS INVOLVING CARBON

The main reactions involving carbon in the lower furnace belong to two classes. Carbon is released from combusting black liquor as organic volatiles, through char combustion and then with reduction of sulfate. Possibly also reactions of carbonate and char gasification are significant. Gas stream reactions occurring mainly above the char bed include oxidation of carbon monoxide to dioxide, formation of carbonate.

Some of the carbon reactions occurring in recovery furnace are shown in Figure 5-23 and listed

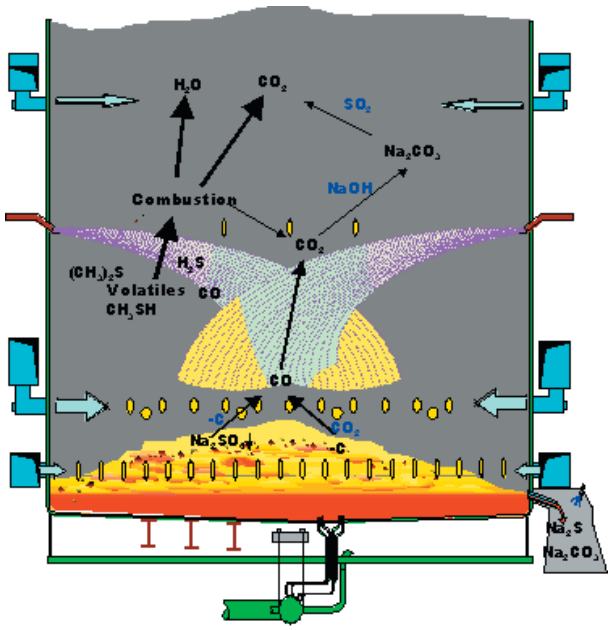

Figure 5-23, Reactions involving carbon in the lower furnace.

below.

$$Na_2S + -OCH_3 \rightarrow CH_3SH,(CH_3)_2S \quad 5\text{-}44$$

$$-C_{(s)} + H_2O \rightarrow CO + H_2 \quad 5\text{-}45$$

$$-C_{(s)} + CO_2 \rightarrow 2CO \quad 5\text{-}46$$

$$2CO + O_2 \rightarrow 2CO_2 \quad 5\text{-}47$$

$$CO + H_2O \rightarrow CO_2 + H_2 \quad 5\text{-}48$$

$$Na_2SO_4 + 4C \rightarrow Na_2S + 4CO \quad 5\text{-}49$$

$$Na_2S + CO_2 + H_2O \rightarrow Na_2CO_3 + H_2S \quad 5\text{-}50$$

$$2NaOH + CO_2 \rightarrow Na_2CO_3 + H_2O \quad 5\text{-}51$$

$$Na_2CO_3 + 2SO_2 + 0.5O_2 \rightarrow Na_2SO_4 + CO_2 \quad 5\text{-}52$$

Main carbon containing products from black liquor pyrolysis in laminar entrained flow reactor tests are tars, CO, CO_2 and various hydrocarbons (Sricharoenchaikul *et al.*, 1995). Main hydrocarbon product was methane which had yield 3 … 6 w-% of carbon. Other smaller hydrocarbon species were methanol, ethylene, acetylene, acetaldehyde, acetone and formaldehyde. McKeough *et al.*, 1995 noted that increasing temperature increased carbon monoxide production.

Char combustion

In recovery boiler furnace the carbon in the char is combusted to CO_2. The required oxygen for char combustion can come from oxygen, O_2, elemental oxygen, O, sodium sulfate, Na_2SO_4, water vapor, H_2O or carbon dioxide, CO_2. For coal combustion the main reactions are the surface C - O_2 and C - CO_2, which produce CO. The CO is used by the gas phase CO - O_2 reaction (Makino, 1990). The reaction rate of C - CO_2 is several orders of magnitude slower than the C - O_2 reaction. In the charbed the oxygen concentration is very small, because CO will consume the oxygen.

$$-C_{(s)} + 0.5O_2 \rightarrow CO \quad 5\text{-}53$$

$$-C_{(s)} + O_2 \rightarrow CO_2 \quad 5\text{-}54$$

Järvinen (2002) has modeled black liquor combustion. During char combustion water vapor and carbon dioxide gasification seem to be the dominant reactions, Figure 5-24. Direct oxidation of char was negligible.

The water vapor can react according to the Langmuir-Hinshelwood kinetics with C to form CO and H_2.

$$-C_{(s)} + H_2O \rightarrow CO + H_2 \quad 5\text{-}55$$

Adomeit *et al.* (1976) noted first the big effect of water vapor on char combustion rate of coal char.

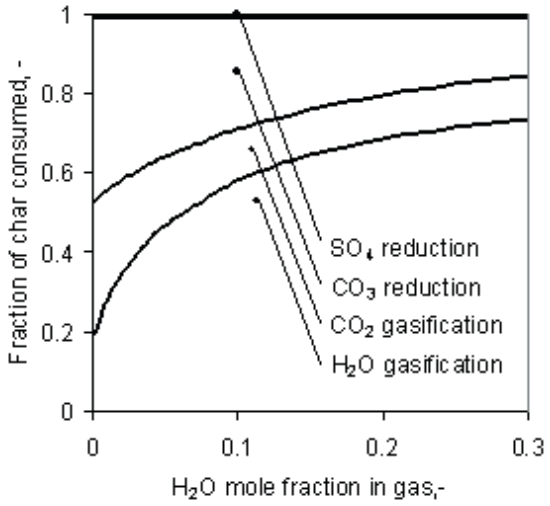

Figure 5-24, Contributions of different mechanisms, 4 % O_2, 12 % CO_2, 3 mm particle, 1200 °C (Järvinen et al., 2001).

In recovery boilers the char combustion by water vapor gasification is one of the largest reactions (Järvinen, 2002). From one third to one half of all char conversion occurs with water vapor. Most of this vapor comes from inside the particle.

The char combustion rate, in flight, for coal particles is independent of surrounding CO_2 concentration (Mitchell and Madsen, 1986).

$$-C_{(s)} + O_2 \rightarrow CO_2 \qquad 5\text{-}56$$

In recovery boilers char gasification by carbon dioxide is one of the main reactions (Järvinen *et al.*, 2001).

Sutinen *et al* (2002) modeled experiments by Brown *et al* (1998). They concluded that an athmosphere with carbon dioxide present will increase the char combustion rate from the char bed surface. Both carbon dioxide and water vapor can react with carbon. Conversely the addition of water vapor seemed to decrease somewhat the char consumption rate. They concluded that presence water vapor increased CO oxidation to CO_2 and thus decreased overall reaction rate.

Reaction rates of carbon at char beds are much lower than the overall combustion rate (Sutinen *et al.*, 2002, Hupa, 2004). Probably more than 60 % of all carbon reactions occur above the char bed. This means that suspension firing is the dominant firing mode.

6 Dimensioning of heat transfer surfaces

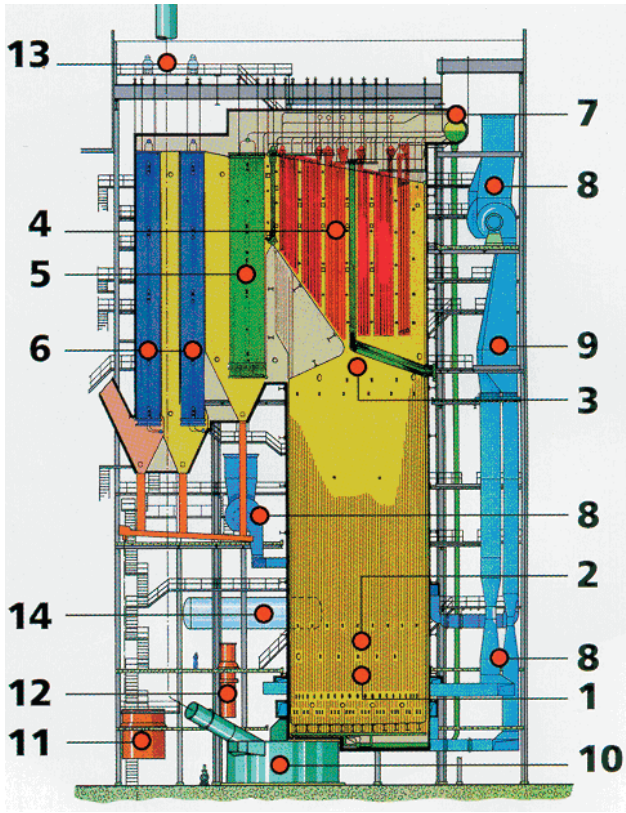

Figure 6-1, Main parts of a recovery boiler.

Recovery boiler dimensioning reflects on the properties of the design fuel, black liquor. The evolution of recovery boiler design follows the evolution of industrial boilers in general. Black liquor is a low calorific fuel, therefore the furnace is large. Fume deposits on surfaces have total emissivity about 0.5 (Wessel *et al.*, 1998). As normal boiler tubes have emissivity of 0.8 this makes radiative heat transfer low. Black liquor has extremely high ash content; therefore the heat transfer surfaces have been designed fouling in mind. Black liquor is corrosive, therefore moderate flue gas temperatures, steam temperatures and steam pressures are used.

As with many industrial devices exact design rules and especially operating margins implemented by different manufactures vary. The recovery boiler design also improves and changes by time. This text aims to present some general guidelines that can be followed when purchasing and projecting a recovery boiler. They can not give for all cases an optimum answer, because of differences in fuels, construction details and materials. So caution should be used when using the presented set of guidelines.

A typical example of modern recovery boiler is shown in Figure 6-1. Pressure parts are made from steel tubing. Lower furnace part (1) is made from compound tube and has start-up burner openings, primary and secondary air ports. Above these in the furnace (2) are liquor guns and tertiary air ports. Example boiler is of single drum (7) design with vertical flow boiler bank (5). Feedwater from feedwater tank (14) is fed to economizers (6) and

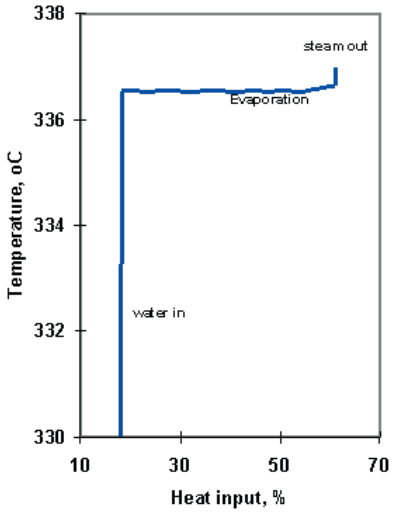

Figure 6-2, Evaporation.

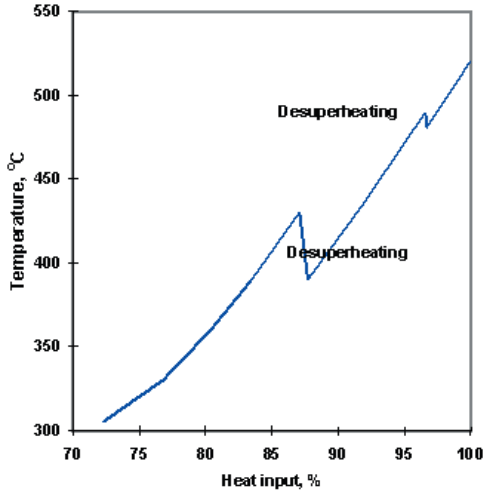

Figure 6-3, Superheating.

further to drum. Steam from drum is superheated in panel superheaters (4). Dolezahls (13) condense steam, which is sprayed to control main steam temperature. Superheaters are protected by screen tubes (3).

Electrostatic precipitator and hopper ash is mixed with black liquor in a mix tank (11). Black liquor temperature is controlled by indirect black liquor heater (12). Air for combustion is supplied by fans (8) and heated by steam air heaters (9). Heated air is inserted to the furnace through air ports. Smelt from furnace flows to the dissolving tank (10).

6.1 MAIN HEAT TRANSFER SURFACES

The main heat transfer surfaces in recovery boiler are evaporative surfaces (2, 3 & 5), superheating surfaces (4) and water preheating or economizing surfaces (6). Each type of surface has its own function in boiler design. The main characteristic of all these surfaces is that they are preliminary made of seamless tube.

There are other heat transfer surfaces that belong to the auxiliary equipment. Dolezahl steam attemperator has typically tube surface. Air preheaters are finned tube surfaces. Smelt spout cooling water and dissolving tank vent circulation exchangers are often plate type surfaces.

Evaporating

In the first steam generators, phase change consumed most of the heat. Phase change from water to steam is called evaporation or boiling. The whole process of evaporation from saturated water to saturated steam takes place at almost constant temperature. At low heat flux conditions this temperature is called the saturation temperature and can be found from e.g. steam tables (Schmidt, 1989, Wagner and Kruse, 1998). Most of evaporation takes place in the furnace below the nose. Less evaporation is done on the upper walls of the furnace. Often about 10 … 15 % of evaporation is done in a dedicated evaporator. This surface is also called boiler generating bank or boiler bank.

Inside heat transfer coefficient for boiling in natural circulation boilers is high. It is in the rage of 30 000 … 120 000 W/m^{2}K. This means that the tube average temperature is close to the saturation temperature.

Because of natural circulation there is no pressure loss across an evaporating surface.

Superheating

Increase of steam temperature from saturated temperature is called superheating. Superheating was first used to dry steam. Soon it was realized that superheating allowed for higher power production (Hills, 1989). Typically the total superheating surface is divided into stages. Large recovery boilers have four to six superheaters. These superheaters are arranged from two to four stages. Water is sprayed to steam between superheating stages to control the final steam temperature.

Steam density is rather low. So the inside heat transfer coefficient in superheaters tends to be low.

Therefore we need high velocities on the order of 10 … 25 m/s to improve heat transfer. Typically superheater inside heat transfer is in the rage of 1 000 … 5 000 W/m^{2}K.

High velocities mean high pressure loss. Typically the pressure loss over the superheating section is more than 10 % of the main steam pressure.

Economizers

If flue gases would leave boiler after the evaporative surfaces they would have temperature of more than 350 °C. Heat in these flue gases can be used to preheat water. Preheating decreases final flue gas temperature and improves boiler heat efficiency. Discovery of this principle in 1800s lead to greater fuel economy. Therefore the water preheating surfaces are called economizers.

Ideally preheating is done up to saturation temperature. In practice some margin for evaporative temperature is needed to prevent boiling. If boiling occurs, unstable water surges can seriously harm boiler operation and even damage it. In practice temperature margin of about 30 °C at MCR is often used.

Water is dense and generally economizers have high inside heat transfer coefficients. Inside heat transfer coefficient in recovery boiler economizers is very low, because the used water velocities are extremely low. Inside heat transfer coefficient is in the rage of 500 … 2 000 W/m^{2}K.

Pressure loss in economizers is very low because of low water velocities. It is often so low that to ensure even water distribution orifices need to be used.

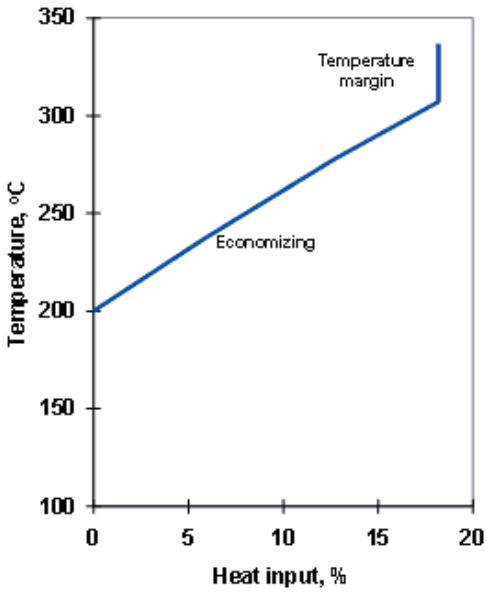

Figure 6-4, Economizing

6.2 HEAT LOAD CALCULATION

The steam boiler design starts with heat load calculation. In heat load calculation each type of heat transfer surface is assigned a load or heat flow based on desired total steam generation.

h-p diagram for water/steam

h-p diagram for water, Figure 6-5 can be used to determine operating conditions and the required heat loads for heat transfer surfaces. Starting from chosen steam outlet pressure and temperature a line is drawn down and right towards desired feedwater inlet pressure and temperature. Enthalpies where saturated steam and saturated water lines are crossed are marked.

Evaporation (boiling)

The first estimation of heat required for transforming water to steam is the difference between the points where the line crosses saturated steam and saturated water lines.

As can be seen there is no phase change above critical pressure (22.12 MPa). This means no evaporative surfaces are needed. Water behaves continuously in this region. In general, lower operating pressure means larger latent heat requirement for the phase change. Higher operating pressure means that more superheat and preheat is required.

Superheat

The first estimation for the heat required to superheat steam is the enthalpy difference between the main steam outlet point and the point where the line crosses saturated steam line, Figure 6-6.

With higher pressures the portion of heat required for superheating increases, up to critical pressure, Figure 6-6. Because of some 1 MPa pressure loss in the superheaters the line angles to the right. This pressure loss slightly increases the superheating heat requirement.

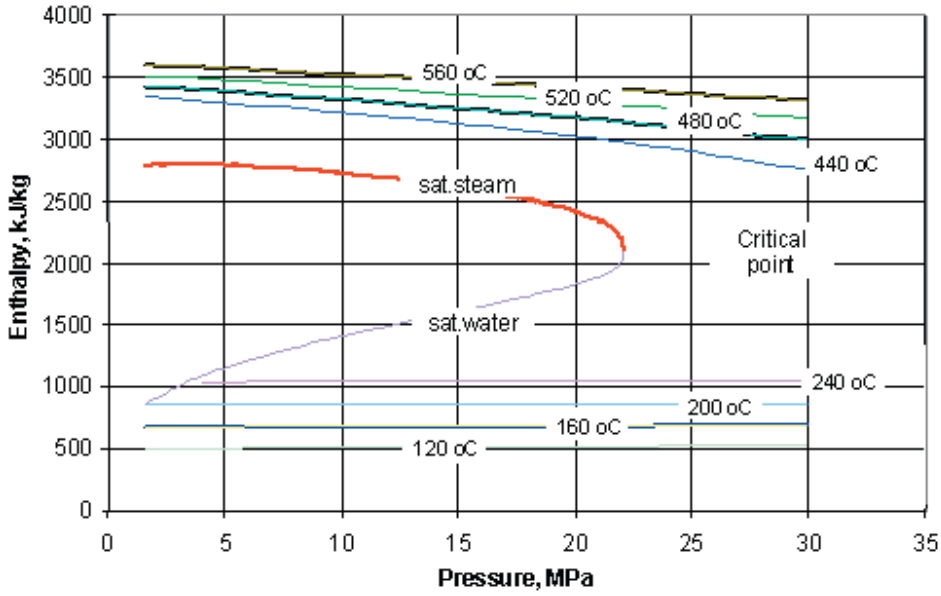

Figure 6-5, h-p diagram for water/steam.

With supercritical cycles the temperature increase from enthalpy corresponding to critical temperature and pressure decreases with increasing pressure. As can be seen the enthalpy needed around critical pressure forms an unstable saddle point. Controlling final temperature is a demanding task there. This is one of the reasons why few boilers operate at close to critical pressure.

Water preheat (economizer)

The first estimation for heat required to bring feedwater to boiling is the enthalpy difference between the points where the line crosses saturated water and the feedwater inlet point.

When pressure increases the portion of heat required for economizers becomes larger.

Temperature - heat input profile

Temperature - heat input profile can then be formed based on heats to each part of the steam water cycle. Figure 6-7 shows a real tempera-

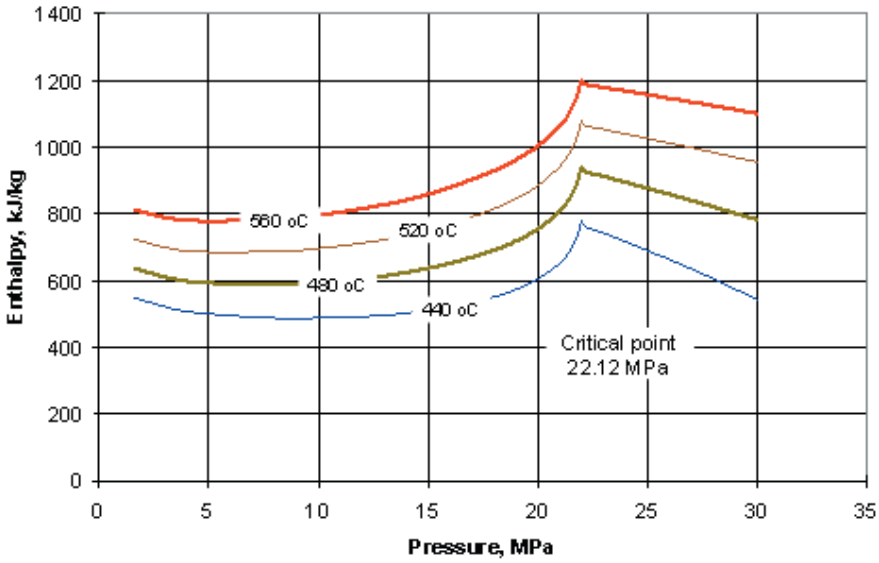

Figure 6-6, Enthalpy for ideal superheat as a function of main steam values.

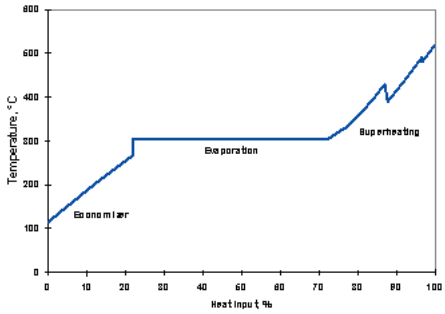

Figure 6-7, Temperature – heat input profile for a natural circulation boiler.

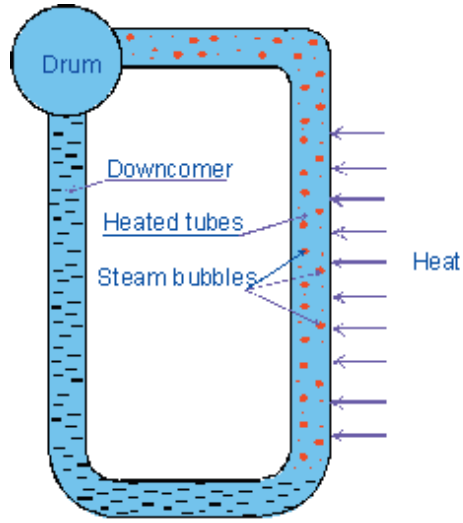

Figure 6-8, Principle of natural circulation.

ture - heat input profile for a natural circulation boiler. In the diagram the individual heat transfer surfaces are arranged in the order of water/steam flow.

The heat required for evaporation is smaller than the initial estimate would give us. Economizing is not usually completed. Part of the water preheating is then replaced by evaporative heat.

There are sharp edges in the superheating part. Between superheating sections water is sprayed to control steam temperature. This is called desuperheating. In practice this means that 30 to 90 °C superheating must be redone. This increases the heat required for superheating and decreases the heat required for economizing and evaporating.

6.3 NATURAL CIRCULATION

Natural circulation is based on the density differences. The same principle can be observed in e.g. room in a cold winter day. Heated air rises on the wall where room is heated and subsequently cooled more dense air falls downwards on the opposite wall.

Natural circulation is caused by the density difference between saturated water and heated water partially filled with steam bubbles. In a natural circulation unit water tubes are connected to a loop, Figure 6-8. Heat is applied to one leg called raiser tubes, where water steam mixture flows upward. Denser saturated water flows downward in unheated leg called downcomer.

Driving force

$$\Delta P_{losses} = (\rho_{water} - \rho_{mixture})gh \qquad 6\text{-}1$$

where

ΔP_{losses}	is the flow losses in the circulation
ρ_{water}	is the density of the water in the downcomers
$\rho_{mixture}$	is the density of the water steam mixture in the heated section
h	is the height of the circulation

Driving force is static head difference between water in downcomers and steam/water mixture in furnace tubes. Saturated water in downcomers weighs more than the steam water mixture in raiser tubes. This creates a force which starts water circulation. Equilibrium is established when pressure losses from friction and pipe fittings equal the driving force. For safety reasons no valves are used in natural circulation arrangement.

Pressure increase decreases driving force because the density difference becomes smaller. When driving force becomes smaller the effect of flow instabilities becomes larger. Maximum pressure where natural circulation boilers have operated is 17,5 MPa (Effenberger, 2000).

Optimization of natural circulation design

Natural circulation design is affected by several design factors. If we increase furnace height the driving head increases. Natural circulation is also

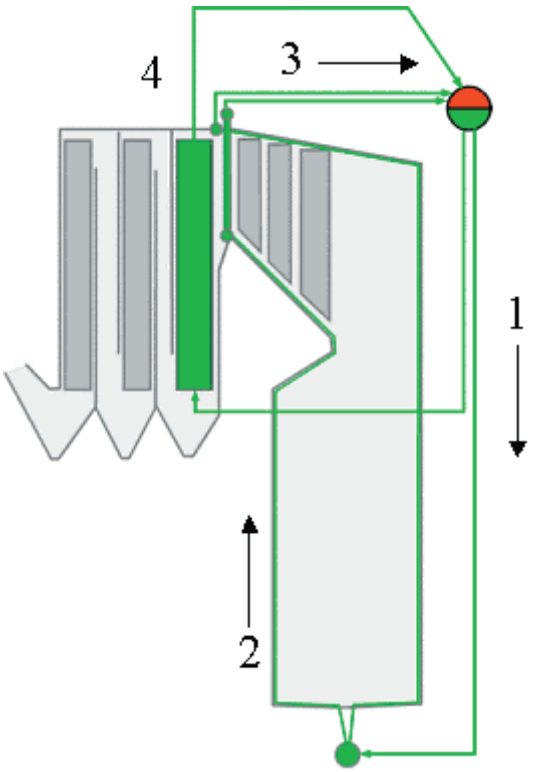

Figure 6-9, Natural circulation arrangement of modern recovery boiler, 1 - water flows down, 2 - steam water flows up water walls, 3 - steam water mixture flows back with risers, 4 - boiler bank has separate downcomers and risers.

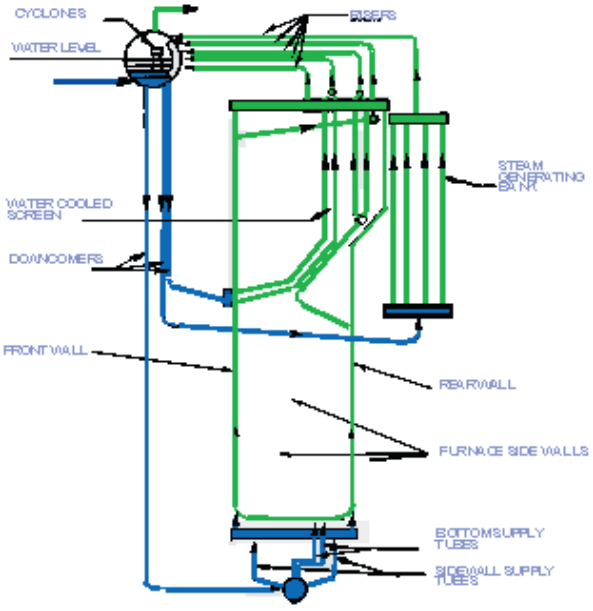

Figure 6-10, Optimization of natural circulation.

improved by higher heat flux in lower part of the tubes. This is one of the reasons that in some older designs boiler bank had upwards flow. Key design success factor is trying to balance flows in all parts of the boiler. This is done by careful arrangement of distribution piping and high enough flow velocity at MCR.

We must try to avoid steam in downcomers. Efficient steam separators reduce the fraction of steam inside the drum. Inserting feedwater to drum at subsaturated state cools down and collapses remaining bubbles. Minimized axial flow inside drum helps creating equal flow in all parts of boilers.

6.4 KEY FURNACE SIZING CHARACTERISTICS

Recovery boiler furnace needs to be sized so that combustion has time to be completed for low emissions. Large furnace lowers furnace outlet temperature, decreases superheater fouling but costs more (MacCallum, 1982). In practice furnace sizing is based on parameters like Effective projected surface area (EPRS), Hearth heat release rate (HHRR) and Hearth solids loading (HSL)

Furnace floor area	=	width*depth
Cross sectional area	=	width*depth
Furnace volume	=	width*depth*height
HSL	=	ds firing rate / floor area
Heat input	=	ds firing rate * HHV
HHRR	=	heat input / floor area
Volumetric input	=	heat input / volume
EPRS	=	projected wall area excluding furnace floor
Heat flux	=	heat transferred / EPRS

In addition furnace performance can be looked at by furnace residence time and furnace gas average velocity. Typical design parameters for modern recovery boiler furnaces are shown in Table 6-1. In boilers with older air systems and low dry solids somewhat more conservative values need to be used.

Table 6-1, *Typical values for recovery boiler furnace design parameters, MCR load.*

Parameter		Value
Heat release rate	kW/m^2	2700 3300
Furnace outlet temperature	°C	950 ... 1000
Generating bank inlet	°C	550 ... 650

Table 6-2, *Effect of dry solids on maximum furnace capacity, if furnace upwards velocity limits capacity.*

Dry solids %	HHRR kW/m^2	Maximum capacity	Velocity m/s	Minimum capacity
65	3 150	100 %	4.5	60 % of max
75	3 750	120 %	4.5	50 % of max
90	4 100	130 %	4.5	40 % of max

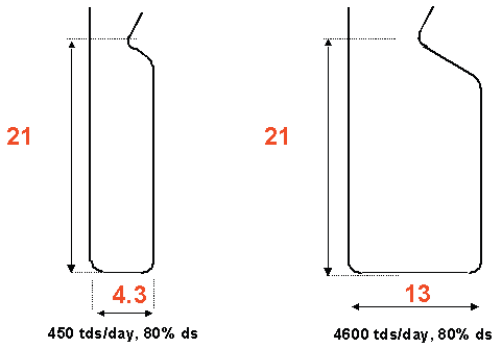

Figure 6-11, Two different size boilers with same residence time.

We know that at least three things can limit the furnace capacity (Adams, 1994). If the flue gas velocity is excessive, then the carryover that accumulates on heating surfaces can plug gas passages. If the char bed combustion rate limit is reached then the char bed growth can be uncontrollable. If there is poor air jet mixing then the emissions from the boiler can be unacceptable.

Major changes have been made to the recovery boiler. Current recovery boilers have improved air systems and so more combustion capacity. The as fired black liquor is in new boilers close to 80 % dry solids concentration. This increases the furnace temperatures and the rate of dry solids burning. New liquor firing practices have increased the fraction of black liquor that is burned in suspension. Finally, a higher char bed temperature is seen. All this has significantly increased the combustion rate. In the following sections we limit the discussion to the modern recovery boilers.

Carryover

The most dramatic effect on furnace capacity has been from the increase in dry solids concentration. Furnace capacity can be limited by carryover. In such a case the average velocity in the lower furnace gives an indication of maximum firing rate. An example of the effect of dry solids can be seen in Table 6-2. The increase in dry solids from 65 to 90 % would increase the dry solids firing capacity from 3150 to 4100 kW/m^2 or 30 %. So even with somewhat increased temperatures the required furnace cross section reduces with

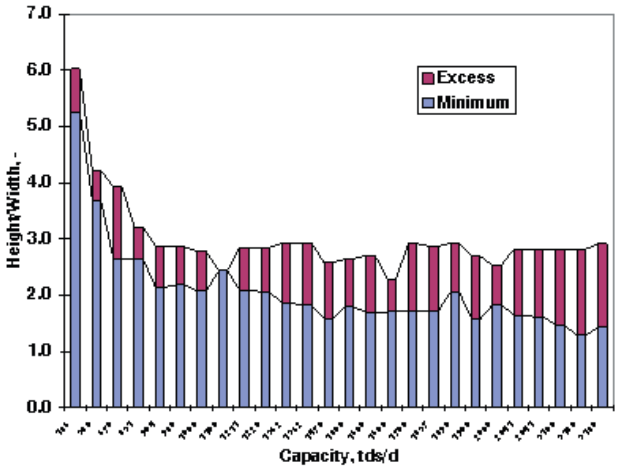

Figure 6-12, Effect of boiler MCR capacity on furnace relative heights.

increased dry solids if we design for a constant lower furnace velocity. This example illustrates why carryover because of an excessive lower furnace velocity should not limit the performance of high dry solids recovery boilers.

Furnace height

Furnace height must provide for the time needed for complete combustion. Furnace height depends on the required residence time. From industry experience it can be determined that approximately 4.5 seconds is required. If we apply this rule to some typical recovery boiler hearth release rates we find that the minimum height corresponding to a 4.5 s residence time increases with increased dry solids, even if the applied hearth heat release rate is higher, Table 6-3.

In practice this would mean that two boilers of same specific loading, but widely different capacity would have an equal height, Figure 6-11.

Does the 4.5-second rule limit recovery boiler capacity? We can plot actual recovery boiler capacity versus their height and the height required for complete combustion at MCR load, Figure 6-12. For nearly all recovery boilers the furnace height seems to be about three times the furnace width.

***Table 6-3**, Furnace height required to ensure a 4.5 s residence time.*

Dry solids %	HHRR kW/m^2	Minimum height m
65	2800	17
75	3300	19
85	3800	22
90	4000	25

If we assume that the design heat flux to the furnace walls is constant, then for same hearth loading the relative height should be constant. On the other hand, the larger the recovery boiler, the lower is the relative height needed for complete combustion. This is because doubling the width quadruples the capacity. If we also double the height then the furnace volume increases eight times. Then there would be two times more time to complete the combustion. Larger boilers have consequently more time to finish combustion.

Mixing of air jets

The penetration depth of a single air jet into the furnace is given by Adams and Frederick (1988)

$$L_p = kD_n \frac{V_n}{V_f}\sqrt{\frac{T_f}{T_n}} \qquad 6\text{-}2$$

where

L_p is the jet penetration length, m
k is an experimental constant, ~1.5
D_n is the hydraulic diameter of air port opening, m
V_n is the jet velocity, m/s
V_f is the furnace gas upward velocity, m/s
T_n is the jet gas temperature, K
T_f is the furnace gas temperature, K

Evaluating the equation we find that most of the parameters are independent of boiler size. The ratio of jet velocity to furnace velocity has increased since modern air systems use higher velocities (pressures) than before. But the design velocities are approximately the same independent of furnace size. Similarly the ratio of furnace temperature to jet temperature is approximately constant.

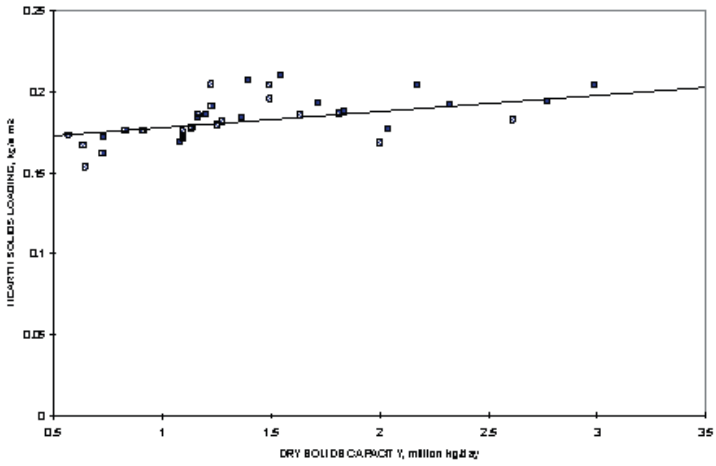

Figure 6-13, Effect of dry solids capacity on HHRR (redrawn after McCann, 1991).

One parameter that changes with boiler size is the hydraulic diameter of air port opening. If we design large and small furnaces with the same hearth loading, then we need the same amount of air per unit of furnace bottom area. The airflow requirement per unit of wall increases linearly with wall width. If we keep the number of airports constant then doubling the wall width would double each air port area. The hydraulic diameter of the air port opening increases as the square root of the wall width increase.

In summary, based on the above equation the single jet penetration depth would increase slower than the furnace size, so at some capacity the mixing would not be enough. Analyses of modern air systems indicate that currently the jet penetration is high enough even for the largest boilers (Adams and Frederick, 1992, Vakkilainen, 2000).

Furnace loading

There is very little data on the effect of recovery boiler size on its performance. McCann (1991) states that the recovery boiler hearth heat release rate, HHRR increases with boiler size. Typical MCR furnace design parameters for new boilers are 2700 … 3300 kW/m^2 (La Fond *et al.*, 1993). If a boiler is well tuned, operates with high dry solids black liquor and is equipped with modern air system, the maximum operating rate is between 3100 and 3700 kW/m^2 (Burton, 2000). The recommended values have increased as design has improved. Barynin and Dickinson (1985) recommended 2680 … 2840 kW/m^2 and superheater inlet temperature below 925 °C. Walsh and Strandell (1992) noted 2500 … 3200 kW/m^2 and superheater inlet temperature 925 … 950 °C.

A major dimensioning criterion for recovery boilers is the furnace floor area. Typical hearth solids loading is close to 0.2 kgds/sm^2 (McCann, 1991), Figure 6-13. Hearth solids loading may be misleading as it does not take into account the variation in liquor properties, especially the heating value. A better indicator is the hearth heat release rate.

Processes in recovery boiler are not limited by the furnace volume. After furnace bottom area has been chosen the furnace height is determined to correspond to desired furnace exit temperature.

Furnace outlet temperature

The adiabatic combustion temperature, Figure 6-14, represents the maximum temperature achievable by black liquor combustion. It is easy to see that a minimum practical operating dry solid is 55 %, where adiabatic combustion temperature is still above 1000 °C.

In recovery furnace the combustion black liquor radiates heat to furnace walls, so maximum temperatures are about a third lower than adiabatic temperatures. Char bed operation requires temperatures in excess of 900 °C. Typical design furnace outlet temperatures are 950 ... 1050 °C, but in highly loaded furnaces they can exceed this by several hundred degrees.

Recovery boiler furnace exit temperature depends strongly on black liquor dry solids and heating value, Figure 6-15. So low MCR loading means lower furnace and high MCR loading requires higher furnace for the same furnace outlet temperature. Furnace outlet temperature affects the

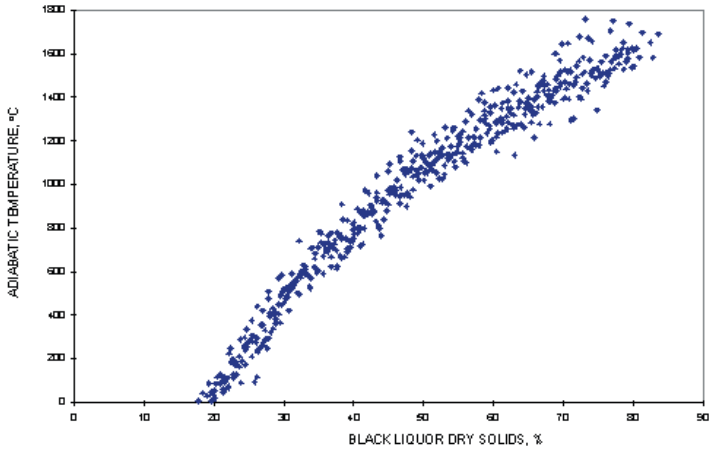

Figure 6-14, Adiabatic combustion temperatures of typical kraft liquors at various concentrations.

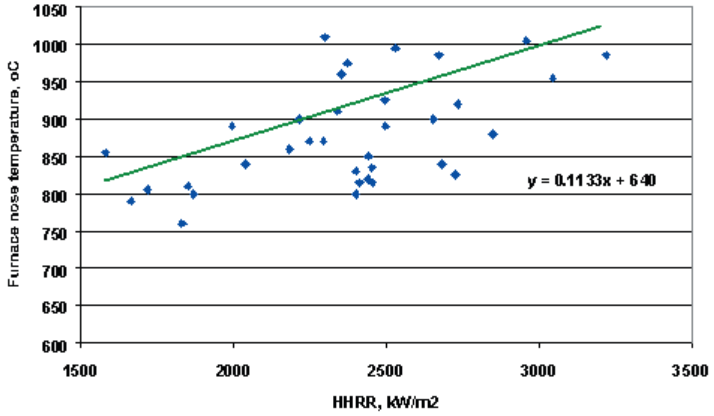

Figure 6-15, Effect of furnace loading on furnace exit temperature.

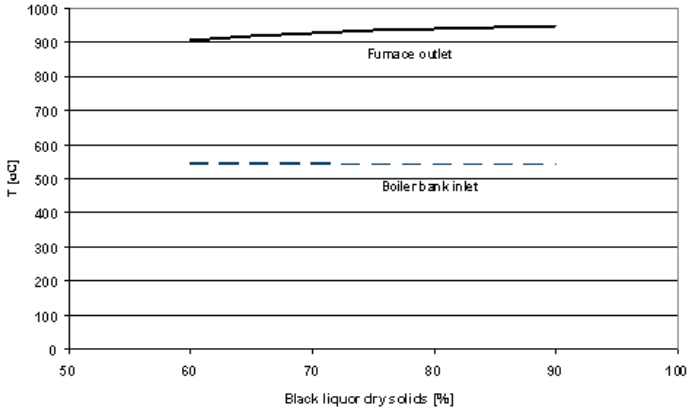

Figure 6-16, Effect of dry solids on furnace outlet temperature (Vakkilainen, 1994).

superheater size. Low furnace outlet temperatures mean large and expensive superheating surface. On the other hand high furnace outlet temperatures mean high heat fluxes to first superheaters and consequently higher corrosion rates and more maintenance.

The choice of furnace outlet temperature affects the ash characteristics. Control of ash behavior and corrosion at superheaters is a key design parameter. Key sizing parameters are first ash melting temperature, ash softening temperature and ash flowing temperature (Hupa *et al.*, 1990).

Furnace outlet temperature affects the dimensioning of the rest of the heat transfer surfaces and has a major effect on emissions. It is often practical to find the proper value through several iterative rounds. Calculating furnace height requires determination of where heat release takes place. This depends on the air splits and liquor firing strategy. Furnace heat flux profiles differ from one boiler manufacturer to another. Typically furnace heights correspond to average heat flux of 60 ... 100 kW/m^2.

One way to look at changes in furnace design is to examine the different design basis for the three recovery boilers discussed earlier, Table 6-4. The nominal furnace loading has increased and will continue to increase. Improved air designs to increase firing rates have been introduced by all major recovery boiler manufacturers. A major factor in helping these innovations has been the use of new three dimensional computational methods for furnace calculation. Raise of black liquor dry solids from 65% to 80% has increased the furnace temperatures. Increase in HSL has been about 30 %, but increase in HHRR has been some 10 %.

The net heat input per unit area of furnace floor increases. The average flue gas flow decreases with less water. This lowers flue gas velocities in furnace by less than 0.5 m/s. The main impact with evolving design is the increase in heat transfer surface required after the furnace. Changing liquor properties require more heat to be transferred especially in the superheating section.

The processes and reactions taking place on the surface and just above the char bed have the greatest impact on boiler operation and performance. About 90% of the total combustion air (equal to all theoretical air required) is introduced at or just above the char bed to maintain a high temperature in the lower furnace. This high temperature leads to low emissions and high reduction efficiency. With increased dry solids concentration the main problem is keeping enough char bed for proper operation, not keeping it hot to achieve low sulfur emissions and high reduction.

Example

Estimate the required furnace dimensions for the 3000 tds/d recovery boiler. The black liquor dry solids is 70 %.

Dry solids firing rate is 3000 / 86.4 = 34.72 kgds/s. If we choose the HSL of 0.2 kgds/(sm^2), then the furnace floor area is 34.72 kgds/s / 0.2 kgds/(sm^2) = 173.6 m^2. This corresponds to 13.2m*13.2m square.

The black liquor higher heating value is 15 MJ/kgds. Heat input is then 15*34.72 = 520.8 MW. (Note! In addition to HHV heat is added with air preheat etc.) The HHRR is then 520800/173.6 = 3000 kW/m^2.

***Table 6-4**, Design basis for the three recovery boilers (For design liquors see Table 2-1).*

	Two drum	Modern	Current
Design dry solids capacity, ton dry solids/day	1700	2400	4000
Design black liquor HHV, MJ/kg dry solid	15.0	13.9	13.0
Design dry solids, %	64	74	80
Design steam temperature, °C	480	480	520
Design steam pressure, bar(absolute)	85	85	104
Steam production, kg steam/kg dry solids	3.584	3.357	3.004
Specific steam production*, kg steam/MJ	0.238	0.242	0.231
Furnace design HSL, ton dry solids/m^2 day	15.6	17.1	20.1
Furnace design HHRR, kW/m^2	2715	2760	3031
Superheater design area, m^2 day/ton dry solids	6.0	5.2	6.8
Boiler bank design area, m^2 day/ton dry solids	3.5	3.0	3.5
Economizers design area, m^2 day/ton dry solids	7.1	10.1	9.1

* steam production per unit of black liquor divided by the HHV of unit of black liquor

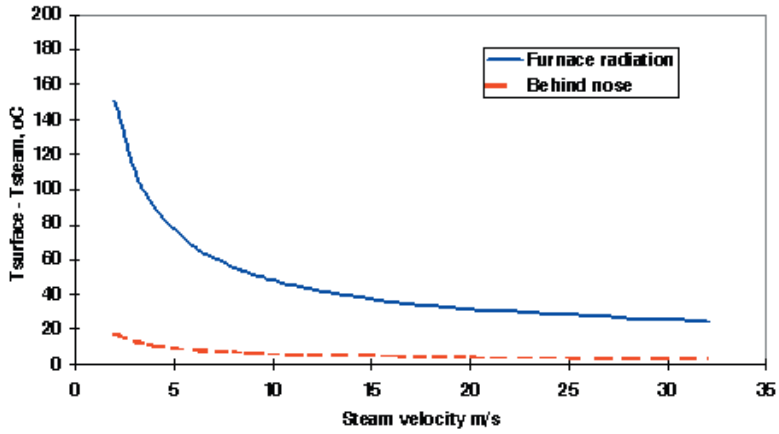

Figure 6-17, Effect of steam velocity on difference between recovery boiler superheater steam and outer tube temperatures.

The area chosen assures that the boiler is of average HSL load. However the HHRR is high. It is in fact higher than what is typical for new boilers. Heat available in the furnace is (13986-1861-290) kJ/kgds*34.72 kgds/s = 410.9 MW

If we choose the furnace exit temperature on the low side, 936 °C, then with flue gas flow of 209.6 kg/s and a c_p value of 1.355, the heat transferred in the furnace is 410900 - 209.6*1.355*936 = 145.1 MW. If the furnace height corresponds to heat flux 80 kW/m^2, then the effective projected area is 1800 m^2. The furnace height is 1800/(13.2+13.2+13.2+13.2) = 34.3 m.

6.5 SUPERHEATER SECTION DIMENSIONING

The superheater surfaces are dimensioned based on radiative heat transfer and ash properties. Superheater dimensioning plays major role in boiler cost. Superheater is one of the most expensive heat transfer surfaces. It is usually made from alloyed steels. Heat transfer in superheaters is mainly radiative, but in the primary superheaters the convection often plays major role.

To achieve good steam temperature control, the last superheater can not have too large temperature rise. Often last superheater section transfers 15 … 33 % of total superheating heat requirement. Placement of superheaters is important. Superheater tubes that receive furnace radiation run much hotter than protected tubes, Figure 6-17.

Superheater design should also be such that temperature differences between adjacent tubes are small. Temperature differences between adjacent tubes can be somewhat controlled by changing tube lengths between passes. Outermost tube which receives the most of radiative heat flux should be shorter than the rest of the tubes. Proper superheater arrangement also eliminates much of the problems with uneven or biased flue gas flow.

Superheater tube does not transfer heat equally around its circumference. Much of the heat transfer is blocked by adjacent tubes and deposits between tubes. Heat transfer is decreased to about the half of the value for clean tubes (Roos, 1968). It is best to use projected heta transfer surface when comparing superheater area. Projected heat transfer surface is calculated assuming the superheater side surfaces are flat. For a superheater element it then equals to element height multiplied by the sum of two times element width and one tube diameter. Use of projected heat transfer area instead of true tube area is further based on the fact that most of the heat transfer is radiative, which is proportional to projected area.

One of the most difficult tasks is to account for uneven temperature and flow fields in the superheater area. An example of upper furnace CFD calculation can be seen as Figure 6-18. Size and placement of bullnose affects flow (Vakkilainen *et al.*, 1992). Typically the superheater needs to be reduced to a series of heat transfer surfaces, which are then solved separately.

Superheater size

Typically the total superheating area is divided into sections for manufacturing reasons, for

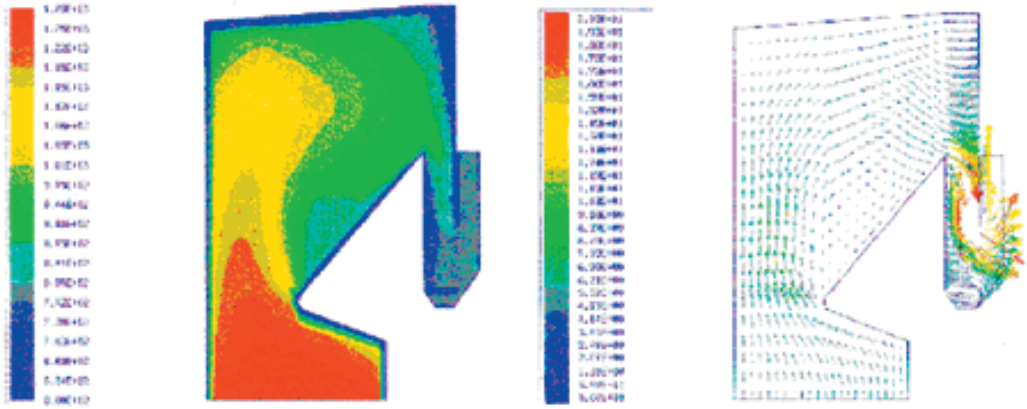

Figure 6-18, Left - temperature profile in a superheater, right – flow profile in the same superheater (Vakkilainen, 2000)

effective sootblowing and to enable desuperheating. Lifting and handling a very large number of tubes during erection is costly. In most cases two desuperheating points are needed. It is customary to call superheaters with roman numerals. All superheating sections have roman numeral I from drum up to first desuperheating, roman numeral II from first desuperheating to second desuperheating etc. The superheating sections in between are numbered alphabetically at direction of steam flow, IA, IB etc.

The amount of superheater surface required depends on the furnace size, steam outlet temperature and desired range of superheating, Figure 6-19. Typically recovery boiler superheaters have specific projected heat transfer surface about 3 $m^2/(tds/d)$.

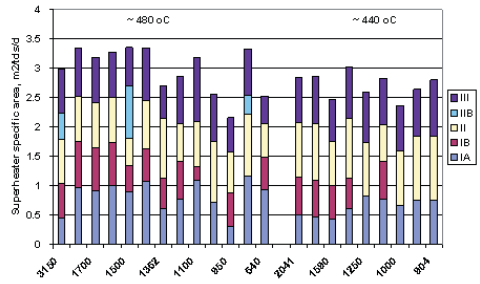

Figure 6-19, Effect of furnace size and superheater outlet temperature on specific superheater projected area.

Effect of load to superheating

Decreasing load (as fired black liquor dry solids rate) decreases flue gas flow and temperatures to and from the superheater, 6-20. Thus the superheating reduces because both the heat transfer coefficient and the available temperature difference decrease. Usually this means that at some 70 % of MCR load the recovery boiler does not superheat enough to reach MCR main steam temperature.

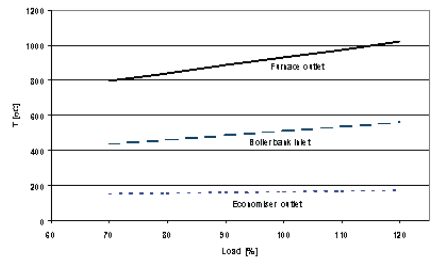

Figure 6-20, Effect of load to temperatures (Adams and Frederick, 1988, Haynes et al., 1988)

Superheater spacing

Typical superheater spacing can be seen in Figure 6-21. For low temperature, nonfouling zone tight spacing can be used. For high temperature, where fouling is probable, wide spacing is used.

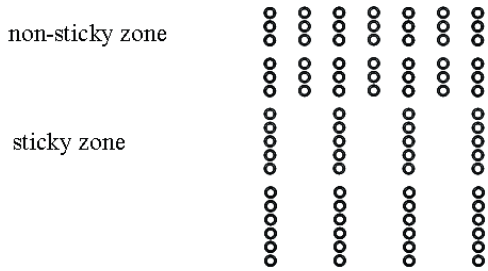

Figure 6-21, Superheater spacing (Singer, 1981)

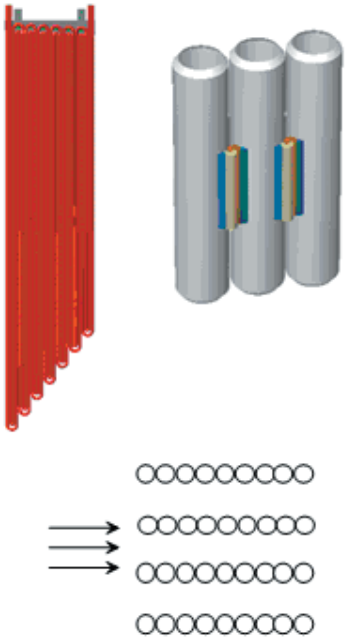

Figure 6-22, Panel superheater

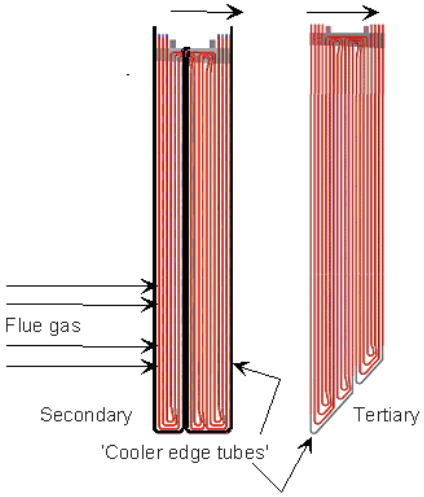

Figure 6-23, Cooler edge tubes.

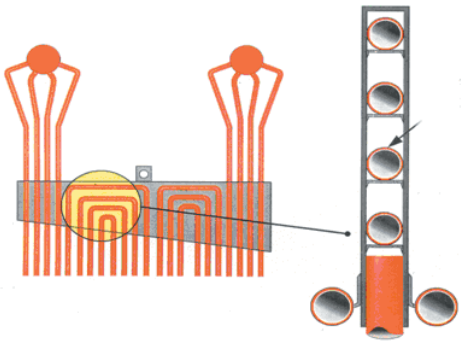

Figure 6-24, Superheater hanging.

Recovery boiler screens and superheater area have typically spacing from 300 to 400 mm. Wider spacing is less resistant to fouling, but leads to more expensive boiler. Recovery boiler vertical flow boiler banks have spacing from 150 to 250 mm. Economizers have spacing from 100 to 150 mm.

Panel superheater

When tubes in an inline superheater are placed close to each other in gas flow direction a panel or platen superheater is created, Figure 6-22. Panel superheaters were introduced to use in 1952 by Combustion Engineering.

In panel superheaters the tube longitudinal spacing is smaller than 1.25 *$Ø_d$. Panel superheater is resistant to fouling and can withstand high heat flux. It is used in most demanding applications, typically as the first gas side superheater.

Arrangement of parallel tubes

Often to limit the steam side pressure loss in a superheater one must use several parallel tubes. Each of these tubes has for construction reasons different length, different total heat absorbed and necessarily somewhat different outlet temperature.

For corrosion reasons one often uses arrangement that results in shorter length of the outermost tube, Figure 6-23. First, outermost or edge tube receives more radiation heat especially from furnace than the other tubes. Also often the corrosive ash has the most difficult properties in the first tube. Shorter flow path helps keep first tube cooler than the others and decreases the first tube corrosion, but increases corrosion of the rest of the tubes.

Superheater hanging

To limit the amount of ash that can escape through superheater openings in the boiler roof, protective boxes are used, Figure 6-24. They seal the opening to the roof to form gas tight construction.

Superheaters need to be supported, so they hang from these boxes. Hanger rods connect boxes to secondary beams. This arrangement helps to control the stresses caused by tube heating and cooling.

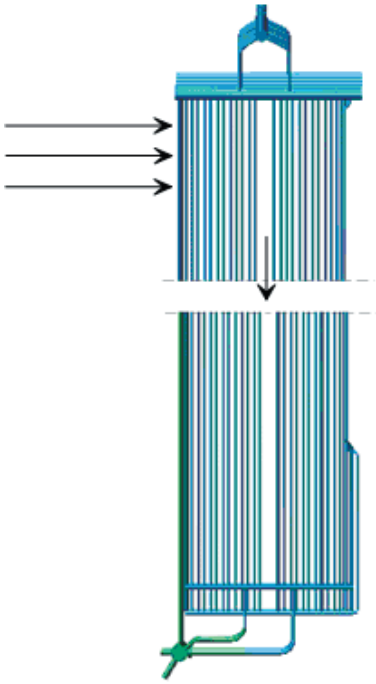

Figure 6-25, Vertical boiler bank.

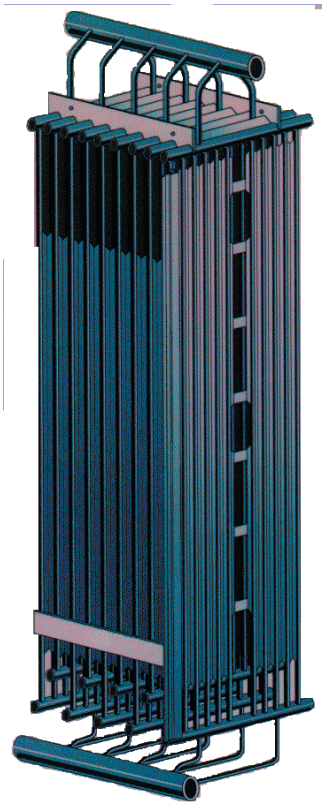

Figure 6-26, Vertical flow economizer.

6.6 VERTICAL BOILER BANK DESIGN

Most boiler banks are of vertical design, Figure 6-25. Earlier generating banks had common upper and lower headers. Modern boiler banks are formed from finned tube panels. Panels are then connected to common headers. This stiffens the construction and limits tube movement, which was problem in the earlier non finned designs.

Ample space is reserved for sootblowing. All major recovery boiler manufacturers use straight sootblowing space. Some place flow distribution plates to this space to improve heat transfer. Flow in the space is hotter and faster that flow in the rest of the surface, which decreases heat transfer (Vakkilainen and Anttonen, 1994).

B&W reports that they have increased the cross flow spacing from original 152.4 mm first to 203.2 mm and then to 228.6 mm to improve fouling behavior (Dickinson *et al.*, 2000). Minimum spacing has varied a lot but new boilers are bought with spacing of 164 ... 230 mm.

Typically boiler generating bank inlet temperature is 540 ... 600 °C. Maximum flue gas velocity should be under 20 m/s (Recovery, 1993). Typical design flue gas mass flow densities at MCR are 6 … 8 kg/sm^2. Special emphasis should be placed on achieving low inlet velocities. Normally in modern boilers the free flue gas flow area is 0.17 … 0.23 m^2/m$^2_{bottom}$ and the finned heat transfer surface area is 45 … 70 m^2/m$^2_{bottom}$.

Boiler bank inlet temperature is one of the key design factors. High inlet temperature means that dust entering boiler bank is still considerably molten. Low inlet temperature mens heavy investment to superheating surface. Barynin and Dickinson (1985) recommend maximum entering gas temperature 625 … 700 °C. McCann (1991) recommends 565 … 625 °C if Cl and K are present.

6.7 VERTICAL ECONOMIZERS

Most economizers are of vertical design, Figure 6-26. They are formed from finned tube panels connected to common headers. Special openings are reserved for sootblowing. In modern large, high dry solids boilers the sootblowing requirement for economizers is very minimal.

Typically economizer inlet temperature is 350 ... 450 °C. Maximum flue gas velocity should be under 30 m/s. The design flue gas mass flow density at MCR are 8 … 10 kg/sm^2. The free flue

gas flow area is typically 0.13 … 0.17 m^2/m^2_{bottom} for economizer 2 and 0.11 … 0.16 m^2/m^2_{bottom} for economizer 1. The total finned heat transfer surface area in both economizers is 150 … 230 m^2/m^2_{bottom}. Minimum spacing has varied a lot but new boilers are bought with economizer spacing of 110 ... 180 mm. Inlet velocity is important. High inlet velocity leads to plugging. Sandquist (1987) reports that reduction of inlet velocity by 30 % solved economizer plugging at Leaf river mill. Barynin and Dickinson (1985) recommend using MCR design velocities lower than 11 m/s and entering gas temperature below 425 °C.

Economizers with low design flue gas mass flow densities and wide spacings are less prone to fouling. Low flue gas velocities lead to low heat transfer rates and high heat transfer areas.

6.8 HEAT TRANSFER IN BOILERS

The purpose of this section is to give the reader an overview of some possible methods to calculate heat transfer in boilers. The treatment is short and the reader is requested to study other material if he is interested in heat transfer phenomena in detail (Blokh, 1988, Brandt, 1985, Rahtu, 1990, Brandt, 1999),

Overall heat transfer

Overall heat transfer in a boiler heat transfer surface can be expressed with the general heat transfer equation as

$$Ø = kA\Delta T \qquad 6\text{-}3$$

where

- Ø is the heat transferred, W
- k is the overall heat transfer coefficient, W/m²K
- A is the heat transfer surface, m²
- ΔT is the temperature difference, K

The overall heat transfer coefficient k is a function of convective and radiative heat transfer.

$$k = \frac{f_o}{\frac{1}{k_i} + \frac{1}{k_o} + \mathbf{F}(\lambda, d_o, d_s, s)} \qquad 6\text{-}4$$
$$k_o = f_n k_c + k_r + k_{ex}$$

where

- f_n is the form correction (correction for number of rows, correction for arrangement, etc.), -
- f_o is the overall correction (fouling correction, etc.), -
- k_i is the inside heat transfer coefficient referred to the outside surface, W/m²K
- k_o is the outside heat transfer coefficient, W/m²K
- k_r is the radiative heat transfer coefficient, W/m²K
- k_{ex} is the external heat transfer arranged to represent a heat transfer coefficient, W/m²K
- k_c is the convective heat transfer coefficient, W/m²K
- λ is the heat conductivity of tube material
- d_o is the outside tube diameter, m
- d_s is the inside tube diameter, m
- s is the tube wall thickness, m

The correction for number of rows, f_n can be expressed as

$$f_n = \begin{cases} \dfrac{(n_r - 1)^2 - 1}{(n_r - 1)^2} & ; n_r > 1 \\ 0.75 & ; n_r = 1 \end{cases} \qquad 6\text{-}5$$

The correction for overall fouling, temperature deviations, flow deviations etc. f_o, is usually dependent on fuel type and properties, steam generator configuration, type of surface and expected calculation error. The exact numerical value must so be determined empirically from previous experimental data.

The heat transfer resistance through a tube of uniform material for a tubular construction where tubes are separated from each other is

$$\mathbf{F}(\lambda, d_o, d_s, s) = \frac{1}{\frac{d_o}{2\lambda} \ln \frac{d_o}{d_i}} \qquad 6\text{-}6$$

Radiation heat transfer

Radiation heat transfer can be calculated according to the formulas specified in VDI – heat atlas, Kc1-Kc12 (1993). Even though the concept of radiation heat transfer coefficient has only a very weak connection to physical reality, it is used here so that the radiative heat transfer can be expressed with the convective heat transfer.

Radiation heat transfer coefficient can be determined through radiation heat flow.

$$k_r = \frac{\Phi_r}{A_{eff}(T_g - T_w)} \qquad 6\text{-}7$$

Radiation heat flow Φ_r can be expressed if temperatures and emissivities are known as

$$\Phi_r = A_{eff} \frac{\varepsilon_w}{\alpha_{dg} + \varepsilon_w - \alpha_{dg}\varepsilon_w} \delta(\varepsilon_{dg} T_g^4 - \alpha_{dg} T_w^4) \quad 6\text{-}8$$

where

ε_w is the emissivity of the wall, for fully oxidized boiler tubes 0.8 is typical
ε_{dg} is the emissivity of the dusty gas
α_{dg} is the absorptivity of the dusty gas

For dusty gas we can express the emissivity and absorptivity assuming no band overlapping, through pure gas and pure dust emissivities

$$\varepsilon_{dg} = \varepsilon_g + \varepsilon_d - \varepsilon_d\varepsilon_g \quad 6\text{-}9$$

$$\alpha_{dg} = \alpha_w + \varepsilon_d - \alpha_w\varepsilon_d \quad 6\text{-}10$$

The emissivities and absorptivities of pure gas mixtures can be calculated with pure gas properties

$$\varepsilon_g = \varepsilon_{H2O}(T_g, sp_{H2O}) + \varepsilon_{CO2}(T_g, sp_{CO2}) + \varepsilon_{SO2}(T_g, sp_{SO2}) - \Delta\varepsilon_g(\varepsilon_{H2O}, \varepsilon_{CO2}, \varepsilon_{SO2}) \quad 6\text{-}11$$

$$\alpha_{dg} = \alpha_{H2O} + \alpha_{CO2} + \alpha_{SO2} - \Delta\alpha_g \quad 6\text{-}12$$

where

$\Delta\varepsilon_g$ is the overlapping correction for emissivity, .
$\Delta\alpha_g$ is the overlapping correction for absorptivity, -
p_x is the partial pressure of substance x, MPa
s is the radiation beam length, m

As no better approximations have been developed we must express absorptivities through emissivity functions, applicable when total gas side pressure is about 0.1 MPa.

$$\varepsilon_g = (0.595 - 0.00015 * T_G)(1 - e^{-0.824\, sp_{tot}}) + (0.275 - 0.000115 * T_G)(1 - e^{-25.907\, sp_{tot}}) \quad 6\text{-}13$$

$$p_{tot} = p_{H2O} + P_{CO2} + p_{SO2} \quad 6\text{-}14$$

$$\alpha_{H_2O} = \left(\frac{T_g}{T_w}\right)^{0.45} \varepsilon_{H_2O}\left(T_g, sp_{H_2O}\frac{T_w}{T_g}\right) \quad 6\text{-}15$$

$$\alpha_{CO_2} = \left(\frac{T_g}{T_w}\right)^{0.65} \varepsilon_{CO_2}\left(T_g, sp_{CO_2}\frac{T_w}{T_g}\right) \quad 6\text{-}16$$

$$\alpha_{SO_2} = \left(\frac{T_g}{T_w}\right)^{0.50} \varepsilon_{SO_2}\left(T_g, sp_{SO_2}\left(\frac{T_w}{T_g}\right)^{1.5}\right) \quad 6\text{-}17$$

The individual emissivity functions can be mathematically approximated as

$$\varepsilon_{CO2} = \alpha_o + \alpha_1\mu + \alpha_2\mu^2 + \alpha_3\mu^3 \quad 6\text{-}18$$

$$\mu = \mu(T_g) \quad 6\text{-}19$$

$$\varepsilon_{H_2O} = \varepsilon_a\left(1 - \varepsilon^{(f(ps)g(ps,T_g))}\right) \quad 6\text{-}20$$

$$\alpha_i = \alpha_i(p_{CO2}, s) \quad 6\text{-}21$$

$$\varepsilon_{SO_2} = \alpha(1 - e^{kT-b})(sp_{SO_2})^{0.87} \quad 6\text{-}22$$

where

ε_a is the background emissivity, -

For dust emissivity ε_d a fully dispersed approach is used

$$\varepsilon_d = 1 - \varepsilon^{-\alpha_d B_d s} \quad 6\text{-}23$$

where

α_d is the absorption coefficient of dust
B_d is the dust loading, kg/m^3
s is the radiation beam length, m

The exact expression for radiation beam length s is very complicated and involves integrating in space of surface element. Usually graphical approximations can be found to all relevant problems.

Kraft recovery boiler deposits have low emissivity, Figure 6-27 (Wessel *et al.*, 1998, Sinquefield *et al.*, 1998, Baxter *et al.*, 2004). Care should be taken to obtain true surface properties.

Outside convection heat transfer

Convection heat transfer is calculated by e.g. Gnielinski equation VDI – heat atlas, Gf1-Gf3 (1993)

$$Nu = f_A\left(0{,}3 + \sqrt{(0.664\sqrt{\mathrm{Re}}\sqrt[3]{\mathrm{Pr}})^2 + \left(\frac{0.037\,\mathrm{Re}^{0.8}\,\mathrm{Pr}}{1 + 1.2443\,\mathrm{Re}^{-0.1}(\mathrm{Pr}^{2/3} - 1)}\right)^2}\right) \quad 6\text{-}24$$

The correction factor fA for outside heat transfer is an empirical coefficient. It is dependent of fuel type and properties, steam generator configuration, type of surface and expected calculation error. The exact numerical value must so be determined empirically from previous experimental data.

Gas side pressure drop, inline

Gas side pressure drop can be calculated according to the Gaddis equation in VDI – heat atlas, Ld1-Ld7 (1993).

$$\Delta p_{gs} = \Delta p_{gf} \quad 6\text{-}25$$

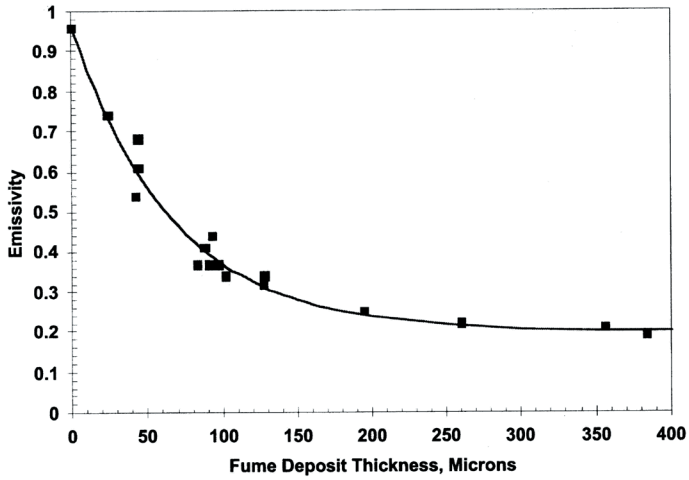

Figure 6-27, Effect of deposit thickness on emissivity, fume deposited on top of tube (Sinquefield et al., 1998).

gas side pressure losses = friction losses

For in line arrangement the pressure drop coefficient for heat transfer surface with horizontal tubes is

$$\Delta p = n_r \zeta_r \Delta p_d \qquad 6\text{-}26$$

where

- n_r is the number of rows in heat transfer surface
- Δp_d is the dynamic pressure, calculated at the gas side mean temperature and smallest area

The single row pressure drop ζ_r for in line tubes is sum of laminar and turbulent coefficients

$$\zeta_r = \zeta_l + \zeta_t \left(1 - e^{-\frac{Re-1000}{2000}}\right) \qquad 6\text{-}27$$

$$\zeta_l = \frac{280\pi((s_l^{0.5} - 0.6)^2 + 0.75)}{(4 s_t s_l - \pi) s_t^{1.6}\, Re} \qquad 6\text{-}28$$

$$\zeta_t = \frac{10^{0.47(s_l/s_t - 1.5)} \left[0.22 + 1.2 \frac{(1 - \frac{0.94}{s_l})^{0.6}}{(s_t - 0.85)^{1.3}} \right] + 0.03(s_t - 1)(s_l - 1)}{Re^{0.1(s_l/s_t)}} \qquad 6\text{-}29$$

where

- ζ_l is the laminar part of the pressure drop coefficient, -
- ζ_t is the turbulent part of the pressure drop coefficient, -
- s_l is the dimensionless transverse pitch,
- s_t is the dimensionless longitudinal pitch,
- Re is the Reynolds number, calculated at the gas side mean temperature and smallest area, -

Inside heat transfer, fluid inside tube

Turbulent convection heat transfer for steam and water flowing inside an circular tube can be calculated according to the Hausen equation; $2300 < Re < 107$, $0.6 < Pr < 500$, $d << L$, $T_w \sim T_f$ (Hausen, 1974)

$$k_i = \frac{\lambda Nu}{d_o} \qquad 6\text{-}30$$

$$Nu_i = 0.0235(Re^{0.8} - 230)(1.8Pr^{0.3} - 0.8) \qquad 6\text{-}31$$

For laminar flow case, $Re < 2300$ a value of

$$Nu_i = 3.64 \qquad 6\text{-}32$$

can be used, Hausen (1974)

Usually no correction for inside fouling is used, as tube inside is kept relatively clean by normal boiler operation.

6.9 EXAMPLE CALCULATION OF HEAT TRANSFER SURFACE

We have a single heat transfer surface arrangement, Figure 6-28, consisting of main heat transfer surface and side walls situated transverse to the gas flow. We can make the following simplifications applicable to most of the cases in practice

- dust is dispersed uniformly to the gas flow
- temperatures of the dust T_{di} and T_{do} are equal to the respective temperatures of the gas flow T_{gi} and T_{go}
- temperature of the side walls T_{sw} can be treated as constant i.e. $T_{gi} - T_{go} >> T_{swo} - T_{swi}$

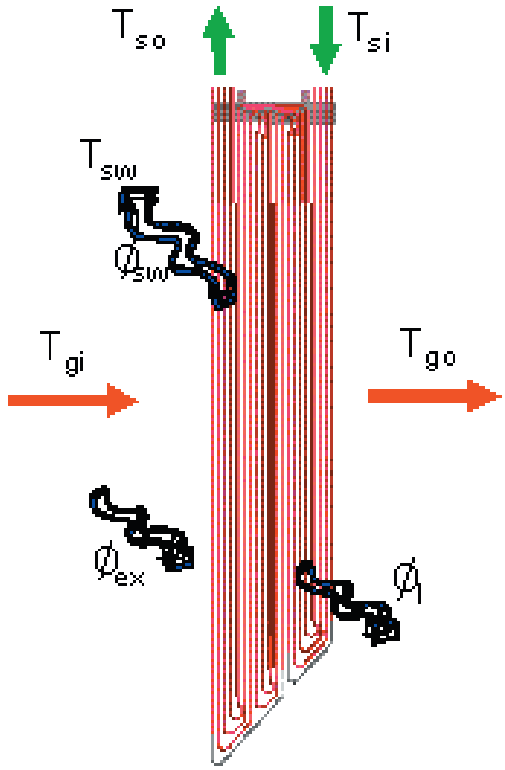

Figure 6-28, Recovery boiler superheater arrangement

- no combustion inside the heat transfer surface volume
- heat losses Φ_l and external heat flow Φ_{ex} can be determined separately from the superheater heat transfer calculations

We want to determine the heat transfer from the flue gas flow to the steam flow. The basic equation involved is

$$\Phi_s = \int k(T_g - T_s)dA \qquad 6\text{-}33$$

For the case of superheaters we usually determine an overall heat transfer coefficient kt which is treated as an independent value. The temperature distribution as reference to area can be solved for simple parallel and counterflow cases. Usually we express the solved equation in basic form.

$$\Phi_s = \int k_t \theta_{ln} A_{eff} \qquad 6\text{-}34$$

heat to steam flow = overall heat transfer coefficient * logarithmic temperature difference * effective heat transfer surface

where

$$\theta_{ln} = \theta_{ln}(T_{gi},T_{go},T_{si},T_{so}) \qquad 6\text{-}35$$

To aid us in heat transfer calculations, when solving unknown temperatures for known area and overall heat transfer coefficient we use nondimensional heat transfer parameters ε, R and z (Ryti, 1969).

$$\varepsilon_{ln} = \varepsilon_{ln}(T_{gi},T_{go},T_{si},T_{so}) \qquad 6\text{-}36$$

$$R_{ln} = R_{ln}(T_{gi},T_{go},T_{si},T_{so}) \qquad 6\text{-}37$$

$$z_{ln} = z_{ln}(T_{gi},T_{go},T_{si},T_{so}) \qquad 6\text{-}38$$

We do this by starting from the definition of the heat flow to the steam.

$$\Phi_s = q_{ms} c_{ps} (T_{so} - T_{si}) \qquad 6\text{-}39$$

For the simple no external heat flow case the heat flow to the steam equals the heat flow from the flue gas

$$\Phi_g = q_{mg} c_{pg} (T_{gi} - T_{go}) = \Phi_s \qquad 6\text{-}40$$

Then the parameters describing the heat transfer can be defined

$$G = k_t A_{eff} \qquad 6\text{-}41$$

$$C_{max} = Max(q_{mg}c_{pg}, q_{ms}c_{ps}) \quad 6\text{-}42$$

$$C_{min} = Min(q_{mg}c_{pg}, q_{ms}c_{ps}) \quad 6\text{-}43$$

$$\Delta T_{max} = Max(T_{gi} - T_{go}, T_{so} - T_{si}) \quad 6\text{-}44$$

$$\Delta T_{min} = Min(T_{gi} - T_{go}, T_{so} - T_{si}) \quad 6\text{-}45$$

$$\theta = \Delta T_{max} - \Delta T_{min} \quad 6\text{-}46$$

$$\varepsilon = \Delta T_{max}/\theta \quad 6\text{-}47$$

$$R = \Delta T_{min}/\Delta T_{max} \quad 6\text{-}48$$

$$z = G/C_{min} \quad 6\text{-}49$$

Then we can express the heat flow to steam also with the dimensionless parameters

$$\Phi_s = \Phi_s(\varepsilon, R, z) = q_{ms}c_{ps}(T_{so} - T_{si}) \quad 6\text{-}50$$

For the complex heat transfer situation occurring in the recovery boiler superheaters, where there is also several additional heat flows, we can redefine the nondimensional heat transfer parameters with aid of correction factor b to be able to treat this multi heat flow case as single heat flow case in the heat transfer calculations (Vakkilainen, 1994)

$$G = k_t A_{eff} \quad 6\text{-}51$$

$$\theta = T_{gi} - T_{si} \quad 6\text{-}52$$

$$R = \frac{b(T_{so} - T_{si})}{T_{gi} - T_{go}} \quad 6\text{-}53$$

parallel flow

$$\theta_{ln} = \frac{(T_{gi} - T_{si}) - (T_{go} - T_{so})}{\ln \frac{T_{gi} - T_{si}}{T_{go} - T_{so}}} \quad 6\text{-}54$$

$$\varepsilon = 1 - \frac{1 - e^{-z(1+R)}}{1 + R} \quad 6\text{-}55$$

countercurrent flow

$$\theta_{ln} = \frac{(T_{gi} - T_{so}) - (T_{go} - T_{si})}{\ln \frac{T_{gi} - T_{so}}{T_{go} - T_{si}}} \quad 6\text{-}56$$

$$\varepsilon = 1 - \frac{1 - R}{e^{z(1+R)} - R} \quad 6\text{-}57$$

$$\theta_{sw} = \frac{T_{gi} - T_{go}}{\ln \frac{T_{gi} - T_{sw}}{T_{go} - T_{sw}}} \quad 6\text{-}58$$

$$z = G/c_{pg}q_{mg} \quad 6\text{-}59$$

It must be noted that above is valid only for the case when flue gas heats the steam.

Heat balance

For the superheater the first principle must hold true

$$\Phi_g - \Phi_s - \Phi_{sw} + \Phi_{ex} - \Phi_l = 0 \quad 6\text{-}60$$

heat from gas - heat to steam - heat to sidewalls + external heat - heat losses = 0
where

$$\Phi_s = G\theta_{ln} = q_{ms}c_{ps}(T_{so} - T_{si}) \quad 6\text{-}61$$

$$\Phi_g = (q_{mg}c_{pg} + q_{md}c_{pd})(T_{gi} - T_{go}) \quad 6\text{-}62$$

$$\Phi_{sw} = k_{sw}\theta_{sw}A_{sw} \quad 6\text{-}63$$

External heat Φ_{ex} and heat losses Φ_l are usually constant, fixed values.

Heat capacities

To make use of the dimensionless parameters ε, R and z possible we must refer the heat transfer situation to the simple two massflows exchange heat case with the aid of correction factor b. We have chosen the steam side heat flow to be the determining heat flow. Then for recovery boiler superheaters

$$C_{min} = q_{mg}c_{pg} \quad 6\text{-}64$$

$$C^*_{min} = q_{ms}c_{ps} \quad 6\text{-}65$$

$$C^*_{min} = bq_{mg}c_{pg} \quad 6\text{-}66$$

$$R = C^*_{min}/C^*_{min} \quad 6\text{-}67$$

$$b = \frac{c_{pg}q_{mg} + \frac{\Phi_{ex} - \Phi_l - \Phi_{sw}}{T_{gi} - T_{go}} + c_{pd}q_{md}}{c_{pg}q_{mg}} \quad 6\text{-}68$$

6.10 EFFECT OF HIGH DRY SOLIDS TO RECOVERY BOILER DIMENSIONING

The lower furnace plays a key role in terms of lowering emissions and raising capacity (Borg

Table 6-5, *Furnace operating conditions for example boiler, constant HHRR.*

Liquor dry solids, %	60	65	70	75	80	85
Sum of heat inputs, MW	559.4	557.9	556.7	555.6	554.7	553.8
Heat in furnace, MW	393.0	402.6	410.9	418.1	424.4	430.0
c_p gas, kJ/kg°C	1.391	1.372	1.355	1.340	1.324	1.314
Liquor flow, kg/s	57.9	53.4	49.6	46.3	43.4	40.9
Flue gas flow, kg/s	221.0	216.9	212.8	209.5	206.7	204.2
Furnace outlet temp., °C	913	926	936	943	949	953
Firing capacity, kg dry solids/m²s	0.2	0.2	0.2	0.2	0.2	0.2
HHRR, MW/m²	3.0	3.0	3.0	3.0	3.0	3.0
Heat release rate, MW/m²	2.26	2.32	2.37	2.41	2.44	2.48

et al., 1974). The key is to control the reactions taking place in the lowest part of the furnace, on the bed surface and just above it. Increasing black liquor dry solids will increase lower furnace temperatures (Backman *et al*., 1995, Ryham and Nikkanen, 1992, Haynes *et al*., 1988). Temperature will have a significant impact on emissions, reduction efficiency and on the fouling and corrosion of the convective heat surfaces.

The air system introduces most of the combustion air into the lower furnace, just above the furnace floor. As the dry solids increases, the penetration of air jets increases. With increasing dry solids and improved design, emissions have been reduced significantly. The nominal furnace loading changes only slightly with an increase in black liquor dry solids content. The furnace loading is usually determined by either the hearth heat release rate (HHRR) or the firing capacity. Because the higher black liquor heating value and the dry solids rate remain constant, these indicators show constant loading. The hearth heat release rate in the furnace remains constant.

As we raise dry solids from 65 % to 80 %, the total heat input per plan area is reduced. This is caused by a reduction in the black liquor sensible heat input. The net heat input to the furnace increases noticeably, as less water needs to be evaporated. The average flue gas flow decreases as less water vapor is present. If the furnace temperature remained constant, this would reduce the flue gas flow rates, but by less than 0.5 m/s.

Loading values for the example 3000 tds/d recovery boiler for a furnace of similar size are listed in Table 6-5. Steam generation with higher dry solids increases. The steam generation with 80 % dry solids equals the steam generation at 106.9 % flow of the 65 % dry solids content black liquor.

If we were to fire at the same steam flow, the furnace loading would be higher with the 65 % dry solids content black liquor than with the 80 % dry solids black liquor. Higher furnace loading indicators include hearth heat release rate, solids loading, total heat input and net heat input. This is because the flue gas losses are high for the 65 % liquor.

Liquor heat treatment reduces the furnace loading. The net heat input remains almost constant. The liquor dry solids flow decreases, as does the black liquor volumetric flow. The average flue gas flow falls more than 10 %. The hearth heat release rate falls by 11 %, and the nominal firing capacity by 8 %. Because the higher black liquor heating value and the dry solids firing rate decrease, the net heat release rate remains constant. Even by a conservative estimate, the furnace bottom area could be reduced by 4-8 %.

Furnace temperature profiles have been published by Jones (1989) and Jutila *et al* (1978). A heat release profile can be found through fitting to achieve a known temperature profile. Making correct furnace outlet temperature predictions require fine tuning to available measurements.

In typical furnace temperature profiles the temperature reaches a maximum in the lower furnace ant then starts dropping toward the nose. The lower furnace temperature increases about 100 °C with an increase in dry solids from 65 % to 80 %. This is significantly less than the 200 °C change in adiabatic flame temperature. On the other hand, the radiative heat flux to the walls increases by about 20 %. Increased lower furnace temperatures can speed up local corrosion in recovery boilers.

The furnace outlet temperatures increase as the dry solids content rises from 65 % to 80 %. The measured increase is 20-35 °C. It must be borne in mind that the measurement error of furnace outlet temperatures is at least +20 °C. The increase

Table 6-6, *Heat available for superheating.*

Liquor dry solids, %	60	65	70	75	80	85
Flue gas flow, kg/s	221.0	216.9	212.8	209.5	206.7	204.2
Furnace exit temperature, °C	913	926	936	943	949	953
Cp gas, kJ/kg°C	1.391	1.372	1.355	1.340	1.324	1.314
Steam flow, kg/s	122.8	126.6	129.9	132.8	135.3	137.5
Heat for superheat, MW	109.9	110.4	109.7	108.8	107.5	106.4
Heat for superheat, kW/kg	894.6	871.3	844.0	819.2	794.3	773.6
If furnace outlet temperature constant = 926 °C						
Heat for superheat, MW	113.9	110.4	106.8	103.9	101.2	99.1
Heat for superheat, kW/kg	927.5	871.3	821.7	782.5	748.1	721.2

in furnace outlet temperatures is caused by changes in the mass flow and the net heat input to the furnace.

The calculated furnace outlet temperature variations for a fixed-size furnace are shown in Table 6-5. Understandably, liquor heat treatment lowers the furnace exit temperature. The change in furnace exit temperature will show up, albeit with reduced magnitude, in the flue gas temperature entering the boiler bank.

The basic dimensioning of recovery boiler superheaters will not change much in response to the change in black liquor dry solids content. As these surfaces are radiative surfaces, their heat transfer does not depend on flue gas velocity. The radiative heat transfer at the superheaters increases by 10-20% along with the increase in black liquor dry solids. The heat flow increase will not require changes in the design of the superheater. More important than the change in radiative heat transfer is the change in fouling of superheater surfaces.

With increasing dry solids content there should be no obstacle to increasing the furnace exit temperatures. For new recovery boilers, less than 1000 °C is typically specified even though nose temperatures of up to 1100 °C have been measured. With higher dry solids the observed superheater corrosion rates are much reduced. A possible cause is the lack of reducing conditions and the increase in carbonate content in deposits.

The flue gas flow is lower with higher dry solids liquor and the heat flux required to superheat steam increases. This means that the temperature drop of flue gas across superheater will increase. To maintain constant superheating either the furnace outlet temperature must be increased or the boiler bank inlet temperature can be lowered.

If the boiler bank inlet temperature is reduced, the average temperature difference between the flue gas and the steam is also reduced. This reduces heat transfer and we need substantially more superheating surface. Heat treatment changes the heat available for superheating, Table 6-6. This behavior is similar to the decrease in superheating with falling boiler load.

Mixed measurements on the effect of high dry solids on superheating have been presented. Jones has recorded a significant superheating temperature drop with the Arkansas Kraft boiler (Jones and Anderson, 1992). The Metsä-Sellu Äänekoski boiler does not show such behavior (Ryham and Nikkanen, 1992). One possible reason for this is the smaller amount of fouling of heat transfer surfaces.

Example

During operation with 65 % dry solids and at 90 bar steam drum pressure, total superheating equals to 230 °C of which 50 °C is used for attemperating. If we assume that furnace exit temperature remains constant at 950 °C and boiler bank inlet temperature is now 580 °C, how would superheating change when black liquor dry solids is 80 %.

We can use non dimensional calculation and assume heat transfer coefficient does not change.

Total temperature difference θ is about

950 - 310 = 640 °C.

Temperature difference of flue gas is

950 -580 = 370 °C.

Temperature difference of steam is

480 - 310 = 170 °C.

Non dimensional parameters for the current case are

$R = 170/370 = 0.459$

$\varepsilon = 370/640 = 0.578$

then

$R\varepsilon = 0.459*0.578 = 0.266$

and we can solve z

$z = \ln((1-R\varepsilon)/(1-\varepsilon))/(1-R) = 1.025$

Now the flue gas flow will decrease 5 % (Figure 6-3) , so z will decrease 5 % to 0.974. The steam flow will increase 7%, so R will decrease by 7% and by 5 % to 0.406.

We can then solve the new ε by assuming that z remains constant

$\varepsilon = 1-(1-R)/ (e^{-z(1-R)}-R) = 0.569$

then

$R\varepsilon = 0.406*0.569 = 0.231$

so heat to superheat decreases

1-1.05*0.231/*0.266 = 9 % or 20 °C.

Example

How would then increase in furnace exit temperature by 23 °C affect the boiler bank inlet temperature and heat to superheat.

We can again use non dimensional calculation and assume that heat transfer coefficient does not change.

Total temperature difference θ is

973 - 310 = 663 °C.

All dimensionless parameters, R, ε and z remain constant so from previous example R = 0.406, ε = 0.569 and z = 1.025

Temperature drop of flue gas from nose to boiler bank inlet is $\varepsilon\theta = 0.569*663 = 377$ °C. The boiler bank inlet temperature is then 973 - 377 = 596 °C. The heat capacity ratio R is the same so heat to steam increases by 377/370-1 = 2 %.

From table 6-6 we see that for example boiler the available heat to superheat decreased 107.5/110.4 = 2.6 %, steam flow increased 135.3/126.6 = 6.9 % and superheating decreased 20 °C. Our assumption of constant heat transfer coefficient caused underprediction of change.

7 Recovery boiler processes

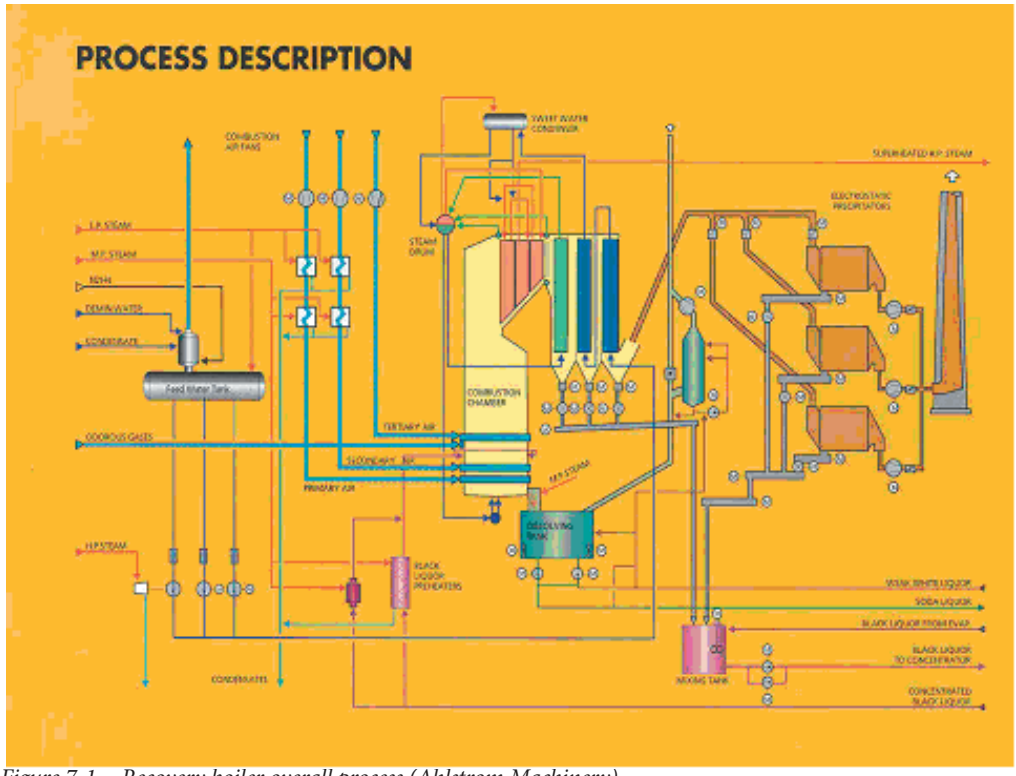

Figure 7-1, Recovery boiler overall process (Ahlstrom Machinery).

The processes occurring in boilers are divided according to the main media to several subprocesses. The main categories are air system, flue gas system, black liquor system and water and steam system. The ash system takes care of the ESP and convective surfaces ashes.

Recovery boiler has processes that are typically missing from other types of boilers. Green liquor system handles smelt and vent gas system handles wet exhaust from green liquor system. Starting and stopping black liquor recovery boiler requires auxiliary fuel firing, which is usually oil or gas.

Kraft process produces smelly odorous gases. These gases classified as concentrated NCG and diluted NCG are often burned at recovery boiler.

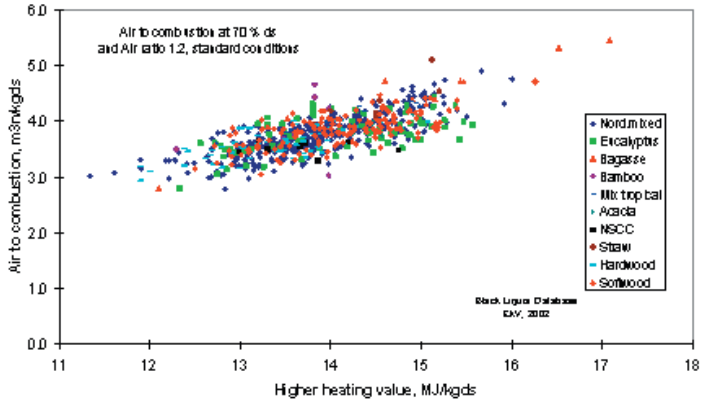

Figure 7-2, Specific air for black liquor combustion as function of black liquor higher heating value.

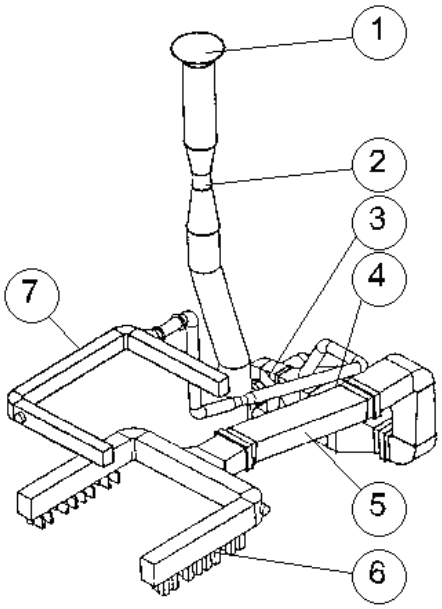

Figure 7-3, Air system for a small boiler.

7.1 AIR SYSTEM

Black liquor consists of combustible organic material and inorganic material that react in the furnace. To be able to sustain combustion air is needed. As the organic content in the black liquor increases more air is needed per unit of black liquor dry solids. The main requirements for boiler air system are maximum mixing and proper air distribution.

Air is typically delivered at several horizontal elevations to ensure complete combustion and minimize emissions. A typical boiler air system, Figure 7-3, consists of 1 - inlet duct with silencer, 2 - venturi for air flow measurement, 3 - air blower, 4 - air heater, 5 - distribution ducts, 6&7 - air ducts. In addition pressure and temperature measurement devices are installed to proper locations.

Air flow is controlled with dampers in furnace openings and by control of air blowers. The air flow trough blowers can be controlled by damper in the duct, changing of rotative speed of the blower or by inlet vane control dampers. The air flow control with dampers in furnace openings produces high duct air pressures. This increases blower power consumption but ensures uniform flow though each opening.

Air intake is typically located high inside the boiler house. This ensures even temperature profile in the boiler house and utilization of heat losses. Upstream location of air blower from air preheaters decreases air blower power consumption. After air heater the air is split into separate ducts for even distribution to different sides of the boiler. It is important to use low design velocities as even small variations in parallel air duct lengths otherwise cause large differences.

Air temperature is controlled by air heaters. There are several air heater types. When flue gas is relatively clean it can be used to preheat air. In bark

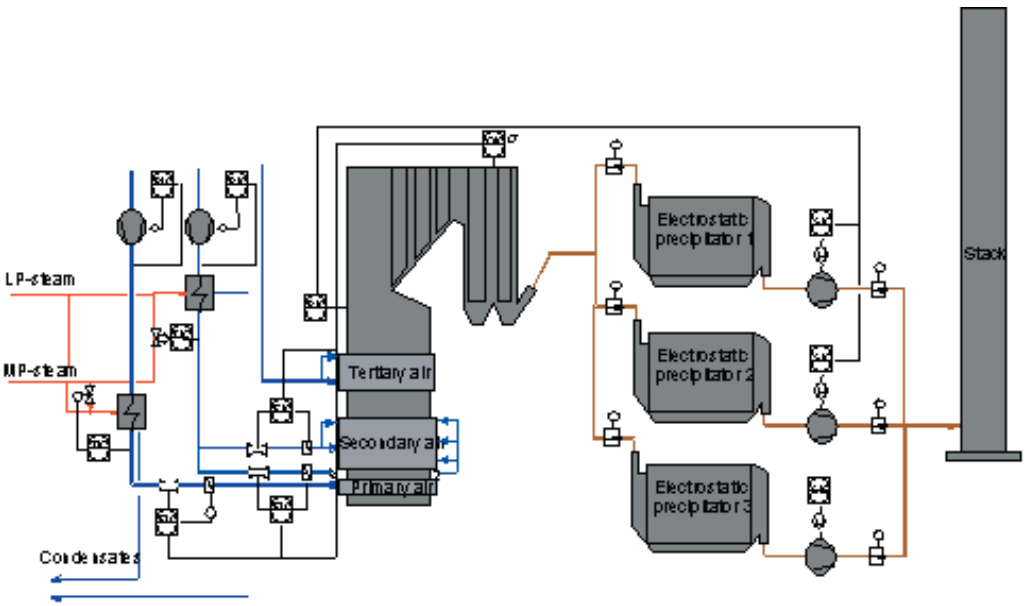

Figure 7-4, Air and flue gas process diagram.

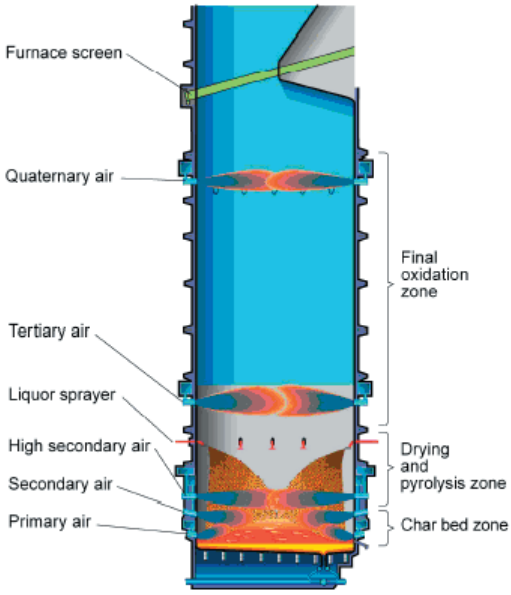

Figure 7-5, Furnace of a large recovery boiler (Mäntyniemi and Haaga, 2001).

boilers several pass steel tube cross flow air heaters are used. In dirty environments, recovery boilers, steam and feedwater air heaters are used. The role of air heater is to increase the furnace temperature which decreases required heat transfer surfaces and increases heat transfer to steam.

Air is typically delivered at several horizontal elevations to ensure complete combustion and minimize emissions, Figure 7-5. Forced draft fans are used to supply air to furnace. Airflow is controlled with dampers in furnace openings and ducts and by control of air fans. Damper in the duct can control the airflow to furnace. The same can be done by changing of rotative speed of the blower or by inlet vane control dampers. The air flow control with dampers in furnace openings produces high duct air pressures. This increases blower power consumption but ensures uniform flow though each opening.

Air intake is typically located high inside the boiler house. This ensures even temperature profile in the boiler house and utilization of heat losses. Upstream location of air blower from air preheaters decreases air blower power consumption. After air heater the air is split into separate ducts for even distribution to different sides of the boiler. It is important to use low design velocities as even small variations in parallel air duct lengths otherwise cause large differences.

Air heaters control air temperature. There are several air heater types. When flue gas is relatively clean it can be used to preheat air. In bark boilers several pass steel tube cross flow air heaters are used. In dirty environments, recovery boilers, steam and feedwater air heaters are used. The role of air heater is to increase the furnace temperature which decreases required heat transfer surfaces and increases heat transfer to steam.

Air system - requirements

The newest air systems introduce most of the combustion air into the lower furnace, just above the furnace floor. The main target is to maintain a high temperature and uniform gas velocity distribution in the lower furnace. Most of the innovative new air systems concentrate on increasing the mixing and jet penetration in the lower furnace (Wallen *et al*., 2002).

Higher black liquor dry solids content increase the furnace temperature. With a higher temperature difference the penetration of air jets increases. Improved understanding of mixing requirements in the lower furnace led to redesign of the airports. All secondary airports are designed for both pressure and flow area control. This allows the operator to change airflow pattern depending on the changes in black liquor properties for improved lower furnace control. Airport shapes are chosen to maximize operating life and minimize fouling.

The main target of the design of the air system is to maintain a high and uniform temperature and gas distribution in the lower furnace. With optimized air introduction the emissions are low and the reduction efficiency is constantly high. With a proper design the combustion takes place in the lower part of furnace. The whole height is effectively utilized for cooling the flue gases before they enter the superheaters.

The combustion air is introduced into furnace from at least three air levels; primary, secondary and tertiary. The primary and secondary are located close to the furnace floor beneath black liquor guns. The tertiary air is introduced above liquor guns. With this system reducing conditions are maintained close to the char bed in the lower part of the furnace. Effective oxidizing environment in the upper part is generated. This means that 80 to 90% of total air is introduced through primary and secondary air nozzles and the rest and excess air via tertiary air nozzles.

Each air level has a separate air fan (forced-draft fans). In smaller boilers only two air fans are used; one for primary and one for both secondary and tertiary. Having separate fans for each level, air pressure in windbox and airflow can be controlled

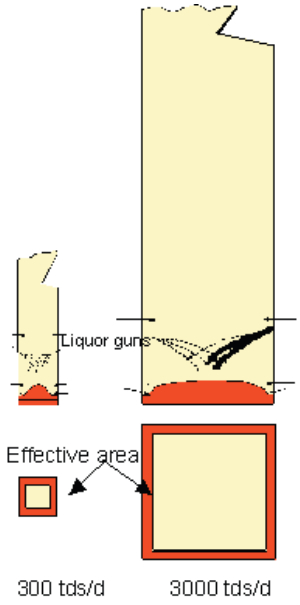

Figure 7-6, Area of penetration for primary air.

independently. Variable inlet vanes or speed of the fans controls desired windbox pressure.

Each air level has usually own air ducts. These are located symmetrically around the centerline of the furnace. Much attention is paid to design of air ducts. Several inlet locations and low design velocity are targeted. This arrangement ensures a uniform air distribution to all walls eliminating the risk for uneven loading of the upper furnace. In older systems the airflow can vary up to 30% between two adjacent nozzles at the same wall.

Air flow used in airport calculations is a theoretical air plus excess air (10 … 20 %), from which sum the infiltration air (4 … 8 %) is subtracted.

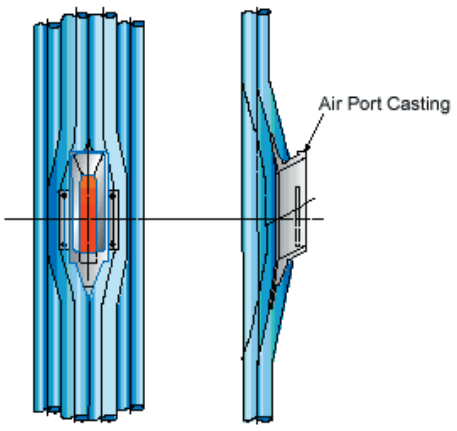

Figure 7-7, Cast primary airport opening (Shenassa et al., 2002).

Depending on the black liquor analyses a typical value of specific airflow is 3.6-4.0 $m^3n/kgds$. While calculating the actual volumetric air flow the temperature, pressure and altitude corrections have to be made. In order to increase the controllability 20 to 30% design margin is used at the primary and secondary air levels. When operating at design load the airports are about 80 percent open. At the tertiary air level design margin is up to 100%. The big margin is due to willingness to control the share of tertiary air in wide scale. Design margin is also needed to take into account possible changes in black liquor composition. If the calculated air flow from given black liquor analysis differs a lot from typical specific value wider design margins have to be reconsidered.

Windbox pressure is a function of boiler capacity. Different design pressures at different size furnaces are used so that secondary and tertiary air jets reach the center of furnace. Design static pressure in a primary air windbox varies between 800 …1500 Pa. The lower value is the minimum necessary to avoid char bed and smelt intrusion. Secondary and tertiary air windbox pressures vary between 3000 … 5000 Pa. Due to furnace draft the pressure drop over the nozzle is a little higher (+200 … 400 Pa). For larger boilers higher windbox pressures are used. High windbox pressure means high jet velocity, high mixing, high efficiency combustion and higher electricity usage.

Primary air system - design

The primary air should be delivered at constant pressure and velocity to maintain combustion stability. It should be delivered uniformly to the boiler to create symmetry (Adams, 1988). Primary airflow has lesser effect to furnace combustion than other air levels. With primary air charbed is kept away from the walls by increasing burning at the edges of the char bed. The effective area of primary air reaches only to about 1 m from the wall, Figure 7-6.

Primary air openings are equally spaced on each wall. Higher spacing requires higher primary air pressure. Side spacing of up to about 650 mm has been successfully used. Side spacing in the corners of the furnace is 300 … 700 mm. In that way accumulation of black liquor in the corners is prevented. This charred heap can collapse and flow through primary air openings to the air duct and even into the boiler house. The airports are designed so that height (straight portion) to width ratio is 1.5 … 2. Plugging tendency of modern wide openings is lower than the narrower ones. Use of high pressure and individual dampers de-

creases the possibility of primary air plugging.

The primary air openings are directed from 10 to 45° downwards. The purpose of this is to prevent smelt flowing to air openings. Higher opening angled leads to 'hole digging' in front of the ports. Molten areas can be seen, which lead to low reduction and in extreme cases possibly to primary port damage.

Secondary air system - design

Secondary air is introduced just above the char bed to maintain a specified temperature in the lower furnace. By controlling this temperature low emissions and high reduction efficiency can be maintained. If the boiler is using high dry solids the main challenge is often how to keep a high enough char bed, not how to keep it hot. With a proper design the combustion takes place on the lower part of the furnace. The whole furnace height is thus effectively utilized for cooling the flue gases before they enter the superheaters. This improved temperature profile (reduced furnace outlet temperature variation) reduces fouling of heating surfaces and the risk for superheater corrosion. Stable combustion in the lower furnace requires efficient mixing by high velocity jets. Adjustable dampers and precise flow control enable operation at low load levels.

Secondary air level has the biggest effect on recovery boiler furnace operation. Its main purpose is to burn up flowing gases rising from the char bed. This burning radiates heat back to the bed, which helps to maintain high char bed temperature. In addition the secondary air prevents the char bed from growing too high. Complete combustion means that the mixing of the combustibles and the air should be as effective as soon as possible above the whole char bed. Upper section heat surface plugging can be decreased by proper introduction of secondary air. Using improved secondary air arrangement can decrease carryover, lower furnace exit temperature, lower gaseous emissions and increase hearth temperatures (Jones and Chapman, 1992).

The secondary airport arrangement should be as flexible as possible. Then different air distribution models can be used during boiler operation. The secondary airports are usually placed along the whole length of the wall. Most modern air systems use two wall secondaries. The idea of secondary air port arrangement is to get as high coverage of the horizontal cross sectional area as possible. Another item is to decrease the collisions of the air jets in the corners of the furnace. Air port shape has little effect on jet penetration (Blackwell and Hastings, 1992). After few hole diameters the jet has coalesced to round one.

The first openings are placed at 0,5 … 2 m distance from the corner. The spacing between secondary openings can vary up to 2.5 m. The larger the opening the larger is the optimum spacing (Tse *et al*., 1994). When planning secondary airport opening arrangement the number and placement of start-up burners has to be taken into consideration. The number of secondary airports is often equal in the opposite walls. Unequal number causes an uneven gas flow at the furnace outlet. It is also recommended that the number of the secondary airports at each wall is even.

Tertiary air system - design

The tertiary air burns the remaining combustibles rising from the lower section. Its effective area should extend to center of furnace. In practice this is quite easy because the tertiary air is unheated and provided at high velocity.

Tertiary openings are located typically on the front and rear wall. Maximum spacing between nozzles can be up to 3.5 m. The number of the tertiary airports can be uneven. Often front wall has one port more than rear wall. The tertiary airports are then interlaced. Interlacing increases mixing (Jones in Adams *et al*., 1997). By introducing more air through front wall the upflow is forced to rear wall side. Properly designed nose can then function as effective flow turner.

Opening shape does not play a major role. Jet penetration is function of port hydraulic diameter (Collin and Vaclavinec, 1989).

Often the number of tertiary airports tends to increase with boiler size, Figure 7-8. It should be remembered that 3/2 and 4/3 arrangements are the best for mixing (Adams, 1994).

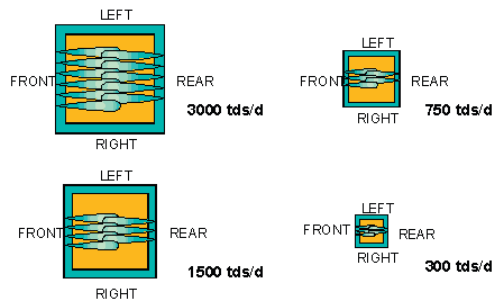

Figure 7-8, Different tertiary airport placements.

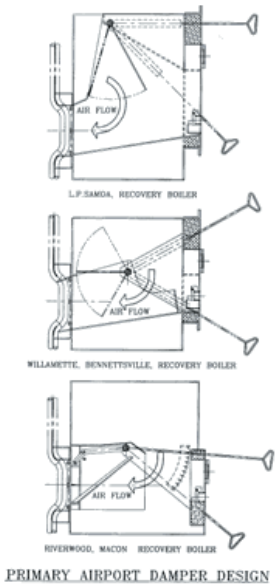

Figure 7-9, Different primary air airport damper arrangements (Ahlstrom Machinery).

Airport flow adjustment

Airflow to each level is accurately measured with a venturi either on fan inlet or on fan outlet. Airflow is controlled with dampers in furnace openings and by control of air blowers.

In all the airports the adjusting takes place smoothly just in front of the furnace wall. Adjusting is performed by dampers. In addition, those are protected at the primary air level ring duct in the case of a falling char bed. Guillotine type dampers can also be used. In Figure 7-9 several types of Ahlstrom Machinery primary air airports are shown.

The airflow through primary airports is adjusted either individually or in groups. Secondary and tertiary airports are adjusted independently.

Airports at the secondary and tertiary air levels should be as open as possible. If a number of openings needs to be throttled it is more preferable to close a few airports in order to get others more open. Dampers are needed at the primary air level. With them a lower windbox design pressure can be utilized. Leaving them out leads in problems with low load operation.

During boiler operation pressures fluctuate at the primary air level +-200 Pa, at the secondary air level +-500 Pa and at the tertiary air level +-700 Pa. Reason for the fluctuation is that the airports are getting dirty. When automatic airport rodders are installed this deviation can be kept below 100 Pa.

The individual dampers of secondary and tertiary airports are connected to a governor shaft that runs along each wall. The system is provided with an actuator and the dampers can be operated remotely wall by wall. Since the connection to the shaft is adjustable it is still possible to individually adjust a damper even if it is connected to the main shaft. Governor shaft can be used in air controlling if requested.

Multilevel air systems

Theoretically multilevel air looks nice but in practice it is difficult to operate, because the flow conditions in the furnace are not stable. Especially at the low load the penetration of the air jets decreases considerably. In literature and in practice four level air can be introduced by doubling the

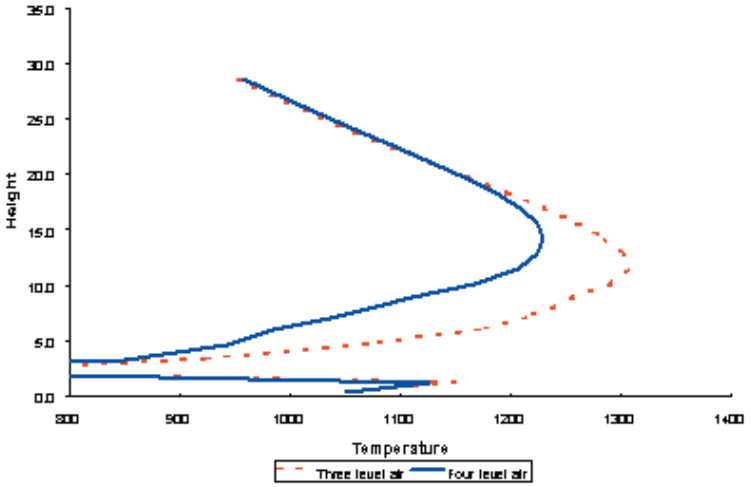

Figure 7-10, Furnace temperature with three and four level airs.

secondary air level or by doubling the number of tertiary air level.

The most typical application of multilevel air is NOx control. By increasing the number of air levels we can shift the combustion down. The lower furnace temperatures decrease increasing with lower stoichiometry the sulfur species concentration. This arrangement is beneficial for NOx control, but detrimental for SOx and reduction control.

Low concentration NCG systems

Typically dedicated nozzles are used to burn HVLC NCG (or DNGC). These nozzles are of special design. To allow rodding of each airport during operation ball valves and tightly closeable disk valves are used to separate each nozzle from NCG stream. Figure 7-11 shows and example of DNCG nozzle design, courtesy of Andritz. Another mandatory requirement is condensate removal lines. DNCG's contain often 20 – 30 % moisture.

High concentration NCG systems

Dedicated burners are used for LVHC NCG (or CNCG), turpentine and methanol. Typically all three are burned using same burner opening. Turpentine and methanol are fired at liquid form using lances.

High concentration odorous gases increase sulfur load in the furnace. This increase can be up to 30 % of all sulfur released in the furnace. If high concentration odorous gases are fired, then high dry solids (>75%) is preferred. The main criterion is that LVHC NCG can be fired without plugging of economizer section.

Burning dissolving tank vent gases

There are several recovery boilers in operation that introduce dissolving tank vent gases to the recovery boiler furnace. In a typical system a fan draws vent gas from dissolving tank. Condenser is used to reduce moisture. Controlling moisture levels is essential. Adding water vapor to furnace unnecessarily cools down flue gases and ads to flue gas volume.

A scrubber is sometimes used to reduce particulate loading and to keep ducts from plugging. Before introduction to furnace these gases are heated to prevent accidental introduction of water to recovery boiler furnace. When the system is not in use vent gases are routed trough scrubber to roof or stack. Figure 7-12 shows and example dissolving tank vent gas system courtesy of Kvaerner.

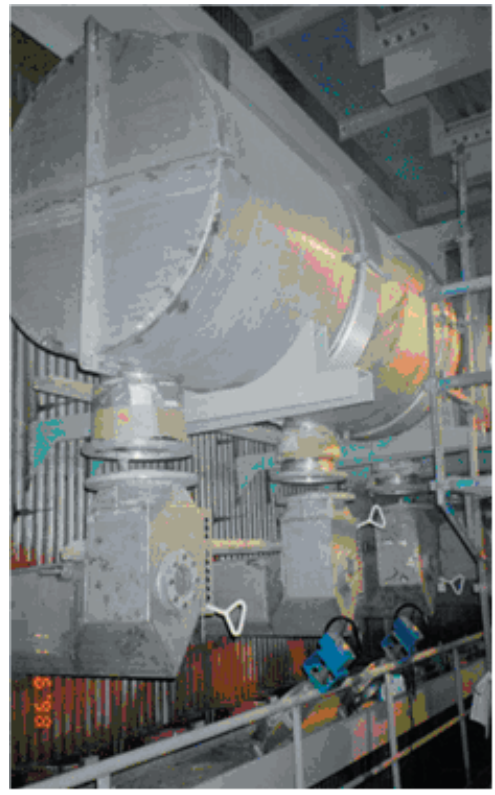

Figure 7-11, Example of HVLC NCG system before insulation and installation of separation valves.

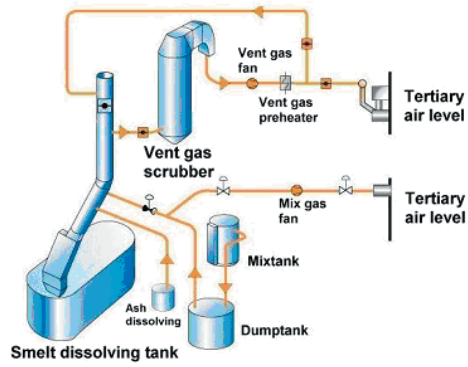

Figure 7-12, Example of dissolving tank vent gas system.

7.2 FLUE GAS SYSTEM

The flue gas system transports combusted material from the furnace safely to the atmosphere. Flue gases from the furnace pass through heat transfer surfaces. The flue gas then flows through flue gas ducts, dampers, flue gas fan, electrostatic precipi-

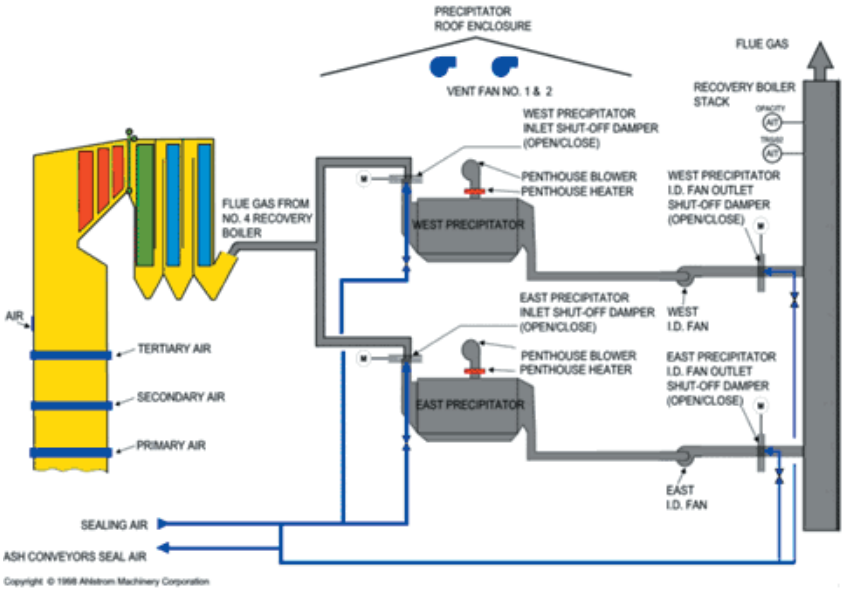

Figure 7-13, Flue gas system of a recovery boiler (Ahlstrom Machinery, 1998).

tator, possible scrubber and stack.

Natural draft caused by density differences in stack is not adequate to draw flue gases out from recovery boiler furnace. The flue gas flow is controlled by induced draft of ID fans. Flue gas fan controls also the furnace draft. The furnace pressure at liquor gun level must be kept below boiler house pressure.

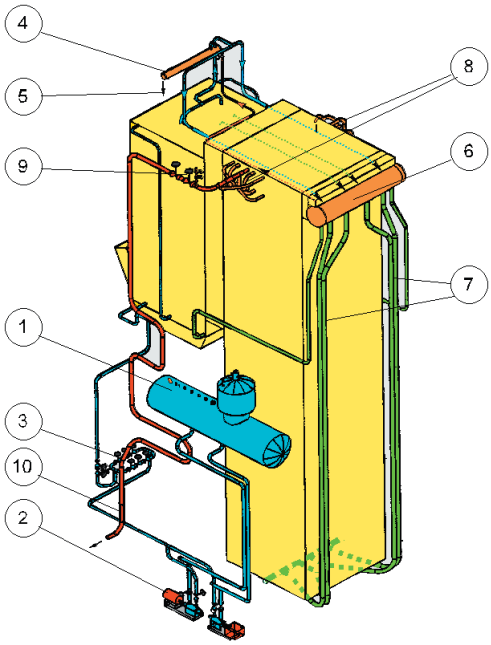

Figure 7-14, Water circulation system.

Flue gas system of an example boiler is shown in figure 7-13. Similarly to air system flue gas fans draw air from the furnace to the stack. In old days draft in the stack was enough. Flue gas ducts connect pieces of equipment. Electrostatic precipitators and other emission reduction equipment are employed to decrease pollution.

7.3 WATER AND STEAM

Boiler water and steam circulation starts with low pressure feedwater and ends with high pressure and temperature steam. The water and steam circulation components transport, pressurize, preheat, vaporize and superheat the water into steam, Figure 7-14.

The starting point of boiler water and steam circulation is the feedwater system. For reliable operation of boiler the feedwater must be low in oxygen and minerals. The feedwater system consists of feedwater tank-1, deaerator, boiler feedwater pump-2, control valve and the feedwater piping-3. The feedwater enters then first heat transfer surface, economizer.

The economizer recovers heat available in the flue gases. This heat is used to preheat the water close to the boiling point. Recovery boilers surfaces foul easily so typically vertical gas flow is used. Counterflow arrangement where hot flue gases and cold feed water enter at opposite ends, is preferentially used.

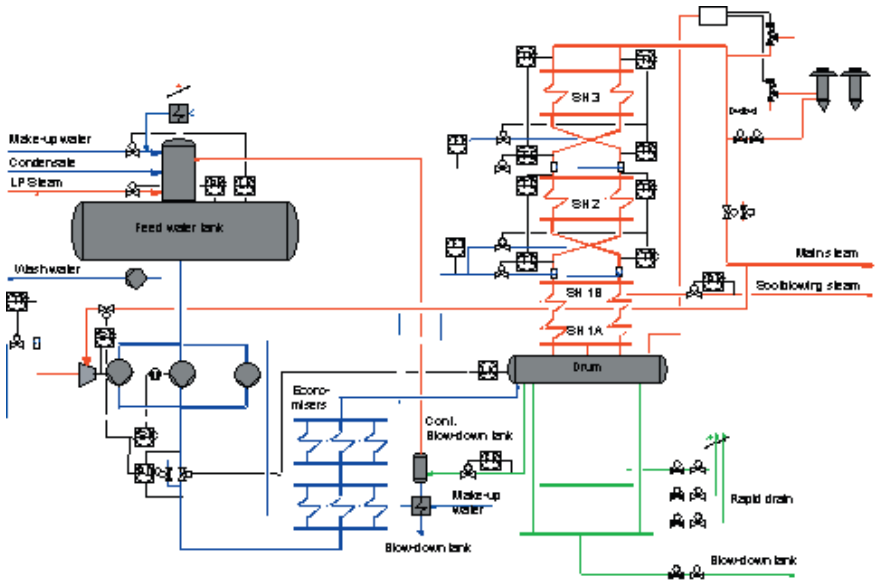

Figure 7-15, Steam and water process diagram.

The water from the economizer is used to generate clean attemperating or desuperheating water-5 from steam in a sweet water condenser-4. The feedwater then flows to the steam drum-6. In steam drum steam is separated from water. Separation is achieved by gravitation, screens and cyclone separators.

Downcomers-7 feed saturated water to evaporative surfaces. Partially evaporated water is collected with risers to the steam drum. Furnace walls do most of evaporation. Depending of boiler operating pressure between 10 to 25 % evaporation is done in boiler bank. The two predominant boiler bank arrangements are vertical and horizontal flow. Both can be used for dirty and clean gases.

Saturated steam exits from drum and flows through superheaters. The role of superheaters is to heat the steam well above the saturation-8. Because turbines can only operate down to some 95 % steam content, proper choice of main steam pressure and temperature is required. Steam flow is controlled by main steam valves-9. The steam from superheaters flows trough main steam line-10 to turbine.

The steam temperature control is done by attemperating. Either condensed steam or feedwater is sprayed into steam line between superheaters. Typically only a two stage desuperheating is used. The source of the spray water must be determined by the available feedwater purity.

Recovery boiler has a risk of smelt/water explosion due to the presence of molten smelt in a porous char bed. To minimize possible damage an emergency system, rapid drain system is installed. The rapid drain system consists of fast valves and pipes to major pressure parts. If the rapid drain is opened pressure inside boiler drives water from the pressure part. In rapid drain system there are separate lines from furnace walls, from the boiler generating bank and from economizers. Water is left at the lowest part of the furnace to provide cooling for the floor tubes. If all water from floor tubes is drained, the heat from char bed damages the tubes.
Water circulation is caused by density difference between steam filled heating surfaces and downcomers. The circulation is limited by friction losses in surfaces, headers, risers and downcomers. Increasing boiler operating pressure decreases the driving force, density difference. High pressure operation requires either pump assisted circulation or once through operation.

Downcomers and raisers

Downcomers are tubes that start from the drum and lead water to lowest points of furnace walls and boiler banks, Figure 7-16.

Downcomers can be divided to main downcomers and connecting tubes. It is customary that from two to five large tubes go straight down from the drum. From these tubes smaller tubes take water to wall headers.

Separate downcomers are often constructed to the boiler bank and sometimes also to the side

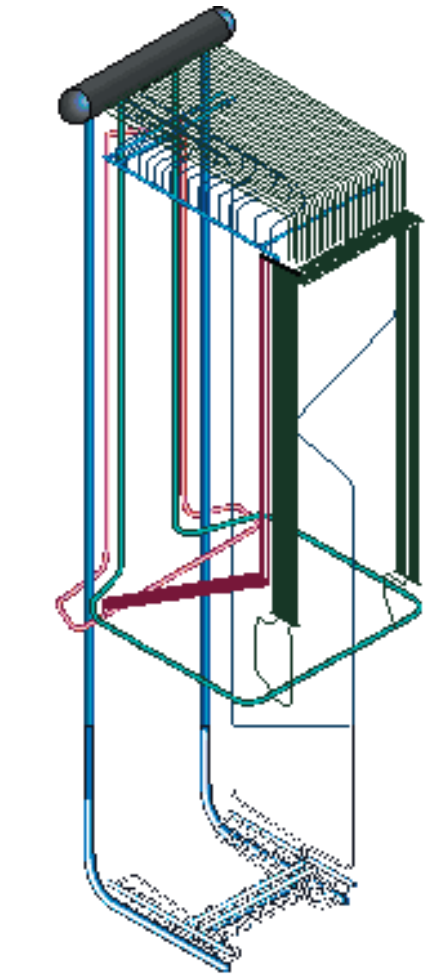

Figure 7-16 Main tubes in a recovery boiler (Kvaerner).

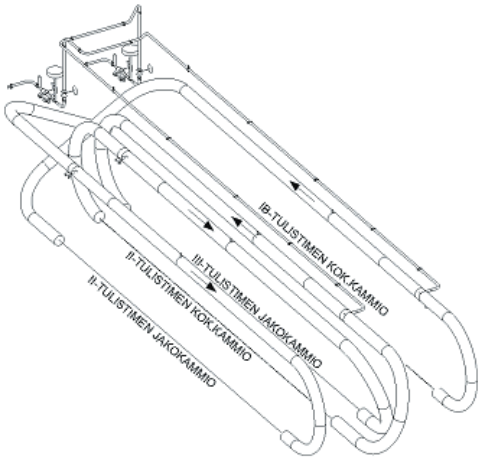

Figure 7-17, Superheater connection tubes

wall extension between furnace tubes proper and boiler bank.

Wall tubes

Wall tubes are the membrane wall tubes that extend from the lower headers to the upper headers. Usually front and back wall are bent together to form the furnace bottom, Figure 7-16. In addition front wall is often bent towards the boiler bank to form the furnace roof. In lower furnace compound membrane construction is used. In middle and upper furnace carbon steel membrane construction is almost always used.

For airports, manholes, liquor gun openings, sootblower openings, smelt spout openings and instrument openings tubes must often be bent.

Headers

Typically each heat transfer surface starts and ends with header, Figure 7-16. Headers are larger tubes that connect all parallel tubes of a heat transfer surface together. Their role is to divide the incoming liquid evenly to all tubes. They also try to collect the fluid without causing uneven flow.

Headers were earlier of various shapes. Even square cross section was used. Nowadays only tubular headers are used.

External pipes

Most of the parts of the pressure vessel belong to the heat exchanger surfaces and circulation system. There are is a system of pipes, equipment and vessels that handles the feedwater. There is also a system of pipes that handles main steam. In addition there are pipes that belong to the desuperheating system, blowdown system, air preheating system, draining system, air venting system and piping assisting the operation of the safety valves. All these tubes and pipes are called external pipes.

Feedwater system

Feedwater system consists of piping tanks and equipment that pump water to the inlet of the economizer, Figure 7-15. Demineralized water is pumped to the feedwater tank. Feedwater tank has a storage capacity corresponding to 15 … 45 minutes of feedwater usage at MCR. In addition to storage, deaeration is carried out to the incoming water. The purpose is to remove all traces of gases especially oxygen and carbon dioxide from the water

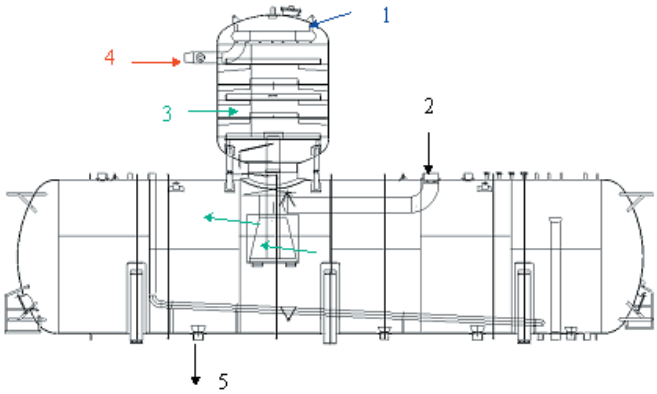

Figure 7-18, Feedwater tank, 1- deaerator, 2 - steam in, 3 – trays, 4 - water in, 5 - water out.

Feedwater is pumped from the feedwater tank to the economizers with feedwater pumps. Typically the feedwater pumps are driven by electric motors. To ensure safety during pump failure there are usually more than one pump. Feedwater flow is controlled by feedwater valves.

Superheater connecting tubes

Each superheater must be connected to the following superheater. To even out left right flow and temperature imbalances connecting tubes cross sides.

Feedwater tank

Feedwater tank sits usually in the middle of the boiler room. Feedwater tank is situated at height of 10 – 30 meters so that the feedwater pumps can have the necessary head to operate. Feedwater is stored in the feedwater tank, Figure 7-18. Returning condensate is mixed with make-up water. The feedwater flow is not even and the boiler can have disturbances. The tank capacity needs to correspond to some 20 minutes to 1 hour reserve water calculated from MCR feedwater.

Feedwater tank is also used to separate gases from the feedwater. This is done by steam stripping incoming water in the deaerator.

Feedwater pump

Feedwater pumps are commonly centrifugal pumps, Figure 7-19. To ensure high enough head, several even dozens of individual pumps have been arranged in series to same axle. A feedwater pump is most often driven by electric motor for energy efficiency. Often also a spare steam turbine driven feedwater pumps included for safety reasons.

To ensure adequate feedwater flow a boiler must have at all times a little bit of higher capacity for feedwater than for steam generation. Feedwater

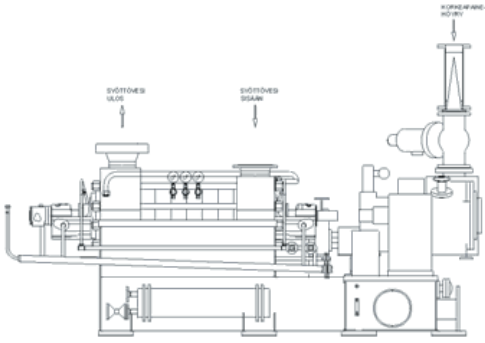

Figure 7-19, Feedwater pump

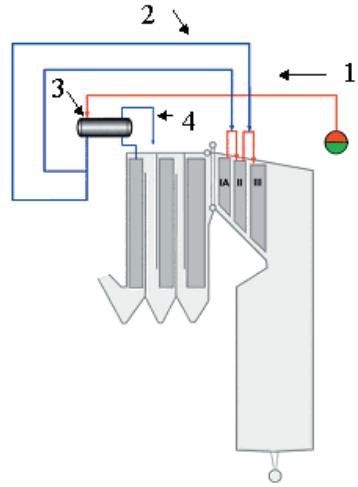

Figure 7-20, Dolezahl – attemperator, 1 - Steam flows from drum, 2 - condensation in heat exchanger, 3 - condensate sprayed to desuperheat, 4

Figure 7-21, Spray water group

pumps can be common for several boilers. For safety normally one needs full feedwater flow even if one feedwater pump fails.

Dolezahl – attemperator

Dolezahl attemperator is used especially in the industrial boilers where feed water quality is lower than in the utility boilers. In a Dolezahl feedwater condenses steam. This condensate is sprayed using the static head formed to attemperate the produced steam. Normally saturated steam is used. High quality of spray water is ensured as saturated steam has much higher purity than corresponding feedwater.

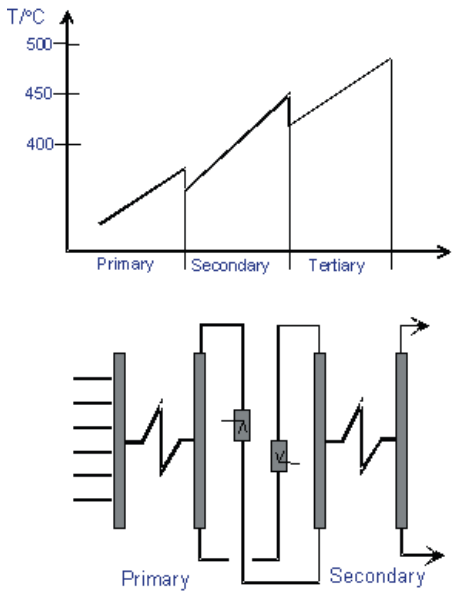

Figure 7-22, Operation of attemperating group

Spray water group

In a spray water group feed water is injected into steam. This increases the steam massflow and decreases the steam temperature. Typically spraying to different tubes is arranged close to another for maintenance purposes. Also automatic spray water valve is usually doubled or tripled with hand valves. Often, because of location airing and emptying valves need to be installed.

Steam temperature increases in each superheating surface. Between surfaces water is sprayed to control final steam temperature. Forcing steam flow to change sides helps balance uneven temperatures.

Drainage and air removal

When boiler is brought to operation it must be

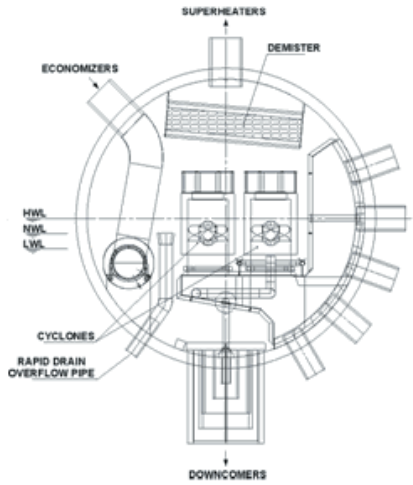

Figure 7-23, Steam drum.

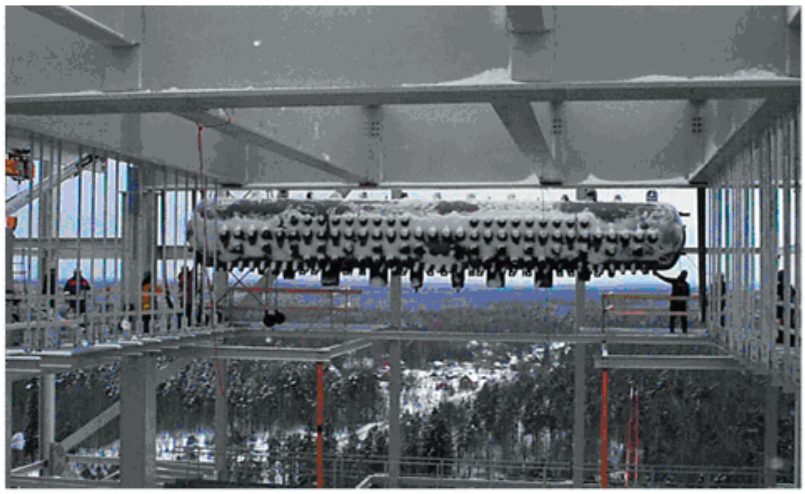

Figure 7-24, Erection of steam drum under wintery conditions.

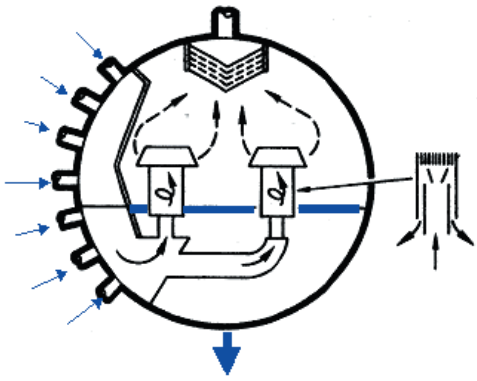

Figure 7-25, Operation of drum.

filled with water and air removed. All top points of each heat exchanger surface need to be equipped with small lines with a hand valve to be able to remove air from the pressure vessel.

Steam drum

Steam drum consists of a circular section welded from bent steel plate with two forged ends. Circular section has a number of inlets and outlets. A drum can be made of a single thickness sheet if the pressure is low or with plates of multiple thicknesses if pressure is high. One reason for different thicknesses is that sections where are openings need to be thicker than sections without openings. Steam water mixture enters from raisers. Cyclone separators force water down. Steam exits through

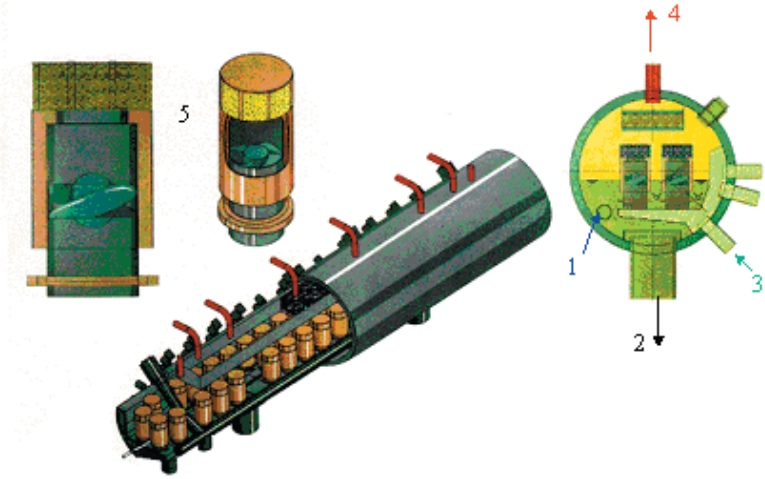

Figure 7-26, Placement of water separators in a drum, 1- feed water in, 2 – downcomers, 3 – raisers, 4 - steam out, 5 - droplet separator.

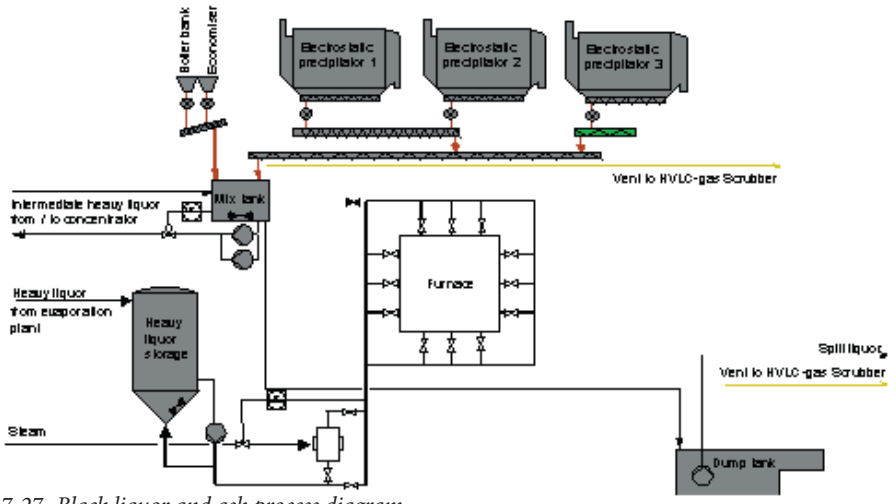

Figure 7-27, Black liquor and ash process diagram

baffle separators from top. Water exits through downcomers. Additional separation is done by a wire mesh or baffles at the top of the steam drum.

Only <<0.01 % water in steam is allowed. Water contains impurities. Impurities deposit on tubes and cause superheater overheat. Especially carbonate (CO_3) and sulfate (SO_4) form hard to remove deposits with low thermal conductivity. Impurities will also deposit on turbine blades. Na + K are the most harmful impurities for turbine.

As the steam drum is the heaviest piece of equipment it is often lifted as the first piece of pressure part equipment.

7.4 BLACK LIQUOR AND ASH

In modern recovery boiler the black liquor from heavy black liquor storage is pumped through heavy liquor pipe to ring header. Ring header is a large diameter pipe that circles the furnace. The purpose of the ring header is to ensure equal flow to all liquor guns. Collected fly ash form precipitator is mixed with about 50 % dry solids liquor in a mix tank and pumped back to the evaporator. Ash recycle helps evaporator operation in high solids.

Black liquor system of an example boiler is shown in figure 7-28. It needs to have flow, temperature and pressure measurement. Typically there are more than one insertion points of the black liquor into the furnace, with black liquor guns.

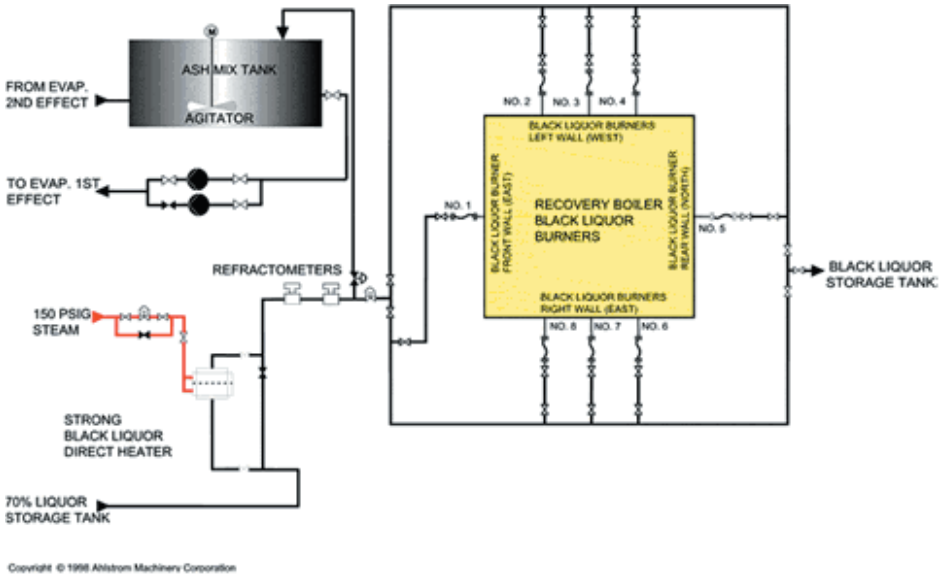

Figure 7-28, Black liquor system of a recovery boiler (Ahlstrom Machinery, 1998).

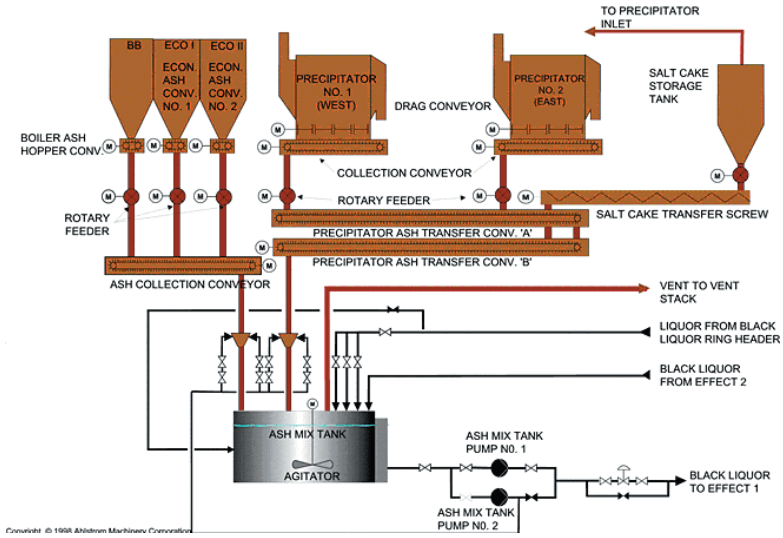

Figure 7-29, Ash system of a recovery boiler (Ahlstrom Machinery, 1998).

To control the liquor temperature the liquor can be heated in a liquor heater. Heating is done either directly with steam or indirectly with a heat exchanger.

Black liquor system design is thoroughly covered by standards and safety recommendations. This is because if it malfunctions, fire or explosion outside or inside the furnace could happen with loss of life and property.

When we burn black liquor chemical ash is formed. Ash system of an example boiler is shown in Figure 7-29. Ash system consists of ash transport equipment like screws and conveyors. There are hoppers where ash is collected. Rotary feeders are used to control ash flow. Ash can is handled dry or sluiced and pumped away.

In older boilers make up chemicals were added to mixing tank. Now as there often is excess sulfur in the mill the make up is added as sodium hydroxide.

7.5 OIL/GAS SYSTEM

Oil/gas fired fuel system of an example boiler is shown in Figure 7-30. If several fuels are used each fuel has its own fuel system.

Oil firing system has built in safety systems. Each

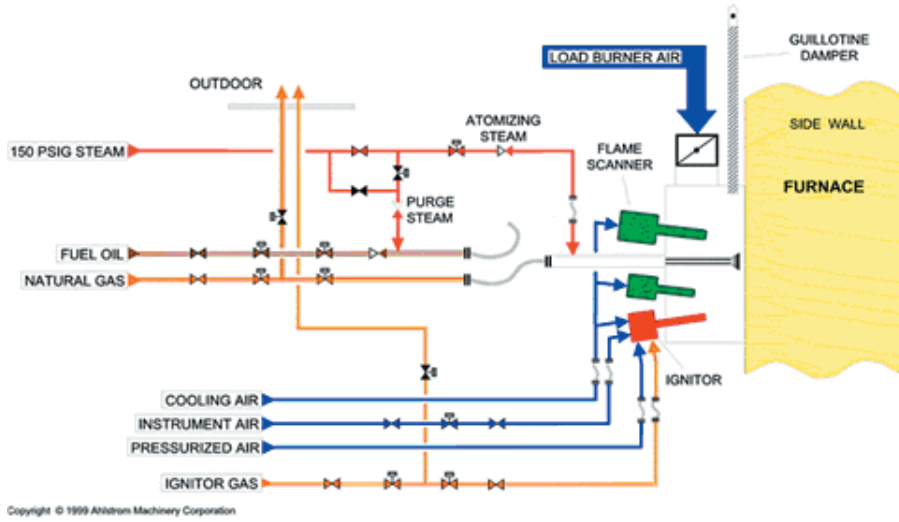

Figure 7-30, Oil/gas fired fuel system of a recovery boiler (Ahlstrom Machinery, 1998)

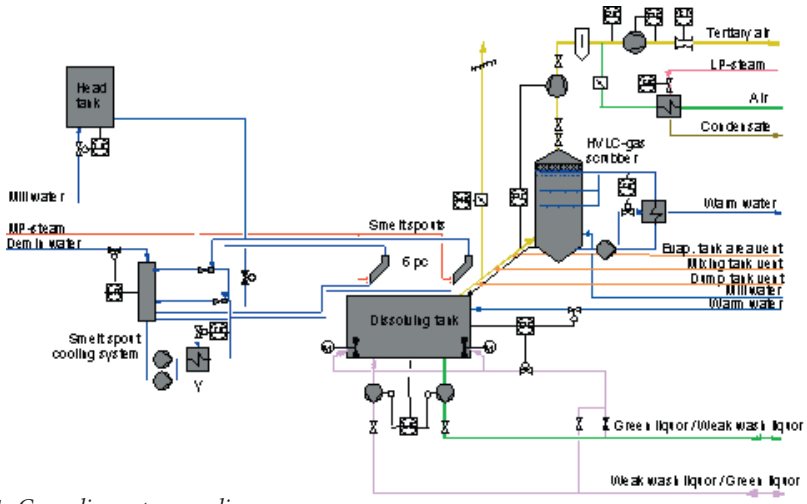

Figure 7-31, Green liquor process diagram.

burner needs it own flame monitoring. Instead of main flame monitoring an auxiliary or support flame can be monitored. Normally double valve arrangement is required to ensure closing of oil line.

Flame is lighted with an igniter. Often gas igniters are used. Especially heavy fuel oil is heated to lower its viscosity. To ensure sufficient atomization of oil pressurized air or steam is used to assist atomization.

If natural gas is used as fuel, venting to air is often used to ensure that gas leak to furnace is impossible.

7.6 GREEN LIQUOR

Green liquor is formed when smelt and weak white liquor are mixed at dissolving tank. Green liquor gets its name from iron oxide impurities which color green liquor.

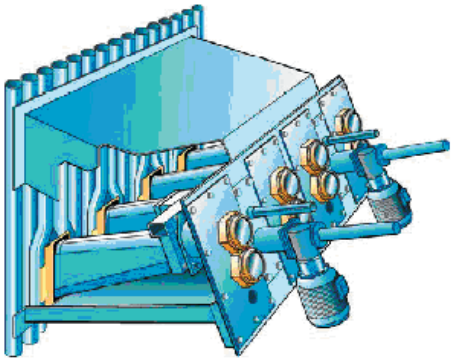

Figure 7-32, Roddingmaster automatic primary port air rodders (Sheyneassa et al., 2002).

Mixing molten inorganics to water creates heat. In a 3000 tds/d boiler the heat input is more than 10 MW. Heat usually escapes dissolving tank as steam. With steam green liquor droplets and H_2S gases formed escape. To reduce gas volume, dust and TRS content the vent gases are scrubbed with alkaline liquid.

Smelt spouts run from furnace to dissolving tank transporting molten smelt. They are cooled by ~60 °C water that circulates inside them.

Because green liquor forms pirssonite that will quickly block transport pipes, weak wash and green liquor pipes are exchanged to one another once a shift.

7.7 AUXILIARY EQUIPMENT

Recovery boiler needs for operation a number of equipment in addition to main equipment. This equipment is called auxiliary equipment. There are number of recent changes and additions to recovery boiler auxiliary equipment that are improving the process.

Automatic cleaning system

The target of airport cleaning system is to keep all the airports as open as possible most of the time. The port rodders are typically provided to airports below liquor guns. Sometimes it has also been provided to secondary airports. They are not used at all levels primarily because of expensive price. Plugging tendency at tertiary and quartenary air levels is low because of bigger airports and higher pressure.

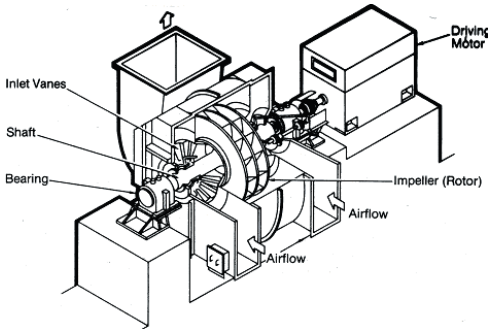

Figure 7-33, Radial air fan (Singer, 1981).

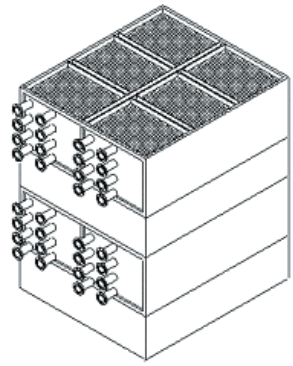

Figure 7-34, Steam air preheater.

The primary airports are cleaned in groups of two or three openings. At the secondary air level they are cleaned separately. All this is performed according to pre-programmed intervals.

Pyrometers and char bed cameras

Separate pyrometers are not needed if bed cameras are used. Instead cameras with integrated pyrometer should be used. Cameras and pyrometers are located in secondary air openings. One camera on a side wall close to rear wall and the other one in the opposite corner in the front wall.

Air fans

In boiler plants, fans supply primary and secondary air to the furnace. The air is primarily used for combustion of fuels, but can also be utilized in pneumatic transport of fuels and other solid materials to the furnace. The induced draft (ID) fans exhaust combustion gases from the boiler.

In operation, they normally cause a small under pressure into the furnace.

The selection of fan is made with the performance curves provided by the fan manufacturer. The curves are based on experiments that the manufacturers have made in laboratories for different types of fans. The curve illustrates the change in the total pressure created by the fan as a function of volume flow and speed of rotation. When choosing a fan, the required volume flow and pressure difference must be known. Other factors influencing the choice are

- Efficiency
- Required space
- Shape of the characteristic curve for the fan.

Most recovery boiler fans are radial type. Sometimes two sided air inlet is preferred. Axial fans are avoided as more expensive.

Steam air preheater

Steam air preheaters are used to preheat steam.

Figure 7-35, Retractable sootblower.

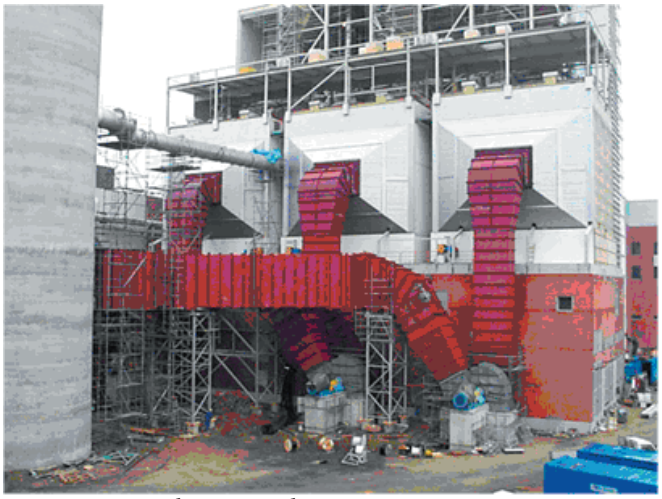

Figure 7-36, Electrostatic precipitator being erected.

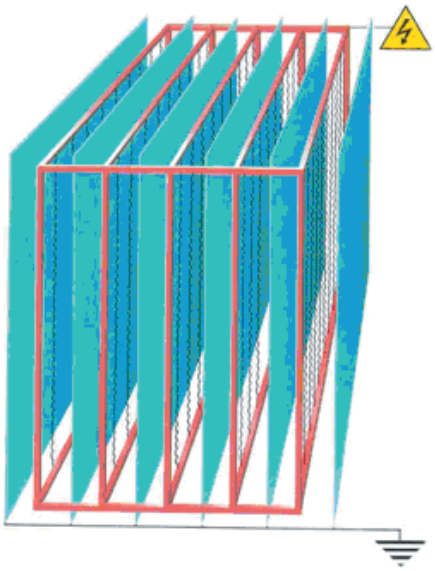

Figure 7 37, Schematic arrangement of collecting surfaces with electrodes (F.L.S. Miljø, 2002).

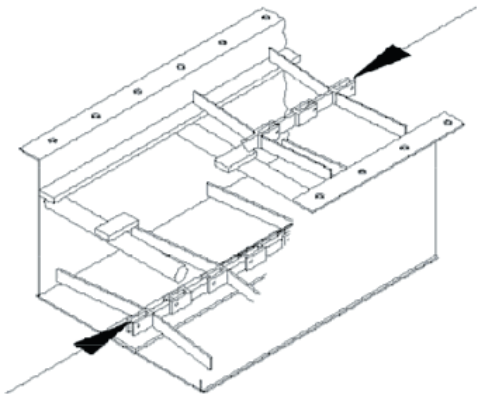

Figure 7-38, Section of an ash conveyor.

Steam flows inside tubes. Air flows outside finned or bare tubes and is heated by the condensing steam. Condensate flows out from the bottom headers.

Sootblowing

Most typical sootblower in the recovery boiler has a rotating lance which is inserted from wall to the heat exchanger surface, Figure 7-35. Tip of the lance has a hole. Steam at sonic speed is injected from tip. Sootblowers are pulled outside the boiler, when not in use.
This type of sootblower gradually rotates around while it is inserted and retracted. The sootblower is then able to clean a large area of a heat exchanger surface.

The steam mass flow through the nozzle is directly linear to the steam pressure (Jameel *et al.*, 1994). Nozzle design and flow area at nozzle throat affect the mass flow.

Electrostatic precipitators

Electrostatic precipitator efficiency depends on

$$\eta = 1 - e^{-\left(\frac{Aw}{V}\right)^k} \qquad 7\text{-}1$$

Where
e is the collection efficiency, -
A is the collector surface, m^2
w is the collection migration velocity, m/s
V is the actual gas flow, m^3/s
k is an empirical constant (0.4 .. 0.5 ..0.6), -

The principle of electrostatic precipitator is simple. Figure 7-37. Dust laden flue gas flows along col-

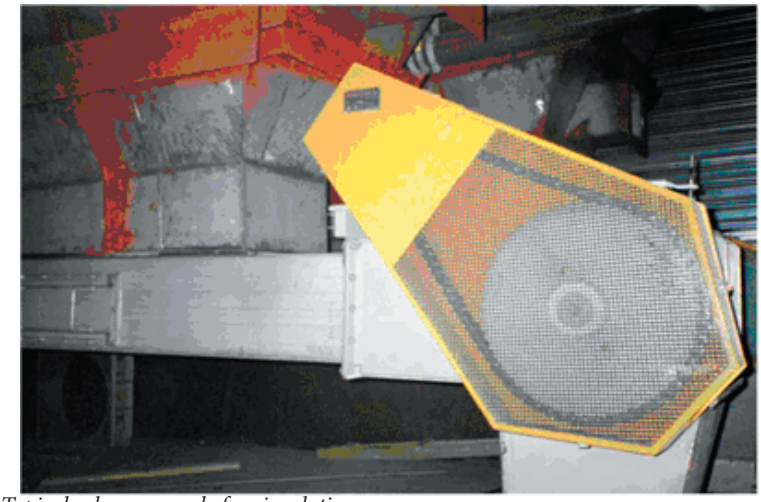

Figure 7-39, Typical ash conveyor before insulation.

lecting surfaces formed of plates. Strings of wire are suspended between the platens. When high voltage electric current is applied between the electrodes (-) and the collector plates (+), the dust particles become charged. The charge draws them towards the collecting plates where they deposit.

Ash conveyors

Ash is collected to hoppers. Motors turn ash conveyors. Collected ash is dropped to ash chutes.

Figure 7-39 shows a section of an ash conveyor. Ash is dropped to the conveyor from the top. It is dragged along the bottom to the right with moving scraper blades. These are attached to a belt. The belt returns on the top of the conveyor.

The return leg can be also below the conveyor bottom.

Mixing tank

Ash from electrostatic precipitator, economizers and boiler banks is mixed with 50 … 65 % black liquor. Recovery boiler ash is reusable chemicals, mostly sodium sulfate. The amount of recovery boiler ash is 5 … 12 % of black liquor dry solids flow. Higher ash flow corresponds to higher black liquor dry solids. In the older designs the black liquor from the mix tank was sprayed to the boiler furnace. In more modern, high dry solid designs the black liquor is returned to the evaporation plant for final concentration. If black liquor dry solids inside the mix tank gets too high the black liquor stops flowing out from the mix tank. If black liquor dry solids is too low the ash is dissolved into the black liquor. Increasing dissolved sulfate in black liquor makes it more fouling and

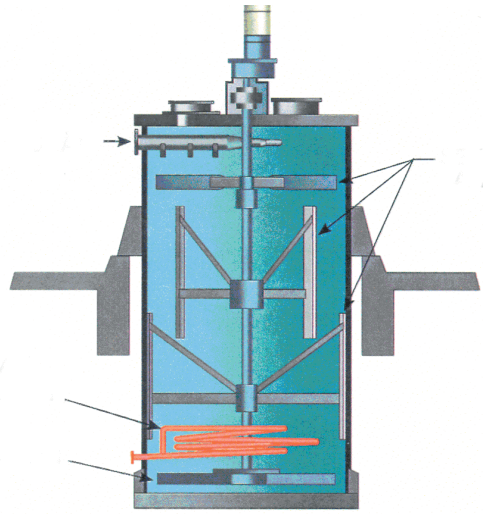

Figure 7-40, Ash mixing tank.

causes problems in the evaporation.

Boiler bank, economizer and electrostatic precipitator salt ash is dropped from the top through one or several openings to the mix tank. Incoming black liquor is sprayed from special nozzle so that it wets the ash at the liquid surface, Figure 7-40. Rotating rotor, often with blades mixes ash with black liquor. Ash containing black liquor is drawn through a screen plate (not shown in the picture) with a pump and pumped back to the evaporator.

Mixing hot ash with black liquor causes evaporation of water. At the same time sulfur containing gases in the black liquor are released. Formed NCG's must be removed from the mix tank and treated appropriately. Part of the ash is coming from economizer hoppers which operate under

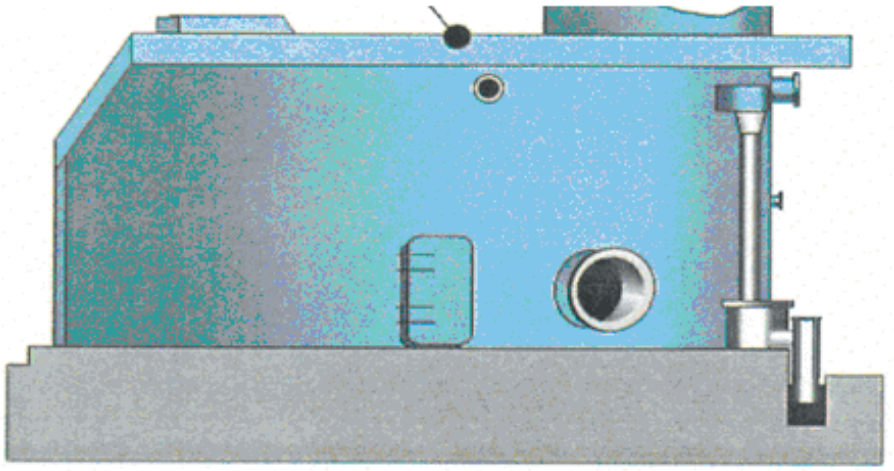

Figure 7-41, Dissolving tank.

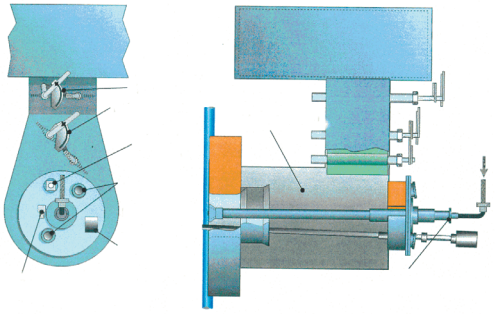

Figure 7-42, Startup burners.

atmospheric pressure. To prevent backflow all ash chutes are equipped with rotary feeders and air purge. Mix tank operates at about 115 °C. To prevent condensation and plugging all surfaces must be insulated.

Dissolving tank

The molten smelt flows from the recovery boiler furnace through smelt spouts to the dissolving tank, Figure 7-41. When dissolved to water or weak wash the smelt forms green liquor. Constant level and constant alkali content are maintained by pumping in weak white liquor to replace out pumped green liquor. Control of alkali content is done by measuring the density of the out flowing green liquor.

Dissolving is a violent action with noise, heat and vibration. This is because a smelt droplet is a poor heat conductor. After it drops to the tank the liquid cools the surface of the droplet. Cool surface contracts, but hot molten inside doesn't. When tension becomes high the smelt droplet pops open like popcorn. This popping action is responsible for the noise. To decrease the noise the dissolving tank is often lined with concrete. In addition steam jets or green liquor jets are used in trying to disperse smelt from smelt spouts to make very small smelt droplets.

Dissolving tanks often operate at high enough alkali content so pirssonite is formed at all surfaces (Frederick *et al.*, 1990). To limit scaling incoming weak white liquor and outgoing green liquor pipes are exchanged once a shift. Heat in smelt forms vapor in dissolving tank. This vapor contains small droplets of green liquor and TRS. This stream must be treated before it is burned of released to atmosphere.

Sometimes an operating error leads to a large smelt flow. This flow can cause a dissolving tank explosion. A dissolving tank stack is constructed so that it will lead pressure wave away from the boiler room. To prevent personnel accidents a concrete platform is built above the dissolving tank.

Startup burners

Startup burners are placed usually at all four walls, close to the recovery boiler bottom. The role of the recovery boiler startup burners is to heat up the char bed during startup and low loads. In addition the startup burners are used to burn away excess charbed before the boiler shutdown.

Startup burners use light fuel oil or natural gas.

Direct contact evaporator

There are still many boilers that use direct contact

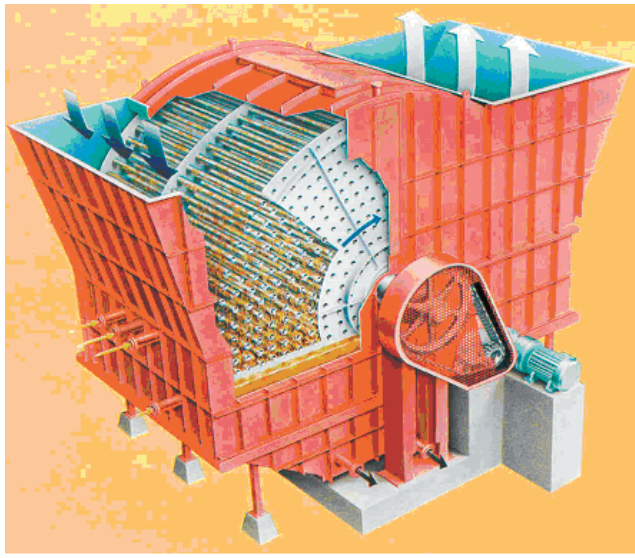

Figure 7-43, Cascade evaporator (Tampella).

(DCE) or cascade evaporators, Figure 7-43. Cascade evaporator looks like old mill's waterwheel, where flat surfaces are replaced with rows of tubes. Incoming black liquor sticks to the tubes when they are submerged in a black liquor pool. When these tubes emerge from the black liquor, flue gases evaporate water from the liquor that sticks to the tube surface. Black liquor dry solids 70 … 74 % can be reached. Cascade evaporator was a rather cheap way of increasing black liquor concentration at a time when multiple effect evaporators could produce only 45 to 50 % dry solids.

A big problem with cascade evaporators is that TRS in the black liquor is released during the process. Even if black liquor oxidation, which decreases the TRS levels to close to the 10 ppm level, is used the resulting sulfur emission is considered unacceptably high for a modern mill.

Other problems that plagued the cascade evaporator were fire (black liquor is burnable after all) and crusting of liquor to tubes because of too high flue gas temperatures.

There was another type of direct contact evaporator promoted by Babcock & Wilcox. In it the black liquor was sprayed to flue gases in a cyclone. Because this type is based on equilibrium and the CE type is based on countercurrent drying the B&W type achieved lower solids 60 … 65 %.

Last new boiler to be equipped with cascade evaporator started operating 1991 in US. At that time cascade evaporator was almost phased out in Scandinavia. Boilers with cascade evaporators have been supplied recently to India and China.

8 Fouling

Black liquors contain inorganic chemicals. During combustion and reduction reactions significant amounts of alkali compounds vaporize. Small char fragments and liquor particles may entrain to flue gas flow. These phenomena cause deposits on heat transfer surfaces.

The heat flow in a heat transfer surface can be expressed as function of heat transfer area and temperature difference between flue gas and steam/water. As the heat transfer surface gets fouled this heat flow decreases. Reduction in performance is caused by the increased heat transfer resistance of deposits.

Fouling and fouling related phenomena have long been of concern in recovery boiler design and operation. Several studies of recovery boiler plugging and fouling mechanisms have been reported (Tran *et al*., 1983, Tran, 1988). Even with improved air systems and advances in recovery boiler design, fouling remains one of the big operating problems.

It is typical to talk about recovery boiler fouling as it would be a consistent type of process with a single cause. Like many industrial problems there are number of different causes that lead to same end condition. To determine the cause of fouling the exact location and the fouling rate should be determined. It is also recommended to look at black liquor properties and changes in the pulping process. Changes in sulfidity, chloride and potassium levels of black liquor will cause changes in recovery boiler fouling.

For a modern recovery boiler the crucial piece of equipment is often the boiler bank. When black liquor dry solids is over 70 %, the economizers plug far less often. Superheater fouling has dramatically reduced. Modern recovery boilers have less superheater deposits because the new improved air systems have halved the carryover.

Finding the cause for recovery boiler fouling can be started by examining fouling at that boiler. There are several questions that need to be answered; How fast is the recovery boiler fouling. What measurements indicate the progress of fouling. Is the fouling continuous or are there equilibrium stages. Are there any upset or abnormal operation conditions that correlate with times of fast fouling. Does the furnace operate smoothly and well.

Often a cause for fouling can be found by looking at black liquor properties and changes in the pulping process. Especially changes in sulfidity, chloride and potassium levels can cause increased fouling.

To combat fouling black liquor properties can be changed. Decreasing flue gas temperatures or carryover rate helps. Improving surface cleanability or more frequent sootblowing can be used to reduce fouling. Their ability to solve the current fouling problem should be weighed carefully.

8.1 ASH DEPOSITS ON HEAT TRANSFER SURFACES

To understand fouling the first step is to identify the location and growth rate of the problematic deposit. Then one needs to find the cause for the problem. It is often difficult to clearly identify the degree of fouling without shutting down the boiler, but instrumentation can help in pinpointing the progress of fouling (Vakkilainen, 2000).

The two main methods to observe the fouling of the heat transfer surfaces are visual observation of the heat transfer surfaces by experienced operators and prediction of fouling from operating parameters; i.e. temperature and pressure measurements (Vakkilainen and Vihavainen, 1992). Prediction of fouling through estimation from operating parameters is the most frequently used method in modern sootblowing control systems (Bunton and Moskal, 1995, Jameel *et al*., 1995). The main fouling indicators are pressure loss measurements, flue gas temperature measurements and steam / water temperature measurements.

Modern CFD-programs offer some help in estimating the amount of carryover that ends up to superheater area (Fakhrai, 1999, Kaila and Saviharju, 2003). The amount of carryover is subject to changes in air distribution, black liquor properties and liquor gun operating practices. Because of limitations in input CFD can only be used to highlight the direction of changes to carryover and not to predict actual operating levels.

Several groups have attempted to formulate equations describing deposit properties in recovery boiler heat transfer surfaces (Backman *et al*., 1996, McKeough and Vakkilainen, 1998, Frederick *et*

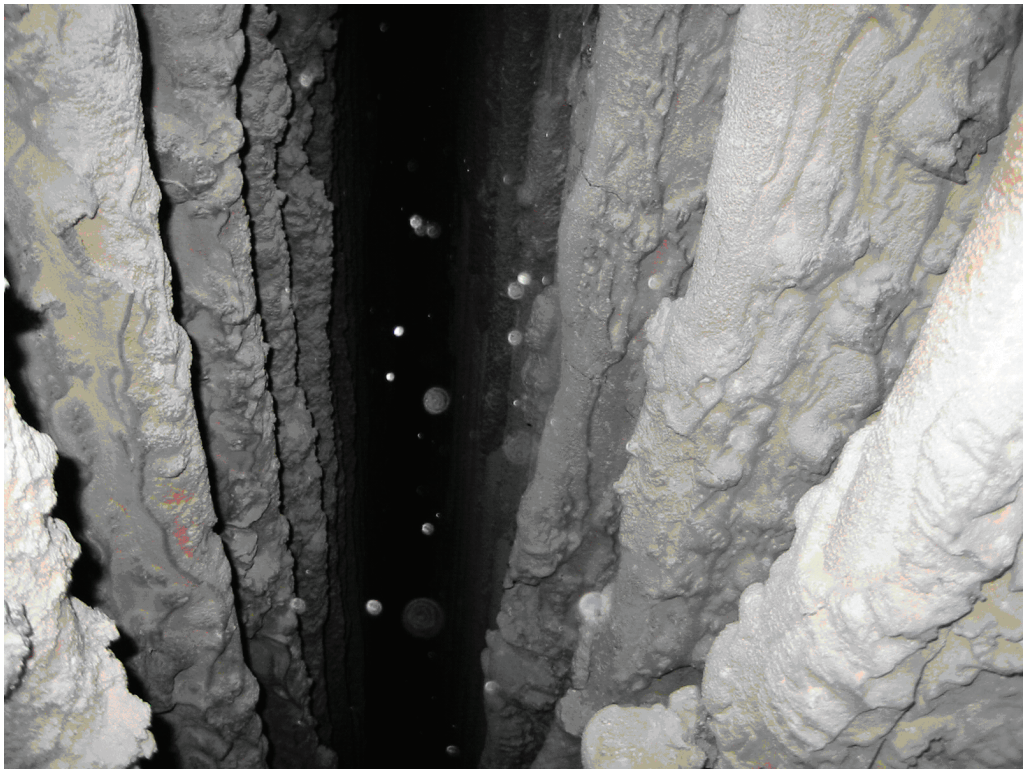

Figure 8-1, Deposits on superheaters seen along cavity between SH3 and SH2.

al., 2001, Janka *et al*., 2004). With the aid of these programs and measured black liquor properties one is able to predict from given operating conditions which surfaces are prone to fouling (Forssén *et al*., 2000).

As the heat transfer surface gets fouled the build-up of deposits decreases available gas flow area. This causes an increase in flue gas flow velocity and pressure loss across a heat transfer surface. The pressure loss is often more important for maintaining operation than the decreasing heat transfer. Usually the recovery boiler maximum capacity is limited by the flue gas side pressure loss. Fouling increases until the flue gas fan can not supply enough pressure and flow. Then the recovery boiler load must be decreased or the boiler shut for water washing.

Superheater fouling

Superheater deposits are formed mainly by two mechanisms, inertial impaction and fume deposition (Backman *et al*., 1987). Deposit properties vary widely depending on the location of sampling. The high carbonate and sulfide contents as well as low chloride and potassium enrichment can be explained by assuming different mixing ratio of carryover and fume (Vakkilainen and Niemitalo, 1994, Janka *et al*., 1998).

The flue gas velocities at superheater area are rather low 3 – 5 m/s. This creates good conditions for separation of large particles. For particles over 10 µm the collection efficiency at superheater surfaces is high (Jokiniemi *et al*., 1996).

Superheater deposits decrease the heat transfer and lower the steam temperature. Low superheater main steam temperature requires boiler to be shut down for water was. Superheater deposits can significantly reduce the recovery boiler availability (Clement *et al*., 1995). As superheater heat transfer decreases the temperature entering boiler bank increases. Superheater deposition can thus negatively influence the fouling in downstream heat transfer surfaces.

Boiler bank fouling

Boiler bank is the crucial piece of equipment for a modern recovery boiler. Especially after increased mill closure the boiler bank plugging has been the most problematic fouling in modern recovery boilers.

There are several indicators for boiler bank plugging. Some of the typical ones are low melting

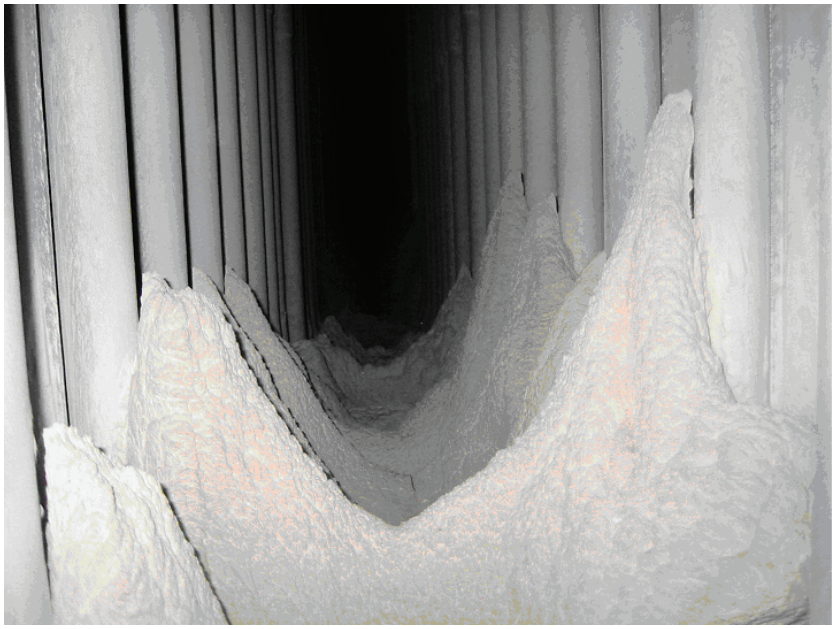

Figure 8-2, Deposition in the middle of the boiler bank.

temperature of ash deposited, increased black liquor chloride content, too high flue gas temperature into boiler bank and fast sintering rate of deposits (Frederick *et al.*, 2001). All of these indicators point to problems in controlling the fouling rate.

Economizer fouling

Economizer fouling is typically caused by low ash pH. Higher dry solids increases lower furnace temperature. Increased lower furnace temperature increases sodium and potassium release (Frederick *et al.*, 1998). As sulfur release stays rather flat (Perjyd and Hupa, 1984) the excess shows as carbonate in ash, Figure 8-3.

With low dry solids firing there is no carbonate. As less and less sodium is released there is excess of sulfur. Part of the dust remains sodium bicarbonate (Backman *et al.*, 1984). Increased sodium bicarbonate decreases pH of dust. Figure 8-4 shows actual simultaneous mill measurements of dust carbonate and pH. To keep dust pH above 10 one needs at least 2 to 3 % of carbonate in ash.

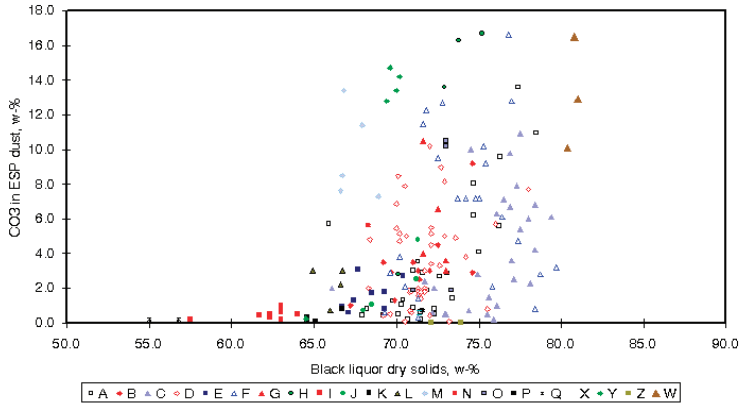

Figure 8-3, Carbonate in ESP ash as a function of dry solids.

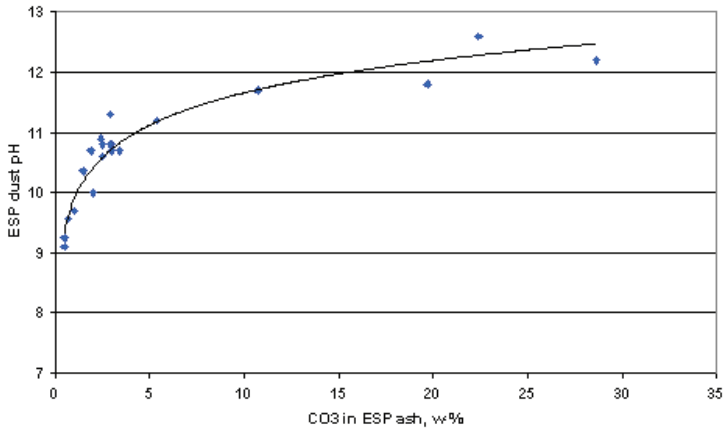

Figure 8-4, Effect of dust carbonate to pH of ESP ash.

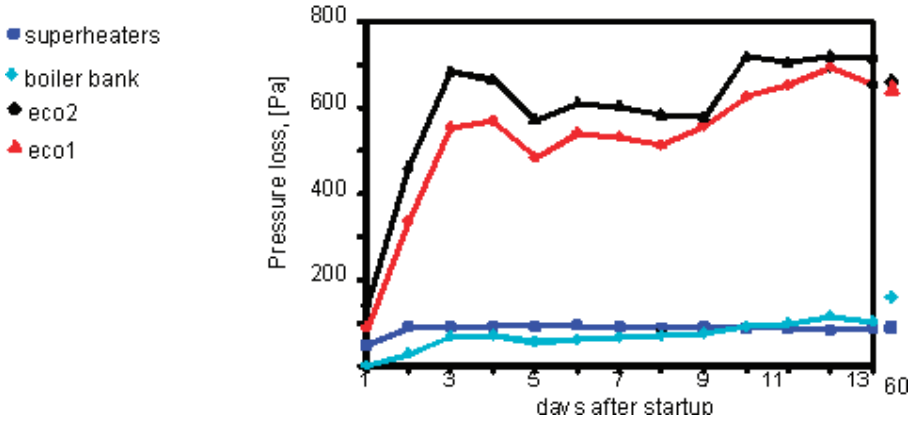

Figure 8-5, Pressure losses in heat transfer surfaces during 14 days after startup, 60 equals situation after 60 days (Vakkilainen and Niemitalo, 1994).

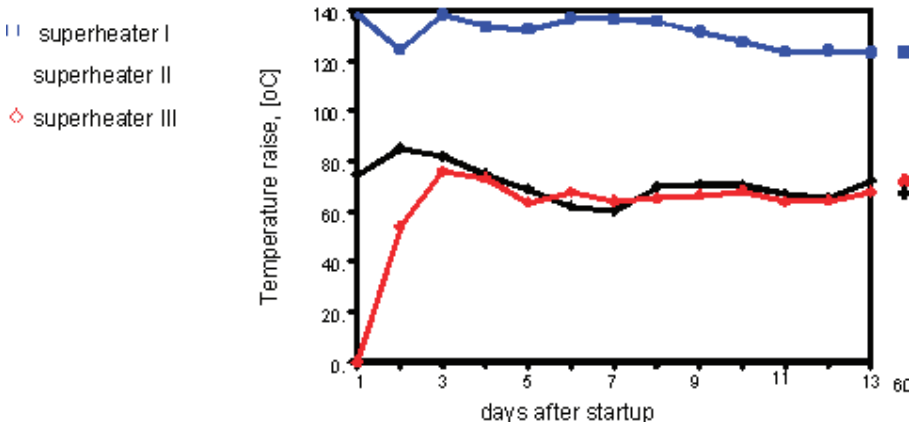

Figure 8-6, Temperature raises in superheaters during 14 days after startup, 60 equals situation after 60 days (Vakkilainen and Niemitalo, 1994).

It has been found that ash with low pH is sticky and hard to remove form surfaces (Tran, 1988, Uloth *et al*., 1996). In practice it has been found that economizer ash is not sticky and is easy to remove if the pH of 10 % of dust in water solution is at least 10.

With higher dry solids the economizers plug far less often and are seldom the cause of serious problems.

Use of temperature measurements to predict fouling

Flue gas temperatures are measured in several locations. These typically include char bed temperatures, furnace temperatures from different heights, boiler bank inlet and flue gas exit temperatures. The furnace temperature measurements are done mainly for operating purposes and are not normally used to predict fouling. Temperature measurements at superheaters, boiler bank and economizers can be used to predict fouling. Operating temperatures rise when heat transfer surfaces get fouled. The main difficulty in predicting fouling with flue gas side temperature measurements is the limited number of measuring points. Accurate prediction of fouling at individual superheaters needs far more gas side temperature measurements than are usually available.

Use of pressure measurements to predict fouling

If we position two gas side pressure measurement elements one before the heat transfer surface and one after the heat transfer surface we can use the pressure difference information to indicate fouling. Measured pressure loss is affected also by the flue gas flow. The flue gas flow can be assumed to be directly proportional to the boiler load. The most reliable boiler load measurement is main steam flow. To compensate for the changes in boiler load, the measured pressure differences can be scaled with the square of the steam flow as follows:

$$d_p^* = d_p \, (q_{nom} / q_{steam})^2 \qquad 8\text{-}1$$

where

d_p^* is the scaled pressure difference, Pa
d_p is the measured pressure difference, Pa
q_{steam} is the measured steam flow, kg/s
q_{nom} is the nominal steam capacity, kg/s

In practice only the pressure drops of economizers and boiler bank are significant, Figure 8-5 (Vakkilainen and Niemitalo, 1994). The pressure drops of superheater section are always lower than 10 Pa. The pressure losses in economizers and boiler bank increase during the first few days after start-up because boiler load is increasing. Then a level of stable pressure difference is achieved. The pressure difference in the superheater area and economizers changes only a little after that. Vakkilainen and Niemitalo (1994) observed that after two months of operation no significant change in superheater, economizer and boiler banks had occurred, Figure 8-5. The boiler bank fouling seems to be slower and a more continuing process. This increase is often very slow. With modern instrumentation the overall fouling of boiler banks and economizers can be predicted by pressure loss measurements. The pressure loss measurement does not tell where exactly in the heat transfer surface is fouling.

Predicting superheater fouling

Superheater fouling can be predicted by using steam side temperature raise. These temperatures are reliably and easily measured. At a constant steam flow rate, the steam temperature raise is directly proportional to the heat flow to that surface. When the superheating decreases, the fouling in that heating surface has increased.

The daily averages of superheating right after the start-up of a recovery boiler are presented in Figure 8-6, (Vakkilainen and Niemitalo, 1994). It shows that each superheater achieves its equilibrium fouling degree in two weeks. After that the superheating in all superheaters is fairly constant.

The attemperating flow is another good index of overall superheater fouling. As the heat flow to superheaters decreases less attemperating is needed. The attemperating water flow describes how much the superheated steam has to be cooled to keep the main steam flow temperature constant. Clean heat transfer surface conducts heat better and the superheating is more effective. Attemperating can also be measured as the temperature decrease between one superheater outlet to next inlet.

Figure 8-7 (Vakkilainen and Niemitalo, 1994), presents the attemperating flows between the superheaters as daily averages after start-up. The lowest curve, attemperating flow I, is between primary and secondary superheaters. The middle, attemperating flow II, is between secondary and tertiary superheaters. The highest curve is the sum of these two. Directly after start-up, when the superheaters are clean, the attemperating flow is at its maximum. Then the attemperating starts decreasing as superheaters are fouled. The changes in attemperating flow are small after two weeks of

operating. The boiler operating mode affects the superheating and attemperating flow.

8.2 FORMATION OF ASH PARTICLES IN RECOVERY BOILER

In kraft recovery boilers the ash is formed by several mechanisms. It is known that black liquor properties, operation practices and furnace conditions affect the ash content and ash properties in the flue gases (Frederick and Vakkilainen, 2003, Hupa, 1993, Janka *et al*., 2004, Tran *et al*., 2000, Vakkilainen, 2002).

Alkali metals in burning black liquor droplets vaporize. They subsequenly react with furnace gases and condense to small particles. This process is called fume formation. Most of the ash in recovery boiler flue gases is fume. Almost all ash collected in the electrostatic precipitators is fume.

Some of the black liquor fired into recovery boiler furnace gets caught with flue gas. Furnace gases drag these burning particles with them out of the furnace. This process is called carryover particle formation . Rate of carryover depends on firing practices especially droplet size. In addition material that can form carryover is physically ejected from burning black liquor droplets (Verrill and Wessel, 1998). Most of the ash depositing to superheater surfaces is carryover.

It has also been observed that during char combustion intermediate size particles. are formed in the char bed (Kochesfahani *et al*., 1998). They probably contribute both to fume and carryover formation and deposit on superheater and boiler bank(Mikkanen, 2000).

Fume

In the kraft recovery furnace the alkali elements are vaporized. When flue gases are cooled the vapors become supersaturated. Another mechanism of supersaturation is formation of species by reactions. E. g. sodium hydroxide and sulfur dioxide may react to form sodium sulfate, which has lower vapor pressure than the reactants (Jokiniemi *et al*., 1996).

Supersaturated vapors may form particles via two mechanisms. In homogeneous nucleation two vapor molecules stick together to form a small particle. For this a vapor pressure much higher than unity is needed. Vapors then start to condense on these particles. In recovery boiler furnace there are small metal oxides and other impurities present, which will serve as starting nucleus for the vapors. This process is called heterogeneous condensation. After formation of nucleus the vapor condensation to these particles keeps supersaturation low.

Formed very small particles grow to a uniform size. Much of the particle size growth is result of agglomeration. Small liquid particles collide with each other and form new spherical particles. Resulting particle size is less than 10 µm. Measured mass averaged fume particle average sizes are 0.5 … 1.3 µm, Figure 8-8 (Bosch 1971). Furnace conditions especially the black liquor dry solids with load and liquor species affect the average particle size (Mikkanen, 2000).

Measurements of fume particle mass distribution indicate that the mean particle size does not change from the size seen at the furnace outlet level (Mikkanen *et al*., 1999, Baxter *et al*., 2001). After flue gas temperature decreases below about 550 °C fume particles that hit each other do not stick. But particles that touch each other can grow together through a process called sintering (Duhamel *et al*., 2004). Sintering takes place at particles deposited on heat transfer surfaces. There fume can form large agglomerates. These agglomerates can re-entrain to flue gas when sootblowed. They show as larger 20 … 30 µm particles at electrostatic precipitator inlet, Figure 8-9 (Mikkanen, 2000, Janka *et al*., 2000). Amount of re-entrained dust is 10 … 30 % of total dust flow (Tamminen *et al*., 2000).

Fume deposits at tube surfaces consist initially of fine filaments with large aspect ratios and high porosity (Frederick and Vakkilainen, 2003, Baxter *et al*., 2004).

Most of the fume tends to end up in electrostatic precipitator. Figure 8-10 shows ESP dust as function of black liquor dry solids from about twenty recovery boilers. Furnace temperature increases with increased black liquor dry solids. This increases sodium and potassium release (Frederick *et al*., 1995). ESP ash flow forms an estimate of fume formation in recovery boiler. Black liquor sodium and potassium release depends also on the liquor i.e. wood species and the pulping conditions (Backman *et al*., 1999). In addition the firing conditions affect the lower furnace temperature. As can be seen the actual fume formation rate as a function of black liquor dry solids can vary a lot.

Dust (or fume) formation is almost directly propotional to the black liquor firing rate, Figure 8-11 (Tamminen *et al*., 2002). Chemical equilibrium

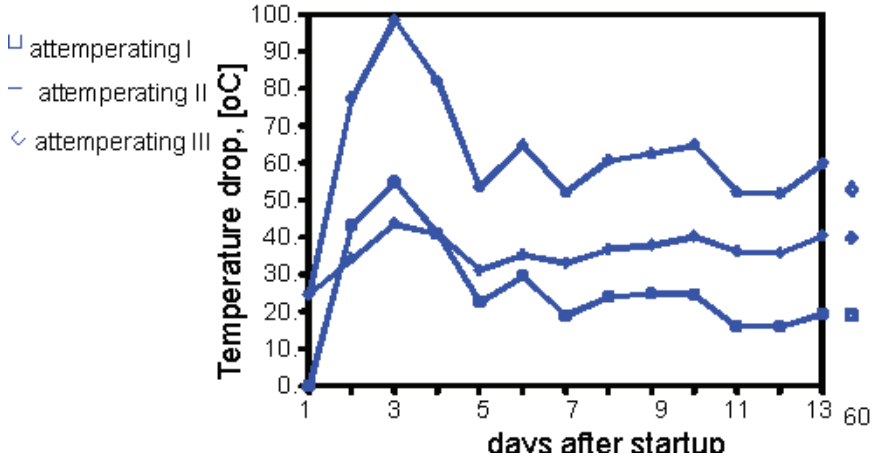

Figure 8-7, Attemperating flow as the sum of temperature drops between the superheaters II - III and IB – I (Vakkilainen and Niemitalo, 1994).

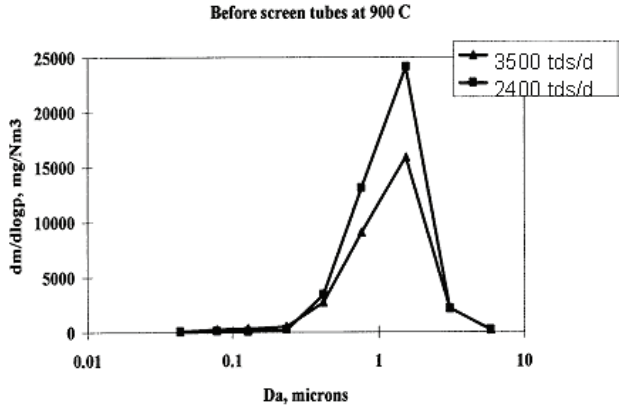

Figure 8-8, Measured fume size distribution from the furnace, sampled at nose before screen tubes (Mikkanen et al., 1999).

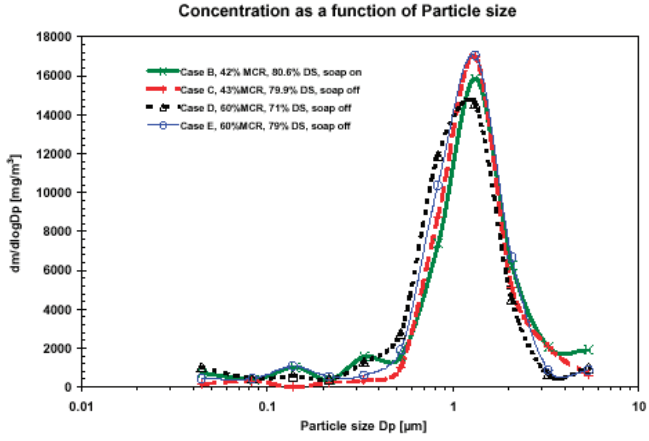

Figure 8 9, Size distribution of dust samples, collected before electrostatic precipitator, at different operating conditions (Janka et al., 2000).

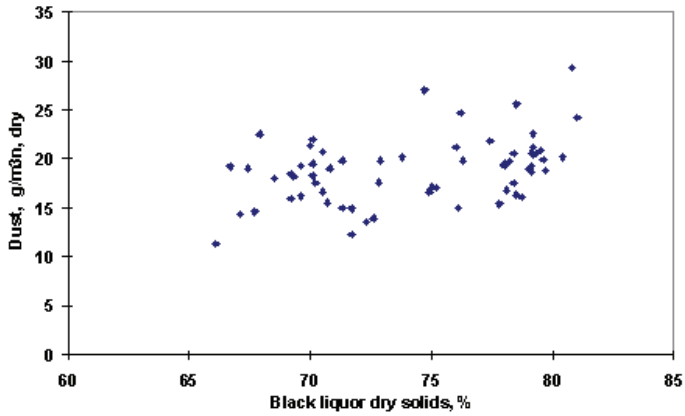

Figure 8-10, Measured ESP dust concentration from recovery boilers.

calculations (Perjyd and Hupa, 1984) suggest that fume formation increases as the lower furnace gas temperature increases. This is shown as slightly upward trend in the figure 8-10.

Briscoe *et al.* (1991) reported that in their measurements chemical fume production remained about constant even though lower furnace gas temperature varied. Increased temperatures in lower furnace didn't result in decreased TRS emissions.

Carryover

Carryover is burned and unburned particles that get caught with the flue gases. Very small particles burn fast and form liquid droplets which don't get entrained with the flue gas. Large particles do not have time to swell and hit furnace walls or char bed before they entrain. It is the fraction around initial 1 mm size that is responsible for entrainmet (Horton and Vakkilainen, 1993).

For kraft recovery boilers running close to MCR equipped with modern air systems the typical carryover rate is 2 – 4 g/m^{3}n (Kaila and Saviharju, 2003). The amount of carryover depends on the air flow settings and the chosen air model (Costa *et al.*, 2004). Typically carryover decreases for lower loads. At about 85 % load and 70 % dry solids liquor carryover rates in three boilers were 0,5 – 1,5 g/m^{3}n (Backman *et al.*, 1995). For older boilers with conventional air systems carryover rates can be as high as 5 – 8 g/m^{3}n (Metiäinen, 1991).

Carryover can be broadly classified into two distinct groups. Carryover that is still burning when it reaches the boiler nose elevation can be seen as light streaks against darker background. Detection devices to monitor combusting carryover are available and are widely used. Flue gas temperatures drop fast after the boiler nose. This means that the carbon reactions practically stop when the carryover particle reaches superheater. Carryover that is combusting at nose shows as unburned carbon residue in the deposits. It can be seen as black color on boiler bank ash coming out of hoppers. Carryover that has combusted totally has high reduction and contains sodium sulfide. Even if combustion was over early, sulfation of sulfide is slow for carryover size droplets (DeMartini, 2004). High flow of fully combusted carryover can be seen as pink or red color at superheater sootblower lances. In modern high dry solids boilers carryover carbon content is very low. Carryover particles are depleted of potassium and chlorine (Khalaj *et al.*, 2004).

Intermediate size particles

The actual coarse material that is seen on superheater section is very diverse. There are particles that are larger than fume but smaller than the residue of medium sized black liquor droplet. These particles are called the intermediate size particles. In industrial measurements (Mikkanen *et al.*, 2001) at least five different types of intermediate particles have been identified based on their assumed formation path.

1. Large agglomerates which consist of 0.3±0.7 µm diameter primary particles. These particles form when the fine fume particles deposit onto the heat exchangers, sinter and re-entrain to the flue gas.
2. Extensively sintered irregular particles 30±250 µm in diameter. The appearance

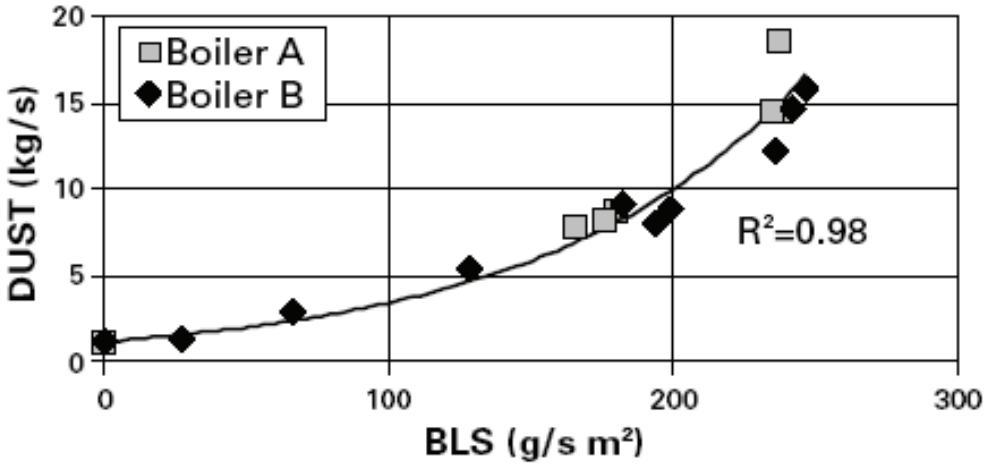

Figure 8-11, Dust generation as a function of boiler load (Tamminen et al., 2002).

and the composition of these particles suggest that they were formed from extensively sintered fine fume particles and subsequently removed from the heat exchangers by soot blowing.

3. Spherical particles 5±100 µm in diameter, which appeared highly porous inside. These particles are enriched in potassium. Formation of these particles is most likely through residue of burning black liquor.
4. Dense spherical particles 5±250 µm in diameter. These particles are enriched in Na and K and depleted in Cl and C. Furthermore, these particles deposit efficiently in the superheater area.
5. Irregular, rough particles 3±40 µm in diameter. These particles have Si, Ca and sometimes traces of Mg in their spectra suggesting that they originate from the mineral impurities in the black liquor. Some of these particles might have formed on the evaporator.

Type four intermediate particles can form two ways. Small particles can be physically ejected during black liquor droplet combustion (Verrill and Wessel, 1998). During char combustion release of 10 to 100 µm char fragments happens in laboratory experiments and pilot plant tests (Kochesfahani *et al*., 1998). In mill trials this size particles have been found, Figure 8-12 (Kochesfahani and Tran, 2000, Mikkanen *et al*., 2001).

The release of ISP from combusting black liquor has not yet been measured. Verrill *et al.* (1994) measured sodium loss from combusting black liquor droplets and found 5 … 20 % of sodium was released during the first seconds. They attributed most of this loss to physical ejection during drying and volatilization. The release of ISP from char bed seems to increase with increasing char bed temperature (Verrill and Lien, 2003). Total mass release at 1000 °C seems to be about 8 % of initial char mass. About 75 % of the released mass seemed to be ISP (Kochesfahani *et al*., 1998). This would mean that 10 … 30 % of Na loss or 2 … 4 g/m^{3}n is ISP from char bed.

The amount of intermediate size particles in typical recovery boilers is still somewhat open. Wessel and Kaufman (2000) indicated in their recovery boiler model that about half of all particles could be ISP. In field studies at two US boilers between 1 and 2 g/m^{3}n have been found (Schaddix *et al*., 2003, Baxter et al., 2001, Lind et al., 2000). In another set of field studies at three North American boilers 20 to 40 % of large material at superheater inlet was ISP (Kochesfahani and Tran, 2000). The measured ISP amount equaled 1 … 3 g/sm^2. Mass averaged size of ISP was about 50 µm.

8.3 DEPOSITION OF PARTICLES AND VAPORS

Deposition of particles and vapors on heat transfer surfaces can occur through multiple pathways (Goerg-Wood and Cameron, 1998). Thermophoresis or temperature gradient between flue gas and deposit surface transfers small particles to surface. Larger particles are deposited by inertial or turbulent impaction.

Vapor or gaseous species can condense on the surface and react with deposits on the surface. Concentration differences play role near the heat

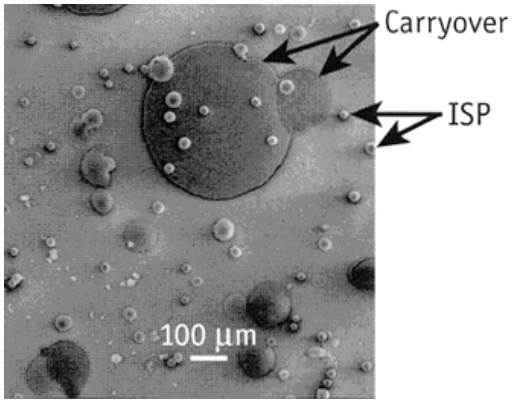

Figure 8-12, Intermediate size particles (Kochesfahani and Tran, 2000).

transfer surface. For very small particles (<0.1 µm) molecular diffusion and Brownian motion can play a role. Eskola *et al.* (1998) have presented formulas of deposition rates.

Thermophoresis

Thermophoresis plays significant role in capturing the small 0.2 … 1 µm fume particles suspended in the flue gas. When hot flue gas flow past colder heat transfer surfaces temperature gradient forms. This temperature gradient forces small particles towards cold surface. Thermophoretic deposition rate is proportional to the temperature gradient, particle diameter and particle concentration (Goerg-Wood and Cameron, 1998).

$$D_T = KB_d d_p (T_g - T_s)/T_l \qquad 8\text{-}2$$

and

K	is constant, -
B_d	is dust concentration, kg/m^3
d_p	is particle diameter, m
T_g	is gas temperature, K
T_s	is surface temperature, K
T_l	is gas temperature on the outer edge of the laminar layer, K

Inertial impaction

For particle sizes larger than about 20 µm the main deposition mechanism is the inertial impaction. The capture efficiency of a collector(cylinder) in a cross flow of combustion gases is mainly determined by inertia, which can be characterized with the Stokes number

$$Stk = l_p/R_c \qquad 8\text{-}3$$

As can be seen, the Stokes number is defined as the ratio of the particle stopping distance, l_p, to the characteristic cylinder dimension, that is to the cylinder radius R_c. Impaction of particle on the cylinder surface will occur only, when Stk > 0.125 (Friedlander, 1977). The stopping distance is a finite distance, which a particle will travel before coming to rest as $t \to \infty$, when the particle is projected into a stationary fluid with a velocity $U_{p,0}$. The stopping distance is usually calculated by applying Stokes linear drag law (Friedlander, 1977)

$$l_p = U_{p,0}\tau \qquad 8\text{-}4$$

where τ is the particle relaxation time, defined as

$$\tau = m_p/3\pi d_p \eta = \rho_{pb} d_p^{\,2}/18\eta \qquad 8\text{-}5$$

and where

m_p	is particle mass,
d_p	is particle diameter,
η	is the dynamic viscosity of host gas and
ρ_{pb}	is the particle bulk density.

However, when particles do not obey Stokes linear drag law, that is when $Re_p > 1$, stopping distance also depends on the particle Reynolds number, defined as

$$Re_p = Ud_p/\nu \qquad 8\text{-}6$$

where U is the free stream velocity. Fortunately, this dependency can also be taken into account, when stopping distance is defined as (Israel and Rosner, 1983)

$$l_p(\mathrm{Re}_p) = \frac{4}{3}\left(\frac{\rho_{pb}}{\rho}\right) d_p \int_0^{\mathrm{Re}_p} \frac{d\,\mathrm{Re}_p'}{C_D(\mathrm{Re}_p')\,\mathrm{Re}_p'} \qquad 8\text{-}7$$

where r is the gas density. Using this form of the stopping distance, we are able to generalize the Stokes number for particles, which do not obey Stokes linear drag law. This new effective Stokes number is defined as

$$Stk_{eff} = \frac{l_p(\mathrm{Re}_p)}{R_c} = \Psi(\mathrm{Re}_p)\,Stk \qquad 8\text{-}8$$

where $\Psi(Re_p)$ is the non-Stokesian drag correction factor (Israel and Rosner, 1983, Wessel and Righi, 1998), which is monotonously decreasing function of Re_p and Stk is the same Stokes number, which was already defined in equation (8-4).

Collection efficiency, which is our interest, is defined as a ratio of the actual particle mass collection rate of the collector to the rate at which

mainstream particles flows through the projected area of the target, that is

$$\eta_{coll} = \frac{-\dot{m}_{p(i),c}}{\rho_{p(i),\infty} U A_{proj}} \qquad 8\text{-}9$$

where $\rho_{p(i),\infty}$ is the mass content of particles in a flue gas. Next we need to be able to form the following relationship between collection efficiency and effective Stokes number:

$$\eta_{coll} = f(Stk_{eff}(Re_p)) \qquad 8\text{-}10$$

Fortunately, using a potential flow field approximation to the fluid motion about the collector, the collection efficiency of the cylindrical target has been calculated numerically (Israel and Rosner, 1983, Wessel and Righi, 1998) as a function of effective Stokes number. These numerical results have also been correlated as a function of Stkeff. One recommended collection efficiency curve-fit equation for $Stk_{eff} > 0.14$ is (Israel and Rosner, 1983):

$$\eta_{coll}(Stk_{eff}) = \{1+1.25(Stk_{eff}\text{-}0.125)^{-1}\text{-} 0.014(Stk_{eff}\text{-}0.125)^{-2}+ 0.508*10^{-4}(Stk_{eff}\text{-}0.125)^{-3}\}^{-1} \qquad 8\text{-}11$$

However, more accurate two-equation correlation for the collection efficiency of the cylinder is given by (Wessel and Righi, 1998). They give a correlation for the local collection efficiency, which enables to calculate local deposition rates on the cylinder surface as a function of cylinder angle.

Turbulent eddy impaction

When host gas and particles flow over the plane parallel with in the isothermal system, one can observe notable deposition of large particles although Brownian diffusion coefficient of these large particles is very small. This is possible, not by way of Brownian or turbulent diffusion, but by way of turbulent impaction, which is important deposition mechanism for large particles, when boundary layer between surface and host flow is turbulent. Inside the turbulent boundary layer turbulent eddies have velocity components, which are normal to the main flow and are capable to give enough momentum for particles to cross the laminar sub-layer and finally deposit on the wall. This phenomenon can be understood using previously defined stopping distance model. In this case eddies lose momentum

$$m_p \overline{(u'^2)}^{\frac{1}{2}} \qquad 8\text{-}12$$

for a particle and particles initial velocity in the model is the same as mean fluctuation velocity in the fluid mainstream, $\overline{(u'^2)}^{\frac{1}{2}}$. Particles fluctuation-imparted stopping distance, calculated at the outer edge of laminar sub layer, is

$$l_{pf} = \overline{(u'^2)}^{\frac{1}{2}}\ t. \qquad 8\text{-}13$$

Because gas turbulent velocity is negligible in the laminar sub-layer, particle can deposit at the wall only if

$$l_{pf} > l \qquad 8\text{-}14$$

where is the thickness of the laminar sub-layer. Substituting equation (8-14) into equation (8-15) we get a following form

$$\overline{(u'^2)}^{\frac{1}{2}} > \frac{l}{\tau} = \frac{18\mu l}{\rho_{pb} d_p^{\ 2}} \qquad 8\text{-}15$$

This inequality clearly shows that the smaller the particles are, the greater is the mean fluctuation velocity in the fluid mainstream $\overline{(u'^2)}^{\frac{1}{2}}$, required for their deposition at the wall. Theoretical models for particles turbulent impaction, which are shown in the literature, are modelled assuming fully developed turbulent flow in pipes. All of these models include parameters, which are based on experiments. Most of these models fall close to the experimentally determined dimensionless deposition velocity. Comprehensive treatment of particles turbulent impaction used in our calculations can be found from (Im and Chung, 1993).

Vapor deposition

Vapors may condense by direct condensation on heat transfer surfaces or on the particles inside the boundary layer. Condensing vapor may also react with surfaces. For direct vapor condensation flux to the surface we get a following expression (Eskola *et al.*, 1998)

$$I_v = Sh(T_g)\frac{\left[D_v(T_g)D_v(T_w)\right]^{1/2}}{d_c R_g}\left(\frac{p_v(T_g)}{T_g} - \frac{p_{v,s}(T_w)}{T_w}\right) \qquad 8\text{-}16$$

where

Sh	is Sherwood number,
D_v	is vapor diffusivity,
d_c	is cylinders characteristic dimension,
R_g	is the gas constant,
p_v	is actual vapor pressure,
$p_{v,s}$	is the saturation vapor pressure
T_g	is gas temperature, K
T_w	is wall temperature, K

Deposition to surfaces

Deposition rate is controlled by particle size distribution, temperature difference, heat transfer surface construction and ash content in the flue gases. It is therefore obvious that deposition rate to different recovery boiler surfaces is not constant but varies.

Fume tends to deposit on economizers and boiler banks, Figure 8-13 (Jokiniemi *et al.*, 1996). Fume deposition occurs mainly through thermophoresis. Carryover tends to deposit on superheater surfaces. If we look at deposits on these surfaces we see a clear difference on particle size that forms these deposits. Boiler bank dust contains larger, carryover particles mixed with smaller fume, Figure 8-14. Economizer deposits tend to contain mostly fume, small submicron size spheres.

8.4 PROPERTIES OF RECOVERY BOILER ASH

Deposits in recovery boiler heat transfer surfaces are not static but depend on process conditions. The ash deposition is often time dependet i.e. the ash properties change in a deposit cross section. The most important ash property is its strength. It depends on ash melting behavior and sintering rate.

First melting temperature

Melting behavior of deposits in kraft recovery boiler heat transfer surfaces determines many of the deposit properties. The first melting temperature (FMT) is the temperature at which the melt appears in a recovery boiler deposit. The temperature where deposit melting appears marks also the region where fouling problems occur. Understanding and predicting first melting temperature is particularly important in terms of superheater corrosion (Tran *et al.*, 1999).

Liquid content

When recovery boiler dust is heated it at first behaves like solid. At first melting temperature liquid appears. Above that temperature there exists a state where the deposit is partially molten and partially solid. Depending on the type of system after small or larger temperature difference the whole system is molten.

Figure 8-16 presents two typical binary systems. Left is eutetic mixture. Typical eutetic mixtures are for example systems Na_2SO_4-Na_2S and Na_2SO_4-NaCl. At right there is a minimum melting system. Typical minimum melting systems are for example systems Na_2SO_4-K_2SO_4 and Na_2SO_4-Na_2CO_3. In eutetic mixtures the components do not mix together but remain separate through heating and cooling. In minimum melting mixtures the compounds are reasonably similar so they can form a complete solid structure with each other.

It is typical that in salt systems melting temperatures of mixtures are lower than individual melting temperatures. In Figure 8-16 the melting

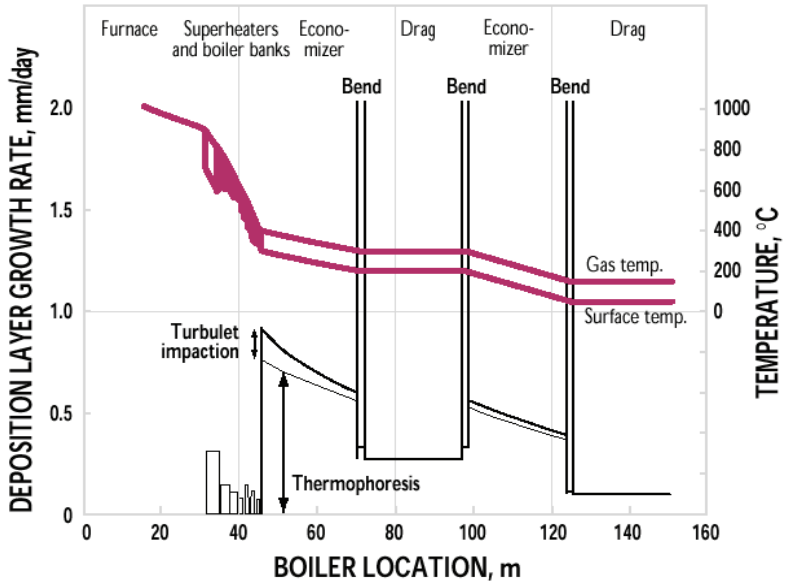

Figure 8-13, Fume deposition on recovery boiler heat transfer surfaces (Jokiniemi et al., 1996).

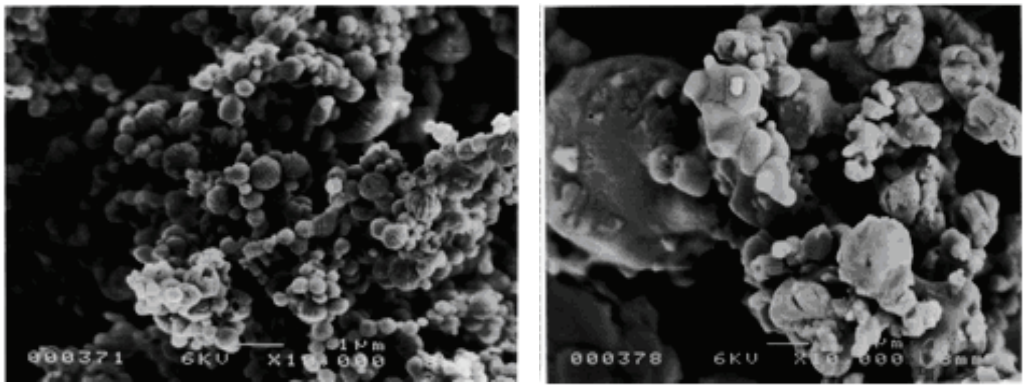

Figure 8-14, At the left precipitator dust (small spheres), at the right boiler bank dust (mixture of different sizes).

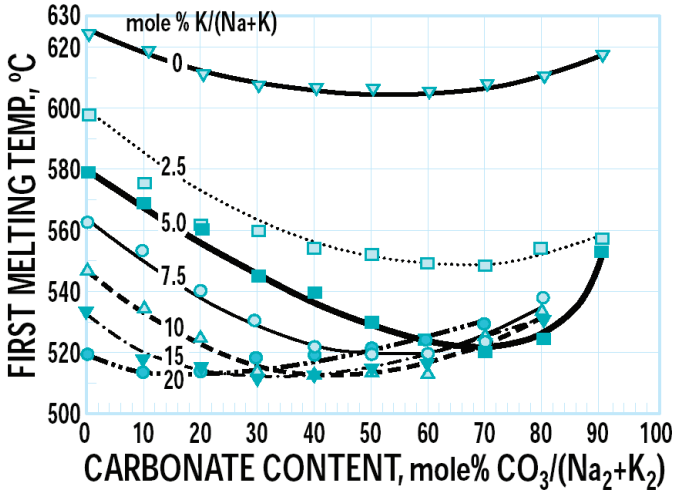

Figure 8-15, Effect of carbonate content to first melting temperature of synthetic dust containing chloride at various potassium contents (Tran et al., 1999).

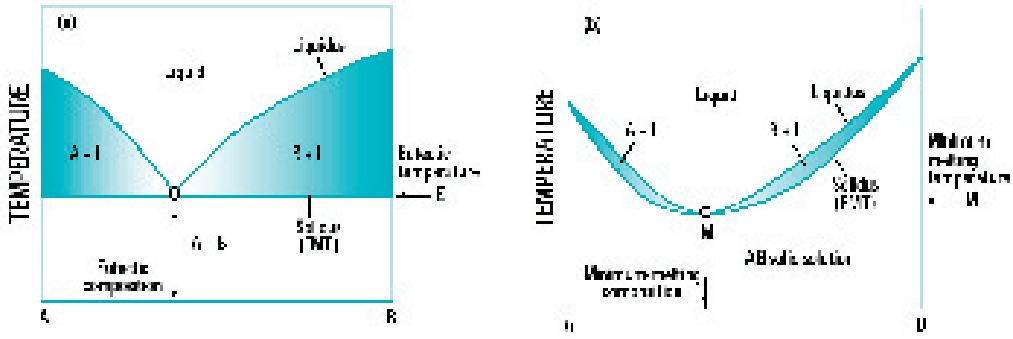

Figure 8-16, Basic phase diagrams for binary systems: left eutectic and right minimum melting (Tran et al., 1999).

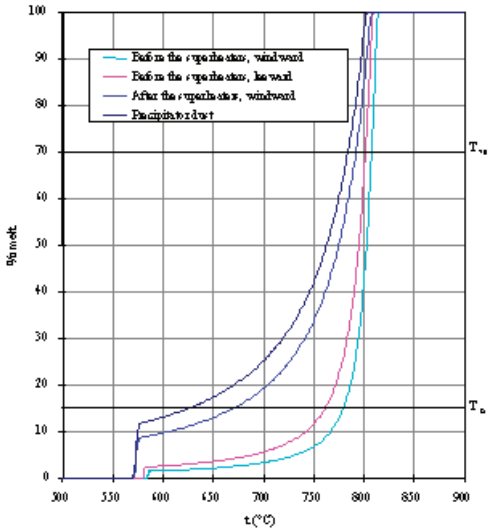

Figure 8-17, Predicted liquid contents as a function of temperature for recovery boiler dusts (Backman et al., 1996).

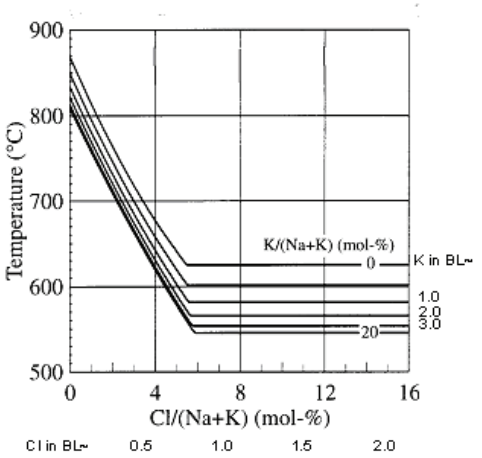

Figure 8-18, Effect of potassium and chloride on recovery boiler dust sticky temperature (Backman et al., 1995)

temperatures of component B is higher than component A and the mixture melting temperatures are well below the melting temperature of pure compound B.

The temperatures where 15 w-% of the deposit is at molten state and 85 w-% is at solid state is called T_{15} or sticky temperature. The temperatures where 70 w-% of the deposit is at molten state and 30 w-% is at solid state is called T_{70} or flow temperature. Recovery boiler dusts tend to stick to the heat transfer surfaces and form hard deposits when they are between T_{15} and T_{70}. An example showing the effect of water content on material behavior is plaster. If it is dry it will fall off from the wall. If there is too much water the plaster will again will fall off the wall But between these states the plaster will stick to the wall.

Liquid content can be predicted with computer programs (Backman *et al*., 1996).

Sintering

Sintering is a process where dust particles that have stuck to a heat transfer surface gradually densify and harden. Originally loose and porous material becomes solid almost crystal like. As deposits densify, their strength increases exponentially, and they become more difficult to remove

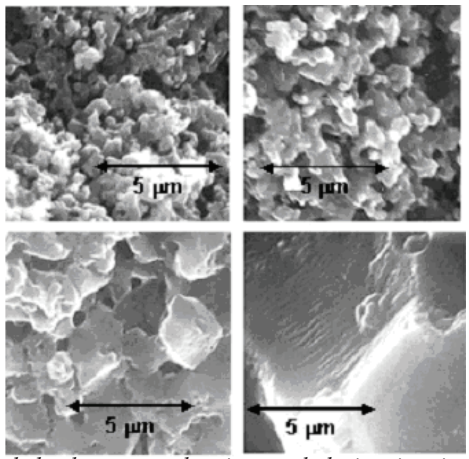

Figure 8-19, Progression of neck development and grain growth during sintering of an ash sample from the electrostatic precipitator of a kraft recovery boiler. Conditions were 450 °C for three minutes upper right fifteen minutes lower left, and sixty minutes lower right (Frederick et al., 2001).

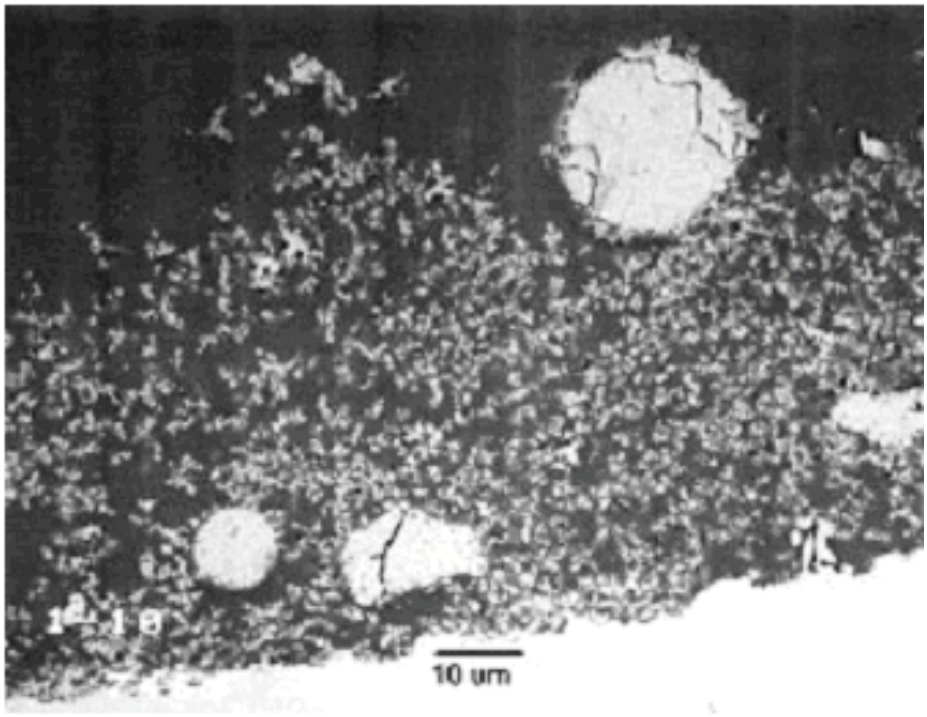

Figure 8-20, SEM photomicrograph of a cross-section of a deposit formed on a deposition probe inserted in the mid-boiler bank region of an operating kraft recovery boiler (Frederick et al., 2001).

by sootblowing. Because of the end product the process is often called deposit hardening.

Fume particles sinter at temperatures above 300 °C (Tran *et al*., 1988). The rate of sintering increases rapidly with temperature (Skrifars *et al*., 1991). The recovery boiler deposits sintering and hardening is affected also by deposit packing density, dust and flue gas composition.

These fine particles apparently sinter and harden into difficult-to-remove boiler bank deposits by two mechanisms: (a) evaporation of sodium chloride from the particles and recondensation, forming a neck at the point of contact between two particles, and (b) transport of mass from the particles to the neck by solid-state diffusion (Frederick *et al*., 2001). Figure 8-19 illustrates the changes that occurred during sintering of fine particles. As sintering proceeds, the neck between the fine particles grows until ultimately individual particle shapes can not be seen. Beyond that point the grain size of the structure grows as mass from smaller, individual particles is transported to the larger ones. These phenomena have been observed both in laboratory studies (Skrifars *et al*., 1991, Tran *et al*., 1988) and in deposits formed in operating recovery boilers (Frederick and Vakkilainen, 2003).

In real recovery boiler deposits the sintering behavior is much more complex. These deposits, Figure 8-20, contain fine fume, large carryover particles and intermediate particles. Each particle type has its own composition and so its own sintering behavior. The actual deposit sintering behavior is then sum of sintering of all of these different materials.

$$\frac{\Delta L}{L} = \frac{k_{\sin t}}{r^{2/3}} \left(\frac{t^{1/3} p_o^{1/3}}{T^{0.5}} \right) \qquad 8\text{-}17$$

Lien *et al*. (1999) measured the rate of linear shrinkage (ΔL/L) of pellets pressed from particles collected in the electrostatic precipitators of eight different recovery boilers. They correlated the linear shrinkage data with the chloride content of the dusts, the temperature at which the particles were sintered, and time. Equation 8-17, the correlating equation, was adapted from Kingery and Berg (1955), who used it to correlate sintering rates for particles that sintered by the evaporation-condensation mechanism. Raoult's law was used to express p_o, the partial pressure of NaCl in this case, in terms of the pure component vapor pressure of NaCl and the mole fraction NaCl (y_{NaCl}) in the dusts.

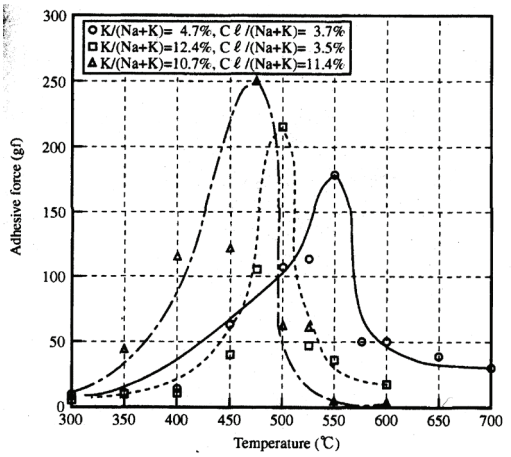

Figure 8-21, Examples of ash adhesive forces as function of temperature (Fujisaki et al., 2003).

Strength of deposits

Deposit strength depends only on its porosity (Kaliazine *et al.*, 1997). The following equation has been derived by fitting the bending strength versus porosity data of Piroozmand *et al.* (1998) for sintered pellets made from recovery boiler ESP catch (Frederick *et al.*, 2003)

$$\sigma = 42800\ e^{6.64\,P} \qquad 8\text{-}18$$

where

P is the deposit porosity, -
σ is the deposit strength, Pa

At some temperature a part of the deposit starts to melt and forms liquid. This point is called the initial melting point or the first melting temperature (FMT). Compression strength reaches its maximum around the first melting temperature, Figure 8-21.

8.5 DEPOSIT BEHAVIOR

In recovery boiler furnaces alkali metals are vaporized. They react with sulfur, chloride and carbon to form fume. In combination with combustion residue from lower furnace they combine to form deposits on boiler surfaces. Several studies of recovery boiler plugging and fouling mechanisms have been reported. The effect of potassium and chloride on recovery boiler fouling mechanisms has been studied by (Backman *et al.*, 1987, Tran, 1988, Skrifvars, 1989). A preliminary experimental investigation of potassium and chloride enrichment was reported by (Reis *et al.* 1994).

Significant progress has been made in understanding recovery boiler fouling. When recovery boiler capacity is limited, it is important to find out how different operating parameters affect the fouling.

Enrichment of potassium

Potassium compounds are more volatile than sodium compounds. They are typically enriched in the precipitator dust (Vakkilainen *et al.*, 1995). The amounts of sodium and potassium depend on the amounts of other compounds in the sample. Therefore potassium content is typically expressed as the molar ratio of potassium to the sum of sodium and potassium. The enrichment or enrichment factor is usually defined as the ratio the of potassium content of the dust sample to the potassium content in virgin black liquor, i.e.

$$E_K = K_{sample}/(Na_{sample}+K_{sample}) \,/\, K_{BL}/(Na_{BL}+K_{BL}) \qquad 8\text{-}19$$

where

K_{xx} is the potassium content at xx as mol-%
Na_{xx} is the sodium content at xx as mol-%

Vakkilainen *et al.* (1995) indicated that potassium enrichment factors range from 1 to 2.5. This means that the weight fraction of potassium in ESP dust is about 2.5±0.5 times the potassium in virgin black liquor. Another way to express this is the mole ratio of potassium to the sum of sodium and potassium in ESP dust is about 4.6±0.9 times the mass weight percent of potassium in virgin black liquor.

The data from twenty-one operating boilers, Figure 8-22, show that the potassium enrichment decreases with increasing carbonate content. This data implies that the potassium enrichment decreases with increasing furnace temperature. They found no correlation between potassium enrichment and other operating variables.

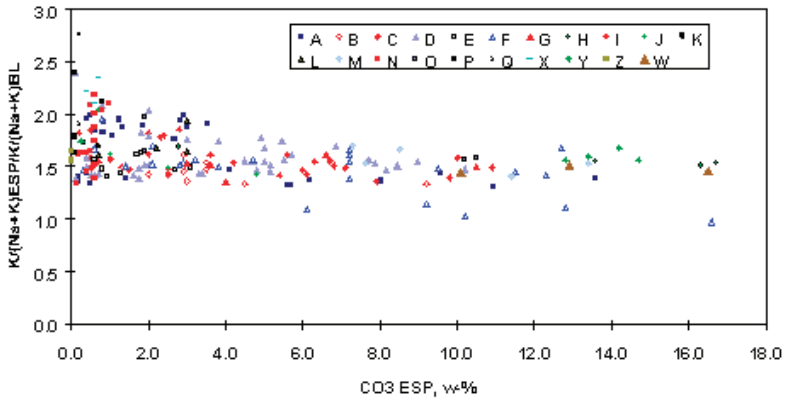

Figure 8-22, Potassium enrichment factors in ESP dust versus carbonate.

Enrichment of chloride

Chloride compounds in the lower furnace have higher vapor pressures than other sodium and potassium compounds (Hupa, 1993). They are typically enriched in the precipitator dust. Chloride content is typically expressed as molar ratio of chloride to sum of sodium and potassium. The enrichment or enrichment facor is usually defined as the ratio of chloride content in dust sample to chloride content in virgin black liquor, i.e.

$$E_{Cl} = Cl_{sample}/(Na_{2,sample}+K_{2,sample}) \,/\, Cl_{BL}/(Na_{2,BL}+K_{2,BL})$$

where

Cl_{xx} is the chloride content at xx as mol-%

The data from twenty-one operating boilers, Figure 8-23 shows that in these boilers the chloride enrichment ranges from 0.3 to 6. The average chloride enrichment is 2.9 with standard deviation of less than 1.5. Another way to express this is the mole ratio of chloride to the sum of sodium and potassium in ESP dust is about 8±1 times the mass weight percent of cloride in virgin black liquor. This means that the weight fraction of chloride in ESP dust is about 4±2 times the chloride in virgin black liquor. As with the potassium enrichment factors, this is less than data reported in other sources (Tran and Reeve, 1991, Adams and Frederick, 1988).

Chloride enrichment versus furnace temperatures indicated by the CO_3 content of the dust gives two separate enrichment regions. When the ESP dust CO_3 content was below 4 weight-% the data was scattered. Above an ESP dust CO_3 content of 4 weight-%, the data were much less scattered and a decrease in enrichment with increasing carbonate content was noted. This implies that chloride enrichment decreases with increasing temperature. Smaller fume particles are enriched in chloride

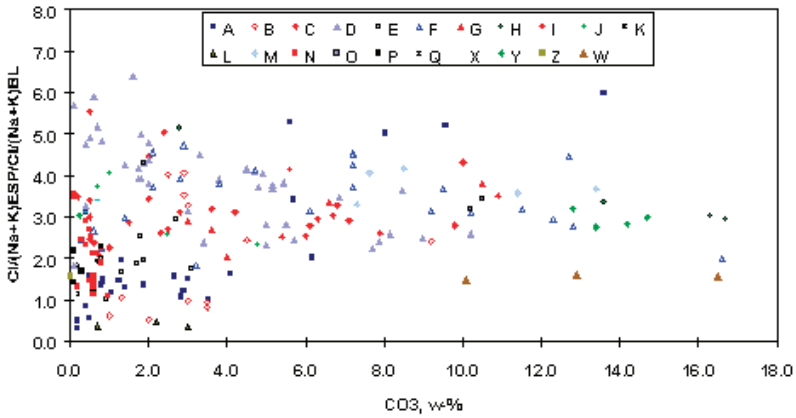

Figure 8-23, Chloride enrichment factors in ESP dust versus carbonate

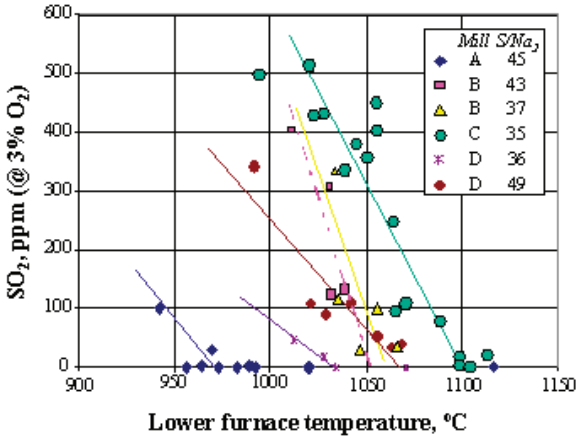

Figure 8-24, SO_2 content of gases concentrations at the boiler flue gas exit level versus temperature at the secondary air level for four different kraft recovery boilers.

(Mikkanen, 2000, Välimäki and Salmenoja, 2004).

Effect of SO_2 on chloride enrichment

(Frederick *et al.*, 1998) reported data on SO_2 concentrations at the boiler flue gas exit level and temperature at the secondary air level (~2.5 m) in the lower recovery furnace for four kraft recovery boilers. The SO_2 concentration decreased with increasing temperature in the lower furnace for each boiler, Figure 8-24. These characteristic SO_2 versus temperature curves were shifted to different locations along the temperature axis for the different boilers. The probable reason for the shift is the different sulfur release rate for each liquor.

Using data from Figure 8-24 and measurements of chloride enrichment factors in a laboratory combustor Frederick *et al.* (1998) studied how SO_2 and furnace temperature affected the chloride enrichment.

Replotted Figure 8-25, shows enrichment values that first decrease to less than unity and then increase sharply when SO_2 decreases to 0 to start another decline with further temperature increase. This is consistent to data presented in Figure 8-23. In real boilers, because of mixing limitations and non uniformity of temperature fields the sharp increase should be much more gradual.

ESP dust enrichment

Based on more than 200 tests with analysis of ESP dust and black liquor, it is possible to predict ESP dust composition as a function of black liquor composition and dry solids;

- Prediction of SO_2 is based on (Maso, 1988)
- Depending on lower furnace temperature

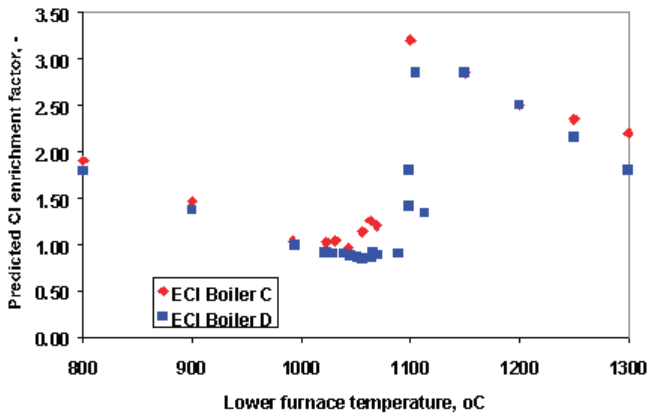

Figure 8-25, Prediction of enrichment of chloride to dust as function of lower furnace temperature.

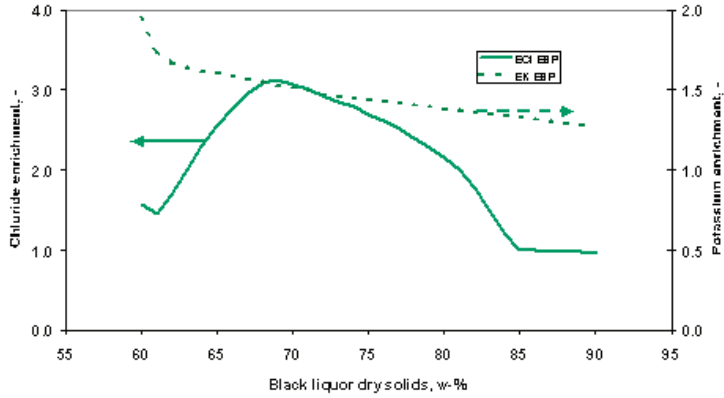

Figure 8-26, Prediction of potassium and chloride enrichment in a recovery boiler as a function of black liquor dry solids.

there are two operating regions; with and without SO_2

- When boiler operates without SO_2 then ESP dust analysis is based on enrichment versus carbonate content data (Vakkilainen *et al.*, 1995)
- When boiler operates with SO_2 then enrichment data is based on (Frederick *et al.*, 1998)

Predicted enrichment, Figure 8-26, shows gradual decrease of potassium enrichment as a function of black liquor dry solids for a recovery boiler with $S/(Na_2+K_2)$ = 27 mol-%, Cl/(Na+K) = 0.90 mol-%, K/(Na+K) = 12 mol-% and black liquor dry solids 75 %. This is consistent with data from (Reis *et al.*, 1994). The chloride enrichment shows a minimum enrichment at 62 % dry solids, followed by an increase and then decline. The enrichment behavior of chloride at very high dry solids seems to reach a plateau. Lack of industrial operating data prevents from verifying this trend.

BB dust enrichment

Boiler bank dust has a composition which is a mixture of fume and carry-over. Carry-over particles deplete the potassium and chloride levels in dust (Vakkilainen and Niemitalo, 1994). The mixture assumption seems to fit a wide range of liquors and boilers (Janka *et al.* 1998, Mikkanen *et al.*, 1999). By setting carry-over to a known level, we can calculate the properties for this mixture in a typical recovery boiler (Eskola *et al.* 1998).

The predicted enrichment behavior, Figure 8-27, seems to fit the data presented by (Janka *et al.* 1998). The notable exception is the 60 % dry solids black liquor. Because of chloride losses as HCl the chloride enrichment should drop down as shown. Trends like this need more industrial verification.

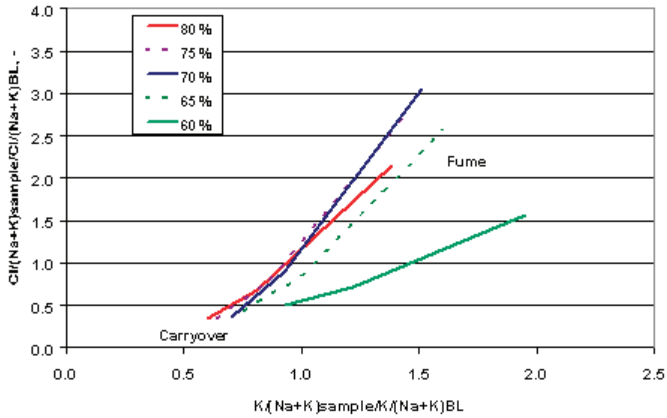

Figure 8-27, Prediction of potassium and chloride enrichment for carryover and fume for several black liquor dry solids levels. Lower left carryover, middle boiler bank, upper right ESP ash.

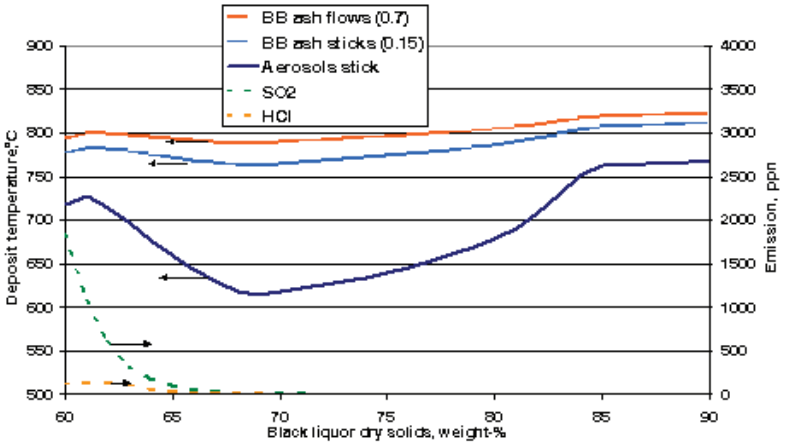

Figure 8-28, Prediction of effect of dry solids to boiler bank dust properties in a recovery boiler, sulfidity = 27 %.

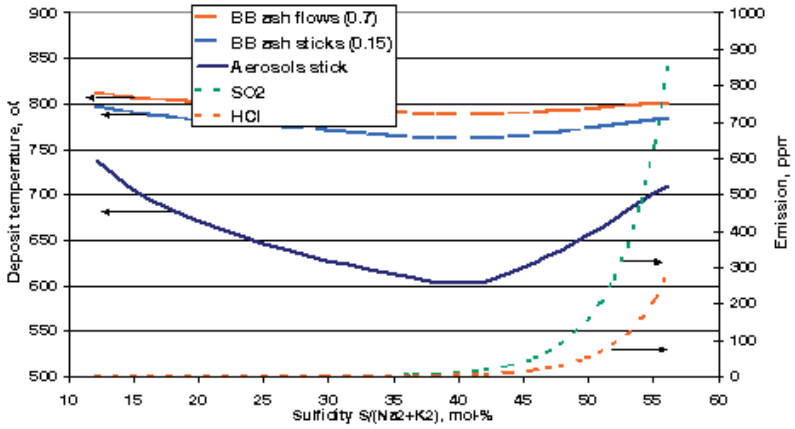

Figure 8-29, Prediction of effect of sulfidity to boiler bank dust properties in a recovery boiler, dry solids =75 %.

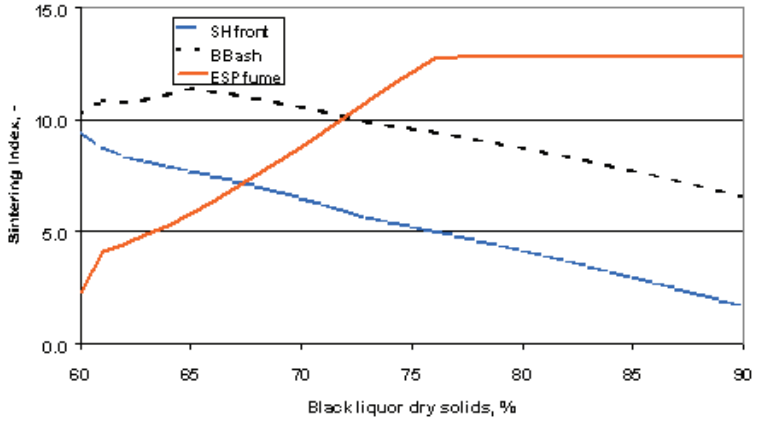

Figure 8-30, Prediction of sintering index as a function of dry solids.

Based on the above described assumptions the model has been used to predict the effect of changes in black liquor properties on different fouling indicators. The predictions should not be assumed to show absolute values, but rather show trends which are applicable to interpreting operating data on recovery boilers.

Dust properties, such as sticky temperature can be predicted based on data from (Backman *et al.*, 1995). In the model flow temperature T_{70}, sticky temperature T_{15} and first melting temperature T_0 are based on ash chloride, potassium and carbonate contents. Changes in these temperatures have been show to correlate with changes in fouling behavior (Tran, 1988).

Effect of dry solids to boiler bank dust properties

Figure 8-28 shows boiler bank ash behavior as a function of dry solids for $S/(Na_2+K_2)$ = 27 mol-%, Cl/(Na+K) = 0.90 mol-% and K/(Na+K) = 12 mol-%. Increasing dry solids eliminates SO_2 and HCl emissions after about 65 % dry solids. One sees the sticky and flow temperatures in this recovery boiler to be well above industry practice for designing boiler bank inlet temperatures (McCann, 1991). If the aerosol fume would strongly affect the boiler bank fouling then this kind of limit would make sense.

Effect of sulfidity to boiler bank dust properties

Sulfidity affects the recovery boiler fouling through the same mechanism as dry solids. Increase in sulfidity shows the same way as decrease in dry solids, Figure 8-29. The figure seems to suggest that for boiler that operate at low SO_2 emissions, lowering sulfidity might mean lower fouling. There are no industry cases where this has been tried. Higher solids firing should at first increase chloride enrichment as gaseous HCl is converted to NaCl as sodium becomes available. After a zero SO_2 level is reached, enrichment should decrease because higher furnace temperatures cause higher sodium release (Vakkilainen, 2000b). Potassium enrichment should decrease with increasing dry solids because of the higher release.

Higher solids firing should affect recovery boiler the same way than decreasing sulfidity. Higher dry solids should worsen the economizer fouling, contrary to industry observation, unless the fouling is mainly controlled by the ash pH (Skrifars, 1989). In high solids boilers there seems to be low sulfide content in deposits (Raukola and Haaga, 2004).

Predicting deposit behavior

In addition to traditional indicators, ash sintering index can be calculated (Frederick *et al.*, 2004). Ash sintering index is based on the model by (Lien *et al.*, 1999). In their model the sintering index was mainly a function of the first melting temperature. Lowest sintering rate was set as unity and higher sintering rates are shown as ratios to the lowest rate. Figure 8-30 shows the effect of the dry solids on this sintering index for a recovery boiler.

Dust sintering index seems to increase for ESP dust. This is because of higher chloride and potassium enrichment factors. Industrial practice seems to indicate that in spite of this economizers do not show increased fouling. It might be that because of low temperature the economizer fouling is not controlled by sintering rate. Figure 8-30 shows decreasing sintering rates with increasing dry solids for boiler bank and superheaters. Industrial practice indicates that boiler bank fouling decreases with increasing dry solids.

8.6 DEPOSIT REMOVAL

Sootblowing steam exits the sootblower at or above the sonic speed of steam. The velocity degrades fast, Figure 8-31. Decay is caused by the interaction of turbulent jet with surrounding gas (Tandra *et al.*, 2001). As can be seen the effective cleaning radius of a sootblower jet is 1 … 1,5 m.

One of the most problematic cases are the older types of heat transfer surfaces. Wrongly designed tube anti vibration ties and too large distance between sootblowers can cause problems. The remaining solution is to add more sootblowers to the offending heat transfer surface.

Superheater deposit removal can be improved by chill-and-blow. Stopping black liquor firing but using auxiliary burners decreases superheater temperatures. Because of differences in thermal expansion stresses are created with superheater deposits and superheater tubes. Deposit removal can then be done by mechanical means or by using sootblowers extensively at superheater area.

After recovery boiler has been on line for some time the recovery boiler economizer area fouling appears to level out. Sootblowing does not seem to affect the heat transfer but lack of sootblowing

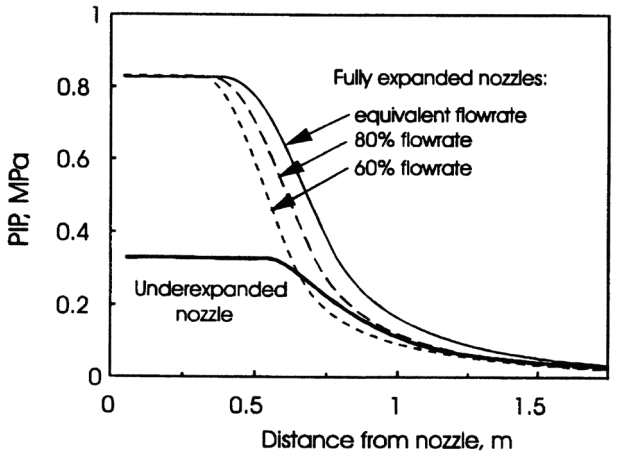

Figure 8-31, Decline of exit velocity of supersonic turbulent sootblower jet (Kaliazine et al., 1998).

leads to fast increase of draft loss (Uloth *et al.*, 1996b).

8.7 HOW TO DECREASE FOULING RATE

Fouling rate is a combination of three parameters; amount of incoming particles, their ability to stick to the surface and the removal rate by sootblowing (Tran, 2004). Many of these parameters relate to the patrticle composition especially potassium and chlorine content. There are several measures that can be used to decrease fouling in a recovery boiler. Their effectivity to solve the current fouling problem should be weighed carefully. The categories are; affect the liquor properties, decrease flue gas temperatures, decrease carryover rate and improve surface cleanability.

Change black liquor properties

Black liquor properties affect the fouling rate of a recovery boiler. The three main options are increasing dry solids, decreasing chloride content in black liquor or lowering sulfidity. In addition to these, changes in pulping can affect the black liquor combustion properties, which, in turn, affect the furnace outlet temperature and so recovery boiler fouling. An example of development of potassium and chloride levels in a Scandinavian mill is shown in Figure 8-32

Increasing potassium and chloride content will increase recovery boiler dust sintering rate at temperatures above 450 °C (Skrifars, 1989, Hupa *et al.*, 1990). Chloride concentration in white liquor can be calculated from the approximate mill balance;

$$Cl_{wl} = 0.25*Cl_{in}*(1-\eta_S)/[1-(1-\eta_S)(1-\eta_W)] \qquad 8\text{-}21$$

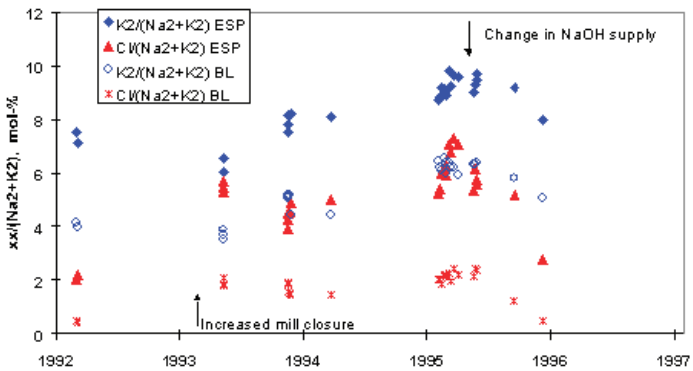

Figure 8-32, Potassium and chloride levels in a Scandinavian mill.

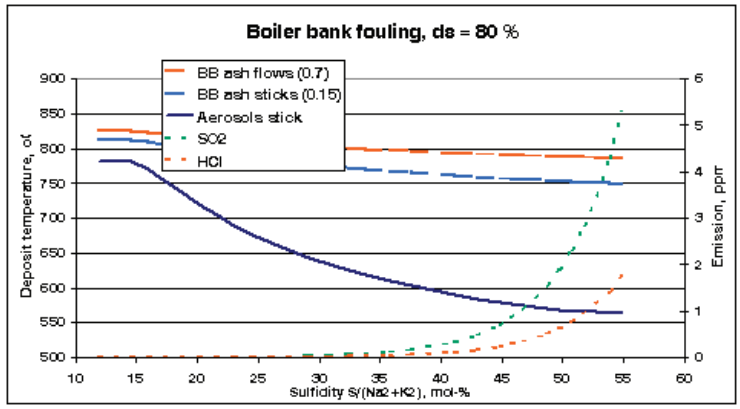

Figure 8-33, Effect of sulfidity to boiler bank ash properties.

where

Cl_{wl} is the white liquor chloride content, g/l
Cl_{in} is the chloride input, kg Cl/tpulp, (1 … 6)
η_S is the fraction of chloride lost through recovery boiler stack loss, (0.00 … 0.02)
η_W is the fraction of chloride flow lost through washing loss, (0.005 … 0.02)

The best way to affect the chloride level is to try to reduce the chloride input to the mill. Typically the main source of chlorides is the chips (Ferreira, 2003). Surprisingly in many problematic cases the main input has been as impurity in purchased NaOH. Chloride level can also be reduced by increasing losses. The most used method is to purge ESP dust (Nunes *et al.*, 1995). Chloride can be purged as HCl if SO_2 emissions to stack are allowed (Ibah, 1995). If chloride input to mill is high, then the chloride removal process should be considered. If the chloride is less than 0.5 w-% in black liquor dry solids, no extra measures are usually required.

Sulfidity affects the recovery boiler fouling through the same mechanism as dry solids. Increase sulfidity shows the same way as decrease in dry solids, Figure 8-33 (Vakkilainen, 2000b).

Dry solids increase decreases fouling, (Niemitalo, 1993). The main improvement comes as the SO_2 emission is eliminated. Typically high sulfur emissions indicate low ash pH.

Decrease temperatures

Decreasing temperatures in the flue gas side of the recovery boiler decreases the deposit strengths. Most effective means of reducing temperatures is to reduce boiler load. If furnace performance can be improved by a new air system of better liquor firing, then furnace nose temperatures can be decrease. Addition of heat transfer surface helps situation downstream.

The fact is that many older recovery boilers are operated more than +30% over design capacity. Often the upper furnace heat surface area is too small for this capacity. The boiler bank inlet temperature will be too high no matter how well the furnace is operating.

Decrease carryover

Improving furnace behavior by decreasing carryover rates is often very beneficial. Carryover affects the fouling through two phenomena. Possible sulfide decreases dramatically dust sintering temperature. Increased flow increases superheater deposit rate, which can lead to increased fouling.

Improve sootblowing

If fouling is local the first priority is to improve cleanability at that site. This can be done by improving sootblowing. Improvement can be achieved with additional sootblowers, high efficiency nozzles and a change in the sootblowing program. In practice the location and timing appear to be the most important factors when determining the sootblowing efficiency (Uloth *et al.*, 1996).

9 Firing black liquor

Figure 9-1, Black liquor gun nozzle.

Black liquor can be fired in a recovery boiler in a number of ways. The aim of firing strategy is to obtain a reasonable fouling rate, operate within the permitted emission limits and maintain stable and secure operation (Poon, 2001). The operator can choose an air model that suits him. With air model it is meant the division of air into the different air levels and also how the ports in each level are configured. The operator can also choose how he wants to fire the black liquor guns.

To illustrate the firing of black liquor a number of simulations has been made using a computer program developed for that purpose (Järvinen, 2002, Järvinen *et al.*, 1997, Manninen and Vakkilainen, 1996, Horton and Vakkilainen, 1993).

9.1 LIQUOR GUN OPERATION

Black liquor is delivered to a recovery boiler furnace by using liquor guns, Figure 9-1. The end part of the liquor gun is called the nozzle. The main types of nozzles are the splashplate nozzle, U- and V-type nozzles, fan nozzle, willow flute and the swirl cone nozzle. There are many other

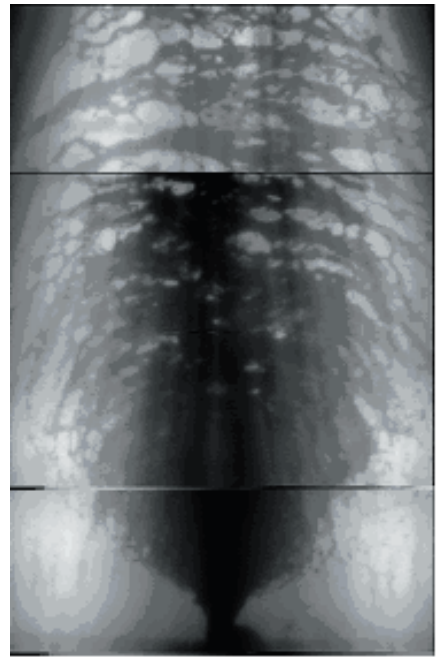

Figure 9-2, Flow from a splash plate liquor gun, spray from middle of the picture upwards (TKK)

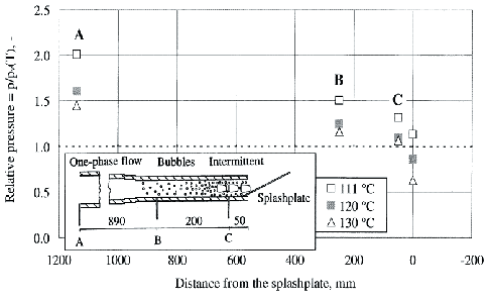

Figure 9-3, Pressure and flow in a liquor gun firing liquor above the BPR (Kankkunen et al., 1998).

types that are used and have been used, but mill experience seems to lean towards these types. Usually, the nozzle size and type varies from one recovery boiler to another. The spray properties from these nozzles differ to a great extent, but every nozzle has an optimum operating point. Nozzles are selected, based on previous experience, to keep the boiler operation effective and the droplet size optimal.

The purpose of the black liquor gun is to from small black liquor droplets to facilitate burning. Liquor flow inside a tube is either constricted or bounced of a plate to form a sheet of liquid, Figure 9-2. This sheet will break up and create droplets. With liquid sheet the droplet formation occurs with two mechanisms. In wavy formation the surface tension and drag help form waves from local instabilities (Dombrowski and Johns, 1963). These waves will break into ribbons, which will collapse into cylindrical strands and ultimately form droplets (Spielbauer and Aidun, 1992). In perforation breakup the liquid sheet forms holes randomly which rapidly enlarge (Spielbauer and Aidun, 1992). Resulting black liquor strands break to droplets. No matter how the droplets form, it seems that the shape of droplet size distribution is the same (Kankkunen and Miikkulainen, 2003).

When hot steam containing liquid is sprayed to atmospheric pressure the steam bubbles play a dual role. They can form an instability that will break a hole into the sheet causing perforation breakup. If the steam amount is sufficient the sheet formation does not occur and liquid droplets are formed directly (Helpiö and Kankkunen, 1995).
When the pressure of black liquor falls in the liquor gun handle under the pressure that corresponds to the boiling temperature, bubbles will begin to form, Figure 9-3. The boiling is not usually sudden, but an increasing part of the black liquor flow is steam bubbles. The increase in the firing temperature will be seen as an increase in the spray velocity and as a decrease in drop size and mass flow, Figure 9-4. Typically this means that larger nozzles are required to maintain load.

Boiling temperature of black liquor is defined as sum of boiling temperature of water at same conditions and black liquor boiling point rise. Boiling point rise is liquor dependent but is mostly a function of black liquor dry solids. Typically constant difference to boiling point temperature produces 'optimum' firing conditions for a particular liquor gun type and black liquor. At very high dry solids this temperature must be increased to compensate for the decrease in water volume in the black liquor, Figure 9-5 and to keep the liquor viscosity low enough for pumping.

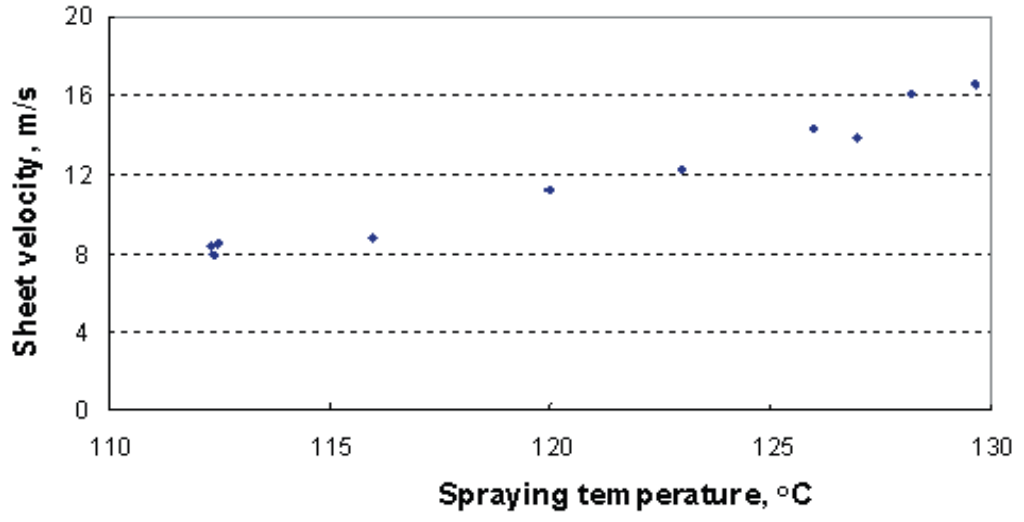

Figure 9-4, Liquor droplet velocity at liquor gun exit as a function of the firing temperature (Vakkilainen and Holm, 2001).

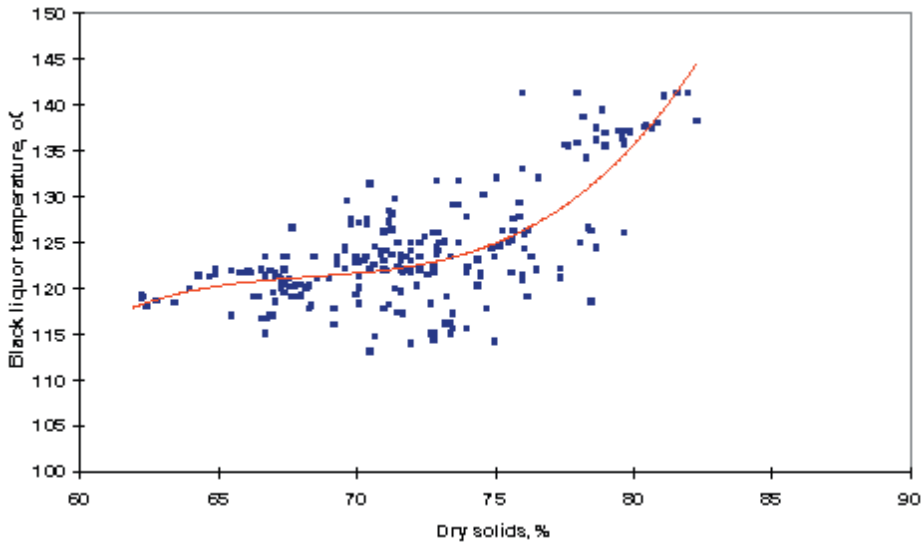

Figure 9-5, Black liquor as fired temperatures as function of black liquor dry solids.

After selecting the nozzle size and type, the liquor flow is controlled by the liquor pressure and temperature. A higher firing temperature has another effect. The liquor flashes in the nozzle tube and causes a bigger pressure loss due to the accelerated velocity, Figure 9-5. Thus, we have to raise the liquor firing pressure to keep the boiler load unchanged.

Flow from black liquor gun

The nozzle pressure loss can be expressed through flow coefficient and flow dynamic pressure at nozzle. The flow coefficient takes into account the friction and acceleration losses (Spielbauer and Adams, 1990).

$$\Delta p_n = C_f \rho u^2/2 \qquad 9\text{-}1$$

where
C_f is nozzle flow coefficient, -

The flow coefficient for industrial nozzles has been correlated with a simple two term equation.

$$C_f = a + bRe_n^{\,c} \qquad 9\text{-}2$$

where
Re_n is Reynolds number at nozzle outlet, -
a, b, c are constants, -

Reynolds number is calculated on the basis of the smallest flow area of the nozzle. The minimum flow area is a function of plate installation angle. The values for the constants a, b and c are presented in table 9-1 (Spielbauer and Adams, 1990).

Table 9-1, *Nozzle flow coefficient constants (Empie et al., 1992).*

Nozzle type	a	b	c
splashplate nozzle	1.17	373	-0.92
fan spray nozzle	1.16	2780	-1.65

Usually, the liquor firing pressure, temperature and volume flow rate are measured in the liquor ring. For some boilers, only the total flow rate is measured. A better knowledge and controllability of liquor firing is achieved by measuring and controlling the volume flow rate on each wall or even through each of the liquor guns.

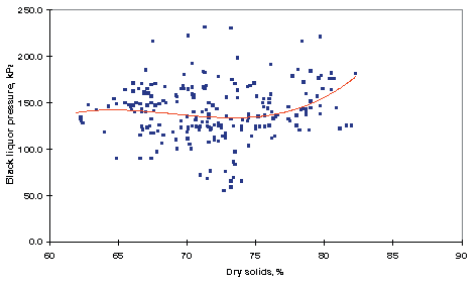

Figure 9-6, Black liquor as fired pressures as function of black liquor dry solids.

Effect of black liquor type

Black liquor has different properties in different mills; even the same mill can have quite variable liquor properties. Chemical cooking and wood source affect the liquor properties. To illustrate the effect of firing parameters we can make simula-

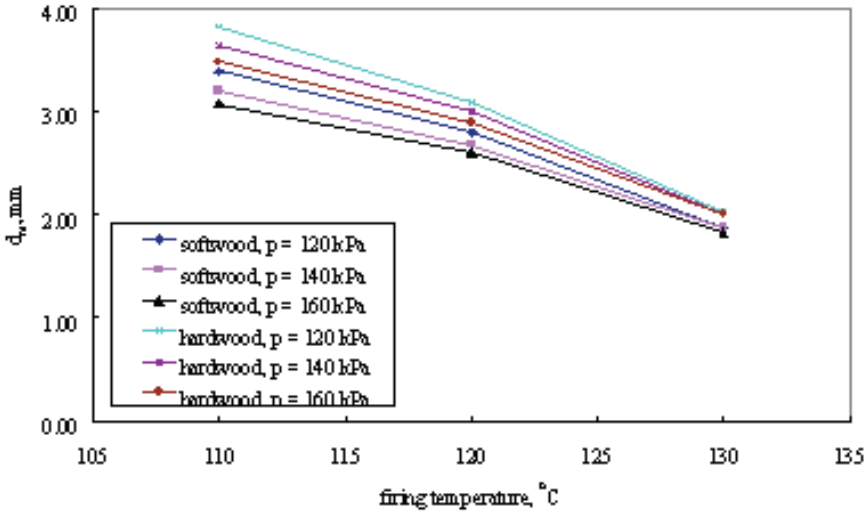

Figure 9-7, Black liquor droplet size for both liquor types and different firing pressures as a function of firing temperature at 70 % dry solids.

tions on gun behavior. Softwood and hardwood liquor were studied (Järvinen *et al.*, 1997). A range of typical values is firing temperature of 110, 120 and 130 °C and pressures of 120, 140 and 160 kPa.

Table 9-2, *Black liquor properties at 70 % dry solids and 110 °C.*

Liquor type	Hardwood	Softwood
Viscosity, mPas	344	206
Diameter ratio during devolatilization, -	2.9	3.2
Boiling point rise, °C	13.9	13.9

A single throttled splashplate nozzle of 27 mm, situated at the level of 6.2 m was used. The dry solids content was 70 % all the time. The reference values of the properties of black liquor are presented in Table 9-2. The diameter ratio during drying was 1.5.

Firing temperature and boiling point rise determine the velocity at gun throat (Helpiö and Kankkunen, 1995). Higher velocity leads to smaller diameter droplets. The mass median droplet diameter is presented as a function of firing temperature, Figure 9-7.

The black liquor droplet size of hardwood liquor is larger than the droplet size of softwood liquor due to its larger viscosity. The droplet size decreases with increasing temperature due to the accelerated flow and the smaller black liquor viscosity. When firing below the liquor boiling point, an increasing firing pressure decreases the droplet size significantly. This is because of a larger mass flow rate and higher outlet velocities.

In order to enlarge the softwood droplet size equal to hardwood values, the firing temperature must to be lowered. Approximately a temperature decrease of 5…7 °C is needed at the firing temperature range of 110…120 °C. A decrease of 2…3 °C with a firing temperature range of 120…130 °C is needed. Another way of enlarging the droplet size is to lower the firing pressure. Thus, the gun load would be smaller.

When flashing, an increasing pressure decreases the nozzle outlet quality meaning that the change of the outlet velocity is less significant. The calculated initial velocities of the black liquor droplets are presented in Figure 9-8.

An increasing firing pressure and temperature

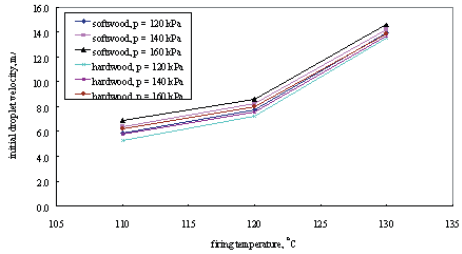

Figure 9-8, Black liquor droplet initial velocities for both liquor types as a function of firing temperature at 70 % dry solids for different firing pressures.

decreases the fraction of the liquor sprayed to the char bed and increases suspension burning and the fraction of the liquor reaching the furnace walls. When firing liquor below the boiling point, hardwood liquor increases the liquor amount reaching the char bed. When firing under flashing condition at 130 °C, fraction of liquor reaching the char bed is smaller with hardwood liquor compared with softwood liquor. This is due to the increased liquor fraction ending up on the furnace walls.

It is known that hardwood liquor swells less that softwood liquor. In order to compare liquor droplet combustion and flight path differences, was combustion of two different droplets with a diameter of 2 and 3 mm simulated. The flue gas upward velocity used was 5 m/s and the droplets were fired horizontally with a velocity of 8 m/s. The flight paths of the droplets are presented in Figure 9-9. Swelling of the black liquor affects the flight path of the droplet. Black liquor swells normally by a factor of 2 to 3 in diameter during devolatilization. Liquors which swell much, loose their momentum faster than non swelling liquors (Manninen and Vakkilainen, 1996).

Due to the larger swelling and the smaller droplet size of softwood liquor, softwood liquor droplets have bigger friction forces with the result that the penetration of the spray into the furnace is smaller. This is considered the reason for the larger hardwood liquor amount ending up on the furnace walls at higher firing temperatures.

Table 9-3, *Spray properties calculated as a function of liquor gun type, q_m = 7.4 kg/s, t_f = 136 °C, dry solids content 83.5 %*

Nozzle size, mm	Firing press., kPa	Outlet velocity, m/s	Droplet size, mm	Outlet quality, %
38	100	11	3.07	0.055
33	128	12	2.66	0.039
28	184	14	2.22	0.024

The effect of the liquor gun type on black liquor combustion can be modeled. Järvinen *et al.* (1997) studied firing with three different size liquor guns. The boiler process values and dimensions were based on typical Scandinavian practice. The objective was to find out how gun size affects firing. The firing pressure was adjusted to keep the gun load unchanged, i.e. the smaller the nozzle, the higher the firing pressure. The firing temperature was kept constant. A single throttled splashplate nozzle, situated at the level of 8.6 m from furnace bottom, was used. The liquor firing parameters are presented in Table 9-3.

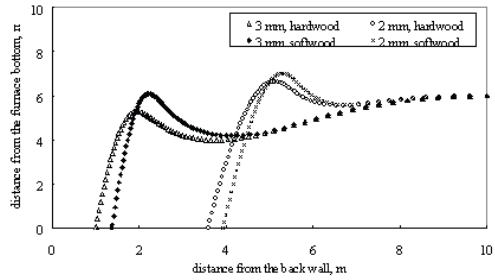

Figure 9-9, Flight paths of hardwood and softwood liquor droplets as a function of droplet size, t = 120 °C, u = 8 m/s, horizontal spraying.

The larger the nozzle, the larger the droplet size and the smaller the nozzle outlet velocity. The lower values of the quality with the smaller nozzles results from a higher pressure in the nozzle inlet. On the basis of these results, combustion simulations for each case were made. The amount of the liquor sprayed to the walls, to the char bed and the carryover amount were calculated.

There are no significant differences in drying. The droplet has not swollen yet so the droplets tend to stay in the same vertical plane. Water is released further away from the liquor gun as the droplet size increases.

The center of gravity of carbon release is presented in Figure 9-10. This puts the whole carbon releases to a single point so half of release occurs below and half above. Similarly half of the release occurs behind and half in front of the point. A larger nozzle size moves combustion towards the opposite wall of the liquor gun due the longer combustion times. A smaller nozzle size moves the combustion up higher. Smaller droplets tend to burn faster, break faster and are more carried with upflowing flue gas.

The amount of liquor reaching furnace walls and char bed is presented in Figure 9-11. The amount of the liquor hitting the furnace walls decreases as

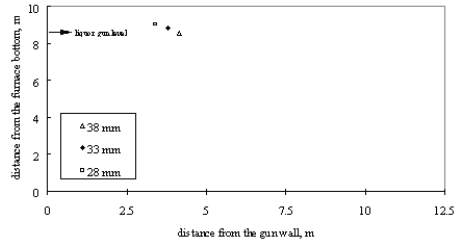

Figure 9-10, Center of gravity of carbon release as a function of gun size, q_m = 7.4 kg/s, t = 136 °C.

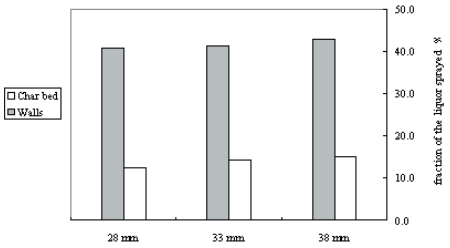

Figure 9-11, Fraction of the black liquor sprayed to the char bed and on furnace walls as a function of liquor gun size, q_m = 7.4 kg/s, t = 136 °C.

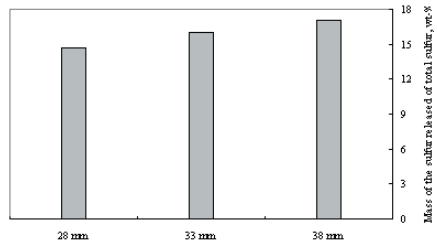

Figure 9-12, Fraction the sulfur released of the total sulfur during devolatilization.

a function of decreasing droplet size. This is because of the shorter combustion times due to the smaller droplet size. The amount of liquor hitting walls could also be controlled by gun type and spraying angle, but here these were kept constant.

The release of sulfur during the devolatilization was studied by calculating the total sulfur amount released for each case. The result is presented in Figure 9-12. The larger the nozzle, i.e. the larger the droplet size, the larger the sulfur release.

9.2 LIQUOR GUN TYPE

Järvinen *et al.* (1997) have studied the effect of liquor gun type to the firing of typical softwood black liquor. Boiling point rise is a function of black liquor dry solids content. Black liquor sheet velocity increases due to liquor flashing in the nozzle opening. Typical droplet burning parameters for softwood are listed in Table 9-4.

Table 9-4, *Softwood liquor burning properties.*

Swelling factor during drying	$1.54*D_o$
Devolatilization swelling factor	$2.3*D_o$
Boiling point rise	16 °C

The firing temperature used was 123 °C, which is typical for recovery boilers firing softwood liquor at 73 % dry solids. This temperature is above the atmospheric boiling point of the liquor.

The liquor was sprayed from guns without vertical velocity distribution. The sheet velocities, droplet sizes and liquor mass flow distributions for all nozzles were modeled as continuous functions of spray angle. These models are based on interpolation and extrapolation of experimental measurements. Use of data from small scale model work was needed for some parameters.

Five different nozzle types were studied (Helpiö and Kankkunen, 1995b, Adams, 1994, Helpiö and Kankkunen, 1994, Empie *et al.*, 1995). Nozzles one, two, three and five were of the splashplate type. The orifice diameter and the position of the splashplate varied depending on the manufacturer. Nozzle four was a fan spray nozzle. The dimensions of the nozzles are presented in Table 9-5. Operating parameters of the nozzles were selected by Reynolds number criteria i.e. the same value for Re was used for every nozzle. In all cases, only one nozzle was used which was placed at the center of the front wall and at height of 6 m. The vertical spraying angle used was constant for every case and it had a value of -10°.

The horizontal direction of liquor droplets is determined by the liquor mass flow distribution. If the nozzle opening angle is wide, liquor is usu-

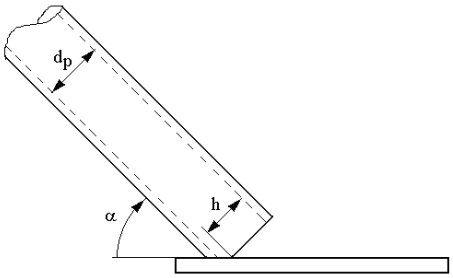

C27

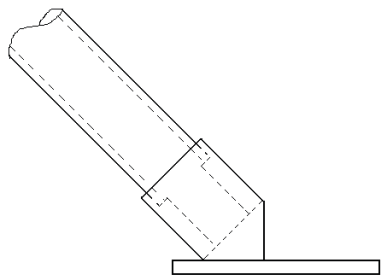

D28

Figure 9-13, Two typical splash plate liquor guns, left partially blocked, right totally open (TKK).

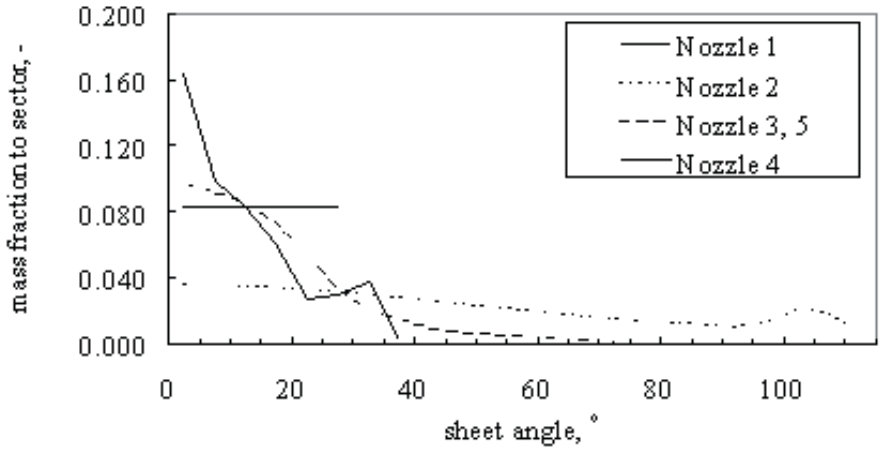

Figure 9-14, Mass flow distribution of the nozzles at 123 °C, Re = 3400, sector width 5 °.

Table 9-5, *Nozzle properties.*

Type	Description	Opening angle, °	Plate angle, °	Diameter, mm
1	Splashplate throttled	85	25	21.6
2	Splashplate nonthrottled	210	35	15
3	Splashplate at a distance	120	25	15
4	Fan spray nozzle	60	-	15.5
5	Splashplate at a distance	120	25	42

Table 9-6, *Mass median diameter, MMD of the nozzles.*

Nozzle type	MMD, mm
1 Ahlstrom	1.89
2 Kvaerner	1.79
3 Pantsar	1.79
4 CE	1.97
5 B&W	3.78

ally sprayed to adjacent furnace walls. Mass flow distributions of the nozzles are presented in Figure 9-12. The mass flow distribution of the nozzle 5 was similar to nozzle 3. The mass flow distribution varies between geometrically different nozzles. Especially, the fan spray nozzle differs from the others because of the small opening angle used. Another exception is the nozzle type 2. Because of wide angle of spray a great deal of liquor is sprayed close to walls. The mass flow rate distribution of a splashplate nozzle is shaped as a triangle while the fan nozzle has a flat distribution.

Droplet size

One of the most important parameters in controlling recovery boiler furnace operation is the droplet size. Plenty of research work has been done in order to study black liquor droplet formation and liquor sheet disintegration. Full scale measurement data was available for the droplet sizes of nozzles 1 and 2. The droplet size of nozzle 5 was calculated based on nozzle 1. The droplet sizes of nozzles 3 and 4 were based on measurements with small scale models. Droplet sizes were then scaled to full size values based on scaling criteria from small and full scale measurement results using dimensional analysis, Table 9-6. The nozzle 5 has a droplet size much bigger than the others.

Release of water

The evaporation of water consumes energy. If the droplets are not dry when reaching the char bed, the temperature of the bed will decrease causing unstable furnace operation. In the worst case, the water in the bed may lead to bed extinction.

It was observed that the water reaching the char bed was insignificant with the nozzles spraying smaller size droplets. Only the largest nozzle 5 delivered some water to the char bed, 5 % of total water amount. The maximum spraying of black liquor to adjacent walls occurred with nozzle 2 due to a wide opening angle. The amount of water landing the walls with this nozzle was 13.5 % of total water.

The drying takes place in the vicinity of the nozzle. With all nozzles, most of the water is released within the first second. With increasing droplet size, the drying moves farther from the nozzle in

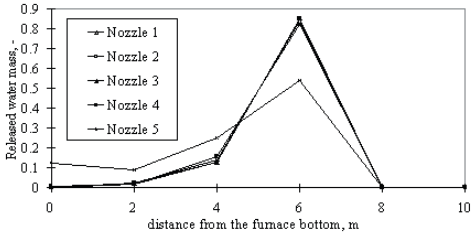

Figure 9-15, Release of water in vertical direction.

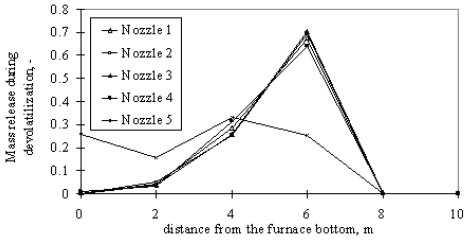

Figure 9-16, Release of mass during devolatilization in vertical direction.

horizontal direction.

Devolatilization

During devolatilization gases are released from the black liquor droplet and the diameter of the black liquor droplets increases by a factor of 3 (Horton *et al*., 1992). This means larger drag forces due to larger cross-sectional area. If the friction forces are high enough, entertainment takes place.

A clear difference between the nozzles can be seen in the mass release during devolatilization, Figure 9-14. With nozzles 1, 2, 3 and 4, devolatilization is completed in flight. With nozzle 5, many droplets are still going through pyrolysis when they reach the char bed.

With the small nozzles devolatilization occurs at the vicinity of the liquor gun. The release distribution is flatter with bigger droplet size.

Sulfur release

The release model from (Manninen and Vakkilainen, 1995) was used for calculating sulfur release during pyrolysis. It can be seen that the larger the droplet size, the lower in the furnace the sulfur release occurs, Figure 9-17.

When comparing the total release of sulfur in the furnace nozzle 2 released sulfur closest to the wall. At the same time, the release distribution is flatter. With wider opening, the maximum release point moves towards the liquor gun wall.

The minimum sulfur release occurred with nozzle 5. The reason for this is the larger droplet size. Calculated sulfur release was cut off when droplets landed on the char bed. When the droplet size is bigger, the release point of sulfur moves towards the opposite wall from the liquor gun.

Sulfur release seems to occur along the flight path, Figure 9-19. Sulfur release starts when the droplet surface is dry. With larger MMD of droplets the sulfur release occurs farther away from the liquor

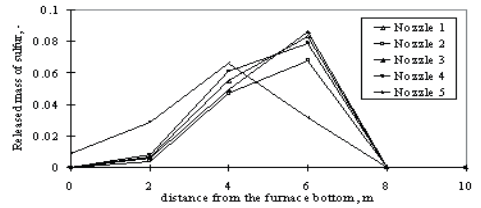

Figure 9-17, Release of sulfur in vertical direction.

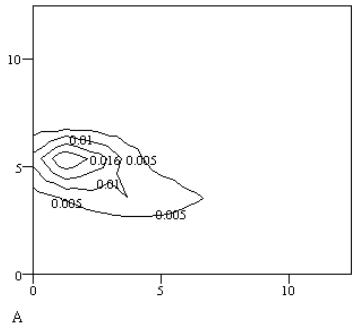

Figure 9-18, Release of sulfur in vertical plane, nozzle 2.

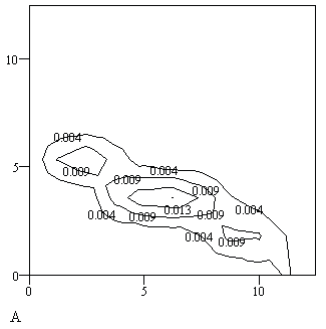

Figure 9-19, Release of sulfur in vertical plane, nozzle 5.

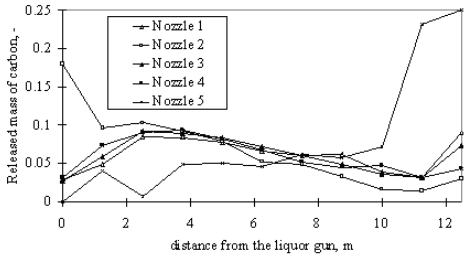

Figure 9-20, Release of carbon in the direction of nozzle center line.

gun.

Char combustion

Char combustion is important for proper furnace operation. If the droplet size is too small the char combustion is completed before the droplets reach the char bed. When liquor is fired with small nozzles, the maximum release point is at the level of liquor gun. When droplet size is bigger, the release point moves lower and more carbon is delivered into the char bed.

Horizontal mass flow pattern affects how efficiently the furnace cross sectional area is utilized. The wider the opening angle and the bigger the droplet size, the better one liquor gun covers the whole furnace. This is why gun 5 can be large.

Figure 9-20 shows the carbon release as a function of distance from the liquor gun. With the small nozzles the release is rather flat. With bigger guns much of the release occurs at the vicinity of the opposite wall and char bed.

The carbon release patterns for nozzle types 1 and 3 are fairly similar. There are two main release locations. For small and medium size droplets the release occurs at the vicinity of the liquor gun. Larger droplets have just completed evaporation and started devolatilization as they hit the opposite wall. The fan spray nozzle 4 behaves like splashplate nozzles 1 and 3. Most of the carbon release is at the liquor gun level. Nozzle 2 releases carbon fairly close to the gun. The liquor is sprayed in wide angle so carbon release occurs along the liquor gun wall. This type of spraying decreases the penetration of the liquor spray to the center of the furnace.

The biggest nozzle 5 seems to have a different type of operation. A lot of the droplets land on char bed without significant carbon release during flight in the furnace. In practice, low char bed temperatures and uncontrollable char bed growth would result.

9.3 AIR DISTRIBUTION

Air is added to lower furnace for the combustion and gasification reactions to proceed. There is typically less than stoichiometric air added to keep up reducing atmosphere. Because of the limited reaction speeds there is however some 3 ... 12 % of O_2 in the lower furnace gases.

Air addition happens typically in three stages.

- Primary air, which is added at the root of the char bed.
- Secondary air, which is added at height of 1 ... 3 m above primary air.
- Tertiary air, which is added some 3 ... 6 m above the liquor gun level.

The two level air staging is in use only in older boilers. It typically produces higher emissions and results in lower operating furnace loads than the three level air.

There have been some reported schemes to increase the number of air levels from three to five by splitting the primary and secondary air into two levels. No benefits of these tries have been reported.

There are many conflicting results on how air distribution affects sulfurous gas and particulate emissions. If we assume that combustion is mixing limited in the recovery boiler furnace, then changing air flow rates and patterns affects the location of the main combustion zone. This affects the furnace temperature pattern and so the char bed temperature distribution. It is the temperature profile that then controls the emissions.

Primary air

The role of the primary air is to shape the bed so that the sides angle towards the juncture of the furnace wall and the bottom and provide air for char burning. There have been other tasks attributed to primary air such as keeping the TSR emissions low (Jutila *et al.*, 1978) and controlling the loading level.

The amount of primary air flow depends on the boiler manufacturer and the way the boiler is operated. Range of reported operating values is as high as 25 ... 60 % primary air of total air (Kippo, 1979). In modern boilers with high dry solids the primary air is usually well below 30 % of all air.

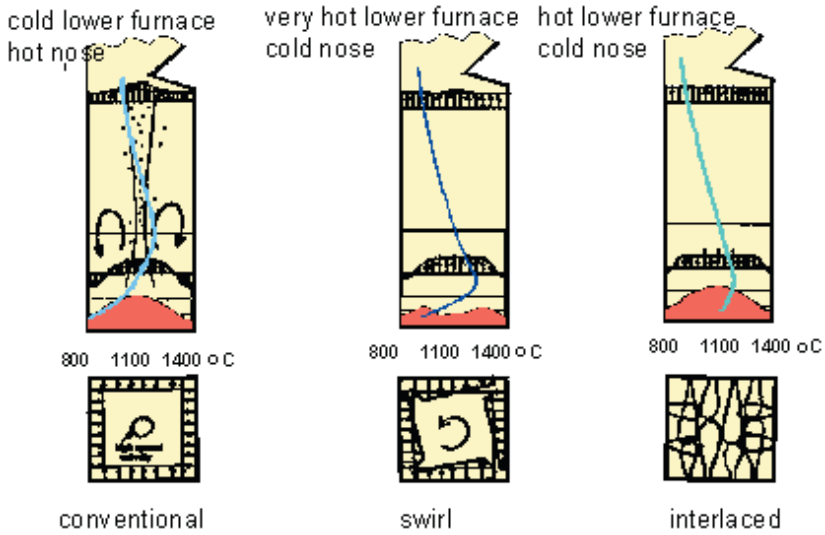

Figure 9-21, Effect on secondary air model on furnace temperature.

Table 9-7, *Effect of air model on deposition rate at nose level*

Air model	Softwood, mm/h	Hardwood, mm/h
Straight	7 - 9	5 – 7
Swirl	3 - 5	4 - 5
Interlaced	3 - 5	3 - 4

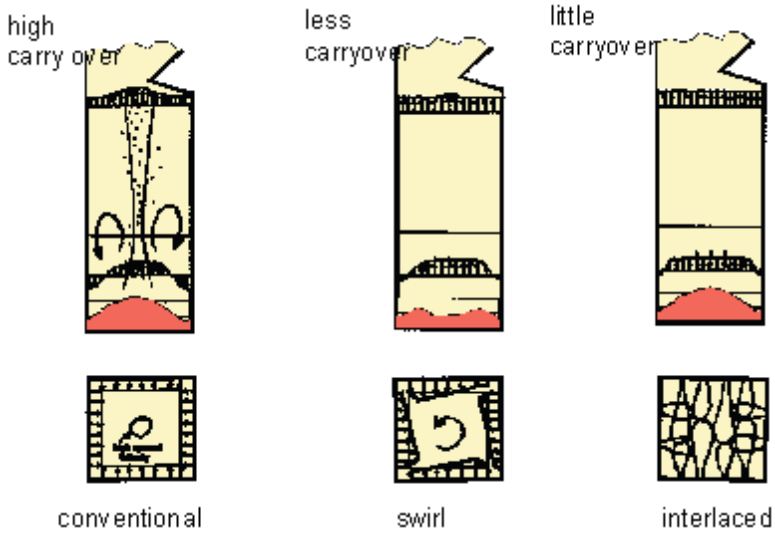

Figure 9-22, Effect on secondary air model on carryover.

Depending on boiler operation both increasing and decreasing primary air temperatures have been reported in the literature. Harrison and Ariessohn (1985) report that char bed surface has a maximum temperature corresponding a primary air value. Both higher and lower primary air flows result in lower char bed temperatures. This phenomenon has been attributed by (Adams and Frederick, 1988) to the limited reaction rate. If air more than what is needed to produce only CO_2 is provided, then the excess will cool the bed. It has been observed that high air flow will blow off and prevent light char particles from landing.

Secondary air

The main tasks of secondary air are to keep the size of the char bed desired and provide air for volatiles burning and for the combustion reactions on the top section of the char bed. Secondary air is the main air responsible for mixing in the furnace (Adams, 1994a). Secondary air is the main control air level.

Furnace behavior can be affected by changing secondary air model (Metiäinen, 1991). The main effects are seen at the furnace temperatures and the amount of carryover. The swirl seems to increase lower furnace temperatures significantly, Figure 9-21 (Vakkilainen, 1996). Even modest adjustments in air port damper settings change the temperature profile. It is possible to decrease the flue gas temperature at nose level by some 20 - 30 °C. In the beginning of 1990 some boilers used very much swirl (Bergman and Hjalmarson, 1992). Increasing swirl too much results in very high temperature imbalance between left and right superheater sections. High swirl deposits unburned material on air and liquor openings thus increasing corrosion.

Interlaced models seem to give much of the swirl benefits without its adverse effects. Left and right superheater section temperatures can be kept fairly even. The carryover measurements show that high velocity core exists with conventional firing, Figure 9-22. This increases carryover and decreases furnace effective cross section. Swirl firing seems to decrease carryover because of disappearance of the high velocity core. According to the measurements, Table 9-7, interlaced pattern can minimize carryover.

Tertiary air

The role of the tertiary air is to provide mixing of unburned flue gas with air to complete the combustion and even temperature distribution at the bullnose level. Tertiary air has little effect on char bed operation.

Optimum operating temperature

Many of the lower furnace operating parameters depend on the lower furnace temperature. Low furnace temperatures cause high TRS emissions. Increasing lower furnace temperature decreases the sulfur dioxide and TRS emissions. But when the sulfurous emissions are lowered the nitrogen oxides increase and the hydrochloric acid emissions decrease.

High sulfur emissions cause increased lower furnace corrosion. High furnace temperatures increase heat fluxes and corrosion caused by high metal temperatures. High heat fluxes decrease or even remove the protective frozen char bed and smelt layers covering the tubes. Composite tube floor cracking can be partially caused by low char

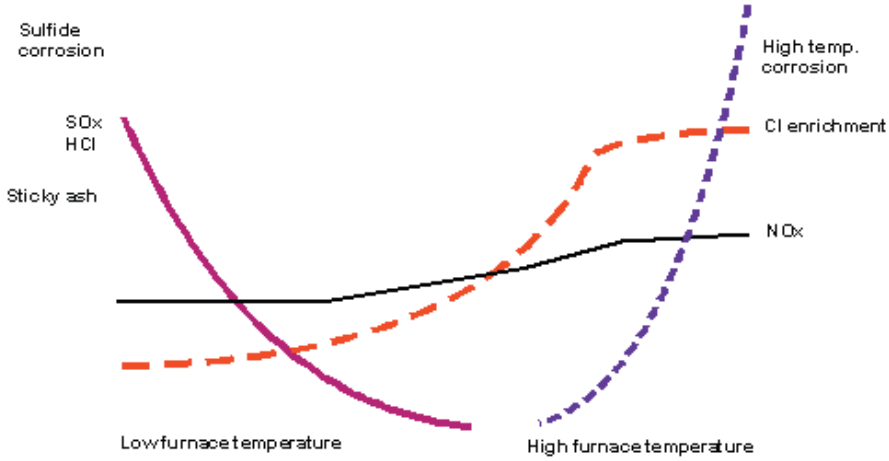

Figure 9-23, Optimum temperature window.

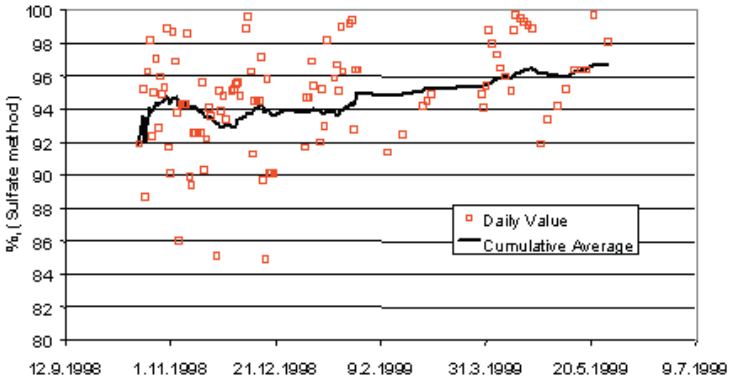

Figure 9-24, Reduction efficiency after new boiler startup (Vakkilainen and Holm, 2000).

bed height.

High sulfur dioxide emissions mean sticky, low pH, sodiumbisulfite containing dust that is fouling. Increased lower furnace temperature and sodium release binds the SO_2 and creates excess sodiumcarbonate. Resulting dust is non sticky and easy to remove. A further increase in the lower furnace temperature increases chloride enrichment in dust causing boiler bank pluggage and superheater corrosion.

9.4 REDUCTION CONTROL

Good reduction efficiency requires high temperature, lack of oxygen and presence of carbon. For good reduction proper char bed that covers smelt is essential. After new boiler startup the reduction rate will initially vary a lot, Figure 9-24. Modern boilers can achieve reduction efficiencies of 95 … 97 mol-% measured in smelt.

There are several reasons for poor reduction. Reduced smelt can reoxidize. If char bed does not cover the smelt spout openings, air will react with molten smelt. Low char bed temperature will result in low reduction and high sulfur emissions. Suspension firing with too small droplets will affect reduction. Droplets will burn fast and furnace can be hot, but lack of carbon will slow down reduction reactions.

Lower load will reduce furnace temperatures and decrease reduction (Verloop and Jansen, 1995). Often low loads are run with high excess air levels. This further decreases reduction.

9.5 NOX CONTROL IN RECOVERY BOILERS

Wood contains some 0.05 … 0.15 w-% of nitrogen (Verveka *et al.*, 1990). During kraft cooking most of it is released and transferred to black liquor. It seems that dissolution of nitrogen containing compounds occurs easily during the first stages of cooking (Niemelä and Ulmgren, 2002). Very little nitrogen exits with pulp (Kymäläinen *et al.*, 1999). Most of the ammonia and other volatile condensates in black liquor is released during evaporation and ends up in methanol and NCG. Heat treatment can increase this release of nitrogen (Aho *et al.*, 1994).

Some of the main forms of nitrogen in black liquor are pyrrole, pyridine and amino acids (Niemelä, 2001), Figure 9-25. Different wood species have nitrogen in different forms. In pine (pinus sylvestris) about fifteen different amino acids can be found.

Nitrogen release from black liquor during combustion

About two thirds of nitrogen in black liquor is released as ammonia during volatiles release (Aho *et al.*, 1993). The rest remains in char and exits the recovery furnace with smelt probably as sodium cyanate NaOCN (Kymäläinen *et al.*, 2002). In recovery boiler furnace nitrogen in black liquor has three pathways. It ends up as NO, elemental nitrogen or nitrogen in smelt, Figure 9-26.

The formation of NOx in coal, gas and oil flames has been extensively studied. The main chemical mechanisms that can be used to control formation

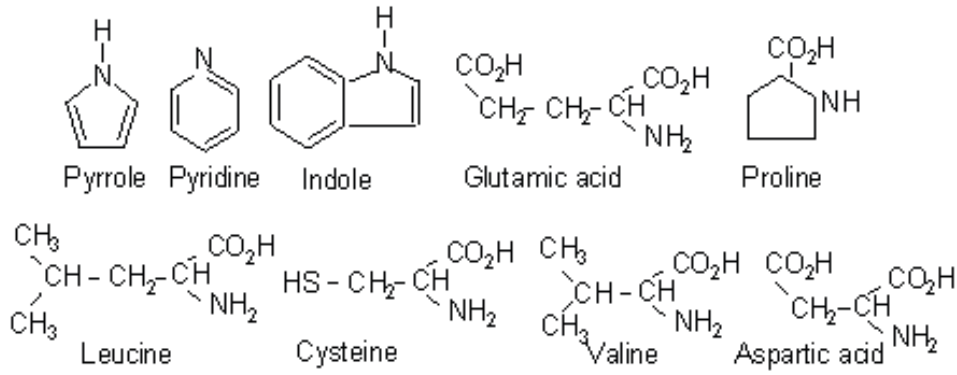

Figure 9-25, Some of the nitrogen compounds in black liquor.

and reduce formed NO have been established for some time now. These same principles apply to kraft recovery boilers. The effect of the presence of volatile alkali metals such as sodium and potassium seem to have minor effect. The main sources of NOx in boilers are fuel and thermal NOx. The fuel NOx is formed during pyrolysis and volatiles evolution. The source is the nitrogen in the fuel.

Example

Calculate NOx from nitrogen in black liquor using typical values for recovery boiler material and energy balance and a typical nitrogen content of 0.1 w-% in the dry solids. We can get for possible NO generation per 100 kg of dry solids.

Nitrogen oxides moles

$$M_{NOx} = 0.001^{kg}/_{kgds} * 100kgds/14^{kg}/_{kmol} = 7.1mol$$

Nitrogen oxides volume

$$V_{NOx} = 7.1mol * 22.4^{m^3}/_{kmol} = 0.16\ m^3$$

Flue gas volume

$$V_{fg} = 663.5 * 22.4^{m^3}/_{kmol} / 27.4^{kg}/_{kmol} = 542\ m^3$$

Nitrogen oxides

$$V_{NOx}/V_{fg} = 0.16\ m^3 / 542\ m^3 = 300\ ppm$$

The typical NOx emissions from a recovery boiler are about 100 ppm. We can conclude that there is enough fuel nitrogen in the black liquor to produce all of the NOx emissions if the conversion is 25 ... 30 %. Similar conversion fractions have been measured in laboratory conditions. This fraction seems to be about constant for black liquor of various wood species, type of cook and dry solids concentration (Forssén *et al.*, 1997).

Thermal NOx is formed during combustion. The source is the elemental nitrogen coming in with the air. Typically about up to 60 % of NOx emissions in PFC boilers are from thermal NOx. The temperatures in recovery boiler furnace are

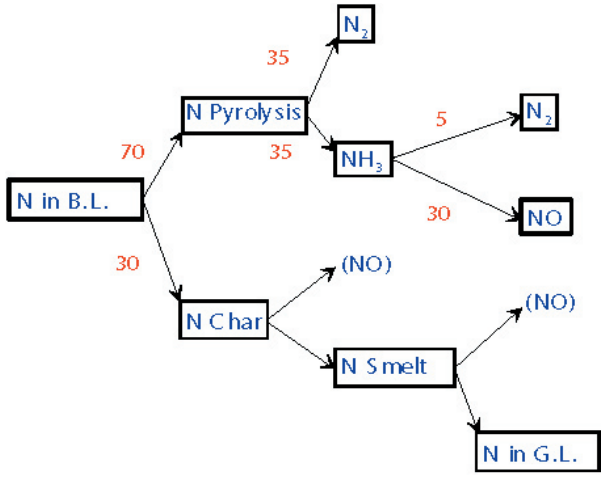

Figure 9-26, Nitrogen reaction paths from black liquor.

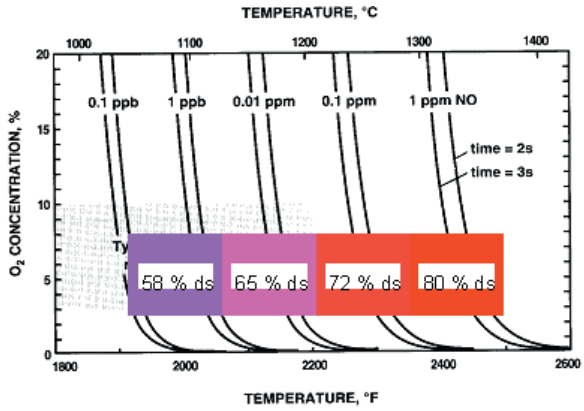

Figure 9-27, Formation of thermal NO in recovery boilers (after Nichols et al., 1993).

too low for significant thermal NOx production (Nichols *et al.*, 1993). Formation of thermal NOx is very low until the furnace temperatures reach 1400 °C, Figure 9-27. Even increase of black liquor dry solids from 67 to 80 % does not in typical boiler produce significant amounts of thermal NOx (Adams et al., 1993).

Other smaller sources of NOx, such as prompt or Fennimore NOx can be ignored for recovery boilers.

NOx destruction in recovery boilers

The main effort on NOx control has concentrated on firing and air system modifications as these offer almost the only viable option (Anderson and Jackson, 1991). NOx formation is affected by the amount of air and combustible products. The lower portion of recovery boiler furnace is at or little below stoichiometric level. The fluctuating concentrations, temperatures and velocities affect strongly to the formation of NOx.

The recovery boiler differs from typical coal and oil fired boilers in the respect that the inert fraction in the fuel is very large. In addition the fuel heating value is low. So the temperatures encountered in recovery boilers are low (1000 - 1400 °C).

Some of the possible main pathways for NOx reduction are

- reduction by hydrocarbons
- reduction by CO
- reduction by H_2
- reduction by H_2S
- reduction by residual carbon in char
- reverse Zeldovich mechanism
- reduction by sodium species

Ernola *et al.* (1989) have presented an extensive study on NOx reduction using CHEMKIN computer code in coal combustion. They found H_2 and CO to be effective reducing agents. They concluded that the main destructive reactions were

$$NO + CO \rightarrow N + CO_2 \qquad 11\text{-}3$$

$$NO + H_2 \rightarrow N + H_2O \qquad 11\text{-}4$$

Lyon *et al.* (1989) have studied the effect of H_2 as NOx destruction agent in a pilot scale tower furnace. They found hydrogen to be less effective than propane. In the presence of CO and when temperature is over 1400 °C, the NO formed will react to N fairly rapidly (less than 100 ms) (Aho *et al.*, 1993).

Thompson and Empie (1993) have proposed that some reaction of NO by sodium species to $NaNO_3$ could take place. Analyses of mill ESP samples have shown this to be of minor importance.

Effect of fuel nitrogen content to NOx emissions

When boilers are run with liquors from pulping of different wood species, high nitrogen containing woods (hardwood) produce more NOx than softwood liquors. Field tests support the conclusion that recovery boiler NOx emissions correlate with nitrogen in the black liquor (Clement and Barna, 1993). The highest reported nitrogen content has been 0.5 w-% of bagasse black liquor dry solids (Aho, 1994). The detection accuracy of nitrogen in the fuel from commercial laboratories is very poor so direct correlations are often misleading. For example two black liquors of nitrogen content 0.072 and 0.114 mass % get both typically a value of 0.1 mass-%.

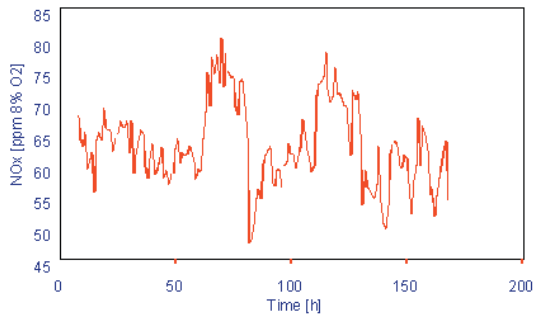

Figure 9-28, NO during trials at a North American mill.

Aho *et al.*, (1994) studied the reduction of nitrogen in the black liquor. One can somewhat change the nitrogen content by treating chips, making cooking changes and treating black liquor. The results however have so far showed this to be uneconomical.

Part of the nitrogen in black liquor is in the form of NH_3 and so easily vaporized. Parts of nitrogen can then be extracted from black liquor in the stripper area. This product may enrich to some parts of the recovery cycle so great care should be taken when this waste stream is destroyed.

Effect of operating parameter changes to NOx emissions

Changing air and liquor distribution affects NOx levels. In trials done in a North American boiler the NOx level could be varied from 75 to 55 ppm. The nitrogen content in the black liquor was low. 20 to 30 % reduction from highest values can be done by proper air staging and firing.

General observations of mill trials seem to indicate that

- flue gas dust content and NOx emissions have no significant correlation
- black liquor HHV and NOx emissions have no significant correlation
- air split between primary and secondary level has no significant effect to NOx
- air pressure has no significant correlation with NOx
- CO emissions affect NOx
- staging air higher (to tertiary) can reduce NOx a little
- adding a upper tertiary or quaternary air level can reduce NOx

Decreasing furnace temperature seems to decrease NO. This change can be attributed to higher SO_2 formation. In trials with actual operating recovery boilers typically after SO_2 emissions go to zero an increase in NOx emissions is seen, Figure 9-29.

In the NOx tests performed by manufacturers the

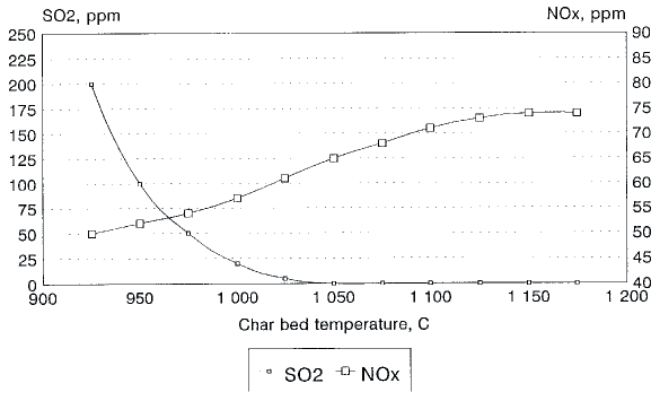

Figure 9-29, Effect of furnace temperature to NO during trials at a North American mill.

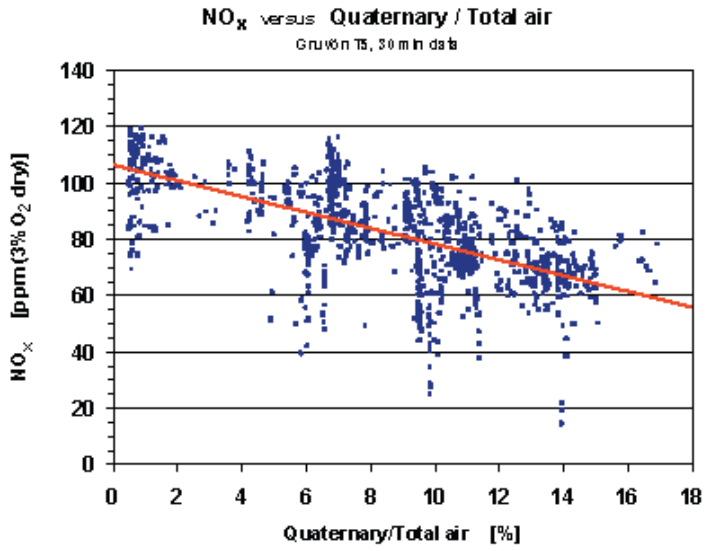

Figure 9-30, Effect of quaternary air flow to NO during trials at a Scandinavian mill (Wallén et al., 2002,).

number of liquor guns hasn't affected the NOx emission level. This means that for typical kraft recovery boilers the uneven fuel and oxidant mixing isn't a significant source of NOx emissions. However in some tests it has been seen that uneven firing can cause increase in other nitrogen emissions than NO. High gun pressure and resulting small black liquor droplet size has also been suggested as source of some reports of high NO excursions (Björklund and Warnqvist, 1989). Recovery boiler load increase has been reported to increase NOx emission (Salmenoja 1998).

Trials in Sweden with oxygen enriched air to recovery boiler have resulted in unchanged concentration of NOx in flue gas. As flue gas flow is reduced, the total emission of NOx per ton of pulp did reduce (Verloop *et al.*, 2001).

Reduction of NOx in the upper furnace

Recovery boiler NOx emission can be decreased by applying air in stages (Forssen *et al.*, 2000a). Typically this has been done by adding fourth level of air. The effect of amount of quaternary air can be seen in Figure 9-30. More than 10 % of total air is needed to achieve significant reduction.

Also residence time in furnace before the final air injection seems to play a role, Figure 9-31. More than 10 s residence time was needed for NOx removal. This seems to indicate that sufficiently low temperature is reached before the final combustion takes place. Brink *et al.* (2004) predict that long residence time between the black liquor gun

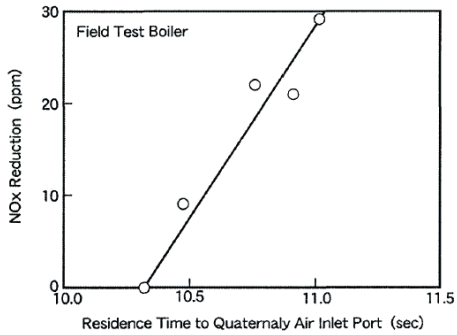

Figure 9-31, Effect of residence time to quaternary air to NO reduction during trials at a Japanese mill (Wallén et al., 2002).

level and the first tertiary air level improve NOx removal.

NOx behavior in a large Scandinavian boiler has been studied by Vakkilainen *et al.* (1998a). The recovery boiler employs partially interlaced secondary air injection model. This type of air model is capable of achieving high mixing rates in the lower furnace resulting at a fairly even temperature profile. The average temperature at the furnace exit is about 950 °C.

The modelling results showed fairly typical flow, temperature and gaseous species concentration patterns. Nitrogen is released primarily during the pyrolysis phase. Half of the fuel nitrogen was assumed to be released during pyrolysis as ammonia and half as molecular nitrogen, Figure 9-32. The nitrogen release occurs between the secondary

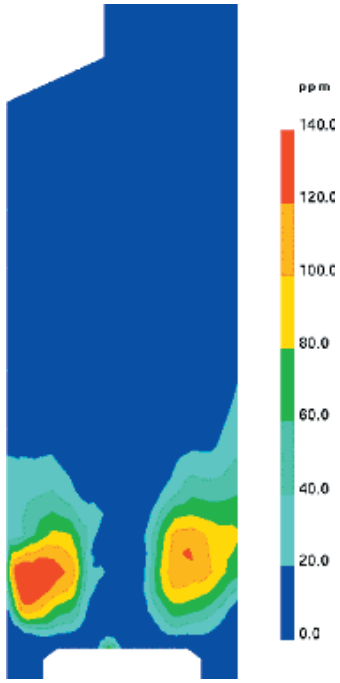

Figure 9-32, Furnace vertical NH_3 concentration profile, dry gases.

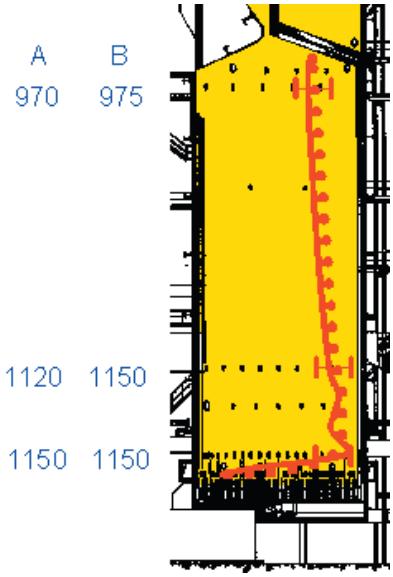

Figure 9-33, Furnace temperature measurements.

and tertiary air levels at a rather large furnace cross section. This would indicate that lower furnace conditions are the most relevant to nitrogen oxides formation and possible reduction reactions. There is a small peak in the middle of the char bed surface showing a local release of nitrogen containing species. This is not indicative of char nitrogen, which was not modelled, but of liquor droplets landing onto the char bed at this site.

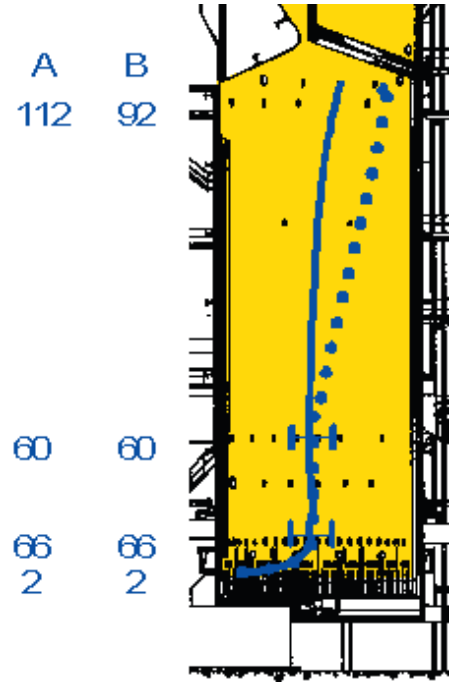

Figure 9-34, Furnace NO- measurement profile converted to dry gases and 3 % O_2.

This boiler was fitted with upper tertiary air to reduce NOx emissions. The retrofit was done in a pre planned three day shut down. Results from the calculations were compared to measurements performed on two days A and B. For practical reasons the experimental cases differ to some extent from simulated case. The furnace measurements were conducted by inserting an air cooled sampling tube through air ports, 2,5 m into the furnace at the primary, secondary and tertiary air levels. The temperatures were measured by a shielded thermocouple and the NO profile by an on-line analyzer. The measured temperatures for two days A and B are shown as Figure 9-33 and the furnace NO profile for the same cases as Figure 9-34.

The experimental temperatures show a fairly constant lower furnace temperature. The computed temperature field is consistent with the experimental data. The nitrogen species measurements in the furnace reached similarly only the furnace perimeter. Main nitrogen species measured by the on-line analyzer was NO. Significant NO_2 concentrations could not be found. It was not possible to measure NH_3 nor HCN concentrations at the same time so the values reported at Figure 9-34 show only NO. The NO concentration is very small at the primary air level. This indicates that the portion of NO released from the char bed is fairly low. The overall exit NO concentration (92

- 112 ppm) represents typical values when operating with mixed wood liquors.

The measurements showed that NOx reduction is practical with splitting the tertiary air into two or more separate levels (in vertical direction). In practice the NOx can be lowered by 10 … 15 % compared to traditional system.

The study shows that this kind of modeling can be applied to a 3150 tds/d recovery boiler. The modeling results increased the understanding of the in-furnace processes and helped in interpretation of the measurements and of the observations in the operation of the boiler. The results also support the role of fuel nitrogen as a major source of the recovery boiler NO emissions.

Other means of controlling NOx emissions

We can control the formation of NOx by.

- Reducing the free oxygen concentration (Boström, 1990). This decreases both the thermal and fuel NOx generation. All new improved air systems use this as part of their NOx reduction strategy. Reduction of oxygen level should be continued until unacceptable CO emissions result.
- Reducing the mean and the peak temperature levels in the boiler. This reduces the thermal NOx.
- Improving mixing, which affects temperature and concentration profiles decreases usually NOx emissions.
- Staging the air to more levels than conventionally.

Some studies indicate that increasing black liquor droplet size might have a beneficial effect to NO emissions. In modelling studies fine black liquor droplets produces more NOx than coarse black liquor droplets (Forssén *et al.*, 2000b).

Table 9-8, *Effect of solids increase to recovery boiler operation*

Dry solids	%	65	77
Capacity	tds/d	2130	2130
Steam temp.	°C	480	480
Steam pressure	bar	86	86
Economizer exit	°C	168	157
Reduction eff.	%	93–96	96-97
Sootblowing steam	%	2.5 – 3	<2
SO_2 emission	ppm	200 – 300	0
CO emission	ppm	~100	30 - 60
NOx emission	ppm	60 – 80	~70
HHRR	MW/m^2	3.1	3.1
Gross steam	%	100	105.5

9.6 SO_x AND TRS CONTROL

In the early 1980's it was discovered that increasing black liquor dry solids decreased the sulfur emissions (Maso, 1988). It was quickly understood that this happened because increased dry solids increased furnace temperatures. This increased sodium release, which then could bind sulfur dioxide to sodium sulfate (Perjyd and Hupa, 1984).

Increased furnace temperatures also increase reaction rates decreasing the reduced sulfur emissions. Lankinen *et al.* (1991) have outlined how the third

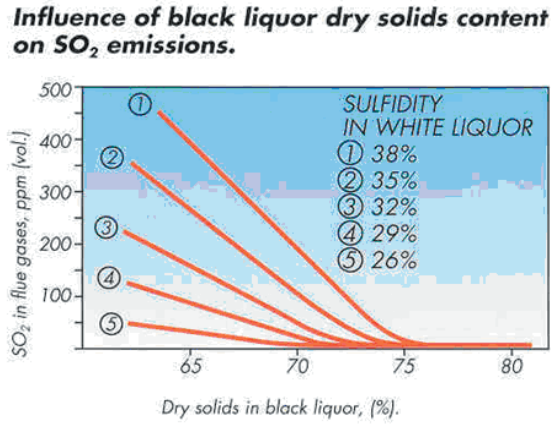

Figure 9-35, Effect of black liquor dry solids content to sulfur emissions (A. Ahlstrom Oy).

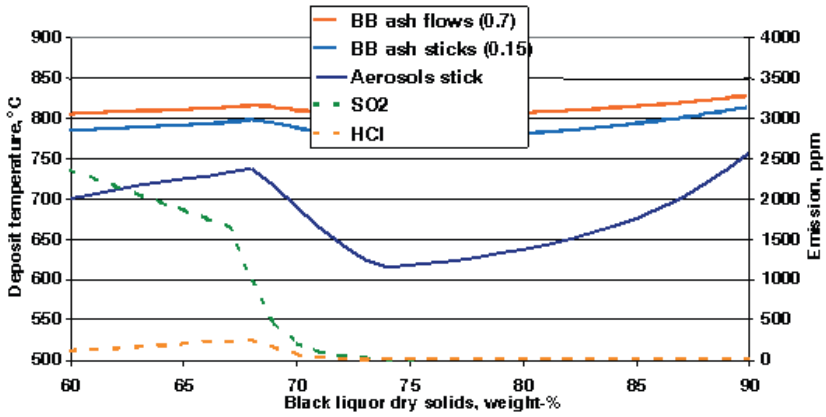

Figure 9-36, Effect of black liquor dry solids on ash behavior and emissions of SO_2 and HCl (Vakkilainen, 2000).

generation recovery island will affect the boiler operation, Table 9-8. How the char bed processes will be affected is not as obvious.

Earlier it was common practice to oxidize black liquor. Oxidation decreased TRS emissions from black liquor. With modern air systems and higher dry solids, black liquor oxidation is becoming obsolete.

In recent years the dry solids concentration from evaporators has increased from 65 to about 80 % dry solids. Increasing the black liquor dry solids concentration does not change the combustion air flow or the black liquor dry solids flow (Vakkilainen, 2000). The flue gas flow decreases as less water enters the furnace. The same amount of heat from burning organics can increase the flue gas temperature. Even a moderate increase in black liquor dry solids increases the lower furnace temperature and decreases the SO_2 emission, Figure 9-35 (Ryham and Nikkanen, 1992, Vakkilainen *et al.*, 1998).

It is also obvious from Figure 9-35 that increasing sulfidity increases sulfordioxide emissions. Even boilers that fire 80 % dry solids will have sulfur emissions if sulfidity is high enough (Ibach, 1995).

Sulfur dioxide and NOx have cross correlation. This cross correlation exists also with high dry solids boilers (Jones and Stewart, 1993). Increasing furnace temperatures decreases sulfur dioxide emission. Increase of NOx emissions is not because of thermal NO formation. Recovery boiler furnace temperatures hardly reach required 1400 °C (Nichols *et al.*, 1993). NOx emissions increase because H_2S is much better scavenger of oxygen.

Björkman and Warnquist (1985) claimed that non dried liquor droplets will have only a marginal influence on reaction and temperature conditions. They based this assumption on the large mass and high temperature of the char bed. The modern use of char bed imagining cameras has concluded that even small low temperature areas will significantly increase sulfur emissions. Practical experience with char bed imagining cameras indicates that creation of 'cool spots' in the bed correlates with increased SO_2 emissions. If poor mixing or low temperatures prevail in furnace also higher TRS emissions result.

Firing high dry solids black liquor has decreased recovery boiler fouling (Vakkilainen, 2000, Vakkilainen *et al.*, 1995). This effect can be attributed to decreased sulfur emissions and the diluting effect of sodium carbonate, Figure 9-36. It should be noted that there are two regimes of fouling; low solids fouling is controlled by SO_2, and high solids fouling is controlled by the ash sticky temperature.

9.7 FIRING BLACK LIQUOR – MILL EXPERIENCE

Actual black liquor firing practices differ between different boilers. This is illustrated by studying firing practices in five modern boilers (Järvinen *et al.*, 1997). These boilers are large and from both main Scandinavian vendors. The furnace dimensions and liquor gun locations for each boiler are presented in Table 9-9. Dimensionless height is the actual height divided by the square root of bottom area.

Firing parameters

To record operating practices inquiries were sent to operators and then the answers were reviewed

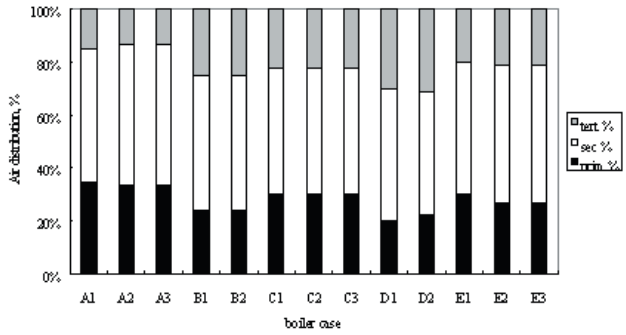

Figure 9-37, Air distribution models of the boilers (Järvinen et al., 1997).

***Table 9-9**, Boiler geometries, gun locations and loads.*

Boiler	Furnace width	Furnace depth	Furnace height	Liquor gun height	Load, tds/d
A	10.1	10.4	27.8	6.0	2550
B	12.6	11.8	34.5	9.0	3300
C	9.9	9.9	23.0	4.8	2200
D	12.6	11.8	34.5	8.6	3500
E	10.9	10.8	31.6	6.2	2750

***Table 9-10**, Liquor parameters.*

Boiler	Firing press. kPa	Firing temp. °C	Liquor -	Dry solids %	Diff. to BP °C
A_1	150	124	softw.	68.6	+10.7
A_2	150	124	hardw.	68.6	+10.7
A_3	150	124	mixed	68.6	+10.7
B_1	95	118	mixed	74.4	+2.0
B_2	125	125	mixed	74.4	+9.0
C_1	220	133	softw.	75.0	+16.7
C_2	220	133	hardw.	75.0	+16.7
C_3	202	133	mixed	75.0	+16.7
D_1	170	136	softw.	83.5	+15.2
D_2	100	134	mixed	83.5	+13.2
E_1	140	125	softw.	72.6	+9.8
E_2	120	115	hardw.	72.6	-0.2
E_3	130	120	mixed	72.6	+4.8

and discussed with copies of parameters from automation systems. Typical liquor firing parameters at full load are shown in Table 9-10. All of the mills pulp several wood species and operators use different parameters to fire black liquor from pulping of different wood species. These values reflect the actual average values in use at the mill, and are not necessarily manufacturer's recommendations.

Black liquor dry solids in use at these mills reflect the Scandinavian practice. Older mills have dry solids close to 70 %. The newest mills have dry solids in excess of 80 %. It is also typical that the target black liquor dry solids is the same for all wood species. In addition the difference of firing temperature to boiling point temperature at atmospheric pressure is shown. Boiling point rises were based on actual liquor analysis at mill and represent averages of analysis for the mill in question.

There are four different types of liquor guns in use at these five mills. It is usual that liquor guns differ from one mill to another. Liquor gun selection at a mill is typically based on long time learning curve. Mills A and E use splashplate with a narrow liquor firing angle. Mills B and D use splashplate with a large diameter and wide liquor firing angle. Mill C uses small size liquor gun

Difference between liquor firing temperature and the atmospheric boiling point temperature describes the flashing tendency. As can be seen in Figure 9-3, the black liquor partly forms steam inside the liquor gun if the operating temperature is above the atmospheric boiling point. The larger the value of temperature difference, the larger the driving force of evaporation. If firing temperature exceeds the liquor atmospheric boiling temperature, flashing occurs. Practically all boilers operate above the atmospheric boiling temperature.

In order to compare the liquor droplet combustion and flight path between different boilers, an average flue gas velocity was calculated. Flue gas density was scaled with respect to the adiabatic flame temperature. The furnace temperature when firing high solids black liquor is higher due to a smaller flue gas amount. Furnace temperature has a great effect on char bed processes and on droplet combustion. The liquor mass flow rates and flue

gas flow parameters are presented in the Table 9-11.

It can be seen that there are no significant differences between the mean flue gas velocities. The calculated adiabatic flame temperatures differ mainly because of different dry solids. This means that some furnaces will naturally operate somewhat hotter that the others.

The air distribution models differ from boiler to boiler. The model is typically changed when firing different types of liquors. The air distribution models for the boilers are presented in Figure 9-37. As can be seen there is a marked difference between the different primary air flows and tertiary air flows.

Liquor spray properties

As it was previously observed, the boilers differ from each other as far as liquor firing is concerned. Various types of nozzles are used. There are differences in the boiler geometry and the liquor dry solids content. The liquor spray properties; nozzle outlet velocity and mean droplet size were calculated with respect to the real operating parameters. The results are presented in Table 9-12.

Black liquor combustion height

Differences in black liquor firing practices can be observed if we use CFD calculations to look at where black liquor burns. For the presented five boilers this was done (Järvinen *et al.*, 1997). Black liquor combustion was calculated for one nozzle, situated at the center of the front wall, for every boiler and each wood species. Actual liquor gun operating height position and vertical spraying angle were used. The sheet velocity was assumed to be constant as a function of sheet angle. The mass flows varied as a function of sheet angle.

Carbon combustion is important for a proper furnace operation. For example, the reduction requires carbon to proceed. If carbon combustion is completed before the droplets reach the char bed, there is no reducing carbon for the reactions in the char bed.

The black liquor combustion level was calculated on the basis of the vertical carbon release distribution in the furnace. The results are presented as a function of the liquor droplet size, Figure 9-38. A clear correlation between the combustion level and the droplet size can be seen. The larger the droplet size, the lower the combustion level.

If combustion of different wood species is compared, the effect of the liquor type is obvious. Softwood liquors burn at a higher level compared to hardwood liquors. This is because of softwood liquor swells more.

The horizontal carbon release level is presented

***Table 9-11**, Black liquor and flue gas flows (Järvinen et al., 1997).*

Boiler	Gun / d_o / h_o - /mm/mm	mass flow kg/s	No of guns -	Flue gas flow m^3n/s	Flue gas velocity m/s
A_1	sA/27 /22	3.98	8	101.0	4.5
A_2	sA/27 /22	3.98	8	101.0	4.5
A_3	sA/27/22	3.98	8	101.0	4.5
B_1	sB/30/30	5.25	8	132.0	4.3
B_2	sB/30/30	5.25	8	132.0	4.3
C_1	pp/22.5/19	3.96	7	91.0	4.6
C_2	pp/22.5/19	3.96	7	91.0	4.6
C_3	pp/22.5/19	3.96	7	91.0	4.6
D_1	sB/38/38	5.72	8	139.0	4.9
D_2	sB/38/38	5.72	8	139.0	4.9
E_1	sA/27/22	4.33	8	114.0	4.7
E_2	sA/27/22	4.33	8	114.0	4.7
E_3	sA/27/22	4.33	8	114.0	4.7

sA = splashplate type A, sB = splashplate type B, pp = "willow flute" type, d_o = nozzle tube diameter, h_o = height of the nozzle opening

***Table 9-12,** Liquor spray properties (Järvinen et al., 1997).*

	Firing temp. °C	Firing press. kPa	Nozzle velocity m/s	Droplet size mm	Furnace temp. K
A_1	124	150	11	2.05	1400
A_2	124	150	11	2.09	1400
A_3	124	150	11	2.08	1400
B_1	118	95	6	3.91	1455
B_2	125	125	7	3.32	1455
C_1	133	220	17	1.39	1468
C_2	133	220	17	1.49	1468
C_3	133	220	17	1.44	1468
D_1	136	150	10	3.34	1545
D_2	134	100	8	3.96	1545
E_1	125	140	10	2.20	1441
E_2	115	120	6	3.31	1441
E_3	120	130	8	2.72	1441

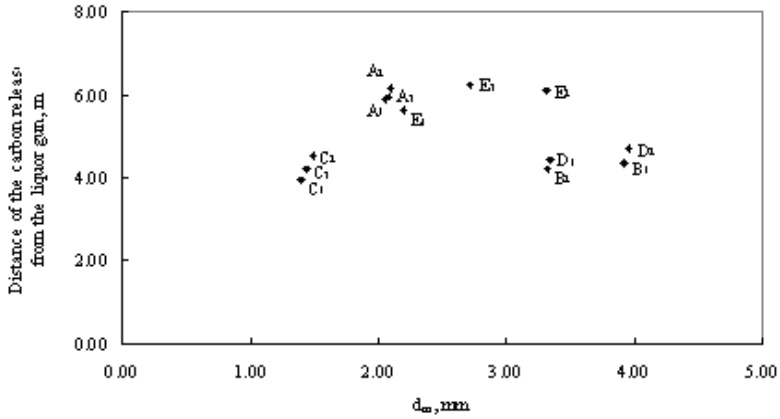

Figure 9-39, Horizontal distance of carbon release from the level of the liquor gun as a function of droplet size for the different boilers.

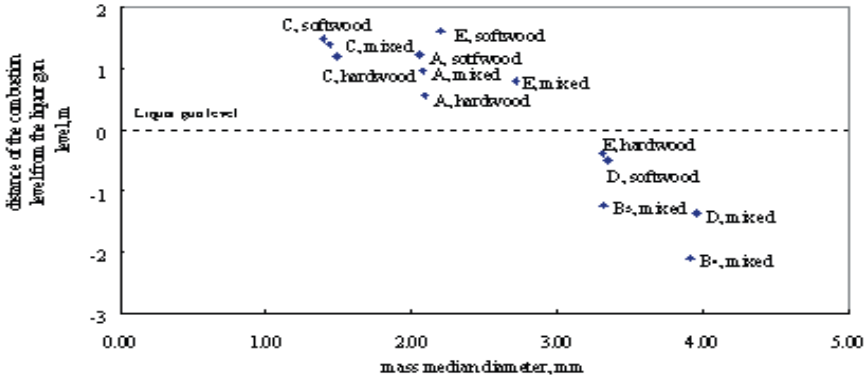

Figure 9-38, Vertical carbon release level as a function of droplet size.

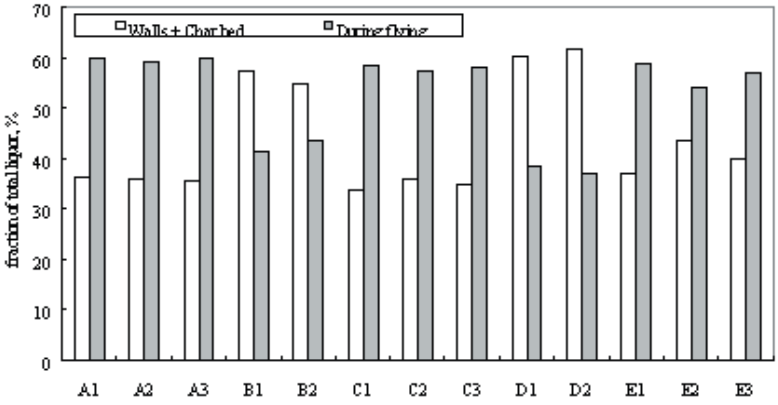

Figure 9-40, Fraction of the liquor delivered to the char bed and the fraction of the liquor burned in suspension.

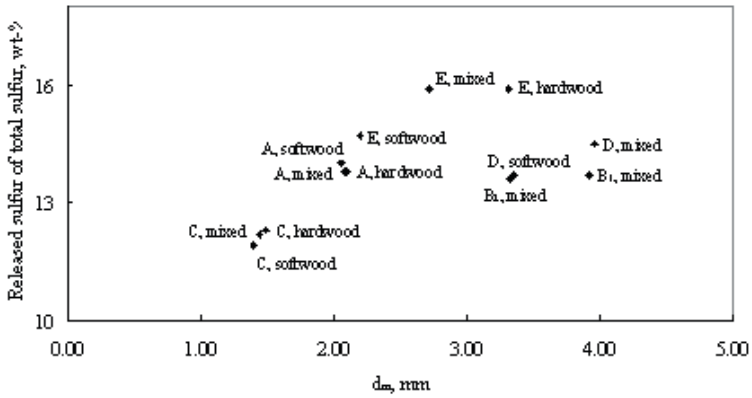

Figure 9-41, Total amount of sulfur released during devolatilization as a function of droplet size.

in Figure 9-39. The general trend in the horizontal carbon release location seems to be that the smaller the droplet size, the closer the location of the carbon release from the liquor gun. In boilers B and D, with wide angle guns and large droplet size, the liquor is burned closer to the nozzles. This is due to the larger opening angle of the nozzles used in these boilers. In them a greater liquor amount is sprayed near the adjacent furnace walls of the liquor gun, which reduces the penetration of the spray into the furnace. When liquor types are compared, the softwood liquor, that swells more, seems to burn closer the liquor gun wall due to larger drag forces and the smaller droplet size.

Combustion in suspension, in char bed and on furnace walls

The amount of liquor reaching the char bed, the furnace walls and the fraction of liquor forming carryover were calculated on the basis of the droplet flight path data. The results are presented in Figure 9-40.

There are major differences between the boilers. The boilers B and D seem to spray liquor to the furnace walls to a great extent. The boilers A and E show the opposite trend.

There is a variation between suspension burning and bed burning. In the boilers A, C and E approximately 60 % of the liquor combustion takes place during flying and the rest of the combustion occurs in the char bed. With the boilers B and D the fraction of the inflight combustion is approximately 40 % of the total liquor and the bed and wall burning consumes nearly 60 % of the liquor sprayed.

Sulfur release

The release of sulfur in different boilers was studied. The total amount the sulfur released was calculated. The result is presented in Figure 9-41. Generally, the amount of sulfur released seems to increase with increasing droplet size. Boilers B and D show an opposite trend, as before, during char combustion. The reason for a smaller amount of sulfur released is wall spraying.

In these calculations sulfur release is cut off when the liquor hits the wall. In reality, the release continues on the furnace wall and as the liquor droplet falls from the furnace wall to the char bed. This means a large part of the sulfur release is probably unaccounted for.

Firing 90 % liquor in a recovery boiler

Tests at the mill level to spray very high dry solids black liquor were performed in the Stora-Enso mill at Varkaus (Vakkilainen and Holm, 2000). In these tests different dry solids black liquors were sprayed in to the furnace. Mass flow and liquor gun types were varied. Typical commercial nozzles were used. The evaporative potential of the black liquor at the very high dry solids is small. Therefore it was noticed, perhaps unexpectedly, that the liquor sheet formed from firing 90% black liquor looked quite similar to the corresponding sheet at firing 75% black liquor.

Burning of 80 to 85% dry solids black liquor is in commercial operation in several kraft recovery boilers. Spraying of the very high dry solids black liquor has not led to any unsolvable problems.

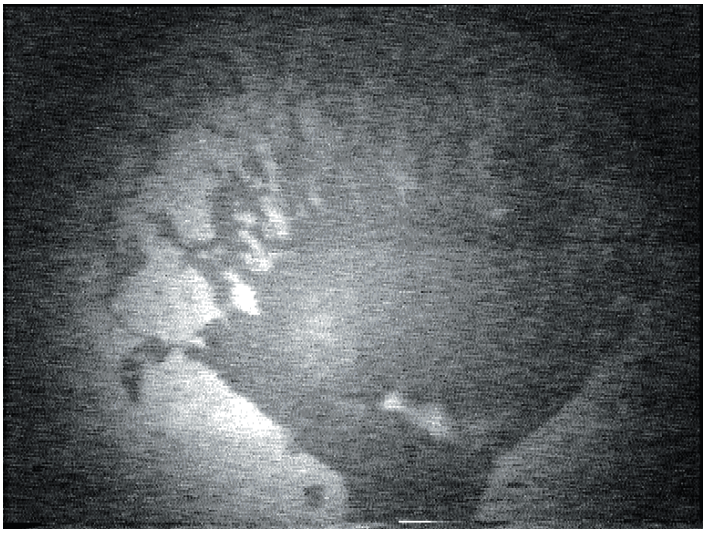

Figure 9-42, Picture of 90 % liquor sprayed at recovery boiler furnace with liquor gun type B22 (Vakkilainen and Holm, 2000).

The main advantage of the very high dry solids is that black liquor can be fired at substantially lower partial loads (Mäntyniemi and Hartley, 1999). The char bed is more stable and easily controlled and the boiler is able to handle process disturbances more smoothly (Vakkilainen and Holm, 2001). In addition emissions can be controlled also when burning odorous gases (Mäntyniemi and Haaga, 2001).

Some problems in burning of very high dry solids black liquor have been that the membrane material of manometers does not last long, valves tend to stick and they have other mechanical problems and there are difficulties to get big enough droplet sizes.

9.8 BURNING WASTE STREAMS IN A RECOVERY BOILER

Modern boilers that burn waste streams have typically liquor dry solids at least in the 70's and a modern or modernized air system that comprises of primary, secondary and often two-level tertiary air. One noticeable feature in these air systems is that they have been improved by using larger and wider spaced airports. Modern air system is a necessity. Excess streams require high furnace temperature and rather stable combustion.

Firing methanol and turpentine

Turpentine and methanol can be fired in recovery boiler furnace. Most often turpentine and methanol are fired at liquid form using separate lances using the CNCG burner opening. Turpentine is more typically fired in the lime kiln. Main use of methanol has lately been as a support fuel for CNCG burner. There are mainly positive experiences from this type of operation. However from the mill energy balance point of view also methanol could be better used at the lime kiln to reduce fossil fuel consumption.

Removal of turpentine from NCG is important because turpentine is very explosive. Collection lines that contain turpentine are prone to explosion hazard. Several incidents with NCG in Finland have probably been caused by high turpentine concentrations. If NCG contains gaseous turpentine, the line should have droplet separation and flame arrester for safety reasons.

Firing soap

Soap has been separated from black liquor as it naturally ascends to the surface of a black liquor tank since 1910's (Niemelä, 2004). Modern mills have often so low sulfur loss that it is uneconomical to manufacture tall oil from soap by acidification with sulfuric acid. In several mills firing soap mixed with black liquor has been practiced with good success.

Black liquor that contains soap burns slower. Soapy liquor also swells less. Soapy liquor needs to be fired with smaller droplet. It is harder to achieve zero SO_2.

It is important to note that soap affects the refractometer reading, Figure 9-43.

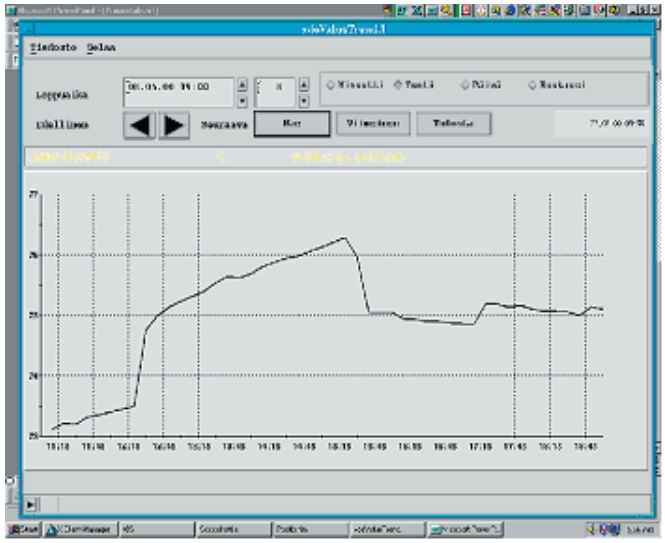

Figure 9-43, Effect of addition of soap to black liquor dry solids reading by refractometers.

Burning biosludge

Biosludge has been burned successfully in several recovery boilers by mixing it with black liquor (Dahlbom, 2003). Biosludge contains organic dead bacteria. This makes water removal very difficult. Biosludge dry solids is typically only 5-15 g/l from waste water plant. It needs to be concentrated with e.g. centrifuges to > 10 % dry solids.

Biosludge contains inorganic residue from waste water and chloride from bleaching. It has a negative effect to fouling, plugging and corrosion.

Combustion of bleach plant effluent

There have been mill trials of combustion of bleach plant effluents in US and Sweden. The aim is to decrease bleach plant effluent loading by recycling part of black plant effluent to recovery. Mill water usage can decrease significantly.

The main concern has been the increased NPE load to recovery cycle. Especially the high chloride content of bleach plant effluents has been mentioned.

Adding bleach plant effluents to black liquor seems to affect the liquor viscosity and combustion properties only slightly (Ledung and Ulmgren, 1998, Ledung and Ulmgren, 1997, Nichols, 1992,). The results were similar to both acidic and alkali stage additions. This is because the composition of bleach plant filtrate is fundamentally similar to black liquor.

Effect of waste stream burning to sulfur emissions

Whether dry solids is enough is easily checked. Assume that sulfur input with NCG forms SO_2. Further assume that SO_2 is reacted to sulfate replacing carbonate in ESP ash. Check that there is enough carbonate remaining in the ash to keep pH high, Figure 9-44, even after high concentration odorous gases are being fired.

Boiler SO_2-emission and so carbonate in ESP ash can be additionally controlled by air model, liquor gun type and air ratios. Mill sulfur balance will affect the sulfur release and the recovery boiler operation. High sulfidity means LVHC NCG can not be fired. It has been found that even with +80 % dry solids in as fired black liquor, LVHC NCG burning was impossible when sulfidity was over 45 %.

Burning HVLC NCG or DNCG in a recovery boiler has only a minor but negative effect on recovery boiler sulfurous gases emissions, if black liquor dry solids is over 68 %. It has been found that in most cases when sulfidity is below 40 % and the black liquor dry solids is over 72 %, DNCG can be burned with minimum sulfur emissions. Finnish recovery boiler committee does not recommend burning NCG in a recovery boiler if sulfur emissions increase significantly.

Effect of waste stream burning to NOx

CNCG, biosludge and methanol can contain sig-

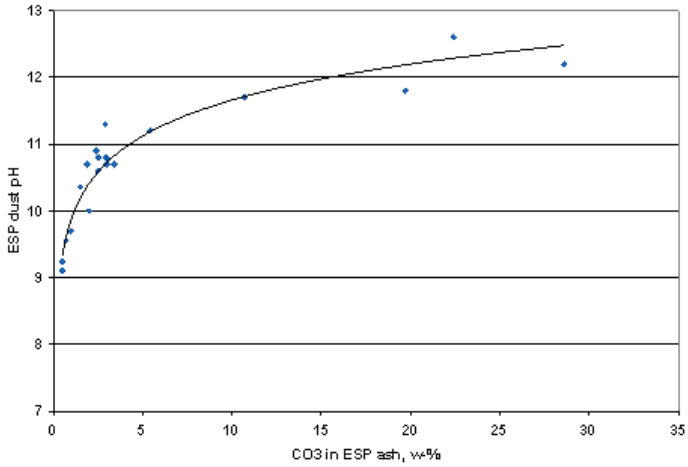

Figure 9-44, Effect of carbonate on ESP ash pH.

nificant amounts of nitrogen compounds.

LCHV NCG has not been reported to affect the NOx levels in recovery boilers. HCLV NCG contains sometimes up to 2000 ppm of nitrogen compounds, mostly ammonia. The flow if high concentration odorous gases is between 0,2 and 3 % of total flue gas flow. If one assumes all nitrogen compounds to react to NOx then the NOx level would increase less than 5 ppm.In practice the measured increase has been 2 ppm or less.

Crawford and Jain (2002) found that in thermal oxidizers at temperatures above 850 °C about 25 to 30 % of ammonia in CNCG and stripper off gas was converted to NOx.

Recommendations for combustion of waste streams

Burning waste streams in a recovery boiler causes risks. Analysis of accidents with NCG burning helped to quantify these risks. The following risks were identified; leaking of toxic streams to working environment, disruptions in condensate removal, explosion in line or duct containing gases, gaseous explosion in recovery boiler furnace, smelt-water explosion in recovery boiler furnace and corrosion in ducts, lines or pressure parts.

Several recovery boiler users associations including BLRBAC, Swedish and Finnish associations have approved recommendations concerning combustion of waste streams in recovery boilers. The target has been to avoid accidents that can happen when NCG are

Figure 9-45, Example of how recovery boiler looks after NCG handling accident.

burned in a recovery boiler, Figure 9-45.

The recommendations deal exclusively with waste stream combustion in a recovery boiler. Collection of waste streams and handling them in other systems (e.g. lime kiln) are not covered by the recommendations.

9.9 AUXILIARY FUEL FIRING

Auxiliary fuel can be fired in a recovery boiler from startup burners and load burners. Typical auxiliary fuels are natural gas, light and heavy fuel oil.

Startup burners are located near furnace floor. They help to heat recovery boiler char bed during startup. Autonomous black liquor firing needs lower furnace temperatures in excess of 800 °C.

Startup burners need to be used when char bed is out of control or blackout is eminent. Char bed can if the black liquor droplet size landing on the bed is too large to grow uncontrollably. The remedy is to decrease black liquor firing rate and start using startup burners until the situation is under control again. If the bed growth proceeds too long, a blackout result. This means liquor firing must be stopped and bed burned away.

10 Material selection and corrosion

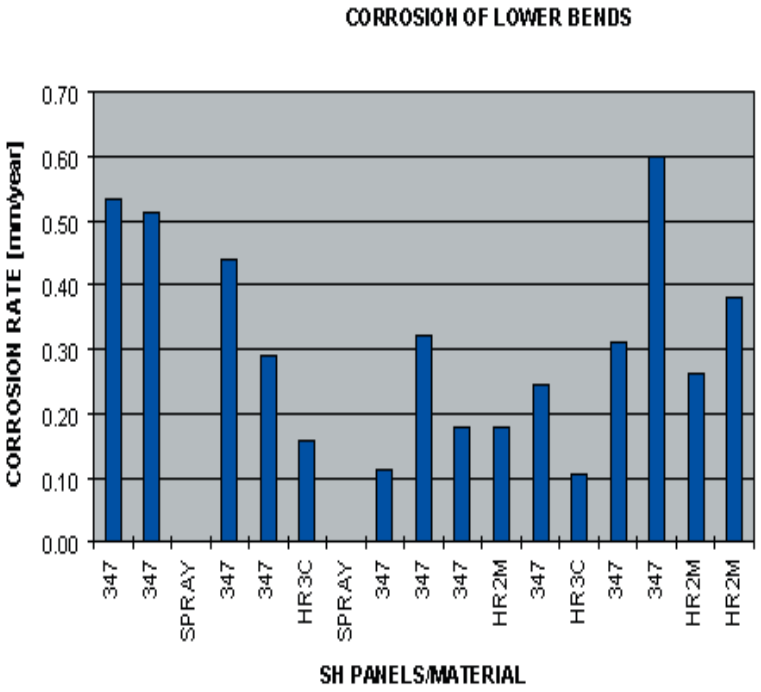

Figure 10-1, Corrosion rate of a row of superheater lower bend tubes.

When recovery boilers are designed one of the most difficult questions that arise is; what kind of materials should one use for different parts of the boiler. Corrosion is typically divided into areas based on location of corrosion; water side corrosion, high temperature corrosion and low temperature corrosion

Water side corrosion occurs in the steam/water side of the boiler tubes. Most often the cause is impurities in the feedwater. High temperature corrosion occurs typically in the superheaters. Low temperature corrosion occurs in the economizers and air heaters. Low temperature corrosion is often associated with formation of acidic deposits.

10.1 GAS SIDE CORROSION OF HEAT TRANSFER SURFACES

Gas side corrosion in recovery boilers is caused by formation of deposits, which have corrosive properties. A typical cause is formation of molten alkali phase. Gas side corrosion can also be caused by gaseous components and is then usually associated with reducing atmosphere.

If corrosive environment is known proper material can be selected. Often only experience can give the answer to this. The recovery boiler is physically large. Corrosion rate in one side of the boiler can significantly differ from corrosion on another side, Figure 10-1.

Normal tube environment

Before we start the discussion about corrosion, we should look at how a normal tube surfaces in a

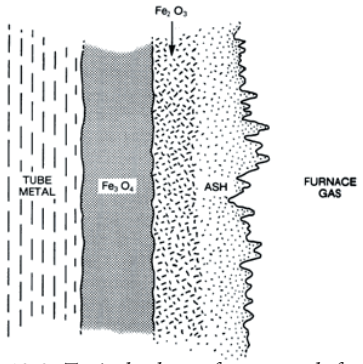

Figure 10-2, Typical tube surface towards furnace (MPSP, 1991).

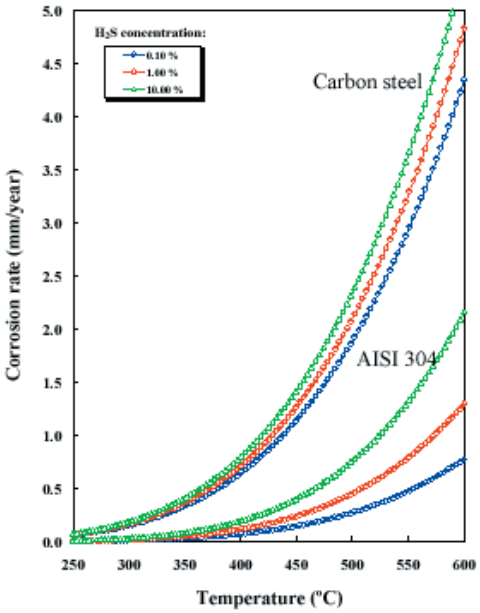

Figure 10-3, Effect of temperature and H_2S concentration on corrosion rate of carbon steel and alloy AISI 304 (Salmenoja and Tuiremo, 2001).

typical boiler look like.

In Figure 10-2, we see that the boiler tube oxidizes fast and forms protective iron oxide (Fe_3O_4) layer. Protection is typically higher if tube Cr, Ni and Mn content is increased. Increase in corrosion prevention is often associated with tighter deposits, which prevent passage of corrosive agents. Specifying a proper alloy and thus a proper protective layer composition helps to protect against known corrosive environment.

Often the outermost tube is corroded iron oxide (Fe_2O_3). This is porous and flaky, so gases can easily pass through. Corroded iron oxide has very low strength. It then flakes and breaks away at fast rate. Often there forms an ash layer on the tubes, especially superheater tubes. Ash is formed through direct deposition of ash particles, condensation of vapours and reaction of gaseous species with deposited material. Depending on conditions this layer is thin and reactive or thick and rather static. For corrosion the layer closest to the tube is the most important.

Sulfidation

Sulfidation is the most common form of corrosion in the lower furnace, in openings and in superheater tubes. In particular hydrogen sulfide (H_2S) contents close to the wall in the lower furnace can be around twenty mole percent (Singh *et al.*, 1999). In modern, high solids boiler the concentration close to the wall above the tertiary air is only some tens of ppm (Vakkilainen and Holm, 2001). In sulfidation the iron reacts with sulfur in the gas phase forming iron sulfide FeS. This means that the protective oxidized surface of metal tube reduces in presence of sulfur containing species.

Corrosion due to gaseous H_2S is low up to 250 °C, but at carbon steel it increases rapidly above 310 °C, Figure 10-3. Metal temperatures of the furnace tubes are typically 15-30 °C hotter than the saturation temperature of the boiler water. Sulfidation

Figure 10-4, Corroded superheater tube (Suik, 2001).

corrosion decreases when chrome containing metals are used. Sulfidation corrosion does not occur at significant rates with stainless steel until ~480 °C is reached. Stainless steel 304L is the most typical metal used to control sulfidation corrosion.

Sulfidation attack can be seen in a tube as rough uneven wear on tube surface, Figure 10-4. Corrosion pattern is often uneven, Tube surface is rough and larger, deeper pockets can be found (Eilersson *et al.*, 1995). Without adequate protection sulfidation corrosion occurs fast under partially dried black liquor at furnace walls (Bruno, 2003).

High temperature corrosion

Figure 10-5 shows thinning of superheater tube side surfaces. Ash is sticking to the windward side of the tube. Molten layer exists at tube sides.

Fuels contain minor amounts of impurities. These impurities can cause high temperature corrosion in the superheaters. Especially vanadium, sulfur and alkali metals cause high temperature corrosion. Figure 10-6 shows actual deposits on a superheater. As can be seen many different types of particles exist.

One of the most typical means of fighting high temperature corrosion is to use alloyed materials. Figures 10-7 and 10-8 show the effect of chromium to a corrosion rate. Other popular metals to add are nickel and molybdenum. Choice of proper material is in practice often a matter of trial and error.

Alkali corrosion

Recovery boiler ash in contact with the tubes is normally solid. Sodium and potassium may form ash with low melting points 500 … 600 °C. Contact of tube surface with molten alkali salts causes fast corrosion. This is because chemical reactions

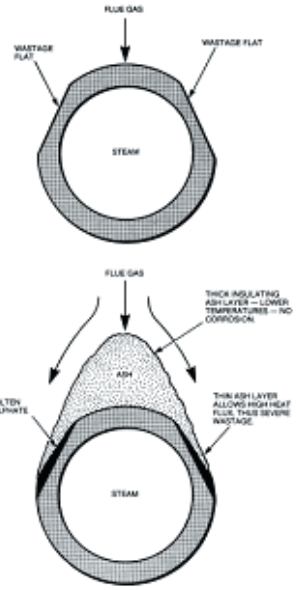

Figure 10-5, Superheater corrosion (MPSP, 1991).

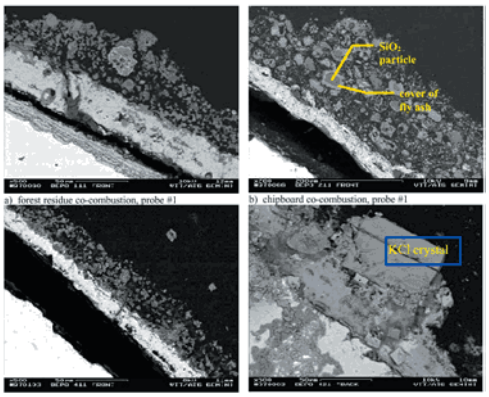

Figure 10-6, Forest residue superheater ash FB (Kurkela et al., 1998).

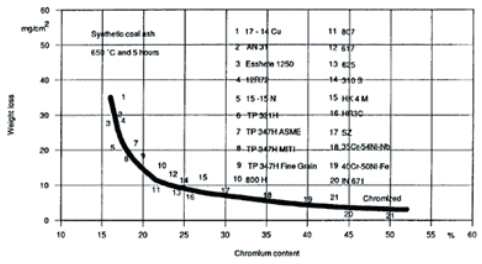

Figure 10-7, Effect of chromium on corrosion.

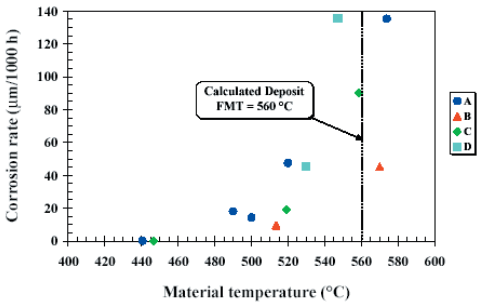

Figure 10-8, Effect of material temperature on corrosion rate, A – D different materials (Salmenoja and Tuiremo, 2001).

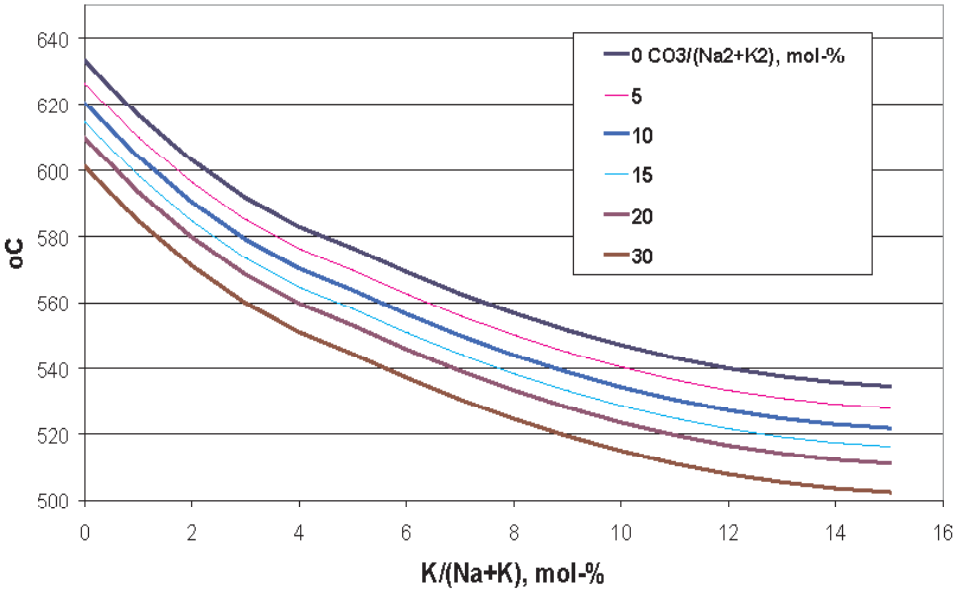

Figure 10-9, First melting temperature of recovery boiler superheater deposit containing some chloride.

occur faster with molten than solid phase, a liquid phase provides an electrolyte for electrochemical reactions, a liquid phase can readily dissolve the corrosion products and liquid phase can fluidize the ash. Carbon steel corrodes very fast in molten smelt, 1 … 3 mm/h. So maintaining protective, frozen layer is essential for safe operation.

Typical first melting temperatures of recovery boiler deposits are shown in Figure 10-9. With high enough liquid content ash flows down the superheater surface. First melting point is a function of boiler operation. Increasing lower furnace temperature increases fuming and carbonate in deposit (Stead *et al.*, 1995). Alkali corrosion usually leaves a smooth, even surface. Uniform thinning can be seen in e.g. superheater tube bends. A special case for alkali corrosion prevention is the smelt spouts. By keeping tube temperature close to 100 °C carbon steel can survive the molten, free flowing smelt.

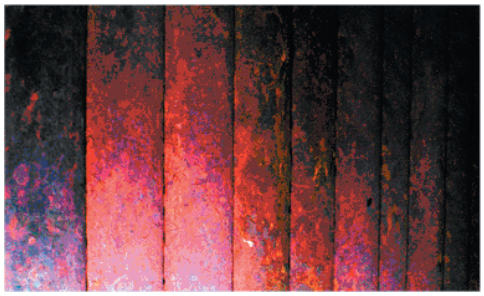

Figure 10-10, Chloride corrosion in superheater bank (Koivisto, 2000).

Chloride corrosion

Chloride in fuel forms NaCl, Cl_2 and HCl in gaseous from. In active oxidation these gases react with iron to $FeCl_2$ (Grabke *et al.*, 1995). This when in contact with oxygen, reacts back to Fe_2O_3 releasing chloride in gas form. Reformed iron oxide layer is porous and does not offer protection from corrosion. Released chloride can react with fresh iron oxide and the cycle repeats. Active oxidation leads to rapid waste of superheater tubes, Figure 10-10.

Chloride corrosion needs continuous gaseous chloride species present to proceed. Salmenoja *et al.* (1999) found in laboratory tests that it took some 20 min to start the corrosion and some 15 min to stop when HCl in oxidizing conditions was used.

Chloride corrosion has been studied a lot in connection with waste burning and recovery boilers. It can be identified from sharp chloride layer between deposit and the uncorroded tube (Nishio *et al.*, 2001), Figure 10–11.

Chloride corrosion is affected by gaseous chloride content near superheaters, Figure 10-12. Even with higher chloride content at deposits the high carbonate (i.e. high dry solids) boiler shows lower chloride corrosion rate (Koivisto, 2000). Laboratory studies show that chloride corrosion rate below

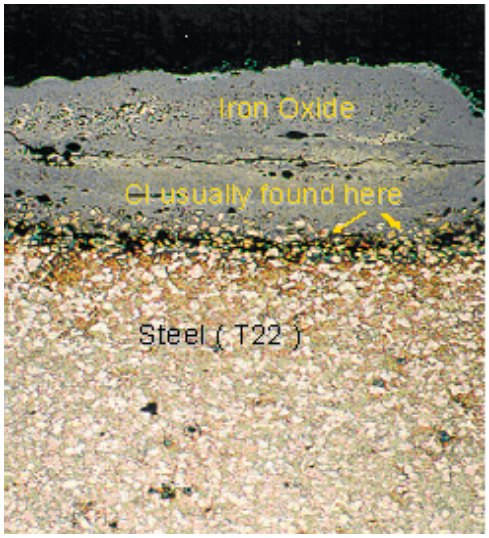

Figure 10-11, Chloride corrosion in superheater bank (Koivisto, 2000).

450 °C is very low (Salmenoja, 2000). Salmenoja *et al.* (1999) report that chloride corrosion rate is low if metal chrome content is above 12 w-%.

Laboratory studies done by Japanese boiler maker Mitsubishi show that deposit properties affect the chloride corrosion rate. Decreasing deposit melting temperature from 580 to 520 °C by adding potassium to carbonate containing deposit, with SO_2 present in flowing gases doubled corrosion rate. Increasing chloride content in the deposit from 1 to 5 w-%, which decreases FMT by 4 … 6 °C increased corrosion rate only marginally (Nishio *et al.*, 2001).

Molten hydroxide corrosion

Typically in the furnace conditions sodium hydroxide vapor reacts with available sulfur and chloride species. It can also react with carbon dioxide

$$2NaOH(l) + CO_2(g) \rightarrow Na_2CO_3(s) + H_2O(g) \quad 10\text{-}1$$

Close to air and liquor ports the carbon dioxide partial pressure can be low. There it is possible that sodium hydroxide condenses to the tube surface. Lately it has been suggested that hot fluxing of metal into the salt (Holcomb, 2001) can cause this attack.

$$Fe_2O_3 + Na_2O \rightarrow 2NaFeO_2 \quad 10\text{-}2$$

This kind of corrosion has been found especially behind the furnace tubes close to air ports where gases can leak. In addition it has been found at liquor gun openings. Stainless steel 304L has about 10 times the corrosion rate in molten hydroxide than normal carbon steel. In high pressure boilers the wastage of composite layer can occur in less than two years (McGurn, 1993). Alloys with high nickel to chrome ratio seem to be able to resist this corrosion (Paul *et al.*, 1993).

Acidic sulfate corrosion

Boilers running at high sulfur dioxide emission can experience acidic sulfate corrosion. Formation of acidic sulfates, sodium bisulfate or pyrosulfates occurs at flue gas temperatures below 400 … 450 °C and causes problems especially in boiler banks (Backman *et al.*, 1984). Formation of acidic sulfates is reduced by running boiler with low level of

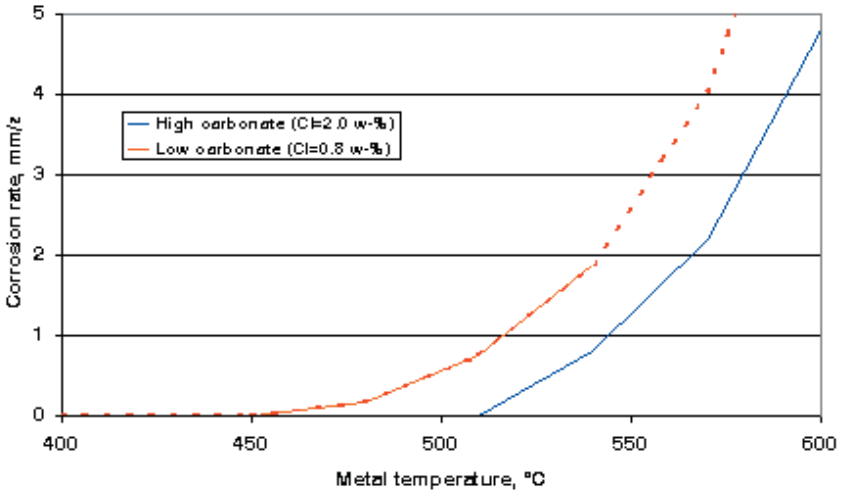

Figure 10-12, Effect of operating conditions on corrosion rates of superheater tubes from two boilers.

Figure 10-13, Cracked 304L floor.

excess air and low sulfur dioxide emissions.

Sulfur dew point

When flue gases cool their capability of holding species in gaseous form weakens and such species start condensing. The temperature where condensed species appear is called dew point temperature. Acid dew point means conditions where this condensate is acidic. Typically sulfur dew point refers to conditions where sulfur trioxide starts condensing. Also HCl condensation is possible.

10.2 FURNACE CORROSION

Recovery boiler furnace walls needs to be water-cooled, gas tight, easy to maintain, very safe, low cost and easy to manufacture (Björklund 1963). Even today the furnace walls lack in safety, cost and ease of manufacture. Main reason for this is the difficult process conditions.

One of the most researched corrosion phenomena in recovery boilers has been furnace wall and floor tube corrosion. The first major corrosion problems emerged in early 1960s. Heavy wall corrosion in two recovery boilers at Kaukopää mill was discovered in 1961 and later in others (Soodakattiloiden, 1968). Recovery boiler furnace walls were corroding rapidly and corrosion rates of up to 1 mm/year were recorded. At that time there were number of accidents and wall tubes of new higher pressure boilers were experiencing short lifetime. Sulfidation of iron oxide layer was found to be the main cause. Several means of control were attempted to reduce corrosion in carbon steel walls. Studding the wall or using refractory helped, but required extensive maintenance. It wasn't until the composite tubing appeared after 1972 that this problem decreased. In late 1980's it was thought that corrosion with composite tubing was non existent (Sandquist, 1987).

The second wave of large problems hit when composite floor tubes started cracking, Figure 10-13, in the late 80's. In the beginning it was thought to be only a specific problem occurring in some individual boilers, but around 1990 it was recognized that it was a wide spread industry problem. Much progress has been made. Several possible reasons for cracking of stainless steel 304 have been discovered. Alloy 825 and modified alloy 835 (Sanicro 38) tubes seem much less prone to cracking in floor conditions than 304L.

The third wave of furnace problems hit in the 1990's, when primary airport cracking started causing large problems (Falat, 1996). Currently this is still a question awaiting answer. Use of highly alloyed steels (e.g. alloy 825 or alloy 625) has not solved this problem.

Cracking of floors

After 70s almost all recovery boiler floors were made of 304L. Cracking of 304L was first identified in Scandinavia and then in early 90s in North America (Keiser *et al.*, 2004). Klarin (1993) attributed the cause of these attacks to higher black liquor dry solids and mill closure. These changes

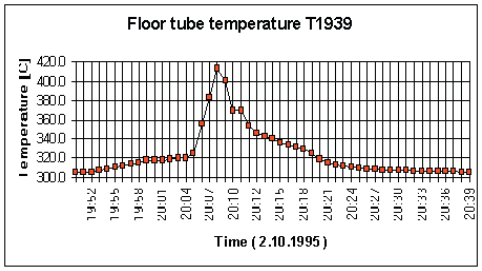

Figure 10-14, Floor tube temperature excursion.

work to create hotter shallower char bed which is richer in potassium and chloride. All this will increase the probability of smelt tube contact.

304L and carbon steel have different thermal expansion behavior. Therefore stresses occur when composite tubes made of 304 are subjected to thermal cycles, Figure 10-14. Thermal spikes during operation were found (Abdullah *et al.*, 1999). This caused early suspicion that thermal stresses were the main cause for floor tube cracking. Thermal stress may assist, but is no longer considered the main culprit (Keiser *et al.*, 2001).

The cause of thermal spikes in the recovery boiler floor remain unknown. At first it was assumed that problems in water circulation were causing thermal spikes. Extensive bottom monitoring has found no correlation between abnormal flow and thermal spikes (Hogan, 1999). Current theory assumes that cracks in the frozen layer cause vertical smelt flow in the bed, which is seen as thermal spikes in bed.

Most of the analyzed cracks seem to exhibit stress corrosion cracking (SCC). In SCC strain in the tubes aids progression of chemical corrosion. For the time being nobody has proved which chemical is causing it and how this corrosion can proceed under the frozen smelt layer.

Some researchers attribute floor tube cracking to phenomena during water wash. During a water wash there is a liquid electrolyte (water + bed material especially sulfide). This solution has been show to cause SCC in laboratory conditions (Tran *et al.*, 1999).

There is evidence that sulfur, chlorides and potassium enrich to recovery boiler tube surface (Backman *et al.*, 2002). All these can lower the melting temperature of the smelt. They can make the frozen layer thinner and easier for the smelt to penetrate. They also decrease the viscosity of the molten smelt, which then is able to flow more easily towards the floor tubes. Especially polysulfides that form can form a molten phase in floor tube operating temperature.

Poor flow at some floor tubes has been suspected to cause high temperatures and floor cracking. Simultaneous measurements of tube temperature excursions and flow at the same tubes have confirmed that in measured boilers there is flow at all times in the tubes exhibiting temperature peaks (Koivisto and Holm, 1998).

General corrosion

Kraft recovery boiler furnace has very reducing environment. Water shift reaction causes high levels of carbon dioxide and hydrogen. In addition the burning black liquor droplets can cause very high levels of reductive gases. But general corrosion seems not to be the limiting factor of current recovery boiler furnace life.

Smelt corrosion in floors

In kraft recovery boiler floors there appear large patches of metal loss. These spots are so big that it cannot be called pitting. One probable cause is molten smelt corrosion. If steel tubes are subjected to molten sodium compounds, very rapid corrosion occurs. Normally contact is prevented by a frozen layer of smelt on the tubes.

Layer on the tubes can melt if subjected to high heat flux e.g. from startup burners. There is smelt flowing along the tubes and out from smelt spouts. Large flow could eat away protective smelt layer.

The layer close to the tubes can contain low melting compounds and so corrodes the tubes. There is evidence that high sulfidities are found at the surface of floor tubes. This indicates in turn that polysulfides exist. Smelts with polysulfide in them have very low melting temperature (Backman *et al.*, 2002).

Galvanic effects

It's well known that carbon steel floor tubes corrode fastest close to the weld to composite tubing, Figure 10-15. This is one disadvantage of carbon steel floors. Koivisto and Holm (2000) made studies with different material combinations trying to find out how strong this so called galvanic effect is in each case. Results show that compared to 304L, Sanicro 38 is slightly better but Sanicro 65 increases the corrosion of carbon steel significantly. One coating (45CT) was also tested and its' effect on corrosion was similar to that of Sanicro 65 (i.e.

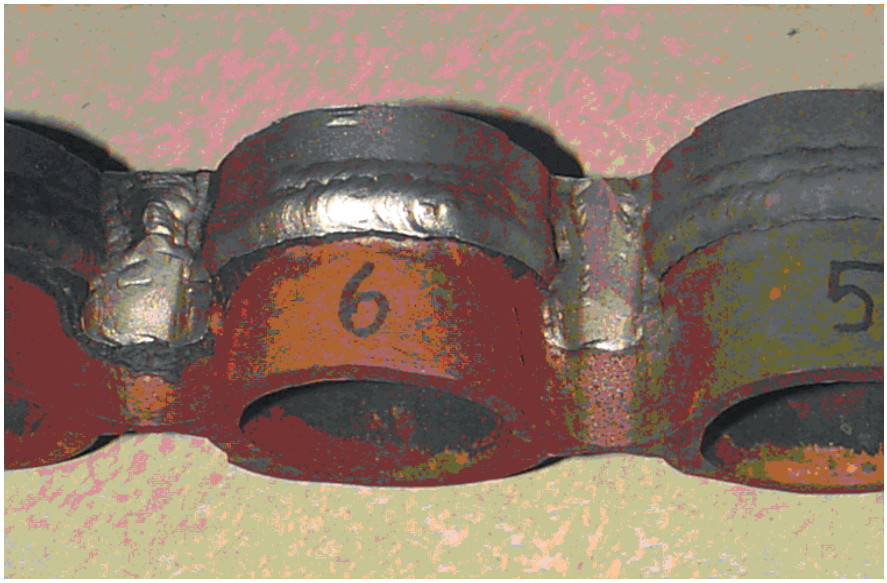

Figure 10-15, Galvanic corrosion of carbon steel.

strong galvanic effect).
The experience is that with an adequately protected and properly cooled floor the corrosion rate of the carbon steel floor is low. Highest rates that have been measured are of the order of 0.3 mm/a near the weld to the composite (304L). Thinning can be monitored with regular thickness measurements and necessary precautions can be taken when they are needed.

When the lower walls are of Sanicro 38 type composite then the corrosion of carbon steel due to galvanic effect will be even smaller according to laboratory tests.

Thermal fatigue

Thermal cycles take place in recovery boiler floors. A cycle is initiated each time boiler is shut down and started up. Such spikes have also been observed during normal operation. Cracks can be created when a certain amount of cycles has occurred. The higher the stresses or strains associated with a thermal cycle the fewer cycles are needed for a crack to initiate.

Typical thermal fatigue cracks, Figure 10-16, are found in recovery boiler walls. Normally these failures can be traced to occurrence of very large temperature peaks. The main risk with thermal fatigue is the fracture doesn't stop at the interface between carbon steel and cladding but continues to grow into the carbon steel.

Test results show that Sanicro 38 type composite material can withstand three times the number of thermal cycles as compared to 304L type composite before cracks are initiated (Karhula, 1992). This is in accordance with the thermal expansion properties of the cladding materials i.e. the bigger the difference in the thermal expansion between the substrate and the cladding, the lower the fatigue limit is. If carbon steel is used, then thermal stresses are of much less concern.

Furnace environment

Floor tube cracking is in most cases found to be environmentally assisted. This means that there

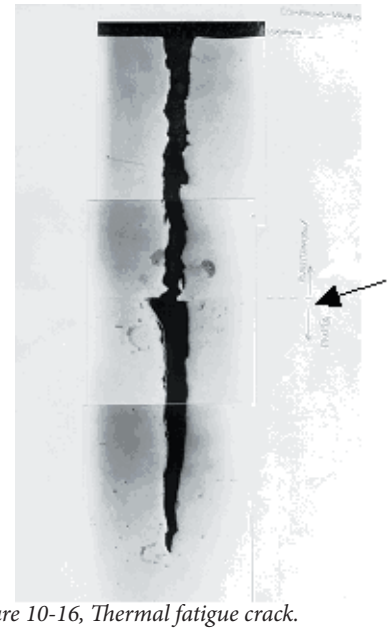
Figure 10-16, Thermal fatigue crack.

must be some chemicals, which at certain temperature assists crack initiation and propagation. In addition to this chemical and temperature an electrically conductive electrolyte is needed.

The Savcor company in Finland has measured the bed electrical resistance with a probe they have developed and they have seen that bed resistance varies a lot from "normal" between 2 and 5 k cm to as low as 0.1 k cm and sometimes even lower (Laitinen *et al.*, 1998). This indicates the existence of molten phases in the bed material during normal steady state operation.

Doug Singbeil and his group in Paprican have made SCC tests in simulated water wash conditions both with artificial salt mixtures and with real smelt taken from a boiler. Tests show that these environments (salt + water) can cause cracking at temperatures ~170 °C. They have found a threshold stress about 170 MPa and a threshold temperature about 160 °C for 304L (Keiser *et al.*, 2001). It seems that the presence of sodium sulfide will prevent complete dryout until about 180 °C (Tran *et al.*, 1999).

Preet Singh from IPST has made numerous tests in different artificial water wash solutions using the slow strain rate test method. These experiments show that 304L steel may suffer from SCC already at very low temperatures like 50 °C. These tests, however, show only if the alloy is prone to SCC in test environment but don't tell if SCC really takes place in real recovery boiler water wash environment.

Airport corrosion

Recovery boiler airports suffer corrosion. Some of the recorded corrosion phenomena include cold side corrosion, membrane cracking and recently tube cracking (Keiser *et al.*, 2004).

Cold side corrosion is caused by molten hydroxide corrosion. There vaporized sodium hydroxide deposits on cold back side of air port tubes. Especially boilers with cast air tubes have suffered from this corrosion mechanism. As rate with compound is much higher than with carbon steel, this doesn't normally present great concern.

At upper and lower end of air ports there is larger width of membrane, because of tube bends. This membrane is then at higher temperature and exhibits higher corrosion rates. Corrosion can be augmented by periodic temperature excursions (Tay *et al.*, 2004).

There are differences with external conditions between air ports even close to each other. The following affect the corrosive environment: presence of molten smelt on the char bed surface, flow of molten smelt towards the air port tubes and presence of large pieces of char near primary air ports. It has been suggested that a combination of several events may lead to tube temperature excursions at primary air ports (Vafa, 2003).

10.3 EROSION

Gas side heat transfer surfaces in boilers are subjected to passage of ash particles. Erosion is caused as these particles hit the heat transfer surface. Erosion rate increases with kinetic energy of the particles. Erosion depends strongly on ash

Figure 10-17, Corroded load burner sleeve.

***Table 10-1**, Requirements for boiler feed water according to DENÅ requirements.*

Drum maximum pressure	MPa(a)	2.5	3.6	6.8	9.1	12.6	16.1
Superheated steam pressure	MPa(a)	2.3	3.3	6.3	8.5	11.1	14.1
pH25 upper limit		15.1	15.0	13.5	12.8	11.8	10.5
pH25 lower limit		9.5	9.5	9.0	9.0	8.5	8.5
p-value	mval/kg	8.0	6.0	2.0	0.75	0.20	0.05
p-value if phosphates	mval/kg	1…8	1…6	1…2			
Conductivity25	mS/m	400	350	80	40	15	4
Na+K	mg/kg	800	650	150	80	30	8
PO_4	mg/kg	10…20	<15	<15	2…6	2…6	2…6
Silicates	mg/kg	108	56	7.0	3.0	1.0	0.35

characteristics and local velocity field.

The erosion problems caused by ash in recovery boilers are small. Firstly the flue gas velocities are moderate (4 … 12 m/s). Secondly the ash in kraft recovery boilers is typically rather soft.

A significant source of erosion in recovery boilers is erosion caused by sootblowers. Sootblowing steam contains condensate droplets. When blown these droplets hit the tubes. If the distance to the tube is short (velocity is high) tube erosion will occur. Erosion can be partly controlled by adding high resistance erosion control plate on top of the tubes.

In addition to heat transfer surface erosion the fuel transport and handling equipment suffer from erosion. There are number of cases related to erosion corrosion in black liquor pipes especially in elbows and contractions.

10.4 WATER SIDE CORROSION

The water side of boiler system is subject to several types of corrosion. These types of corrosion can result in severe damage that will affect the safety and operational reliability of the boiler. To prevent corrosion feedwater purity has strict limits, Table 10-1.

Oxygen corrosion causes pitting of tube inside surface. Rapid failure of a tube can occur with relatively small overall metal loss. Even small amounts of dissolved oxygen can cause severe damage.

Acid corrosion occurs when feedwater has too low pH. This corrosion is characterized by a general wastage of the metal.

Caustic corrosion occurs when feedwater has too high pH. This corrosion is characterized by loss of magnetite film, irregular patterns and is often referred to as “caustic gouging”.

Hydrogen attack results in loss of metal strength. There are no visible signs to indicate wether this is happening.

Main means of steam/water side corrosion protection is creation of a protective oxide film on the metal surface. Steam/water circuits in power plant depend on such films for their integrity. The prime aim of water treatment is to maintain conditions where these protective oxide films are formed and are stable (MPSP, Vol. E, 1992).

Oxygen corrosion

Oxygen corrosion causes pitting of tube inside surface. Rapid failure of a tube can occur with relatively small overall metal loss. Even small amounts of dissolved oxygen can cause severe damage. Oxygen is extremely corrosive when present in hot water. Components that raise water temperature rapidly, such as feedwater heaters and economizers are particularly susceptible to an oxygen corrosion attack. The temperature increase provides the driving force that accelerates the corrosive reaction.

Out of service boilers are also susceptible to an oxygen corrosion attack. Such an attack may typically be found at the water/air interface. If boiler is shut down for longer periods, special procedures such as using nitrogen are necessary to avoid corrosion.

Almost complete removal of dissolved oxygen is necessary. Oxygen is removed mechanically in deaerator and chemically by a suitable chemical dosage. Small residual oxygen content is needed to prevent flow assisted corrosion.

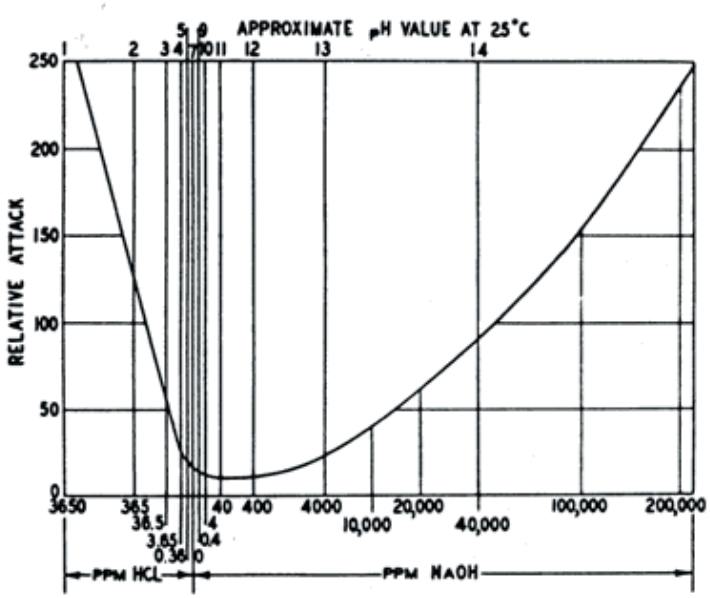

Figure 10-18, Rate of corrosion of carbon steel in boiler water as a function of pH, (Navitsky and Gabrieli, 1980).

Acid corrosion

When low pH water attacks steel, the attack is characterized by a general wastage of the metal, as opposed to the localized pitting nature of an oxygen attack. Since acidic conditions during the operation will produce rapid and severe corrosion, pH control of the boiler water is critically important.

In normal operating pH range of boiler water very little corrosion occurs. Under these conditions, steel readily reacts with water to form magnetite:

$$3Fe + 4\,H_2O \rightarrow Fe_3O_4 + 4H_2 \qquad 10\text{-}3$$

Magnetite forms as a thin, tenacious film on boiler tube. This film protects boiler steel against attacks. Highly acidic or caustic conditions can dissolve the magnetite film.

If pH in boiler water decreases below 4.5 magnetite film is loosened from the tubes. ESP is required as separated magnetite layer will block tubes.

pH control in high purity feedwater systems is problematic. Feedwater as such is subject to extreme pH swings from minor changes in acid or in alkali concentrations. Usually some buffer-ingchemical is used. A typical primary constituent of internal chemical treatment is phosphate. Phosphate will serve to buffer the deionized water to dampen pH swings.

To control acid corrosion in the high-pressure boilers, the pH will be maintained above 8.5. One typical method of control is to feed caustic solution into the feedwater.

Caustic corrosion

High pH boiler water can be equally as corrosive as acid. High-pressure boilers are more susceptible to caustic attack than the acidic attacks. Deionized feedwater provides no buffering capacity to react with the OH-ion and inhibit caustic concentration. Predominate contaminate in demineralized makeup is sodium hydroxide (caustic).

The caustic will concentrate under scale where evaporation of water occurs. As steam contains almost no caustic the caustic concentration is increased. The concentrated caustic readily "dissolves" the protective magnetite film, forming complex caustic-ferritic compounds. The exposed

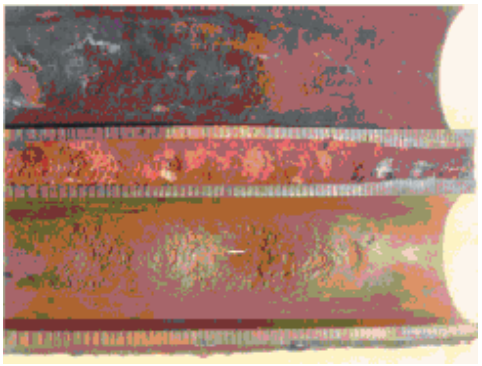

Figure 10-19, Caustic corrosion of carbon steel tubes (Kearns et al., 2001).

steel then reacts with water to reform the magnetite film, which is again dissolved by the caustic. The attack on the boiler steel continues for as long as the concentrated caustic exists.

The resultant metal loss assumes irregular patterns and is often referred to as "caustic gouging". When deposits are removed from the tube surface during examination, the characteristic gouges are evidence of caustic corrosion. The gouges are accompanied by a typical white salt deposit which is a combination of sodium carbonate (which is the residue of the caustic after contact with the carbon dioxide in the air) and crystallized sodium hydroxide.

Prevention of caustic corrosion is obtained by maintaining both proper pH and a control of molar ratio of sodium in the boiler water.

Flow assisted corrosion

Flow assisted corrosion (FAC) causes wall thinning in carbon steel. Wall thinning occurs as protective oxide layer is dissolved into the water. This process is continuous and can be seen if tube inside is examined. FAC has caused a lot of condensate line problems, economizer leaks and boiler shutdowns for repairs. Flow assisted corrosion does not affect superheated steam lines.

Flow assisted corrosion rate increases with increasing water velocity. Especially bends, orifices and headers, where flow is turbulent are prone to FAC. Corrosion rate is affected by temperature. The highest rates have been recorded between 100 and 250 oC. If steels with more than 0.5 w-% are used the rate is much lower. Lower pH promotes FAC. Presence of 10 to 20 ppb oxygen will help maintaining protective layer and reduce corrosion rate.

Corrosion control

A major factor in preventing water/steam side corrosion is keeping internal surfaces clean. Major contributors to the formation of a heat deterrent scale or deposit are contaminating elements present in the makeup water, metal oxides transported to the boiler with feedwater, contaminants from rest of the plant introduced into the condensate returned to the boiler and solids present in condenser leakage. Having clean surfaces means operating boiler with feedwater and boiler water within the applicable guidelines. The blowdown flow must be sufficient to prevent furnace side deposits.

To prevent feedwater related problems demineralization equipment must be operated with care. Good control of demineralizer operation, regeneration and maintenance is needed to ensure minimum sodium and silica leakage. There needs to be a pH buffer in the boiler water. This is done with dosing continuously with suitable chemical. Some internal water treatment chemicals provide an operating range.

High pressure boilers with high makeup are prone to deposits from the precipitation of chemical compounds. Substances such as calcium bicarbonate if not properly removed from the makeup water will decompose in the boiler water to form calcium carbonate as follows:

$$Ca(HCO_3)_2 \rightarrow CaCO_3 + CO_2 + H_2O \qquad 10\text{-}4$$

Calcium carbonate has very limited solubility and thus, the precipitated particles will agglomerate at the heated surfaces to form a scale. Other substances such as calcium sulfate are also scale producing. In this case, the scaling mechanism is, however, a function of a retrograde solubility or a decrease in solubility in water with an increase in temperature. These substances have a low thermal conductivity, and if left untreated, even a thin scale will overheat the boiler tube.

***Table 10-2**, Summary of waterside corrosion (adapted from Makkonen, 1999).*

Cause	Corrosion mechanism
Salts	General corrosion
Oxygen	General corrosion, pitting
Too low pH	Acid corrosion
Too high pH	Base corrosion
Non heterogeneous oxide layer	Pitting
Insufficient pre treatment	General corrosion, pitting
Chlorides	General corrosion, pitting
Stress	Stress corrosion cracking
Vibrations	Corrosion fatigue
Undesired turbulence / high velocity	Erosion corrosion

Summary of waterside corrosion

Summary of waterside corrosion is shown in Table 10-2. Waterside corrosion is generally understood

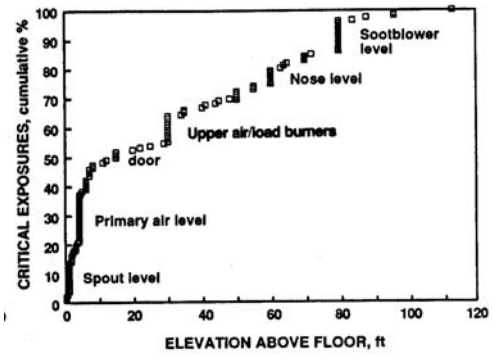

Figure 10-20, Critical exposures as function of elevation (Bauer and Sharp, 1993).

well. In spite of this waterside corrosion causes problems frequently because the operators tend to ignore all waterside issues. Keeping the feedwater purity high is essential.

10.5 FURNACE DESIGN AND MATERIALS

Recovery boiler furnace walls and floors have long been under investigation for better materials. Especially the floor construction and materials affect the recovery boiler safety Figure 10-20 (Bauer and Sharp, 1991). Most of the critical leaks in the furnace occur in the lowest 3 m of furnace walls. Figure 10-20 shows some of the used possibilities for lower furnace construction.

The lowest is studding and refractory. Corrosion protection with studs is excellent, but this solution requires large amount of maintenance and repair work. The middle picture shows membrane wall with welded corrosion protection of alloyed material. Welded furnace wall is of comparable price to

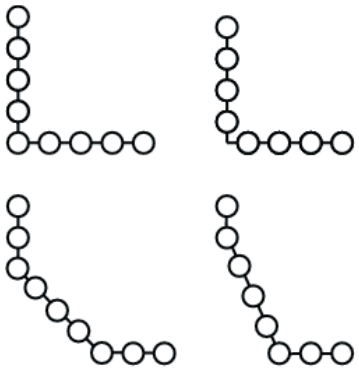

Figure 10-22, Different recovery boiler corner designs; upper left corner tube completely blocked from heat ransfer, upper right no corner tube, lower left rounded corner, lower right another rounded corner.

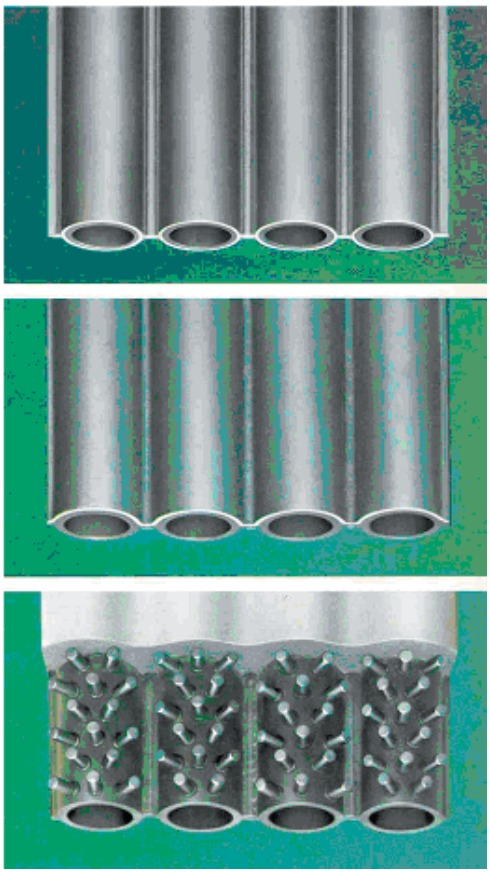

Figure 10-21, Different recovery boiler walls, lowest refractory with studs, middle protective welded cladding, highest finned membrane wall made from composite tubes (Tampella).

compound tubing, top, which is the most used recovery boiler wall construction. All new recovery boilers are of membrane design. Tangent tubing was phased out late 1980's (Sandquist, 1987).

It is important to protect the floor tubes from high temperatures. Proper design of water circulation lowers maximum temperatures. Sufficient water flow needs to be maintained in the tubes to cool them and to remove created steam bubbles. Usually the requirement is flow velocities $\geq$ 0.5 m/s in all tubes.

The floor angle in modern boilers needs to be upwards with the flow. As bottom tubes are supported by steel beams they hang a little. Floor angle helps to avoid parts where steam bubbles could get stuck. Depending on the distance between the support tubes, the angle needs to be from 2.5 to 4 degrees. Smelt spouts need to be high enough so that all floor is covered with frozen smelt layer. Especially critical is the area farthest from the smelt spouts and the area right in front of the smelt spouts. In practice it seems that 200 ... 300 mm

***Table 10-3**, Properties of typical floor tube materials.*

	Carbon steel	304L	Sanicro 38 (Alloy 825)	Sanicro 65 (Alloy 625)
Main elements	Fe	20Cr–10Ni	20Cr–40Ni	20Cr–60Ni
Thermal expansion, 10^{-6} /°C	13.5	17.5	14.9	13.9
Thermal cond., W/m°C	41	19	16	14
SCC resistance	Excellent	Low	High	Excellent
Corrosion resistance	Low	Moderate	Excellent	High

is enough. Too much height will cause problems when we try to empty the bed for shutdown.

Four different corner designs are shown in Figure 10-22. The amount of heat transferred to corner tubes differs from one design to another. Of the different recovery boiler corner designs only the design at the upper left is not recommended. The lower designs are safer than the upper designs.

Furnace tube materials

Some of the most typical furnace tube materials are listed in Table 10-3. Many more have been tried and for one reason or another abandoned. Carbon steel was the material of choice before the compound tubing. Upper furnace from above the highest air level is always made from carbon steel. Carbon steel seems to resist most corrosive conditions at oxygen rich conditions. But bare carbon tubes can not resist black liquor burning on them nor smelt contact. Most modern recovery boilers use highly alloyed compound tube as floor construction. Carbon steel has also been lately used as floor material, Figure 10-23. Floors with carbon tube are not susceptible to SCC corrosion.

Extensive research in Finland has been carried out where the corrosion of different materials in molten polysulfides was studied. This research showed that Sanicro 38-type composite material had the best corrosion resistance among the steels studied (Mäkipää and Backman, 1998). Test panels made of Sanicro 38 installed in 1991 and 1994 have not shown any alarming corrosion. Nor have there been any reported cracking found in recovery boiler bottoms made from Sanicro 38 since 1995. This highly alloyed material seems to have good corrosion resistance, but it is fairly expensive.

Stainless steel 304L seems to last well in the furnace walls above the char bed. It is very resistant to sulfidation. SCC in the tubes at the furnace bottom tubes has made manufactures and recovery boiler owners search for replacement materials in that area (Keiser *et al.*, 2000).

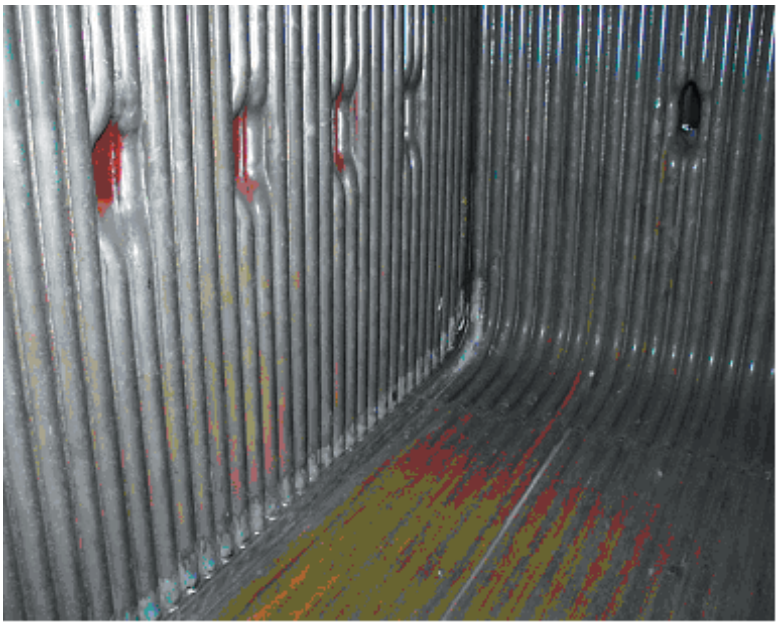

Figure 10-23, Modern carbon steel furnace bottom (Andritz).

Suppliers' current recommendations are to use modified alloys in the front and rear bends and close to the side walls. To facilitate weld inspection the whole lower furnace is often made of modified alloys up to and over the primary air ports. The present favorite is Sanicro 38 composite tube. In addition of high content of chrome and nickel the tube has about the same thermal expansion coefficient that the carbon steel.

Sanicro 65 (Alloy 625) composite tubing is another possibility. It has very favorable properties considering thermal fatigue and stress corrosion cracking. There are some reports of failure. So use of 625 needs more study at the moment. Another area under study is the air port cracking (Keiser *et al.*, 2002, Keiser, *et al.*, 2004). Primary air ports and smelt openings seem to exhibit cracking. Thermal cycling and smelt contact are suspected causes.

Use of compound tubing has about 30 year history in recovery boilers. Compound tubing is expensive and the selection of materials is limited. Some competing alternatives are chromizing of tubes (Plumley *et al.*, 1989, Labossiere and Henry, 1999). Another popular method is spray of plasma coating. Compound surface can also be replaced by welded surface. Of all above methods quality control is easiest with compound tube.

Membrane materials

Membrane materials should be similar to the tube material used. Carbon steel fin is used in case of carbon steel tubes. Either composite membrane or totally stainless steel membrane is used in case of composite floor tubing.

Fins receive thermal radiation and need to conduct heat to the tube proper. Fin surface is thus at higher temperature than the tube surface. In high heat flux areas and with wide fins this can lead to tube cracking, Figure 10-24. A composite membrane has better thermal conductivity as compared to solid material, which is important especially in case of wide tube spacing.

Refractory and studs

Small studs can be welded to tube and then covered with refractory, Figure 10-25. Refractory is also a fair corrosion protection. It should be remembered that both refractory and studs need regular replacement. It is also impossible to inspect a floor for faults after it has been studded. Because of this neither refractory nor studs is anymore widely used in recovery boilers.

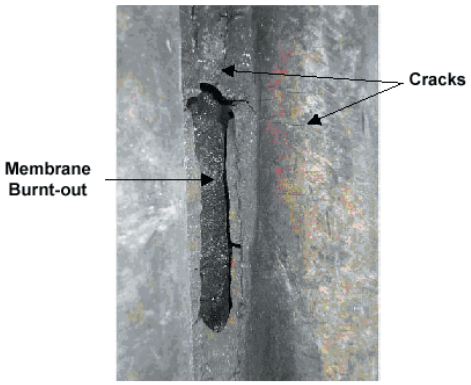

Figure 10-24, Burning of membrane material (Rivers et al., 2002)

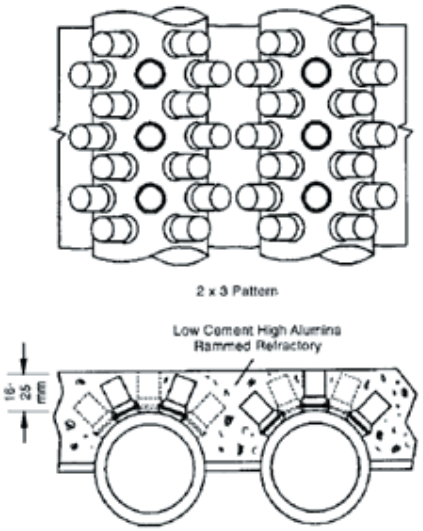

Figure 10-25, Refractory with studs to protect the furnace wall (Quest Integrated Inc)

10.6 SUPERHEATER DESIGN AND MATERIALS

Recovery boiler superheaters suffer from corrosion, design issues and operation issues. Operation problems that cause superheater failure can be (McMillan, 2004)

1) Condensate blocked tubes during start up
2) Water from hydrotest not being evacuated during start up
3) Water carryover from the drum
4) Desuperheater spray water quality control issues
5) Sootblower action
6) High temperature cycling caused by poor superheating control

Even the most modern recovery boilers suffer

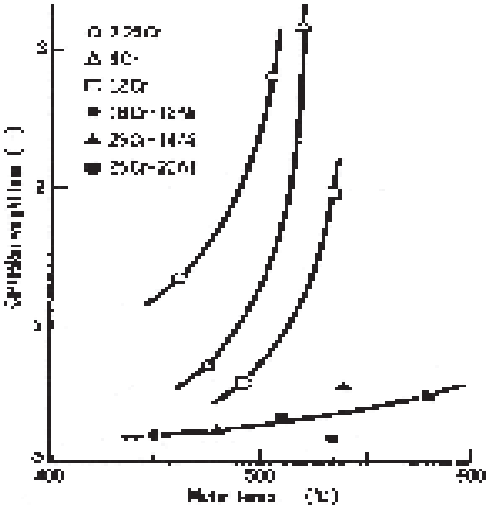

Figure 10-26, Effect of material and temperature on recovery boiler superheater corrosion, effect of tube temperature on corrosion rate in field tests (Fujisaki et al., 1994).

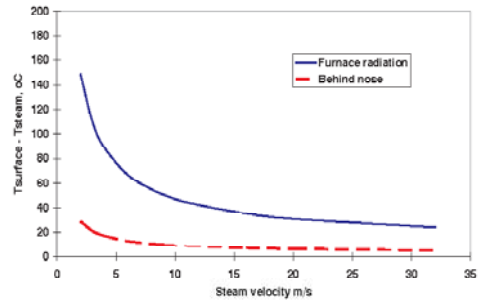

Figure 10-27, Effect of steam velocity and tube position on superheater tube surface temperature, 51 mm tube, behind nose calculated with average heat flux, furnace radiation calculated with heat flux from furnace.

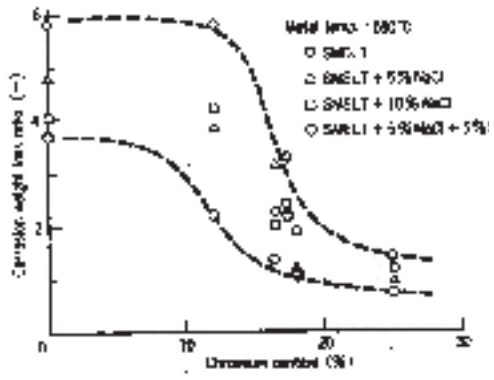

Figure 10-28, Effect of chromium content on corrosion rate in laboratory tests, (Fujisaki et al., 1994).

from superheater corrosion (Salmenoja, 2004). Corrosion is the main problem that limits the ability of kraft recovery boiler to produce electricity (Bruno, 1997). In e.g. coal fired boilers much higher superheater temperatures are typically used. In comparison to coal fired boilers kraft recovery boilers have higher rates of alkali metals, chloride in gaseous form and often highly reducing conditions caused by carryover particles On the other hand levels of some high temperature corrosion causing substances like antimony, vanadium and zinc are typically low.

Loss of tube thickness can be caused by sulfidation, alkali or chloride corrosion. Typically superheaters exhibit higher corrosion resistance if their tube materials have higher contents of chromium (Blough *et al.*, 1998).

Effect of steam outlet temperature

Main steam temperature is the main parameter that affects the choice of superheater materials. The rule of thumb is to keep the superheater surface temperature below the first melting temperature of deposits (Salmenoja and Tuiremo, 2001). Corrosion rates in final superheaters are increased because superheater material temperatures are highest, Figure 10–26. As can be seen there typically is some temperature range where the corrosion rate is acceptable. Increasing tube temperature by some tens of degrees can significantly increase corrosion rate.

Steam side heat transfer coefficients in typical recovery boiler superheaters are low. Superheater surface temperature can be tens of degrees higher than the bulk steam temperature, Figure 10-27. It can easily be seen that surface temperatures and thus corrosion rates are greatly affected by superheater positioning. Furnace radiation can effectively be reduced by placing a screen to block radiation heat flux. Therefore placing the hottest superheaters behind the nose or screen will significantly decrease corrosion.

Typical materials

Typical primary superheater materials, when they are protected from direct furnace radiation are carbon steel. Secondary and tertiary superheater materials contain often 1 to 3 % Cr. These kinds of materials are easy to weld and have good corrosion protection. T22/10CrMo910 material can usually be used up to 495 °C steam outlet

***Table 10-4**, Example compositions of various superheater materials (Note that actual composition will vary depending on the tube manufacturer and the production batch).*

	Cr	Ni	Mo	Si	Cu	Al	Mn	C	Fe	Other
15Mo3	0.3	0.3	0.3	0.26	0.3		0.65	0.16	97.6	
SA213 - T12	1.0		0.5	0.45			0.45	0.1	97.5	P,S
13CrMo44	1.0	0.3	0.3	0.26	0.3		0.55	0.14	97.1	
SA213 - T11	1.25		0.50	0.75			0.45	0.15	96.9	P
10CrMo910	2.3		1.00				0.50		96.1	
SA213 - T22	2.25		1.00	0.75			0.45	0.15	95.4	P
X10CrMoVNb91	9,0	0,3	1,00	0,40			0,50		88,7	V, Nb
SA213 - T91	9,0	0,33	0,99	0,24		0,03	0,45	0,11	88,7	Cb, N
HCM 12	12.0		1.00						86.9	V, Nb
X20CrMoV121	12.0	0.5	1.00	0.50			0.50	0.23	85.2	V
AISI 304	19.0	9.5							71.4	
SS3338	18.0	12.0		0.72			0.15		69.2	Nb, Ta
AISI 316	17.0	11.0	2.70						69.2	
AISI 321	18.5	10.2		0.75			2.00	0.06	68.5	
AISI 347	17.5	10.3		1.30		0.70	1.60	0.08	68.4	Nb, Ta
253 MA	21.0	11.0		1.70					66.2	N, Ce
2205	22,0	5,5	3,20	1,00			2,0		66.2	
Esshete 1250	16.0	11.0	1.25	1.00			7.0		62.5	V, Nb
AISI 309	23.0	14.5		0.70			1.50	0.10	60.2	P
HR2M	22.2	14.4	1.49	0.55			3.14	0.03	58.1	N
YUS170	24,4	13,2	1,50	0,78			0,58	0.02	59.5	N, P
AISI 310	25.0	20.5		0.50				0.08	53.8	
Alloy 800 HT	21.0	32.5		0.50	0.40	0.40	0.75	0.05	44.3	Ti
HR3C	25.0	29.5		0.42	1.28		1.10	0.06	42.6	N
AC66	27.0	32.0		0.25		0.02	0.8	0.06	39.2	Ce, Nb
Sanicro 28	27.0	31.0	3.50		1.00		0.05	0.01	37.3	
Sanicro 38	21.0	38.0	2.50	0.30	1.70		0.80		35.6	Ti
Alloy 825	22.0	39.0	3.50	0.36			0.50		34.5	Ti
HR11N	28.5	41.2	1.06	0.12			0.50	0.01	28.6	N
Nicrofer 45 TN	27,0	46,9		2,70		0,20		0,08	23,0	Re
Super 625	21.0	52.7	8.97	0.21		0.28	0.20	0.01	15.8	Nb
Alloy 600	15.5	74		0.25	0.26		0.50	0.07	9.3	V, Nb
Sanicro 65	21.0	61.0	8.40	0.35			0.38		8.8	
Alloy 625	21.0	58.0	9.0	0.50		0.4	0.50	0.10	5.0	Nb,Ti

temperatures (Clement, 1990). With higher temperatures and higher chloride and potassium contents in the black liquor it is advisable to use higher chromium containing tubes.

Fujisaki *et al.* (1994) found that recovery boiler superheater corrosion is much reduced when chrome content of the superheater tube is increased, Figure 10-28. Similar trend was found from Swedish studies in Norrsundet recovery boiler (Eriksson and Falk, 1999). They found that alloyed austenitic materials 304L and Sanicro 28 had much better corrosion resistance than high alloyed ferritic materials SS2216 and X20.

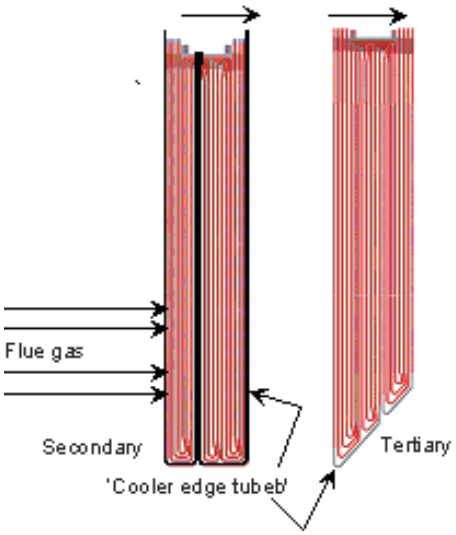

Figure 10-29, Outermost tube temperature can be decreased by arranging shorter flow path.

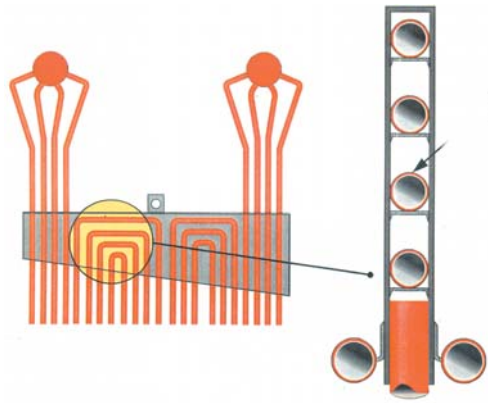

Figure 10-30, Superheater roof seal box arrangement.

Stainless steel lower bends in hottest superheaters have been used for tens of years. From field tests it seems that no appreciable corrosion occurs up to the metal temperature of 540 °C (Arakawa *et al.*, 2004).

Effect of tube arrangement

Recovery boiler superheaters typically consists of some 10 … 40 panels that have some 20 ... 40 tubes each. To control steam velocity in the tubes and so the pressure loss, parallel tube passes are used. Most typically from three to five tubes are used. These superheater tube parallel passes are often all of same or close to same length.

Some control of tube surface temperatures can be made by choosing shorter and longer tube routes, Figure 10-29. The longer routes will have higher pressure loss, lower mass flow and higher end temperature. The shorter routes will have lower pressure loss, higher mass flow and lower end temperature. We can balance corrosion by using shorter routes for outside bends. These outside tubes experience high heat flux and have thus higher temperature difference between tube and steam. But reduced path can lower steam temperature and balance corrosion rate. This procedure is in more detail described by LaFond et al (1992).

Sealing the roof

Superheater tubes and the furnace roof need to for a gas tight construction. This is usually done by box made of steel plate, Figure 10-30. If the sealing is not tight or leaks corrosive salt builds on top of the roof. Superheaters need to be supported. Hanger rods are tied to seal box. Individual tubes hang from horizontal supports inside the box. Thermal movement needs to be accounted for. This means that superheater tubes can not hang from headers.

10.7 SCREEN DESIGN AND MATERIALS

Screens are built as first heat transfer surface after the furnace to protect other heat transfer surfaces from radiation and carryover. Screens are typically just tube panels, where tube spacing is very narrow. Most of the screens are made of carbon steel as their temperature is close to the tube wall temperature. Corrosion of screen tubes is low because of the material temperature.

The most problematic screen design element is the damage that can be caused by falling deposits (Villarroel *et al.*, 2004). Especially at the corner of front wall and roof large deposits can build up. If a deposit drops from the roof down to a screen it can break the tubes. Deposit damage can be minimized but not eliminated by building fins or extra thickness to screen top surface.

10.8 BOILER BANK DESIGN AND MATERIALS

Two drum boiler banks have very good reliability record. They, however, suffer form mud drum corrosion (Labossiere and Henry, 1999). This type of corrosion is caused by steam from sootblowing wetting the salt at tube joints in lower drum. The progress of the near drum corrosion can be monitored with ultrasonic equipment (Soar *et al.*, 1994). Two drum boiler banks are made with

plain tubes tapered at both ends. The joints can be made without welds up to the pressure of over 8.0 MPa.

Another problematic failure type is caused by vibrations from gas flow or sootblowing. The longer the free tube length the higher the resulting stress at joins. Industry practice states that maximum length of free tubes is about 8 meters. Typically longer tubes are too flexible and will vibrate too much. This will create cracks and faults in few years. All larger recovery boilers have vertical boiler banks.

Vertical boiler banks consist of hundreds of tubes. Often you find from 60 to 100 tube rows between sidewalls. Each tube row consists of tubes welded together with wide fins to improve heat transfer and create rigidity. In modern boilers the vertical boiler bank has one or two sootblowing cavities open from top to bottom.

Finned design causes temperature differences between fin and tube. This will create high stresses at fin ends. To prevent these stresses cut fins are preferred, Figure 10-31.

Some pluggage problems have been reported on boiler bank lower end (Sandquist, 1987). If lower headers are located too close to each other they trap falling material. Placing a sootblowers close to the lower end is also critical to keep it free from fouling.

10.9 ECONOMIZER DESIGN AND MATERIALS

Modern economizers are of vertical design. Earliest horizontal economizers had severe plugging problems and were replaced by cross flow design. Cross flow economizer had lower heat transfer coefficients and was more prone to plugging than the modern vertical economizer.

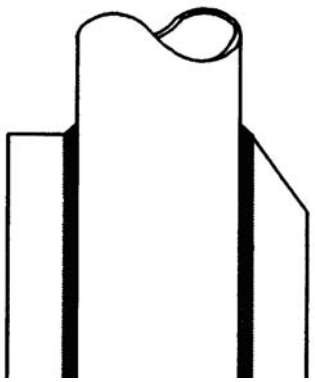

Figure 10-31, Upper end of vertical flow boiler generating bank showing left straight fin and right cut fin, which minimizes thermal stresses around weld (Bruno and Hägerström, 1998).

In economizers the loss of tube thickness can be caused by gas side corrosion; sulfidation and acid dew point corrosion or water side erosion corrosion.

Lower ends of economizers in recovery boilers suffer from water side erosion corrosion. Typically the symptoms are worst in the first few meters of economizer tube.

Recovery boiler economizers have hundreds of weld joints. Each weld even after inspection is potentially problematic. Therefore the preference was to avoid unnecessary welds and use only continuous tubes without butt welds. Largest boilers have economizer lengths of 27 meters. Carbon steel tubes maximum length is some 23 meters. So in the newest boilers this preference can not be adhered to. Attention should be paid to qualification of welds in economizer tube joints.

11 Emissions

Environmental issues matter to the pulp and paper industry (Vasara, 2001). In reducing emissions to air the performance of the recovery boiler is the key factor. The pulp and paper industry has in the recent past significantly reduced emissions from recovery boilers (Bruce and Van der Voored, 2003). Total elimination of all emissions to air is impossible, but proper recovery boiler design and operation can minimize the impact of harmful emissions.

Emissions to air from recovery boilers can be broadly categorized with the age of the boiler, the black liquor dry solids and the boiler load. But emissions do not only depend on the process conditions and the type of equipment. Significant emission decreases can be achieved when trained, educated and motivated personnel run a properly maintained unit with high level process control optimization (IPPC, 2001).

11.1 TYPICAL EMISSIONS

Kraft recovery boiler is the largest producer of gaseous effluents from the pulp mill. Typical emission levels of main controlled substances are shown in Table 11-1 (IPPC, 2001). It is evident from that table that at present stage some kraft pulp mills still produce significant sulfurdioxide and dust releases. The NOx levels from kraft pulping are well below the average NOx releases from energy production. Kraft pulping gets accused of producing bad smell. The smelly component release (TRS) from recovery boilers is however of minor magnitude.

When determining emission levels it is often advantageous to look at total emissions from pulp mills. BAT emission levels from kraft pulping process and recovery boilers are shown in table 11-2 (IPPC, 2001). These figures should include lime kiln, NCG-combustion and uncontrolled gaseous releases. In integrated mills the bark and auxiliary boiler emissions are not typically included to pulp mill releases, because modern pulp mills can produce all their heat from just black liquor.

***Table 11-1**, Typical emissions (dry, 3 % O_2) to air from recovery boilers (IPPC, 2001).*

	ppm	mg/m^{3}n	mg/MJ	kg/ADt
Sulphur dioxide	35 - 275	100 - 800	60 - 250	1 - 4
TRS	< 7	< 10	< 5	< 0,05
NOx	50– 125	100 - 260	50 - 80	0,8 – 1,8
Dust		10 - 200		0,1 – 1,8

***Table 11-2**, BAT emission levels from kraft pulping process and recovery boilers (IPPC, 2001).*

Emission		Kraft pulping	Recovery boiler
Particles	kg/ADt	0.2 … 0.5	0.2 … 0.5
SO_2	kg(S)/ADt	0.2 … 0.4	< 0.1
NOx	kg(NO_2)/ADt	1.0 … 1.5	0.7 … 1.1
TRS	kg(S)/ADt	0.1 … 0.2	< 0.1

It is possible to reduce the sulfur dioxide emissions from recovery boilers to near zero levels. Additional sulfur releases occur from lime kiln, NCG-boiler and as uncontrolled gaseous releases. The role of uncontrolled gaseous releases in TRS emissions can clearly be seen. Lime kiln contributes some 25 … 35 % of the mill NOx release. A significant source of mill ammonia is the green and white liquor system (Kymäläinen *et al.*, 1999).

11.2 REDUCED SULFUR SPECIES

Reduced sulfur species are smelly gases. They include hydrogen sulfide, methyl mercaptan, dimethyl sulphide and dimethyl disulphide. The main reason for limiting their emission is to improve local environment around the mill. The main source of TRS in modern kraft pulp mills are uncollected vent gases and other points where mill liquors are handled in contact with the air. Therefore in addition to NCG, the mixing tank vent gases and dissolving tank vent gases need to be burned in the furnace.

The TRS emission is often caused by cold char bed and poor mixing in the furnace. When black liquor dry solids is increased furnace temperature

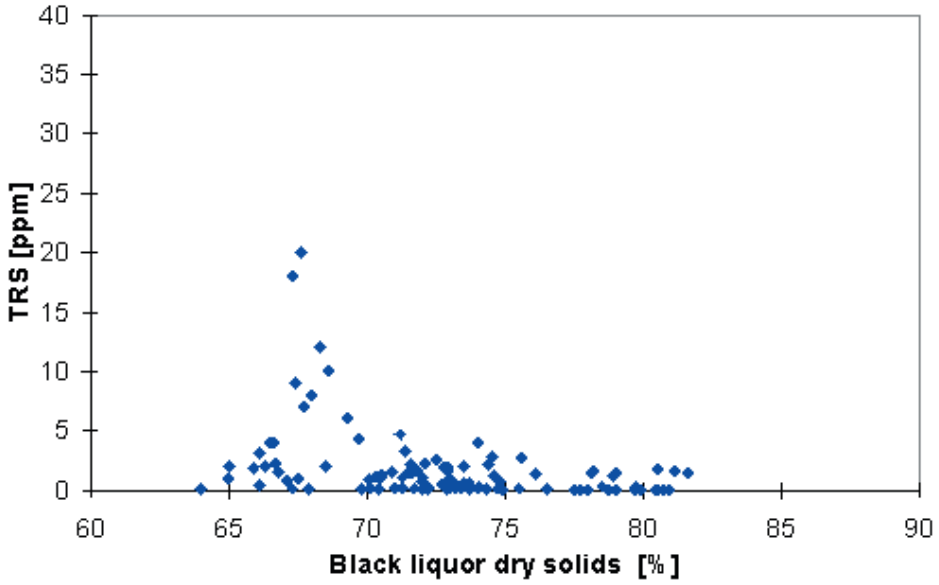

Figure 11-1, TRS emissions from modern recovery boilers.

gets higher. Typical emission levels for modern recovery boiler main stack at over 65 % liquor are 1 … 5 mg/m^{3}n or 5 ppm at 3 % O_2 and dry gas, Figure 11-1. Reduced sulfur species (TRS) will oxidize in a modern furnace to sulphur dioxide. This requires sufficient temperature and mixing. Improving recovery boiler air system below the liquor gun level can be used to lower TRS emissions (La Fond *et al.*, 1994).

11.3 CARBON MONOXIDE

Incomplete combustion produces carbon monoxide (CO). It is a colorless, odorless, poisonous gas. CO formation increases dramatically when black liquor is burnt at very low excess oxygen conditions. Carbon monoxide is emitted from all combustion sources including motor vehicles, power stations, waste incinerators, domestic gas boilers and cookers.

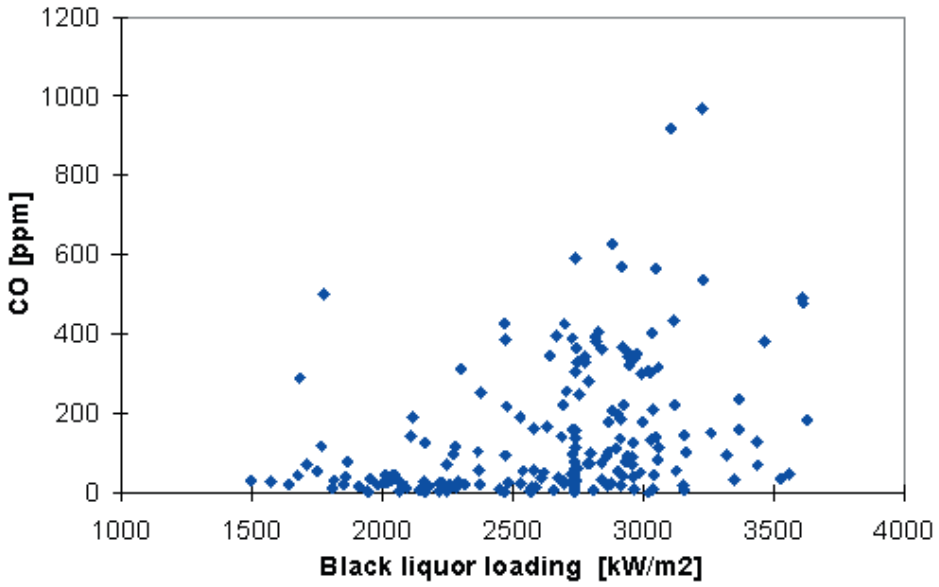

Figure 11-2, Typical carbon monoxide levels from modern boilers.

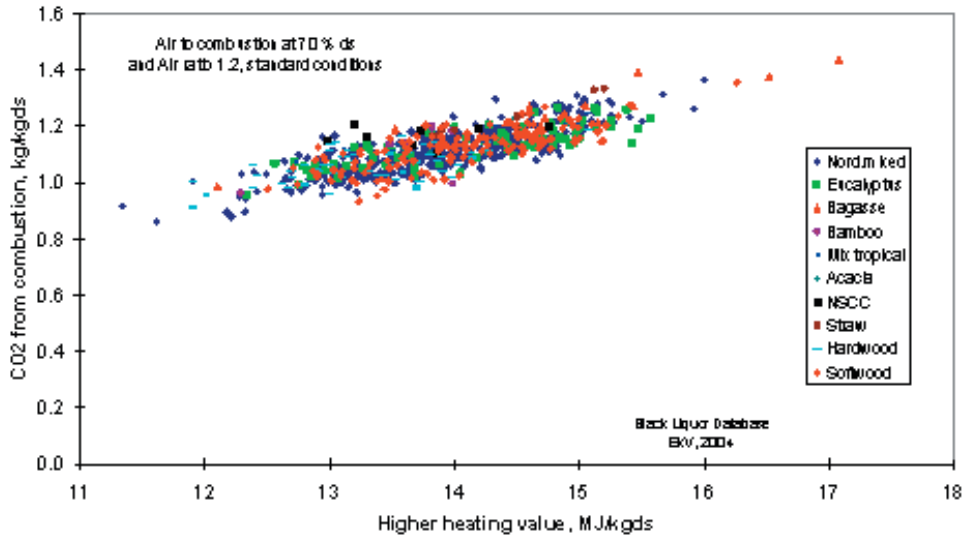

Figure 11-3, Renewable carbon dioxide from black liquor combustion.

Carbon monoxide has limited effect on human health. It attaches itself to red blood cells preventing the up-take of oxygen. Carbon monoxide contributes indirectly to an enhancement of global warming through reactions with other gases in the lower atmosphere.

CO correlates well with O_2 content in the flue gases. The higher the air ratio and the better the mixing the lower is the CO emission. Higher furnace temperature and longer residence time decrease CO emission. The NOx and TRS emission increase with decreasing CO (Vakkilainen and Holm, 2000). It is typically advantageous to run at some hundreds of ppm of CO to lower other emissions and keep reasonable flue gas heat losses.

With modern large boilers the CO level is not greatly affected by as fired black liquor dry solids or boiler load. In small retrofitted boilers the furnace residence time might be too low to complete combustion.

11.4 CARBON DIOXIDE

Carbon dioxide (CO_2) is odourles gas that is not harmful to humans. Carbon dioxide absorbs radiation. It has been postulated that increasing carbon dioxide levels in atmosphere cause global warming. Therefore reduction of carbon dioxide production is of importance.

Black liquor is a biofuel. Carbon dioxide produced when burning organics from wood on black liquor is assumed to be reabsorbed back to organic matter in forests. Therefore the only fossil carbon dioxide production from kraft recovery boilers is from use of auxiliary fuel during startup, upsets or for extra steam production.

11.5 NOX

Nitrogen oxides (NOx) emissions from recovery boilers are mainly nitric oxide (NO). In the atmosphere it reacts to nitrogen dioxide (NO_2). Nitric oxide is a colorless, odorless gas. Nitrogen dioxide is a reddish-brown gas with a pungent odor. Nitrogen oxides contribute to acid rain formation. Nitrogen dioxide affects human respiratory system aggravating asthma and other lung diseases.

Major man-made releases of nitrogen oxides are from automobiles and fuel combustion. Forest fires and biological processes in soils and waters produce also NOx.

NOx levels in recovery boilers are typically 70 … 120 ppm at 3% O_2.(Aho 1994). The emissions from Swedish recovery boilers in 1998 were between 60 and 140 ppm with average 92 ppm at 3% O_2 (Kjörk and Herstad, 2000). Typical emission from modern recovery boiler is 60 ... 80 mg/MJ. This level is significantly lower than most of the coal and oil fired boilers can achieve.

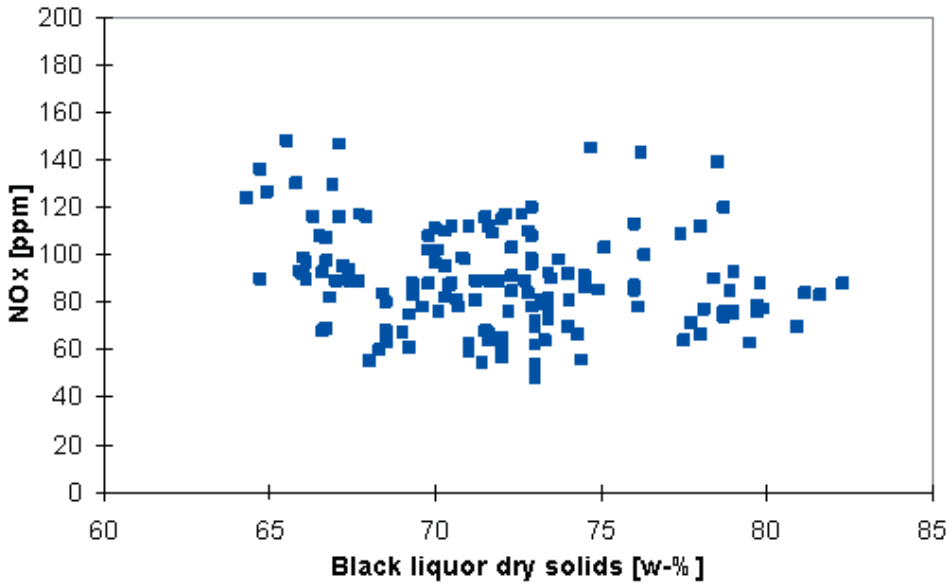

Figure 11-4, Typical recovery boiler NOx emission values.

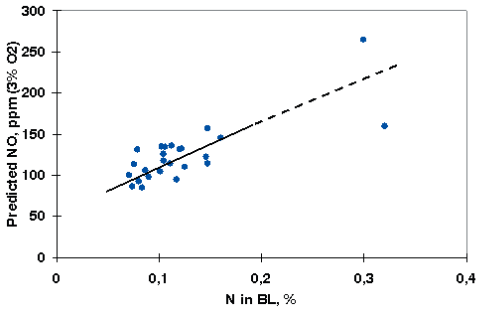

Figure 11-5, Correlation of NO emissions in recovery boilers to nitrogen in fuel (Plotted from data in Forssén et al, 1997).

Recent changes in recovery boiler operation have increased the NOx level. Examples are; increasing black liquor dry solids, combustion of NCG in recovery boiler furnace and combustion of dissolving vent gases in the recovery boiler.

Effect of fuel nitrogen content to NOx emissions

When boilers are run with liquors from pulping of different wood species, high nitrogen containing woods (hardwood) produce more NOx than softwood liquors. Field tests support the conclusion that recovery boiler NOx emissions correlate with nitrogen in the black liquor (Clement and Barna, 1993). Laboratory tests show that the nitrogen release from black liquor seems to be independent of wood species and cooking method (DeMartini *et al.*, 2004). The highest reported nitrogen content has been 0.5 w-% of bagasse black liquor dry solids (Aho, 1994). The detection accuracy of nitrogen in the fuel from commercial laboratories is very poor so direct correlations are often misleading. For example two black liquors of nitrogen content 0.072 and 0.114 mass % get both typically a value of 0.1 mass-%.

Aho *et al.* (1994) studied the reduction of nitrogen in the black liquor. One can somewhat change the nitrogen content by treating chips, making cooking changes and treating black liquor. The results however have so far showed this to be uneconomical.

Part of the nitrogen in black liquor is in the form of NH_3 and so easily vaporized. Parts of nitrogen can then be extracted from black liquor in the stripper area. This product may enrich to some parts of the recovery cycle so great care should be taken when this waste stream is destroyed.

NOx - reduction

The following reduction means have been tried in recovery boilers in an industrial scale

- Optimisation of the feeding of air and fuel
- Increasing number of air levels
- Feeding of the ammonia to the top of the furnace
- Vertical air
- Oxidation /reduction processes

Several other methods can be used to reduce the NOx of recovery boilers. Among the methods known from the general combustion processes are the following

- electron beam method
- catalytic conversion (SCR)

SCR can not be used in recovery boilers as the fine aerosol particles and the sodium containing gases pose challenges to the lifetime of the catalyst (Anderson and Jackson, 1991).

Selective noncatalytic reduction

Selective noncatalytic reduction is the next possibility to reduce NOx from recovery boilers. The use of noncatalytic reduction is difficult in recovery boilers as it requires a rather narrow operating temperature range around 950 oC to function. NOx is removed by injecting some reducing substance into flue gas. Typical chemical components used are ammonia, urea and their derivatives. The main reaction path is.

$$2NH_3 + 2NO + {}^1/_2O_2 \rightarrow N_2 + 3H_2O \qquad 11\text{-}1$$

Ahlstrom Machinery and Gotaverken have tried the feeding of the ammonia to the top of the furnace in a recovery boiler (Lövblad *et al.*, 1991). During the trials the gas temperature at injection point was about 1000 °C. With this technique a 15 … 35 % or 22 … 60 ppm reduction was reached. The NOx level in the flue gases lowered from depending on how much reducing agent is used and how big ammonia slip is allowed. To restrict the ammonia, discharge below 5 ppm level only about 25% reduction was reached.

***Table 11-3**, Achievable NOx reduction levels*

Nitrogen	Normal			Reduced		
w-%	ppm	mg/m3n	mg/MJ	ppm	mg/m3n	mg/MJ
0,08	83	170	55	62	128	41
0,10	97	200	65	73	150	49
0,15	130	266	87	97	200	65

With the spraying of the ammonia there exists always some ammonia slip caused by the unevenness of the spraying and NOx. Ammonia is known to cause low temperature corrosion and is in itself a corrosive agent.

A recovery boiler has 100 ppm of NOx at dry flue gases and dry flue gases 3,86 m^3n/kgds. Level of ammonia in flue gases is 100 ppm/m^3n. The ammonia content is then 1 ppm of NH_3 to 1 ppm of NO. 1 ppm NH_3 = 0.771 mg(asNH_3)/m^3n.

Ammonia consumption is at 3000 tds/d

NH_3 kg/24h = 3000*3,86*0,771*100/1000 = 893 kg/24 h

NOx removal is

NO_2 kg/24h = 3000*3,86*2,053*25/1000 = 594 kg/24 h

This comes as about 1,5 tons of NH_3 per one ton of NO_2 removed.

Approximate operating cost is then 2.000 – 2.500 €/t NO_2. Ammonia in water solution costs 2 – 3 € per kg of ammonia. For a 3000 tds/d recovery boiler the operating cost of ammonia would be about 3 million Euro per year.

Oxidation-/reduction processes

From chemical industry there are known several methods to oxidize NO to NO_2 followed by capture of NO_2 and reduction to N_2. Known oxidizers are peroxide, ozone and chlorinedioxide. This process can occur in a recovery boiler (Janka *et al.*, 1998). The scrubber material needs to be able to withstand the oxidizer. Published operating costs are from 2.300 to 3.100 €/t NO_2. Trials of this process have been conducted in several mills.

Use of chlorine dioxide is about 4 ppm for 1 ppm of NOx.

ClO_2 kg/24h = 3000*3,86*3,149*400/1000 = 14586 kg/24 h

Removed NOx is

NO_2 kg/24h = 3000*3,86*2,053*75/1000 = 1786 kg/24 h

required chlorine dioxide is about 8 tons per removed ton of NO_2.

Chlorine addition to recovery cycle would be

Cl kg/t pulp = 14586 kg/24 h / 1670 t / 24h = 9 kg/ t pulp

Normal chlorine input is 1 - 2 kg/ t pulp, so the addition might increase the chloride level in the mill significantly. In one Finnish mill the chlorine level in black liquor would have increased from 0.3 w-% to 1.8 w-%. So the additional capacity reduction in recovery boiler must be considered if chlorine based oxidizer is used.

Typical mill emission levels

Typical emission levels of NOx (and SO_2)in Scandinavia are listed in Tables 11-4 and 11-5.

***Table 11-4**, NOx and SO_2 emissions from Finnish pulp mills in 2001 (Environmental report, 2002).*

	Production ADt/a	NOx t/a	SO_2 t/a	NOx kg/ADt	SO_2 kg/ADt
Äänekoski	397000	963	465	2.43	1.17
Sunila	300000	594	106	1.98	0.35
Kaskinen	368000	705	587	1.92	1.60
Joutseno	334000	618	377	1.85	1.13
Kemi	443000	801	22	1.81	0.05
Varkaus	178000	323	322	1.81	1.81
Valkeakoski	142000	243	107	1.71	0.75
Pietarsaari	527000	852	155	1.62	0.29
Kuusankoski	420000	666	69	1.59	0.16
Uimaharju	560000	844	155	1.51	0.28
Lappeenranta	678000	1011	392	1.49	0.58
Rauma	470000	681	433	1.45	0.92
Kemijärvi	178000	248	69	1.39	0.39
Veitsiluoto, Kemi	312000	421	10	1.35	0.03
Imatra	727000	981	410	1.35	0.56
Oulu	299800	353	24	1.18	0.08
Kotka	121000	83	280	0.69	2.31
Average	379694	611	234	1.61	0.62

The emissions per ton of pulp produced vary a lot from mill to mill. The national average mill size and the average emissions per ton of pulp produced are very close to each other. If we count only those mills that achieve sulfur emission below 0,5 kg/ADt, the corresponding NOx emission is 1,2 … 1,8 kg/ADt.

The lowest emission of NOx per ton of pulp produced has been achieved at a mill where the corresponding sulfur emissions are the highest. The nitrogen oxide emissions can be plotted. Tables 11-4 and 11-5 have been plotted as function of total pulp production and scaled to 100 %.

Nitrogen oxide emissions from pulp mills Tables 11-4 and 11-5 are plotted as function of total pulp production and scaled to 100 % in Figure 11-6. One can see from that typical nitrogen oxide emissions are around 1.5 kg / ton of pulp. Normal emission limits from pulp mills can be seen in Table 11-6.

***Table 11-5**, NOx and SO_2 emissions from Swedish pulp mills in 2001 (Collected from company web pages in 2002).*

	Production ADt/a	NOx t/a	SO_2 t/a	NOx kg/ADt	SO_2 kg/ADt
Husum	591000	1199	768	2.03	1.30
Väröbacka	327000	660	400	2.02	1.22
Piteå	395000	743	126	1.88	0.32
Billingsfors	50621	93	49	1.84	0.97
Iggesund	308000	558	508	1.81	1.65
Munksund	215000	360	76	1.67	0.35
Skärblacka	395000	654	356	1.66	0.90
Karlsborg	275000	449	377	1.63	1.37
Aspabruk	159555	243	87	1.52	0.55
Valvik	169400	256	142	1.51	0.84
Norrsundet	245000	351	384	1.43	1.57
Obbola	241000	336	271	1.39	1.12
Gruvö	630000	871	109	1.38	0.17
Östrand	395000	541	537	1.37	1.36
Mörrum	390000	520	360	1.33	0.92
Skutskär	467000	613	602	1.31	1.29
Mönsterås	658000	770	350	1.17	0.53
Frövi	222400	213	61	0.96	0.27
Gävle	654500	622	196	0.95	0.30
Skoghall	528000	489	321	0.93	0.61
Average	340776	524	309	1.54	0.91

***Table 11-6**, Nitrogen oxide emissions from pulp mills as kg/ADt.*

	Range	Average
Finland 2001	1,2 – 2,0	1,61
Sweden 2001	1,0 – 2,0	1,54
USA (Pinkerton, 1998)		1,38
IPPC BAT	1,0 – 1,5	
New pulp mill, hardwood		1,4
New pulp mill, softwood		1,2

Addition of nitrogen containing flows

Burning of NCGs and dissolving tank vent gases will increase the nitrogen flow to furnace. Changes in N to furnace are directly related to NOx emissions.

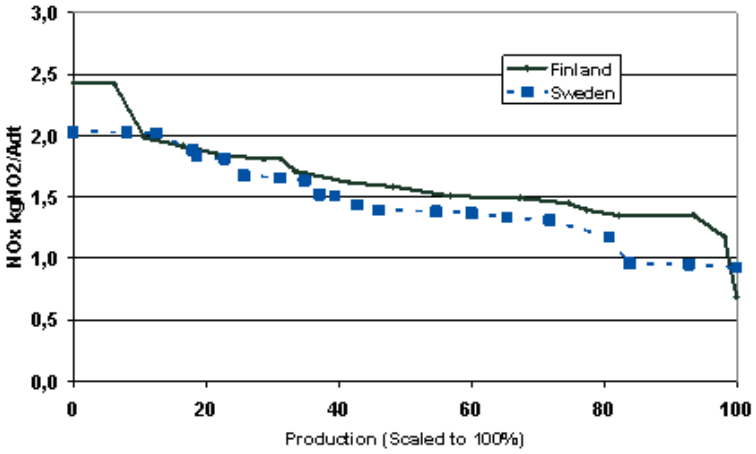

Figure 11-6, Nitrogen oxide emissions from pulp mills Tables 11-4 and 11-5 plotted as function of total pulp production and scaled to 100 %.

Dissolving vent gases

Dissolving vent gas flow is about 0.25 m^3n(dry)/kgds. Dissolving vent gases containing nitrogen as ammonia at about 100 ppm/m^3n(dry). One can assume that 30 % ammonia is converted to NOx (Crawford and Jain, 2002). The increase in NOx emission from recovery boiler is in the order of

NOx+ % = (3,67*100 + 0,30*0,25*100)/(3,67*100) * 100 -100 = ~2 %

DNCG

The flow of high volume low concentration NCG is typically 5 … 10 % of total air flow. The nitrogen in DNCG gases is mainly ammonia. Level of nitrogen compounds in DNCG can be assumed to be 10 ppm/m^3n(dry) (Janka, and Tamminen, 2003). One can assume that 30 % ammonia is converted to NOx even if the CNCG burner is installed above the liquor guns. The increase in NOx emission from recovery boiler is in the order of

NOx+ % = (3,67*100 + 0,30*0,1*3,67*10)/(3,67*100) * 100 -100 = <1 %

CNCG

The flow of low volume high concentration NCG is 0,010 … 0,025m^3n/kgds. The nitrogen in CNCG gases is mainly ammonia. Level can be assumed to be 2000 ppm/m^3n. One can assume that 30 % ammonia is converted to NOx. The increase in N to boiler is

NOx+ % = (3,67*100 + 0,30*0,025*2000)/(3,67*100) * 100 -100 = ~4 %

Emissions

***Table 11-7**, BAT NOx emissions from recovery boilers (IPPC report, 2001).*

Mill	Country	kg/ADt
Äänekoski	Finland	1,748
Pöls	Austria	1,600
Värö	Sweden	1,510
Iggesund	Sweden	1,500
Vallvik	Sweden	1,440
Kaskinen	Finland	1,366
Örstrand	Sweden	1,360
Aspa	Sweden	1,290
Skutskär	Sweden	1,260
Dynäs	Sweden	1,240
Bäckhammar	Sweden	1,220
Husum	Sweden	1,210
Enocell	Finland	1,186
Skoghall	Sweden	1,140
Sunila	Finland	1,029
Obbola	Sweden	1,020
Stora Celbi	Portugal	1,020
Joutseno	Finland	1,013
Frövi	Sweden	1,010
Mönsteras	Sweden	0,950
Huelva	Spain	0,880
Wisaforest	Finland	0,864
Oulu	Finland	0,810
Skärblacka	Sweden	0,660

***Table 11-8**, Volatile organic emissions from US kraft recovery boilers with dry bottom ESP and without direct contact evaporator (NCASI, 2001).*

MILL #		C1	C2	J	K	M	Avg.
Acetaldehyde	ppm			1.8-2.3	0.5-0.9	0.2-0.4	0.5
Methanol	ppm	7-22	4.70	2.4-2.8	4.3-9.7	1.7-2.0	2
Acetone	ppm	0.14-0.21	0.33	0.17-0.20	0.10-0.29	0.1-0.2	0.1
Methyl ethyl ketone	ppm	0.35	0.29	0.09-0.30		0.07-0.1	0.1
Benzene	ppm	0.26-0.27	0.72	1.79	0.3-2.7		0.5
Methyl isobutyl ketone	ppm		0.81				0.5
Toluene	ppm	0.12		0.02-0.03			0.5
m,p-xylene	ppm			0.04		0.03	0.05
o-xylene	ppm			0.04		0.02	0.05
Xylenes	ppm	0.09	0.18				0.1
Styrene	ppm	0.06	0.12	0.08			0.1
Alpha-pinene	ppm	0.10					0.1
Beta-pinene	ppm	0.06-0.21					0.1
Terpenes	ppm			0.11-0.38	0.13-2.3	0.14-0.17	0.3
Formaldehyde	ppm			0.98			1
VOC	ppm		152	119	3-193		100

BAT recovery boiler NOx emission

BAT recovery boiler emission levels in Europe are listed in Table 11-7. The best recovery boilers achieve emissions little below 1.0 kg/ADt. NO emission strongly correlates with N-content in the fuel.

11.6 VOC

Volatile organic compounds (VOC) contributes to the formation of ground-level ozone in the atmosphere. Some high molecular mass VOC are carcinogens (Froste, 1996). Common sources of VOC emissions include vehicle exhausts and the chemicals industry, with other minor releases also occurring naturally from forest fires. The majority of industrial emissions to air are from leaks during production, use, storage, transport and disposal of carbohydrates. Volatile organic compound emissions from recovery boilers are low and mainly of low molecular weight.

Most of the measured VOC (C_xH_y, C_xH_zOH, …) emission seems to come from the mixing tank vent gases and dissolving tank vent gases.

11.7 DUST EMISSIONS

Dust or particulate matter is small particles suspended in the air. They are one of the most noteworthy air quality problems in urban areas (Ohlström *et al.*, 2000). Typically particulate matter comes from a variety of different sources. Especially smaller particle size can directly affect human blood through respiratory system. Particulate matter comes from combustion sources, road traffic, dusts, sea salt and biological particles. Particulate matter is usually reported as total solid mass flow. Additionally small size particular matter is reported as PM10 or PM2.5 (particles with diameter less than or equal to 10 or respectively 2.5 micrometers). 80 … 99 % of recovery boiler particulate matter emission belongs to PM2.5 category (Mikkanen *et al.*, 1994, Mikkanen *et al.*, 2001).

$$\eta = 1 - e^{\left(\frac{-Aw}{V}\right)^k} \qquad 11\text{-}1$$

where

e is the collection efficiency, -
A is the collector surface
w is the collection migration velocity, m/s
V is the actual gas flow, m^3/s
k is an empirical constant (0.4 .. 0.5 ..0.6), -

Even at high dry solids the emission after the recovery boiler economizer is typically below 20 g/m^3n. The dust emission is strongly dependent on boiler load. It has been noted that firing with high black liquor droplet velocities and small droplets

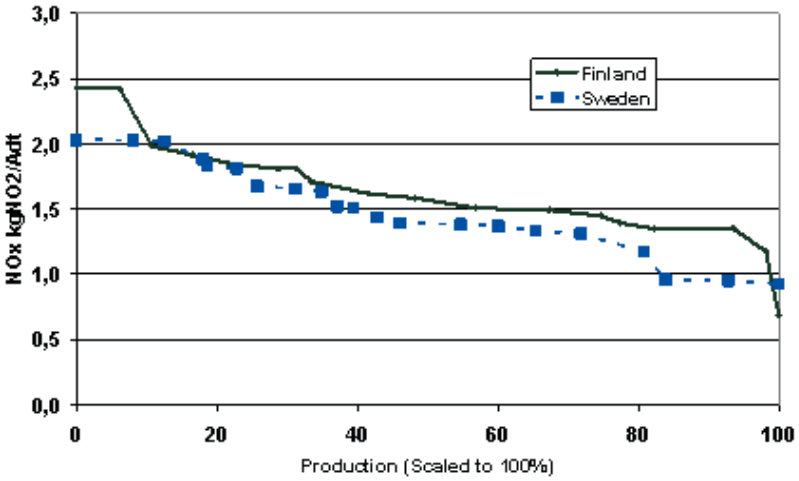

Figure 11-7, Total uncontrolled dust emission from recovery boiler furnace.

causes excess carryover and high dust loading. Dust emission can be reduced by using electrostatic precipitators.

Effect of operating conditions to dust emissions

In kraft recovery boilers the ash is formed by several mechanisms. Most of the ash is formed through fume formation. Almost all ESP ash is typically fume. Some of the black liquor fired into recovery boiler furnace gets caught with flue gas. Furnace gases then drag these particles with them out of the furnace. It has also been postulated that during char combustion some intermediate size particles are formed.

In the kraft recovery furnace the alkali elements are vaporized. When flue gases are cooled the vapors become supersaturated. Another mechanism of supersaturation is formation of species by reactions. E. g. sodium hydroxide and sulfur dioxide react to sodium sulfate, which has lower vapor pressure than the reactants (Jokiniemi *et al.*, 1996). Resulting particle size is 0.5 … 1.3 µm.

In recovery boiler furnace there are small metal oxides and other impurities present, which will serve as starting nucleus for the vapors. This process is called heterogeneous condensation. After formation of nucleus the vapor condensation keeps then supersaturation low.

Much of the particle size growth is result of agglomeration. Small liquid particles collide with each other and form new spherical particles. After flue gas temperature decreases below about 550 oC fume particles that hit do not stick to each other. Sintering can occur at heat transfer surfaces. There fume can form large agglomerates. These agglomerates can re-entrain to flue gas when soot-blowed. They show as larger 20 … 30 µm particles at electrostatic precipitator inlet (Mikkanen, 2000, Janka *et al.*, 2000). Amount of re-entrained dust is 10 … 30 % of total dust flow (Tamminen *et al.*, 2000).

Chemical equilibrium calculations (Perjyd and Hupa, 1984) suggest that fume formation increases as the lower furnace gas temperature increases. When boilers are run with higher dry solids the furnace temperature increases (Vakkilainen and Holm, 2000). Higher dust emission is then a trade off to lower sulfur emissions.

Most of the fume tends to end up in electrostatic precipitator. Figure 11-7 shows ESP dust as function of black liquor dry solids. Furnace temperature increases with increased black liquor dry solids, which increases sodium and potassium release (Frederick *et al.*, 1995). ESP ash flow forms an estimate of fume formation in recovery boiler. Black liquor sodium and potassium release depends also on the liquor i.e. wood species and the pulping conditions (Backman *et al.*, 1999). In addition the firing conditions affect the lower furnace temperature. As can be seen then the actual fume formation rate can vary a lot.

Typical mill emission levels

Typical emission levels in Scandinavia are listed in Tables 11-9 and 11-10.

***Table 11-9**, Dust emissions from Finnish pulp mills in 2001 (Environmental report, 2002).*

	Production ADt/a	Dust t/a	Dust kg/ADt
Äänekoski	397000	304	0,77
Sunila	300000	133	0,44
Kaskinen	368000	227	0,62
Joutseno	334000	93	0,28
Kemi	443000	29	0,07
Varkaus	178000	158	0,89
Valkeakoski	142000	547	3,85
Pietarsaari	527000	647	1,23
Kuusankoski	420000	125	0,30
Uimaharju	560000	161	0,29
Lappeenranta	678000	87	0,13
Rauma	470000	191	0,41
Kemijärvi	178000	127	0,71
Veitsiluoto, Kemi	312000	87	0,28
Imatra	727000	37	0,05
Oulu	299800	98	0,33
Kotka	121000	87	0,72
Average	379694	185	0,67

***Table 11-10**, Dust emissions from some Swedish pulp mills in 2001 (Collected from company web pages, 2002).*

	Production ADt/a	Dust t/a	Dust kg/ADt
Husum	591000	428	0,72
Väröbacka	327000	840	2,57
Billingsfors	50621	36,9	0,73
Iggesund	308000	141	0,46
Munksund	215000	531	2,47
Obbola	241000	157	0,65
Östrand	395000	163	0,41
Mörrum	390000	220	0,56
Mönsterås	658000	140	0,21
Gävle	654500	215	0,33
Average	340776	295	0,98

Table 11-11, *Typical dust emissions from recovery boilers (IPPC report, 2001).*

Location		Emission
after ESP	mg/m^3n	10 … 200
	kg/ADt	0.1 … 1.8

BAT recovery boiler emission levels

The typical emissions, according to the IPPC document, from recovery boiler are shown in Table 11-11.

BAT recovery boiler emission levels in Europe are below 50 mg/m^3n. The best recovery boilers achieve emissions little below 0.2 kg/ADt.

11.8 SULPHUR DIOXIDE

Sulphur dioxide (SO_2) is a colorless gas. About half of world sulphur dioxide emissions are from burning of fossil fuels (Lefohn *et al.*, 1996). Large part of the rest comes from emissions from metal production and large industrial plants. Pulp mills used to be a major source of sulfur emissions, with most of it coming from recovery boiler.

Sulphur dioxide is a major contributor to acid rain. Sulphur dioxide irritates the eyes and air passages. It may increase asthma or lung disease symptoms. Sulphur dioxide is transported by air for long distances.

The sulphur dioxide emissions are dependent on the dry solids and the black liquor sulphur to sodium and potassium molar ratio (Wallén *et al.*, 2004). The higher the dry solids the higher sulfur emission one can produce. Similarly the higher the sulfidity the higher is the possible emission. Sulfur emissions from about 30 different boilers running different loads at different dry solids and black liquor sulfidities are shown in Figure 11-9. Even at high sulfidities the sulfur dioxide emissions tend to decrease to levels below 10 ppm.

Correlating black liquor sulfidity and dry solids to sulfur dioxide emission results in a graph like 11-10. In it we can see three trends. Sulfur emission is steadily decreasing until at some point it rapidly falls to a very low figure. For increased sulfidity this fall point is at higher solids.

If the boiler load decreases the furnace temperature decreases. The lower the furnace temperature the lower is the alkali release. It seems that below 2500 kW/m^2bottom the furnace starts to cool and SO_2 emission increases, Figure 11-10.

11.9 HCL

Chlorine can be found in ESP dust as NaCl and KCl and in recovery boiler flue gases as HCl. The enrichment factor of chlorine is 1-4.5 from BL

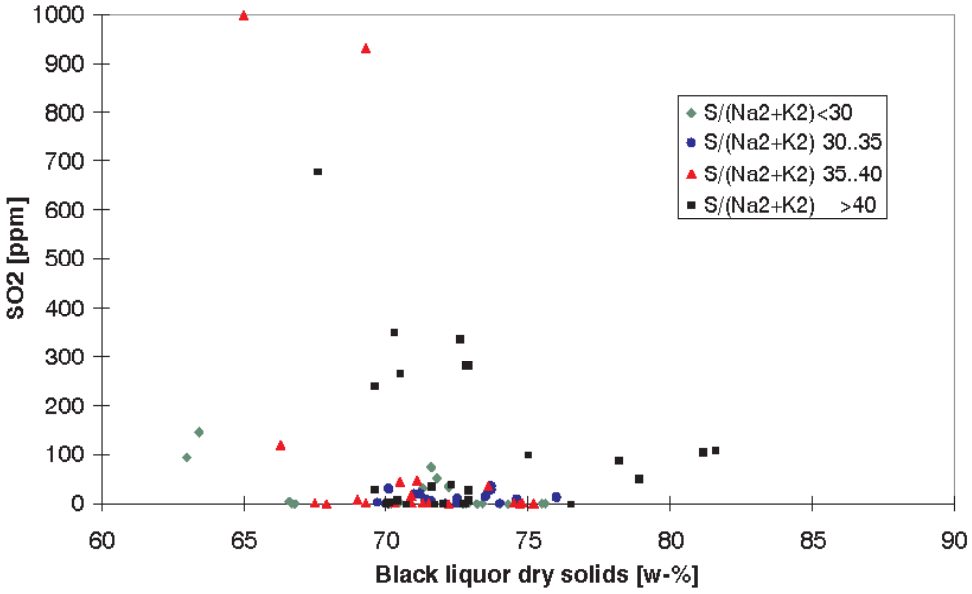

Figure 11-8, Typical sulfur dioxide emissions at different dry solids levels.

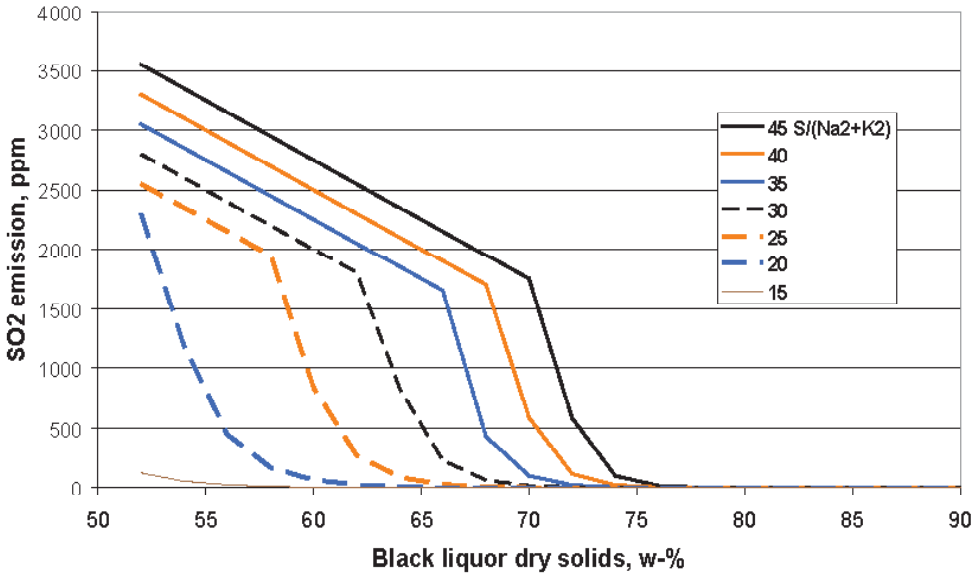

Figure 11-9, Correlation of sulfur dioxide emissions with dry solids.

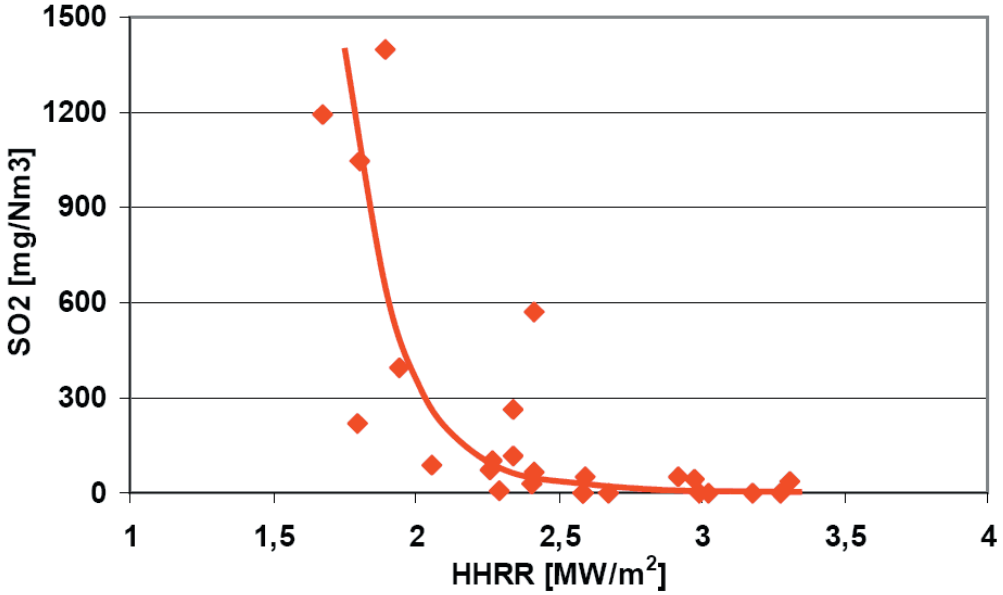

Figure 11-10, Correlation of sulfur dioxide emissions with Heart Heat Release Rate at sulfidity between 40 to 45 % (Wallén et al., 2004).

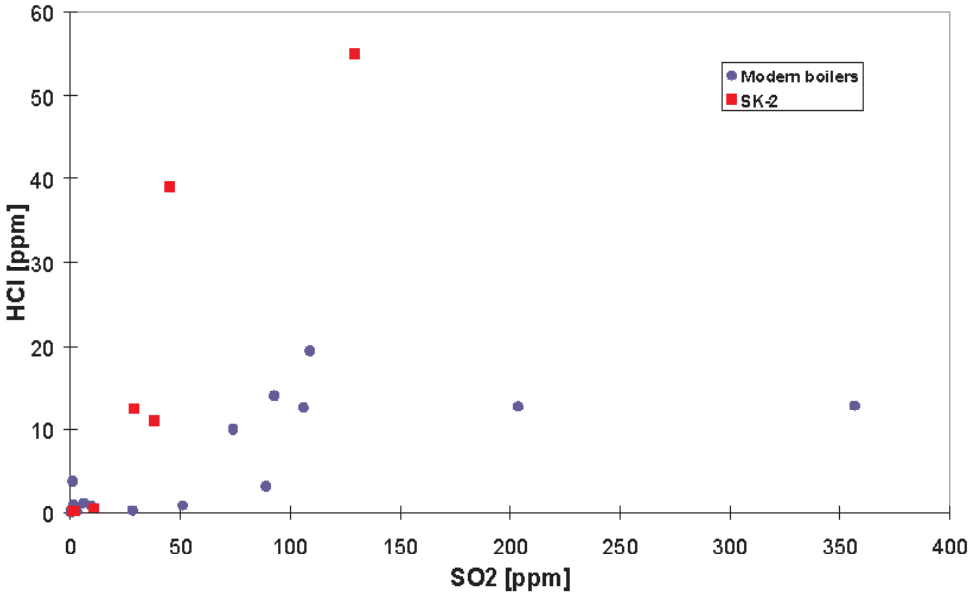

Figure 11-11, Examples of measured HCl concentrations in recovery boiler flue gas.

to ESP dust. Released chlorine in the recovery furnace reacts to form HCl. If there is residual free sodium after sulfur species have reacted then HCl will react to NaCl. NCASI has found HCl to be about one third of SO_2 emission. In modern Scandinavian boilers the level of HCl was lower for the same sulfur dioxide emission. The probable cause is better mixing.

concentrations in recovery boiler flue gas. Sonnenberd and Nichols (1995) studied the effect of adding bleach plant effluents to the black liquor. They found that only about 5 % of chlorine in bleach plant effluent was released as HCl. Most organic chlorine is trapped as NaCl rather than emitted as HCl during pyrolysis of bleach plant solids that contain a molar excess of sodium over chlorine.

Rules of thumb
1 wt-% of Cl in black liquor is 3.0 mole-%
1 wt-% of Cl in ESP dust is 2.0 mole-%
HCl emission is less or about 1/3 of SO_2 emission.

Calculation of chlorine emission per unit mass of black liquor fired

10 ppm HCl => 4.5 m^3n*10*10-6*1.63 kg/ m^3n*35.5/36.5 = 71 mg
250 mgdust/ m^3n and 0.5 m-% Cl in BL => 4.5 m^3n*250*0.005*3*4.5/2 = 38 mg
Total emission = (71+38)= 110 mg/kgblds

11.10 MISCELLANEOUS MINOR EMISSIONS

One can in addition to major emissions measure some very little streams that are of environmental interest.

Sulfuric acid

Sulfuric acid, H_2SO_4 emissions correlate with SO_2 emissions. Some of the sulfur dioxide in flue gases reacts with molecular oxygen in the recovery furnace and forms SO_3. Typically the amount of SO_3 is much less than 5 %. During sampling or at surface the SO_3 reacts with water vapor to form H_2SO_4.

In some measurements the sulfuric acid content has been found to be tens of ppms if the SO_2 emission is very high. In modern boilers the H_2SO_4 emission is expected to be practically zero.

Dioxins

Organic compounds can combine with available chlorine to form dioxins. No single component can be found. There are hundreds of such elements but only a handful have been analyzed as their content in typical recovery boiler furnace stack is typically very low. The various dioxins can be converted to TCDD equivalent based on their toxicity. The measured dioxin emissions from recovery boilers are about two magnitudes lower than measured emissions from the same mills power boilers (Luthe *et al*., 1997).

NACASI measured dioxin emissions from six recovery boilers. The levels varied from 1.2–2.5 pg TEQ/m^3 (NACASI, 1996). This corresponds to 0.38 to 5.2 pg TEQ /m^3, levels measured by Luthe *et al* (1997). The typical emission level for dioxin emissions is in the order of <100 pg/m^3n at 3 % O_2 or <10 pg(as TCDDequivalent)/m^3n at 3 % O_2. Note! 1 000 000 000 pg = 1 mg

Main components in one measurement were 2,3,7,8-TCDD, 1,2,3,7,8,9-HxCDD and 1,2,3,7,8-PeCDD.

Sonnenberd and Nichols (1995) studied the effect of adding bleach plant effluents to the black liquor. They found that adding 1 mass-% bleach plant effluent to black liquor increased dioxin levels from black liquor droplet combustion by about a decade.

Furans

There are very little reliable measurements on furan contents of recovery boiler emissions. A typical value for furan emissions is in the order of 1000 pg/m^3n at 3 % O_2 or 100 pg(as TCDDequivalent)/m^3n at 3 % O_2. Note! 1 000 000 000 pg = 1 mg.

Main components in one measurement were 2,3,7,8-TCDF, 1,2,3,6,7,8-HxCDD and 1,2,3,7,8-PeCDF.

Fluorine

Fluorine in black liquor can be found as trace metal. The amounts are typically much smaller than 5 ppm. Most of the fluorine in black liquor is expected to be released in the recovery furnace. Because fluorine levels in black liquor are very low the fluorine emission from recovery boiler is expected to be negligible.

11.11 HEAVY METALS

Heavy metal emissions are harmful as they may collect to human body. Especially inhaling small particles can increase heavy metal levels in blood. Heavy metal levels in recovery boiler dusts are very low. Most of the matter in dust is harmless sodium sulfide, sodium carbonate and sodium chloride.

Heavy metals include antimony (Sb), arsenic (As), barium (Ba), beryllium (Be), cadmium (Cd), chromium (Cr), cobalt (Co), copper (Cu), gold (Au), iron (Fe), lead (Pb), manganese (Mn), mercury (Hg), niobium (Nb), nickel (Ni), selenium (Se), silver (Ag), tellurium (Te), thallium (Th), zink (Zn), vanadium (V) and other even more minor elements. They can be found as trace elements in black liquor. The US Environmental Protection Agency has listed eleven metals as hazardous air pollutants. These are antimony, arsenic, beryllium, cadmium, chromium, cobolt, lead, manganese, mercury, nickel and selenium. The European Community has signed a protocol to limit the total annual emissions into the atmosphere of cadmium, lead and mercury. Directive 2000/76/EC list twelve heavy metals that require limits; antimony, arsenic, cadmium, chromium, cobalt, copper, lead, manganese, mercury, nickel, thallium and vanadium. The most problematic ones listed are cadmium, thallium and mercury. Expected levels from recovery boilers are listed in Table 11-2.

The actual level in black liquor varies significantly from mill to mill (Control, 1999). The main source of these trace elements is wood chips. So the inflow is mainly controlled by the soil conditions in

***Table 11-12**, Expected heavy metal emissions.*

Metal	Concentration in BL mg/kgds	Expected tot.emission mg/Adtp	Expected in gas μg/ m^{3}n	Expected in dust μg/ m^{3}n
Al	10 - 350	158	3 - 8	1 - 20
Antimony		1 – 20		
As	1 - 10	<21 0,1 – 200	<3	<0,4 - 2
Au		0,2 – 15		<1
Ba	5 - 30	2 – 4		8 - 12
Be	0 - 10	0,2 – 3		<1
Cb		<15		
Cd	0 - 10	0,92 0,4 – 30	0,04 - 0,13	0,1
Cr	0.1 - 20	8,7 0,5 – 25	0,13 - 0,7	1,5
Cu	1 - 10	3 – 100		<1
F	1 - 10		<100	
Fe	10 - 100	145	3 - 11	2 - 30
Hg		3 1 – 30	0,4 - 0,5	<0,02
Mg	50 - 1000	66	2,4 - 9,7	3 - 40
Mn	20 - 150	22 3 – 40	0,4 - 1,6	1 - 20
Ni	1 - 10	<21 1 – 35	<1,3	<2
Pb	1 - 10	8,8 5 – 70	1 - 1,3	0,1 - 0,3
Se	0 - 10	<6,3 1 – 200	<0,7	<0,3
Tl		<21 <15	<1,7	<1,5
Zn	10 - 40	15 – 40 360		4 - 8

the area where the wood is brought in. Significant increase of levels can be expected if bleach plant effluent is recycled to brown stock washing. main exits are with pulp and dregs. Highest concentrations are with Mg 50 ... 1000 mg/kgblds, Mn 20 ... 150 mg/kgblds and Ba 5 ... 30 mg/kgblds. Lower concentrations are Zn 10 ... 40 mg/kgblds, Cu 0,1 ... 10 mg/kgblds, Cr 0 ... 20 mg/kgblds, Ti 0 ... 4 mg/kgblds, V, 0 ... 2 mg/kgblds, Be 0 ... 8 mg/kgblds. Total concentration is 1000 ... 2000 mg/kgblds.

The emission is mostly as dust in fluegases after ESP. The heavy metals can be divided into three groups based on their volatility (Iisa, 2004). As, Cd and Pb are highly volatile and they vaporize completely or nearly completely (Backman *et al.*, 2004). Se, Sb and Be are of medium volatility. Mn, Ni, Cr and Co are of low volatility.

11.12 DISSOLVING TANK EMISSIONS

Dissolving tank emissions are caused by non reacted material in the smelt and reaction of water with sulfur species. Dissolving tank dust emissions are caused by droplets of green liquor which when dried contain inorganic salts. Dissolving tank flow is about 0,3 - 0,2 m^3n(dry)/kgds or 0,5 - 0,3 m^3n(wet)/kgds (lower values for higher capacities). Most of the dissolving tank flow is thus water vapor. Increasing air infiltration decreases specific emissions (mg/m^3n) but does not affect the emissions as mass per fired solids (kg/tds).

The typical output level for sulfur dioxide is 0.0050 … 0.0075 kg/tds or 8 … 12 mg/m^3n, dry. The typical output level for TRS is 0.0050 … 0.0075 kg/tds or 6 … 10 mg/m^3n, dry. TRS emission can increase if mix tank vent gases are introduced to dissolving tank vent gases, the scrubbing media contains volatile sulphur compounds (e.g. is not condensate) or dissolving tank receives condensates from NCG handling or evaporator.

The typical output level for particulate with scrubbing as only control is 0.035 … 0.050 kg/tds or 100 … 150 mg/m^3n, dry.

12 References

A study of kraft recovery furnace total gaseous non-methane organic emissions, 1996, NCASI, Atmospheric Quality Improvement Technical Bulletin, No. 105, National Council of the Paper Industry for Air and Stream Improvement, New York, NY.

Abdullah, Z., Gorog, J. P., Keiser, J. R., Meyers, L. E. and Swindeman, R.W., 1999, Pattern of thermal fluctuations in a recovery boiler floor. NACE International CORROSION '99, San Antonio, TX, April 25-30, 1999

Water tube boilers and auxiliary installation – Part 15: Acceptance Test on Steam Generators, 2003, 12952-15:2003 E, CEN European Committee for Standardization, 89 p.

Adams, Terry, 2001, Sodium salt scaling control in black liquor evaporators and concentrators. *Tappi Journal*, Vol. 84, No. 6, June 2001, 18 p.

Adams, Terry N., 1994a, Air flow, mixing and modelling for recovery boilers. 30 Years Recovery Boiler Co-operation in Finland, International conference, Baltic sea, 24 - 26 May, pp. 61 - 78.

Adams, Terry N., 1994b, Black liquor spray nozzles for kraft recovery boilers. TAPPI Kraft Recovery Short Course, Orlando, January 9 - 13, pp. 287 - 302.

Adams, Terry N., 1988, Air jets and mixing in kraft recovery boilers. *Tappi Journal*, Vol. 71, No. 1, January 1988, pp. 97 – 100.

Adams, Terry N. and Frederick, William J., 1988, Kraft recovery boiler physical and chemical processes. American Paper Institute, Inc., New York. 256 p.

Adams, Terry N., Frederick, Wm. James, Grace, Thomas M., Hupa, Mikko, Iisa, Kristiina, Jones, Andrew K. and Tran, Honghi, 1997, Kraft recovery boilers. AF&PA, Tappi Press, Atlanta, 381 p. ISBN 0-9625985-9-3.

Adams, Terry N., Stewart, Robert I. and Jones, Andrew K., 1993, Using CFD calculations to estimate thermal-NOx from recovery boilers at 67% and 80% dry solids. Proceedings of 1993 Tappi Engineering Conference, Orlando, Florida, September 20 – 23, Tappi Press, pp. 625 – 634.

Adomeit, G., Mohiuddin, G. and Peters N., 1976, Boundary layer combustion of carbon. Sixteenth Symposium on Combustion. The Combustion Institute, Pittsburgh, pp. 731 - 743.

Ahlers, Per E., 1983, Investigation of alloyed steels for use in black liquor recovery boilers. Swedish Corrosion Institute, Stockholm. Proceedings 1993 Environmental Conference, Tappi press, pp. 643 – 647.

Aho, Kaisa, 1994, Nitrogen oxides formation in recovery boilers. Lic. Tech. thesis, Report 94-7, Combustion Chemistry Group, Åbo Akademi, Åbo. 118 p.

Aho, Kaisa, Hupa, Mikko and Nikkanen, Samuli, 1993, Release of nitrogen compounds during black liquor pyrolysis. Proceedings of 1993 TAPPI Engineering Conference, Orlando, September, pp. 377 - 384.

Aho, Kaisa, Vakkilainen, Esa and Hupa, Mikko, 1994, Fuel nitrogen release during black liquor pyrolysis, Part 1: Laboratory measurements at different conditions. *Tappi Journal*, Vol. 77, No. 5, May 1994, pp. 121 – 127.

Ahtila, Pekka, 1997, Optimization of recovery boiler plant air systems by new design method and process integration. *Acta Polytechnica Scandinavica*, Me, Mechanical engineering series, 127, Finnish Academy of Technology, 137 p. ISBN 952-5148-34-3.

Akiyama, H., Uchimura, M., Osawa, S., Shinohara, M., Hasegawa, T., Iwanaga, T. and Iwahashi, K., 1988, Recovery boiler with higher pressure, temperature and thermal efficiency. *MHI technical Review*, Vol. 25, No. 2, pp. 84 - 90.

Alava, Paavo, 1955, Kokemuksia JMW-soodakatilan käytöstä. (Operation experiences of a JMW recovery furnace) in Finnish, *Paperi ja Puu*, Vol. 37, No. 5, pp. 209 – 215.

Albrecht, Melvin, 2002, Enhancing the circulation analysis of a recovery boiler through the incorporation of 3-D furnace heat transfer results from COMO. Proceedings 2002 TAPPI Fall Technical Conference, September 8 - 11, San Diego, Ca. 7 p.

Alén, Raimo, 2004, Combustion behavior of black liquors from different delignification conditions. 40th Anniversary International Recovery Boiler Conference, Finnish Recovery Boiler Committee, Haikko Manor, Porvoo, May 12-14, 2004, pp. 31 – 42.

Alén, Raimo, 2000, Basic chemistry of wood delignification. in Forest Products Chemistry, editor Stenius, P., Fapet, Helsinki, Finland, pp. 58-102.

Alén, Raimo, 1997, Mustalipeän koostumuksen vaikutus lipeän poltto-ominaisuuksiin. (Effect of black liquor composition to combustion properties) in Finnish, LIEKKI2- yearly report, part II, Åbo Akademi, Department of Chemical Engineering, pp. 751 – 759.

Anderson, Peter H. and Jackson, James C., 1991, An analysis of best available control technology options for kraft recovery furnace NOx emissions. *Tappi Journal*, Vol. 74, No. 1, January 1991, pp. 115 - 118.

Arakawa, Yoshihisa, Taguchi, Yuzo, Maeda, Takayuki and Baba, Yoshitaka, 2004, Experience of high pressure and high temperature recovery boilers for two decades. Proceedings of 2004 International Chemical Recovery Conference, June 6-10 2004, Charleston, South Carolina, USA, pp. 35 - 43.

Arakawa, Yoshisa, Ichinose, Toshimitsu, Okamoto, Akiyasu, Baba, Yoshitaka and Sakai, Toshiyuki, 2003, Application for in-furnace NOx removal system for recovery boilers. *Pulp & Paper Canada*, Vol. 104, No. 2, pp. T42 – T46.

Backman, Rainer V., Wikstedt, Henrik, Skrifvars, Bengt-Johan, Hupa, Mikko M., Ruohola, Tuomo and Haaga, Kari, 2004, Trace element distribution in and around the recovery boiler. Proceedings of 2004 International Chemical Recovery Conference, June 6-10 2004, Charleston, South Carolina, USA, 503-517 p.

Backman, Rainer, Hupa, Mikko, Kymäläinen, Marita and Pulliainen, Martti, 2002, Formation of sulfur-rich melt near the floor tubing of kraft recovery boilers. *Tappi Journal*, Vol. 85, No. 4, April 2002, 7 p.

Backman R., Skrifvars B.-J., Hupa M., Siiskonen P. and Mäntyniemi, J. 1996, Fluegas and dust chemistry in recovery boilers with high levels of chlorine and potassium. *Journal of Pulp and Paper Science*, Vol. 22, No. 4, pp. J119-J126.

Backman. Rainer, Hupa, Mikko, Söderhjelm, Liva, 1996, Mustalipeän polttotekniset ominaisuudet. (Combustion properties of black liquors) in Finnish, Åbo Akademi University, Department of Chemical Engineering, Report 96-9.

Backman, Rainer, Forssén, Mikael, Hupa, Mikko and Uusikartano, Timo, 1996, New black liquor combustion characteristics II. Liekki II, project 511, final report. Finnish Recovery Boiler Committee, SPL-20803-007.

Backman, R., Eriksson, G. and Sundström, K., 1996, The recovery boiler advisor, Combination of practical experience and advanced thermodynamic modeling. 3. colloquium on process simulation, Espoo, Finland, 11-14 Jun 1996, pp. 357.

Backman, Rainer, Hupa, Mikko, Söderhjelm, Liva, 1995, Liquor-to-liquor differences in combustion and gasification processes: alkali release and fume formation. *Journal of Aerosol Science*, Vol. 26, September 1995, pp. S681 - S682.

Backman, Rainer, Skrifars, Bengt-Johan, Hupa, Mikko, Siiskonen, Pentti and Mäntyniemi, Juha, 1995, Flue gas chemistry in recovery boilers with high levels of chlorine and potassium. Proceedings 1995 International Chemical Recovery Conference, Toronto, CPPA, pp. A95 – A103.

Backman, R., Frederick, W. J. and Hupa, M., 1993, Basic studies on black-liquor pyrolysis and char gasification. *Bioresource Technology*, Vol. 46, No. 1-2, pp. 153 - 158.

Backman, Rainer, Hupa, Mikko and Uppstu, Erik, 1987, Fouling and corrosion mechanisms in the recovery boiler superheater area. *Tappi Journal*, Vol. 70, No. 6, June 1987, pp. 85 - 89.

Backman, Rainer, Hupa, Mikko and Uusikartano Timo, 1985, Kinetics of sulphation of sodium carbonate in flue gases. Proceedings of 1985 International Chemical Recovery Conference, New Orleans, Louisiana, Book 3, pp. 445 - 450.

Backman, Rainer, Hupa, Mikko and Hyöty, Paavo, 1984, Corrosion relating to acidic sulfates in kraft and sodium sulfite recovery boilers. *Tappi Journal*, Vol. 67, No. 12, December 1984, pp. 60 - 64.

Barynin, J. A. and Dickinson, J. A., 1985, Considerations for the uprating of recovery boilers. Proceedings of 1985 International Chemical Recovery Conference, New Orleans, Louisiana, Book 1, pp. 49 – 53.

Bauer, Donald G. and Sharp, W. B. A., 1991, The inspection of recovery boilers to detect factors that cause critical leaks. *Tappi Journal*, Vol. 74, No. 9, September 1991, pp. 92 - 100.

Baxter, Larry, Hatch, Greg, Sinquefield, Scott A. and Frederick, Wm. James, 2004, An experimental study of the mechanisms of fine particle deposition in kraft recovery boilers. Proceedings of 2004 International Chemical Recovery Conference, June 6-10 2004, Charleston, South Carolina, USA, pp. 393 - 412.

Baxter, Larry, Lind, Terttaliisa, Rumminger, Marc and Kauppinen, Esko, 2001, Particle size distributions in recovery boilers. Proceedings of 2001 International Chemical Recovery Conference, June 11-14, 2001, Whistler (BC), Canada, pp. 65 - 69.

Berglin, Niklas and Berntsson, Tore, 1998, CHP in the pulp industry using black liquor gasification: thermodynamic analysis. *Applied Thermal Engineering*, Vol. 18, No. 11, November 1998, pp. 947 - 961.

Bergman, Jan and Hjalmarsson, Lennart, 1992, Rotafire – a new recovery boiler operation concept. Proceedings of 1992 International Chemical Recovery Conference, Seattle, Washington, June 7-11, pp. 35 - 43.

Bergroth, Nici, 2004, Char bed processes in a kraft recovery boiler – A CFD based study. M. Sc.

thesis, Åbo Akademi, Kemisk-Tekniska Fakulteten Processkemiska Centret, Report 04-2, 149 p. ISBN 952-12-1331-0.

Bernath, P., Sinquefield, S. A., Baxter, L. L., Sclippa, G., Rohlfing, C. and Barfield, M., 1996, In situ analysis of ash deposits from black liquor combustion. 26. International symposium on combustion, Naples (Italy), 28 Jul - 2 Aug, 1996, 24 p.

Bhattacharya, P. K., Parthiban, V. and Kunzru, D., 1986, *Indian Engineering Chemical Process Design and Development*, Vol. 25, p. 420.

Björklund, Henry, Warnquist, Björn and Pettersson, Bertil, 1991, Inside a kraft recovery boiler - combustion of high-sulphidity black liquor at high dry solids. *Pulp & Paper Canada*, Vol. 92, No. 8. pp. T206 - 208.

Björklund, Henry, 1963, Synpunkter på olika väggkonstruktioner för sodahusaggregat. (Viewpoints of different wall constructions for recovery plants) in Swedish, Sodahuskonferens 1963, ÅF-IPK, Stockholm, pp. A1 – A9.

Björkman, Anders and Warnquist, Björn, 1985, Basic processes in kraft liquor reductive gasification/burning. Proceedings of 1985 International Chemical Recovery Conference, New Orleans, Louisiana, Book 1, pp. 13 - 23.

Blackwell, Brian and Hastings, Calvin, 1992, Simple mathematical analysis of air jets in recovery and power boilers. *Paperi ja Puu* (Paper and Timber), Vol. 74, No. 3, pp. 216 – 222.

Blackwell, Brian and King, Tracy, 1985, Chemical reactions in kraft recovery boilers. Sandwell and Company Ltd. 206 p.

Blokh, A. G., 1988, Heat transfer in steam boiler furnaces, Hemisphere Publishing Corporation, 283 p. ISBN 0-89116-626-2.

Blough, J. L., Seitz, W. W. and Girshik, A., 1998, Fireside corrosion testing of candidate superheater tube alloys, coatings, and claddings - Phase 2 field testing. Technical report, ORNL/Sub-93-SM401/02, Oak Ridge National Lab., TN, United States, 75 p.

Blue, Jerry D., Heiner, Larry A. and Wessel, Richard A., 2000, Advanced combustion and flow modeling: comprehensive model study improves recovery boiler operation. *Tappi Journal*, Vol. 83, No. 7, July 2000, 13 p.

Boiler plant handbook, 1968, Sulzer Brothers Limited, Switzerland, 163 p.

Boniface, Arthur, 1985, Introduction. in Chemical recovery in alkaline pulping processes, editor Hough, Gerald, Tappi Press, Atlanta, pp. 1 – 7. ISBN 0-89852-046-0.

Boonsongsup, L., Iisa, K., Frederick, W. J. and Hiner, L., 1994, SO_2 capture and HCl release at kraft recovery boiler conditions. *AIChE Symp. Ser.*, Vol. 90, No. 302, pp. 39 – 45.

Borg, A., Teder, A. and Warnquist, Björn, 1973, Inside a kraft recovery furnace - studies on the origins of sulfur and sodium emission. *Tappi Journal*, Vol. 57, No. 1, pp. 126 - 129.

Borg, A., Nilsson, C., Teder, A. and Warnquist, B., 1974, Process betingelsernas inverkan på emissionen från sodahusaggregatet. (Effect of process conditions to recovery boiler sulfur emissions) *STFI Meddelande*, serie B nr. 203 (MA B:40).

Bosch, J. C., 1971, *Tappi Journal*, Vol. 54, p. 1871.

Boström, Curt-Åke, 1990. Aktuellt om massaindustrins NOx utsläpp. (News of pulp industry NOx emissions) in Swedish, Sodahuskonferenssen 1990, ÅF-IPK, Stockholm, pp. 103 -108.

Brandt, Fritz, 1999, Dampferzeurger, kesselsysteme energiebilanz stömungstechnik. (Steam generators, boiler systems, energy balances, fluid mechanics) in German, Vulkan-Verlag, Essen, 283 p. ISBN 3-8027-3504-8.

Brandt, Fritz, 1985, Wärmeübertragung in dampferzeugern und wärme-austauschern, (Heat transfer in steam boilers and heat exchangers) in German, Vulkan-Verlag, Essen, 281 p. ISBN 3-8027-2274-4.

Brown, Craig A., Grace, Thomas P., Lien, Steve J. and Clay, David T., 1989, Char bed burning rates - experimental results. *Tappi Journal*, Vol. 72, No. 12, December 1989, pp. 175 - 181.

Brink, Anders, Coda Zabetta, Edgardo, Hupa, Mikko and Saviharju, Kari, 2004, NOx chemistry in recovery boilers under staging conditions. Proceedings of 2004 International Chemical Recovery Conference, June 6-10, 2004, Charleston, South Carolina, USA, 491-501 p.

Briscoe, B., Nichol, M., Blackwell, Brian, Brewis, K. and MacCallum, C., 1991, Application of modern recovery boiler instrumentation.

Bruce, D. and Van der Vooren, T., 2003, Trends in air emission limits for world class mill. *Pulp & Paper Canada*, Vol. 104, No. 7, July 2003, pp. 51 - 54.

Bruno, Fredrik, 2003, Corrosion as a cause for recovery boiler damages. *Pulp & Paper Canada*, Vol. 104, No. 6, June 2003, pp. T 143 - 151.

Bruno, Fredrik, 1999, The significance of superheater tube corrosion on steam temperature on kraft recovery boilers. Proceedings 8th International Symposium on Corrosion in the Pulp & Paper Industry, Stockholm, Sweden, May 16-19, Swedish Corrosion Institute, pp. 138 – 149.

Bruno, Fredrik, 1999, On the influence of

chlorides and sulphurous compounds on the corrosion of superheater tubes in boilers with special consideration on kraft recovery boilers. Technical Report, SVF-664, Värmeforsk Service AB. 36 p.

Bruno, Frederick and Hägerström, Joachim, 1998, Skador på sodapannor i Sverige 97-98. (Incidents at Swedish recovery boilers 97-98) in Swedish, Sodahuskonferens 1998, ÅF-IPK, Stockholm, pp. 33 – 55.

Bunton, Mark A. and Moskal, Thomas E., 1995, Increasing boiler efficiency through sootblower optimization. Proceedings of 1995 TAPPI Engineering Conference, Dallas, Texas, Book 2, pp. 706 - 705.

Burton, Dave, 2000, Practical experiences with ABB recovery boilers. UEF Conference on Behavior of Inorganic Materials in Recovery Boilers, Bar Harbor, Maine, 4 - 9 June 2000. United Engineering Foundation, 28 p.

Bäckman, Kaj, Lindberg, Hans and Sjöberg, Hans, 1999, Recovery modernization at Stora Enso's Skutskär kraft mill. *Tappi Journal*, Vol. 82, No. 12, December 1999, pp. 90 - 98.

Cameron, John, 1998, *Chem. Eng. Comm.* Vol. 59, pp. 243 – 257.

Casale, F. S. and Friz, P. A., 1990, Start up and operation of a high-solids recovery boiler at S.D. Warren Company Westbrook, Maine. Proceedings of 1990 Engineering Conference, Tappi Press. pp. 687 - 688.

Chamberlain, R. E. and Cairns, C. E., 1972, Analysis of recovery unit operation and control. *Pulp and Paper Magazine of Canada*, Vol. 73, No. 1, pp. 97 - 104.

Chemical recovery in the alkaline pulping processes, 1985, a project of the Alkaline Pulping Committee of the Pulp Manufacture Division, editor Gerald Hough, Tappi Press.

Chemical recovery in the alkaline pulping processes, 1992, Prepared by the Alkaline Pulping Committee of the Pulp Manufacture Division, editors Green, Robert P. and Hough, Gerald, TAPPI PRESS. 196 p.

Churchill, S. W., 1972, Friction factor equation spans all fluid regimes. *Chemical Engineering*, November 1972, pp. 91 – 92.

Clay, David T., 1987, Fundamental studies in black liquor combustion. in Proceedings of the Black Liquor Research Program Review Fourth Meeting, editor Sobczynski, Stanley F., July 28- 30, Contract No. DE-AC01-87CE40762, pp. 177 - 225.

Clay, David T., Lien, Steve J., Grace, Thomas M., Macek, Andrej, Semerjian, Hratch G., Amin, N. and Charagundla, S. Rao, 1987, Fundamental studies in black liquor combustion. Report No. 2 - Phase I for the period October 1984 - November 1986, Contract No. AC02-83CE40637, DOE. 227 p.

Clement, Jack L., 1996, Black liquor firing presentation. Presented to: Black Liquor Recovery Boiler Advisory Committee, Spring 1996 Technical Session, April 3, 1996, Atlanta, Georgia, U.S.A.

Clement, Jack L., 1990, High pressure and temperature recovery boilers. Proceedings of Babcock & Wilcox, Pulp & Paper Seminar, February 12 – 14, 1990, Portland, Oregon, 7 p.

Clement, J. L., Hiner, L. A., Moyer, S. C., Cox, C. and Harris, R., 1995, Fundamental approach to black liquor combustion improves boiler operation. Proceedings of 1995 International Chemical Recovery Conference, Toronto Canada, CPPA, pp. A47 – A57.

Clement, Jack L. and Barna, Joan L., 1993, The effect of black liquor fuel-bound nitrogen on NOx emissions. Proceedings of 1993 Tappi Environmental Conference, Tappi Press, pp. 653 – 660.

Clement, J. L., Coulter, J. H. and Duda, S., 1963, B&W kraft recovery unit performance calculations. *Tappi Journal*, Vol. 46, No. 2, p. 153.

Coelho, P. J., 1999, An engineering model for the calculation of radiative heat transfer in the convection chamber of a utility boiler, *Journal of the Institute of Energy*, Vol. 72, pp. 117 – 126.

Colebrook, C. F., 1939, Turbulent flow in pipes with particular reference to the transition region between the smooth and rough pipe laws. *Journal of Institution Civil Engineers,* Vol. 11, 1938/39, pp. 133 – 156.

Collier, J. G., 1983, Boiling and evaporation, in Heat exchanger design handbook, HEDH, Part 2, Fluid mechanics and heat transfer, VDI, Düsseldorf, pp. 2.7.1 – 2.7.4-12. ISBN 3-18-419082-X.

Collin, Rolf and Vaclavinec, Jiri, 1989, Injection of secondary and tertiary air in the spent kraft liquor recovery boiler – model study. The midnight sun colloquium on recovery research, June 14 - 16 1989, STFi, pp. 86 - 96.

Combustion Engineering A reference book on fuel burning and steam generation, 1949, editor de Lorenzi, Otto, Combustion Engineering – Superheater, Inc, New York.

Combustion fossil power, 1991, 4th edition, editor Singer, Joseph G., Asea Brown Boveri, 977 p. ISBN 0-9605974-0-9.

Combustion fossil power, 1981, 3rd edition, editor Singer, Joseph G., Combustion Engineering Inc., 866 p. ISBN 0-9605974.

Compilation of "air toxics" emission data for boilers, pulp mills, and bleach plants, 1993, *NCASI Technical Bulletin* No. 650, National Council of the Paper Industry for Air and Stream Improvement,

New York, NY, June 1990, 128 p.

Consonni, Stefano and Larson, Eric and Katofsky, Ryan E., 2003, Integration issues, performances estimates and environmental benefits of black liquor gasification combined cycles for the pulp & paper industry. Colloquium of black liquor combustion and gasification, Park City, Utah, 13-16 May 2003, 14 p.

Costa, A. O. S., Biscaia, Jr. E. C. and Lima, E. L., 2004, Mathematical description of the kraft recovery boiler furnace. *Computers & Chemical Engineering*, Vol. 28, No. 5, May 2004, pp. 633 – 641.

Crawford, Robert J. and Jain, Ashok K., 2002, Effect of stripper off-gas burning on NOx emissions. *Tappi Journal*, Vol. 85, No. 1, January 2002, 6 p.

Dahlbom, Johan, 2003, Effects of non process elements in the chemical recovery system of a kraft pulp mill from the incineration in the recovery boiler of biological sludge. (Effekter av PFG vid indunstning och förbränning av bioslam i ett massabruks sodapanna) in Swedish, Report Number SVF-798, Project Värmeforsk-S2-226, 42 p.

Darmstad, W. J., Wangerin, D. D. and West, P. H., 1968, Combustion of black liquor. Chapter 3 of Chemical recovery in alkaline pulping process, editor Whitney, Roy P., *TAPPI Monograph series,* No. 32, Mack Printing Company, Easton, Pa., pp. 59 – 99.

Deeley, E. and Kirkby, A. H., 1967, The development of chemical recovery boiler. *Journal of the Institute of Fuel*, September 1967, pp. 417 – 424.

DeMartini, Nikolai, Forssén, Mikael, Niemelä, Klaus, Samuelsson, Åsa and Hupa, Mikko, 2004, Release of nitrogen species from the recovery processes of three kraft pulp mills. *Tappi Journal*, Vol. 3, No. 10, October 2004, pp. 3 - 8.

Demirbaş, Ayhan, 2001, Pyrolysis and steam gasification processes of black liquor. *Energy Conversion and Management*, Vol. 43, No. 7, pp. 877 - 884.

Dickinson, James A., Hiner, Larry A. and Wessel, Richard A., 2000, practical solutions to improving recovery boiler operation. UEF Conference on Behavior of Inorganic Materials in Recovery Boilers, Bar Harbor, Maine, 4 - 9 June 2000. United Engineering Foundation, 15 p.

Directive 2000/76/EC of the European Parliament and of the Council of 4 December 2000 on the incineration of waste. 21 p.

Doležal, Richard, 1967, Large boiler furnaces, Elsevier Publishing Company, 394 p.

Doležal, Richard, 1985, Dampferzeugung: verbrennung, feuerung, dampferzeuger, (Steam generation, combustion, firing, steam boilers) in German, Springer Verlag, Berlin, 362 p. ISBN 3-540-13771-8.

Dombrowski, N. and Johns, W. R., 1963, *Chem. Eng. Sci.*, Vol. 18, pp. 203 - 214.

Donovan, Joe and Brown, Robert, 2003, BLG: Implications for the industrial gases industry. Colloquium of black liquor combustion and gasification, Park City, Utah, 13-16 May 2003, 14 p.

Duhamel, Melanie, Tran, Honghi and Frederick, W. James Jr., 2004, The sintering tendency of recovery boiler precipitator dust. *Tappi Journal*, Vol. 3, No. 10, October 2004, pp. 25 - 29.

Edling, Gustaf, 1937, Några synpunkter beträffande sodahus av olika system. (Some observations concerning different types of recovery) in Swedish, presented in the Swedish Paper and Pulpengineer's winter meeting 6th march 1937, in Sodahuset 1930 – 1945, Ångpannaföreningen, Stockholm, pp. 27 - 36 p.

Edling, Gustaf, 1981, Tekniken i Svenska sodahus 1870 – 1935. Sodahuskonferenssen, Svensk Papperstidning, No. 6, pp. 19 – 26.

Edling, Gustaf, 1983, Sodahuset 1930 – 1945. Ångpannaföreningen, Stockholm, 77 p.

Edwards, Louis L., Shiang, Niann T., Damon, Robert and Strothmann, Brian, 1986, Kraft recovery furnace capacity and efficiency improvement. *Nordic Pulp and Paper Research Journal*, No. 2, pp. 18 - 23.

Effenberger, Helmut, 2000, Dampferzeugung. (Steam boilers) in German, Springer Verlag, Berlin, 852 p. ISBN 3-540-64175-0.

Eilersson, Thomas, Leijonberg, Anders and Praszkier, Paul, 1995, Black liquor recovery boiler superheater gas side corrosion. Proceedings of 8th International Symposium on Corrosion in the Pulp & Paper Industry, Stockholm, Sweden, May 16-19, Swedish Corrosion Institute, pp. 158 – 164.

Empie, Jeff H., Lien, Steven J., Yang, Wen Rui and Adams, Terry N., 1992, Spraying characteristics of commercial black liquor nozzles. Proceedings of 1992 International Chemical Recovery Conference, Seattle, Washington, June 7-11, pp. 429 - 440.

Empie, H.J., Lien, S. J., Yang, W. and Samuels, D. B., 1995, Effect of black liquor type on droplet formation from commercial spray nozzles. *Journal of Pulp and Paper Science*, Vol. 21, No. 2, pp. J63 – J67.

Environmental pollution control pulp and paper industry part 1 Air, 1976, U.S. Environmental protection agency, Technology Transfer, Prepared October 1976, by EKONO Inc. and EKONO Oy, 260 p.

Environmental report statistics for 2001, 2002, editors Sieppi, Susanna and Heino, Petri, Finnish Forest Industries Federation, Kirjapaino Oy West Point, Rauma, 6.2002, ISSN 1236–1097.

Eriksson, Thomas and Falk, Ivan, 1999, Överhettarmaterial för energi-effectivare, miljövänligare och bränsleflexiblare sodahus och barkpannor. (Superheater materials for better energy efficiency, lower emissions and better fuel flexibility in recovery and bark boilers) in Swedish, Studsvik Material AB, S6-615, Värmeforsk Service AB. 47 p.

Ernola, P., Hupa, Mikko, Kjäldman, Lars and Oksanen, P., 1989, Detailed modelling of NOx emissions in fuel staging. Åbo Akademi, Department of Chemical Engineering, Combustion Chemistry Research Group, Report 89 - 9. 16 p.

Eskola, Arkke, Jokiniemi, Jorma, Vakkilainen, Esa and Lehtinen, Kari, 1998, Modelling alkali salt deposition on kraft recovery boiler heat exchangers in the superheater section. Proceedings of 1998 International Chemical Recovery Conference, Tampa, USA, 1 - 4 June 1998, Vol. 3, TAPPI, pp. 469 – 486.

Eskola, Arkke, Jokiniemi, Jorma, Pyykönen, Jouni and Lehtinen, Kari, 1997, Modelling alkali-vapour/particle deposition on cooled surfaces. Proceedings of 1997 European Aerosol Conference. Hamburg 15 - 19 Sept. 1997, *Journal of Aerosol Science*, Vol. 28, No. S1, pp. 453 - 454

Fakhrai, Reza, 1999, Modelling of carry-over in recovery furnaces. Lic. Tech. thesis, Dept. of Metallurgy, Royal Inst. of Tech., Stockholm, Sweden, 68p.

Falat, Lad, 1996, Mechanism and prevention of localized corrosion of recovery boiler tubes at air ports. *Tappi Journal*, Vol. 79, No. 2, February 1996, pp. 175 -185.

Ferguson, Kelly H., 1991, L-P Samoa mill improves air quality with recovery island modernization. *Pulp & Paper*, September, pp. 180 - 185.

Ferreira, Licínio Manuel G. A., Soares, Micaela A. R., Egas, Ana Paula V. and Castro, José Almiro A. M., 2003, Remoção seletiva de cloreto e potássio em fábricas de cellulose kraft. (Selective removal of chloride and potassium in kraft pulp mills) in Portuguese, *O Papel / Tappi Journal*, Vol. 3, No. 1, July 2003, pp. 13 – 20.

La Fond, John, F., Jansen, Johan H. and Eide, Perry, 1994, Upgraded recovery boiler meets low air emissions standards. *Tappi Journal*, Vol. 77, No. 12, December 1994, pp. 75 - 80.

La Fond, John F., Verloop, Arie and Jansen, Johan H., 1993, Recovery boiler fireside capacity: an update of theory and practice. *Tappi Journal*, Vol. 76, No. 9, September 1993, pp. 107 – 113.

La Fond, John F., Verloop, Arie and Walsh, Alan R., 1992, Engineering analysis of recovery boiler superheater corrosion. *Tappi Journal*, Vol. 75, No. 6, June 1992, pp. 101 - 106.

Forssén, Mikael, Backman, Rainer, Wallén, Jonas and Hupa, Mikko, 2000a, Flygaskans sammansättning och nedsmutsande tendens i sodapannan. (Flue gas dust composition and fouling tendency in recovery boilers) in Swedish, SVF-680, Technical Report, Värmeforsk, Stockholm, Sweden, Project Värmeforsk-S6-612, S9-804, ISSN 0282-3772, 78 p.

Forssén, Mikael, Kilpinen, Pia and Hupa, Mikko, 2000b, NOx reduction in black liquor combustion - reaction mechanisms reveal novel operational strategy options. *Tappi Journal*, Vol. 83, No. 6, June 2000, 13 p.

Forssén, Mikael, Hupa, Mikko and Hellström, Peter, 1997, Liquor-to-liquor differences in combustion and gasification processes: Nitrogen oxide formation tendency. *Tappi Journal*, Vol. 82, No. 3, March 1999, pp. 221 - 227.

Forssén, Mikael, Frederick, W. J., Hupa, Mikko and Hyöty, Paavo, 1992, Sulfur release during pyrolysis from single black liquor droplets. AIChE 1991 Forest Products Symposium Proceedings, Tappi Press, Atlanta, pp. 11 – 22.

Frederick, Laurie, Singbeil, Doug and Kish, Joey, 2003, Red hot video of combusting liquor & smelt at primary airports. Proceedings of Colloquium of black liquor combustion and gasification, Park City, Utah, 13-16 May 2003, 9 p.

Frederick, Wm James Jr., Iisa, Kristiina, Sinquefield, Scott A. and Sricharoenchaikul, Viboon, 2004, The role and fate of alkali metals in black liquor combustion. 40th Anniversary International Recovery Boiler Conference, Finnish Recovery Boiler Committee, Haikko Manor, Porvoo, May 12-14, 2004, pp. 43 – 49.

Frederick, Wm. James, Ling, Alisa, Tran, Honghi N. and Lien, Steven J., 2004, Mechanisms of sintering of alkali metal salt aerosol deposits in recovery boilers. *Fuel*, Vol. 18, No. 83, pp. 1659 – 1664.

Frederick, Wm. J. Jr. and Vakkilainen, E. K., 2003, Sintering and structure development in alkali metal salt deposits formed in kraft recovery boilers. *Energy & Fuels*, Vol. 17, No. 6, November 2003, pp. 1501-1509.

Frederick, W. J., Lien, S., Vakkilainen, E. K. and Tran, H., 2001, A method to predict the conditions for boiler bank plugging by sub-micron sodium salt (fume) particles. Proceedings of 2001 International Chemical Recovery Conference, June 11-14, 2001, Whistler (BC), Canada, pp. 311 - 322.

Frederick, W. J. Jr., Dent, Gary and Vakki-

lainen, Esa, 1998, Effects of temperature and SO_2 on chloride and potassium enrichment factors in kraft recovery boilers. Proceedings of 1998 International Chemical Recovery Conference June 1 - 4, Hyatt Westshore, Tampa, Fl, pp. 945 - 954.

Frederick, W. J., Reis, V. V., Wag, K. J. and Iisa, K., 1995, A laboratory study of alkali metal salt aerosol formation in black liquor combustion. *Journal of Aerosol Science*, Vol. 26, September 1995, pp. S693 - S694.

Frederick, W. J., Iisa, K., Wag, K., Reis, V. V., Boonsongsup, L., Forssen, M. and Hupa, M., 1995, Sodium and sulfur release and recapture during black liquor burning. DOE/CE/40936-T2, Oregon State University, Corvallis, OR, United States, 225 p.

Frederick, William J. and Hupa, Mikko, 1993, Combustion properties of kraft black liquors. Åbo Akademi, Department of Chemical Engineering, Report 93-3. 112 p.

Frederick, William J. and Hupa, Mikko, 1992, The effect of swelling on droplet trajectories, carbon burn out, and entrainment in black liquor combustion. Proceedings of 1991 Forest Products Symposium, November 17-22, 1991, Los Angeles, California, Tappi Press, pp. 79 – 89.

Frederick, W. J., Krishnan, R. and Ayers, R. J., 1990, Pirssonite deposits in green liquor processing. *Tappi Journal*, Vol. 73, No. 2, pp. 135-140.

Frederick, William J., 1990, Combustion processes in black liquor recovery: Analysis and interpretation of combustion rate data and an engineering design model, Report no. One. Contract no. AC02-83CE40637, U.S. Department of Energy, DOE/CE/40637-T8. 130 p.

Frederick, William J, Noopila, Taina and Hupa, Mikko, 1989, Modelling of black liquor droplet combustion. Soodakattilapäivä, Helsinki, 19 p.

Fricke, A. L., 1987, Physical properties of kraft black liquors: Interim report Phase II, report No. DOE/CE 40606-T5 (DE88002991), U.S. Dept. of Energy, Washington, 1987, 66 p.

Friedlander, S. K., 1977, Smoke Dust and Haze, John Wiley & Sons, New York. 317 p. ISBN 0-471-01468-0.

Froste, H., 1996, Volatile organic compounds and oxides of nitrogen - Further emission reductions. Technical Report, SNV-4689, Swedish Environmental Protection Agency, Stockholm Sweden, ISSN 0282-7298. 109 p.

Fryling, Glenn R., 1967, Combustion engineering, A reference book on fuel burning and steam generation. 2nd edition, The Riverside Press, Cambridge, Massachusetts, 831 p.

Fujisaki, Akihiro, Tateishi, Masakazu, Baba, Yoshitaka and Arakawa, Yoshisa, 2003, Plugging prevention of recovery boiler by character improvement of the ash which used potassium removal equipment (Part II). *Pulp & Paper Canada*, Vol. 104, No. 1, pp. T1 – T3.

Fujisaki, Akihiro, Takatsuka, Hiromu and Yamamura, Misao, 1992, World's largest high pressure and temperature recovery boiler. Proceedings of 1992 International Chemical Recovery Conference, Seattle, Washington, June 7-11, pp. 1 – 20.

Given, P. H. et al., 1986, Calculation of calorific values of coals from ultimate analysis: Theoretical basis and geographical implications. *Fuel*, June 1986, Vol. 65, No. 6, pp. 849 - 854.

Goerg-Wood, Kristin and Cameron, John H., 1998, Fume deposition with kraft recovery boiler implications. Innovative advances in the forest products industry, the 1997 Forest Products Symposium, editor Brogdon, Brian N., New York, American Institute of Chemical Engineers, *AIChE symposium series* 319, Vol. 94, pp.138 – 145.

Grabke, H. J., Reese, E. and Spigel, M., 1995, The effects of chlorides, hydrogen chloride, and sulfur dioxide in the oxidation of steels below deposits. *Corrosion Science*, Vol. 37, No. 7, pp. 1023 – 1043.

Grace, Thomas M., 2004, A review of char bed processes (What goes on in the char bed). 40th Anniversary International Recovery Boiler Conference, Finnish Recovery Boiler Committee, Haikko Manor, Porvoo, May 12-14, 2004, pp. 21 – 29.

Grace, Thomas M., 2001, A review of char bed combustion. Proceedings of 2001 International Chemical Recovery Conference, June 11-14, 2001, Whistler (BC), Canada, pp. 213 - 220.

Grace, Thomas M., 1997, Char bed process. Chapter 6 in Kraft recovery boilers, AF&PA, TAPPI PRESS, Atlanta, 381 p. ISBN 0-9625985-9-3.

Grace, Thomas M. and Timmer, William M., 1995, A comparison of alternative black liquor recovery technologies. Proceedings of 1995 International Chemical Recovery Conference, Toronto Canada, CPPA, pp. B269 - B275.

Grace, Thomas M., 1990, Char bed burning. Kraft Chemical Recovery, University Center, May 14, 1990.

Grace, Thomas M., Cameron, J. H. and Clay, David T., 1989, Role of the sulfate/sulfide cycle in char burning - experimental results and implications. TAPPI Kraft Recovery Operations Seminar, pp. 159 - 167.

Grace, Thomas M., Cameron, J. H. and Clay, David T., 1988, Role of the sulfate/sulfide cycle in char burning - experimental results and implications. TAPPI Kraft Recovery Operations Seminar,

pp. 157 - 165.

Grace, Thomas M., Cameron, J. H. and Clay, David T., 1985, Role of the sulfate/sulfide cycle in char burning - experimental results and implications. Proceedings of 1985 International Chemical Recovery Conference, New Orleans, Louisiana, Book 3, pp. 371 - 379.

Green, Robert P. and Grace, Thomas M., 1984, A method for calculating the composition and heating value of black liquors from kraft and polysulfide pulping. *Tappi Journal*, June 1984, pp. 94 - 98.

Greenwood, Larry D., Ip, Trevor, Dhak, Janice, Kennard, Gary E., Towers, Michael T., Karidio, Ibrahim, Uloth, Vic C. and Weiss, Klaus, 2000, Reverse superheater fouling in the Al-Pac recovery boiler. Proceedings of 2000 Tappi Engineering Conference, TAPPI Press, Atlanta, 19.

Grönblad, Kjell and Sandegård, Ragnar, 2000, Ombyggnad av sodapanna SP-7 i Skutskär. (Rebuild of recovery boiler SP-7 in Skutskär) in Swedish, Sodahuskonferens, ÅF-IPK, Stockholm, pp. 53 – 62.

Gullichsen, Johan, 1968, Heat values of pulping spent liquors. Proceedings of the Symposium on Recovery of Pulping Chemicals, Helsinki, The Finnish Pulp and Paper Research Institute and Ekono, pp. 211 - 234.

Görner, Von K., 1986, Strömungsvorgänge in feuerräumen von dampferzeugern. (Flow prediction in steam boiler furnaces) in German, *VGB Krafrtwerkstechnik*, Vol. 66, No. 3, March 1986, pp. 224 – 233.

Harila, Pauli, 1993, Biolietteen käsittely, mustalipeän superväkevöinti ja hajukaasujen poltto soodakattilassa. (Biosludge treatment, super-concentration of black liquor and NCG burning in recovery boiler) in Finnish, Report 19.10.1993, Oy Metsä-Botnia Ab, Kemi mill, 10 p.

Harms, T. E., Haynes, Jim B. and Edwards, Louis L., 1990, Evaluation of process alternatives to improve recovery boiler performance. *Pulp & Paper Canada*, Vol. 91, No. 7, pp. T267 - T270

Harrison, Ray E. and Ariessohn, Peter C., 1985, Application of a smelt bed imaging system. Proceedings of 1985 TAPPI International Chemical Recovery Conference, pp. 153 - 158.

Hausen, H., 1974, Erweiterte gleichung für den wärmeübergang bei turbulenter strömung. (Expanded equation for heat transfer in turbulent flow) in German, *Wärme- und Stoffübertragung*, Vol. 7, pp. 222 – 225.

Haynes, Jim B., Adams, Terry N. and Edwards, Lou L., 1988, Recovery boiler thermal performance. Proceedings of 1988 Tappi Engineering Conference, Book 2, pp. 355 - 367.

Heinävaara, Antero, 1991, Recovery boiler analysis. Ahlstrom Machinery, Internal report.

Hellström, Bengt, 1982, En-doms sodapanna. (Single-drum recovery boiler) in Swedish, Sodahuskonferensen ‘82, ÅF-IPK, Stockholm, pp. 133 – 135.

Hellström, Bengt, 1977, Styr sodapannans lufttillförsel. *Kemisk Tidskrift*, No. 9, pp. 112 - 114.

Hellström, O., 1970, Rapport från verksamheten inom den amerikanska kommittén för sodahusfrågor (BLRBAC) under 1970. (Report of action in the american committee for recovery boiler questions (BLRBAC) in 1970) in Swedish, Sodahuskonferens 1970, ÅF-IPK, Stockholm, pp. A1 – A15.

Helpiö, Tomi and Kankkunen, Ari, 1995, The effect of black liquor firing temperature on atomization performance. Proceedings of 1995 TAPPI Engineering Conference, Dallas, 11 - 15 September, pp. 717 - 722.

Helpiö, T. and Kankkunen, A., 1995b, Measurements of the Effect of Black Liquor Firing Temperature on Atomization Performance, Part 2: Drop Size Distributions, Helsinki University of Technology, Laboratory of Energy Engineering and Environmental Protection. 34 p.

Helpiö, T. and Kankkunen, A., 1994, Measurements of the Effect of Black Liquor Firing Temperature on Atomization Performance, Part 1: Nozzle Flow Properties and Sheet Breakup. Helsinki University of Technology, Laboratory of Energy Engineering and Environmental Protection.

Henderson, Pamela, Kjörk, Anders, Ljung, Per, Nyström, Olle and Skog, Erik, 2000, Överhettarkorrosion i bioeldade anläggningar – status. (Superheater corrosion in combustion of biofuels - a status) in Swedish, Technical report, SVF-700, Värmeforsk Service AB. 36 p.

Himmelblau, David M., 1989, Basic principles and calculations in chemical engineering. 5th edition, Prentice-Hall International Series in the Physical and Chemical Engineering Sciences.

Hills, Richard L., 1989, Power from steam. Cambridge University press, 338 p. ISBN 0 521 34356 9.

Hiner, L.A., 1994, Kraft Recovery Boiler Operation for Control of Ash Chemistry. Proceedings of 1994 TAPPI Engineering Conference, Press, Atlanta, GA, p.179 - 186.

Hochmuth, Frank W., 1953, New developments in recovery unit design. *Tappi Journal*, Vol. 36, No. 8, p. 359.

Hoddenbagh, J. M. A., Wilfing, K., Miller, K., Hardman, D., Tran, H. and Bair, C., 2002, Borate autocausticizing: a cost effective technology. *Pulp & Paper Canada*, Vol. 103, No. 11, November

2002, T283 – T288.

Hogan, Edward F., 1999, Investigation of chemical recovery unit floor tube overheat failures. *Tappi Journal*, Vol. 82, No. 2, February 1999, pp. 130 - 137.

Holcomb, Gordon R., 2001, Synergistic air port corrosion in kraft recovery boilers. *Tappi Journal*, Vol. 84, No. 8, August 2001, pp. 35 - 37.

Holmlund, Karl and Parviainen, Kari, 2000, Evaporation of black liquor. Chapter 12 in Chemical Pulping, Book 6, series editors Gullichsen, Johan and Fogelholm, Carl-Johan, Finnish Paper Engineers' Association and TAPPI. ISBN 952-5216-06-3.

Hood, Kenneth T. and Henningsen, Gunnar B., 2002, Black liquor gasification: evaluation of past experience in order to define the roadmap of the future pathway. Proceedings of 2002 TAPPI Fall Technical Conference, September 8 - 11, San Diego, Ca, 17 p.

Hooper, William B., 1984, The two-K method predicts head losses in pipes and fittings. *Chemical Engineering*, August 24, pp. 96 – 100.

Horton, Robert R. and Vakkilainen, Esa K., 1993, Comparison of simulation results and field measurements of an operating recovery boiler. Proceedings of 1993 TAPPI Engineering Conference, Orlando, September, pp. 20 - 23.

Horton, Robert R., Grace, Thomas M. and Adams, Terry N., 1992, The effect of black liquor spray parameters on combustion behaviour in recovery furnace simulations. Proceedings of 1992 International Chemical Recovery Conference, Seattle, Washington, June 7-11, pp. 85 - 99.

Horton, Robert R., 1991, In-flight black liquor combustion modelling. in Black liquor chemical recovery research, Program review meeting, Weyerhaeuser Technology Center, Tacoma, Washington, April 8-9, 15 p.

Horton, Robert R., 1991b, Computer simulation of black liquor combustion. DOE Annual Report on Recovery Furnace Modeling, September.

Huhtinen, Markku, Kettunen, Arto, Nurminen, Pasi and Pakkanen, Heikki, 1999, höyrykattilatekniikka. (Steam boiler technology) in Finnish, EDITA, Helsinki, 316 p. ISBN 951-37-1327-X. 1.

Hultin, Sven O., 1968, Physical properties of Finnish sulphite liquors and black liquors. Proceedings of the Symposium on Recovery of Pulping Chemicals, Helsinki, The Finnish Pulp and Paper Research Institute and Ekono, pp. 167 - 182.

Hupa, Mikko, 2004, Research highlights in recovery boiler chemistry. 40th Anniversary International Recovery Boiler Conference, Finnish Recovery Boiler Committee, Haikko Manor, Porvoo, May 12-14, 2004, pp. 125 – 132.

Hupa, Mikko, Backman, Rainer and Frederick, William J., 1994, Black liquor combustion properties. 30 Years Recovery Boiler Co-operation in Finland, International conference, Baltic sea, 24 - 26 May, pp. 37 - 60.

Hupa, Mikko, 1993, Recovery boiler chemistry – the picture becomes sharper. *Paperi ja Puu*, Vol. 75, No. 5, pp. 310 – 319.

Hupa, Mikko, Backman, Rainer, Skrifvars, Bengt-Johan and Hyöty, Paavo, 1990, The influence of chlorides on the fireside behavior in the recovery boiler. *Tappi Journal*, Vol. 73, No. 6, June 1990, pp. 153 - 158.

Hupa, Mikko, 1989, Recovery boiler chemistry. Kraft Recovery Operations Seminar, Tappi Press, pp. 153 - 158.

Hupa, Mikko, Skrifvars, Bengt-Johan and Moilanen, A., 1989, Measuring the ash sintering tendency by a laboratory method. *Journal of the Institute of Energy*, September, pp. 131 – 137.

Hupa, Mikko and Solin, P., 1985, Combustion behavior of black liquor droplets. Proceedings of 1995 International Chemical Recovery Conference, New Orleans, Louisiana. Book 3, pp. 335 - 344.

Hyöty, Paavo, 1994, The history of recovery boiler. 30 Years Recovery Boiler Co-operation in Finland, International conference, Baltic sea, 24 - 26 May, pp. 9 - 22.

Hyöty, Paavo A. and Ojala, Sakari T., 1987, Super combustion of black liquor. Proceedings of 1987 Tappi Engineering Conference, pp. 49 – 53.

Hänninen, Hannu, Tiitinen, Eero, Tanaka, Toshi and Kiesi, Timo, 2003, Soodakattila tulevaisuudessa – Japanin matkakertomus. (Recovery boilers of future – Trip to Japan) in Finnish, Finnish recovery boiler committee, Lipeätyöryhmä, 84 p.

Hänninen, Hannu, 1994, Cracking and corrosion problems in black liquor recovery boilers. 30 Years Recovery Boiler Co-operation in Finland. International conference, Baltic sea, 24 - 26 May, pp. 121 - 132.

Ibah, Sheldon, 1995, Conversion to high solids firing. Proceedings of 1995 International Chemical Recovery Conference, Toronto Canada, CPPA, pp. A173 – A180.

Iisa, Kristiina, 2004, A comparison of the sulfation rates of different fume species in recovery boilers. Proceedings of 2004 International Chemical Recovery Conference, June 6-10 2004, Charleston, South Carolina, USA, 1043-1057 p.

Iisa, Kristiina, 2004, Emissions of trace elements from recovery boilers. 40th Anniversary

International Recovery Boiler Conference, Finnish Recovery Boiler Committee, Haikko Manor, Porvoo, May 12-14, 2004, pp. 115 – 124.

Iisa, Kristiina, Horenziak, Steven A. and Jing, Qun, 2000, Release of sulfur during gasification of black liquor in CO_2 atmospheres. UEF Conference on Behavior of Inorganic Materials in Recovery Boilers, Bar Harbor, Maine, 4 - 9 June 2000, United Engineering Foundation, 10 p.

Iisa, Kristiina and Jing, Qun, 2000, Effect of liquor composition on potassium and chloride enrichment. UEF Conference on Behavior of Inorganic Materials in Recovery Boilers, Bar Harbor, Maine, 4 - 9 June 2000, United Engineering Foundation, 10 p.

Im, K. H. and Chung, P. M., 1993, Particulate Deposition from Turbulent Parallel Streams. *AIChE J*., Vol. 29, No. 3, p. 498.

Incropera, Frank P. and DeWitt, David P., 1996, Fundamentals of Heat and Mass Transfer. 4th edition. John Wiley & Sons. ISBN 0-471-30460-3.

Integrated pollution prevention and control (IPPC), reference document on best available techniques in the pulp and paper industry, 2001, European Commission, European Integrated Pollution Prevention and Control Bureau, December 2001, 475 p. http://eippcb.jrc.es/pages/FActivities.htm.

Ishigai, Seikan, 1999, Historical development of strategy for steam power. in Steam Power Engineering, editor Ishigai, Seikan, Cambridge University Press, 394 p. ISBN 0 521 62635 8.

Israel, R. and Rosner, D.E., 1983, Use of generalized Stokes number to determine the aerodynamic capture efficiency of non-Stokesian particles from a compressible gas flow. *Aerosol Sci. Technol.* (AAAR), Vol. 2, pp. 45 – 51.

Jameel, M. I., Cormack, Donald E., Tran, Honghi and Moskal, Thomas E., 1994, Sootblower optimization. *Tappi Journal*, Vol. 77, No. 5, pp. 135 – 142.

Jameel, M. I., Schwade, H. and Easterwood, M. W., 1995, A field study on the operational impact of improved sootblower nozzles on recovery boilers. Proceedings of 1995 TAPPI Engineering Conference, Dallas Texas, Book 2, pp. 695 - 705.

Janka, Kauko, Wallén, Jonas and Backman, Rainer, 2004, Prediction of dust content and properties in kraft recovery boilers: comparison of theory and experimental results. *Pulp & Paper Canada*, Vol. 105, No. 1, January 2004, pp. 46 – 50.

Janka, Kauko and Tamminen, Ari, 2003, Recovery boiler furnace as concentrated NCG incinerator. *Tappi Journal*, Vol. 2, No. 2, February 2003, 9 p.

Janka, Kauko, Heinola, Ari, Heinola, Marja, Skrifars, Bengt-Johan and Hupa, Mikko, 1998, The roles of black liquor composition and boiler combustion parameters on the fouling tendency of recovery boiler. Proceedings of 1998 International Chemical Recovery Conference, Tampa, USA, 1 - 4 June 1998, TAPPI Press, Atlanta, pp. 629 – 640.

Janka, Kauko, Ruohola, Tuomo, Siiskonen, Pekka and Tamminen, Ari, 1998, A comparison of recovery boiler field experiments using various NOx reduction methods. *Tappi Journal*, Vol. 81, No. 12, December 1998, pp. 137 - 141.

Jing, Qun and Iisa, Kristiina, 2001, Black liquor devolatilization kinetics. Proceedings of 2001 International Chemical Recovery Conference, June 11-14, 2001, Whistler (BC), Canada, pp. 221 - 229.

Jokiniemi, Jorma K., Pyykönen, Jouni, Mikkanen, Pirita and Kauppinen, Esko I., 1996, Modeling fume formation and deposition in kraft recovery boilers. *Tappi Journal*, Vol. 79, No. 7, July 1996, pp. 171 - 181.

Jokiniemi, Jorma, Kauppinen, Esko and Mikkanen, Pirita, 1993, Rikki ja natrium sitoutuvat soodakattilassa aerosoliin. (Sulfur and sodium are caught to aereosols in a recovery boiler) in Finnish, *Paperi ja Puu* (Paper and Timber), Vol. 75, No. 3, pp. 122 – 125.

Jones, Andrew K., 2004, 70 years of advances in recovery boiler design. 40th Anniversary International Recovery Boiler Conference, Finnish Recovery Boiler Committee, Haikko Manor, Porvoo, May 12-14, 2004, pp. 15 – 20.

Jones, Andrew K. and Chapman, Paul J., 1992, CFD combustion modeling – a comparison of secondary air system designs. Proceedings of 1992 Tappi Engineering Conference, Boston, MA, September 14 – 17, Tappi Press, pp. 559 – 579.

Jones, Andrew K., 1989, A model of kraft recovery furnace. Doctoral Dissertation, Appleton, Wisconsin, The Institute of Paper Chemistry. 157 p.

Jones, Andrew K. and Stewart, R. I., 1993, The high solids breakpoint: a trade off between SO_2 and NOx. *Pulp & Paper Canada*, Vol. 94, No. 12, pp. T479 – T482.

Jones, Andrew K. and Anderson, Michael J., 1992, High solids firing at Arkansas Kraft. 78th Annual Meeting, Technical section, CPPA, pp. A39 - A49.

Jutila, E., Pantsar, Ossi and Uronen, Paavo, 1978, Computer control of a recovery boiler. *Pulp & Paper Canada*, Vol. 79, No. 4, pp. 61 - 65.

Järvinen, Mika, 2002, Numerical modeling of the drying, devolatilization and char conversion processes of black liquor droplets. Ph. D. thesis, *Acta Polytechnica Scandinavia*, Mechanical Engi-

neering Series, 94 p.

Järvinen, Mika, Zevenhoven, Ron and Vakkilainen, Esa, 2002, Implementation of a detailed black liquor combustion model for furnace calculations, *IFRF Electronic Combustion Journal*, Article Number 200206, June 2002, 34 p

Järvinen, M., Forssén, M., Vakkilainen, E., Zevenhoven, R. and Hupa, M., 2000, Black liquor devolatilization and swelling detailed droplet model. UEF Conference on Behavior of Inorganic Materials in Recovery Boilers, Bar Harbor, Maine, 4 - 9 June 2000. United Engineering Foundation, 14 p.

Järvinen, Mika and Kankkunen Ari, 2000, Ideal solution approximation for vapor pressure of water in black liquor using Raoult's law. *To be published*.

Järvinen, Mika, Vakkilainen, Esa and Kankkunen Ari, 1997, Effects of liquor gun type on black liquor combustion. Proceedings of 1997 Tappi Engineering Conference, Nashville, Tennessee, pp. 1349 - 1356.

Jönsson, S-E, 1961, Synpunkter på indunstningsanläggningen och dess ekonomi vid indunstning till högre torrhalt. (Viewpoints of evaporators and their economy with high dry solids evaporation) in Swedish, Sodahuskonferens, ÅF-IPK, Stockholm, pp. 54 – 59.

Kaila, Jarmo and Saviharju, Kari, 2003, Comparison of recovery boiler CFD modeling to actual operations. PAPTAC Annual meeting, January 28, Montreal, Canada, 13 p.

Kaliazine, Andrei, Cormack, Donald E., Eibrahimi-Sabet, Abdolreza and Tran, Honghi, 1998, The mechanics of deposit removal in kraft recovery boilers. Proceedings of International Chemical Recovery Conference. Tampa, USA, 1 - 4 June 1998, Vol. 3, TAPPI, pp. 641 – 654.

Kaliazine, Andrei L., Piroozmand, Farshad, Cormack, Donald E. and Tran, Honghi, 1998, Sootblower optimization II. *Tappi Journal*, Vol. 80, No. 11, pp. 201 – 207.

Kankkunen, Ari, Helpiö, Tomi and Rantanen, Pekka, 1994, Small scale measurement of black liquor spraying with splashplate nozzles. Proceedings of 1994 TAPPI Engineering Conference, San Francisco, 19 - 22 September, pp. 207 - 214.

Karhula, M., 1992, Soodakattilan compoundputkien säröilytutkimus. (Study of recovery boiler compound tube cracking) in Finnish, M. Sc. thesis, Lappeenranta University of Technology, Finland, 79 p.

Kawada, Shin and Ibuka, Hideo, 1991, The newest Babcock-Hitachi recovery boiler. in Japanese, *Japan Tappi Journal*, Vol. 45, No. 6, pp. 644 – 655.

Kays, W. M., 1950, *Transactions of ASME*, Vol. 72, pp. 1067 – 1074.

Kearns, Jim, Levesque, Denise and Navitsky, Gary, 2001, Reducing CRU downtime – a circulation and water chemistry perspective. Proceedings of 2001 TAPPI Engineering/Finishing & Converting Conference, San Antonio, TX. 21 p.

Keiser, James R., Singbeil, Douglas L., Sarma, Gorti B., Kish, Joseph R., Choudhury, Kimberly A., Hubbard, Camden R., Frederick, Laurie A., Yuan, Jerry W. and Singh, Preet M., 2004, Causes and solutions for recovery boiler primary air port composite tube cracking. Proceedings of 2004 International Chemical Recovery Conference, June 6-10 2004, Charleston, South Carolina, USA, 527-542 p.

Keiser, James R., Singbeil, Douglas L., Sarma, Gorti B., Kish, Joseph R., Choudhury, Kimberly A., Frederick, Laurie A., Gorog, Peter, Jetté, François, R., Hubbard, Camden R., Swindeman, Robert W., Singh, Preet M., Yuan, Jerry and Maziasz, Philip J, 2004, Cracking and corrosion of composite tubes in black liquor recovery boilers. 40th Anniversary International Recovery Boiler Conference, Finnish Recovery Boiler Committee, Haikko Manor, Porvoo, May 12-14, 2004, pp. 59 – 89.

Keiser, James, Singbeil, Douglas L., Sarma, Gorti B., Choudhury, Kimberly, Singh, Preet M., Hubbard, Camden R., Swindeman, Robert W., Ely, Thomas, Kish, Joseph, Kenik, Edward, Maziasz, Philip J. and Bailey, Sarah, 2002, Comparison of cracking in recovery boiler composite floor and primary air port tubes. *Tappi Journal*, Vol. 1, No. 2, February 2002, pp. 1 - 7.

Keiser, J. R., Sarma, Gorti B., Wang, Xun-Li, Hubbard, Camden R., Swindeman, Robert W., Maziasz, Philip J., Singbeil, Douglas L. and Singh, Preet M., 2001, Why do kraft recovery boiler composite floor tubes crack? *Tappi Journal*, Vol. 84, No. 8, August 2001, 12 p.

Keiser, J. R., Aramayo, G. A., Goodwin, G. M., Maziasz, P. J. and Gorog, J. P., 2000, Improved materials for use as components in kraft black liquor recovery boilers. Oak Ridge National Lab., Report C/ORNL95-0375, 34 p.

Kelly, P. A., Frederick, William. J. and Grace, Thomas M., 1981, The residence time distribution of inorganic salts in kraft recovery boilers. *Tappi Journal*, Vol. 64, No. 10, October, pp. 85 - 87.

Khalaj, Asghar, Kuhn, David and Tran, Honghi, 2004, Composition of carryover particles in recovery boilers. Proceedings of 2004 International Chemical Recovery Conference, June 6-10 2004, Charleston, South Carolina, USA, 1009-1020 p.

Kiiskilä, Erkki, Lääveri, Anu, Nikkanen, Samuli and Vakkilainen, Esa, 1993, Possibilities for new black liquor processes in the pulping industry energy and emissions. *Bioresource Technology*, Vol. 46, pp. 129 - 134.

Kilpinen, P., Hupa, M. and Aho, M., 1997, Selective non-catalytic NOx reduction at elevated pressures: studies on the risks for increased N_2O emissions. Proc. 7th Int. Workshop on Nitrous Oxide Emissions, Cologne, April 21-23, 1997, Bergische Universität Gesamthochschule Wuppertal, Physikalische Chemie, Bericht Nr. 41, September, 1997.

Kilpinen, Pia, 1992, Kinetic modeling of gas phase nitrogen reactions in advanced combustion processes. Ph. D. thesis, Åbo Akademi University, 350 p, ISBN 951-650-132-X.

Kingery, W. D. and Berg, M., 1955, Study of the initial stages of sintering solids by viscous flow, evaporation-condensation, and self-diffusion. *Journal of Applied Physics*, Vol. 26, No. 10, pp. 1205 - 1212.

Kittredge, C. P. and Rowley, D. S., 1974, Resistance coefficients for laminar and turbulent flow through ½ inch valves and fittings. Transactions of ASME, Journal of Engineering for Power, pp. 1579 - 1586.

Kippo, Asko, 1979, Simulation studies of dynamics and multivariable controllers of the recovery boiler. Lic. Tech. thesis, University of Oulu.

Kjörk, Anders and Herstad Swärd, Solvie, 2000, Atmospheric emission of nitrogen oxide from kraft recovery boilers in Sweden. (Kartläggning av NOx-utsläpp från sodapannor i Sverige) in Swedish, Technical Report, SVF-679, Värmeforsk, Stockholm Sweden, Project Värmeforsk S9-807, ISSN 0282-3772, 58 p.

Klarin, Anja, 1993, Floor tube corrosion in recovery boilers. *Tappi Journal*, Vol. 76, No. 12, December 1993, pp. 183 - 188.

Klarin, Anja, 1992, Analysis of char bed material. in Finnish, Ahlstrom Machinery, Internal report. 3 p.

Knacke, O. Kubaschewski, O. and Hesselmann, K., 1991, Thermochemical properties of inorganic substances. II, Springer-Verlag, Berlin. 2412 p.

Kochesfahani, Saied H. and Tran, Honghi, 2000, Field studies on intermediate sized particles (ISP) in recovery boilers. UEF Conference on Behavior of Inorganic Materials in Recovery Boilers, Bar Harbor, Maine, 4 - 9 June 2000, United Engineering Foundation, 22 p.

Kochesfahani, S. Tran, H. N., Jones, A. K., Grace, T. M., Lien, S. J. and Schmidl, W., 1998, Particulate formation during black liquor char bed burning. Proceedings of 1998 International Chemical Recovery Conference, Tampa, USA, 1 - 4 June 1998, TAPPI Press, Atlanta, pp. 599 - 614.

Koivisto, Lasse, 2002, Recovery boiler corrosion and materials issues. Presentation, Andritz Corporation.

Koivisto, Lasse and Holm, Ralf, 1998, Furnace floor design and materials for recovery boilers. Proceedings of 1998 TAPPI Engineering Conference, September 14-18, 1998, Atlanta, Georgia, pp. 1091 - 1098.

Kraft pulping, 1989, A compilation of notes, editor Agneta Mimms, Tappi Press.

Kulas, Katherine A., 1990, An overall model of the combustion of a single droplet of kraft black liquor. Ph. D. thesis, The Institute of Paper Science and Technology. 159 p.

Kulas, Katherine A., Harper, Frank and Clay, David, 1989, Black liquor burning advances in understanding. The midnight sun colloquium on recovery research, June 14 – 16, 1989, STFi, pp. 11 - 22.

Kulas, Katherine A. and Clay, David T., 1988, An empirical rate equation describing the volatiles burning stage of kraft black liquor. AIChE Forest Products Division, pp. 53 - 57.

Kurkela, J., Latva-Somppi, J., Tapper, U., Kauppinen, E. I. and Jokiniemi, J., 1998, Ash formation and deposition onto heat exchanger tubes during fluidized bed combustion of wood-based fuels. Proceedings of the ABC'98 International Conference on Ash Behaviour Control in Energy Conversion Systems, Yokohama, Japan, March 18-19, 1998, pp. 110 - 118.

Kymäläinen Marita, Forssén Mikael, Jansson, Mette and Hupa Mikko, 2002, The fate of nitrogen in the chemical recovery process in a kraft pulp mill, Part IV: Smelt nitrogen and its formation in black liquor combustion. *Journal of Pulp and Paper Science*, Vol. 28, No. 5, pp. 151 - 158.

Kymäläinen, Marita, Forssén, Mikael and Hupa, Mikko, 1999, The fate of nitrogen in the chemical recovery process in a kraft pulp mill. Part I: A general view. *Journal of Pulp and Paper Science*, Vol. 25, No. 1, pp. 410 - 417.

Källberg, Y., 1982, Simulation of formation and depletion of NOx in high temperatures. in Swedish, M. Sc. thesis, Åbo Akademi.

Labossiere, James and Henry, Jeff, 1999, Chromizing for near-drum corrosion protection. *Tappi Journal*, Vol. 82, No. 9, September 1999, pp. 150 - 157.

Laitinen, A., Pulliainen, M. and Heinävaara, A., 1998, On-line monitoring of recovery boilers. 9th International Symposium on Corrosion in the Pulp and Paper Industry, May 26 – 29, 1998, Ot-

tawa, Ontario, Canada, 199 – 202.

Lankinen, Matti, Paldy, Ivan V., Ryham, Rolf and Simonen, Liisa, 1991, Optimal solids recovery. Proceedings of CPPA 77th Annual meeting, pp. A373 - A378.

Ledung, Lars and Ulmgren, Per, 1998, Viscosity changes in black liquor when bleach plant filtrates are added. Proceedings of 1998 International Chemical Recovery Conference, Tampa, USA, 1 - 4 June 1998, TAPPI Press, Atlanta, pp. 157 - 168.

Ledung, Lars and Ulmgren, Per, 1997, Combustion properties of black liquors containing additions of totally chlorine free bleach plant filtrates. *Nordic Pulp and Paper Research Journal*, Vol. 12, No. 3, pp. 145 - 149.

Ledung, Lars and Kaul, Vikaram, 1996, Sodapanneprocessen: en sammanställning av forskningsresultat från litteraturen. (Recovery boiler process: compendum of research results from litterature) in Swedish, STFI-rapport BF 4, Juni 1996, 67 p.

Lefohn, A. S., Husar, J. D., Husar, R. B. and Brimblecombe, P., 1996, Assessing historical global sulfur emission patterns for the period 1850-1990. Technical report, DOE/ER/30234—1, A.S.L. and Associates, Helena, MT United States. 190 p.

Li, Jian, 1989, Rate processes during gasification and reduction of black liquor char. Ph. D. thesis, McGill University.

Li, Jian and van Heiningen, A. R. P., 1991, Sulfur emissions during slow pyrolysis of kraft black liquor. *Tappi Journal*, Vol. 74, No. 3, March 1991, pp. 237 - 239.

Li, Jian and van Heiningen, A. R. P., 1990, Sodium emission during pyrolysis and gasification of black liquor char. *Tappi Journal*, Vol. 73, No. 1, December 1990, pp. 213 - 239.

Li, Jian and van Heiningen, A. R. P., 1989, Sulfur emission during gasification of black liquor char. Proceedings International Chemical Recovery Conference, CPPA, pp. 209 - 216.

Li, Jian and van Heiningen, A. R. P., 1986, Mass transfer limitations in the gasification of black liquor char by CO_2. *Journal of Pulp and Paper Science*, Vol. 12, No. 5, September, pp. J146 - 151.

Lidén, Jan, 1995, Green liquor dregs, its origin and effects in the lime cycle. Proceedings of 1995 International Chemical Recovery Conference, Toronto Canada, CPPA, pp. A291 – A298.

Lien, Steven J. and Verrill, Christopher L., 2004, Particulate emissions from char bed burning. Proceedings of 2004 International Chemical Recovery Conference, June 6-10 2004, Charleston, South Carolina, USA, 1023-1041 p.

Lien, Steven J., Ling, Alisa, Frederick, Wm. James Jr. and Tran, Honghi, 1999, Sintering and densification rates for recovery boiler fume deposits. Paper 5-5, Proceedings of 1999 Tappi Engineering Conference, September 12 – 16, Anaheim, California.

Lind, Terttaliisa, Rumminger, Marc, Baxter, Larry, Kauppinen, Esko, Wessel, Rick, Roscoe, Bob and Ariessohn, Peter, 2000, A field investigation of recovery boiler salt particle characteristics. UEF Conference on Behavior of Inorganic Materials in Recovery Boilers, Bar Harbor, Maine, 4 - 9 June 2000. United Engineering Foundation, 17 p.

Lindberg, Hans and Ryham, Rolf, 1994, Chemical recovery technology for future fiber production. CPPA 80th Annual meeting, pp. A73 - A78.

Lindblom, Josefina, 1999, Sintering in the kraft pulp mill – studies in the rotary kiln and recovery boiler. Ph. D. thesis, Doktorsavhandlingar vid Chalmers tekniska högskola, Ny serie 1554, Chalmers University of Technology, Göteborg, Sweden, 88 p., ISBN 91-7197-864-X.

Lindsley, David, 2000, Power-plant control and instrumentation: the control of boilers and HRSG systems, Institution of Electrical Engineers, London, 222 p., ISBN 0-85296-765-9.

Llinares, Jr. V. and Chapman, P. J., 1989, Stationary firing, three level air system retrofit experience. Proceedings of 1989 Tappi Engineering Conference, Atlanta, Georgia, September 10-13, 10 p.

Lobben, Peder, 1930, Handboken för mekaniker. (Mechanic's handbook) in Swedish, 4th edition, Albert Bonniers Förlag, Stockholm, 748.

Lobscheid, H., 1965, Dampf Babcok – Handbuch. (Steam Babcock – handbook) in German, 4th edition, Vulkan – Verlag, Essen, 322 p.

Lovo, Augusto Cesar, Puig, Floreal and Santos, Saulo, 2004, Presentation of recovery boiler's retrofits – Aracruz Celulose S/A. Proceedings of 2004 International Chemical Recovery Conference, June 6-10 2004, Charleston, South Carolina, USA, pp. 35 - 43.

Lundborg, Sten, 1977, Undersökning av smältatemperaturer. (Study of smelt temperatures) in Swedish, Sodahuskonferensen ´77, ÅF-IPK, Stockholm, pp. 43 – 50.

Luthe, Corinne E., Uloth, Vic, Karidio, Ibrahim and Wearing Jim, 1997, Are salt-laden recovery boilers a significant source of dioxins? *Tappi Journal*, Vol. 80, No. 2, February 1997, pp. 165 - 169.

Lyon, Rickhard K., Cole, Jerald A., Kramlich, John C. and Chen Shi L., 1989, The selective reduction of SO_3 to SO_2 and the oxidation of NO

to NO_2 by methanol. *Combustion and Flame*, Vol. 81, No. 1, pp. 30 - 39.

Lövblad, Roland, Moberg, Göran, Olausson, Lars and Boström, Curt-Åke, 1991, NOx-reduction from a recovery boiler by injection of an enhanced urea solution. Proceedings of 1991 Tappi Environmental Conference, Tappi Press, pp. 1071 – 1075.

MacCallum, Colin, 1992, Towards a superior recovery boiler air system. Proceedings of 1992 International Chemical Recovery Conference, Seattle, Washington, June 7-11, pp. 45 - 56.

MacCallum, Colin and Blackwell, Brian, R., 1985, Modern kraft recovery boiler liquor-spray and air systems. Proceedings of 1985 International Chemical Recovery Conference, New Orleans, LA, pp. 33 - 47.

MacCallum, Colin, 1982, Tailor-made recovery boilers. Proceedings of Black liquor recovery boiler symposium 1982, Helsinki, August 31 – September 1, The Finnish Recovery Boiler Committee – EKONO Oy, 12 p.

Maddern, K. N., 1988, Mill-scale development of the DARS direct causticization process. *Pulp & Paper Canada*, Vol. 87, No. 10, pp. T395 – T399.

Maddox, R. N., 1983a. Properties of mixtures of fluids. in Heat Exchanger Design Handbook, Part 5. Physical properties. Hemisphere Publishing Corporation, pp. 5.2.1-1 - 5.2.5-4.

Maddox, R. N., 1983b. Properties of superheated gases. in Heat Exchanger Design Handbook, Part 5. Physical properties. Hemisphere Publishing Corporation, pp. 5.5.2-1 - 5.5.2-11.

Magnusson, Hans, 1977, Sodapannan som kemisk reaktor. (Recovery boiler as a chemical reactor) in Swedish, Sodahuskonferensen ´77, ÅF-IPK, Stockholm, pp. 26 – 29.

Makino, A., 1981, A theoretical and experimental study of carbon combustion in stagnation flow. *Combustion and Flame*, Vol. 73, pp. 166 - 187.

Makkonen, Pasi, 1999, Artificially intelligent and adaptive methods for prediction and analysis of superheater fireside corrosion in fluidized bed boilers. Ph. D. thesis, Lappeenranta University of Technology, Acta Universialis Lappeenrataensis, 89, 187 p. ISBN 951-764-375-6.

Manninen, Jussi and Vakkilainen, Esa, 1996, Reduction of sulfur emissions from kraft recovery furnace with black liquor heat treatment. Finnish-Swedish Flame Days, Naantali.

Malmberg, Barry, Edwards, Lou, Lundborg, Sten, Ahlroth, Mikael and Warnqvist, Björn, 2003, Prediction of dust composition and amount in kraft recovery boilers. Proceedings of 2003 TAPPI Fall Technical Conference: Engineering, Pulping & PCE&I, Chicago, Il, USA, 8 p.

Mannola, Lasse and Burelle, Richard, 1995, Operating experience of a 7,270,000 lb d.s./day recovery boiler. *Pulp & Paper Canada*, Vol. 96, No. 3, March 1995, pp. 70 – 72.

Mao, Xiaosong, Tran, Honghi and Cormack, Donald E., 2000, Effects of chemical composition on the removability of recovery boiler fireside deposits. Proceedings of 2000 Tappi Engineering Conference, TAPPI Press, Atlanta, 11 p.

Maso, Vesa, 1988, Formation and reduction of emissions. Seminar on Black Liquor Combustion, February 24 - 25, Lappeenranta, Lappeenranta University of Technology. 12 p.

Masse, M. A., Kiran, E. and Fricke, A. L., 1986, *Polymer*, Vol. 27, p. 619.

Matsuda, Takao, Masuda, Takeharu and Suemitsu, Nobuo, 199x. Outline of the world's largest soda recovery boiler with high pressure and high temperature steam. pp. 234 – 248.

McCann, Colin, 1991, A review of recovery boilers process design. CPPA 77th Annual meeting, pp. A49 - A58.

McCarthy, J. H., 1968, Recovery plant design and maintenance. Chapter 5 of Chemical recovery in alkaline pulping process, editor Whitney, Roy P., *TAPPI Monograph series*, No. 32, Mack Printing Company, Easton, Pa., pp. 159 – 199.

McDonald, Kevin L., 1977, Calorific analysis of spent liquors by carbon analysis. *Tappi Journal*, Vol. 60, No. 12, December 1977, pp. 107 – 109.

McGurn, J. F., 1993, Composite tubes in black liquor recovery boilers: an update. *Pulp & Paper Canada*, Vol. 94, No. 12, December 1993, pp. T428 – T432.

McKeough, Paterson, 2004, Evaluation of potential improvements to BLG technology. Proceedings of PulPaper 2004 Energy and carbon management, 1-3 June 2004, Helsinki Finland, pp. 69 - 76.

McKeough, Paterson, 2003, Evaluation of potential improvements to BLG technology. Proceedings of Colloquium of black liquor combustion and gasification, Park City, Utah, 13-16 May 2003, 12 p.

McKeough, Paterson and Janka, Kauko, 2001, Sulphur behaviour in the recovery boiler furnace: theory and measurements. Proceedings of 2001 International Chemical Recovery Conference, Whistler, PAPTAC Publications, pp. 231 – 237.

McKeough, P. J. and Vakkilainen, E. K., 1998, Effects of black liquor composition and furnace conditions on recovery boiler fume chemistry. Proceedings of 1998 International Chemical Recovery Conference, Tampa, USA, 1 - 4 June 1998,

TAPPI Press, Atlanta, pp. 487 - 504.

McKeough, P. J., Kurkela, M., Arpiainen, V., Mikkanen, P., Kauppinen, E. and Jokiniemi, J., 1995, The release of carbon, sodium and sulphur during rapid pyrolysis of black liquor. Proceedings of 1995 TAPPI International Recovery Conference, Toronto Canada, CPPA, pp. A217 - A226.

McMillan, John, 2004, Superheater problems, their causes and solutions. Proceedings of 2004 International Chemical Recovery Conference, June 6-10 2004, Charleston, South Carolina, USA, pp. 953 – 964.

Merriam, Richard L., 1980, KRAFT, version 2.0 computer model of a kraft recovery furnace, Vol. III: users manual. prepared for The American Paper Institute, New York, Arthur D. Little, Inc., 216 p.

Merriam, Richard L., 1977, KRAFT, version 2.0 computer model of a kraft recovery furnace, Vol. II: engineering manual. prepared for The American Paper Institute, New York, Arthur D. Little, Inc. 136 p.

Metiäinen, Sami, 1991, Soodakattilan ilmansyöttömallien kokeellinen tutkimus. (Experimental investigation of recovery boiler air models) in Finnish, M. Sc. thesis, Lappeenranta University of Technology. 84 p.

Miikkulainen, Pasi, Kankkunen, Ari and Järvinen, Mika, 2002, Mustalipeän ruiskutuskokeet soodakattilassa ja ruiskutuskammiossa. (Black liquor firing tests in recovery boiler and firing test rig) in Finnish, Energy Engineering and Environmental Protection publications, Helsinki University of Technology, Department of Mechanical Engineering, No. 8, 34 p. ISBN 951-22-6026-3.

Mikkanen, P., Jokiniemi, J. K., Kauppinen, E. I. and Vakkilainen, E. K. 2001, Coarse ash particle characteristics in a pulp and paper industry chemical recovery boiler. *Fuel*, Vol. 80, No. 7, pp. 987 – 999.

Mikkanen, Pirita, 2000, Fly ash formation in kraft recovery boilers. Ph. D. thesis, VTT Publications 421, Technical research centre, VTT, Espoo, 116 p. ISBN 951-38-5583-X.

Mikkanen, Pirita. Kauppinen, Esko, Jokiniemi, Jorma, Moisala, Antero, Vakkilainen, Esa K. and Hämäläinen, Jouni, 1999, Ash particle deposition study in an operating recovery boiler. American Aerosol Association Research Conference, October 11-15, 1999, Tacoma, Washington.

Mikkanen, Pirita. Kauppinen, Esko, Pyykönen, Jouni, Jokiniemi, Jorma, Aurela, Minna, Vakkilainen, Esa K. and Janka, Kauko, 1999, Alkali salt ash formation in four Finnish industrial recovery boilers. *Energy and Fuels*, Vol. 13, No. 4, pp. 778 - 795.

Mikkanen, Pirita, Kauppinen, Esko J., Jokiniemi, Jorma K., Sinquefield, Scott and Frederick, William, J., 1994, Bimodal fume particle size distributions from recovery boiler and laboratory scale black liquor combustion. *Tappi Journal*, Vol. 77, No. 12, December 1994, pp. 81 - 84.

Mikkanen, P., Kauppinen, E. I., Jokiniemi, J. K., Sinquefield, S. A., Frederick, W. J. and Mäkinen, M., 1994b, The particle size and chemical species distributions of aerosols generated in kraft black liquor pyrolysis and combustion. *AIChE Symp. Ser.*, Vol. 90, No. 302, pp. 46 - 54.

Milanova, E. and Kubes, G. J., 1985, The combustion of kraft liquor chars. Proceedings of 1985 International Chemical Recovery Conference, New Orleans, Louisiana, Book 3, pp. 363 - 370.

Milanova, E., 1988, Variables affecting the swelling of kraft black liquor solids. *Journal of Pulp and Paper Science*, Vol. 14, No. 4, July, pp. J95 - J102.

Miller, P. T., Clay, David T. and Lonsky, W. F. W., 1986, The influence of composition on the swelling of kraft black liquor during pyrolysis. Proceedings of Tappi Engineering Conference, pp. 225 - 234.

Mitsubishi chemical recovery boiler, 1997, Sales brochure, Mitsubishi Heavy Industries, Ltd. Tokyo, Japan, 18 p.

Moberg, Orvar, 1974, Recovery boiler corrosion. in Pulp and paper industry corrosion problems, National Association of Corrosion Engineers, Houston, Texas, pp. 125 – 136.

Moberg, Orvar, 1973, Sodahusets roll i svavelbalansen. (Recovery boilers role in sulfur balance) in Swedish, Sodahuskonferens, 29 November 1973, Ångpannaföreningen, Stockholm, pp. 8 – 14.

Moberg, Orvar, 1967, Eftereldytornas utformning i sodahusaggregat. (Form of after furnace surfaces in a recovery plant) in Swedish, Sodahuskonferens, 27 November 1967, ÅF-IPK, Stockholm, pp. M1 – M18.

Modern power station practice, Vol. B, Boilers and ancillary plant, 1991, 3rd edition, Pergamon press, Singapore, 184 p. ISBN 0-08-040512-6.

Modern power station practice, Vol. E, Chemistry and metallurgy, 1992, 3rd edition, Pergamon press, Singapore, 576 p. ISBN 0-08-040515-0.

Modern power station practice, Vol. 2, Mechanical boilers, fuel and ash-handling plant, 1971, 2nd edition, Pergamon press, Hungary, 432 p. ISBN 08-016060-3.

Moody, L. F., 1944, Friction factors for pipe

flow. *Journal of Heat Transfer*, Vol. 66, pp. 671 – 684.

Myslicki, T. P. and Orr, Alex, 1992, New 3000 tons high pressure / high temperature recovery boiler. Proceedings of 1992 International Chemical Recovery Conference, Seattle, Washington, June 7-11, pp. 413 – 420.

Mäkipää, M., Kauppinen, E., Lind, T., Pyykönen, J., Jokiniemi, J., McKeough, P., Oksa, M., Malkow, Th., Fordham, R. J. Baxter, D., Koivisto, L., Saviharju, K. and Vakkilainen, E., 2001, Superheater tube corrosion in recovery boilers. VTT Symposium 214, 10th International Symposium on Corrosion in the Pulp and Paper Industry (10th ISCPPI), Helsinki, 21 - 24 August 2001, Vol. 1, editor Hakkarainen, Tero, VTT Manufacturing Technology, Espoo, 2001, pp. 157 – 180. ISBN 951-38-5720-4.

Mäkipää, Martti and Backman, Rainer, 1998, Corrosion of floor tubes in reduced kraft smelts: studies on effects of chlorine and potassium. Proceedings of 9th International Symposium on Corrosion in the Pulp and Paper Industry, May 26 – 29, 1998, Ottawa, Ontario, Canada.

Mäntyniemi, J. and Hartley, C. E., 1999, Widening the operating envelope of recovery boilers by using high dry solids firing, Proceedings of 1999 TAPPI Engineering/Process and Product Quality Conference, Vol. 1, p. 479.

Mäntyniemi, Jussi and Haaga, Kari, 2001, Operating experience of XL-sized recovery boilers. Proceedings of 2001 Tappi Engineering, Finishing & Converting Conference, Tappi Press, Atlanta, GA, 7 p.

NCASI summary of PCDD/F emissions from wood residue and black liquor combustion - Locating and estimating air emissions from sources of dioxins and furans, 1996, U.S. EPA Draft Final Report, January 1996.

Navitsky, G. J. and Gabrieli, F., 1980, Boiler water treatment, feedwater treatment, and chemical cleaning of drum-type utility steam generators. Combustion, August, p. 19.

Nichols, Kenneth M. Thompson, Laura M. and Empie, H. Jeff, 1993, A review of NOx formation mechanisms in recovery furnaces. *Tappi Journal*, Vol. 76, No. 1, January 1993, pp. 119 - 124.

Nichols, Kenneth M., 1992, Combustion of concentrates resulting from ultrafiltration of bleached-kraft effluents. *Tappi Journal*, Vol. 75, No. 4, April 1992, 153 - 158.

Nichols, Kenneth, M., 1987, Nitrogen pollutant formation in a high pressure entrained- coal gasifier. Ph. D. thesis, Department of Chemical Engineering, Brigham Young University. 242 p.

Niemelä, Klaus, 2004, Early history of black liquor research: recovery of by-products and cooking chemicals. 40th Anniversary International Recovery Boiler Conference, Finnish Recovery Boiler Committee, Haikko Manor, Porvoo, May 12-14, 2004, pp. 7 – 14.

Niemelä, Klaus, Järvinen, Risto, Ulmgren, Per, Samuelsson, Åsa, Forssén, Mikael, DeMartini, Nicolai, Kilpinen, Pia, Hupa, Mikko, Saviharju, Kari, Ferreira Pinho and Rebola, João, 2002, Reduction of air emissions at kraft pulp mills - overview of a multidisciplinary EU project. Proceedings of the 7th New Available Technologies Conference, Stockholm, Sweden, June 4-6, 2002, pp. 78 - 81.

Niemelä, Klaus and Ulmgren, Per, 2002, Behaviour of nitrogen during kraft pulping of wood. Proceedings of the 7th European Workshop on Lignocellulosics and Pulp, Turku, Finland, August 26–29, 2002, pp. 71 - 74.

Niemelä, Klaus, 2001, Identification of novel volatile sulfur and nitrogen compounds in kraft pulping process streams. Proceedings of the 11th International Symposium on Wood and Pulping Chemistry, Nice, France, June 11-14, 2001, Vol. I, pp. 125 - 128.

Niemitalo, Hanna, 1993, Soodakattilan likaantuminen ja nuohouksen ohjaus. (Fouling and sootblowing control of recovery boiler) in Finnish, M. Sc. thesis, University of Oulu.

Nikkanen, Samuli, Tervo, Olavi, Lounasvuori, Risto and Paldy, Ivan V., 1989, Experience of recovery boiler modernizations. Proceedings of 1989 International Chemical Recovery Conference, Ottawa, Ontario, pp. 39 - 44.

Nikuradse, J., 1933, Strömungsgesetz in rauchen rohren. (Flow loss in rough tubes) in German, *Forshungsheft* 361, Ausgabe B, band 4, VDI Verlag Gmbh, Berlin NW7.

Nishikawa, Eiichi, 1999, General planning of boiler gas side heat transfer surfaces. in Steam power Engineering, editor Ishigai, Seikan, Cambridge University Press, 394 p. ISBN 0 521 62635 8.

Nishio, Toshiaki, Matsumoto, Hirotoshi, Shinohara, Masatomo and Arakawa, Yoshihisa, 2001, Influence of ash composition on corrosion rate of superheater tubes. Proceedings of 2001 Tappi Engineering, Finishing & Converting Conference, Tappi Press, Atlanta, GA, 6 p.

Noopila, Taina, Alén, Raimo and Hupa, Mikko, 1991, Combustion properties of laboratory-made black liquors. *Journal of Pulp and Paper Science*, Vol. 17, No. 4, July, pp. J105 - J109.

Nunes, Walter R., Puig, Floreal and Lindman, Nils, 1995, Purging of ESP ash to control steam

temperature. Proceedings of 1995 International Chemical Recovery Conference, Toronto Canada, CPPA, pp. A59 – A61.

Näretie, V. and Arpalahti, Esko, 1972, Höyrytekniikka. (Steam technology) in Finnish, 277 p. ISBN 951-1-00009-8.

Ohlström, Mikael O., Lehtinen, Kari E. J., Moisio, Mikko and Jokiniemi, Jorma K., 2000, Fine-particle emissions of energy production in Finland. *Atmospheric Environment*, Vol. 34, No. 22, pp. 3701 - 3711.

Ohtomo, Kenji, 2000, The experience of high temperature and pressure recovery boiler operation. *Japan Tappi Journal*, Vol. 54, No. 1, January 2000, pp. 109-114.

Oulu Osakeyhtiö's new sulphate mill, 1937, *The Finnish Paper and Timber Journal*, Vol. 19, No. 7A, pp. 276 – 278.

Paju, Raimo, 1992, Features of safe and reliable recovery boiler. Premier symposium international, Prevention sur les chaudieres de recuperation a liqueur noire, Bordeaux, France, 10 p.

Pantsar, Ossi, 1988, Comparison of firing methods, Effect of furnace size on the process. Seminar on black liquor combustion, 24 – 25 February 1988, Lappeenranta.

Park, Song Won, 2001, Análise de modelos de calderira de recuperação. (Analysis of recovery boiler models) in Portuguese, 14th Latin-American Recovery Boilers meeting, August 7 – 10, Sao Paulo, Associação Brasileira Technica de Celulose e Papel. 8 p.

Paul, Larry D., Barna, Joan L., Danielson, Michael J. and Harper, Sharon L., 1993, Corrosion-resistant tube materials for extended life of openings in recovery boilers. *Tappi Journal*, Vol. 76, No. 8, August 1993, pp. 73 - 77.

Passinen, K, 1968, Chemical composition of pulping spent liquors. Proceedings of the Symposium on Recovery of Pulping Chemicals, Helsinki, The Finnish Pulp and Paper Research Institute and Ekono, pp. 184 - 210.

Performance test procedure: sodium base recovery units, 1996, CA Report No. 84041601, March 1996, Tappi Press, 54 p. ISBN 0-89852338.

Perjyd, L. and Hupa, Mikko, 1984, Bed and furnace gas composition in recovery boilers - advanced equilibrium calculations. Proceedings of 1984 TAPPI Pulping Conference, San Francisco, November. 11 p.

Pettersson, Bertil, 1983, Korsnäs sodapannor under 40 år. (40 years of recovery boilers at Korsnäs) in Swedish, Sodahuskonferensen '83, ÅF-IPK, Stockholm, pp. 57 – 68.

Pinkerton, John E., 1998, Trends in U.S. pulp and paper mill SO_2 and NOx emissions, 1980–1995. *Tappi Journal*, Vol. 81, No. 4, April 1998, pp. 114 - 122.

Piroozmand, F., Tran, H. N., Kaliazine, A. and Cormack, D. E., 1998, Strength of Recovery Boiler Fireside Deposits at High Temperatures. Proceedings of 1998 Tappi Engineering Conference, TAPPI Press, Atlanta, pp. 169-179.

Plumley, A. L., Lewis, E. C., Barker, T. J. and Esser, F. A., 1989, Chromizing for recovery boiler corrosion protection. Proceedings of 1989 Tappi Engineering Conference, Atlanta, Georgia, September 10-13, 8 p.

Pohjanne, Pekka, Hänninen, Hannu, Mäkipää, Martti and Ehrnsten, Ulla, 1992, Cracking of compound tubes in black liquor recovery boilers. Proceedings of the 17th International Symposium on Corrosion in the Pulp & Paper Industry, Orlando, FL, USA, 16 - 20 November 1992, TAPPI Atlanta, pp. 319 – 324.

Poon, William, Barham, David and Tran, Honghi, 1993, Formation of acidic sulfates in kraft recovery boilers. *Tappi Journal*, Vol. 76, No. 7, July 1993, pp. 187 - 193.

Puumassan valmistus, 1983, (Manufacture of pulp) in Finnish, editor Virkola, Nils-Erik, Suomen Paperi-insinoorien Yhdistyksen oppi- ja käsikirja II, osa 1, 2nd edition, 1106 p. ISBN 951-99117-3-1.

Pyykönen, Jouni, 2002, Computational simulation of aerosol behaviour. Ph. D. thesis, VTT Publications 461, Espoo, 154 p. ISBN 951-38-5977-0.

Pyykönen, Jouni and Jokiniemi, Jorma, 2002, Modelling alkali chloride superheater deposition and its implications. *Fuel Processing Technology*, Vol. 80, No. 3, 15 March 2003, pp. 225 - 262.

Rahtu, Jari, 1990, Lämmönsiirto soodakattilan tulistinalueella. (Heat transfer in recovery boiler superheaters) in Finnish, M. Sc. thesis, Lappeenranta University of Technology, Department of Energy Technology, 92 p.

Raukola, Antti and Haaga, Kari, 2004, Expandable recovery boiler, a novel method for future capacity increase. Proceedings of 2004 International Chemical Recovery Conference, June 6-10 2004, Charleston, South Carolina, USA, pp. 241 - 246.

Raukola, Antti T., Ruohola, Tuomo and Hakulinen, Aki, 2002, Increasing power generation with black liquor recovery boiler. Proceedings of 2002 TAPPI Fall Technical Conference, September 8 - 11, San Diego, Ca, 11 p.

Raymond, Del, 2003, The compelling case for gasification technology in the forest products industry. Proceedings of Colloquium of black liq-

uor combustion and gasification, Park City, Utah, 13-16 May 2003, 14 p.

Recovery boiler design review – Functional design considerations. 1993, Babcock and Wilcox Recovery Boiler Users' Association meeting, September 14 – 15, 1993, Atlanta Georgia, 15 p.

Reis, V. V., Frederick, W. J., Wåg, K. J., Iisa, K. and Sinquefield, S. S., 1994, Potassium and chloride enrichment during black liquor combustion. Paper 104c, 1994 AIChE Spring National Meeting, Atlanta, April 17-21.

Reis, Victor V., Frederick, William J., Wåg, Kaj J., Iisa, Kristiina and Sinquefield, Scott A., 1995, Effects of temperature and oxygen concentration on potassium and chloride enrichment during black-liquor combustion. *Tappi Journal*, Vol. 78, No. 12, December 1995, pp. 67 - 76.

Richards, Tobias, 2001, Recovery of kraft black liquor - alternative processes and system analysis. Ph. D. thesis, Doktorsavhandlingar vid Chalmers tekniska högskola, Ny serie 1732, Chalmers University of Technology, Göteborg, 88 p. ISBN 91-7291-048-8.

Richardson, David L. and Merriam, Richard L., 1977, Study of cooling and smelt solidification in black liquor recovery boilers. Phase I report, prepared for The American Paper Institute, New York, Arthur D. Little, Inc., 133 p.

Richardson, David L. and Merriam, Richard L., 1978, A study of black liquor recovery furnace firing conditions, char bed characteristics and performance. Phase II report, prepared for The American Paper Institute, New York, Arthur D. Little, Inc., 165 p.

Richter, W., 1985, Scale-up and advanced performance analysis of boiler combustion chambers. American Society of Mechanical Engineers winter annual meeting, Miami, FL, United States, 17-21 Nov 1985, 21 p.

Rissanen, Erkki, 1965, Economic design aspects of recovery boilers. *Papper och Trä*, No. 10, pp. 553 – 566.

Rivers, Keith B., Roherty, Arnie, Anderson, Blaine A., Milbury, Cindy A., Mott, Dan C., Piroozmand, Farshad, Tran, Honghi and Vafa, Shermineh, 2002, Modifying boiler operation to reduce primary air port cracking in a recovery boiler. Proceedings of 2002 TAPPI Fall Technical Conference, September 8 - 11, San Diego, Ca, 14 p.

Roschier, R. H., 1952, Sooda osasto. (Soda department) in Finnish, in Hiokkeen ja Selluloosan valmistus, editors Pellinen H. and Roshier, R. H., Suomen Paperi-Insinöörien Yhdistys, Helsinki, pp. 359 – 456.

Roos, Tom, 1963, Senaste erfarenheter av corrosion i sodahuseldstäder i Finland. (Recent corrosion experiences of recovery boiler furnaces in Finland) in Swedish, Sodahuskonferens, ÅF-IPK, Stockholm, pp. C1 – C18.

Roos, Tom, 1968, Design and operation experience of reductive recovery boilers. Proceedings of the Symposium on Recovery of Pulping Chemicals, Helsinki, The Finnish Pulp and Paper Research Institute and Ekono, pp. 437 - 489.

Rosner, D. E., 1986, Transport processes in chemically reacting flow systems. Butterworth-Heinemann, Stoneham, MA.

Rönnquist, Eva-Marie, 2000, Överhettarkorrosion i bioeldad panna - teorier och prov i Västermalmsverket, Falun. (Superheater corrosion in biomass boiler - theories and tests in Västermalmsverket, Falun) in Swedish, Technical report, SVF-708, Värmeforsk Service AB. 94 p.

Rydholm, Sven A., 1965, Pulping processes. Interscience Publishers, a division of John Wiley & Sons, Inc., London. 1269 p. ISBN 0 471 74793 9.

Ryham, Rolf, 1992, A new solution to third generation chemical recovery. Proceedings of 1992 International Chemical Recovery Conference, Seattle, Washington, June 7-11, pp. 581 - 588.

Ryham, Rolf and Nikkanen, Samuli, 1992, High solids firing in recovery boilers. Tappi Kraft Recovery Operations Short Course, pp. 233 - 238.

Ryham, Rolf, 1990, High solids evaporation of kraft black liquor using heat treatment. Proceedings of 1990 TAPPI Engineering Conference, Westin Seattle, Seattle, Washington, September 24 - 27, Book 2, TAPPI Press, pp. 677 - 681.

Ryti, Henrik, 1969, Lämmönsiirto. (Heat transfer) in Finnish, Tekniikan käsikirja, Osa 4, K. J. Gummerus, Jyväskylä, pp. 595 – 600.

Saarinen, P. and Hänninen, H., 1997, Terminen väsyminen soodakattilan kompound-putkissa. Finnish recovery Boiler Committee's Recovery Boiler Day, October 22, 1997, Helsinki, Finland.

Salmenoja, Keijo, 2004, Superheater corrosion in modern recovery boilers. 40th Anniversary International Recovery Boiler Conference, Finnish Recovery Boiler Committee, Haikko Manor, Porvoo, May 12-14, 2004, pp. 103 – 113.

Salmenoja, Keijo and Tuiremo, Johanna, 2001, Achievements in the control of superheater corrosion in black liquor recovery boilers. Proceedings of 2001 Tappi Engineering, Finishing & Converting Conference, Tappi Press, Atlanta, GA, 9 p.

Salmenoja, Keijo, 2000, Field and laboratory studies on chlorine-induced superheater corrosion in boilers fired with biofuels. Ph. D. thesis, Report 00-1, Process Chemistry Group, Åbo Akademi, Turku, Finland, 102 p. ISBN 952-12-0619-5.

Salmenoja, Keijo, Hupa, Mikko and Backman, Rainer, 1999, Laboratory studies on the influence of gaseous HCl on the fireside corrosion of superheaters. *Journal of the Institute of Energy*, Vol. 72, December 1999, pp. 127 – 133.

Salmenoja, Keijo, 1998, The role of the black liquor recovery boiler in the closure of chemical cycles in the pulp mill. *Appita Journal*, Vol. 52, No. 2, March 1998, pp. 88 - 92.

Sandquist, Kent, 1987, Operational experience with single drum recovery boilers in North America. Tappi 1987 Kraft Recovery Operations Seminar, Orlando, Fl, January 11 – 16, pp. 221 – 231.

Sandquist, Kent, 1987, Operational experience of composite tubing in recovery boiler furnaces. Götaverken Energy Systems, technical paper TP-2-87, 15 p.

Saroha, Anil K., Wadhwa, Rajesh K., Chandra, Sandip, Roy, Maheshwar and Bajpai, Pramod, K., 2003, Soda recovery from non-wood spent pulping liquor. *Appita Journal*, Vol. 56, No. 2, pp. 107 – 110.

Saviharju, Kari and Pynnönen, Petri, 2003, Soodakattilan keon hallinta. (Control of kraft recovery boiler char bed) in Finnish, Finnish Recovery Boiler Users Association, Konemestaripäivä, 23.1.2003, Oulu, Finnish Recovery Boiler Users Association, 16 p.

Schaddix, Chris, Holve, Don and Wessel, Rick, 2003, Recent measurements of ISP concentration, size, and chemistry in a recovery boiler. Colloquium of black liquor combustion and gasification, Park City, Utah, 13-16 May 2003, 10 p.

Schmidt, Ernst, 1989, Properties of water and steam in SI-units: 0-800 °C, 0-1000 bar. 4th, enl. pr., Berlin, Springer, 206 p. ISBN: 0-387-09601-9.

Sricharoenchaikul, Viboon, Frederick, Wm. James, Jr. and Agrawal, Pradeep, 2002, Black liquor gasification characteristics, 1. Formation and conversion of carbon-containing product gases. *Ind. Eng. Chem. Res*., Vol. 41, No. 23, pp. 5640 - 5649.

Sricharoenchaikul, Viboon, Frederick, Wm. James and Agrawal, Pradeep, 2002, Black liquor gasification characteristics, 2. Measurement of condensable organic matter (tar) at rapid heating conditions. *Ind. Eng. Chem. Res*., Vol. 41, No. 23, pp. 5650 - 5658.

Sricharoenchaikul, Viboon, Hicks, A. L. and Frederick, Wm. James, Jr., 2001, Carbon and char residue yields from rapid pyrolysis of kraft black liquor. *Bioresource Technology*, Vol. 77, pp. 131 - 138.

Schupe, W. and Jeschar, R., 1975, Simplified calculation of radiant heat transfer in industrial furnaces and comparison with measurements made in an experimental combustion chamber, *Gas Wärme International*, Vol. 24, No. 2, pp. 64 – 75.

Scott-Young, R. E. and Cukier, M., 1995, Commercial development of the DARS process. Proceedings of 1995 International Chemical Recovery Conference, Toronto Canada, CPPA, pp. B263 - B267.

Schunk, M., 1983. Properties of pure fluids. in Heat Exchanger Design Handbook, Part 5 Physical properties, Hemisphere Publishing Corporation, pp. 5.5.2-1 - 5.5.2-11

Sebbas, Eva, Ahonen, Aki and Haasiosalo, Taisto, 1983, Jäteliemien poltto, kemikaalien talteenotto ja keittoliuosten valmistus. (Burning of waste liquors, chemicals recovery and manufacture of cooking liquor) in Finnish, in Puumassan Valmistus (Manufacture of pulp), editor Vikola, Nils-Erik, 2nd edition, Teknillisten tieteiden akatemia, Turku, pp. 1189 – 1300. ISBN 951-99452-0-2.

Shenassa, Reyhaneh, Tuiremo, Johanna and Haaga, Kari, 2002, Primary air port tube integrity - a critical review of primary air port design and the effect of boiler design parameters. Proceedings of 2002 TAPPI Fall Technical Conference, September 8 - 11, San Diego, Ca, 11 p.

Shiang, Niann T., 1986, Mathematical modeling and simulation of recovery furnace. Ph. D. thesis, University of Idaho, Moscow.

Shiang, Niann T. and Edwards, Louis L., 1988, Understanding and controlling fireside deposits in kraft recovery furnaces. Chemical Engineering Technology in Forest Products Processing, AlChE Forest Products Division, Vol. 2, pp. 105 - 114.

Shiang, Niann T. and Edwards, Louis L., 1986, Kraft recovery furnace modeling and simulation: heat transfer and gas flow. Forest Products, AIChE Symposium Series, pp. 85 - 94.

Singh, Preet M., Al-Hassan, Safaa J., Stalder, Sloane and Fonder, Greg, 1999, Corrosion in kraft recovery boilers – in-situ characterization of corrosive environments. Proceedings of 1999 Tappi Engineering Conference, September 12 – 16, Anaheim, California, 14 p.

Sinquefield, S. A., Baxter, L. L. and Frederick, W., J., 1998, An experimental study on the mechanisms of fine particle deposition in kraft recovery boilers. Proceedings of 1998 International Chemical Recovery Conference, Tampa, USA, 1 - 4 June 1998, Vol. 3, TAPPI, pp. 443 – 467.

Sjöber, M. and Cameron, J. H., 1984, *AIChE Symposium Series,* Vol. 80, No. 239, p. 35.

Skrifvars, Bengt-Johan, Hupa, Mikko and Hyöty, Paavo, 1991, Composition of recovery

boiler dust and its effect on sintering. *Tappi Journal*, Vol. 74, No. 6, pp. 185-189.

Skrifvars, Bengt-Johan, 1989, Recovery boiler dust sintering and dust composition. The midnight sun colloquium on recovery research, June 14 - 16 1989, STFi, pp. 8 - 10.

Smith, E. L., 1964, Kraft mill recovery units – the third generation. *Paper Trade Journal*, Vol. 140, No. 44, p. 30.

Soar, Roger J., Bardutz, Ronald W. and Guzi, Charlie E., 1994, Characterizing the wastage on near-drum generator tubes using full-coverage ultrasonic scans. *Tappi Journal*, Vol. 77, No. 8, August 1994, pp. 201 - 209.

Someshwar, Arun V. and Jain, Ashok K., 1995, Hydrochloric acid emissions from kraft recovery furnaces. *Tappi Journal*, Vol. 78, No. 12, December 1995, pp. 77 - 83.

Sonnenberg, Gerhard Siegfried, 1968, Hundert jahre sicherheit. (Hundred years of safety) in German, Technikgeschichte in Einzeldarstellungen, 6, VDI-Verlag, Düsseldorf, 338 p.

Sonnenberg, Lucinda B. and Nichols, Kenneth M., 1995, Emissions of hydrochloric acid, PCDD and PCDF from the combustion of chlorine-containing kraft pulp mill bleach plant waste. *Chemosphere*, Vol. 31, No. 10, pp. 4207 – 4223.

Soodakattiloiden syöpymistutkimus 1965 – 1968, 1968, (Corrosion study of recovery boilers 1965 – 1968) in Finnish, Final report 23.10.1968, Ekono, 151 p.

Spielbauer, Thomas M. and Aidun, Cyrus, K., 1992, Mechanisms of liquid sheet breakup and the resulting drop size distributions, Part 1: types of spray nozzles and mechanism of sheet disintegration. *Tappi Journal*, Vol. 75, No. 2, February 1992, pp. 136 - 142.

Spielbauer, Thomas M. and Aidun, Cyrus, K., 1992, Mechanisms of liquid sheet breakup and the resulting drop size distributions - Part 2: strand breakup and experimental observations. *Tappi Journal*, Vol. 75, No. 3, March 1992, pp. 195 - 200.

Spielbauer, T. M. and Adams, T. N., 1990, Flow and pressure drop characteristics of black liquor nozzles. *Tappi Journal*, Vol. 73, No. 9, September 1990, pp. 169 -174.

Sricharoenchaikul, V., Frederick, W. J. and Grace, T. M., 1995, Thermal conversion of tar to light gases during black liquor pyrolysis. Proceedings of 1995 International Chemical Recovery Conference, Toronto Canada, CPPA, pp. A209 - A216.

Sricharoenchaikul, V., Frederick, W. J., Kymäläinen, M. and Grace, T. M., 1995, Sulfur species transformation and sulfate reduction during pyrolysis of kraft black liquor. Proceedings of 1995 International Chemical Recovery Conference, Toronto Canada, CPPA, pp. A227 - A236.

Stead, N. J., Singbeil, D. L. and Forget, C., 1995, Formation of low melting deposits in a modern kraft recovery boiler. Proceedings of 1995 International Chemical Recovery Conference, Toronto Canada, CPPA, pp. A105 – A109.

Steam its generation and use, 1992, 40th edition, editors Stultz, Steven C. and Kitto, John B., 929 p. ISBN 0-9634570-0-4.

Steam power engineering, 1999, editor Seikan Ishigai, Cambridge University Press, New York, 394 p. ISBN 0-521-62635-8.

Streeter, Victor L. and Wylie. E. Benjamin, 1983, Fluid mechanics. McGraw-Hill Book Company. ISBN 0-07-066578-8.

Suik, Heinrich, 2000, Catastrophic corrosion of superheater tubes. UEF Conference on Behavior of Inorganic Materials in Recovery Boilers, Bar Harbor, Maine, 4 - 9 June 2000, United Engineering Foundation, 13 p.

Sumnicht, Daniel W., 1989, A computer model of a kraft char bed. Doctoral Dissertation, Atlanta, Georgia, The Institute of paper Chemistry, 193 p.

Sunil, Anita, 2003, Fluidity of molten smelt in recovery boilers. Web page at www.pulpandpaper.utoronto.ca/Research/Kraft/Summaries/sunil.html.

Sutinen, J., Karvinen, R. and Frederick, W. J. Jr., 2002, A chemical reaction engineering and transport model of kraft char bed burning. *Industrial & Engineering Chemistry Research*, Vol. 41, No. 6, pp.1477 - 1483.

Suutela, Jukka and Fogelholm, Carl-Johan, 2000, Heat and power co-generation. Chapter 16 in Chemical Pulping, Book 6, series editors Gullichsen, Johan and Fogelholm, Carl-Johan, Finnish Paper Engineers' Association and TAPPI. ISBN 952-5216-06-3.

Swartz, J. N. and MacDonald, R. C., 1962, Alkaline pulping. Chapter 9 in Pulp and Paper Science and Technology, Vol. I, editor Libby, C. Earl, McGraw-Hill, New York, pp. 160 – 239.

Sychev, V. V. et al., 1987a, Thermodynamic properties of nitrogen. National Standard Reference Data Service of the USSR, A Series of Property Tables. Hemisphere Publishing Corporation. 341 p.

Sychev, V. V. et al., 1987b, Thermodynamic properties of methane. National Standard Reference Data Service of the USSR, A Series of Property Tables. Hemisphere Publishing Corporation. 341 p.

Sychev, V. V. et al., 1987c, Thermodynamic properties of oxygen. National Standard Reference

Data Service of the USSR, A Series of Property Tables. Hemisphere Publishing Corporation. 307 p.

Söderhjelm, Liva, Sågfors, Pär-Erik and Kiiskilä, Erkki, 1998, Factors influencing heat treatment of black liquor. Proceedings of 1998 International Chemical Recovery Conference, Tampa, USA, 1 - 4 June 1998, TAPPI Press, Atlanta, pp. 169 – 184.

Söderhjelm, Liva, 1994, Black liquor properties. 30 Years Recovery Boiler Co-operation in Finland, International conference, Baltic sea, 24 - 26 May, pp. 23 - 36.

Talbot, L., Cheng, R. K., Schefer, R. W. and Willis, D. R., 1980, Thermophoresis of particles in a heated boundary layer. *ASME Journal of Fluid Mechanics*, Vol. 101, No. 4, p. 737.

Taljat, B., Zacharia T., Wang X.-L., Keiser J. R., Swindeman R. W. and Hubbard C. R., 1998, Mechanical design of steel tubing for use in black liquor recovery boilers. 9th International Symposium on Corrosion in the Pulp and Paper Industry, May 26 – 29, 1998, Ottawa, Ontario, Canada.

Tamminen, Tarja, Kiuru, Jukka, Kiuru, Reijo, Janka, Kauko and Hupa, Mikko, 2002, Dust and flue gas chemistry during rapid changes in the operation of black liquor recovery boilers: Part 1—Dust composition. *Tappi Journal*, Vol. 1, No. 5, July 2002, pp. 27 - 32.

Tamminen, Tarja, Hupa, Mikko, Kujanpää, Jukka and Tikkanen, Juha, 2000, An on-line method for measuring transient changes in the amount and composition of dust in recovery boilers. UEF Conference on Behavior of Inorganic Materials in Recovery Boilers, Bar Harbor, Maine, 4 - 9 June 2000, United Engineering Foundation, 13 p.

Tandra, Danny S., Kaliazine, Andrei, Cormack, Donald E. and Tran, Honghi, 2001, Numerical simulation of sootblower jet and deposit interaction. 14th Annual Chemical Recovery Research Review Meeting, University of Toronto, November 14-15, 2001, 3 p.

Tavares, Alarick J., Tran, Honghi and Reid, Timothy P., 1998, Effect of char bed temperature and temperature distribution on fume generation in a kraft recovery boiler. *Tappi Journal*, Vol. 81, No. 9, September 1998, pp. 134 - 138.

Tay, Chee Vui, Kawaji, Masahiro, Tran, Honghi and Grace, Thomas M., 2004, Recovery boiler tube temperature excursions caused by smelt contact. Proceedings of 2004 International Chemical Recovery Conference, June 6-10 2004, Charleston, South Carolina, USA, 543-553 p.

Techakijkajorn, U., Frederick, W. J. and Tran, H. N., 1999, Sintering of fume deposits in kraft recovery boilers. *Journal of Pulp and Paper Science*, Vol. 25, No. 3, pp. 73 - 83.

Teir, Sebastian, 2003, Steam boiler technology. 2nd ed, Energiatekniikan ja ympäristönsuojelun laboratorio, Konetekniikan osasto, TKK, Espoo. 216 p. Electronic publication http://eny.hut.fi/library/e-books.htm

Thomas, H.-J., 1975, Thermische kraftanlagen. (Thermal powerplants) in German, 386 p. ISBN 3-540-06779-5.

Thompson, Laura M. and Empie, H. Jeff, 1993, A proposed mechanism for the depletion of NOx in a kraft recovery furnace. Proceedings of 1993 Environmental Conference, Tappi press, pp. 643 – 647.

Tomlinson, C. L. and Richter, F. H., 1969, The alkali recovery system. Chapter 10 in Pulp and paper manufacture, Vol. I, The Pulping of Wood, editors MacDonald, Ronald G. and Franklin, John, H., McGraw-Hill, New York, pp. 576 – 627.

Tran, Honghi, 2004, Fouling of tube surfaces in kraft recovery boilers. 40th Anniversary International Recovery Boiler Conference, Finnish Recovery Boiler Committee, Haikko Manor, Porvoo, May 12-14, 2004, pp. 91 – 101.

Tran, Honghi and Arakawa, Yoshisa, 2001, Recovery boiler technology in Japan. Proceedings of 2001 Tappi Engineering, Finishing & Converting Conference, Tappi Press, Atlanta, GA, 13 p.

Tran, Honghi, Frederick, William J. Jr., Iisa, Kristiina, Tavares, Alarick J. and Villarroel, Roberto, 2000, Relationship between SO_2 emissions and precipitator dust composition in recovery boilers. Proceedings of 2000 TAPPI Engineering Conference, September 17-21, 2000, Atlanta.

Tran, Honghi and Villarroel, Roberto, 1999, Effect of CNCG combustion on recovery boiler operation and dust composition. Proceedings of 1999 Tappi Engineering/Process and product Quality Conference, September 12 – 16, Anaheim, California, pp.179 - 186.

Tran, Honghi, Habibi, Bahman and Jia, Charles, 1999, Drying behaviour of waterwash solution and the effect on composite floor tube cracking in recovery boilers. Proceedings of 1999 Tappi Engineering/Process and product Quality Conference, September 12 – 16, Anaheim, California, pp. 1061 – 1070.

Tran, Honghi, Gonsko, Meredith and Mao, Xiaosong, 1999, Effect of composition on the first melting temperature of fireside deposits in recovery boilers. *Tappi Journal*, Vol. 82, No. 9, September 1999, pp. 93 - 100.

Tran, Honghi, 1988, How does a kraft recovery boiler become plugged. TAPPI 1988 Kraft Recovery Operations Seminar, pp. 175 - 183.

Tran, H. N., Barham, D. and Reeve, D. W., 1988, Sintering of fireside deposits and its impact

on plugging in kraft recovery boiler. *Tappi Journal*, Vol. 70, No. 4, pp. 109 - 113.

Tran, H., Reeve, D. and Barham, D., 1983, Formation of kraft recovery boiler superheater fireside deposits. *Pulp & Paper Canada*, Vol. 84, No. 1, January 1983, pp. 36 - 41.

Truelove, J. S., 1983, Furnaces and combustion chambers. in Heat exchanger design handbook, HEDH, Part 3, Thermal and hydraulic design of heat exchangers, VDI, Düsseldorf, pp. 3.11.4-1 – 9. ISBN 3-18-419082-8.

Tse, D., Salcudean, M. and Gartshore, I., 1994, Multiple jet interaction with relevance to recovery boiler flow fields. *Pulp & Paper Canada*, Vol. 95, No. 2, February 1994, pp. T79 – T82.

Tsuchiya, Keiichi, Yamada, Hidetsugu and Hosoya, Minoru, 2002, Investigation of KP operational conditions in Japanese KP mills (phase 3): chemical recovery process (black liquor evaporator, recovery boiler, recausticizing, lime calcining). Japan *Tappi Journal*, Vol. 56, No. 2, February 2002, pp. 59-74.

Tucker, Paul, 2002, Changing the balance of power. *Solutions!* February 2002, pp. 34 – 38.

Uloth, V. C., Marcovic, C. M., Wearing, T. J. and Walsh, A., 1996, Observations on the dynamics and efficiency of sootblowing in kraft recovery furnaces, part II - Dynamics. *Pulp & Paper Canada*, Vol. 97, No. 7, July 1996, pp. 35 – 38.

Uloth, V. C., Marcovic, C. M., Wearing, T. J. and Walsh, A., 1996b, Observations on the dynamics and efficiency of sootblowing in kraft recovery furnaces, part I: Dynamics. *Pulp & Paper Canada*, Vol. 97, No. 6, June 1996, pp. 59 – 65.

Uppstu, Erik, 1995, Soodakattilan ilmanjaon hallinta. (Control of recovery boiler air distribution) in Finnish, Soodakattilapäivä 1995, Finnish Recovery Boiler Committee, 6 p.

Vafa, Shermineh, 2003, Effect of char bed dynamics on recovery boiler primary air port tube temperature excursions. Web page at www.pulpandpaper.utoronto.ca/Research/Kraft/Summaries/vafa.html.

Vakkilainen, Esa K., Kankkonen, Sebastian and Suutela, Jukka, 2004, Advanced efficiency options - increasing electricity generating potential from pulp mills. Proceedings of 2004 International Chemical Recovery Conference, June 6-10 2004, Charleston, South Carolina, USA, pp. 1 - 12.

Vakkilainen, Esa K., 2004, Future of recovery boiler technology. 40th Anniversary International Recovery Boiler Conference, Finnish Recovery Boiler Committee, Haikko Manor, Porvoo, May 12-14, 2004, pp. 51 – 58.

Vakkilainen, Esa K. and Pekkanen, Markku J., 2002, Burning excess streams in recovery boilers. Proceedings 2002 TAPPI Fall Technical Conference, September 8-11, San Diego, Ca, 9 p.

Vakkilainen, Esa, Holm, Ralf and Simonen, Liisa, 2001, Emission performance of large recovery boilers. Tappi Engineering / Finishing & Converting Conference, September 16-20, 2001, San Antonio, TX, Tappi Press, pp. 118 – 127.

Vakkilainen, Esa K., 2000, Predicting ash properties in recovery boilers. UEF Conference on Behavior of Inorganic Materials in Recovery Boilers, Bar Harbor, Maine, 4 - 9 June 2000. United Engineering Foundation, 11 p.

Vakkilainen, Esa, 2000b, Recovery boiler. Chapter 13 in Chemical Pulping, Book 6, series editors Gullichsen, Johan and Fogelholm, Carl-Johan, Finnish Paper Engineers' Association and TAPPI. ISBN 952-5216-06-3.

Vakkilainen, Esa and Holm, Ralf, 2000, Firing very high dry solids in recovery boilers. Proceedings of 2000 Tappi Engineering Conference, September 17-21, 2000, Atlanta

Vakkilainen, Esa K., Taivassalo, V., Kjäldman, L., Kilpinen, P. and Norström, T., 1998, High solids firing in an operating recovery boiler - comparison of CFD predictions to practical observations in the furnace. Proceedings 1998 International Chemical Recovery Conference, Tampa, USA, 1 - 4 June 1998, TAPPI Press, Atlanta, pp. 245 – 256.

Vakkilainen, Esa, Backman, Rainer, Forssén, Mikael and Hupa, Mikko, 1998b, Effects of liquor heat treatment on black liquor combustion properties. Proceedings 1998 International Chemical Recovery Conference, Tampa, USA, 1 - 4 June 1998, TAPPI Press, Atlanta, pp. 229 – 244.

Vakkilainen, Esa, 1996, Recovery boiler adjustable air. Presentation at Spring BLRBAC, Atlanta, Georgia. 7 p.

Vakkilainen, Esa, Frederick, William J., Reis, V. V. and Wåg, Kaj. J., 1995, Potassium and chlorine enrichment during black liquor combustion. Laboratory and mill measurements and a mechanistic model. Proceedings 1995 International Chemical Recovery Conference, Toronto, CPPA, pp. B63 - B76.

Vakkilainen, Esa, 1994a, Limits of recovery boiler technology. 30 Years Recovery Boiler Cooperation in Finland, International conference, Baltic sea, 24 - 26 May.

Vakkilainen, Esa, 1994b, High black liquor solids changes operation of recovery boiler. *Paperi ja Puu* (Paper and Timber), Vol. 76, No. 8.

Vakkilainen, Esa and Niemitalo, Hanna, 1994, Measurement of high dry solids fouling and improvement of sootblowing control. Proceedings of 1994 Tappi Engineering Conference, San

Francisco, California.

Vakkilainen, Esa and Anttonen, Timo, 1993, Effect of economizer central pass design on thermal performance. Proceedings of 1993 Tappi Engineering Conference, Orlando, Florida, Tappi Press. 14 p.

Vakkilainen, Esa and Vihavainen Esa, 1992, Long term fouling of recovery boiler surfaces. Proceedings of 1992 International Chemical Recovery Conference, Seattle, Washington, June 7 - 11.

Vakkilainen, Esa, Adams, Terry N. and Horton, Robert R., 1992, The effect of bullnose designs on upper furnace flow and temperature profiles. Proceedings of 1992 International Chemical Recovery Conference, Seattle, Washington, June 7-11, pp. 101 - 112.

Vannérus, Torbjörn, Svensson, Gustav and Forslund, Folke, 1948, Ångpannor. (Steam generators) in Swedish, Chapter 19, in Maskinteknik, Ingenjörshadboken 2, Nordisk Rotogravyr, Stockholm, Sweden, pp. 937 – 1072.

Vasara, Petri, 2001, Through different eyes: Environmental issues in Scandinavia and North America. *Tappi Journal*, Vol. 84, No. 6, June 2001, pp. 46 - 49.

VDI heat atlas, 1993, Verein Deutscher Ingenieure, VDI-Gesellschaft Verfahrenstechnik und Chemieingenieurwesen, Düsseldorf, VDI-Verlag, ISBN 3-18-400915-7.

Vegeby, Anders, 1966, Scandinavian practices in the design and operation of recovery boilers. *Tappi Journal*, Vol. 49, No. 7, p. 103.

Vegeby, Anders, 1961, Synpunkter på indunstning till högre torrhalt – inverkan i sodahuset. (Viewpoints of high dry solids evaporation – effect to recovery operation) in Swedish, Sodahuskonferens, ÅF-IPK, Stockholm, pp. 60 – 69.

Verloop, Arie and Jansen, Johan H., 1995, Operating a recovery boiler at reduced solids throughput. Proceedings 1995 International Chemical Recovery Conference, Toronto, CPPA, pp. B1 – B4.

Verrill, Chris and Lien, Steven, 2003, The significance of char bed-generated particulate on recovery boiler fouling relative to other sources of combustion areosols. Proceedings of Colloquium of black liquor combustion and gasification, Park City, Utah, 13-16 May 2003, 9 p.

Verrill, Christopher L. and Wessel, Richard A., 1998, Detailed black liquor drop combustion model for predicting fume in kraft recovery boilers. *Tappi Journal*, Vol. 81, No. 9, September 1998, pp. 139 - 148.

Verrill, Christopher L. and Wessel, Richard A., 1995, Sodium loss during black liquor drying and devolatilization - application of modeling results to understanding laboratory data. Proceedings of 1995 International Chemical Recovery Conference, Toronto, Canada, CPPA, pp. B89 - B103.

Verrill, Christopher L. and Wessel, Richard A., 1995, Model of alkali release during black liquor combustion. *Journal of Aerosol Science*, Vol. 26, September 1995, pp. S171 - S172.

Verveka, Peter, Nichols, Kenneth M., Horton, Robert R. and Adams, Terry N., 1993, The form of nitrogen in wood and its fate during kraft pulping. Proceedings of 1993 Environmental Conference, Tappi press, pp. 777 – 780.

Villarroel, Roberto, Gonçalves, Cláudia and Tran, Honghi, 2004, Experience of screen tube damage caused by falling deposits in kraft recovery boilers. Proceedings of 2004 International Chemical Recovery Conference, June 6-10 2004, Charleston, South Carolina, USA, pp. 341 - 349.

Viteri, João Arlindo, 2001, Recentes rejetos de novas caldeiras de recuperação no Brasil. (Recent projects of new chemical recovery boilers in Brazil) in Portuguese, 14th Latin-American Recovery Boilers meeting, August 7 – 10, Sao Paulo, Associação Brasileira Technica de Celulose e Papel. 10 p.

Välimäki, Erkki and Salmenoja, Keijo, 2004, Measured data for sootblowing optimization. Proceedings of 2004 TAPPI Fall Technical Conference, October 31 - November 3, Atlanta, Georgia, 13 p.

Wagner, Wolfgang and Kruse, Alfred, 1998, Properties of water and steam the industrial standard IAPWS-IF97 for the thermodynamic properties and supplementary equations for other properties tables based on these equations. Berlin, Springer, 354 p., ISBN 3-540-64339-7.

Wallén, Jonas, Ruohola, Tuomo and Aikio, Anne, 2004, Sulfur dioxide emission dependency on kraft recovery boiler operation parameters. Proceedings of 2004 International Chemical Recovery Conference, June 6-10 2004, Charleston, South Carolina, USA, pp. 483-490.

Wallén, Jonas, Viiala, Juhani and Björkström, Ingvar, 2002, Operational performance of Billerud Gruvon's new recovery boiler with environmental friendly solutions. Proceedings of 2002 TAPPI Fall Technical Conference, September 8 - 11, San Diego, Ca, 10 p.

Walsh, Alan R. and Srandell, Olof, 1992, Use of design and operating data to determine recovery boiler upgrade potential. Proceedings of 1992 International Chemical Recovery Conference, Seattle, Washington, June 7-11, pp. 421 – 428.

Walsh, Alan R. and Grace, Thomas M., 1989, TRAC: A computer model to analyze the trajectory and combustion behavior of black liquor

droplets. *Journal of Pulp and Paper Science*, Vol. 15, No. 3, May 1989, pp. J84 - J89.

Warnqvist, Björn, Delin, Lennart, Theliander, Hans and Nohlgren, Ingrid, 2000, Technoeconomical evaluation of black liquor gasification processes. Technical report, S6-614, Värmeforsk Service AB, June 2000, ISSN 0282-3772. 37 p.

Warnqvist, Björn, Ihrén, Niclas and Berglin, Niklas, 1994, Combined power plant technology in the recovery cycle of kraft pulp mills. 30 Years Recovery Boiler Co-operation in Finland, International conference, Baltic sea, 24 - 26 May, pp. 95 – 106.

Warnqvist, Björn, 1994, Char bed and smelt properties mill studies. *Pulp and Paper Canada*, Vol. 95, No. 8, pp. 313 – 315.

Wessel, Richard. A. and Kaufman, Keith C., 2000, Computer modeling of kraft recovery boilers. UEF Conference on Behavior of Inorganic Materials in Recovery Boilers, Bar Harbor, Maine, 4 - 9 June 2000. United Engineering Foundation, 16 p.

Wessel, Richard A., Denison, Martin K. and Samretvanich, Artit, 1998, The effect of fume on radiative heat transfer in kraft recovery boilers. Proceedings 1998 International Chemical Recovery Conference, Tampa, USA, 1 - 4 June 1998, TAPPI Press, Atlanta, pp. 425 – 441.

Wessel, R. A. and Righi, J., 1998, Generalized correlations for inertial impaction of particles on a circular cylinder. *Aerosol Sci. Technol.* (AAAR), No. 9, pp. 29-60.

Westerberg, E. Norman, 1983, Kraft mill recovery units examined. *Pulp and Paper International*, March 1983, pp. 53 – 54.

Whitney, Roy P., 1968, Introduction. Chapter 1 of Chemical recovery in alkaline pulping process, editor Whitney, Roy P., *TAPPI Monograph series,* No. 32, Mack Printing Company, Easton, Pa., pp. 1 – 14.

Whitty, Kevin and Verrill, Christopher L., 2004, A historical look at the development of alternative black liquor recovery technologies and the evolution of black liquor gasifier designs. Proceedings of 2004 International Chemical Recovery Conference, June 6-10 2004, Charleston, South Carolina, USA, pp. 13 - 34.

Whitty, Kevin, Backman, Rainer, Forssén, Mikael, Hupa, Mikko, Rainio, Janne and Sorvari, Vesa, 1997, Liquor-to-liquor differences in combustion and gasification processes: pyrolysis behaviour and char reactivity. *Journal of Pulp and Paper Science*, Vol. 23, No. 3, March 1997, pp. J119 - J128.

Whitty, Kevin, Backman, Rainer, Forssén, Mikael, Hupa, Mikko, Raino, Janne and Sorvari, Vesa, 1995, Liquor to liquor differences in combustion and gasification processes pyrolysis behavior and char reactivity. Proceedings of 1995 International Chemical Recovery Conference, Toronto, CPPA, pp. A245 - A253.

Wozniak, John C., 1985, Measurements of the physical properties of kraft smelt. The Institute of Paper Chemistry, Appleton Wisconsin. 69 p.

Wåg, Kaj J., Reis, Victor V., Frederick, William J. and Grace, Thomas M., 1997, Mathematical model for the release of inorganic emissions during black liquor char combustion. *Tappi Journal*, Vol. 80, No. 5, May 1997, pp. 135 – 145.

Wåg, Kaj J., Grace, Thomas M. and Kymäläinen, Marita, 1995, Sulfate reduction and carbon removal during kraft char burning. Proceedings of 1995 International Chemical Recovery Conference, Toronto, Canada, CPPA, pp. B35 - B50.

Zaman, A. A. and Fricke, A. L., 1995, Effects of pulping conditions and black liquor composition on the heat of combustion of slash pine black liquor. in Advances in pulping and papermaking, *AIChE Symposium Series*, Vol. 91, No. 307, pp. 154 – 171. ISBN 0-8169-0687-4.

Zeldovich, J., 1946, The oxidation of nitrogen in combustions and explosions. *Acta physiochimica U.R.S.S.*, Vol. 21, No. 3, pp. 577 – 628.

Zevenhoven, Ron and Kilpinen, Pia, 2001, Control of pollutants in flue gases and fuel gases. Picaset Oy, Espoo, 298 p. Electronic publication http://www.hut.fi/~rzevenho/gasbook.

Index

A Emission conversions

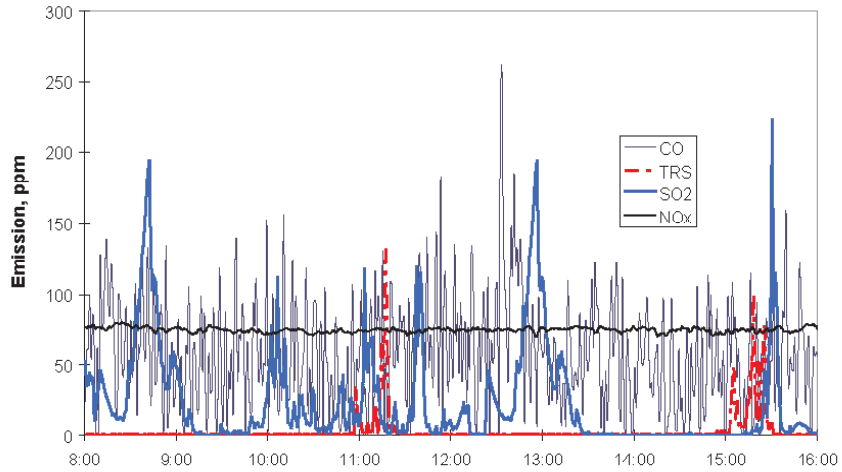

Figure A-1, Typical emissions from recovery boiler.

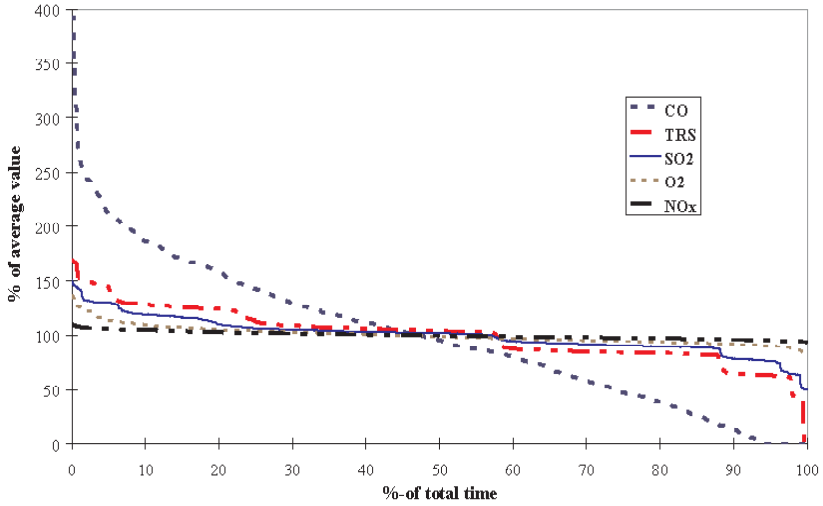

Figure A-2, Same emissions ordered from large to small and scaled so average equals 100.

A.1 CONVERSION OF AVERAGE EMISSIONS TO TIME NOT TO EXCEED

Recovery boiler emissions values are normally based on continuous operation. Short-term values exceed these average values.

When converting average data to peak data at least the corrections in the Table A-1 should be applied. E.g. Average SO_2 emission is 150 mg/MJ. Value for not to exceed for more than 15 min/24h for SO_2 is then 2,00*150 mg/MJ = 300 mg/MJ.

***Table A-1**, Multiplicator for conversion from average to time not to exceed.*

	Time	CO	C_xH_y	TRS	SO_2	NOx	Dust
24 h	100%	1,00	1,00	1,00	1,00	1,00	1,000
8 h/24 h	67 %	1,05	1,03	1,02	1,02	1,01	1,000
1 h/24 h	95 %	2,00	1,70	1,30	1,40	1,05	1,300
30 min/24 h	98 %	2,50	2,20	1,40	1,60	1,07	1,500
15 min/24h	99 %	3,00	2,50	1,60	2,00	1,10	3,000

A.2 CONVERSIONS

The following equations can be used to convert emissions from one value base to another.

Emission from mg/m³n to mg/MJ

$$E[mg/MJ] = 0.24\ n\ k\ E[mg/m^3n] \qquad A\text{-}1$$

where

$E[mg/m^3n]$	is the emission at dry flue gases and air ratio n, mg/m^3n
E[mg/MJ]	is the emission per heat input, mg/MJ
n	is the air ratio at which emission $[mg/m^3n]$ is given
k	is a correction factor to correct emission to lower heating value, -

and

$$k = q_{HHV}/(q_{HHV}\text{-}21.987^{H}/_{100}\text{-}2.443^{(100-x)}/_{x}) \qquad A\text{-}2$$

where

H	is the black liquor hydrogen content as fired, w-%
q_{HHV}	is the black liquor higher heating value as fired, MJ/kgds
x	is the black liquor dry solids as fired, w-%

Example

NO 260 mg/m^3n at 1.2, HHV = 14.0, ds = 75%, H = 3.5%.

k = $14.0/(14.0\text{-}21.987^{*3.5}/_{100}\text{-}2.443^{*(^{(100-75)}/_{75})}$
= 14.0/(14.0-0.77-0.81) = 1.13

$NO[mg/m^3n] = 260*1.2*1.13*0.24 = 85$ mg/MJ

Emission form one O_2 level to another O_2 level

A good approximation of air ratio n is

$$n = 20.9/(20.9\text{-}O_2) \qquad A\text{-}3$$

O_2 is the oxygen content at dry flue gases, vol-%

$$E_Y = E_Z\ (20.9\text{-}O_{2Y})/(20.9\text{-}O_{2Z}) \qquad A\text{-}4$$

where

E_Y	is the emission at dry flue gases and oxygen content Y, mg/m^3n
E_Z	is the emission at dry flue gases and oxygen content Z, mg/m^3n
O_{2Y}	is the corresponding oxygen content Y at dry flue gases, vol-%
O_{2Z}	is the corresponding oxygen content Z at dry flue gases, vol-%

The same equation can be used to change ppm at one O_2 level to another O_2 level at dry flue gases. The emission as mg/MJ at one O_2 level is the same as at another O_2 level (no correction needed).

Emission form ppm to mg/m³n

Emission at dry or wet flue gases can be converted to mg/m3n at the same O_2 level and at dry or wet conditions respectively by multiplying with a coefficient. It is customary that many emissions can be expressed also as equivalent species (e.g. sulfur emissions are often expressed as S or as SO_2).

1 ppm H_2S	= 1.535 mg(as H_2S)/m^3n
1 ppm H_2S	= 1.441 mg(as S)/m^3n
1 ppm CO	= 1.253 mg(as CO)/m^3n
1 ppm NO_2	= 2.053 mg(as NO_2)/m^3n
1 ppm NO	= 2.053 mg(as NO_2)/m^3n
1 ppm NO	= 1.229 mg(as NO)/m^3n
1 ppm NOx	= 2.053 mg(as NO_2)/m^3n
1 ppm NOx	= 1.375 mg(as 95% NO and 5 % NO_2)/m^3n
1 ppm SO_2	= 2.926 mg(as SO_2)/m^3n
1 ppm SO_2	= 1.461 mg(as S)/m^3n
1 ppm HCl	= 1.628 mg(as HCl)/m^3n
1 ppm HCl	= 1.583 mg(as Cl)/m^3n
1 ppm NH_3	= 0.771 mg(as NH_3)/m^3n
1 ppm NH_3	= 2.053 mg(as NO_2)/m^3n
1 ppm CH_4	= 0.719 mg(as CH_4)/m3n
1 ppm H_2SO_4	= 4.375 mg(as H_2SO_4)/m^3n
1 ppm CH_4S	= 2.148 mg(as CH_4S)/m^3n
1 ppm CH_4S	= 2.860 mg(as SO_2)/m^3n
1 ppm CH4S	= 1.428 mg(as S)/m^3n
1 ppm C_2H_6S	= 2.774 mg(as C_2H_6S)/m^3n
1 ppm C_2H_6S	= 2.860 mg(as SO_2)/m^3n
1 ppm C_2H_6S	= 1.428 mg(as S)/m^3n